PEGASOS Refinement Project

Volume 3
SP1 - Seismic Source Characterization -

Evaluation Summaries and Hazard Input Documents

by

Philippe L.A. Renault, Kevin J. Coppersmith,
Robert R. Youngs & SP1 Experts

Olten, 20. December 2013
Rev.1: 28. March 2014

Contents

Part I

General Introduction

by R. Youngs

Chapter 1

Introduction

1.1 Structure of the Report

Analyses Conducted for the SP1 Teams

The following chapters include those calculations and analyses that were conducted by the TFI team at the request of each SP1 team:

Chapter 2, Part II - chapter 2, Part III - chapter 2, Part IV - chapter 2, Part V - chapter 2.

Evaluation Summaries from SP1 Teams

The following chapters include those aspects of the SP1 team models that were revised during the PRP. Unless indicated otherwise, all of the assessments of the original PEGASOS SP1 models remain valid and the reader is directed to the PEGASOS Evaluation Summaries for the unchanged components of the SP1 models (PEGASOS Final Report, Volume 4) or Schmid [2009]; Burkhard and Grünthal [2009]; Musson et al. [2009]; Wiemer et al. [2009], respectively:

Part II - chapter 1, Part III - chapter 1, Part IV - chapter 1, Part V - chapter 1.

Hazard Input Documents

The HIDs are developed to include all of the elements of each team's assessments of importance to the hazard calculations. Although the HIDs provide the information required for the hazard calculations, they do not include any technical explanation or justification for the models or parameters that comprise the models. Those explanations are given in the Elicitation Summaries for each team. The following chapters include the final Hazard Input Documents (HID) for each of the SP1 models:

Part II - chapter 3, Part III - chapter 3, Part IV - chapter 3, Part V - chapter 3.

Hazard Calculations and Feedback for SP1

The appendix A include the results of the hazard calculations and sensitivity analyses that were conducted for each of the SP1 models. The feedback products are first described, followed

by the team-specific considerations. This is followed by the various plots and figures that display the hazard results and sensitivity analyses.

Chapter 2

Supporting Computations

2.1 Introduction

This report describes calculations performed to support the EG1 Expert Team's incorporation of the updated PEGASOS earthquake catalog [SED 2011] into updates to the seismic source models for the PEGASOS Project. The calculations are presented in chronological order beginning with analyses performed for the working meeting in February, 2010 and ending with calculations performed to update each Expert Team's seismic source model seismicity parameters.

2.2 Calculations Performed for January 2010 EG1 Working Meeting

A working meeting was held on January 26, 2010 to present to the EG1 Expert Team's initial assessments of the updated draft ECOS-09 earthquake catalog [SED 2010]. Dr. Stefan Wiemer (member of the EG1d Expert Team) presented initial assessments of catalog completeness and magnitude conversions [Wiemer and Wössner 2010]. As part of their assessment, Wiemer and Wössner [2010] prepared a declustered version of the draft ECOS-09 catalog using the approach preferred by the EG1 Expert Team's. The declustering method used was the approach originally developed by Gardner and Knopoff [1974] but applying the time and distance widows developed by Grünthal [1985] (1985 modified) as published in Burkhard and Grünthal [2009]. This declustered catalog was used to perform exploratory calculations to provide the EG1a, EG1b, and EG1c Expert Team's with initial information on the effect of the updated earthquake catalog on seismicity parameters.

2.2.1 Calculations for EG1a Expert Team

Three sets of comparative calculations were performed for use by the EG1a Expert Team: calculations of catalog completeness, calculations of earthquake recurrence rates, and calculations of maximum magnitude distributions.

2.2.2 Catalog Completeness for EG1a

Comparisons of the completeness of the ECOS-02 and ECOS-09 earthquake catalogs were made by computing "Stepp" plots [Stepp 1972] for each catalog. Stepp plots show the $\lambda(m_i \leq m < m_{i+1}, T_i)$. The declustered catalog is sorted into earthquakes in specific magnitude intervals $m_i \leq m < m_{i+1}$. Starting at the end point of the catalog the earthquake frequency is computed at each point in time when an earthquake occurred. The earthquake frequency is computed by the relationship

$$\lambda(m_i \leq m < m_{i+1}, T_i) = \frac{N(m_i \leq m < m_{i+1}, T_i)}{T_i} \tag{2.1}$$

Where T_i is the length of time from the end of the catalog to the occurrence of the i^{th} earthquake and $N(m_i \leq m < m_{i+1}, T_i)$ is the number of earthquakes in magnitude interval $m_i \leq m < m_{i+1}$ and time period T_i .

The calculations were performed for the earthquakes within each of the catalog completeness regions defined by the EG1a Expert Team. These regions are shown on Figure 2.1. The Stepp plots for each catalog completeness region are shown on Figures 2.2 through 2.7 Each figure contains two panels. The panel on the left shows the Stepp plot for the ECOS-02 catalog and the panel on the right shows the Stepp plot for the ECOS-09 catalog. The magnitude intervals used to create the Stepp plots are those used by the EG1a Expert Team in the PEGASOS project. The vertical dashed lines denote the periods of complete reporting in the ECOS-02 catalog assessed by the EG1a Expert Team for the magnitudes indicated in the legend.

2.2.3 Macro-Zone Seismicity Rates

The EG1a Expert Team divided the study region into eleven macro-zones, as shown on figure 2.8. The ECOS-02 [SED 2002] and ECOS-09 [SED 2011] catalogs were used to compute seismicity rates for each macro-zone using an extension of the maximum likelihood approach developed by Weichert [1980]. The extensions include allowing for variable magnitude completeness within a source region and inclusion of a prior value for the b-value. Assuming that the seismicity rate density is uniform within the source region, variable catalog completeness is incorporated by subdividing the source region into J parts which represent the portions of the source region that lie within the individual catalog completeness regions. The use of a prior value for the b-value is implemented by introducing a penalty term in the likelihood function that penalizes (reduces) the computed likelihood value as the computed b-value deviates from the assigned prior value. The strength of the prior relative to the sample data is controlled by an assigned weight that represents the inverse of the variance of the assigned prior distribution for the b-value. Assuming that the earthquake recurrence relationships is defined by a truncated exponential distribution over the magnitude range of interest, the likelihood function for the observed sample of earthquakes is defined in terms of the earthquake recurrence parameters $N(m \geq m_o)$, the recurrence rate of earthquakes of magnitudes equal to or larger than a specified minimum magnitude m_o , and the Gutenberg-Richter b-value

expressed in natural log units,

$$\beta = b \times \ln(10). \tag{2.2}$$

The likelihood function for the sample data is given by

$$L = \prod_j \prod_i \frac{(\lambda_{ij} T_{ij})^{n_{ij}} \exp^{-\lambda_{ij} T_{ij}}}{n_{ij}!} \times \exp^{-\frac{1}{2} W_p (\beta - \beta_p)^2} \tag{2.3}$$

λ_{ij} = earthquake recurrence rate in subregion j for magnitude range $m_i - m_{i-1}$.

$$\lambda_{ij} = N(m \geq m_o) \frac{A_j}{\sum_j A_j} \left[\frac{\exp^{-\beta^{GR}(m_{i-1} - m_o)} - e^{-\beta^{DR}(m_i - m_o)}}{1 - \exp^{-\beta^{GR}(m - m_o)}} \right] \tag{2.4}$$

T_{ij} = period of completeness in subregion j for magnitude range $m_i - m_{i-1}$

n_{ij} = number of earthquakes in subregion j in magnitude range $m_i - m_{i-1}$

A_j = area of subregion j

β_p = prior on b- value $\times \ln(10)$

W_p = Weight controlling strength of prior

The catalog completeness periods and magnitude intervals used were those defined by EG1a in the PEGASOS Project. For the ECOS-09 catalog the completeness periods were extended by eight years. The maximum likelihood fits to the data allowed for a difference in the earthquake recurrence frequency for the instrumental period (post 1975/01/01) and the historical period (pre 1975/01/01). These initial fits were performed without a prior value for the b-value, $W_p = 0$.

Figures 2.9 through 2.19 show the computed seismicity rates for each macro-zone. The panel on the left of each plot shows the fit to the data for the instrumental period and the panel on the right shows the fit to the data for the historical period.

2.2.4 Macro-Zone Maximum Magnitude Distributions

For the PEGASOS Project, the EG1a Expert Team applied the Bayesian approach Johnston et al. [1994] to develop maximum magnitude distributions for each macro-zone. This approach uses prior distributions for maximum magnitude developed from a world-wide database. The prior distributions are updated using a likelihood function based on the largest observed earthquake, $m_{max-obs}$, and the number of earthquakes with magnitudes $\geq M4.5$ in each

macrozone, $N(m \geq m_o)$. Assuming that the recurrence relationship for earthquakes in a source zone is defined by a truncated exponential distribution with a known b-value, the likelihood function for the maximum magnitude, m^u, is given by

$$L[m^u] = \begin{cases} 0 & \text{for } m^u < m_{max-obs} \\ \left[1 - \exp^{-b\ln(10)(m^u - m_0)}\right]^{-N(m \geq m_0)} & \text{for } m^u \geq m_{max-obs} \end{cases} \tag{2.5}$$

The value of $N(m \geq m_0)$ is corrected for completeness as follows. Assuming that earthquake occurrence rates are stationary in time for the period covered by the catalog, then the maximum likelihood estimate of the rate of earthquakes of magnitude m_i is given by the number of earthquakes, $N(m_i)$ in the completeness period for m_i divided by the length of the completeness period, $T_C(m_i)$. An estimate of the total number of earthquakes of the smaller magnitude that would have been recorded in the completeness period for $m_{max-obs}$ is then given by the estimated rate of occurrence for magnitude m_i multiplied by $T_C(m_{max-obs})$:

$$N_{\text{Completeness Corrected}}(m_i) = N_{\text{In period}T_C(m_i)} \times \frac{T_C(m_{max-obs})}{T_C(m_i)} \tag{2.6}$$

The values of $N_{\text{Completeness Corrected}}(m_i)$ are then summed to provide the completeness-corrected sample size for each domain.

The prior distributions for maximum magnitude used by the EG1a Expert Team are the normal distributions from Johnston et al. [1994] described by a mean and standard deviation. These distributions are then multiplied by the likelihood function defined by equations 2.5 and 2.6 and the result normalized to produce a posterior probability distribution for maximum magnitude. The posterior distribution was then discretized into 0.4 magnitude unit bins. Figures 2.20 through 2.26 show the maximum magnitude distributions computed for each of the EG1a macro-zones using the ECOS-02 and ECOS-09 catalogs. The prior distributions, b-values and completeness periods used were those defined by EG1a in the PEGASOS Project.

2.3 Calculations for EG1b Expert Team

Two sets of comparative calculations were performed for use by the EG1b Expert Team: calculations of earthquake recurrence rates and calculations of maximum magnitude distributions.

2.3.1 Large Zone Seismicity Rates

The EG1b Expert Team divided the study region into eight large source zones, as shown on figure 2.27. The ECOS-02 and ECOS-09 catalogs were used to compute seismicity rates for each macro-zone using the maximum likelihood approach described above in section 2.2.3. The catalog completeness periods and magnitude intervals used were those defined by EG1b in the PEGASOS Project. For the ECOS-09 catalog the completeness periods were extended by eight years. Figures 2.28 through 2.31 show the computed seismicity rates for the large zones.

2.3.2 Large Zone Maximum Magnitude Distributions

For the PEGASOS Project, the EG1b Expert Team applied the Bayesian approach as described above in section 2.2.4 to develop maximum magnitude distributions for each large source zone. Figures 2.32 through 2.35 show the maximum magnitude distributions computed for each of the EG1b large zones using the ECOS-02 and ECOS-09 catalogs. The prior distributions, b-values and completeness periods used were those defined by EG1b in the PEGASOS Project.

2.4 Calculations for EG1c Expert Team

Three sets of comparative calculations were performed for use by the EG1c Expert Team: calculations of catalog completeness, calculations of earthquake recurrence rates, and calculations of maximum magnitude distributions.

2.4.1 Catalog Completeness for EG1c

Comparisons of the completeness of the ECOS-02 and ECOS-09 earthquake catalogs were made by computing "Stepp" plots [Stepp 1972] for each catalog. The calculations were performed for the earthquakes within each of the catalog completeness regions defined by the EG1c Expert Team. These regions are shown on Figure 2.36. The Stepp plots for each catalog completeness region are shown on Figures 2.37 through 2.43. Each figure contains two panels. The panel on the left shows the Stepp plot for the ECOS-02 catalog and the panel on the right shows the Stepp plot for the ECOS-09 catalog. The magnitude intervals used to create the Stepp plots are those used by the EG1c Expert Team in the PEGAOS project. The vertical dashed lines denote the periods of complete reporting in the ECOS-02 catalog assessed by the EG1c Expert Team for the magnitudes indicated in the legend.

2.4.2 Source Zone Seismicity Rates

The EG1c Expert Team divided the study region into source zones, as shown on Figure 2.44. The ECOS-02 and ECOS-09 catalogs were used to compute seismicity rates for each macrozone using least squares (Method 2 used by EG1c in the PEGASOS Project). The catalog completeness periods and magnitude intervals used were those defined by EG1c in the PEGASOS Project. For the ECOS-09 catalog the completeness periods were extended by eight years. The least squares fits to the seismicity data were performed using standard linear regression of the model

$$y_i = A + Bx_i \tag{2.7}$$

$$x_i = m_{i-1} - m_0 \tag{2.8}$$

$$y_i = \log_{10}\left[\sum_{j=1}^{j=i} \lambda(m_{j-1} \geq m > m_j)\right] \tag{2.9}$$

$$\lambda(m_{j-1} \geq m > m_j) = \frac{n_j}{T_j} \tag{2.10}$$

The value of n_j is again the earthquake counts in the specified magnitude interval within the period of catalog completeness for that magnitude interval, T_j. The linear regression fit is performed on the log of the cumulative earthquake rates ignoring the dependence between the data points. Figures 2.45 through 2.49 shows the computed seismicity rates for each source zone.

2.4.3 Source Zone Maximum Magnitude Distributions

For the PEGASOS Project, the EG1c Expert Team applied the Bayesian approach described above in section 2.2.4. The EG1c Team used an uninformative prior (uniform distribution) instead of the normal distributions developed in Johnston et al. [1994]. The prior distributions are updated using a likelihood function based on the largest observed earthquake and the number of earthquakes with magnitudes $\geq M4.5$ in each macro-zone. Figures 2.50 through 2.58 shows the maximum magnitude distributions computed for each of the EG1a macro-zones using the ECOS-02 and ECOS-09 catalogs. The b-values and completeness periods used were those defined by EG1c in the PEGASOS Project.

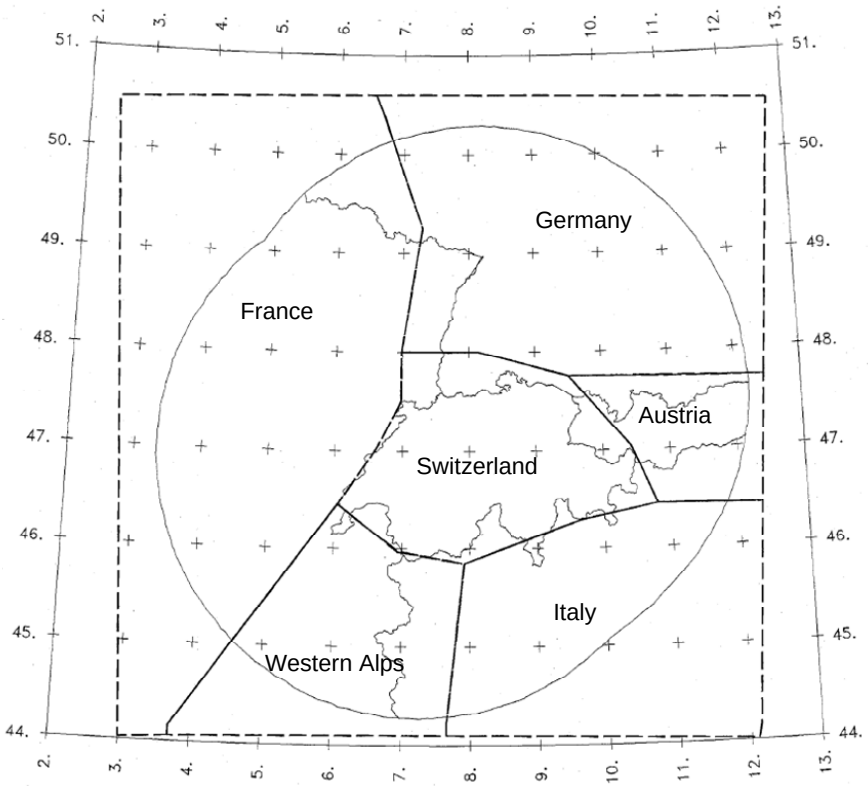

Figure 2.1: Catalog completeness regions defined by Expert Team EG1a.

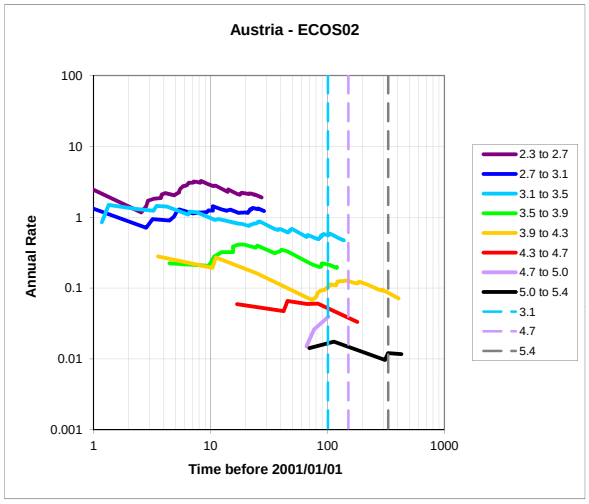

(a) ECOS-02 catalog

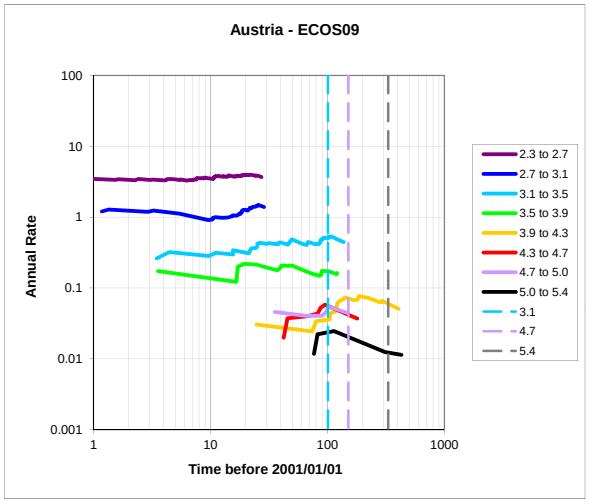

(b) ECOS-09 catalog

Figure 2.2: Stepp plots for EG1a Austria completeness region.

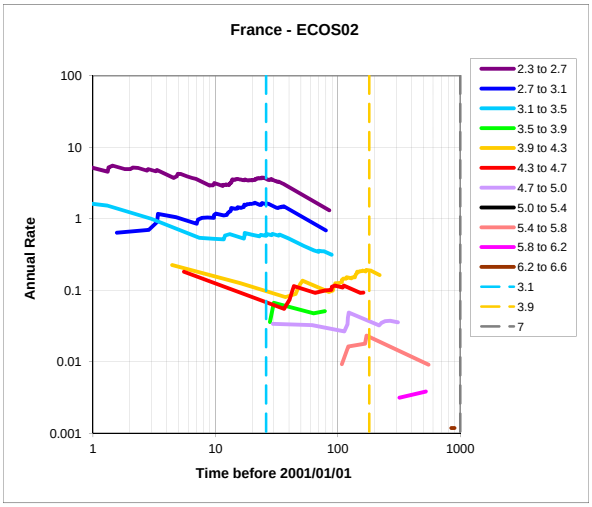

(a) ECOS-02 catalog

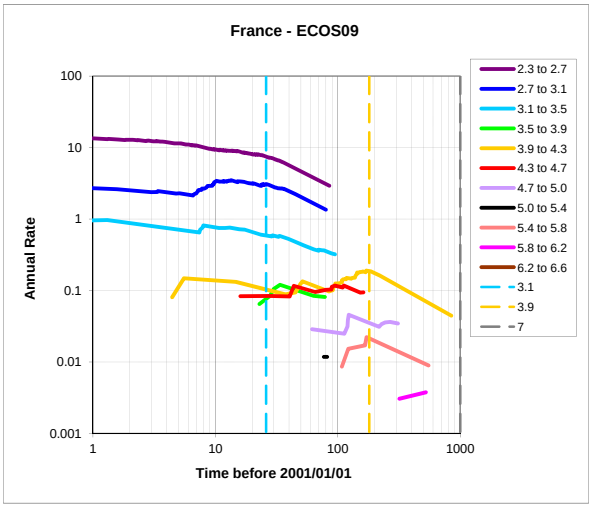

(b) ECOS-09 catalog

Figure 2.3: Stepp plots for EG1a France completeness region.

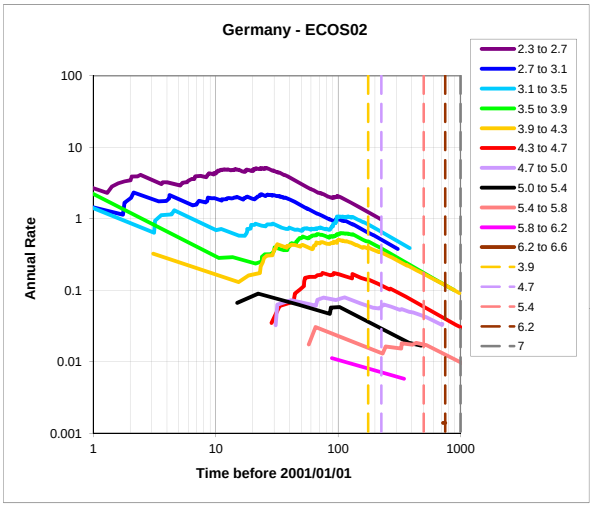

(a) ECOS-02 catalog

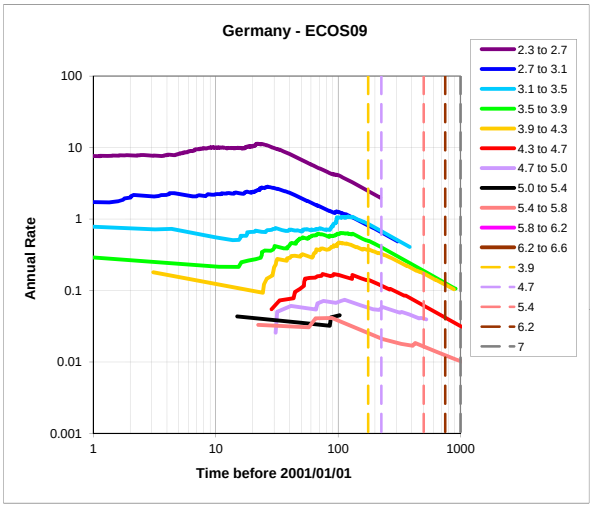

(b) ECOS-09 catalog

Figure 2.4: Stepp plots for EG1a Germany completeness region.

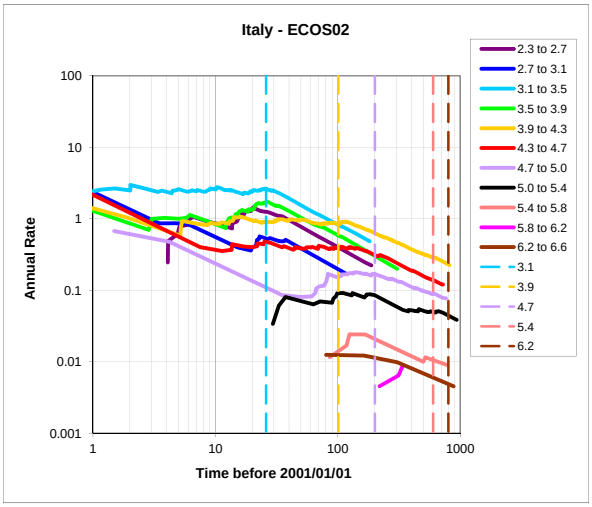

(a) ECOS-02 catalog

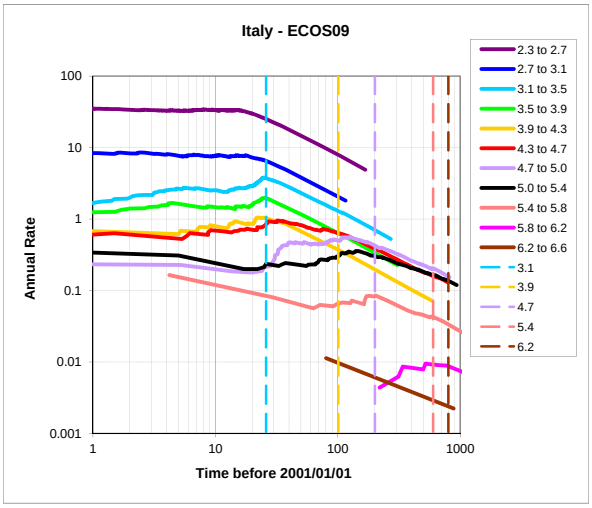

(b) ECOS-09 catalog

Figure 2.5: Stepp plots for EG1a Italy completeness region.

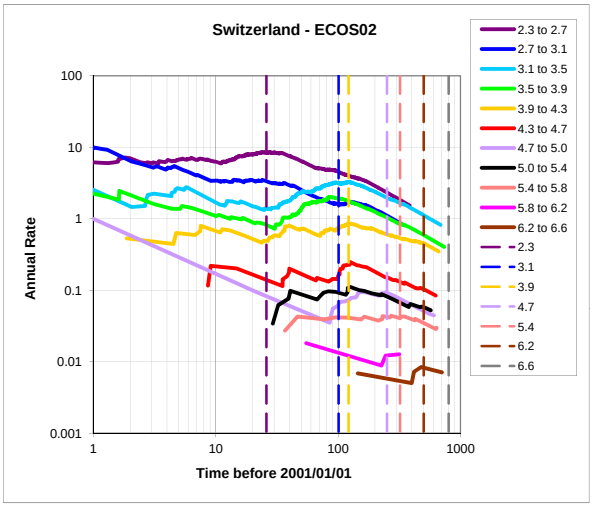

(a) ECOS-02 catalog

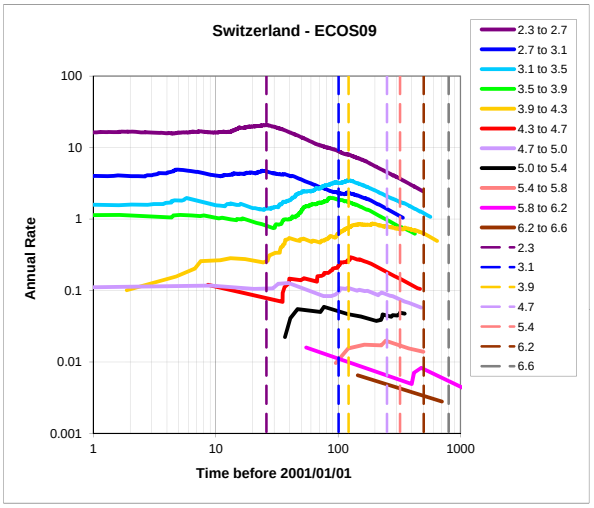

(b) ECOS-09 catalog

Figure 2.6: Stepp plots for EG1a Switzerland completeness region.

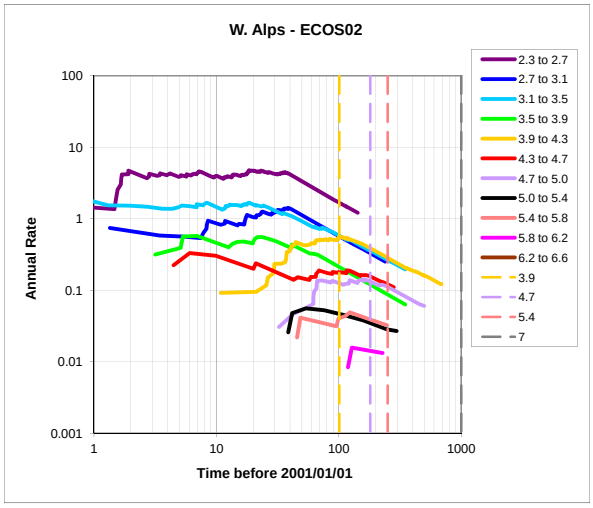

(a) ECOS-02 catalog

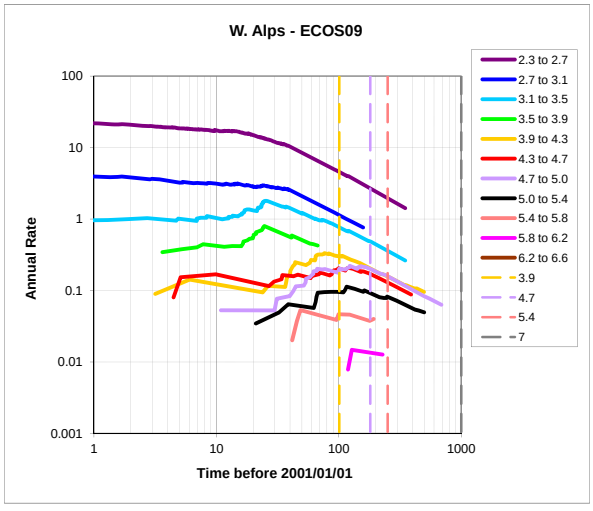

(b) ECOS-09 catalog

Figure 2.7: Stepp plots for EG1a Western Alps completeness region.

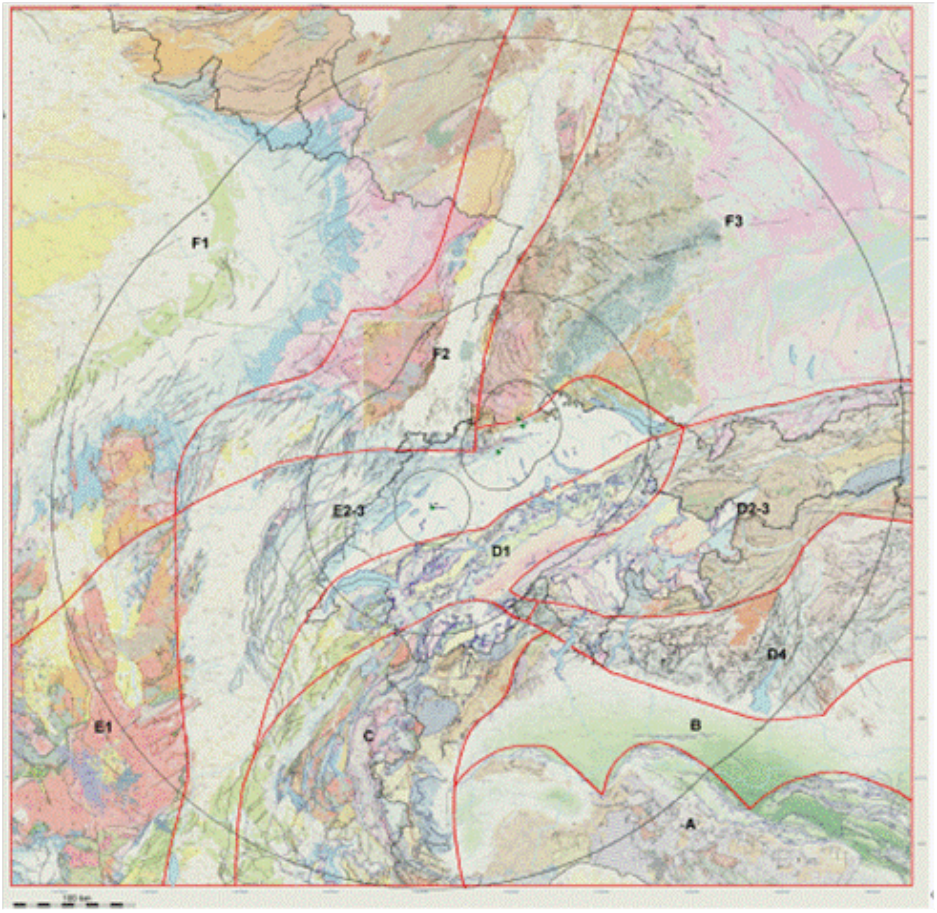

Figure 2.8: Macro-zones defined by EG1a.

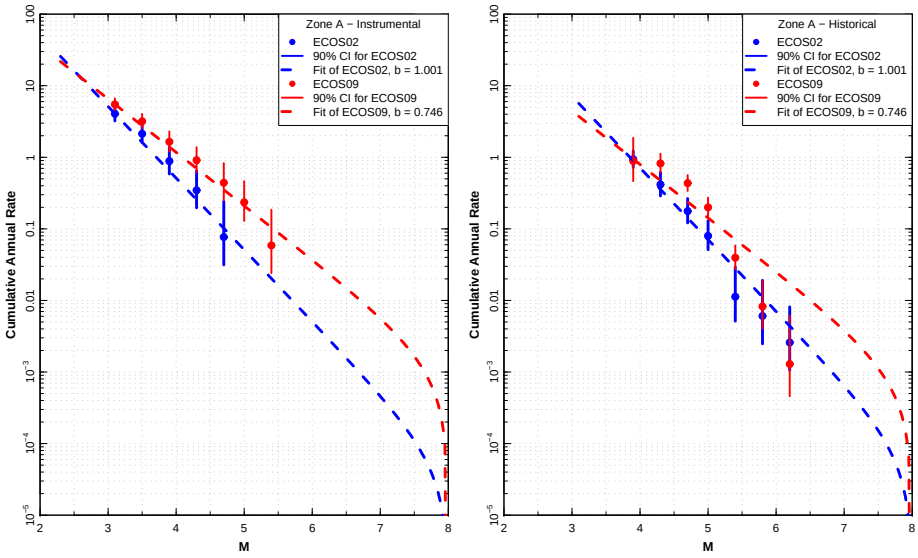

Figure 2.9: Seismicity data and earthquake recurrence rates for EG1a macro-zone A. Left instrumental period, right historical period.

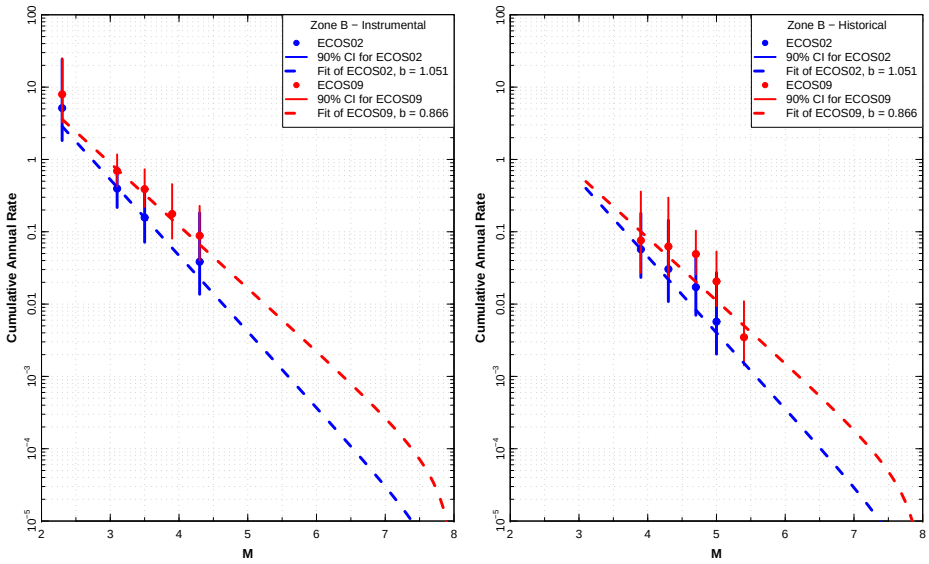

Figure 2.10: Seismicity data and earthquake recurrence rates for EG1a macro-zone B. Left instrumental period, right historical period.

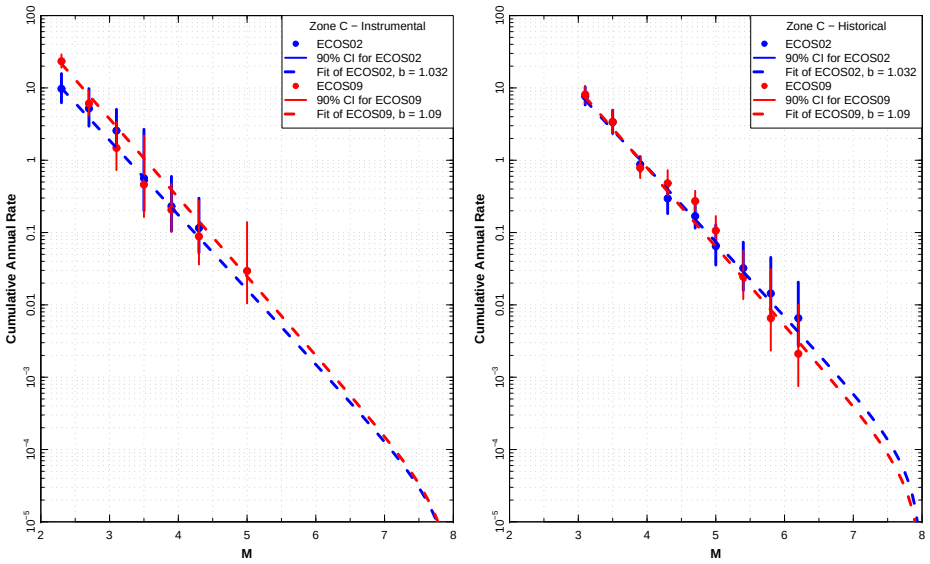

Figure 2.11: Seismicity data and earthquake recurrence rates for EG1a macro-zone C. Left instrumental period, right historical period.

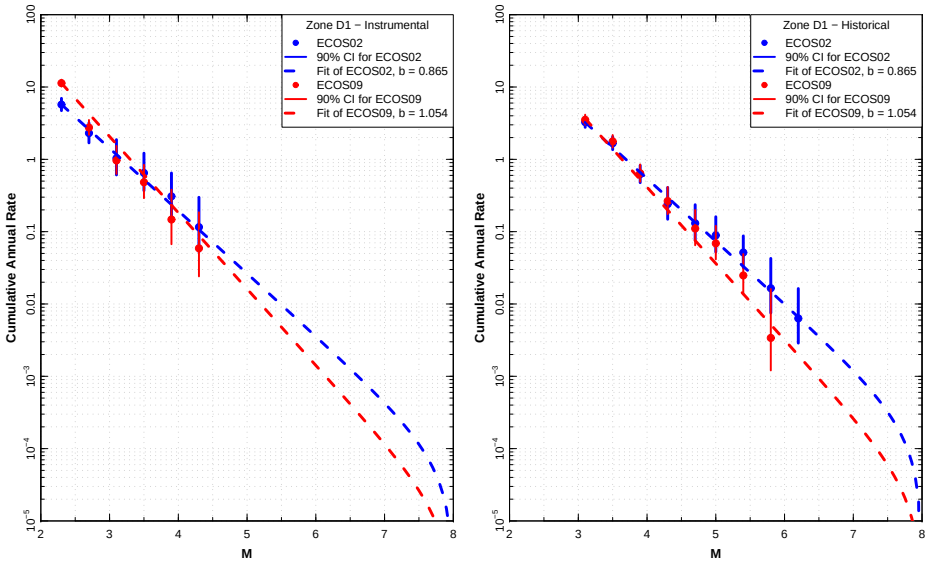

Figure 2.12: Seismicity data and earthquake recurrence rates for EG1a macro-zone D1. Left instrumental period, right historical period.

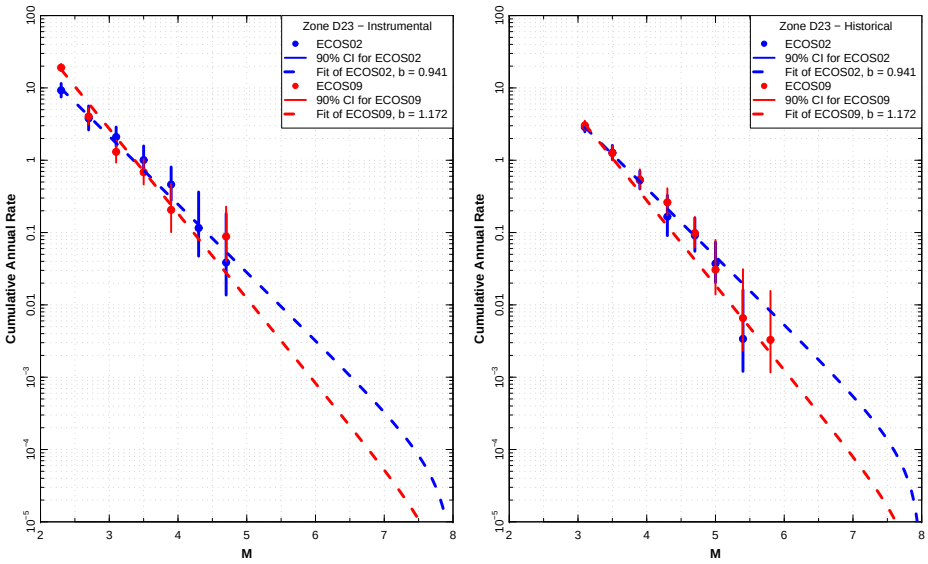

Figure 2.13: Seismicity data and earthquake recurrence rates for EG1a macro-zone D23. Left –instrumental period, right historical period.

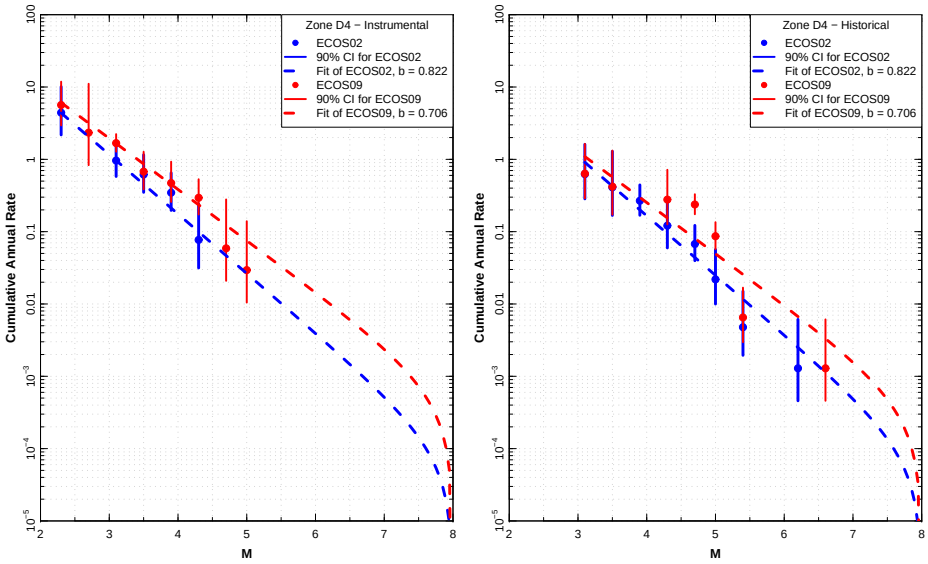

Figure 2.14: Seismicity data and earthquake recurrence rates for EG1a macro-zone D4. Left instrumental period, right historical period.

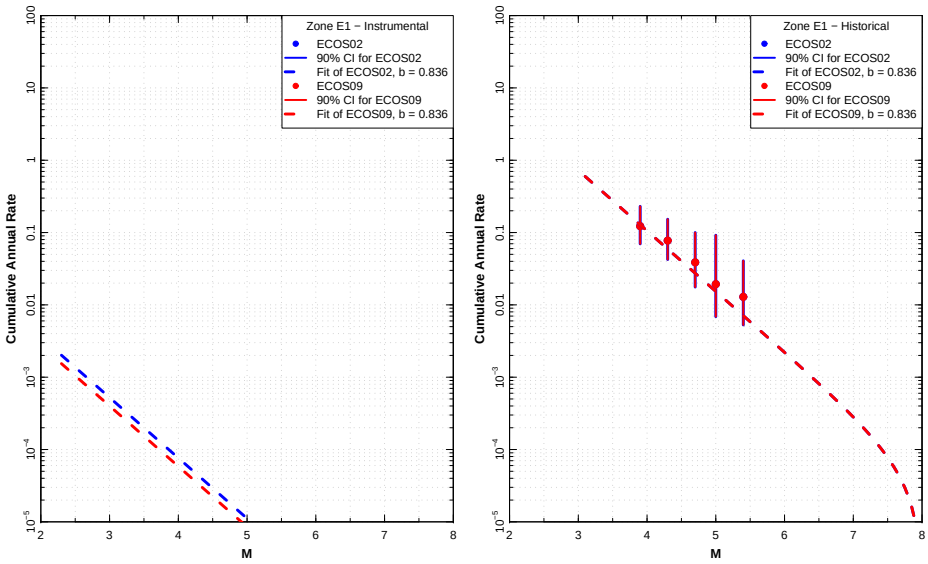

Figure 2.15: Seismicity data and earthquake recurrence rates for EG1a macro-zone E1. Left instrumental period, right historical period.

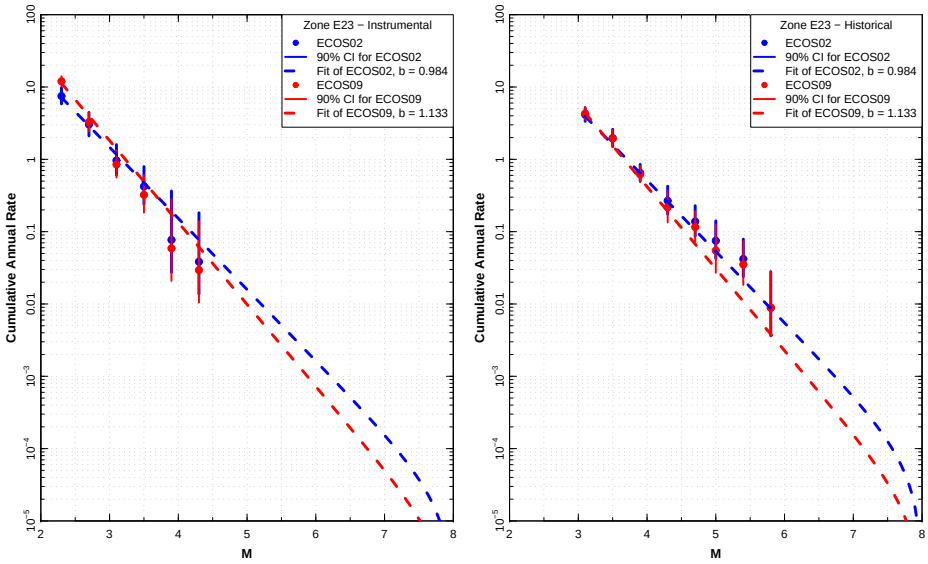

Figure 2.16: Seismicity data and earthquake recurrence rates for EG1a macro-zone E23. Left instrumental period, right historical period.

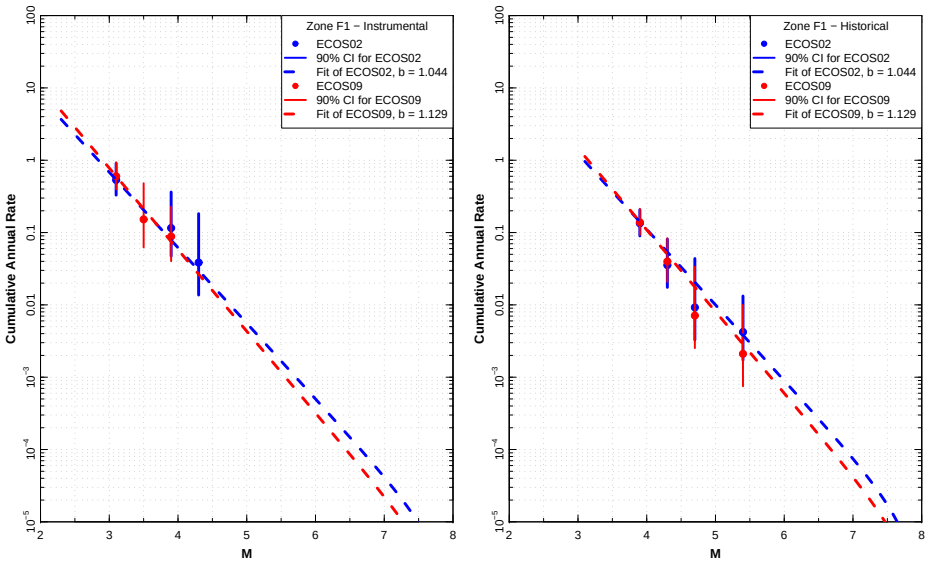

Figure 2.17: Seismicity data and earthquake recurrence rates for EG1a macro-zone F1. Left instrumental period, right historical period.

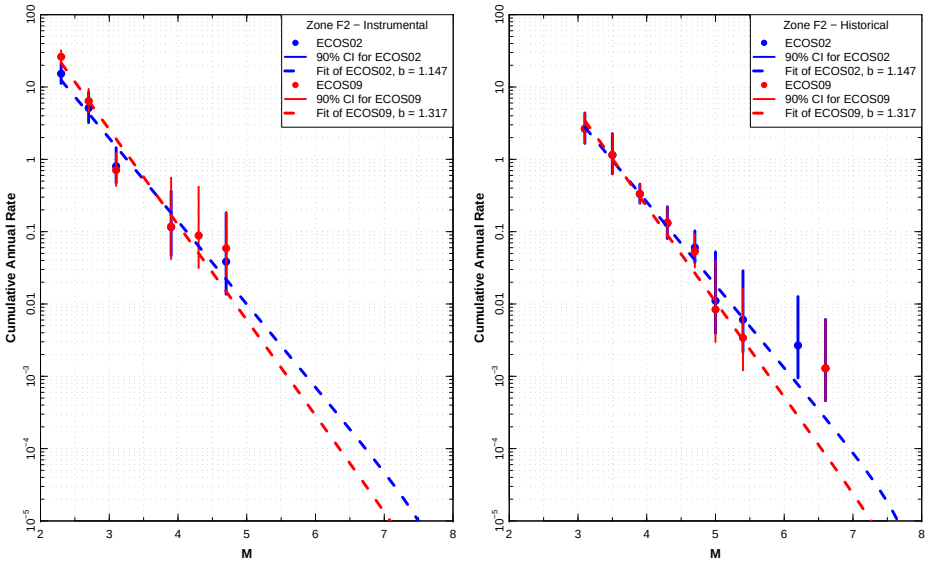

Figure 2.18: Seismicity data and earthquake recurrence rates for EG1a macro-zone F2. Left instrumental period, right historical period.

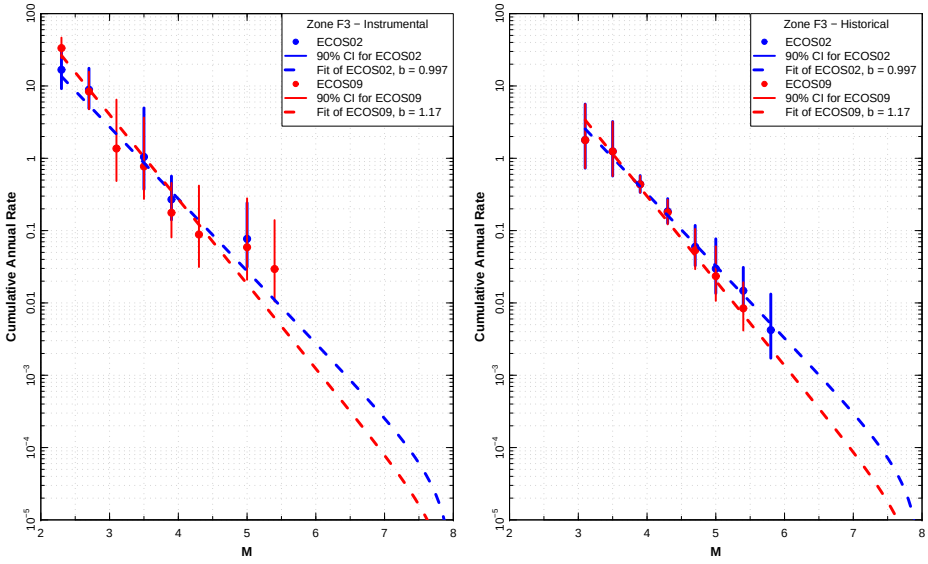

Figure 2.19: Seismicity data and earthquake recurrence rates for EG1a macro-zone F3. Left instrumental period, right historical period.

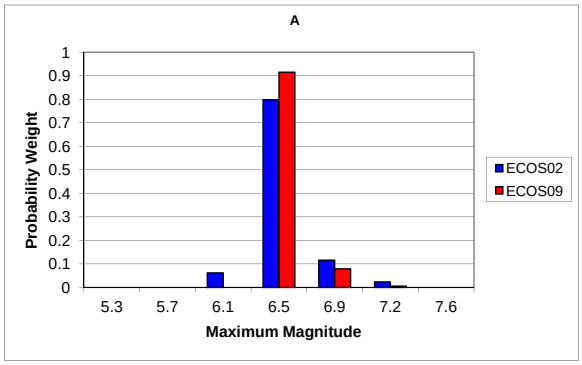

(a) Zone A

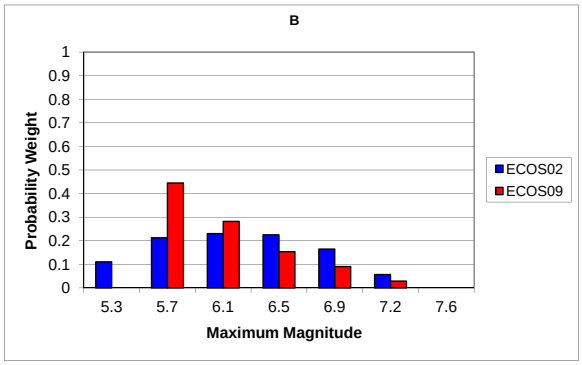

(b) Zone B

Figure 2.20: Maximum magnitude distributions for macro zones A + B.

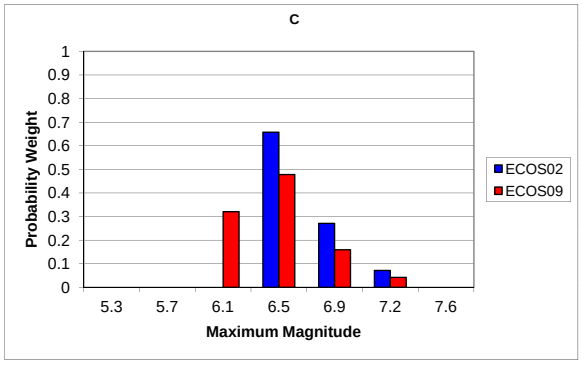

(a) Zone C

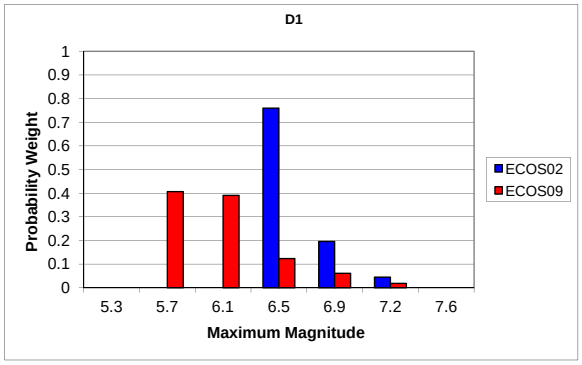

(b) Zone D1

Figure 2.21: Maximum magnitude distributions for macro zones C + D1.

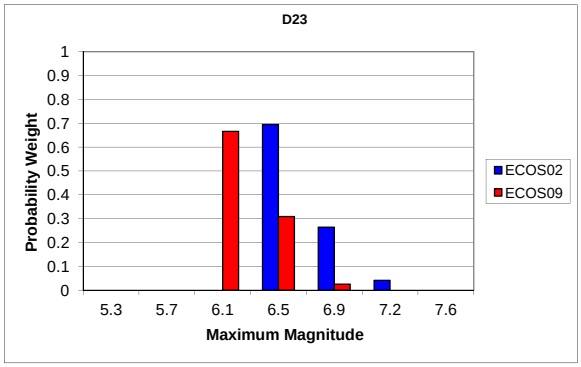

(a) Zone D23

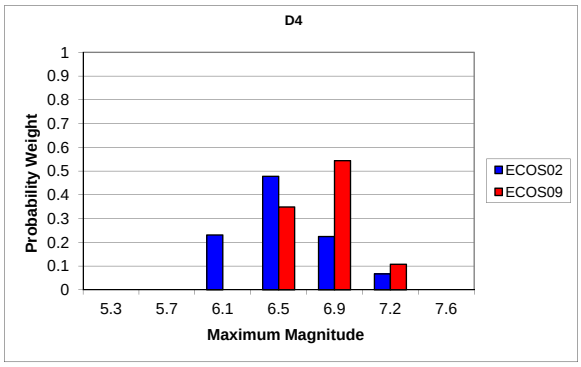

(b) Zone D4

Figure 2.22: Maximum magnitude distributions for macro zones D23 + D4.

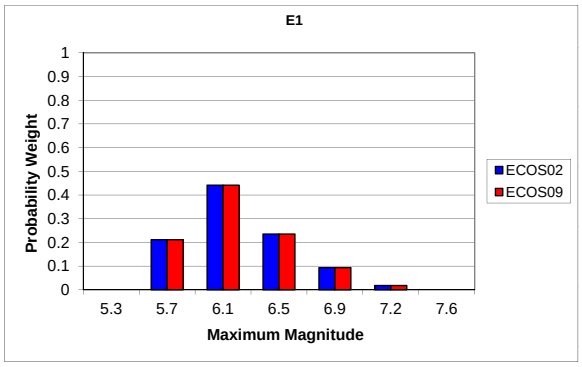

(a) Zone E1

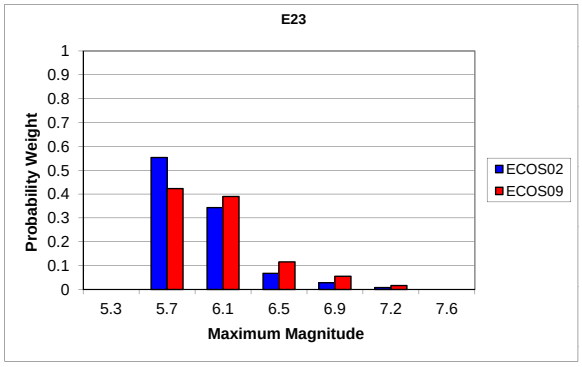

(b) Zone E23

Figure 2.23: Maximum magnitude distributions for macro zones E1 + E23.

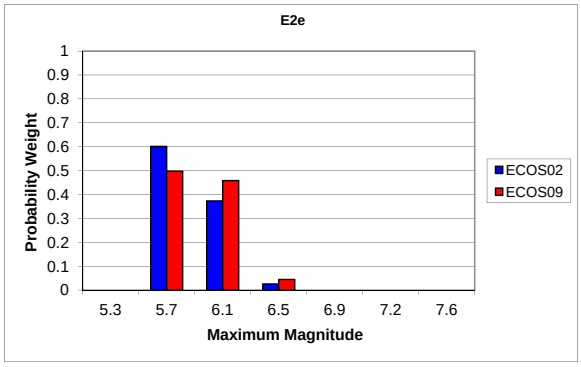

(a) Zone E2e

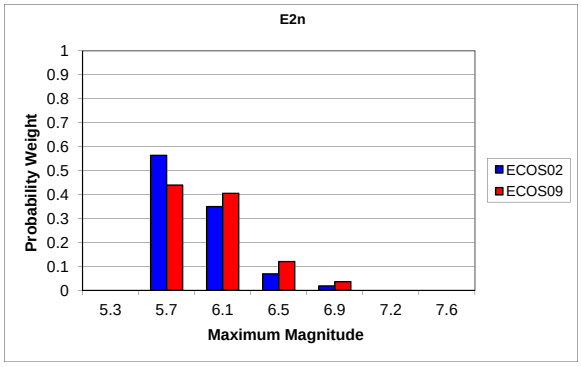

(b) Zone E2n

Figure 2.24: Maximum magnitude distributions for macro zones E2e + E2n.

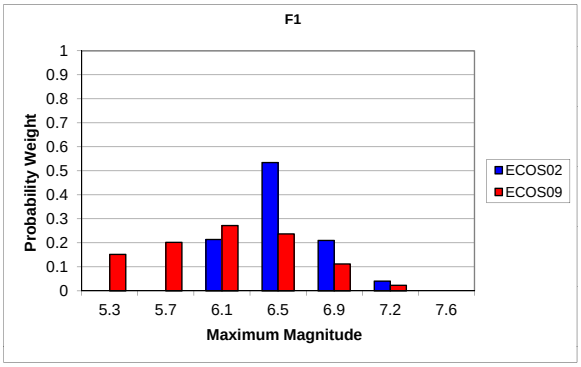

(a) Zone F1

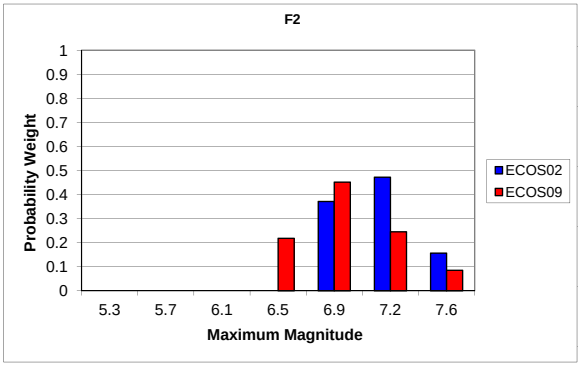

(b) Zone F2

Figure 2.25: Maximum magnitude distributions for macro zones F1 + F2.

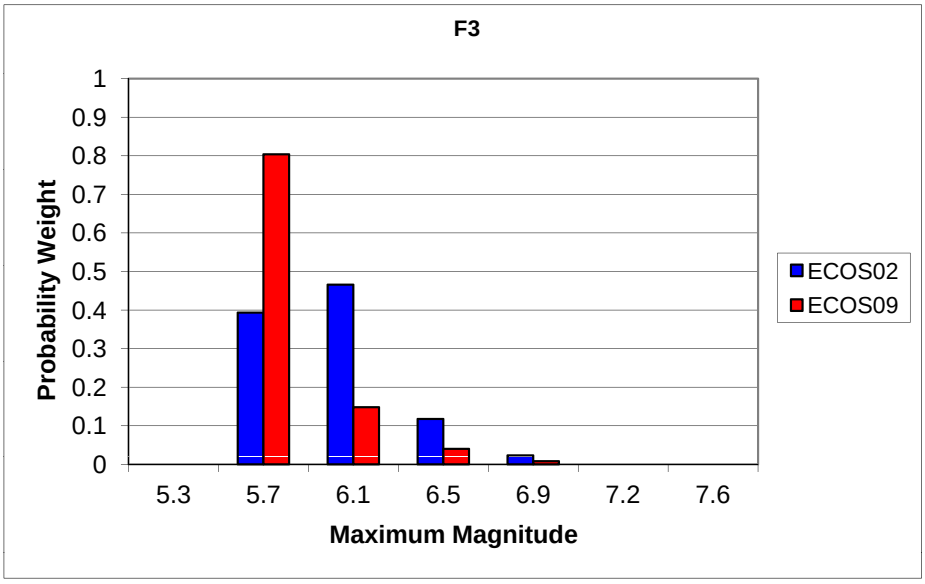

Figure 2.26: Maximum magnitude distributions for macro zone F3.

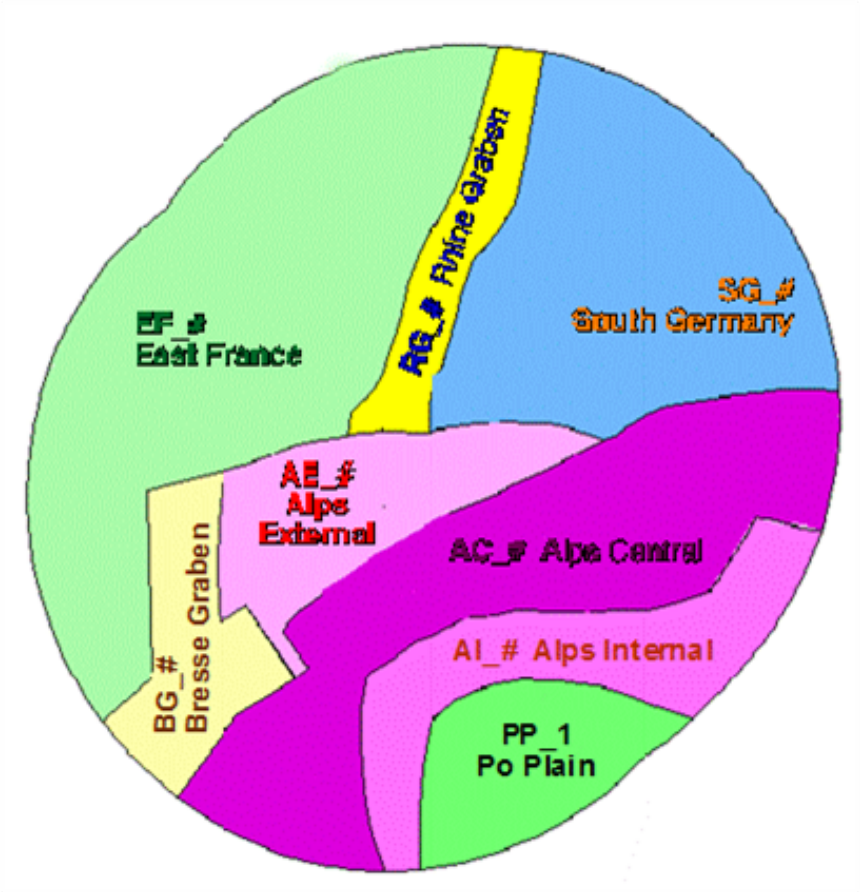

Figure 2.27: Large source zones defined by EG1b.

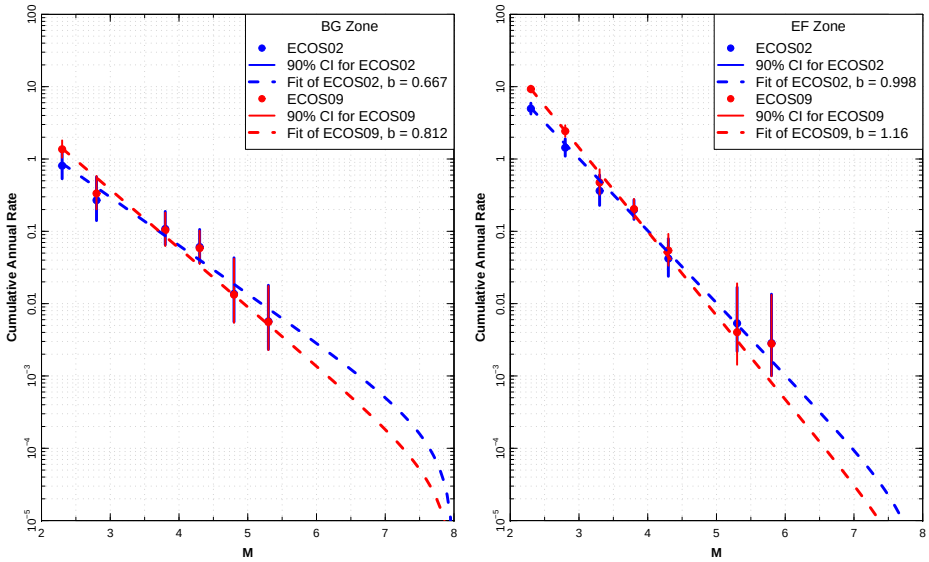

Figure 2.28: Seismicity data and earthquake recurrence rates for EG1b large zones BG and EF.

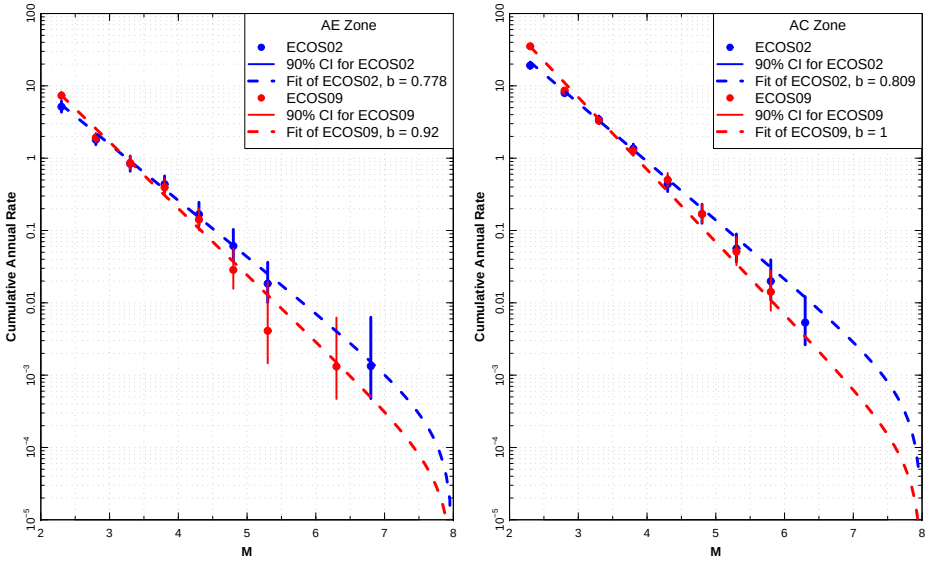

Figure 2.29: Seismicity data and earthquake recurrence rates for EG1b large zones AE and AC.

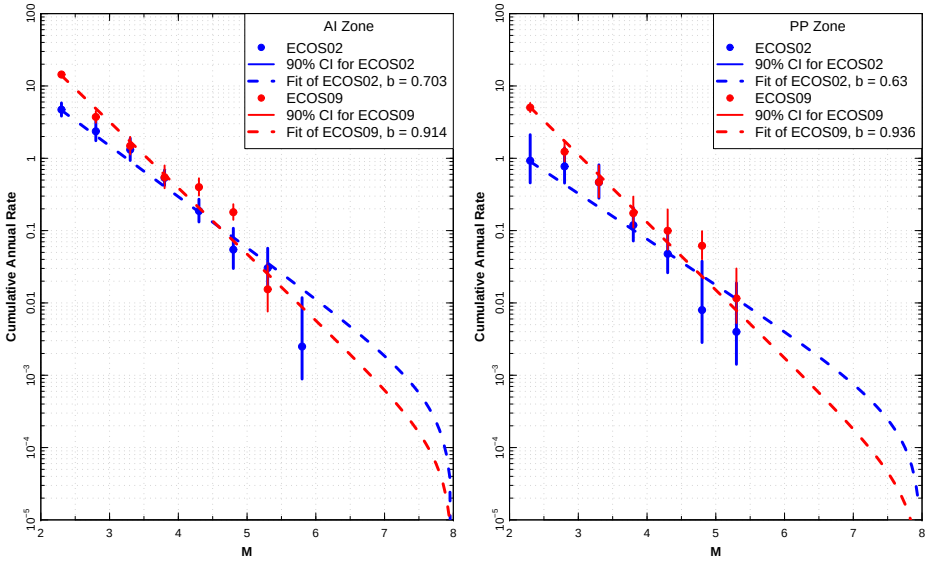

Figure 2.30: Seismicity data and earthquake recurrence rates for EG1b large zones AI and PP.

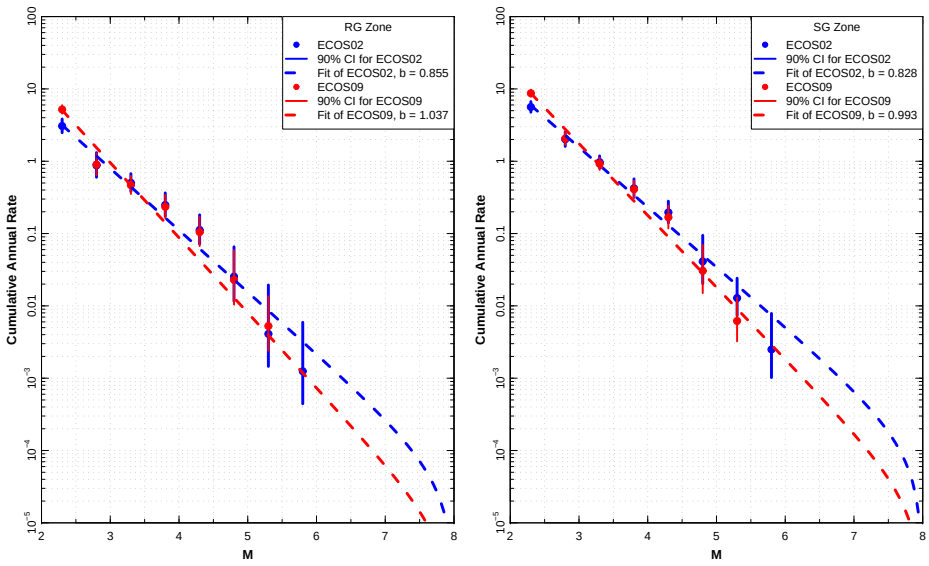

Figure 2.31: Seismicity data and earthquake recurrence rates for EG1b large zones RG and SG.

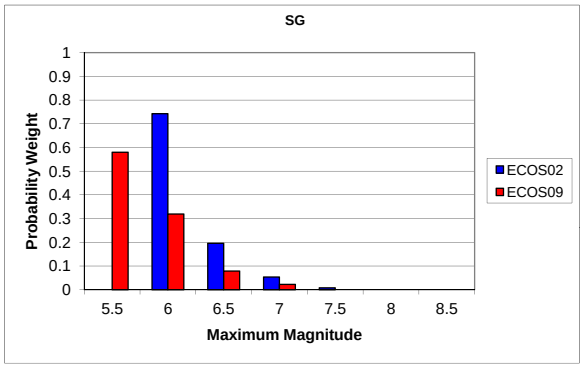

(a) Zone SG

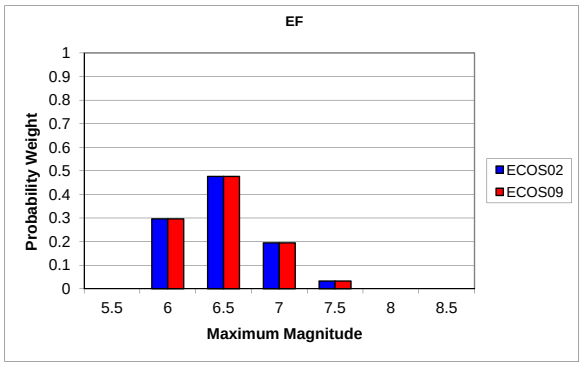

(b) Zone EF

Figure 2.32: Maximum magnitude distributions for EG1b large zones SG + EF.

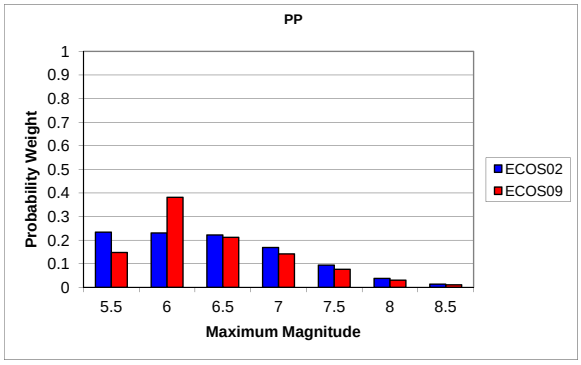

(a) Zone PP

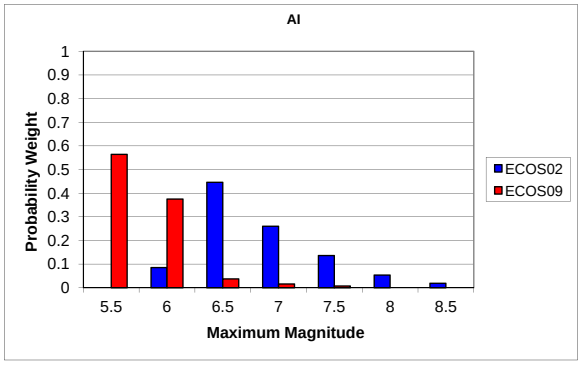

(b) Zone AI

Figure 2.33: Maximum magnitude distributions for EG1b large zones PP + AI.

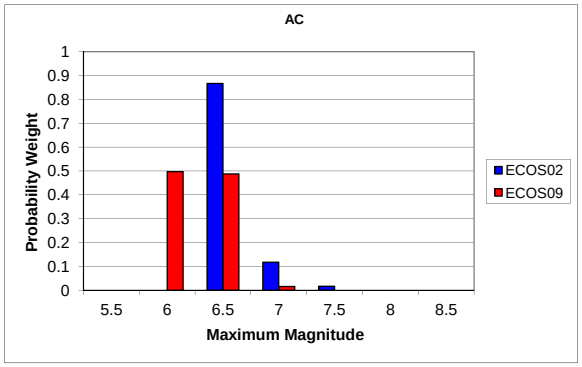

(a) AC

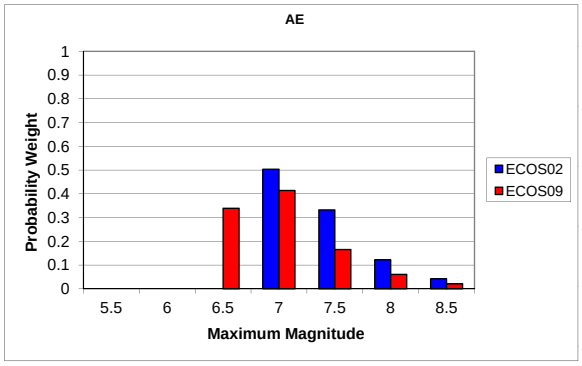

(b) AE

Figure 2.34: Maximum magnitude distributions for EG1b large zones AC + AE.

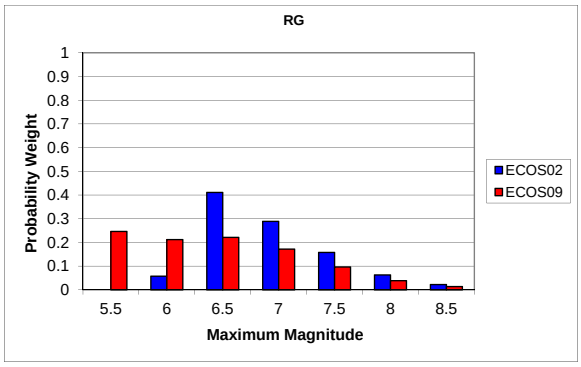

(a) RG

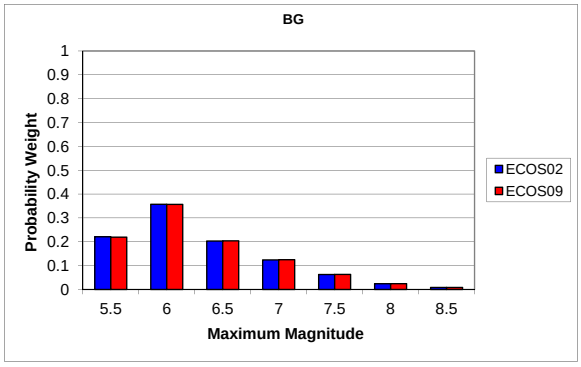

(b) BG

Figure 2.35: Maximum magnitude distributions for EG1b large zones RG + BG.

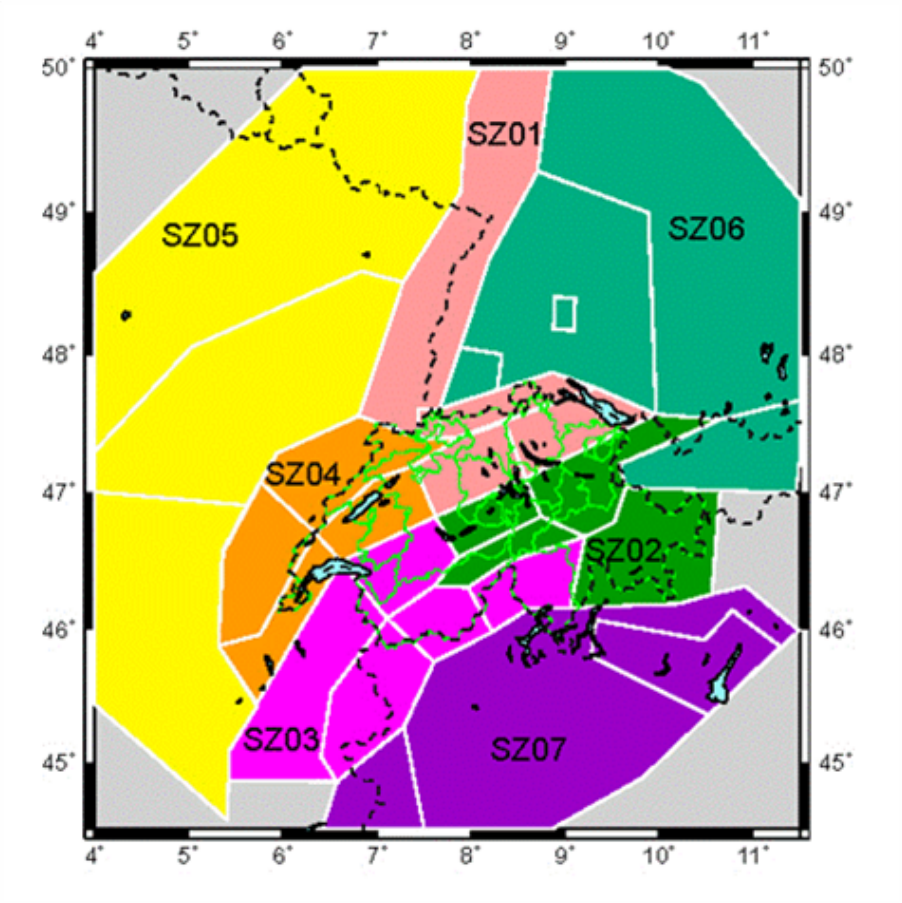

Figure 2.36: Catalog completeness regions defined by Expert Team EG1c.

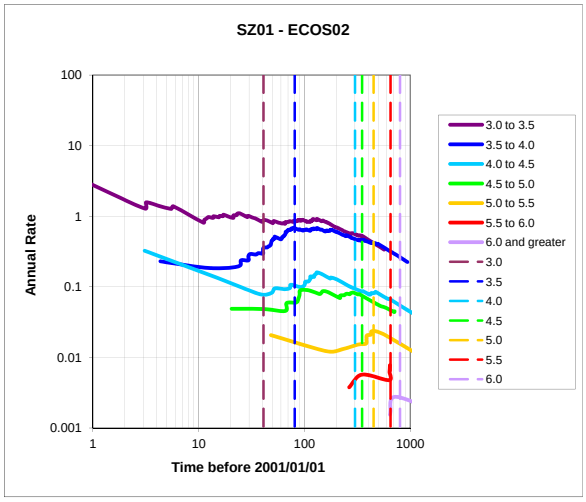

(a) ECOS-02 catalog

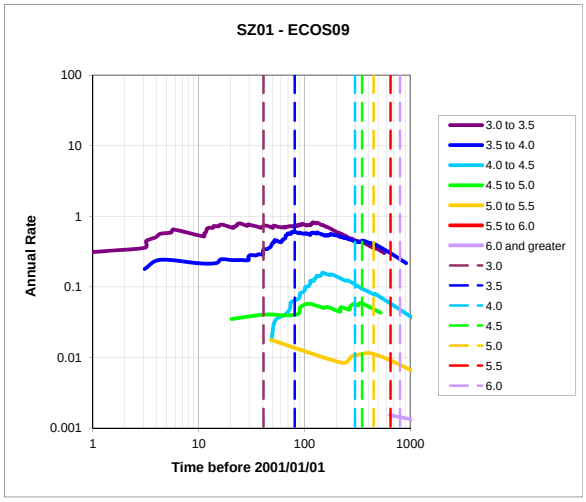

(b) ECOS-09 catalog

Figure 2.37: Stepp plots for EG1a completeness region SZ01.

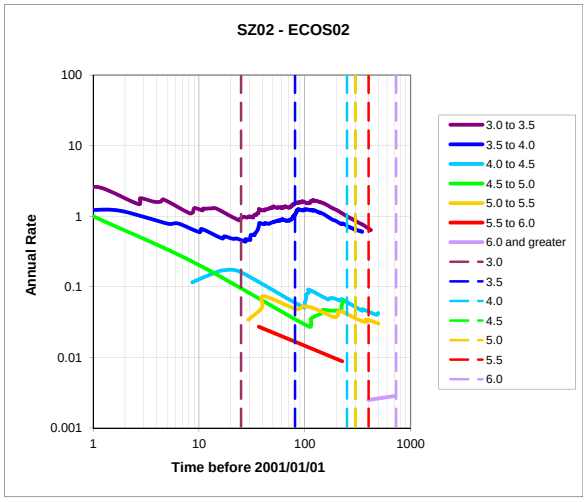

(a) ECOS-02 catalog

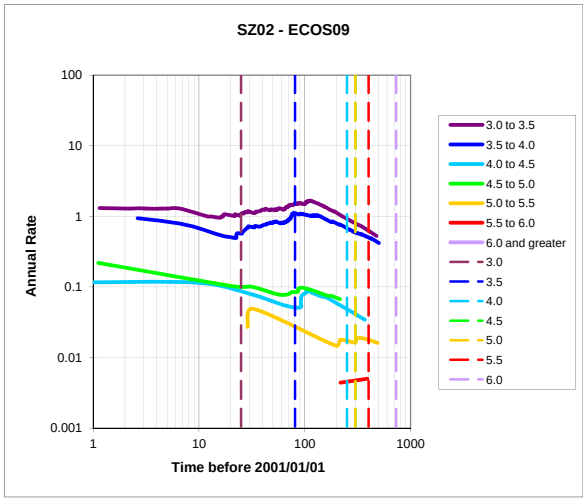

(b) ECOS-09 catalog

Figure 2.38: Stepp plots for EG1a completeness region SZ02.

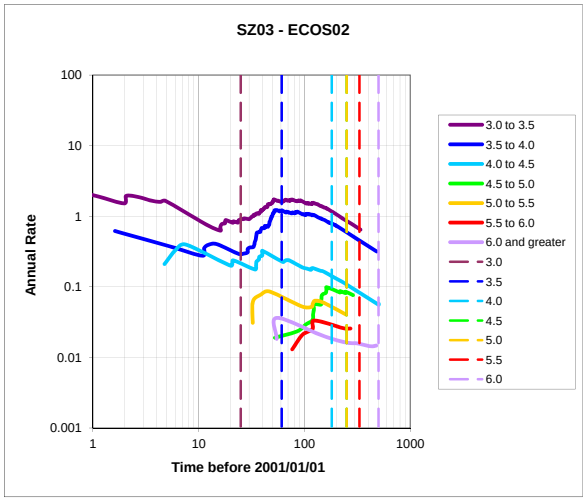

(a) ECOS-02 catalog

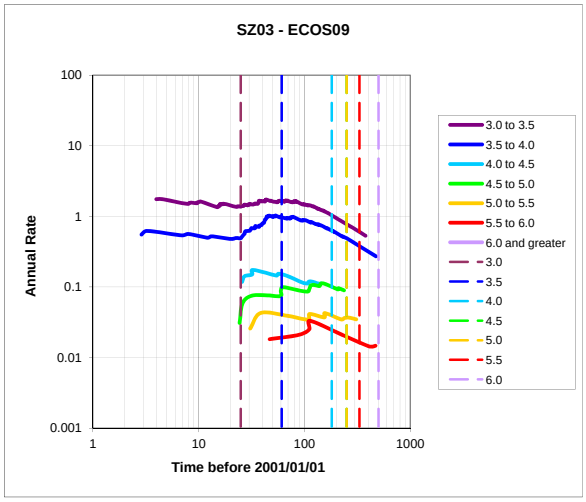

(b) ECOS-09 catalog

Figure 2.39: Stepp plots for EG1a completeness region SZ03.

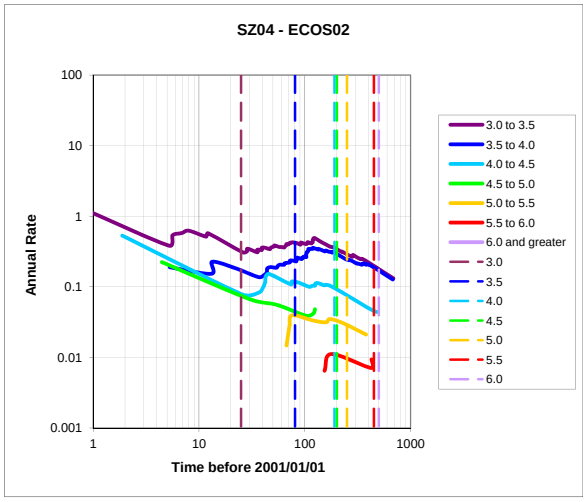

(a) ECOS-02 catalog

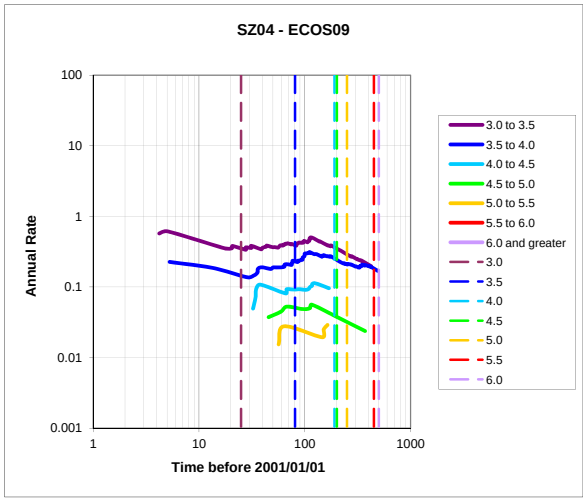

(b) ECOS-09 catalog

Figure 2.40: Stepp plots for EG1a completeness region SZ04.

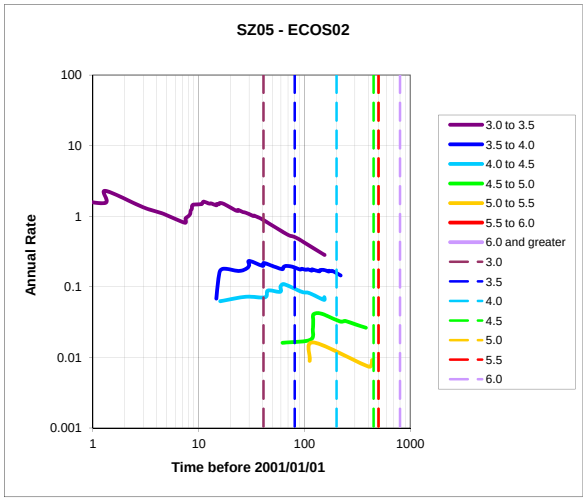

(a) ECOS-02 catalog

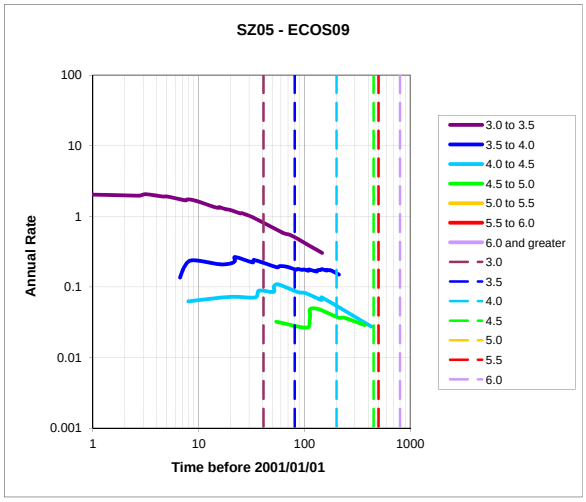

(b) ECOS-09 catalog

Figure 2.41: Stepp plots for EG1a completeness region SZ05.

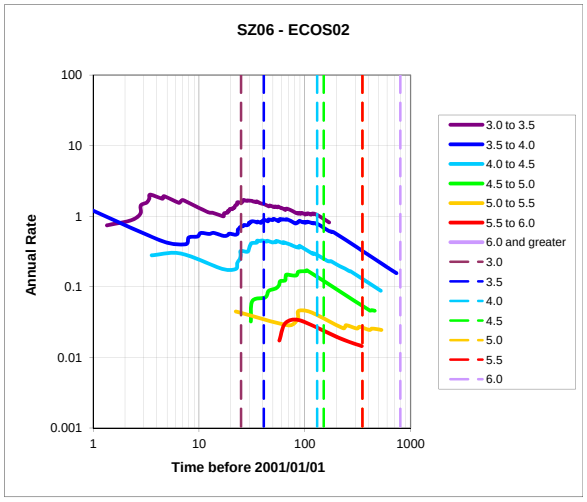

(a) ECOS-02 catalog

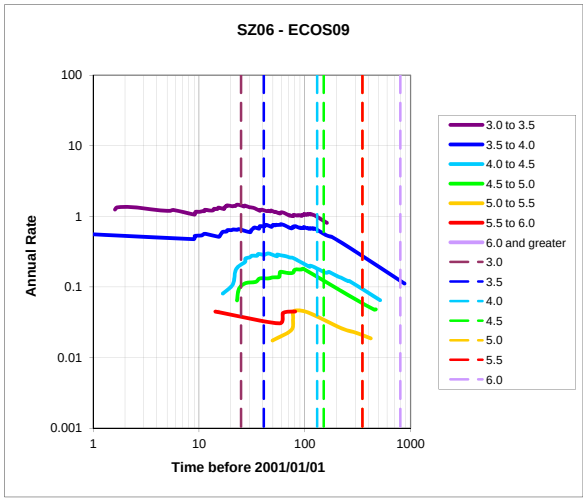

(b) ECOS-09 catalog

Figure 2.42: Stepp plots for EG1a completeness region SZ06.

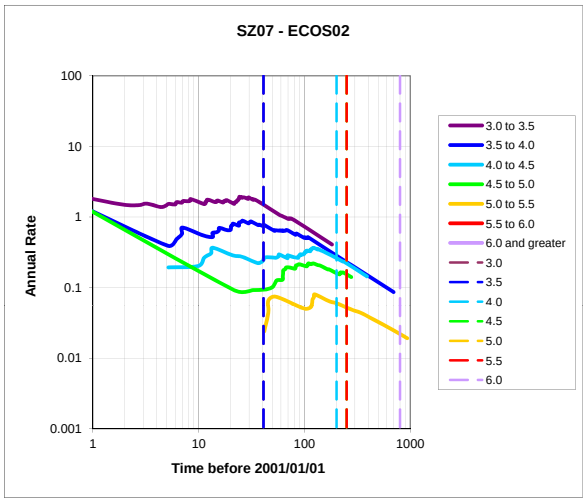

(a) ECOS-02 catalog

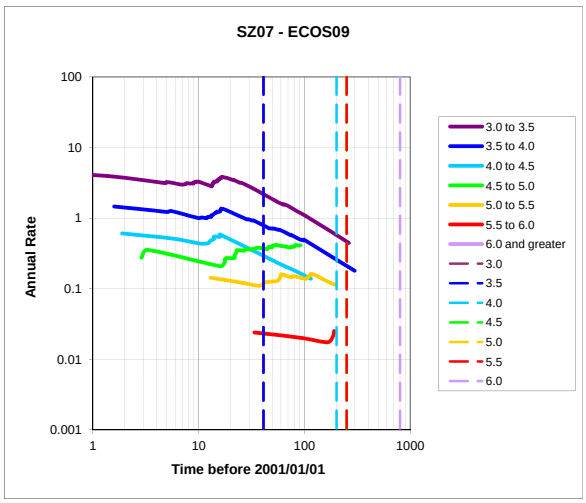

(b) ECOS-09 catalog

Figure 2.43: Stepp plots for EG1a completeness region SZ07.

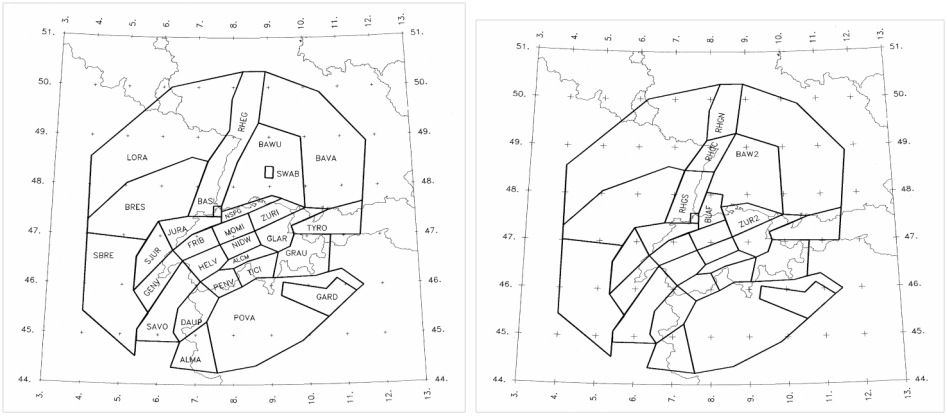

(a) Primary zonation (b) alternative zones

Figure 2.44: Seismic source zones defined by the EG1c Expert Team.

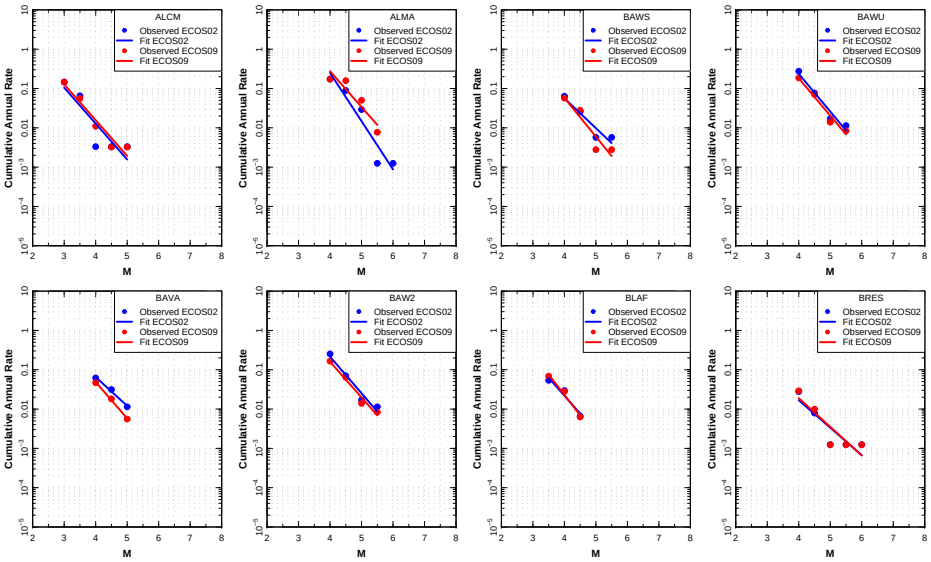

Figure 2.45: Seismicity data and least squares recurrence relationships for EG1c source zones. Seismicity data (1 of 5).

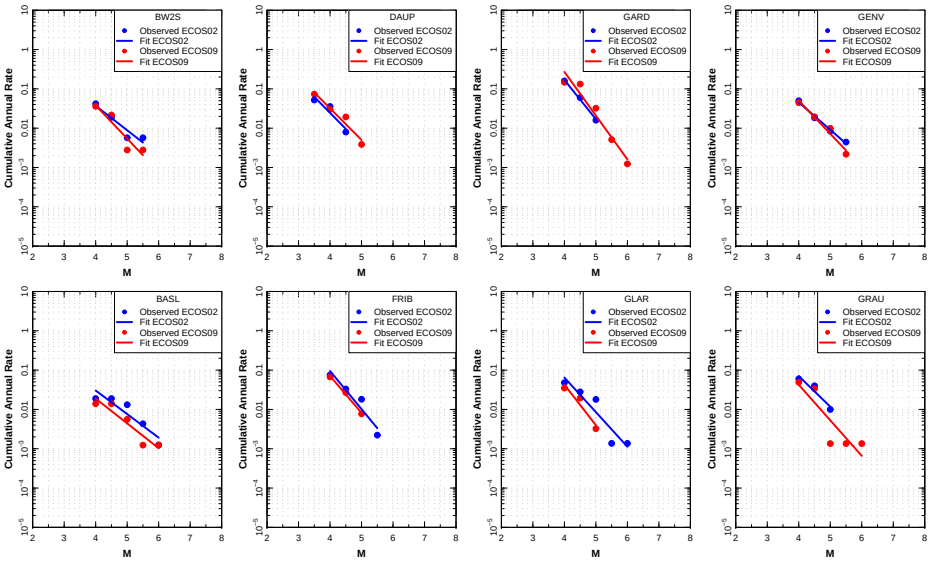

Figure 2.46: Seismicity data and least squares recurrence relationships for EG1c source zones. Seismicity data (2 of 5).

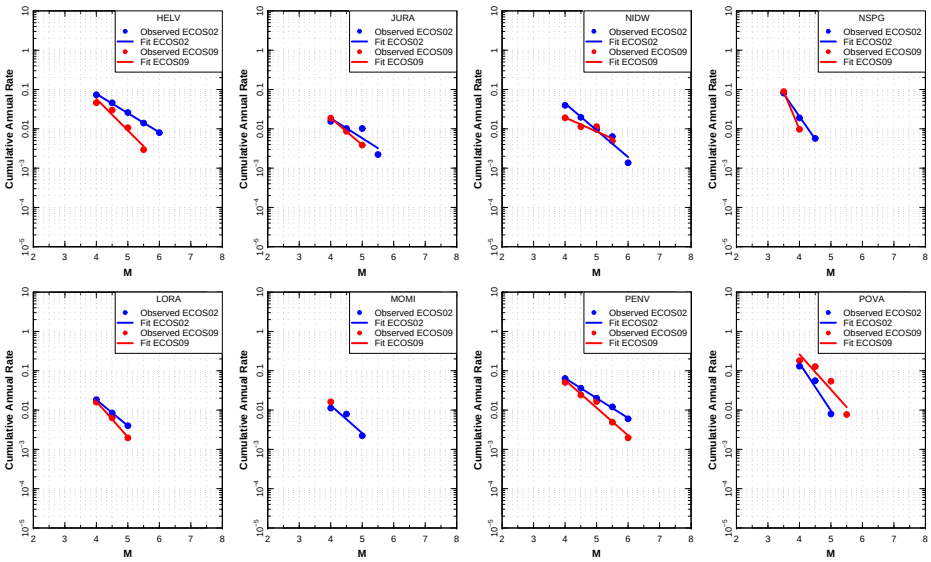

Figure 2.47: Seismicity data and least squares recurrence relationships for EG1c source zones. Seismicity data (3 of 5).

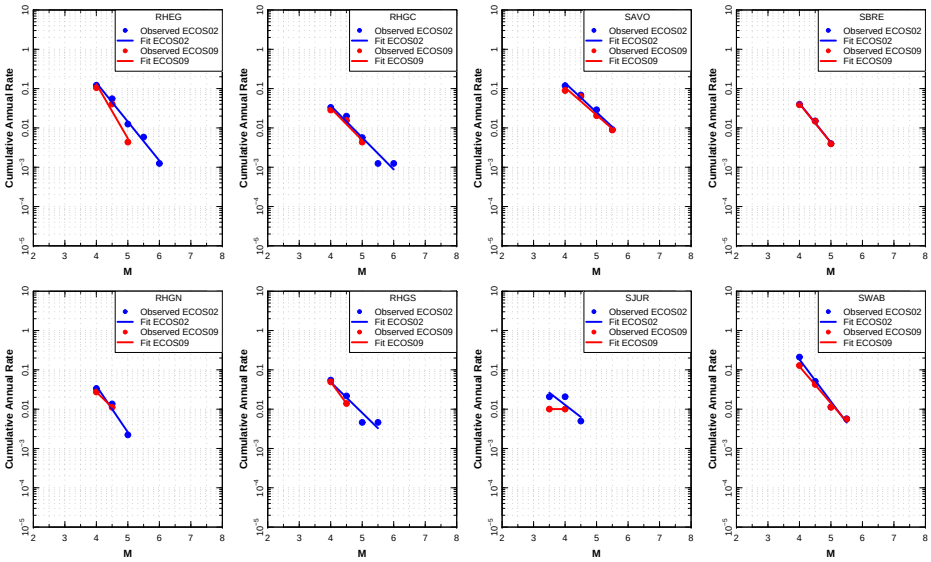

Figure 2.48: Seismicity data and least squares recurrence relationships for EG1c source zones. Seismicity data (4 of 5).

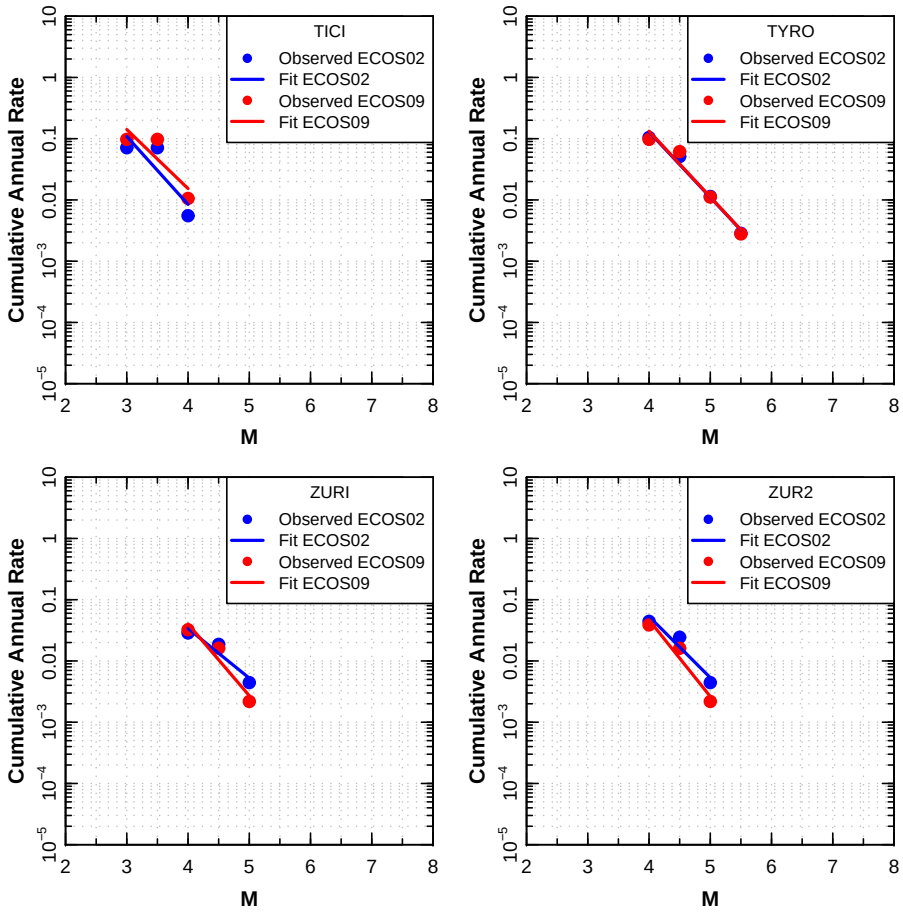

Figure 2.49: Seismicity data and least squares recurrence relationships for EG1c source zones. Seismicity data(5 of 5).

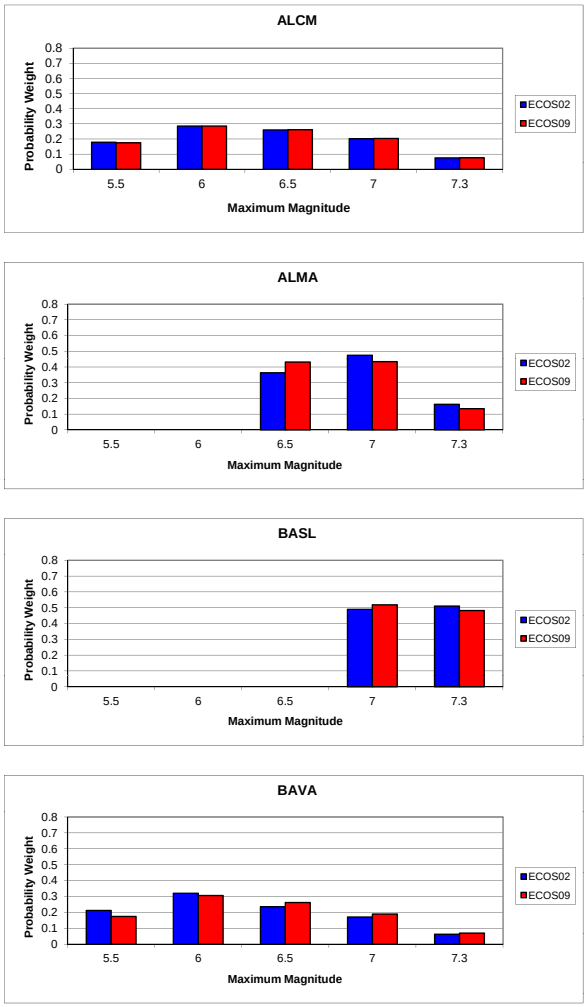

Figure 2.50: Maximum magnitude distributions for EG1c source zones (1 of 9).

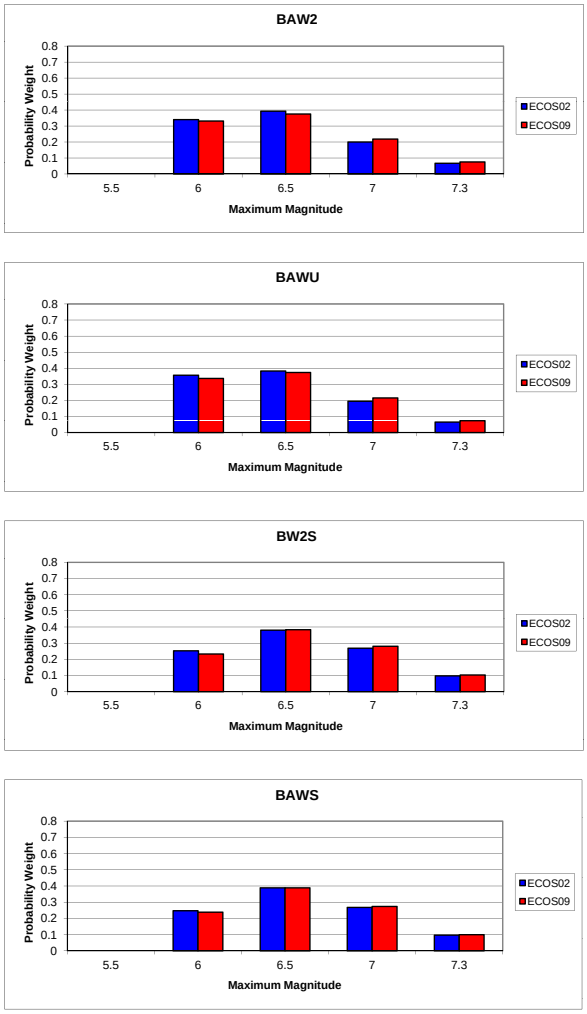

Figure 2.51: Maximum magnitude distributions for EG1c source zones (2 of 9).

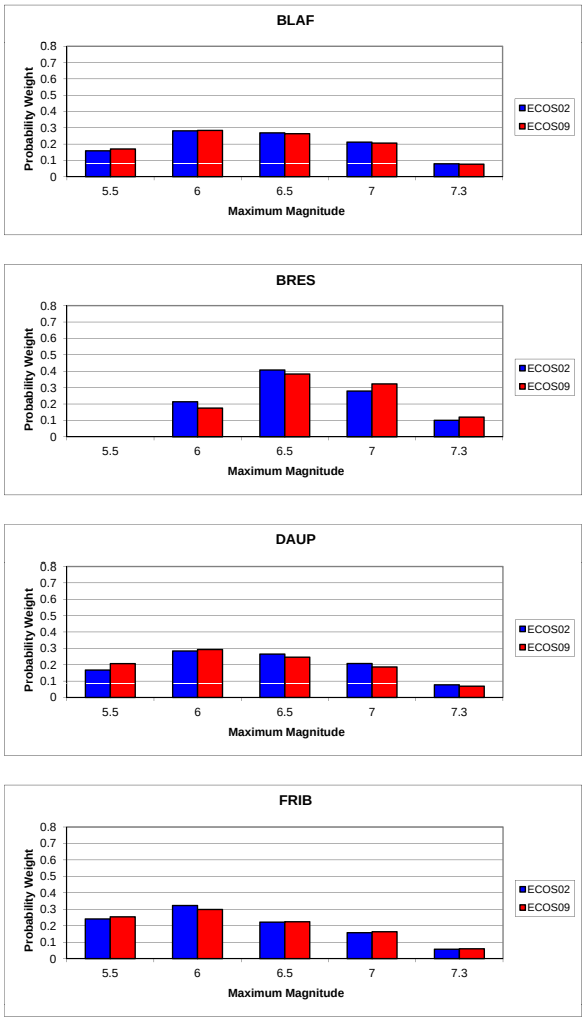

Figure 2.52: Maximum magnitude distributions for EG1c source zones (3 of 9).

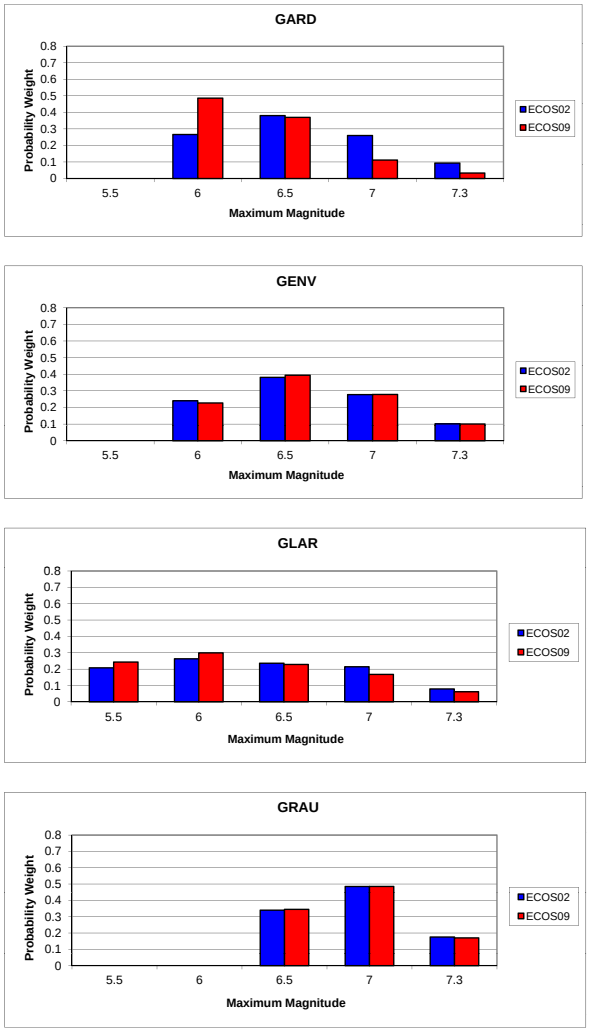

Figure 2.53: Maximum magnitude distributions for EG1c source zones (4 of 9).

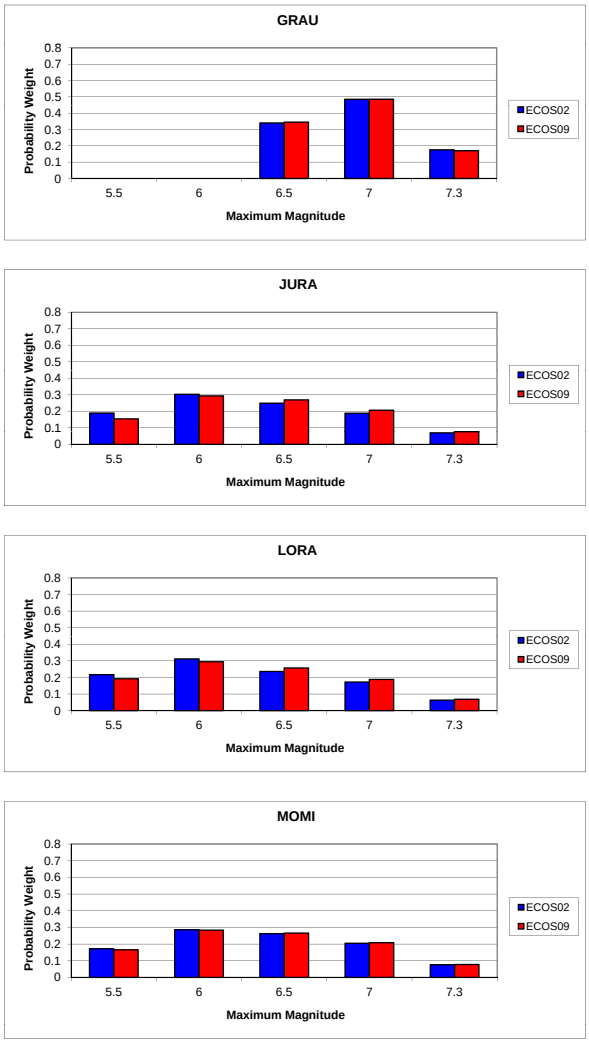

Figure 2.54: Maximum magnitude distributions for EG1c source zones (5 of 9).

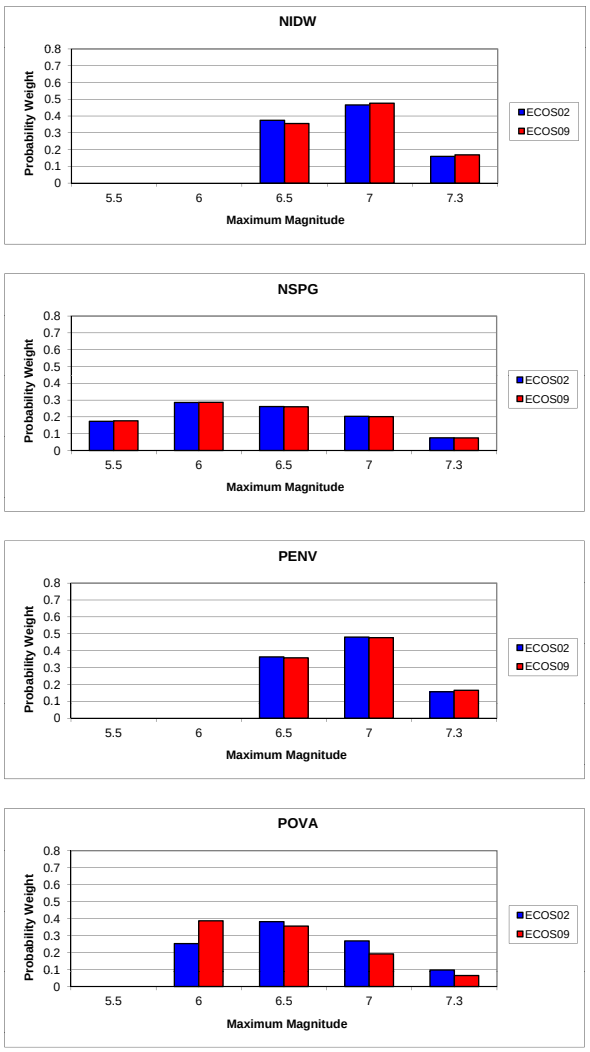

Figure 2.55: Maximum magnitude distributions for EG1c source zones (6 of 9).

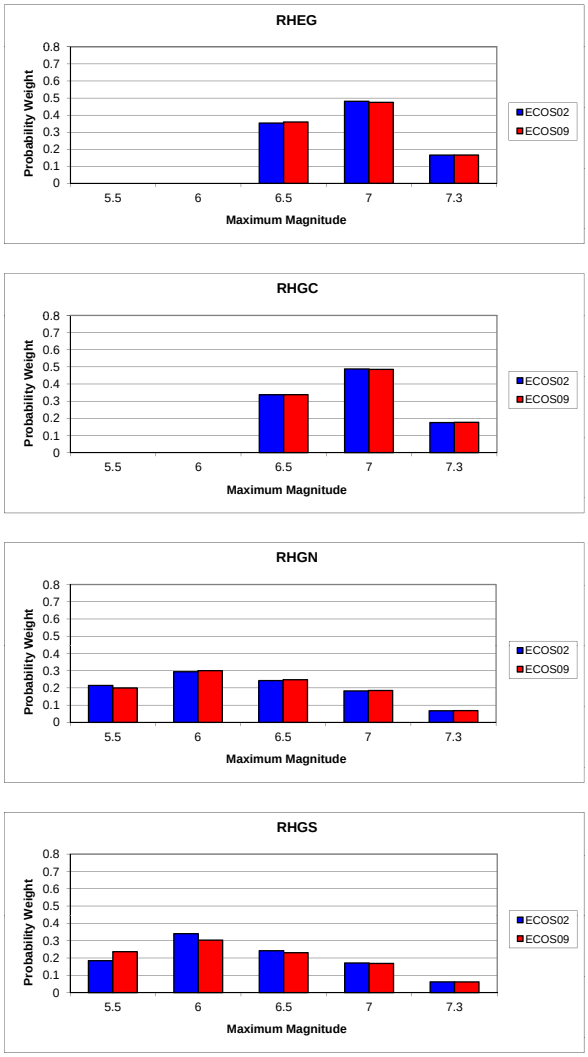

Figure 2.56: Maximum magnitude distributions for EG1c source zones (7 of 9).

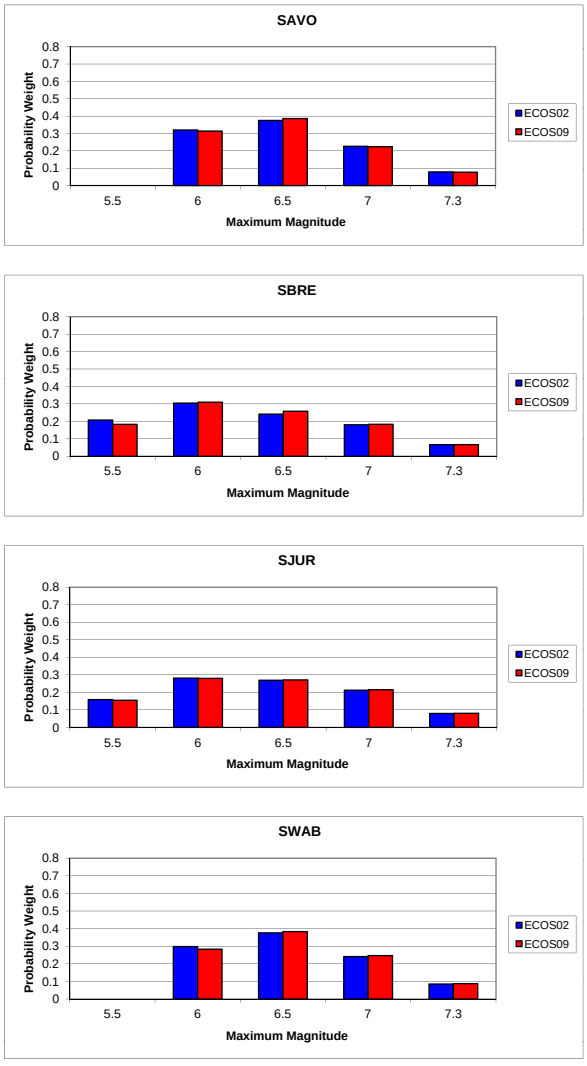

Figure 2.57: Maximum magnitude distributions for EG1c source zones (8 of 9).

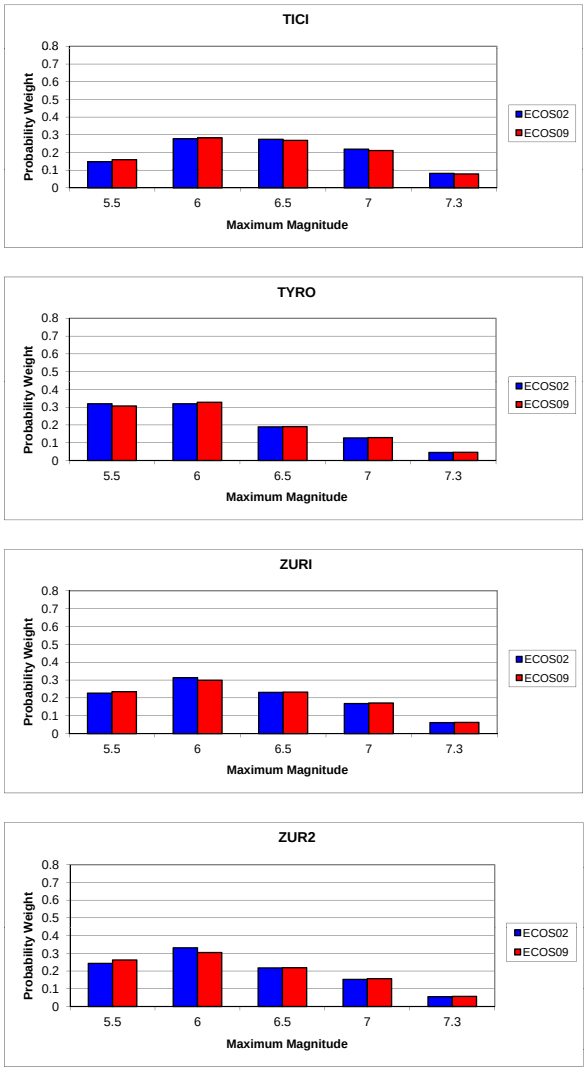

Figure 2.58: Maximum magnitude distributions for EG1c source zones (9 of 9).

2.5 Calculations Performed for February 2010 EG1 Workshop

An EG1 workshop was held in February 2010 to further explore the effect of the updated ECOS-09 earthquake catalog on seismicity parameters (earthquake recurrence and maximum magnitude) for the PEGASOS seismic sources. Calculations of catalog completeness, earthquake recurrence relationships, and maximum magnitude distributions were performed and supplied to the workshop participants. These calculations were performed using the draft ECOS-09 catalog [SED 2011] as declustered by Wiemer and Wössner [2010].

2.6 Earthquake Catalog Completeness

Using the difference in the M_L to M scaling employed in developing the ECOS-02 and ECOS-09 catalogs, the following approximate relationship between the ECOS-02 and ECOS-09 moment magnitudes was derived.

$$M_{ECOS-09} = 1.1038 + 0.594 M_{ECOS-02}, \quad \text{with} \quad M_{ECOS-02} < 1.8 \tag{2.11a}$$

$$M_{ECOS-09} = 1.381 + 0.287 M_{ECOS-02} + 0.085 M^2_{ECOS-02}, \quad \text{with} \quad 1.8 \leq M_{ECOS-02} < 3.8 \tag{2.11b}$$

$$M_{ECOS-09} = M_{ECOS-02} - 0.1, \quad \text{with} \quad M_{ECOS-02} \geq 3.8 \tag{2.11c}$$

Figure 2.59 shows the above relationship.

Comparative plots of catalog completeness were prepared for each of the EG1 Expert Team's catalog completeness regions using equation 2.1. Two sets of Stepp plots were produced. The first utilized the magnitude intervals defined by the EG1a Expert Teams for the ECOS-02 catalog. The second set of Stepp plots were prepared using magnitude intervals adjusted by Equation 2.11 for analysis of the ECOS-09 catalog.

2.6.1 Stepp Plots for EG1a

Figure 2.60 shows the six catalog completeness regions defined by EG1a. Figures 2.61 through 2.72 show the Stepp plots for each catalog completeness region. Part a of each figure compares the earthquake recurrence frequencies computed from the ECOS-02 and ECOS-09 catalogs using the magnitude intervals defined by EG1a for the ECOS-02 catalog. Part b of each figure compares the earthquake recurrence frequencies based on the original magnitude intervals for the ECOS-02 catalog with earthquake recurrence frequencies computed from the ECOS-09 catalog using magnitude intervals adjusted by equation 2.11. For example, the lowest magnitude interval defined by EG1a in the PEGASOS Project for Switzerland was M 2.3 to 2.7. The corresponding magnitude interval adjusted by equation 2.11 is M 2.49 to 2.78. The vertical dashed lines on each plot denote the periods of complete reporting for various magnitude intervals defined by EG1a based on the ECOS-02 catalog.

2.6.2 Stepp Plots for EG1b

Figure 2.73 shows the five catalog completeness regions defined by EG1b. Figures 2.74 through 2.83 show the Stepp plots for each catalog completeness region. Part a of each figure compares the earthquake recurrence frequencies computed from the ECOS-02 and ECOS-09

catalogs using the magnitude intervals defined by EG1b for the ECOS-02 catalog. Part b of each figure compares the earthquake recurrence frequencies based on the original magnitude intervals for the ECOS-02 catalog with earthquake recurrence frequencies computed from the ECOS-09 catalog using magnitude intervals adjusted by equation 2.11. For example, the lowest magnitude interval defined by EG1b in the PEGASOS Project for Switzerland was M 2.3 to 2.8. The corresponding magnitude interval adjusted by equation 2.11 is M 2.49 to 2.85. The vertical dashed lines on each plot denote the periods of complete reporting for various magnitude intervals defined by EG1b based on the ECOS-02 catalog.

2.6.3 Stepp Plots for EG1c

Figure 2.84 shows the seven catalog completeness regions defined by EG1c. Figures 2.85 through 2.98 show the Stepp plots for each catalog completeness region. Part a of each figure compares the earthquake recurrence frequencies computed from the ECOS-02 and ECOS-09 catalogs using the magnitude intervals defined by EG1c for the ECOS-02 catalog. Part b of each figure compares the earthquake recurrence frequencies based on the original magnitude intervals for the ECOS-02 catalog with earthquake recurrence frequencies computed from the ECOS-09 catalog using magnitude intervals adjusted by equation 2.11. For example, the lowest magnitude interval defined by EG1c in the PEGASOS Project was M 3.0 to 3.5. The corresponding magnitude interval adjusted by equation 2.11 is M 3.01 to 3.43. The vertical dashed lines on each plot denote the periods of complete reporting for various magnitude intervals defined by EG1c based on the ECOS-02 catalog.

2.6.4 Stepp Plots for EG1d

Figure 2.99 shows the five catalog completeness regions defined by EG1d. Figures 2.100 through 2.109 show the Stepp plots for each catalog completeness region. Part a of each figure compares the earthquake recurrence frequencies computed from the ECOS-02 and ECOS-09 catalogs using the magnitude intervals defined by EG1d for the ECOS-02 catalog. Part b of each figure compares the earthquake recurrence frequencies based on the original magnitude intervals for the ECOS-02 catalog with earthquake recurrence frequencies computed from the ECOS-09 catalog using magnitude intervals adjusted by equation 2.11. For example, the lowest magnitude interval defined by EG1d in the PEGASOS Project was M 1.8 to 2.2. The corresponding magnitude interval adjusted by equation 2.11 is M 2.17 to 2.42. The vertical dashed lines on each plot denote the periods of complete reporting for various magnitude intervals defined by EG1d based on the ECOS-02 catalog.

2.7 Calculations for EG1a

Earthquake recurrence rate calculations were performed for the EG1a Expert Teams eleven macro-zones. These sources are shown on Figure 2.110. The ECOS-02 and ECOS-09 catalogs were used to compute seismicity rates for each macro-zone using the maximum likelihood approach described in section 2.2.3. The catalog completeness periods and magnitude intervals used were those defined by EG1a in the PEGASOS Project. For the ECOS-09 catalog the completeness periods were extended by eight years. Two sets of calculations were performed for the ECOS-09 catalog. One set used the magnitude intervals defined for the ECOS-02

catalog and the second set used magnitude intervals adjusted by equation 2.11. Figures 2.111 through 2.121 show the computed seismicity rates for each macro-zone. The panel on the left of each plot shows the fit to the data for the instrumental period and the panel on the right shows the fit to the data for the historical period.

2.8 Calculations for EG1b

Two sets of comparative calculations were performed for use by the EG1b Expert Team: calculations of earthquake recurrence rates and calculations of maximum magnitude distributions.

2.8.1 Large Zone Seismicity Rates

Recurrence rate calculations were performed for EG1b Expert Team's eight large source zones, shown on Figure 2.122. The ECOS-02 and ECOS-09 catalogs were used to compute seismicity rates for each macro-zone using the maximum likelihood approach described above in section 2.2.3. The catalog completeness periods and magnitude intervals used were those defined by EG1b in the PEGASOS Project. For the ECOS-09 catalog the completeness periods were extended by eight years. Figures 2.123 through 2.130 show the computed seismicity rates for the large zones.

Four sets of calculations were performed for the ECOS-09 catalog. The first set used the magnitude intervals defined for the ECOS-02 catalog and the second set used magnitude intervals adjusted by equation 2.11. These results are shown on the left hand plots of each figure. The second two sets of calculations used a modified form of the standard truncated exponential distribution that incorporated the curvature in magnitude scaling represented by equation 2.11 and shown on Figure 2.59. These results are shown on the right hand plots of each figure and denoted by the "Modified TE" in the legend.

2.8.2 Large Zone Maximum Magnitude Distributions

For each of the EG1b Expert Team's large zones, the Bayesian approach as described above in section 2.2.4 was used to develop maximum magnitude distributions. Figures 2.131 through 2.138 show the maximum magnitude distributions. Four calculations were performed for each zone. The first calculation used the ECOS-02 and the second calculation used the ECOS-09 catalog. The prior distributions, b-values and completeness periods used were those defined by EG1b in the PEGASOS Project. The third and fourth calculations repeated the first and second calculations including uncertainty in the magnitudes reported in the catalog. Magnitude uncertainty was incorporated by simulating 100 catalogs of earthquakes with magnitudes normally distributed about the reported values using the standard errors for magnitude uncertainty specified in the ECOS-02 and ECOS-09 catalogs. The Bayesian approach was applied to each simulated catalog to obtain a posterior distribution for maximum magnitude. The 100 posterior distributions were then combined with equal weight to produce the composite posterior distribution, denoted by either ECOS02-sim or ECOS09-sim on the plots.

2.9 Calculations for EG1c Expert Team

Recurrence rate calculations were performed for EG1c Expert Team's seven earthquake catalog completeness regions, shown on Figure 2.139. The ECOS-02 and ECOS-09 catalogs were used to compute seismicity rates for each macro-zone using the maximum likelihood approach described above in section 2.2.3. The catalog completeness periods and magnitude intervals used were those defined by EG1c in the PEGASOS Project. For the ECOS-09 catalog the completeness periods were extended by eight years. Figures 2.140 through 2.146 show the computed seismicity rates for the catalog completeness regions. Four sets of calculations were performed for the ECOS-09 catalog. The first set used the magnitude intervals defined for the ECOS-02 catalog and the second set used magnitude intervals adjusted by equation 2.11. These results are shown on the left hand plots of each figure. The second two sets of calculations used a modified form of the standard truncated exponential distribution that incorporated the curvature in magnitude scaling represented by equation 2.11 and shown on Figure 2.59. These results are shown on the right hand plots of each figure and denoted by the "Modified TE" in the legend.

2.10 Calculations for EG1d

Two sets of comparative calculations were performed for use by the EG1d Expert Team: calculations of earthquake recurrence rates and calculations of maximum magnitude distributions.

2.10.1 Regional b-values

Recurrence rate calculations were performed to obtain regional b-values. The ECOS-02 and ECOS-09 catalogs were used to compute seismicity rates for each completeness region using the maximum likelihood approach described above in section 2.2.3. The catalog completeness periods and magnitude intervals used were those defined by EG1b in the PEGASOS Project. For the ECOS-09 catalog the completeness periods were extended by eight years. The EG1d Expert Team defined two sets of earthquake catalog completeness values for each catalog completeness region. The regional b-values were computed by simultaneously fitting all of the data in the study region with a single b-value while allowing different seismicity rates in each of the five catalog completeness regions shown in Figure 2.99. Figures 2.147 and 2.148 show the resulting fits to the ECOS-02 and ECOS-09 catalogs using Completeness Set 1 and Completeness Set 2, respectively. Two fits to the ECOS-09 catalog are shown, one using the magnitude intervals defined for the ECOS-02 catalog and one using magnitude intervals modified by equation 2.11.

Figure 2.149 and 2.150 show the same comparisons as Figure 2.147 and 2.148 except that the modified truncated exponential distribution is used to fit the seismicity data from the ECOS-09 catalog.

Figure 2.151 and 2.152 show the data for the five completeness regions along with simultaneous fits to the data in all regions with a common b-value allowing for differences in the seismicity rate for the instrumental (post 1975) and pre-instrumental (pre 1975) periods.

Figure 2.153 shows the seismicity data from just the Switzerland completeness region. The seismicity data are fit with the standard truncated exponential distribution. Figure 2.154

shows the seismicity data from just the Switzerland completeness region with the ECOS-09 catalog data fit with the modified truncated exponential distribution.

2.10.2 Maximum Magnitude Distributions

Figure 2.155 shows the seismic source zones defined by the EG1d Expert Team. Figures 2.156 through 2.190 show maximum magnitude distributions for each of the source zones and source zone combinations. These maximum magnitude distributions were developed using the Bayesian approach described above in section 2.2.4. Uncertainty in magnitude and earthquake location was incorporated in the assessment by simulation of 100 catalogs using the magnitude and location errors reported in the ECOS-02 and ECOS-09 catalogs.

Each plot shows four maximum magnitude distributions computed as follows

- Using the ECOS02 catalog and the All data b-value of 0.768
- Using the ECOS09 catalog and the All data b-value of 0.999
- Using the ECOS09 catalog with modified completeness magnitude intervals and the ALL data b-value of 0.919
- Using the ECOS09 catalog with modified completeness magnitude intervals and the ALL data b-value of 0.731 for the modified truncated exponential (TE) model

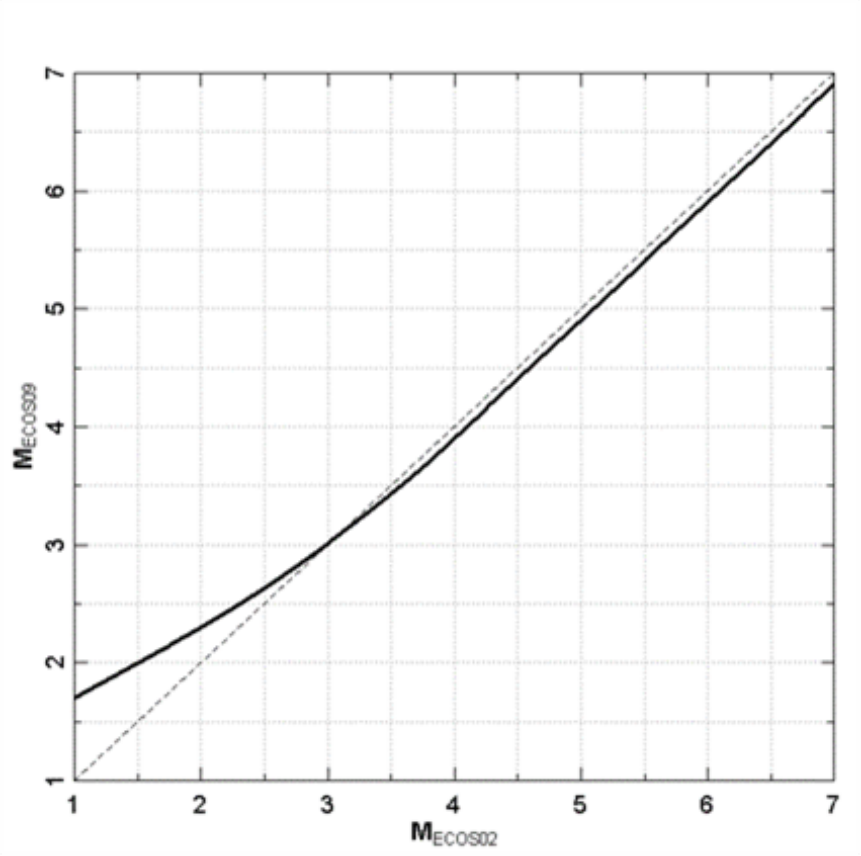

Figure 2.59: Relationship between moment magnitudes in the ECOS-02 and ECOS-09 earthquake catalogs as defined by Equation 2.11.

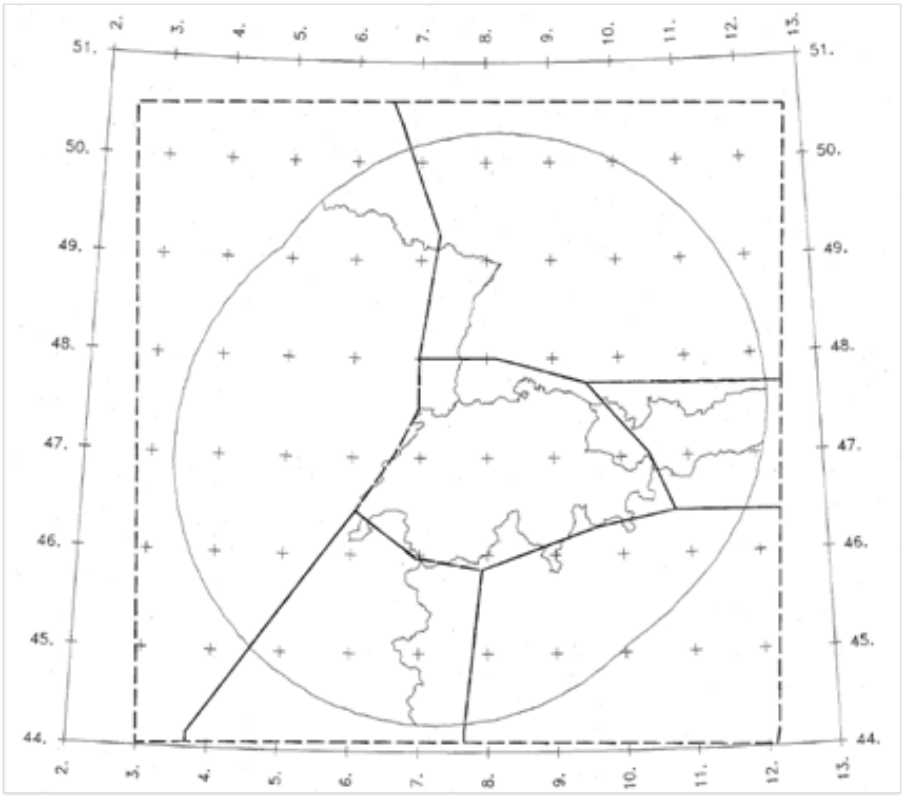

Figure 2.60: Catalog completeness regions defined by Expert Team EG1a.

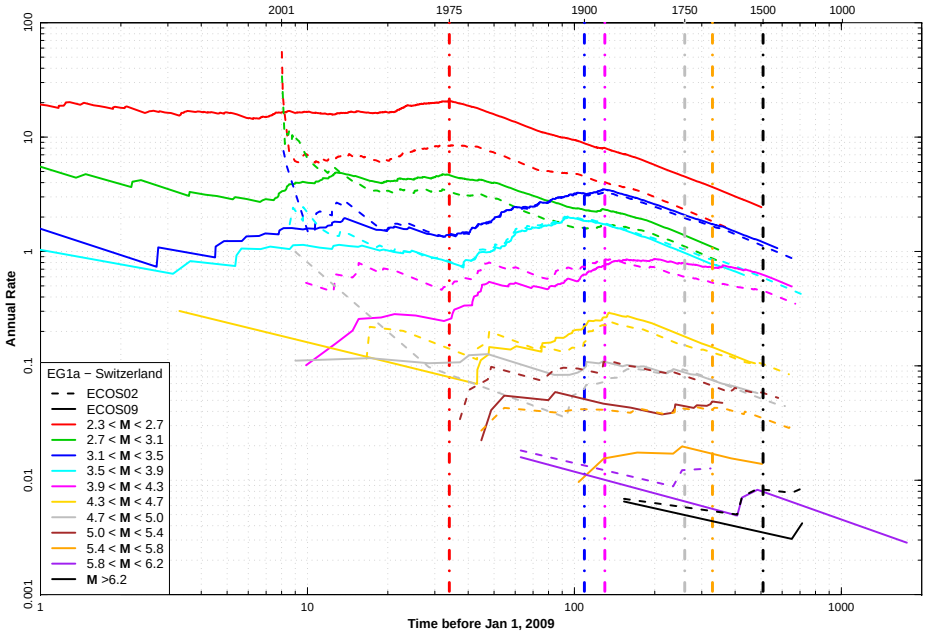

Figure 2.61: Stepp plots for EG1a Switzerland completeness region using magnitude intervals defined for ECOS-02 catalog.

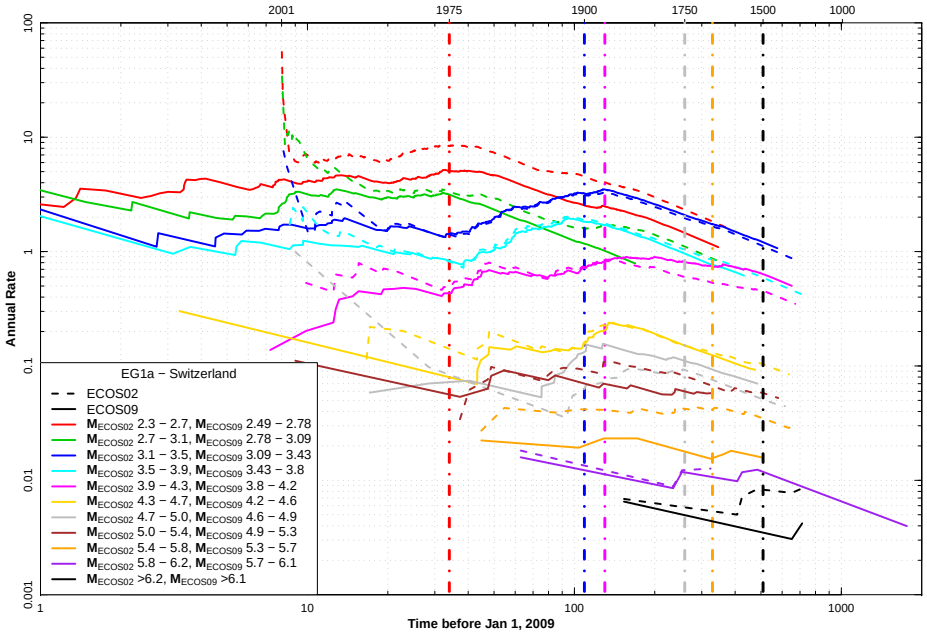

Figure 2.62: Stepp plots for EG1a Switzerland completeness region using ECOS-02 magnitude intervals for ECOS-02 catalog and magnitude intervals adjusted by Equation 2.11 for ECOS-09 catalog.

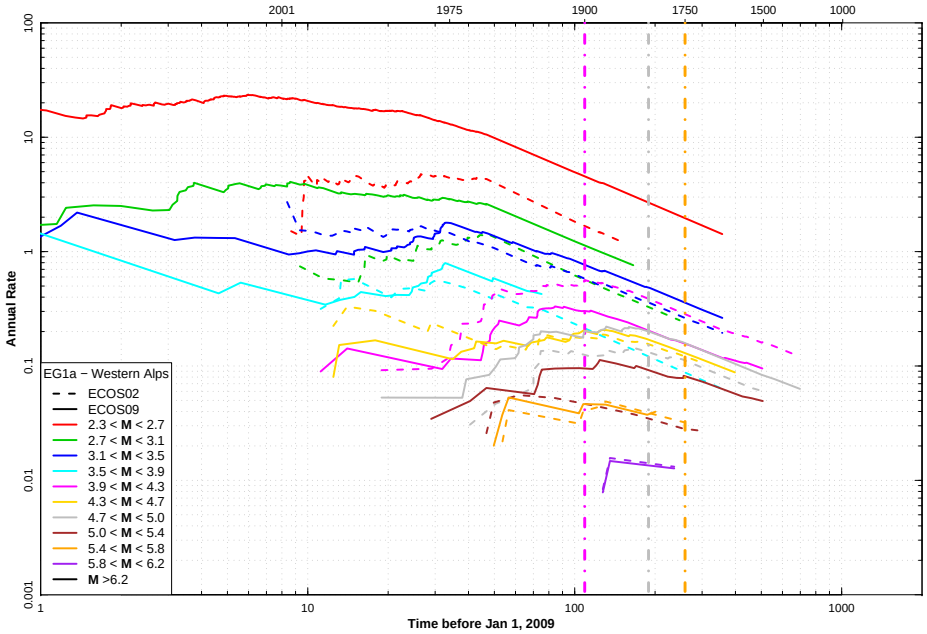

Figure 2.63: Stepp plots for EG1a Western Alps completeness region using magnitude intervals defined for ECOS-02 catalog.

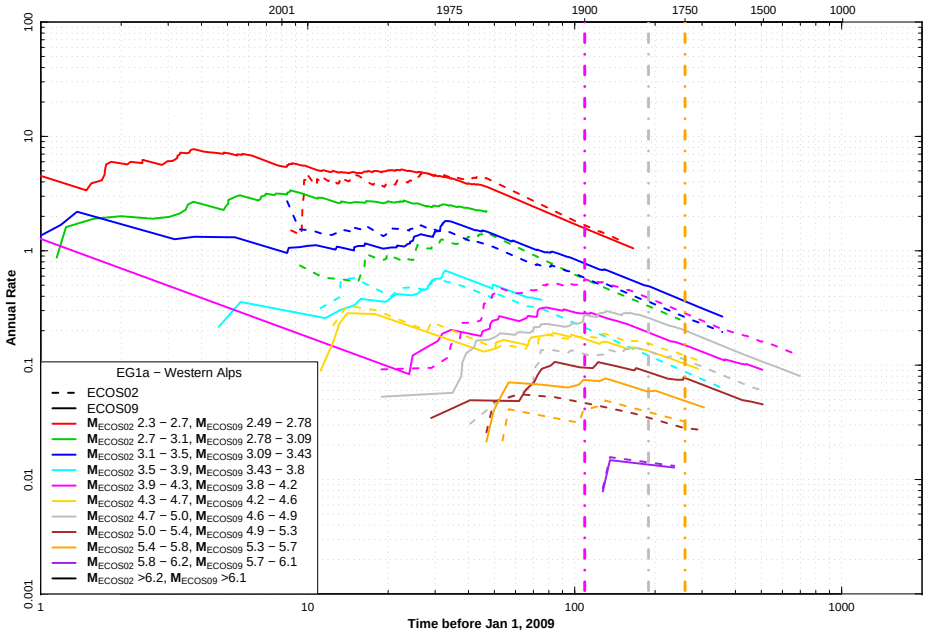

Figure 2.64: Stepp plots for EG1a Western Alps completeness region using ECOS-02 magnitude intervals for ECOS-02 catalog and magnitude intervals adjusted by Equation 2.11 for ECOS-09 catalog.

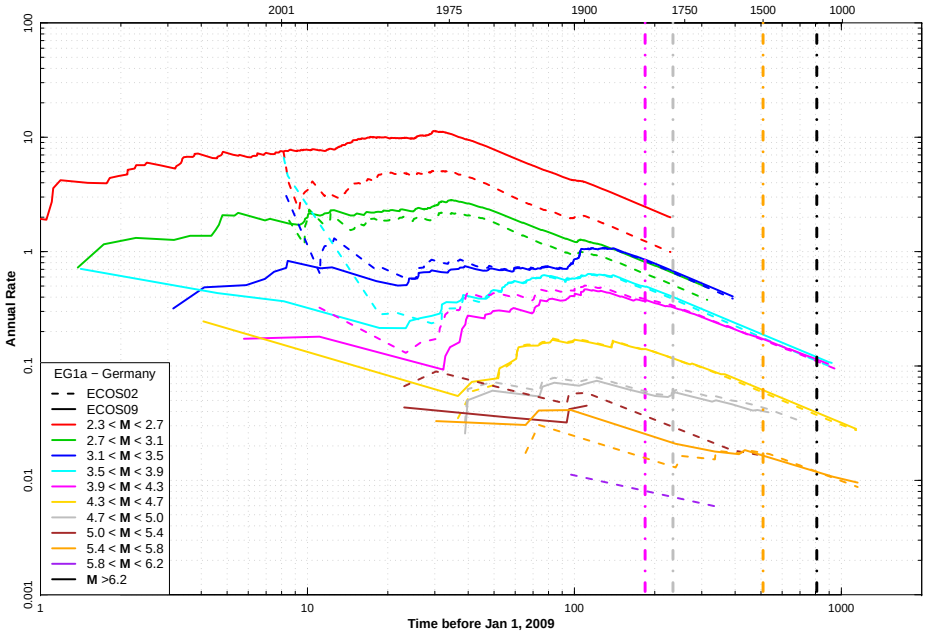

Figure 2.65: Stepp plots for EG1a Germany completeness region using magnitude intervals defined for ECOS-02 catalog.

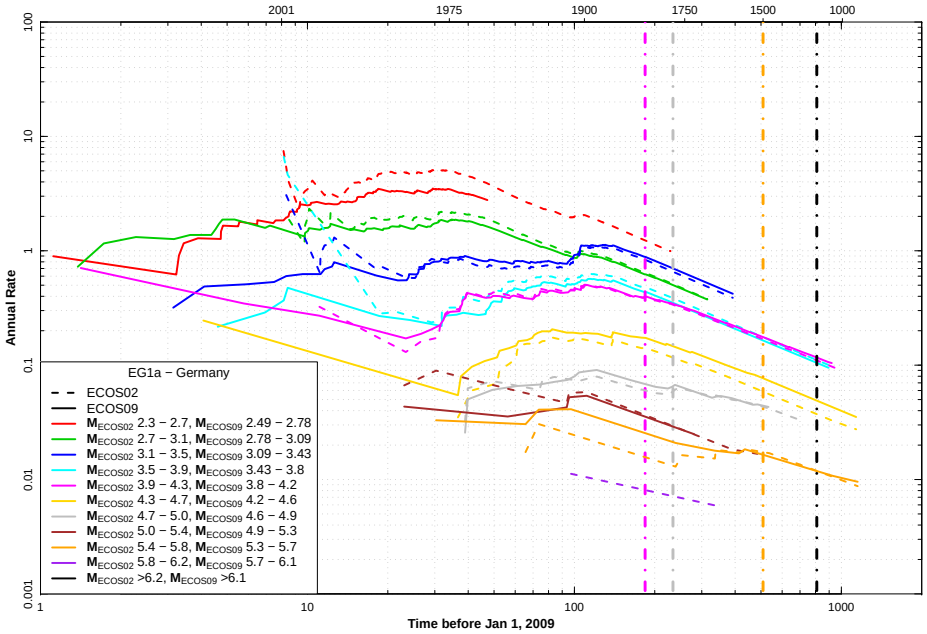

Figure 2.66: Stepp plots for EG1a Germany completeness region using ECOS-02 magnitude intervals for ECOS-02 catalog and magnitude intervals adjusted by Equation 2.11 for ECOS-09 catalog.

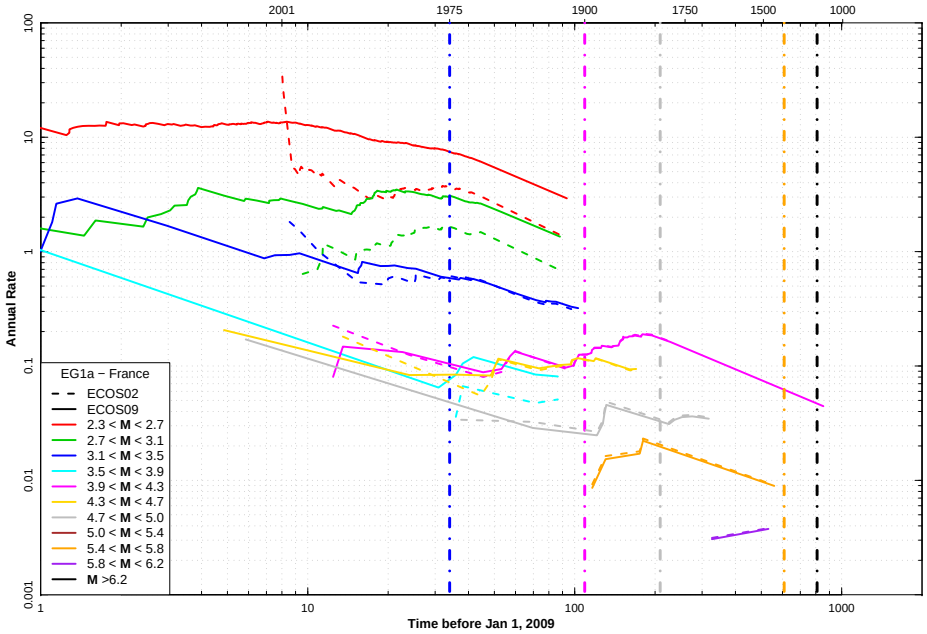

Figure 2.67: Stepp plots for EG1a France completeness region using magnitude intervals defined for ECOS-02 catalog.

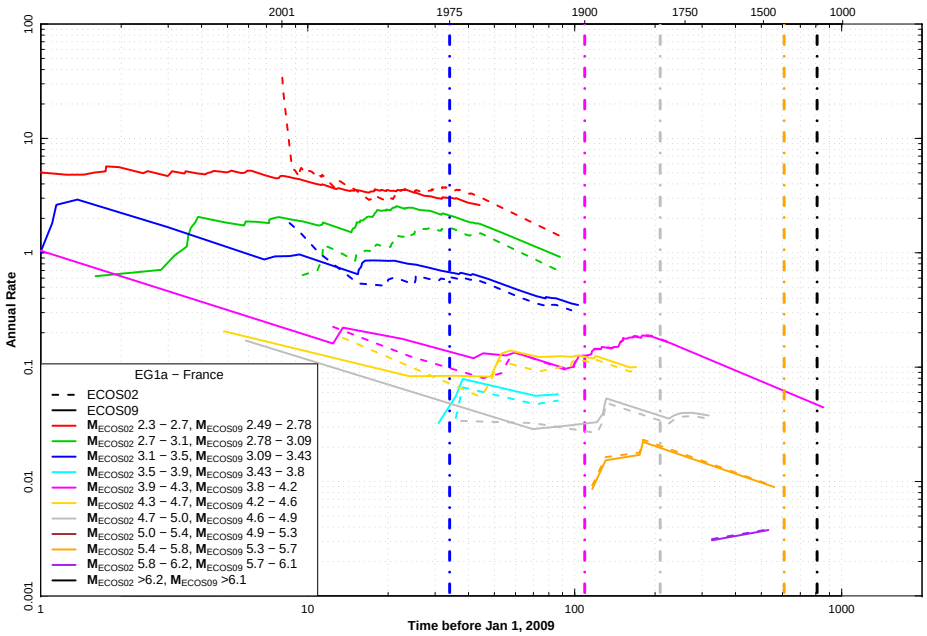

Figure 2.68: Stepp plots for EG1a France completeness region using ECOS-02 magnitude intervals for ECOS-02 catalog and magnitude intervals adjusted by Equation 2.11 for ECOS-09 catalog.

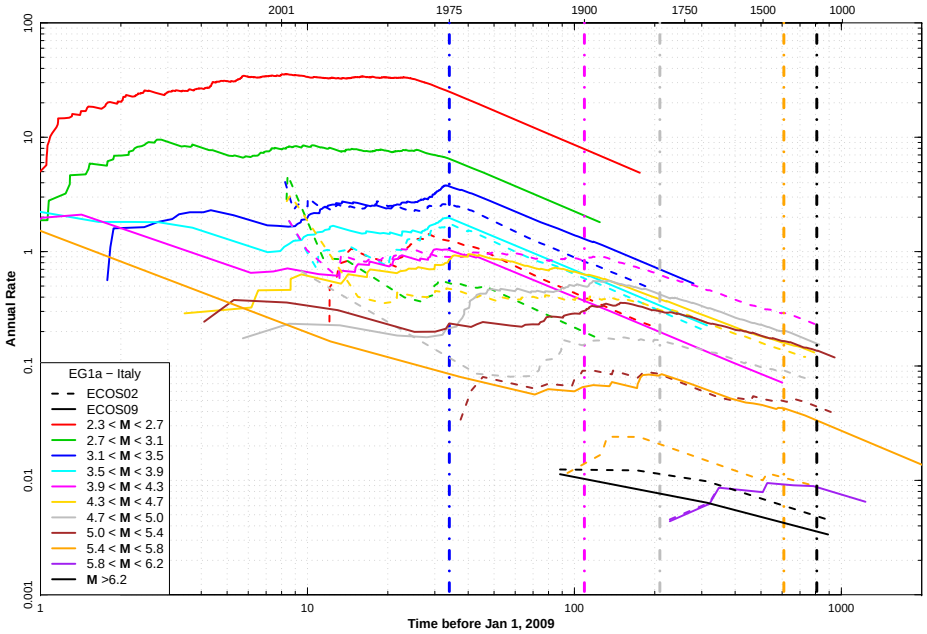

Figure 2.69: Stepp plots for EG1a Italy completeness region using magnitude intervals defined for ECOS-02 catalog.

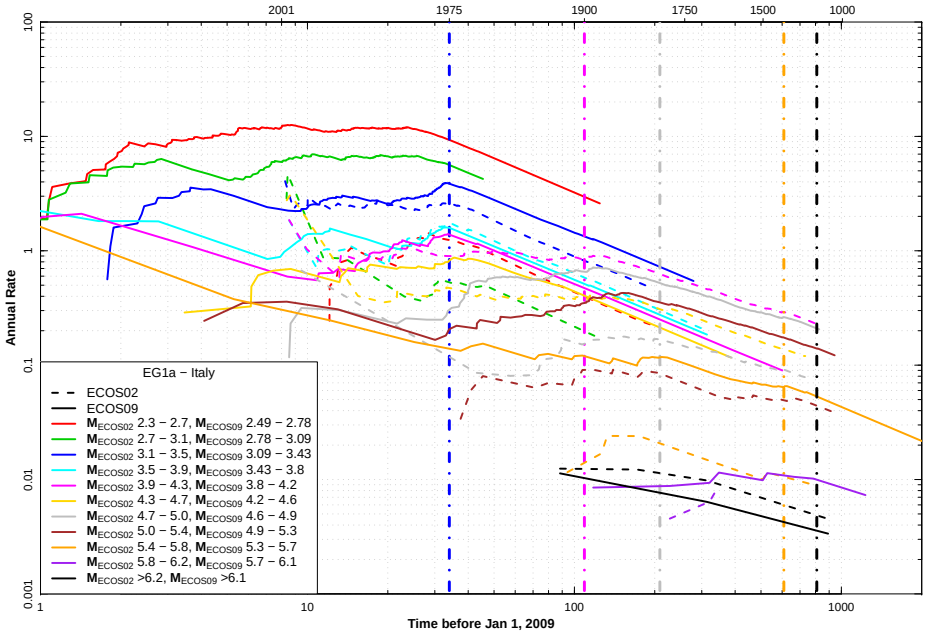

Figure 2.70: Stepp plots for EG1a Italy completeness region using ECOS-02 magnitude intervals for ECOS-02 catalog and magnitude intervals adjusted by Equation 2.11 for ECOS-09 catalog.

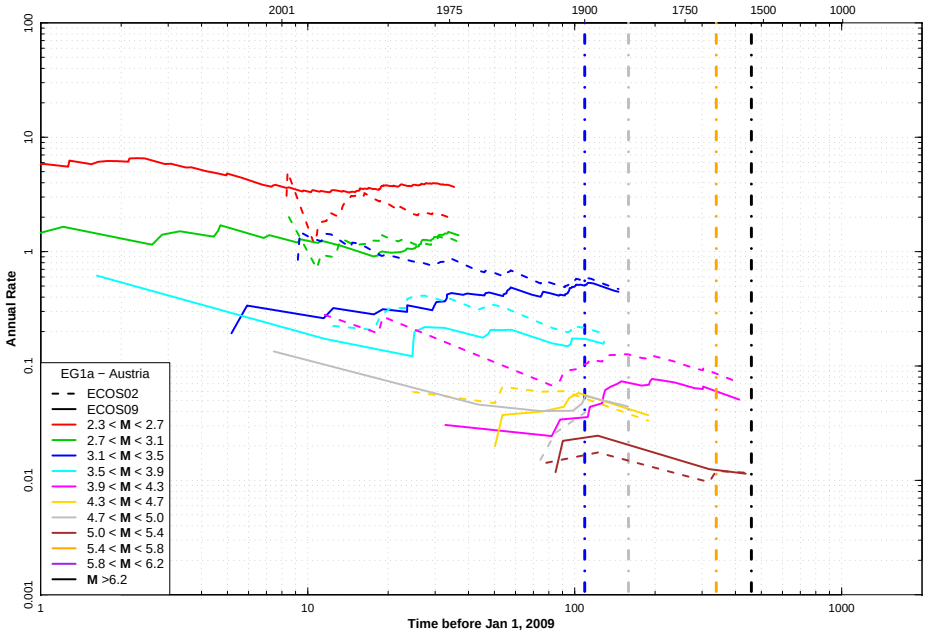

Figure 2.71: Stepp plots for EG1a Austria completeness region using magnitude intervals defined for ECOS-02 catalog.

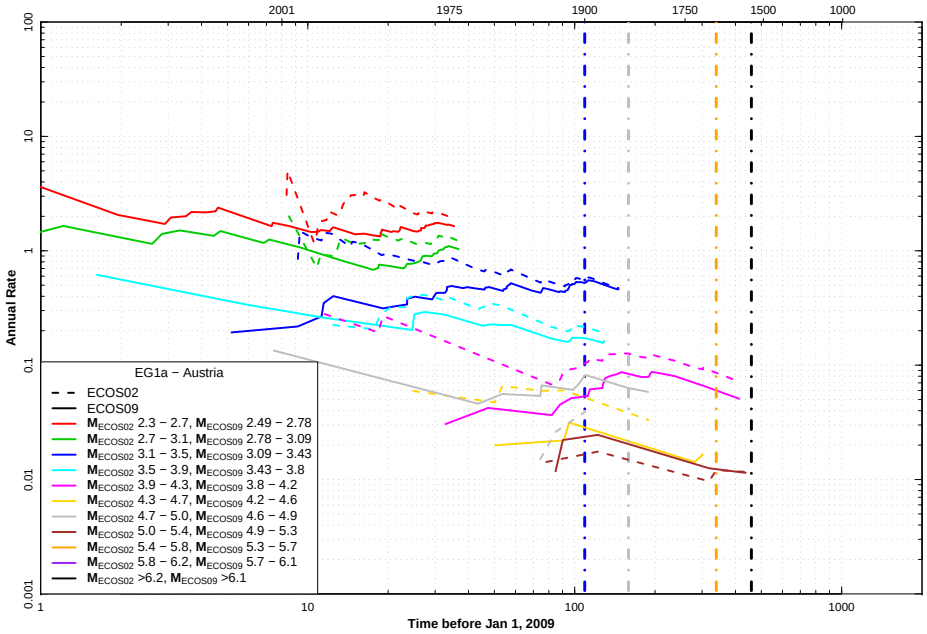

Figure 2.72: Stepp plots for EG1a Austria completeness region using ECOS-02 magnitude intervals for ECOS-02 catalog and magnitude intervals adjusted by Equation 2.11 for ECOS-09 catalog.

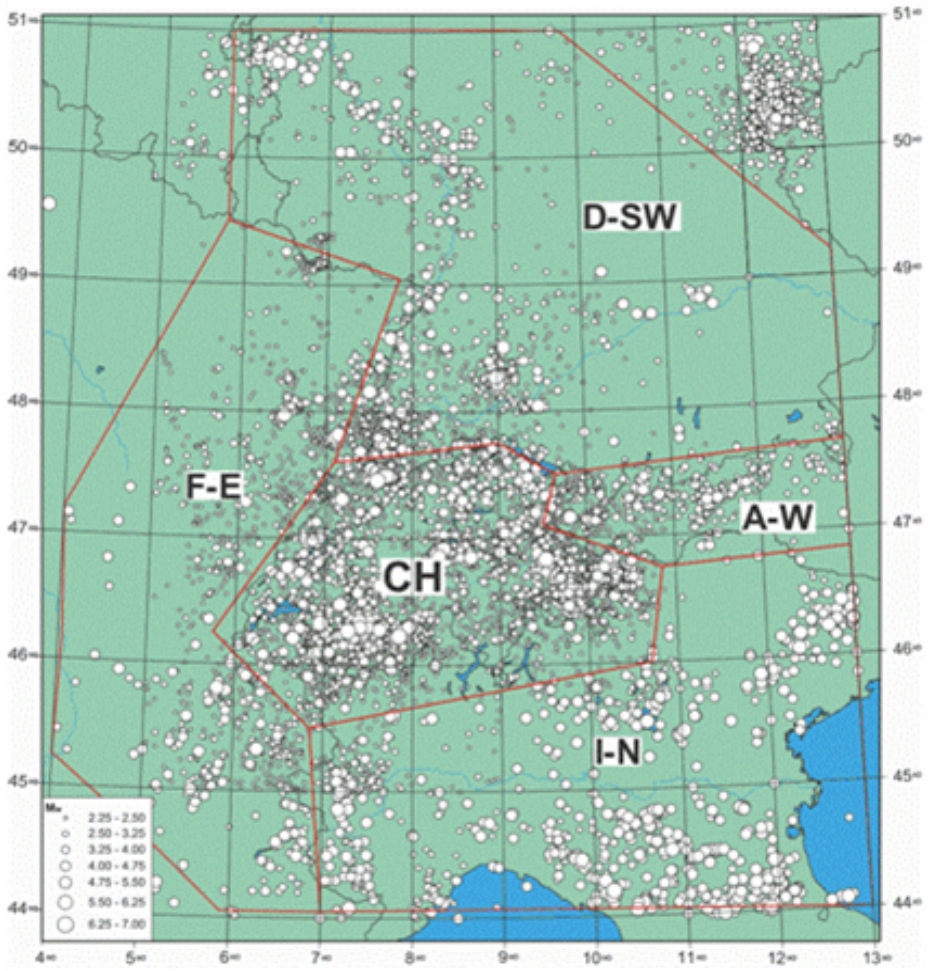

Figure 2.73: Earthquake catalog completeness regions defined by the EG1b Expert Team.

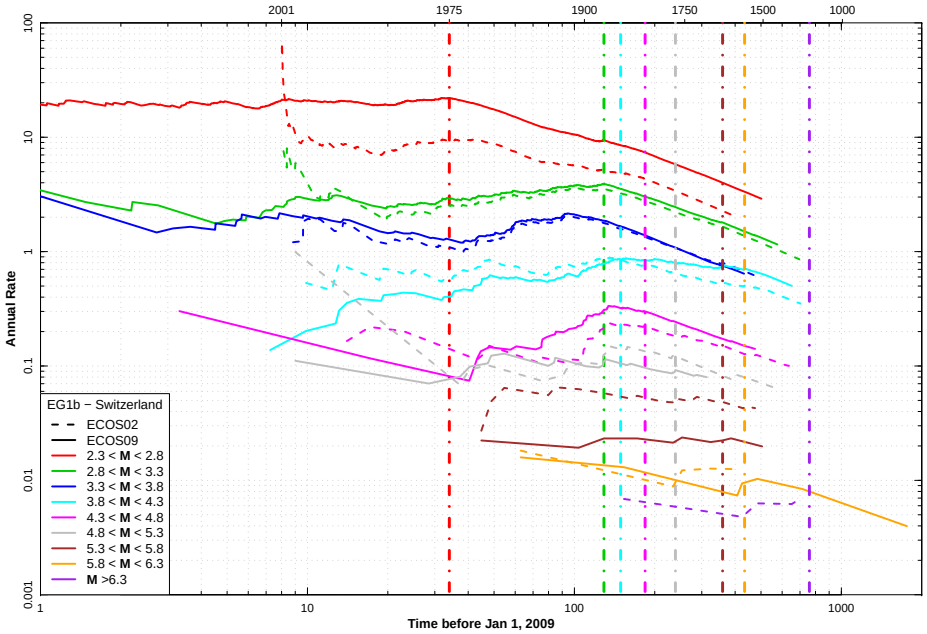

Figure 2.74: Stepp plots for EG1b Switzerland (CH) completeness region using magnitude intervals defined for ECOS-02 catalog.

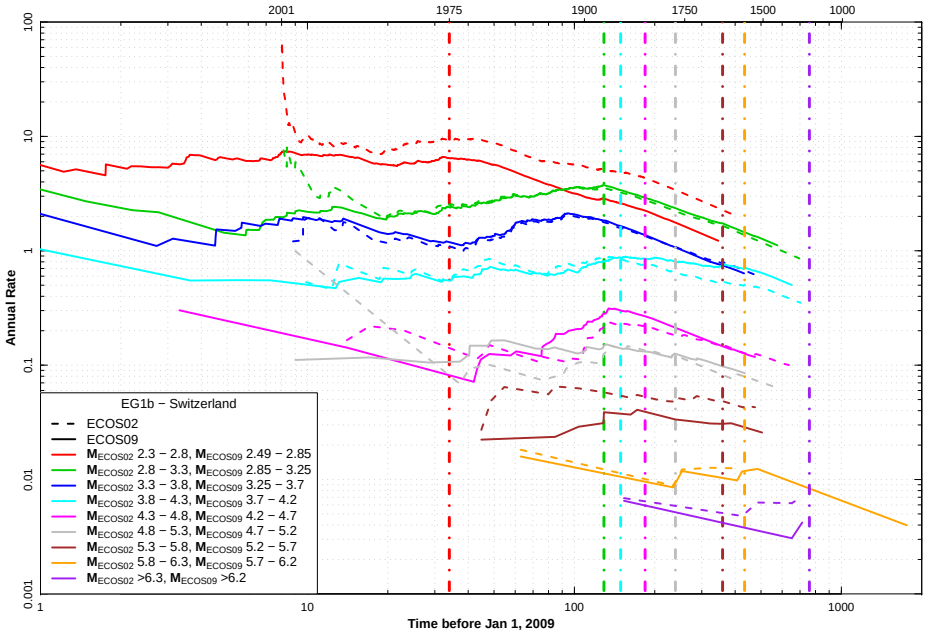

Figure 2.75: Stepp plots for EG1b Switzerland (CH)completeness region using ECOS-02 magnitude intervals for ECOS-02 catalog and magnitude intervals adjusted by Equation 2.11 for ECOS-09 catalog.

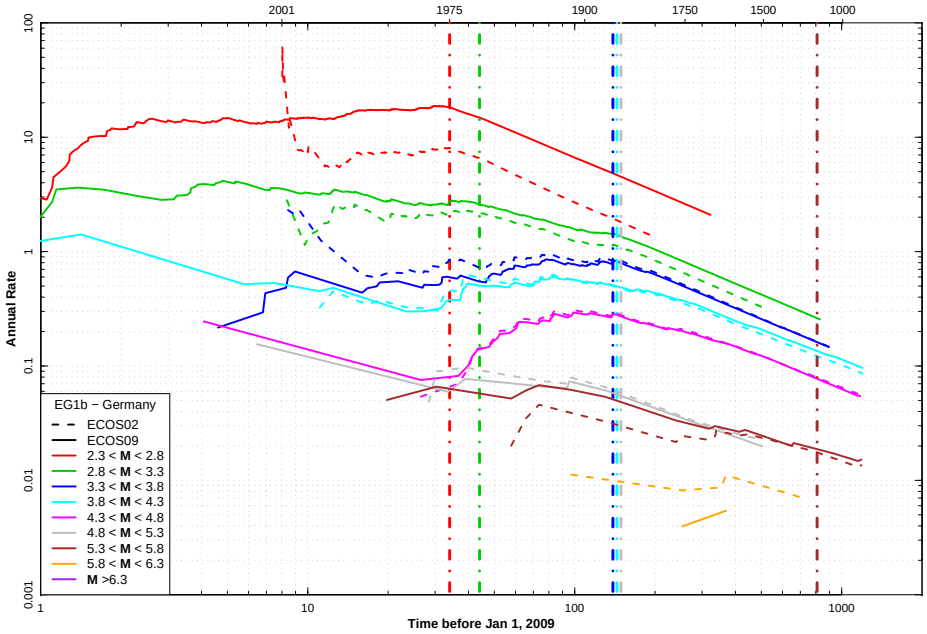

Figure 2.76: Stepp plots for EG1b Germany (D-SW) completeness region using magnitude intervals defined for ECOS-02 catalog.

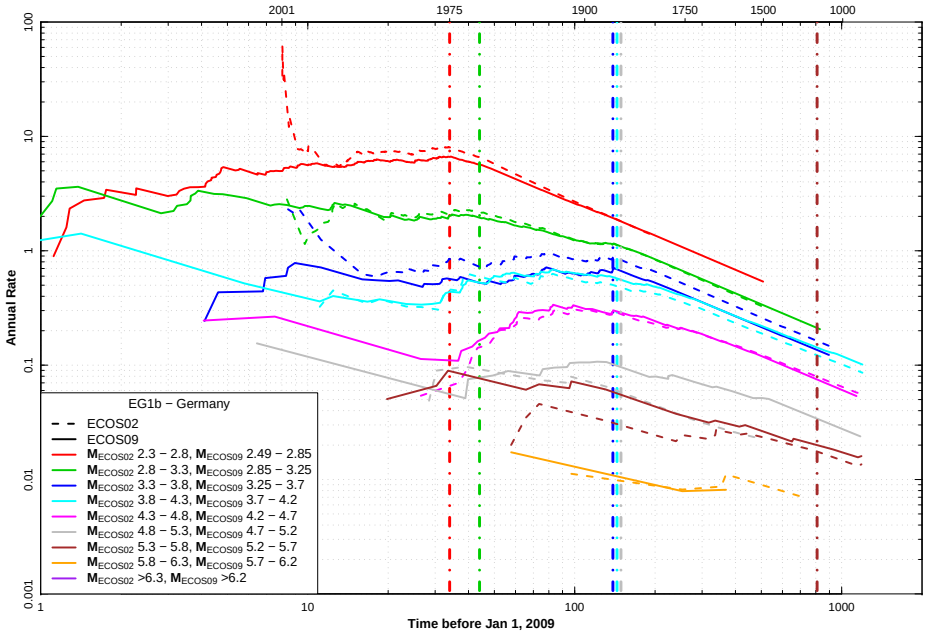

Figure 2.77: Stepp plots for EG1b Germany (D-SW)completeness region using ECOS-02 magnitude intervals for ECOS-02 catalog and magnitude intervals adjusted by Equation 2.11 for ECOS-09 catalog.

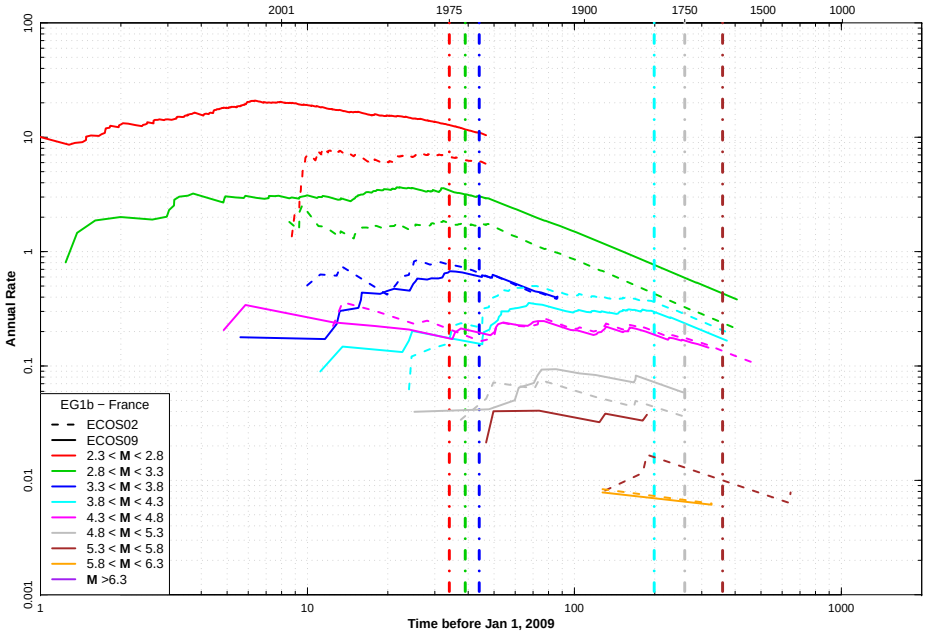

Figure 2.78: Stepp plots for EG1b France (F-E)completeness region using magnitude intervals defined for ECOS-02 catalog.

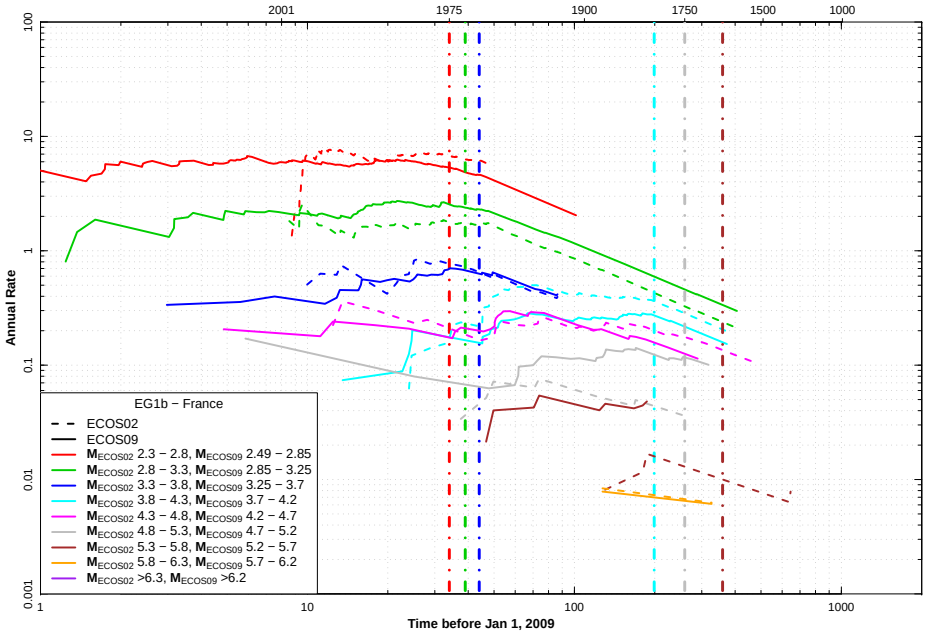

Figure 2.79: Stepp plots for EG1b France (F-E)completeness region using ECOS-02 magnitude intervals for ECOS-02 catalog and magnitude intervals adjusted by Equation 2.11 for ECOS-09 catalog.

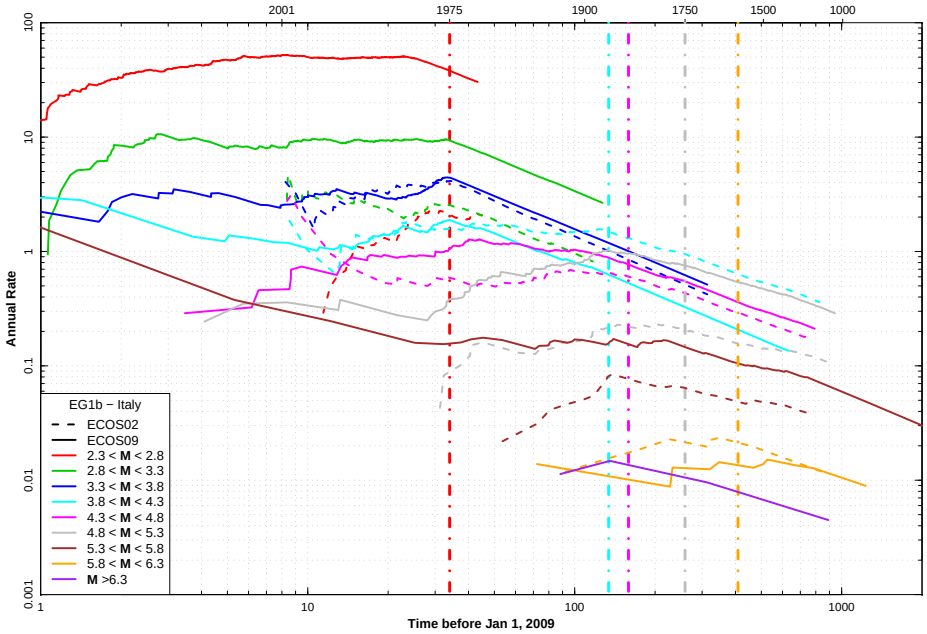

Figure 2.80: Stepp plots for EG1b Italy (I-N)completeness region using magnitude intervals defined for ECOS-02 catalog.

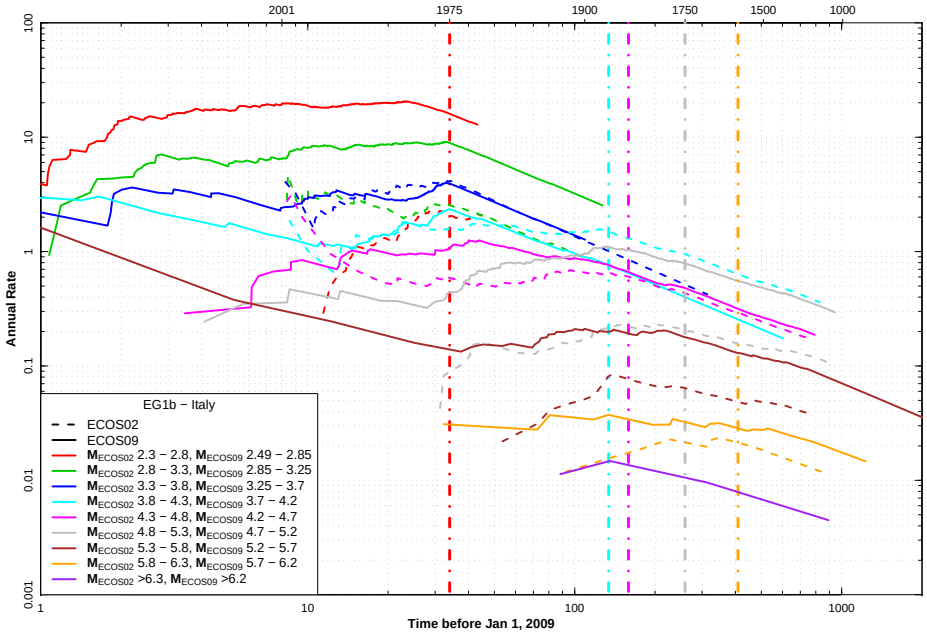

Figure 2.81: Stepp plots for EG1b Italy (I-N) completeness region using ECOS-02 magnitude intervals for ECOS-02 catalog and magnitude intervals adjusted by Equation 2.11 for ECOS-09 catalog.

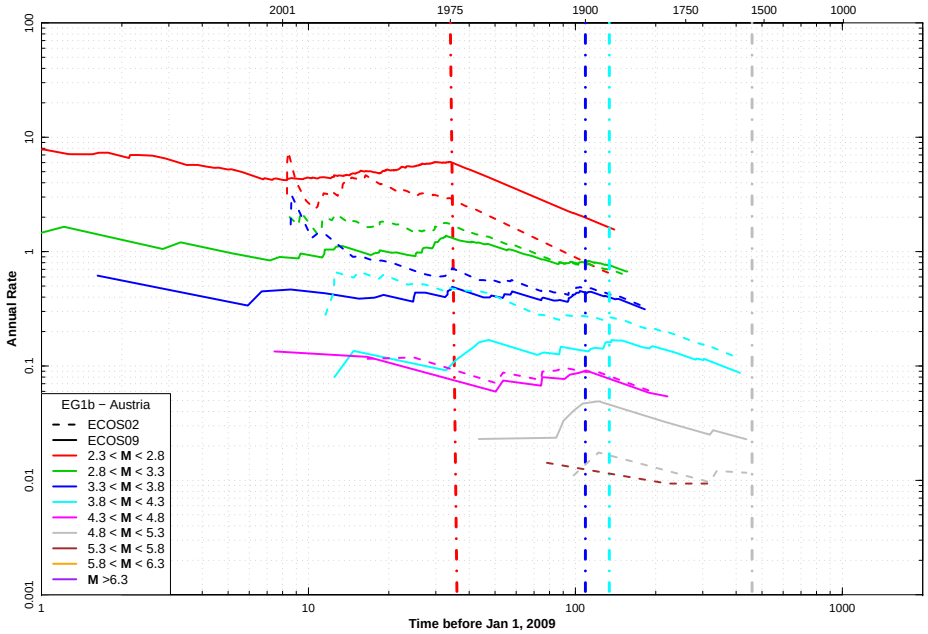

Figure 2.82: Stepp plots for EG1b Austria (A-W)completeness region using magnitude intervals defined for ECOS-02 catalog.

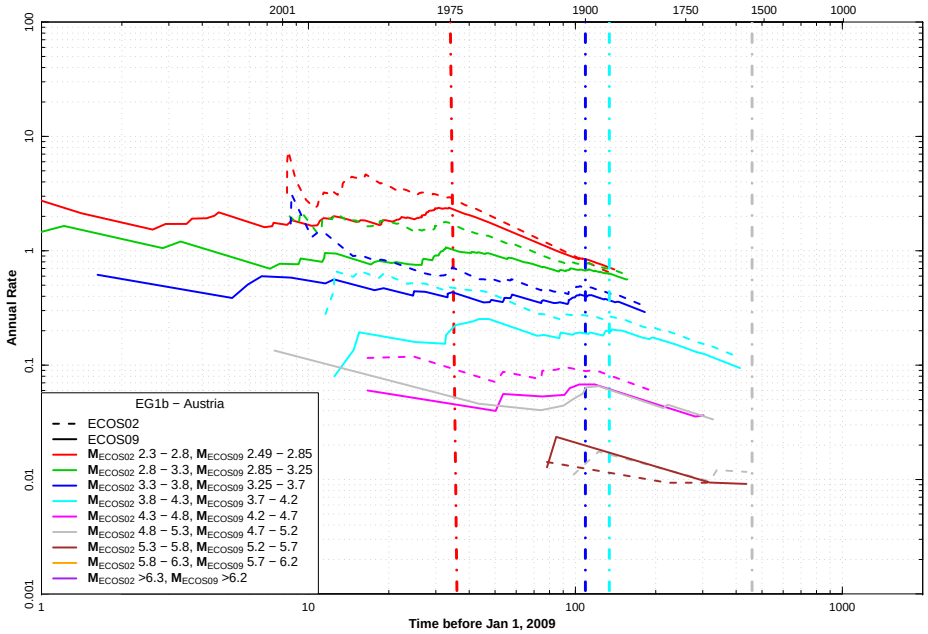

Figure 2.83: Stepp plots for EG1b Austria (A-W) completeness region using ECOS-02 magnitude intervals for ECOS-02 catalog and magnitude intervals adjusted by Equation 2.11 for ECOS-09 catalog.

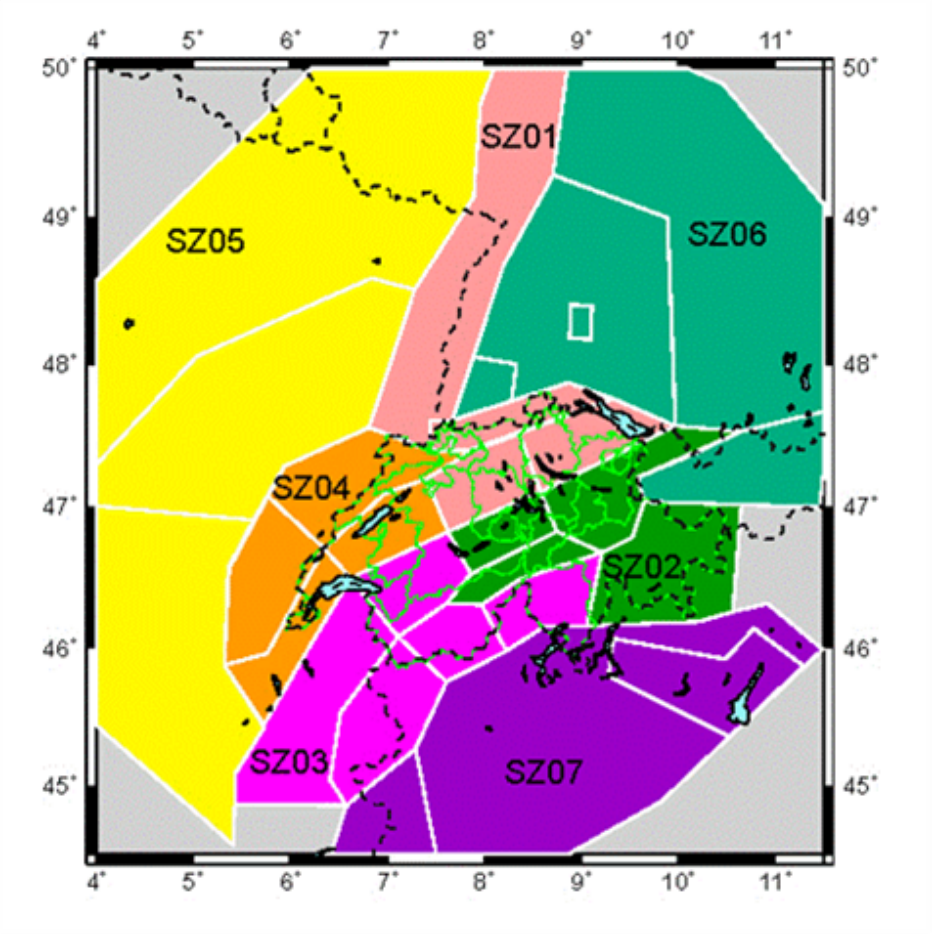

Figure 2.84: Catalog completeness regions defined by Expert Team EG1c.

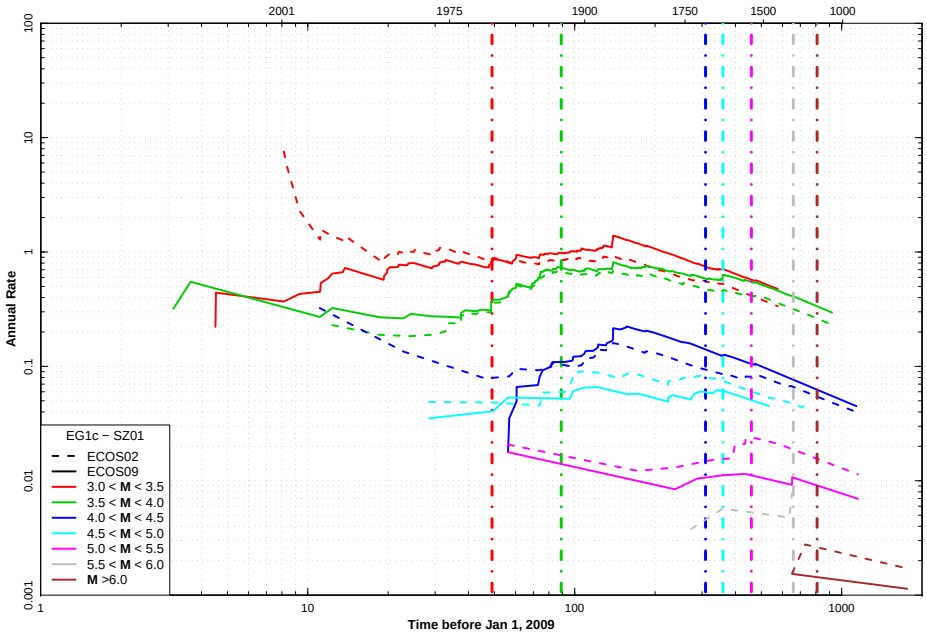

Figure 2.85: Stepp plots for EG1c SZ01 completeness region using magnitude intervals defined for ECOS-02 catalog.

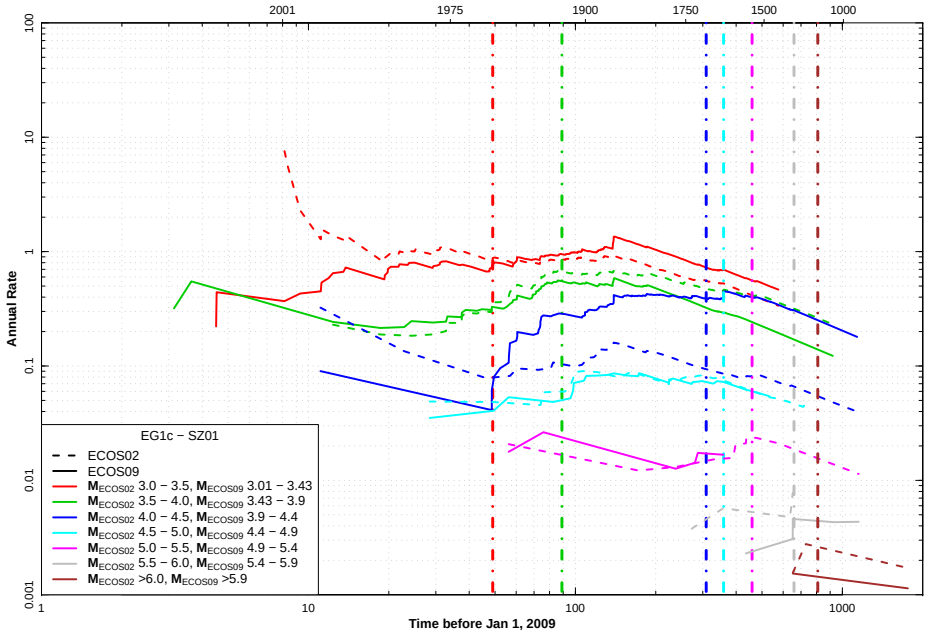

Figure 2.86: Stepp plots for EG1c SZ01 completeness region using ECOS-02 magnitude intervals for ECOS-02 catalog and magnitude intervals adjusted by Equation 2.11 for ECOS-09 catalog.

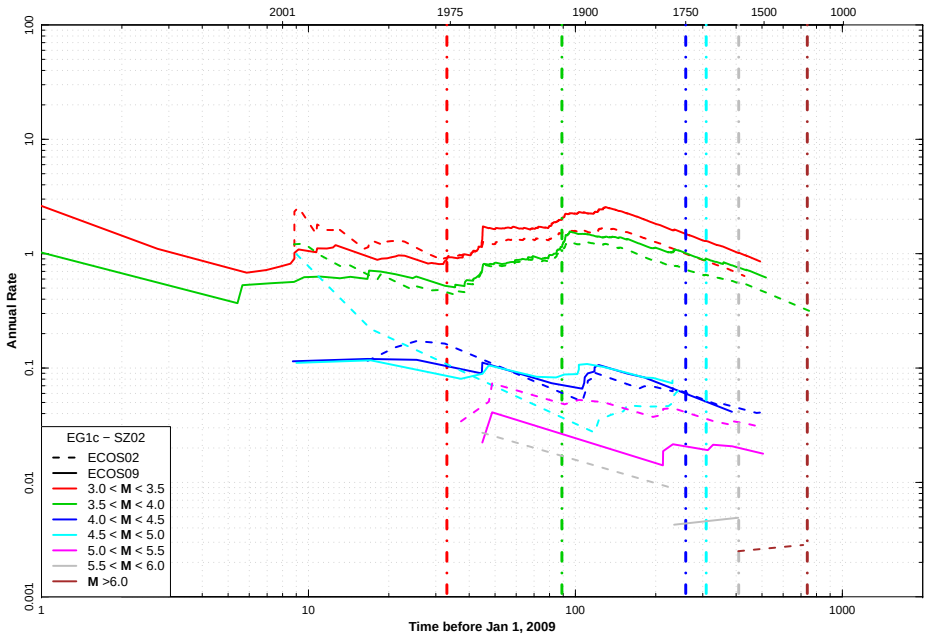

Figure 2.87: Stepp plots for EG1c SZ02 completeness region using magnitude intervals defined for ECOS-02 catalog.

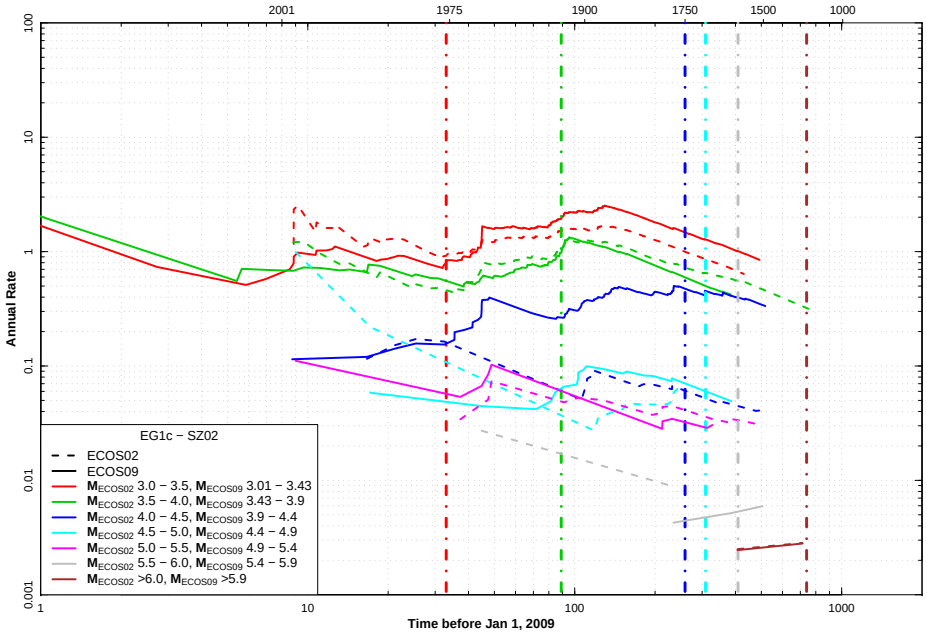

Figure 2.88: Stepp plots for EG1c SZ02 completeness region using ECOS-02 magnitude intervals for ECOS-02 catalog and magnitude intervals adjusted by Equation 2.11 for ECOS-09 catalog.

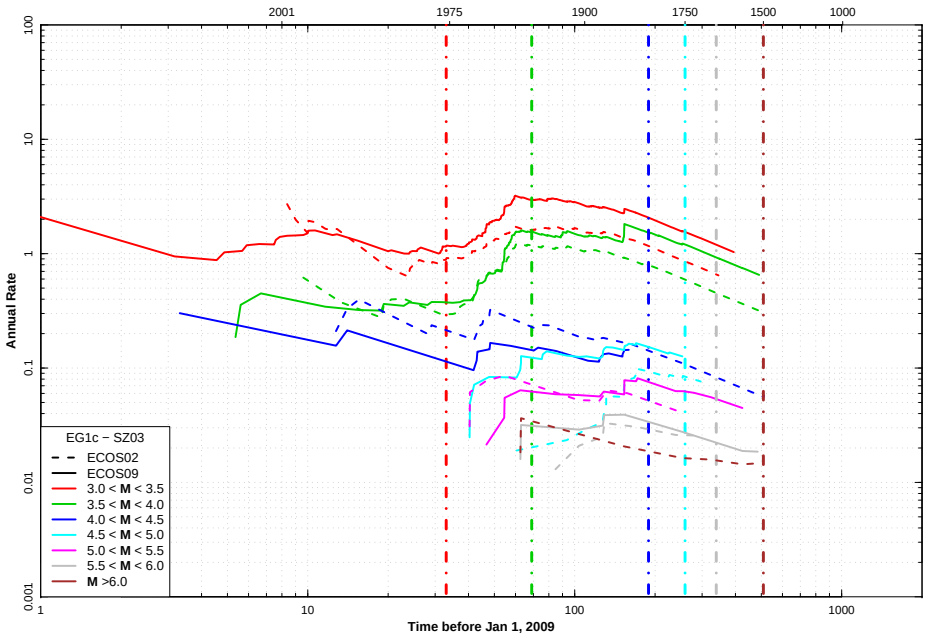

Figure 2.89: Stepp plots for EG1c SZ03 completeness region using magnitude intervals defined for ECOS-02 catalog.

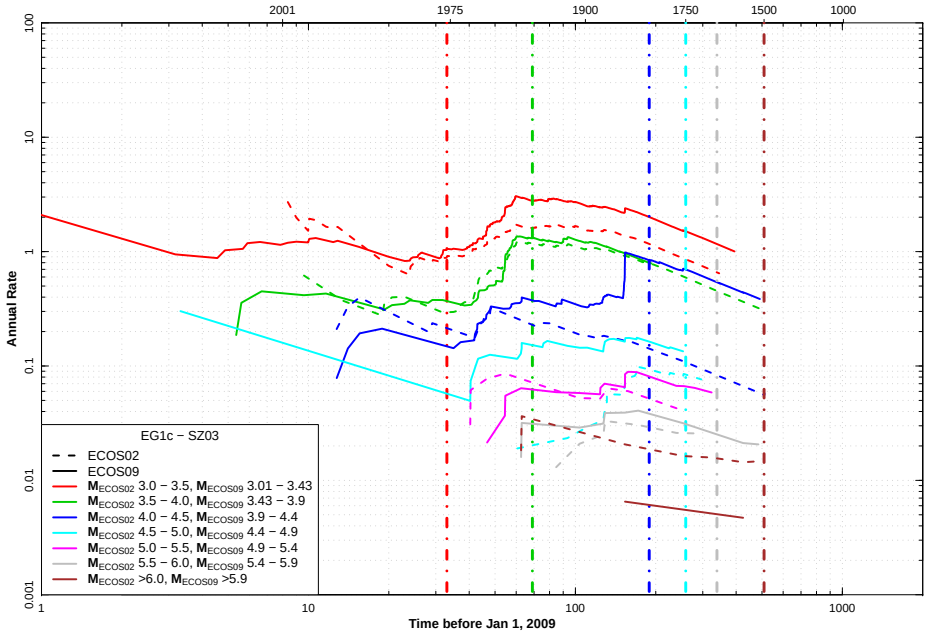

Figure 2.90: Stepp plots for EG1c SZ03 completeness region using ECOS-02 magnitude intervals for ECOS-02 catalog and magnitude intervals adjusted by Equation 2.11 for ECOS-09 catalog.

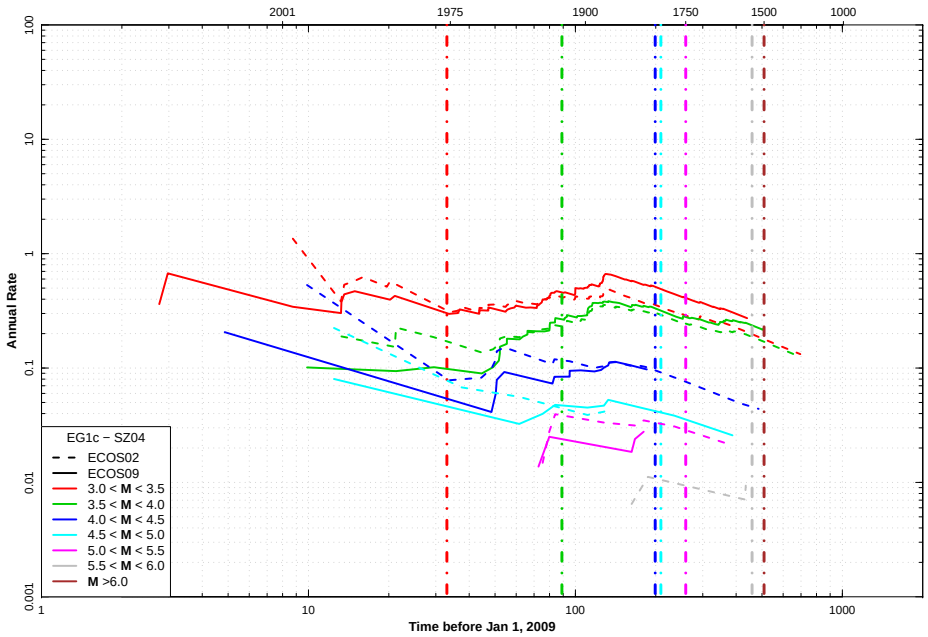

Figure 2.91: Stepp plots for EG1c SZ04 completeness region using magnitude intervals defined for ECOS-02 catalog.

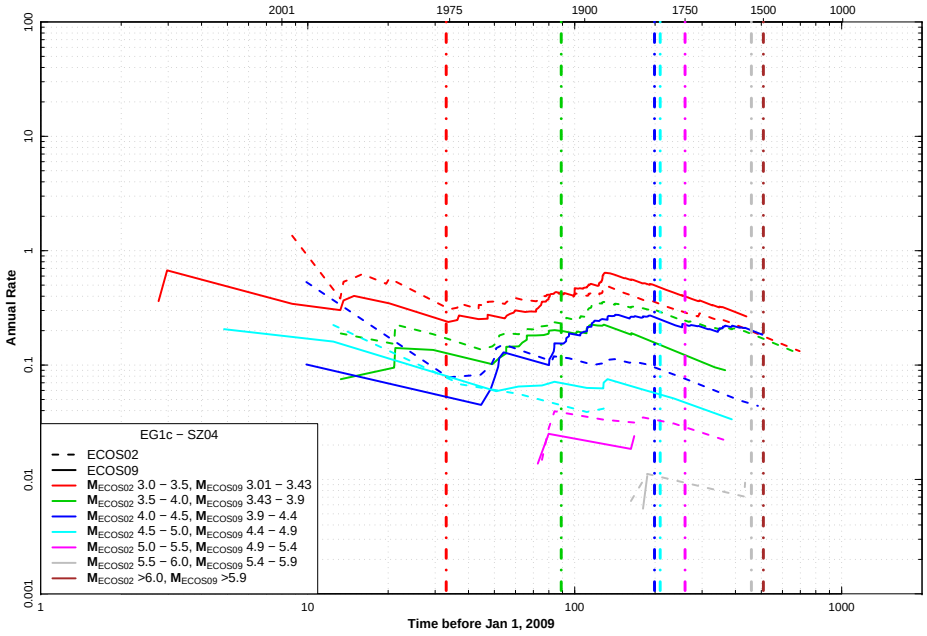

Figure 2.92: Stepp plots for EG1c SZ04 completeness region using ECOS-02 magnitude intervals for ECOS-02 catalog and magnitude intervals adjusted by Equation 2.11 for ECOS-09 catalog.

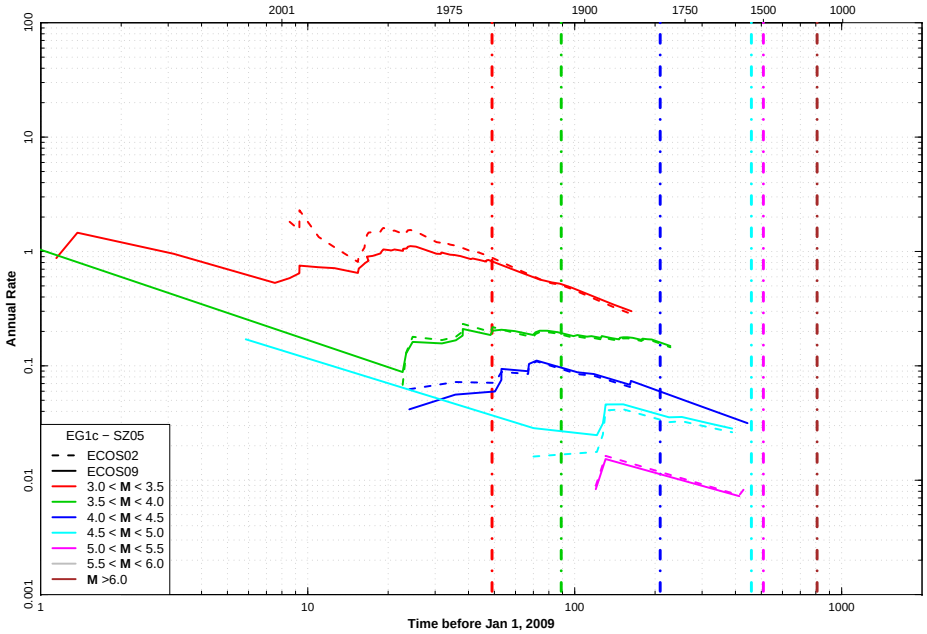

Figure 2.93: Stepp plots for EG1c SZ05 completeness region using magnitude intervals defined for ECOS-02 catalog.

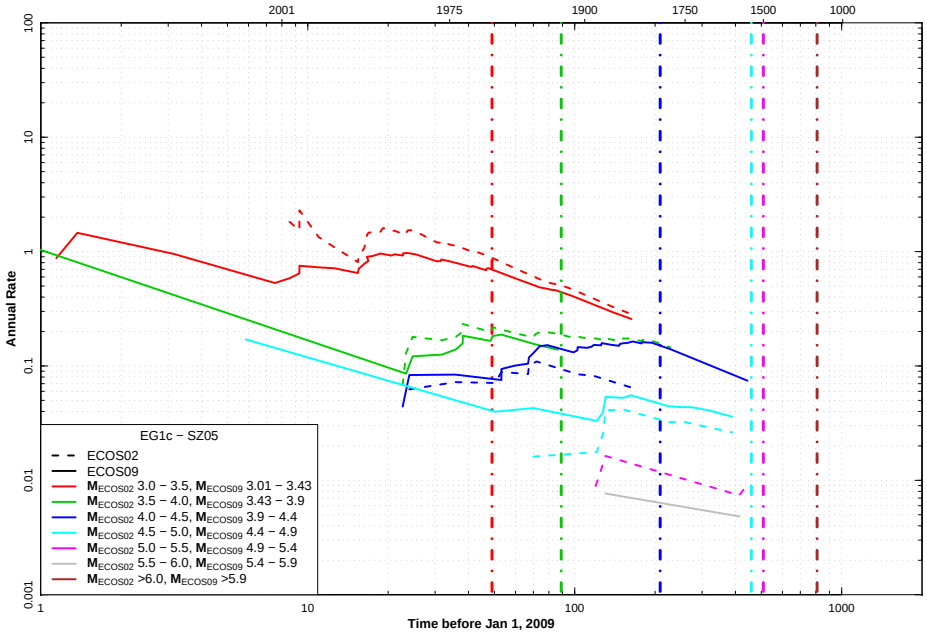

Figure 2.94: Stepp plots for EG1c SZ05 completeness region using ECOS-02 magnitude intervals for ECOS-02 catalog and magnitude intervals adjusted by Equation 2.11 for ECOS-09 catalog.

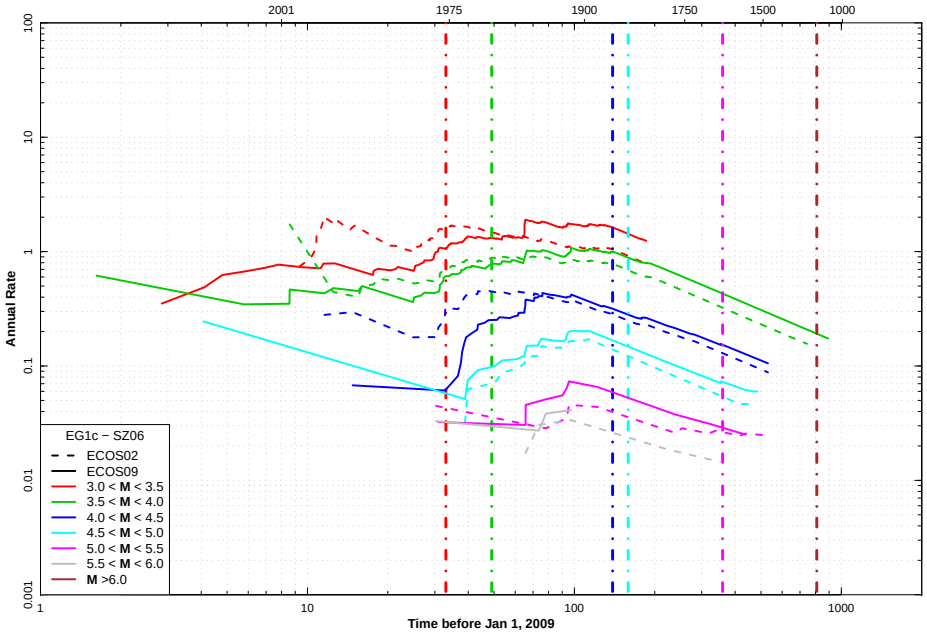

Figure 2.95: Stepp plots for EG1c SZ06 completeness region using magnitude intervals defined for ECOS-02 catalog.

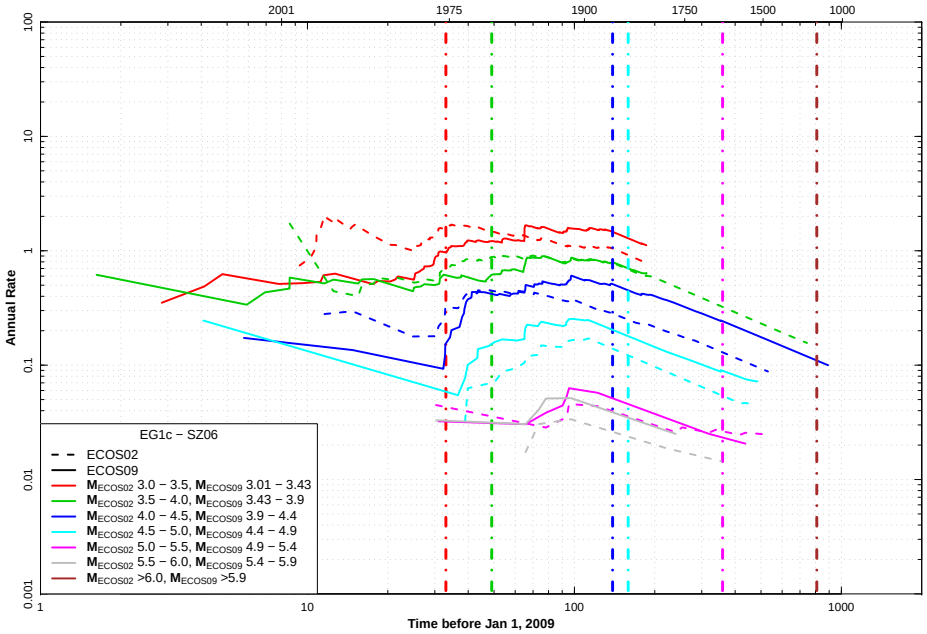

Figure 2.96: Stepp plots for EG1c SZ06 completeness region using ECOS-02 magnitude intervals for ECOS-02 catalog and magnitude intervals adjusted by Equation 2.11 for ECOS-09 catalog.

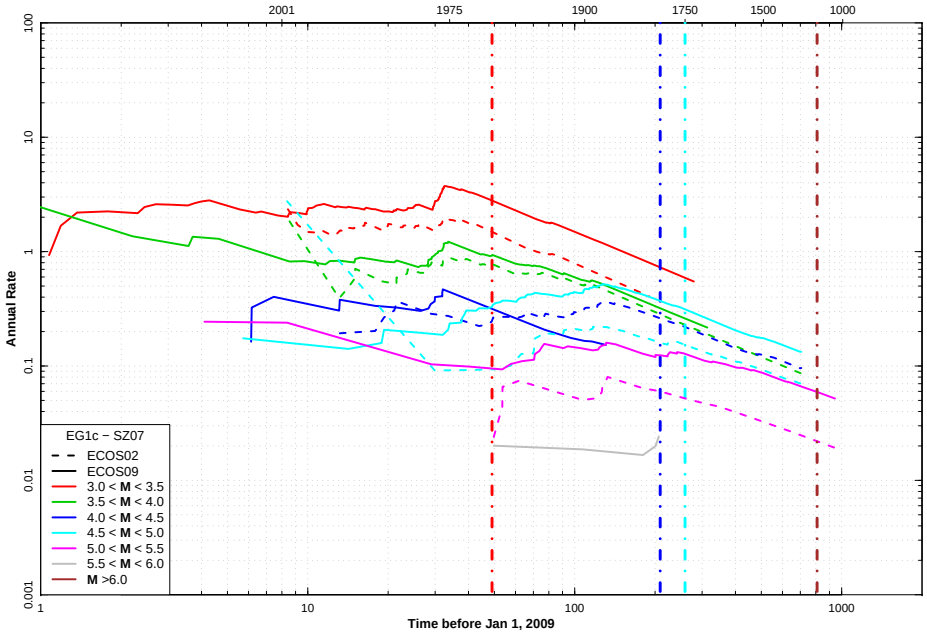

Figure 2.97: Stepp plots for EG1c SZ07 completeness region using magnitude intervals defined for ECOS-02 catalog.

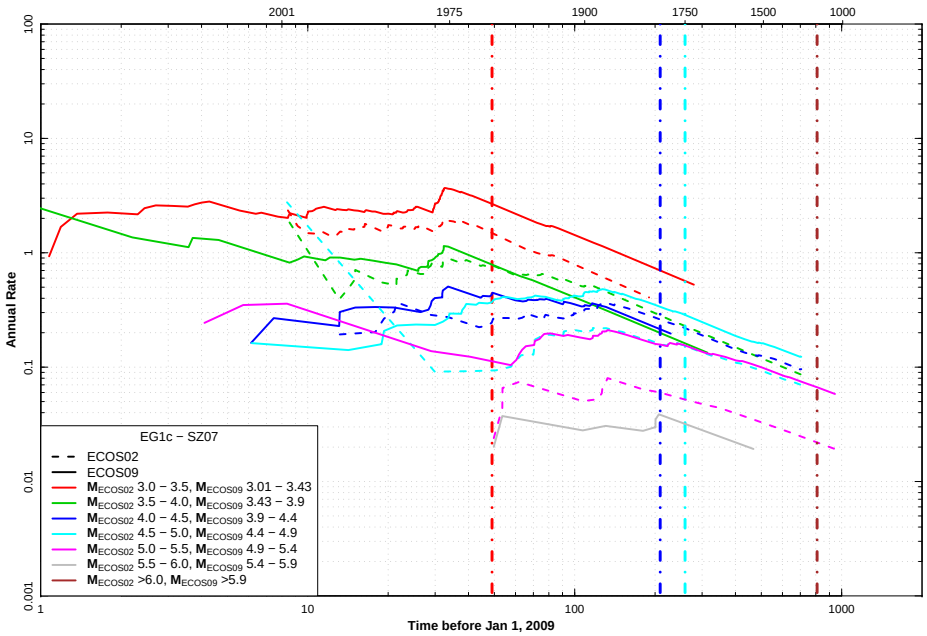

Figure 2.98: Stepp plots for EG1c SZ07 completeness region using ECOS-02 magnitude intervals for ECOS-02 catalog and magnitude intervals adjusted by Equation 2.11 for ECOS-09 catalog.

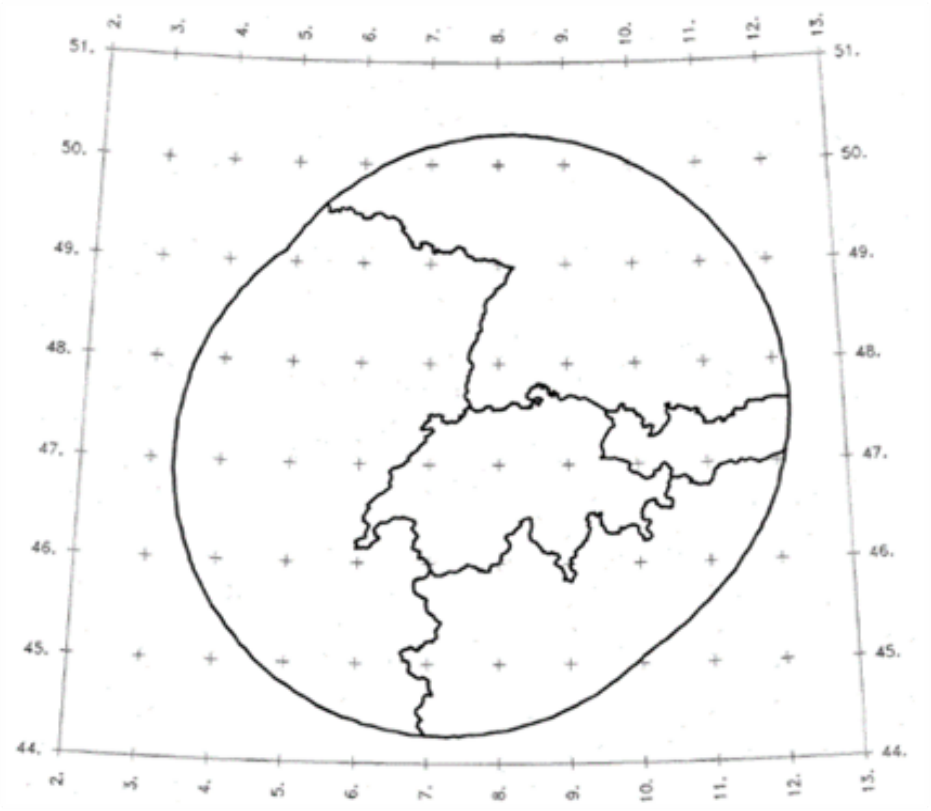

Figure 2.99: Catalog completeness regions defined by Expert Team EG1d.

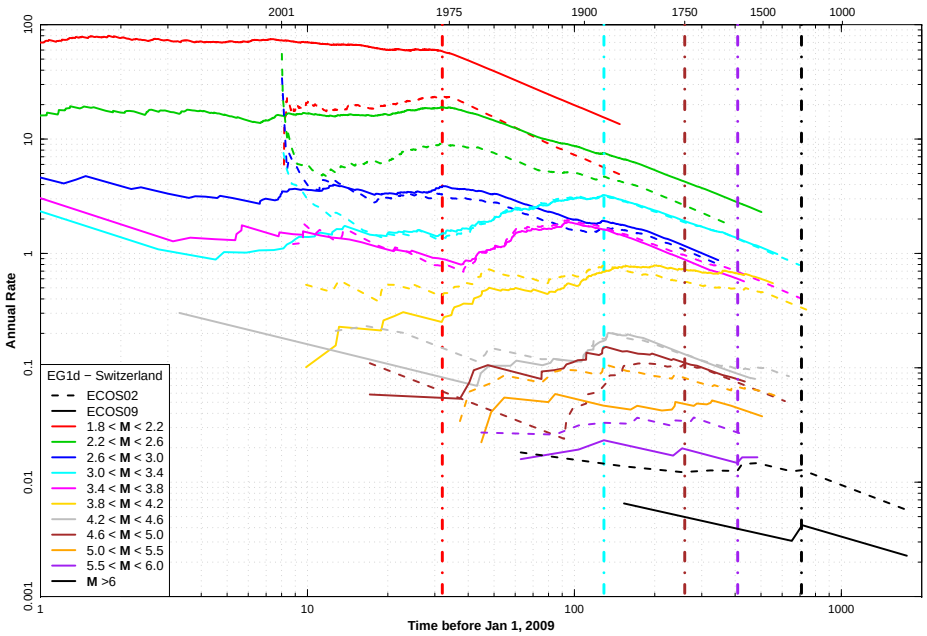

Figure 2.100: Stepp plots for EG1d Switzerland completeness region using magnitude intervals defined for ECOS-02 catalog.

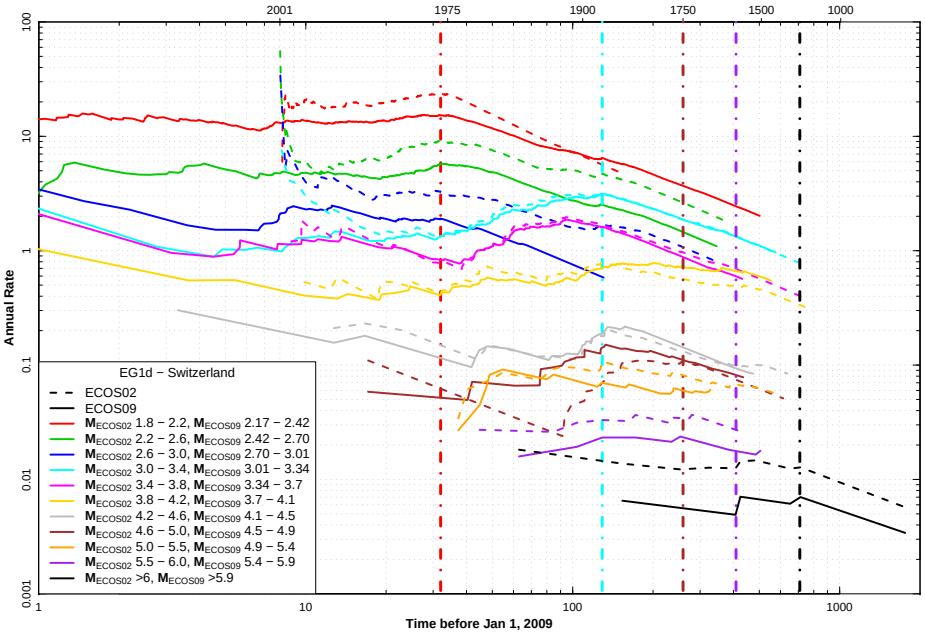

Figure 2.101: Stepp plots for EG1d Switzerland completeness region using ECOS-02 magnitude intervals for ECOS-02 catalog and magnitude intervals adjusted by Equation 2.11 for ECOS-09 catalog.

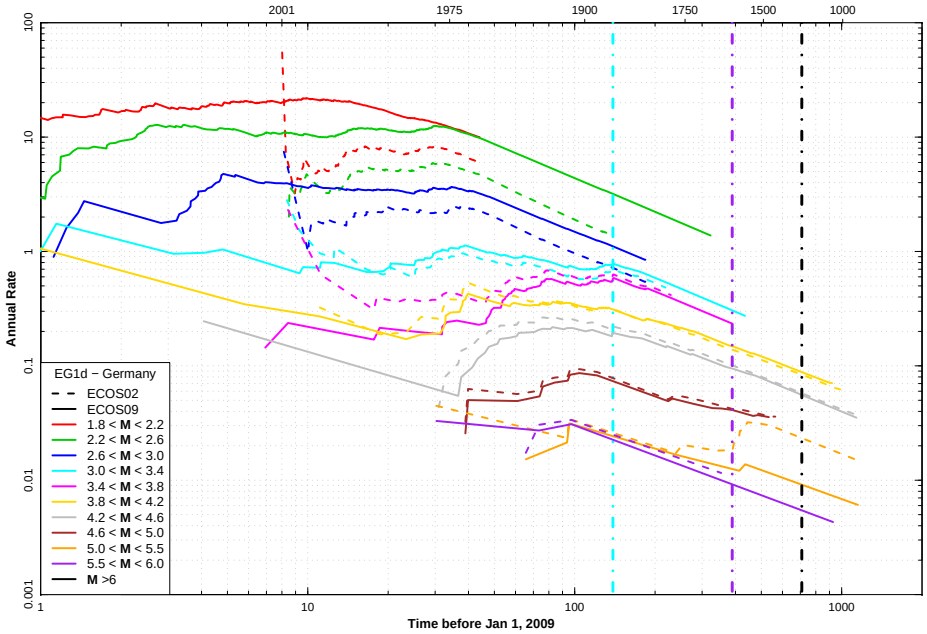

Figure 2.102: Stepp plots for EG1d Germany completeness region using magnitude intervals defined for ECOS-02 catalog.

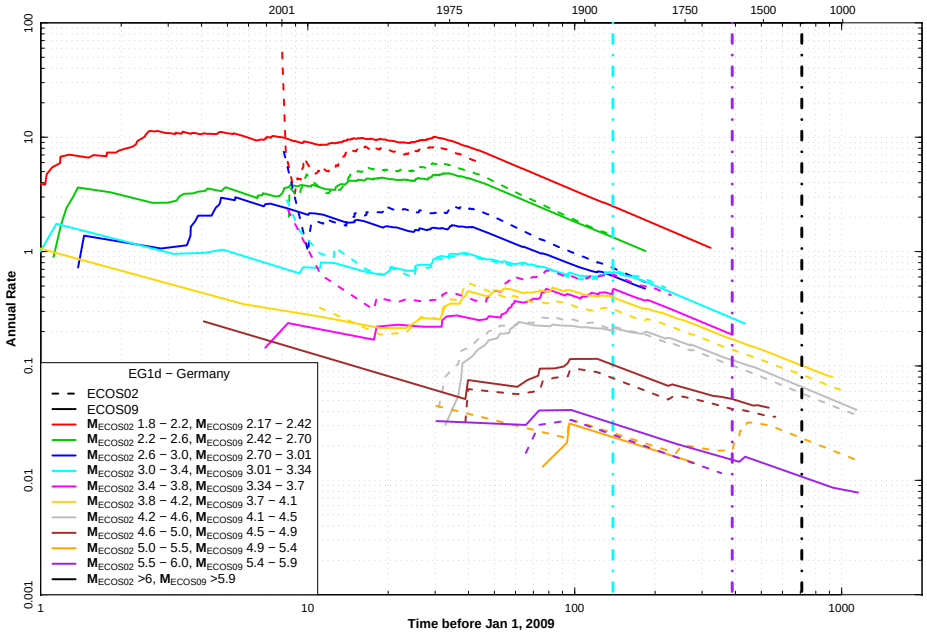

Figure 2.103: Stepp plots for EG1d Germany completeness region using ECOS-02 magnitude intervals for ECOS-02 catalog and magnitude intervals adjusted by Equation 2.11 for ECOS-09 catalog.

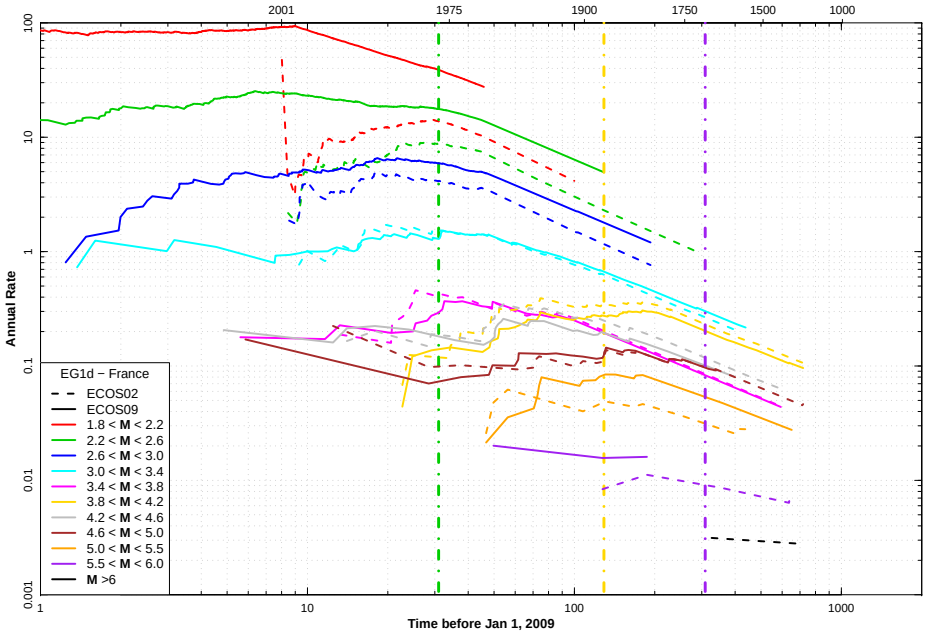

Figure 2.104: Stepp plots for EG1d France completeness region using magnitude intervals defined for ECOS-02 catalog.

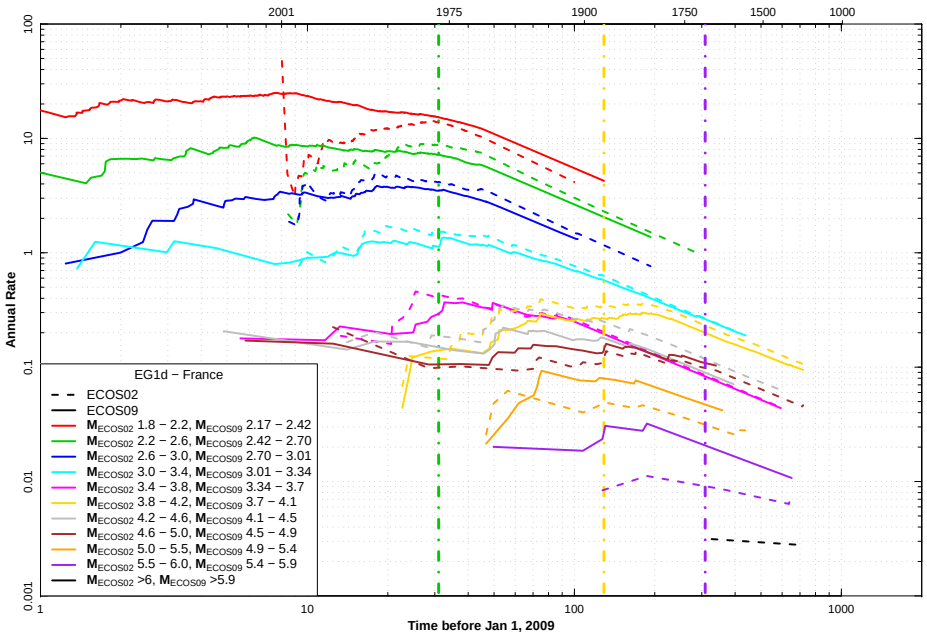

Figure 2.105: Stepp plots for EG1d France completeness region using ECOS-02 magnitude intervals for ECOS-02 catalog and magnitude intervals adjusted by Equation 2.11 for ECOS-09 catalog.

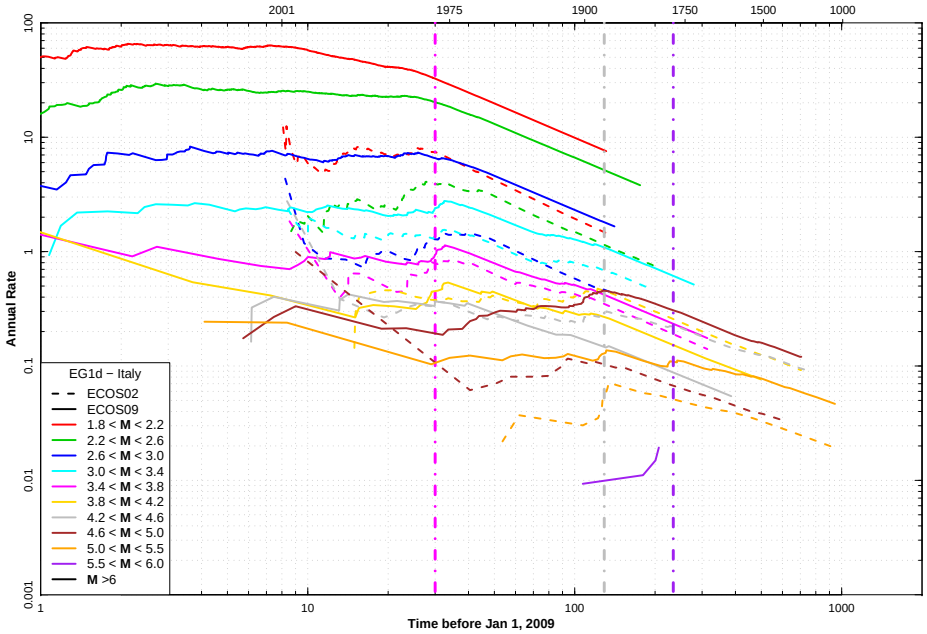

Figure 2.106: Stepp plots for EG1d Italy completeness region using magnitude intervals defined for ECOS-02 catalog.

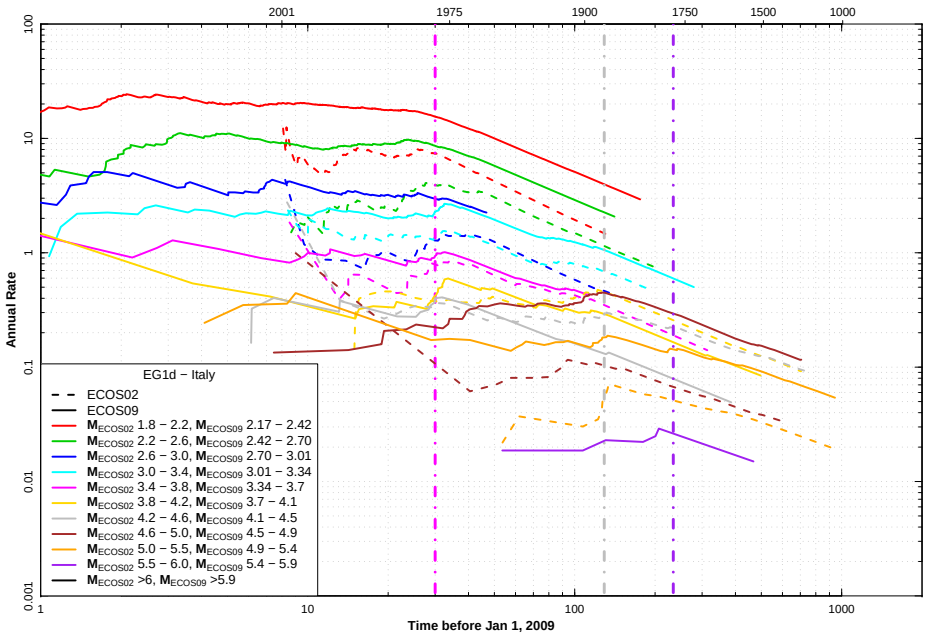

Figure 2.107: Stepp plots for EG1d Italy completeness region using ECOS-02 magnitude intervals for ECOS-02 catalog and magnitude intervals adjusted by Equation 2.11 for ECOS-09 catalog.

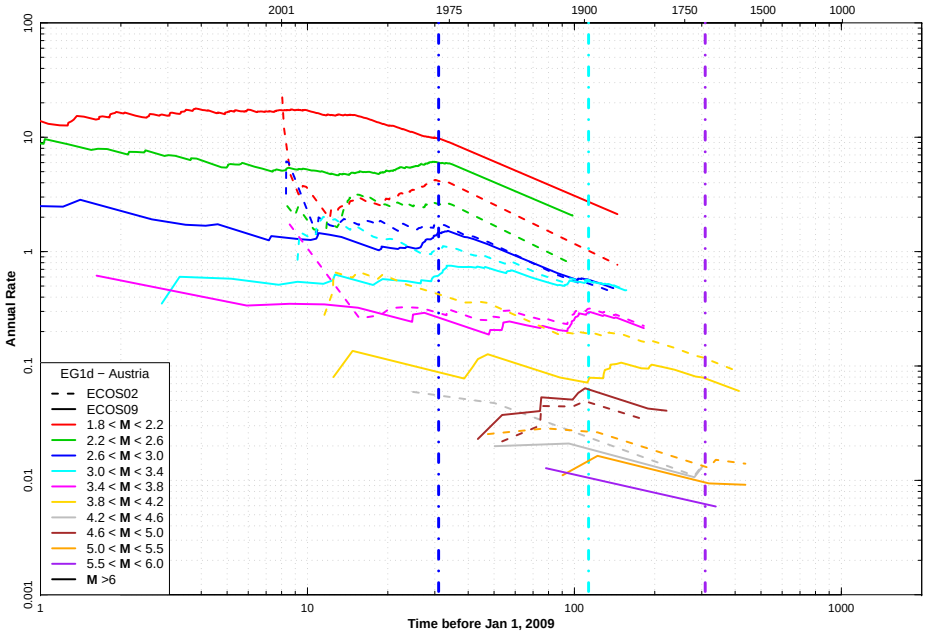

Figure 2.108: Stepp plots for EG1d Austria completeness region using magnitude intervals defined for ECOS-02 catalog.

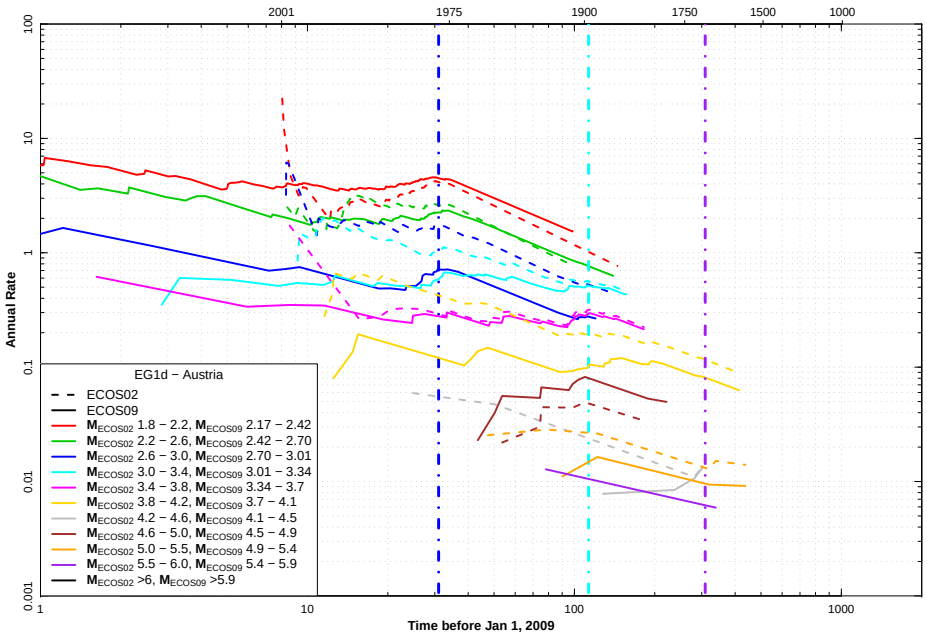

Figure 2.109: Stepp plots for EG1d Austria completeness region using ECOS-02 magnitude intervals for ECOS-02 catalog and magnitude intervals adjusted by Equation 2.11 for ECOS-09 catalog.

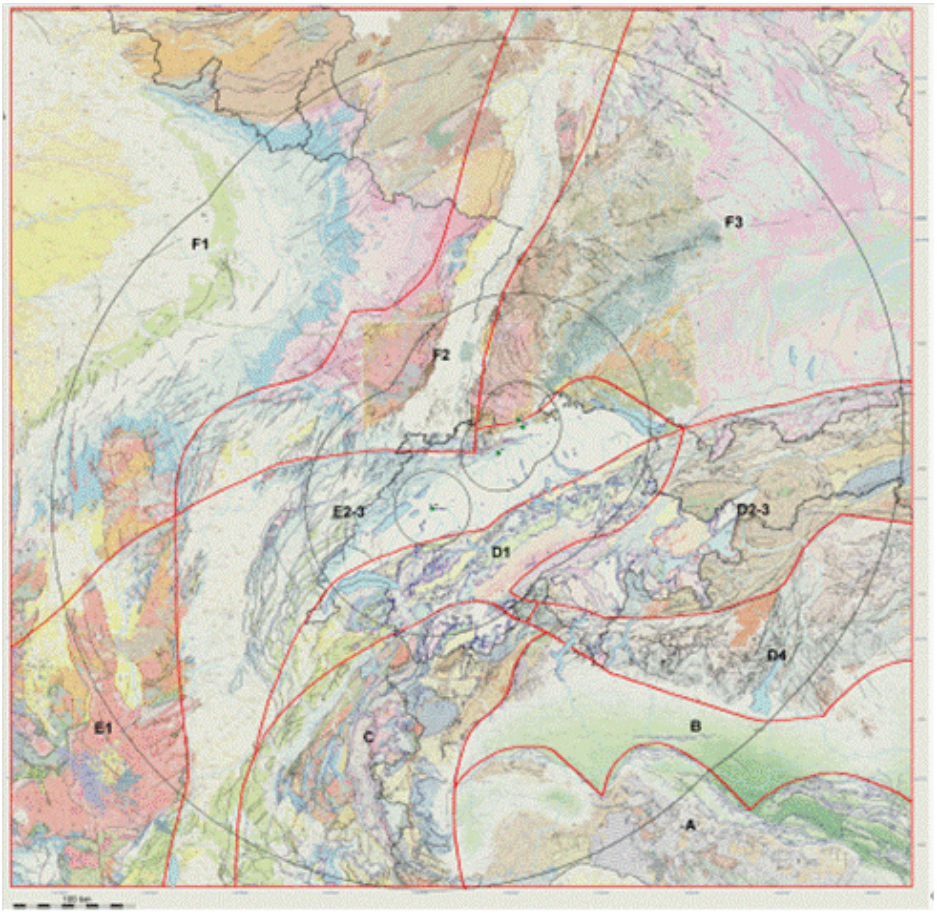

Figure 2.110: Macro-zones defined by EG1a.

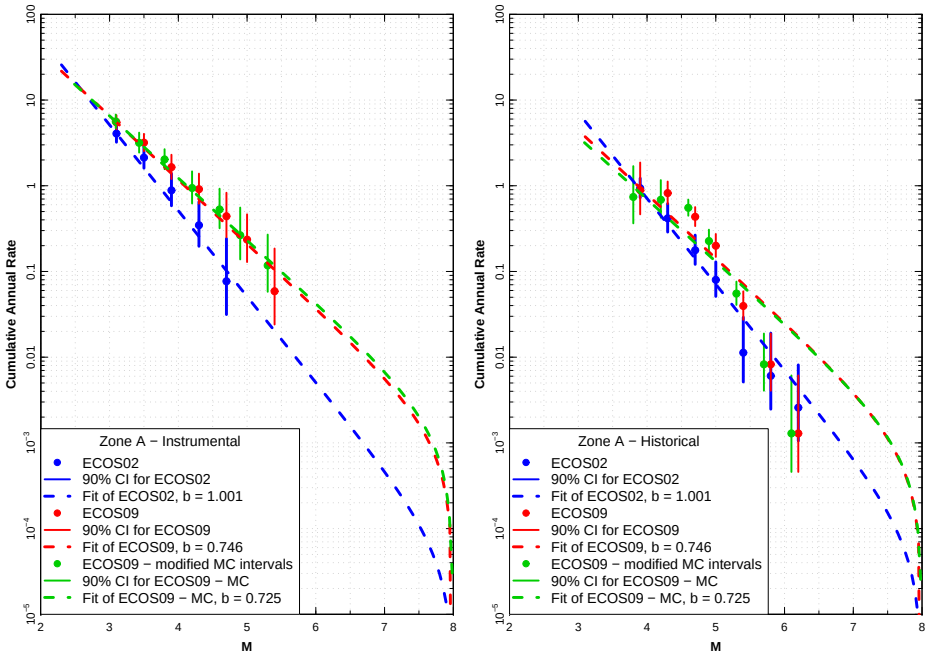

Figure 2.111: Seismicity data and earthquake recurrence rates for EG1a macro-zone A Left instrumental period, right historical period.

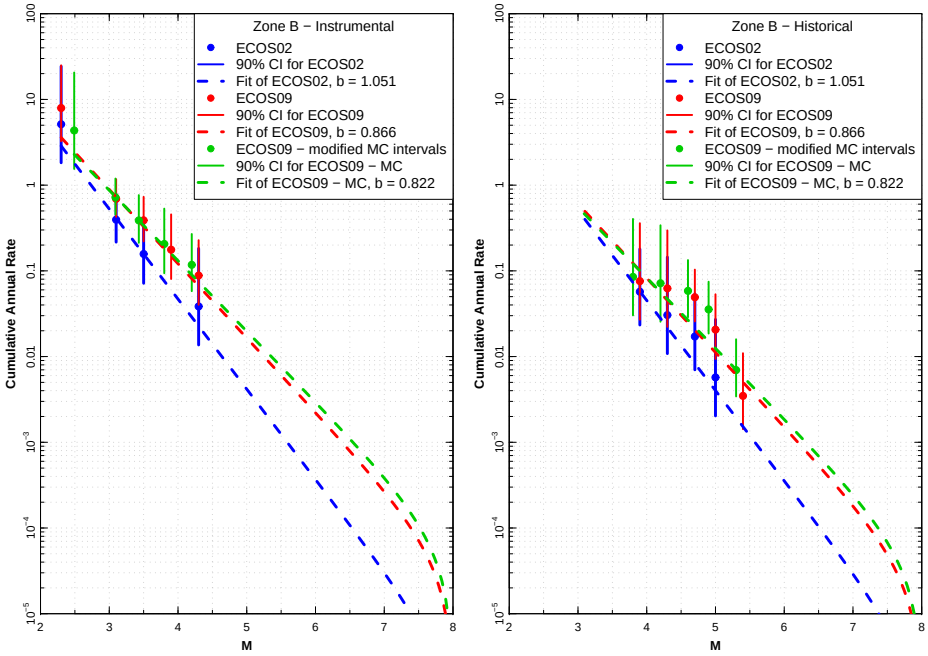

Figure 2.112: Seismicity data and earthquake recurrence rates for EG1a macro-zone B Left instrumental period, right historical period.

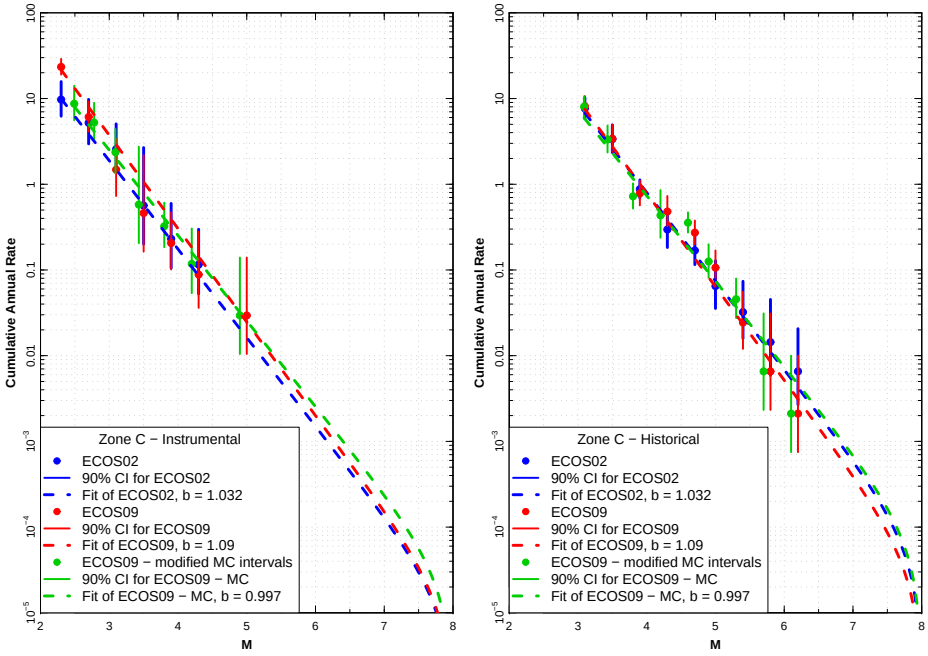

Figure 2.113: Seismicity data and earthquake recurrence rates for EG1a macro-zone C Left instrumental period, right historical period.

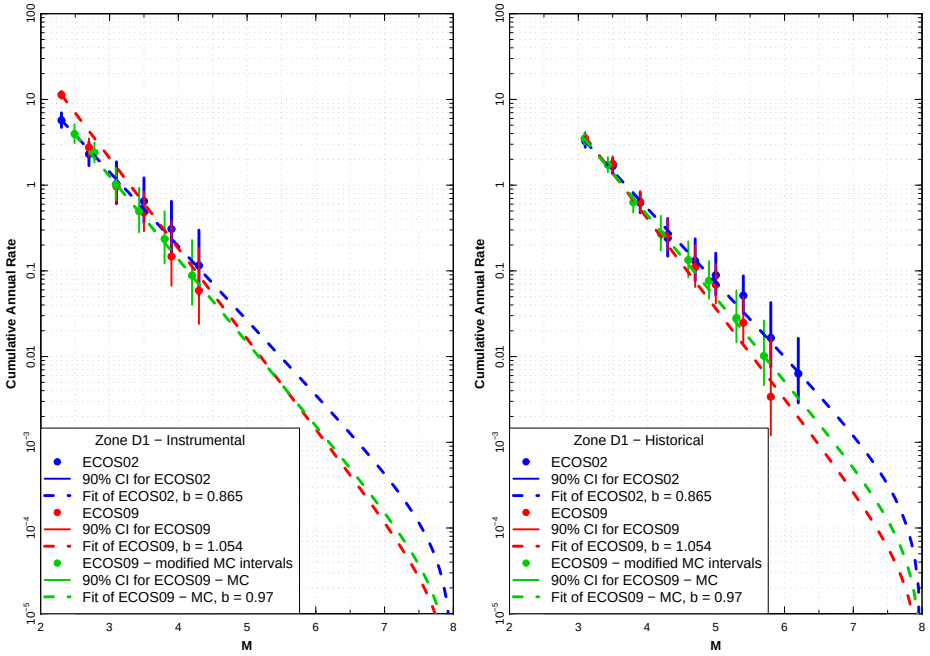

Figure 2.114: Seismicity data and earthquake recurrence rates for EG1a macro-zone D1 Left instrumental period, right historical period.

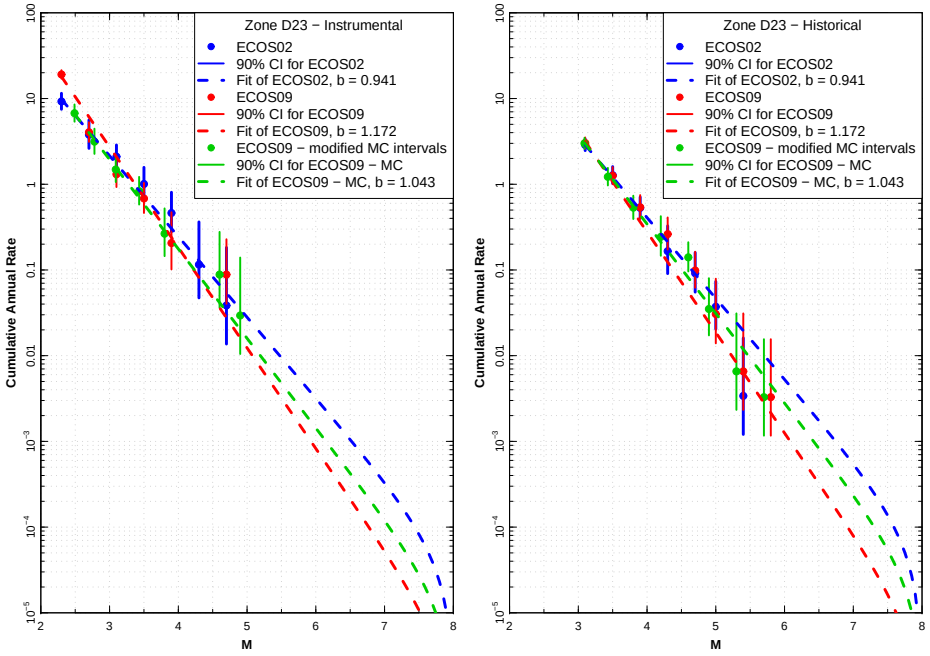

Figure 2.115: Seismicity data and earthquake recurrence rates for EG1a macro-zone D23 Left instrumental period, right historical period.

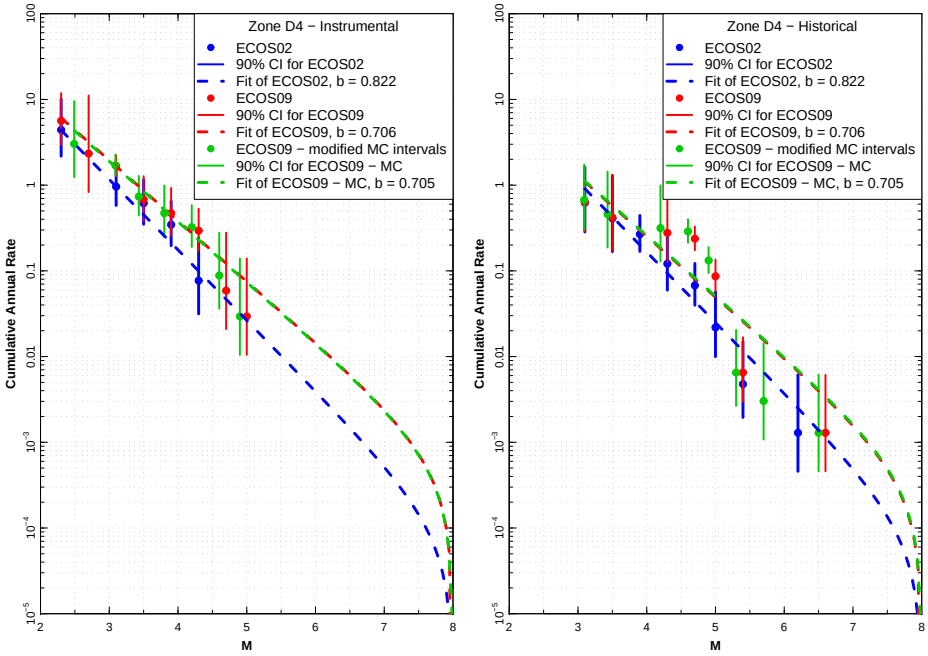

Figure 2.116: Seismicity data and earthquake recurrence rates for EG1a macro-zone D4 Left instrumental period, right historical period.

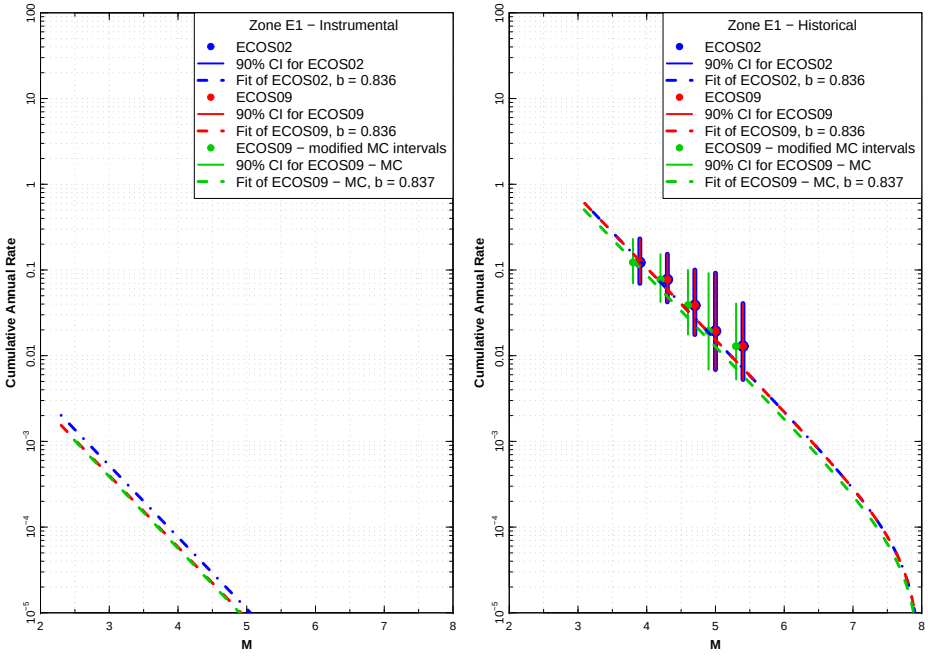

Figure 2.117: Seismicity data and earthquake recurrence rates for EG1a macro-zone E1 Left instrumental period, right historical period.

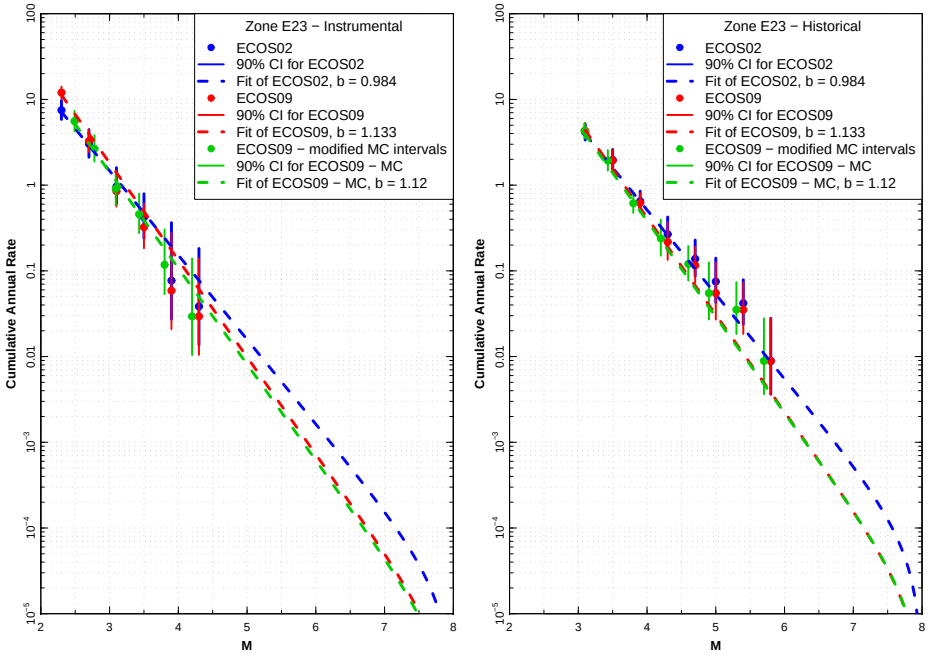

Figure 2.118: Seismicity data and earthquake recurrence rates for EG1a macro-zone E23 Left instrumental period, right historical period.

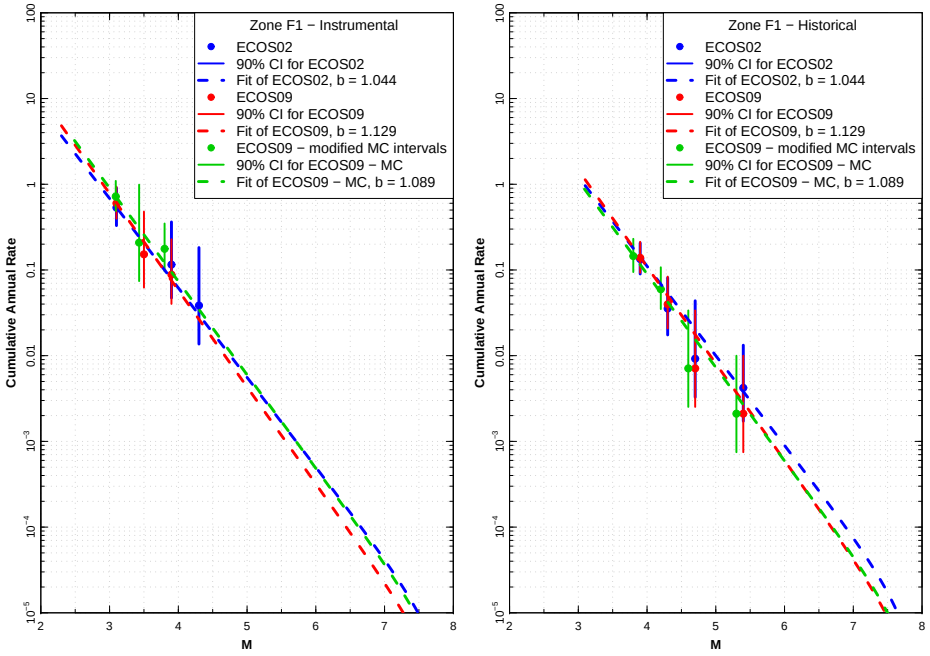

Figure 2.119: Seismicity data and earthquake recurrence rates for EG1a macro-zone F1 Left instrumental period, right historical period.

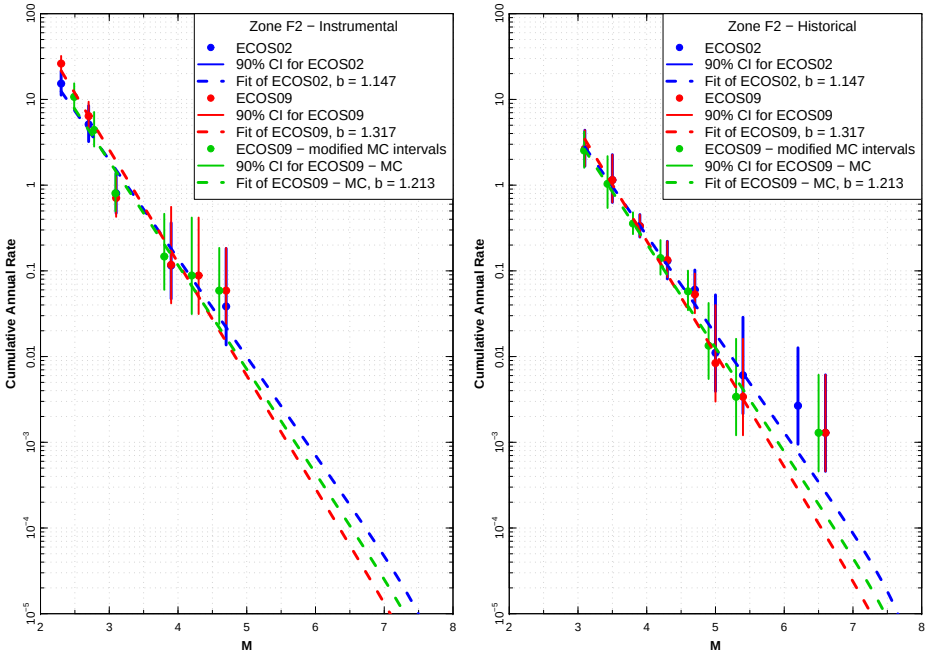

Figure 2.120: Seismicity data and earthquake recurrence rates for EG1a macro-zone F2 Left instrumental period, right historical period.

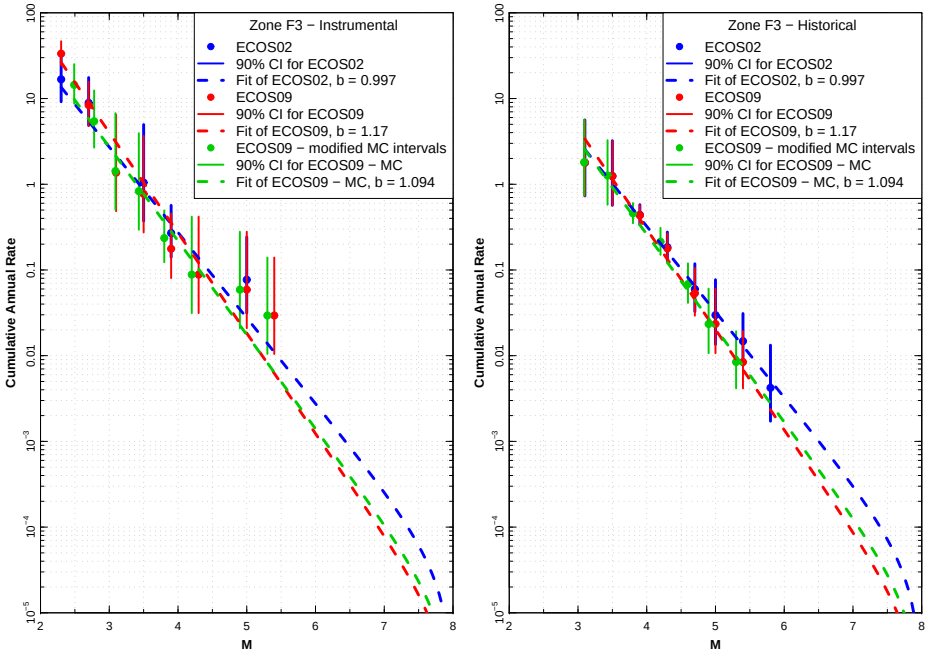

Figure 2.121: Seismicity data and earthquake recurrence rates for EG1a macro-zone F3 Left instrumental period, right historical period.

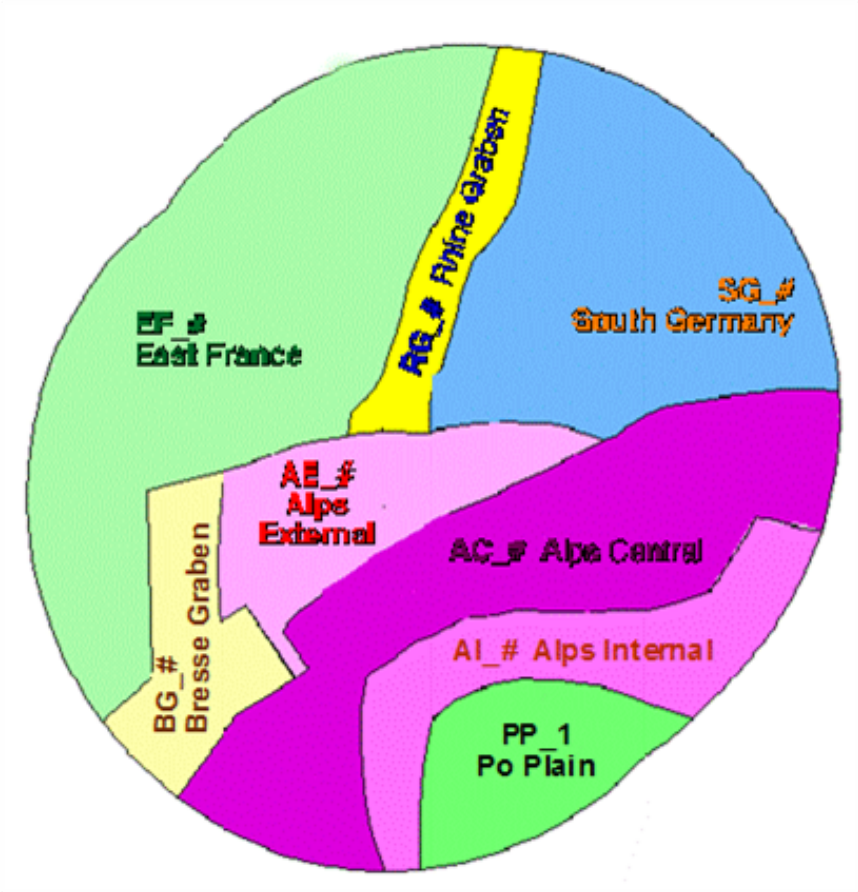

Figure 2.122: Large source zones defined by EG1b

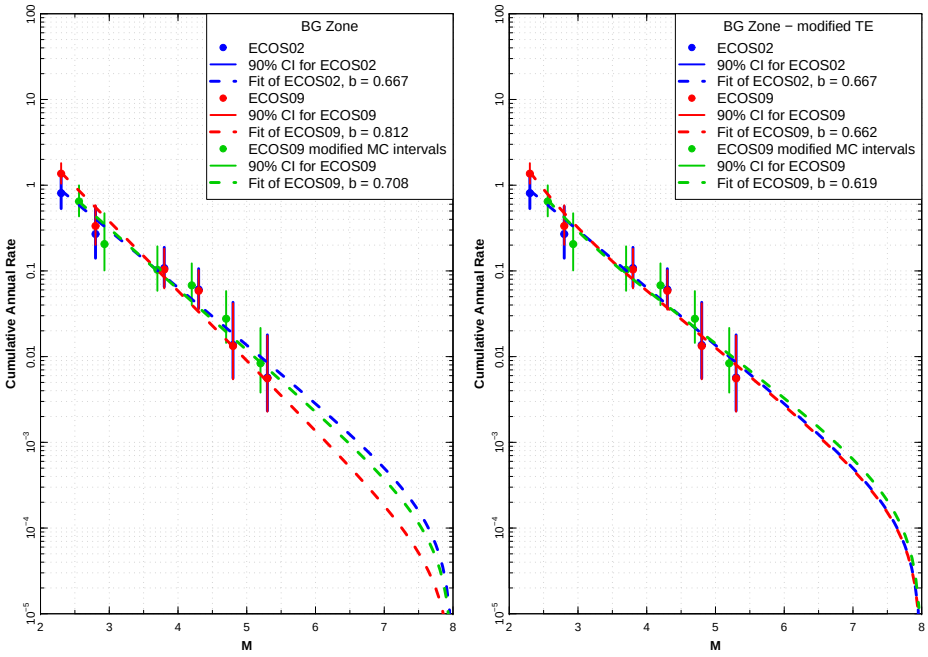

Figure 2.123: Seismicity data and earthquake recurrence rates for EG1b large zone BG Left standard truncated exponential applied to ECOS-09 catalog, Right – modified truncated exponential applied to ECOS-09 catalog.

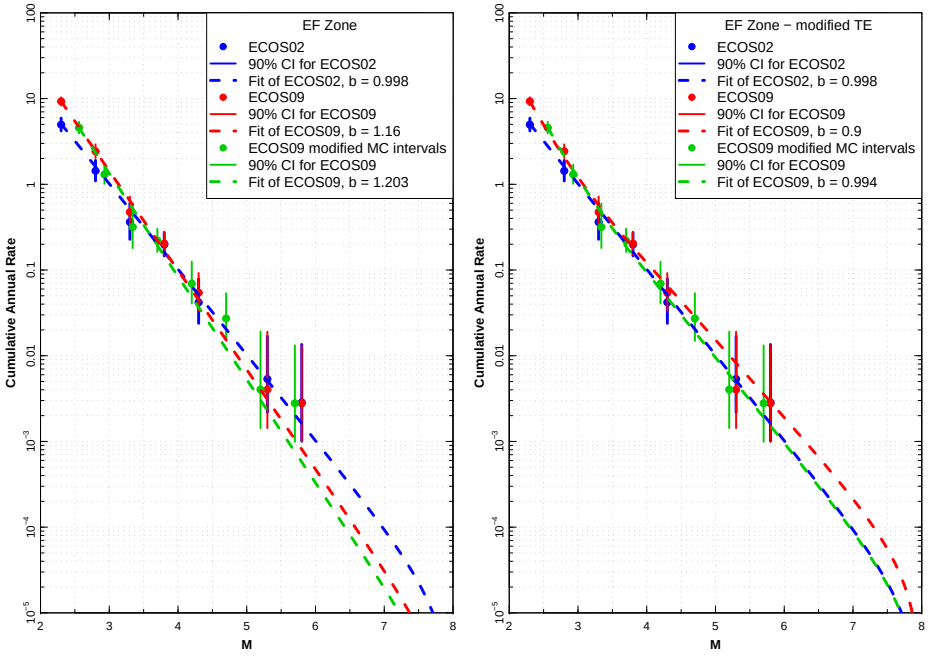

Figure 2.124: Seismicity data and earthquake recurrence rates for EG1b large zone EF Left standard truncated exponential applied to ECOS-09 catalog, Right – modified truncated exponential applied to ECOS-09 catalog.

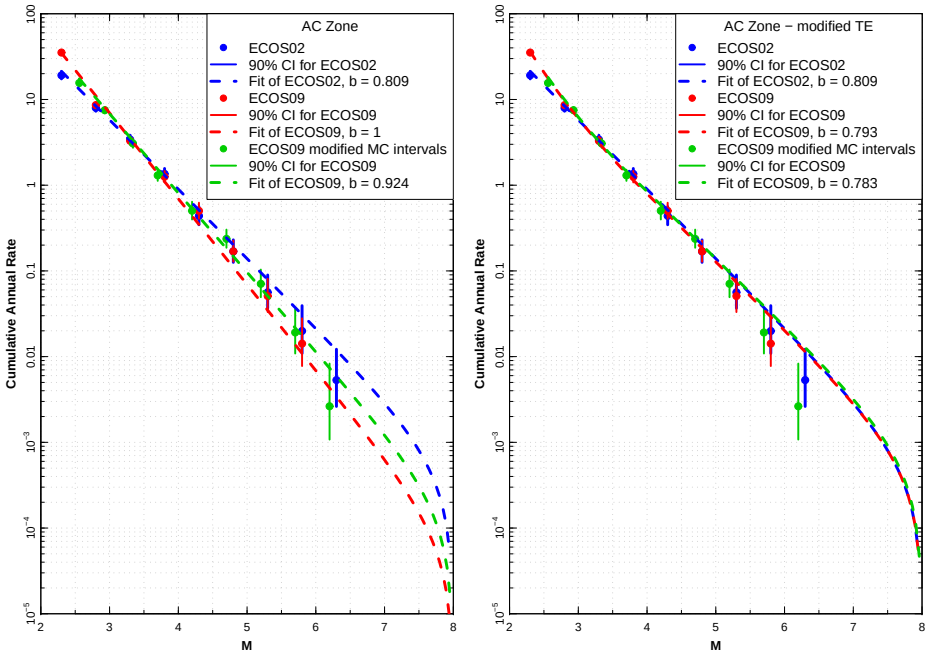

Figure 2.125: Seismicity data and earthquake recurrence rates for EG1b large zone AC Left standard truncated exponential applied to ECOS-09 catalog, Right – modified truncated exponential applied to ECOS-09 catalog.

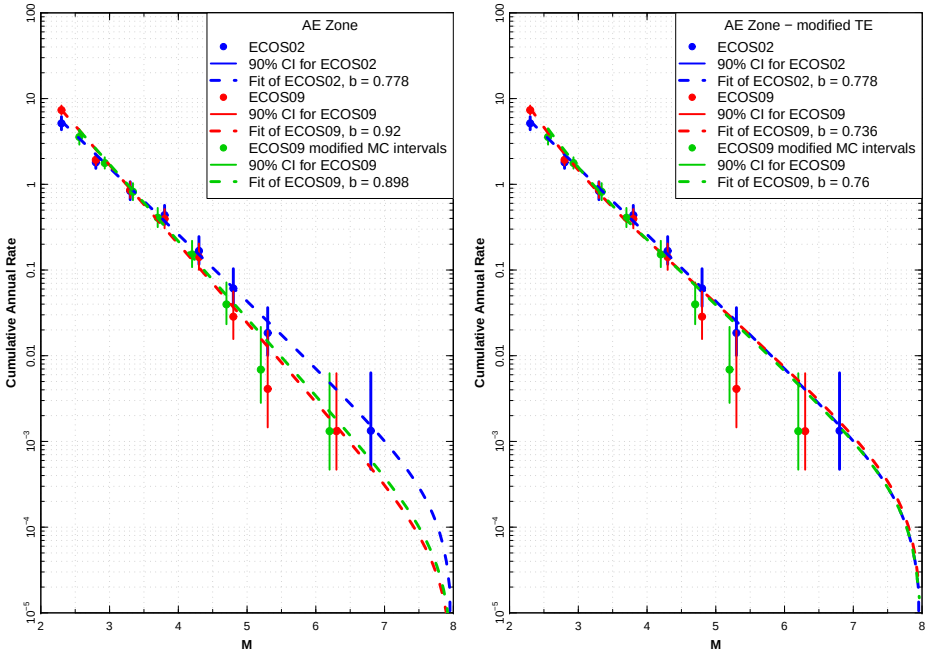

Figure 2.126: Seismicity data and earthquake recurrence rates for EG1b large zone AE Left standard truncated exponential applied to ECOS-09 catalog, Right – modified truncated exponential applied to ECOS-09 catalog.

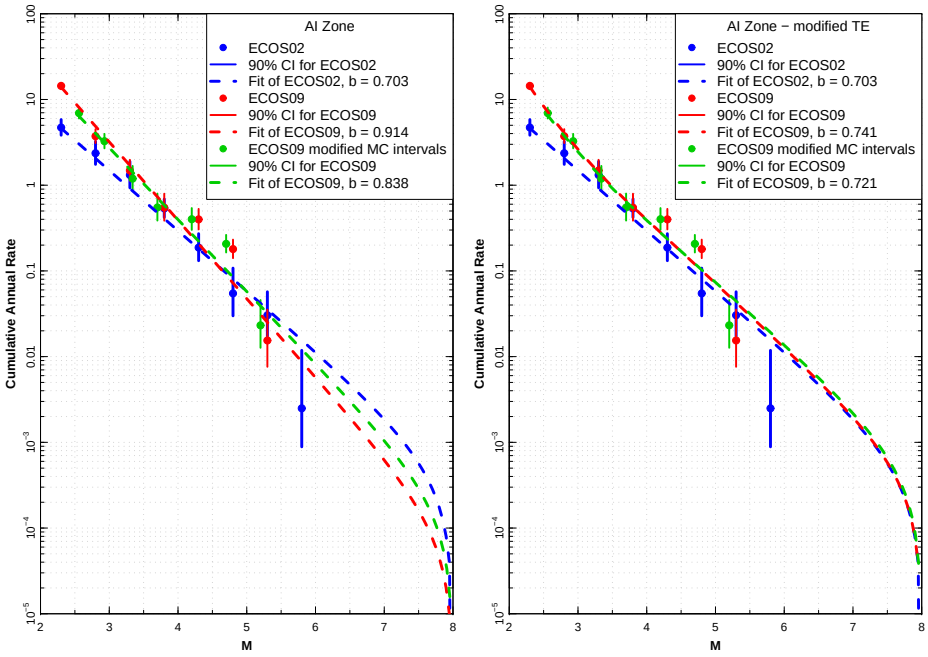

Figure 2.127: Seismicity data and earthquake recurrence rates for EG1b large zone AI Left standard truncated exponential applied to ECOS-09 catalog, Right – modified truncated exponential applied to ECOS-09 catalog.

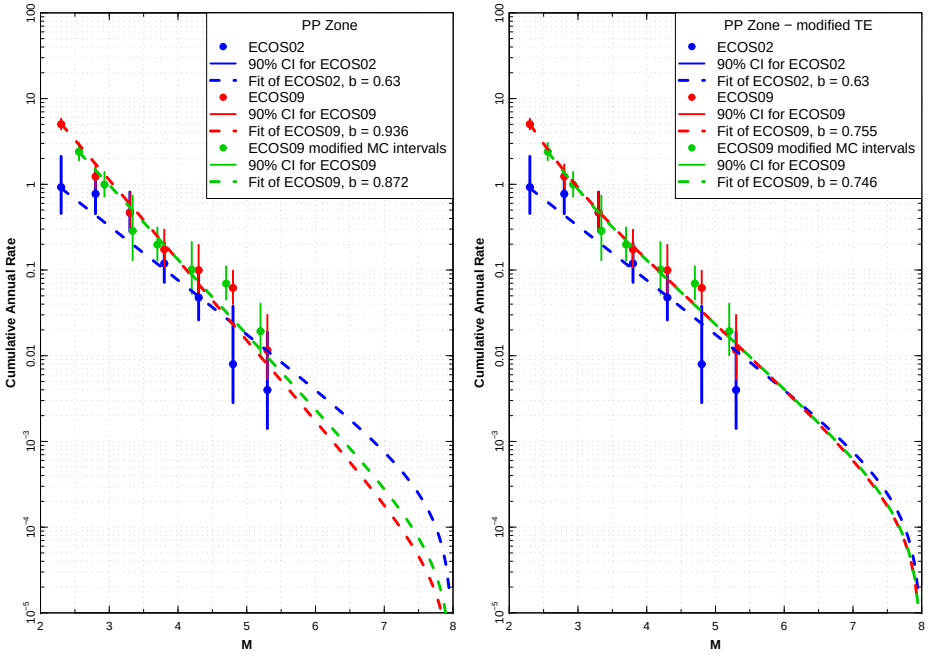

Figure 2.128: Seismicity data and earthquake recurrence rates for EG1b large zone PP Left standard truncated exponential applied to ECOS-09 catalog, Right – modified truncated exponential applied to ECOS-09 catalog.

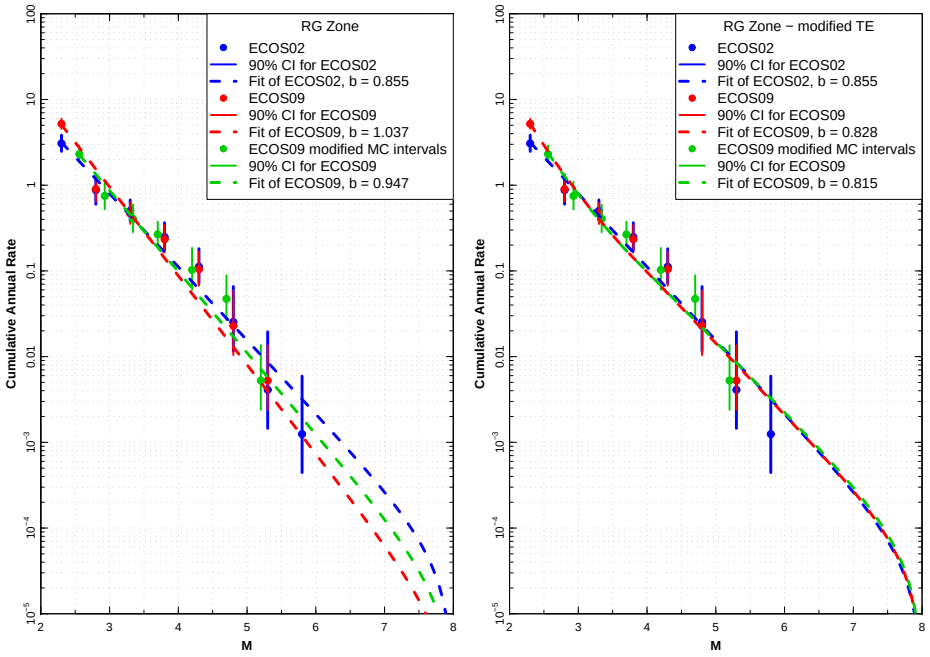

Figure 2.129: Seismicity data and earthquake recurrence rates for EG1b large zone RG Left standard truncated exponential applied to ECOS-09 catalog, Right – modified truncated exponential applied to ECOS-09 catalog.

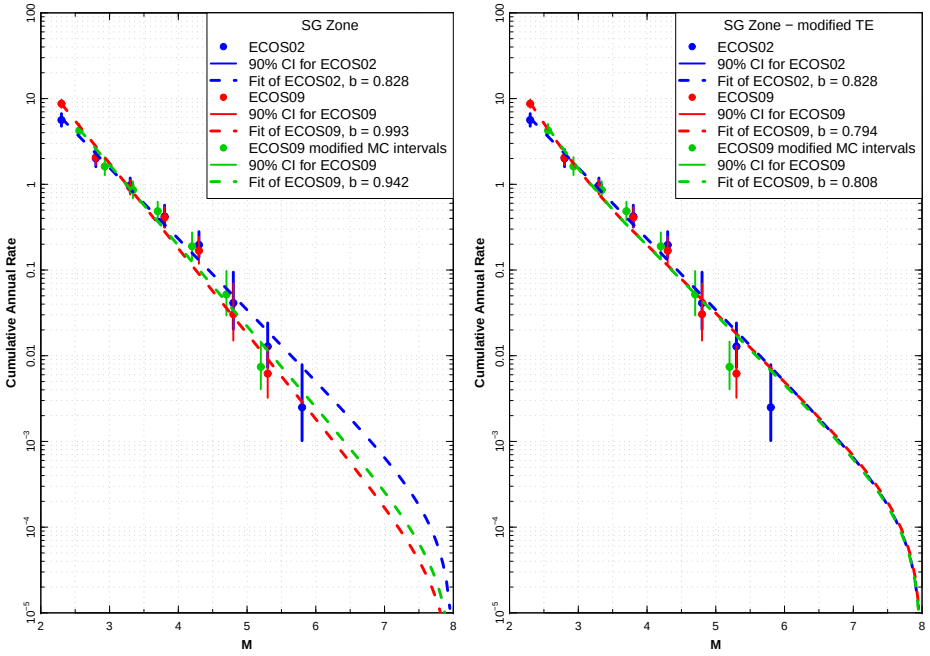

Figure 2.130: Seismicity data and earthquake recurrence rates for EG1b large zone SG Left standard truncated exponential applied to ECOS-09 catalog, Right – modified truncated exponential applied to ECOS-09 catalog.

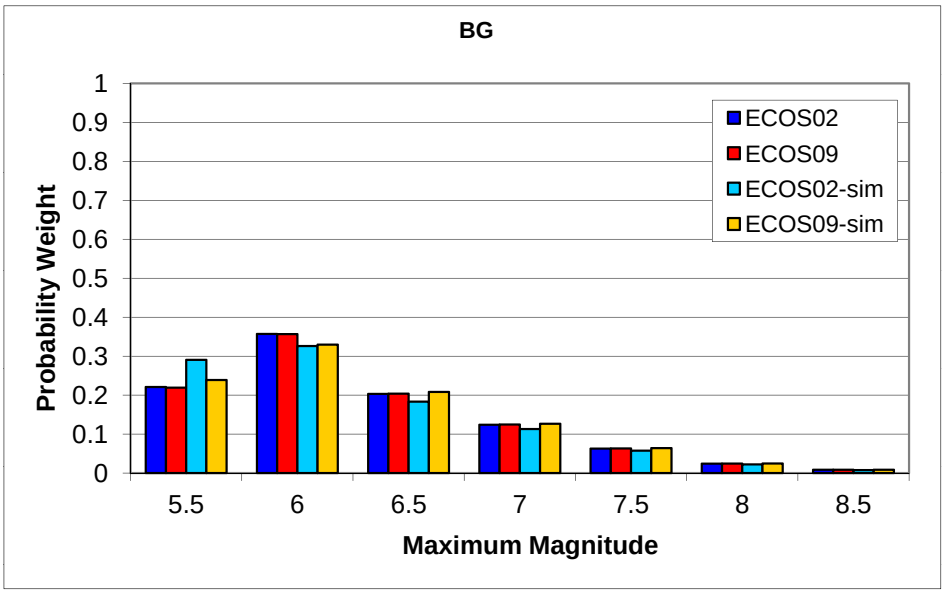

Figure 2.131: Maximum magnitude distributions for EG1b large zone BG.

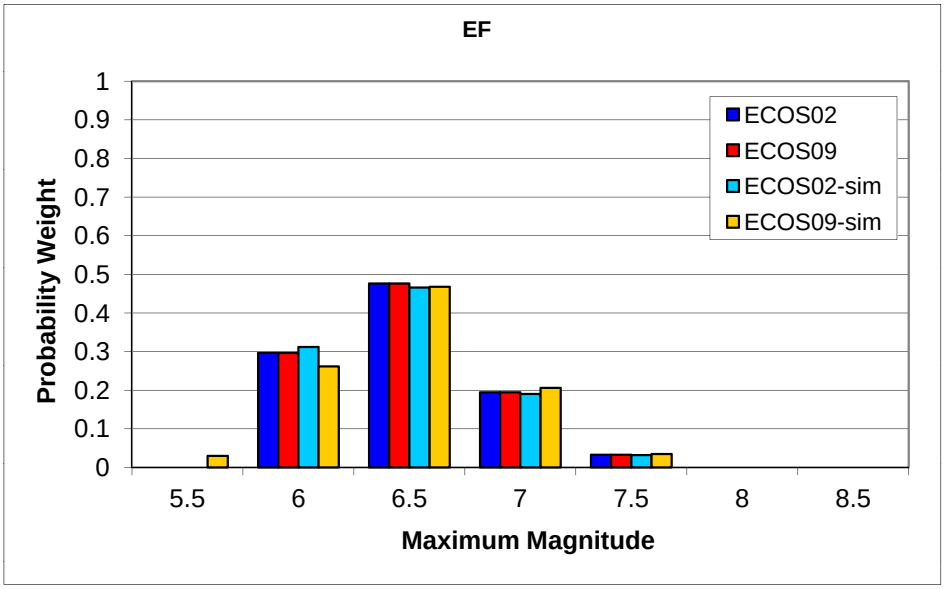

Figure 2.132: Maximum magnitude distributions for EG1b large zone EF.

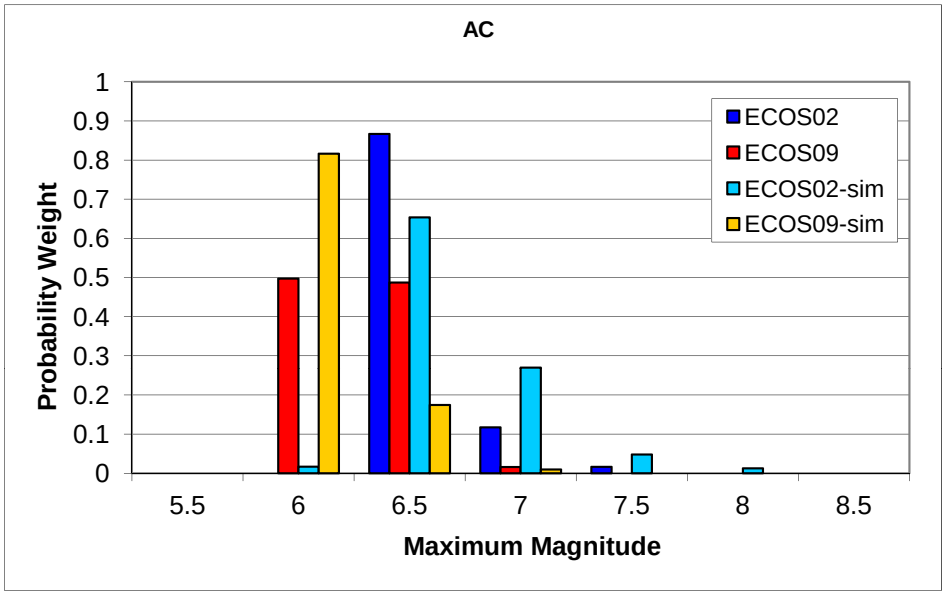

Figure 2.133: Maximum magnitude distributions for EG1b large zone AC.

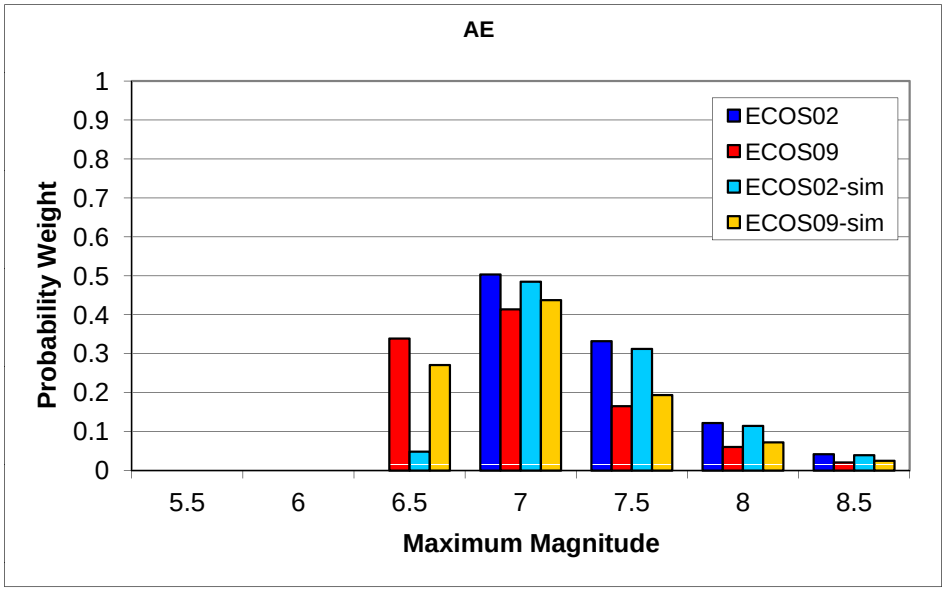

Figure 2.134: Maximum magnitude distributions for EG1b large zone AE.

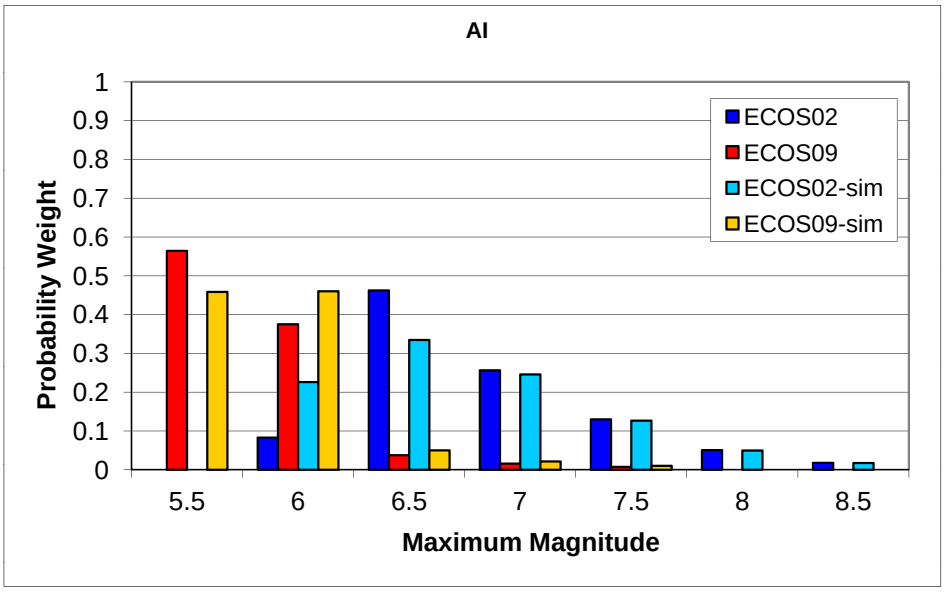

Figure 2.135: Maximum magnitude distributions for EG1b large zone AI.

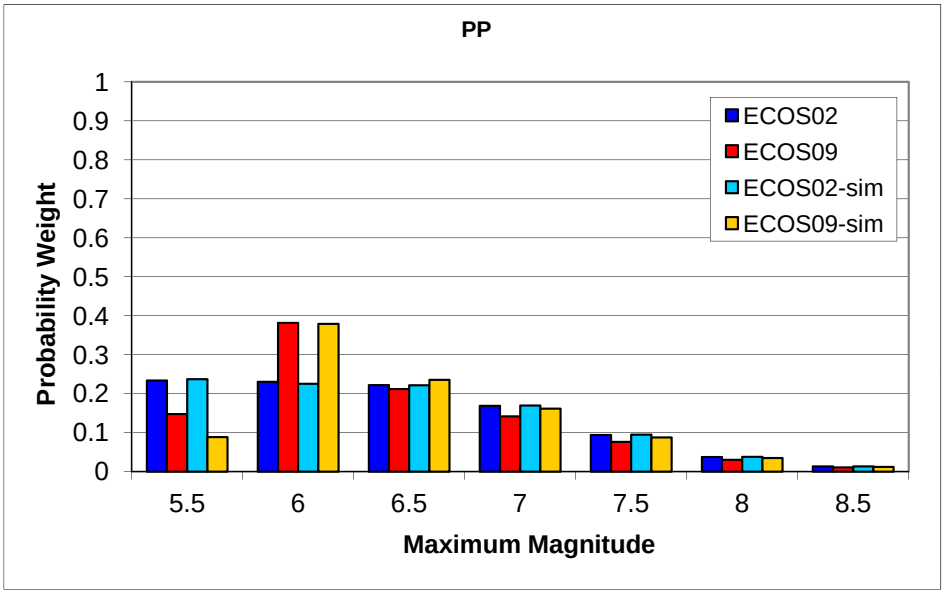

Figure 2.136: Maximum magnitude distributions for EG1b large zone PP.

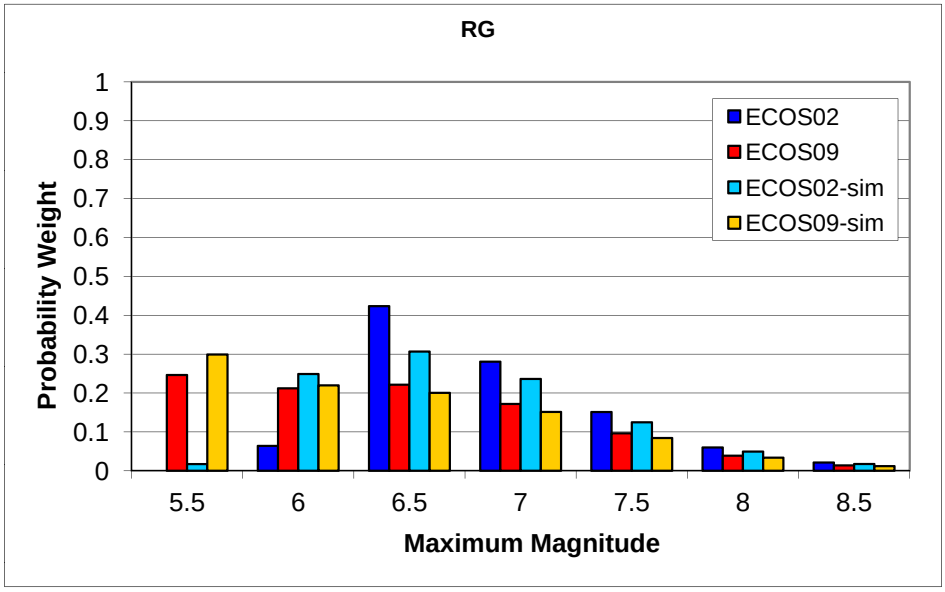

Figure 2.137: Maximum magnitude distributions for EG1b large zone RG.

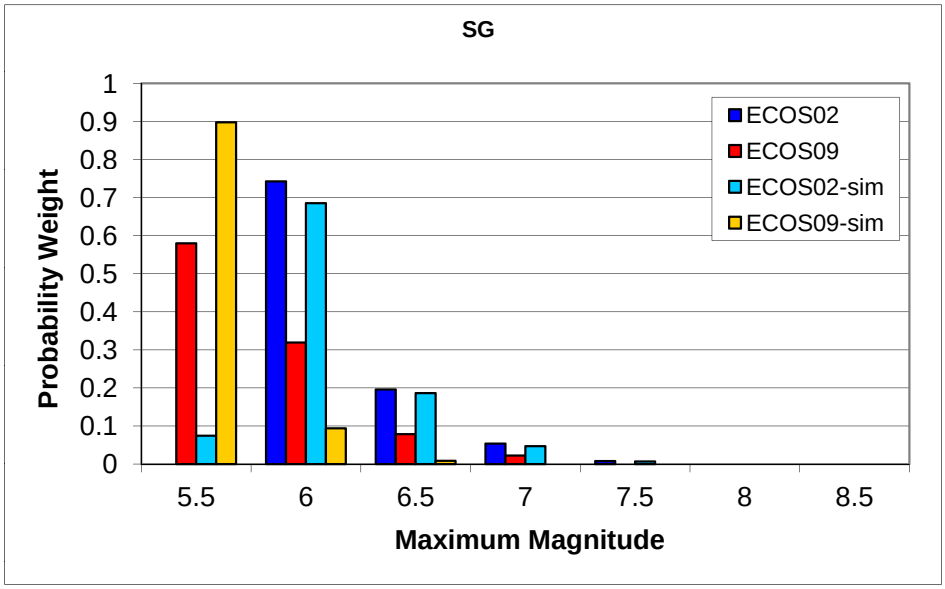

Figure 2.138: Maximum magnitude distributions for EG1b large zone SG.

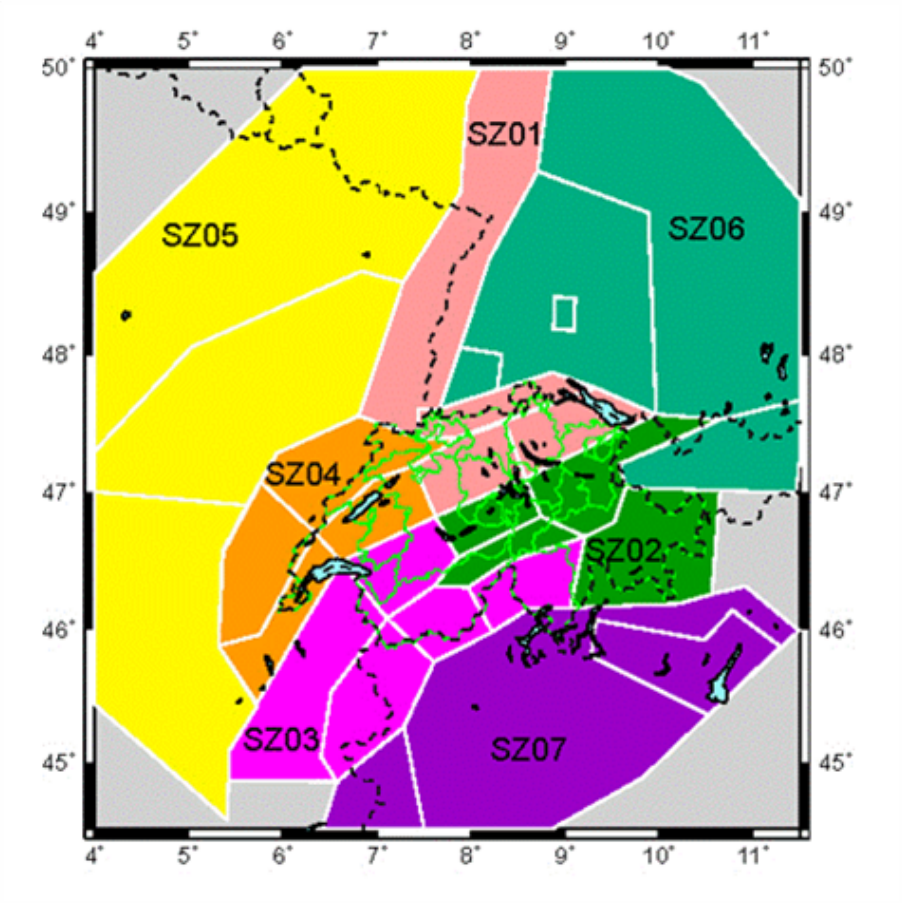

Figure 2.139: Catalog completeness regions defined by Expert Team EG1c.

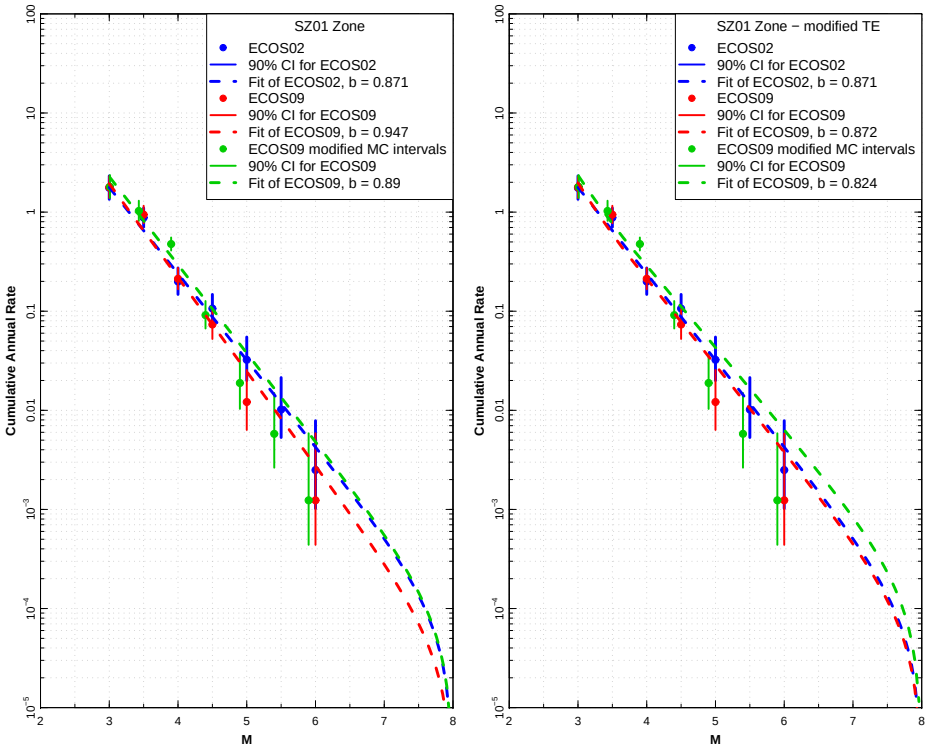

Figure 2.140: Seismicity data and earthquake recurrence rates for EG1c catalog completeness region SZ01. Left standard truncated exponential applied to ECOS-09 catalog, Right modified truncated exponential applied to ECOS-09 catalog.

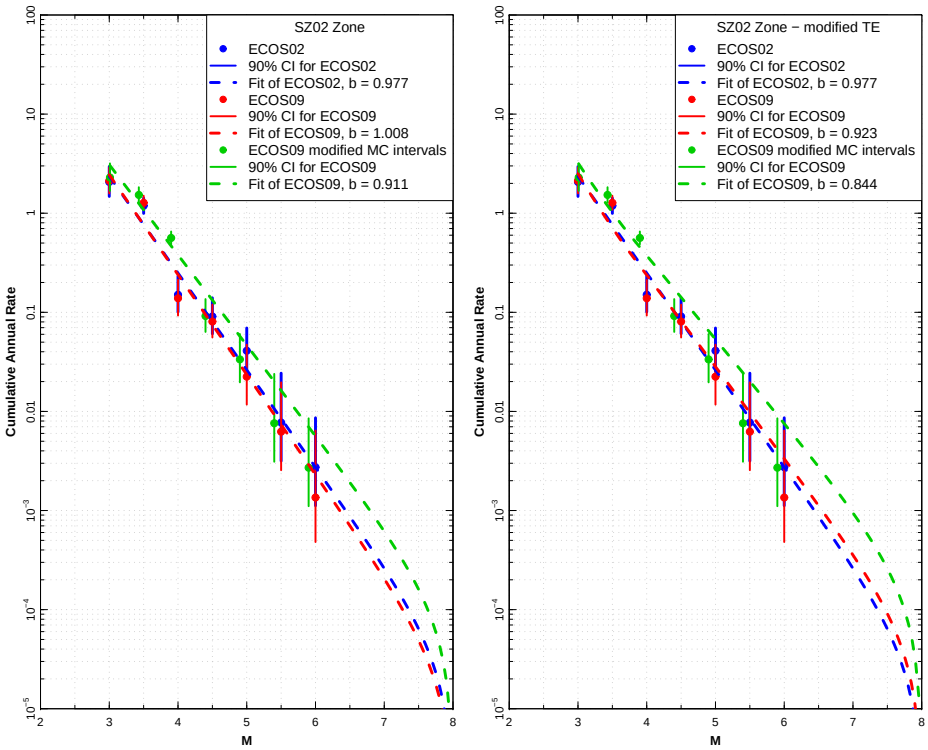

Figure 2.141: Seismicity data and earthquake recurrence rates for EG1c catalog completeness region SZ02. Left standard truncated exponential applied to ECOS-09 catalog, Right modified truncated exponential applied to ECOS-09 catalog.

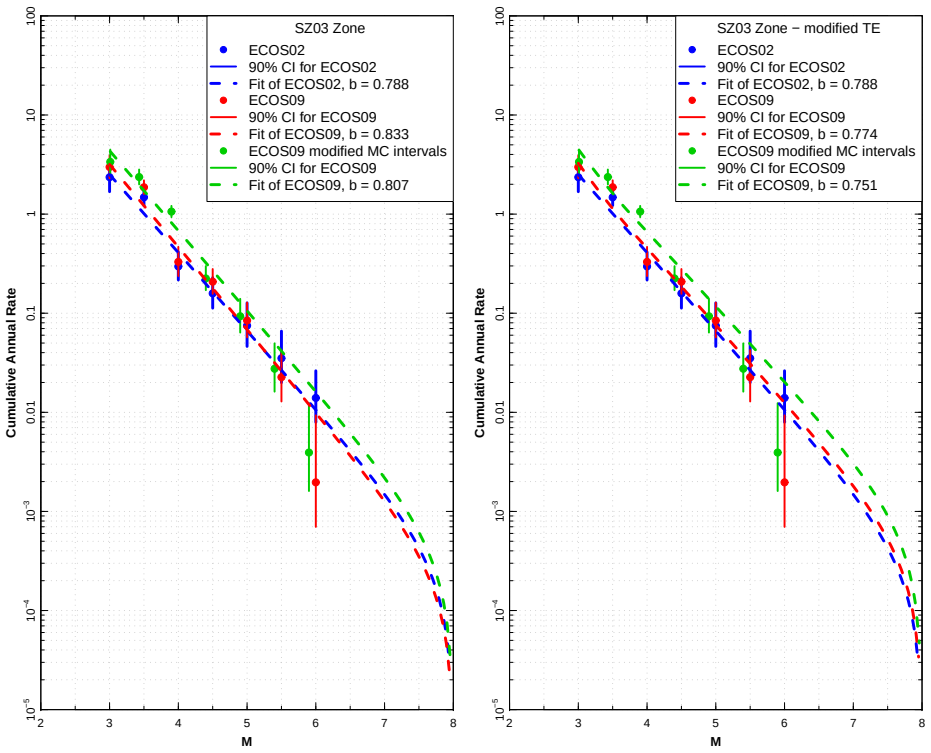

Figure 2.142: Seismicity data and earthquake recurrence rates for EG1c catalog completeness region SZ03. Left standard truncated exponential applied to ECOS-09 catalog, Right modified truncated exponential applied to ECOS-09 catalog.

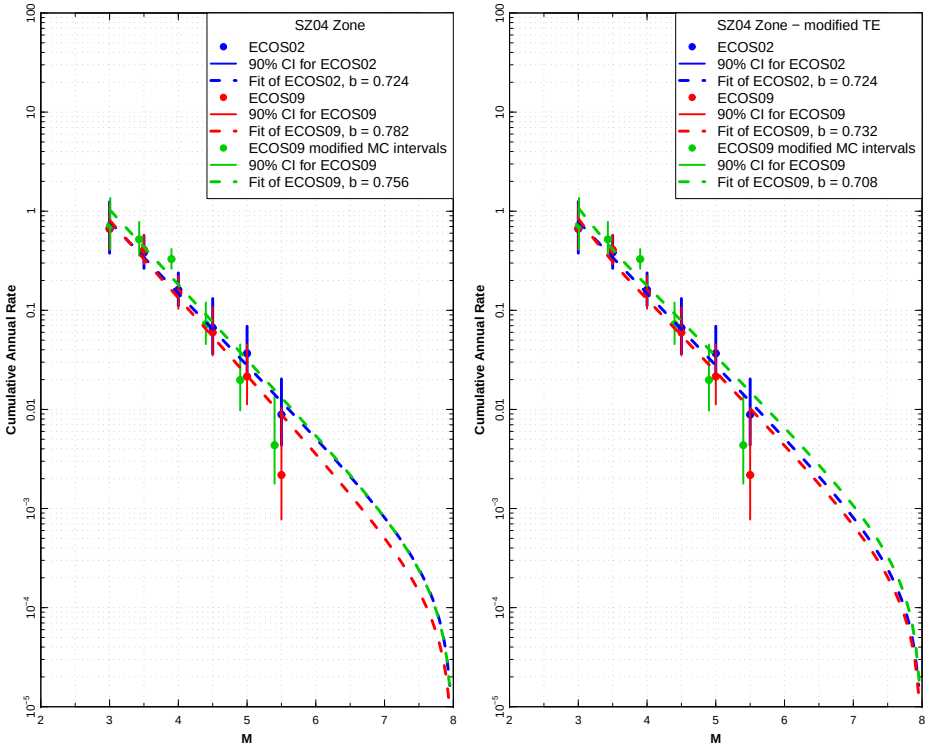

Figure 2.143: Seismicity data and earthquake recurrence rates for EG1c catalog completeness region SZ04. Left standard truncated exponential applied to ECOS-09 catalog, Right modified truncated exponential applied to ECOS-09 catalog.

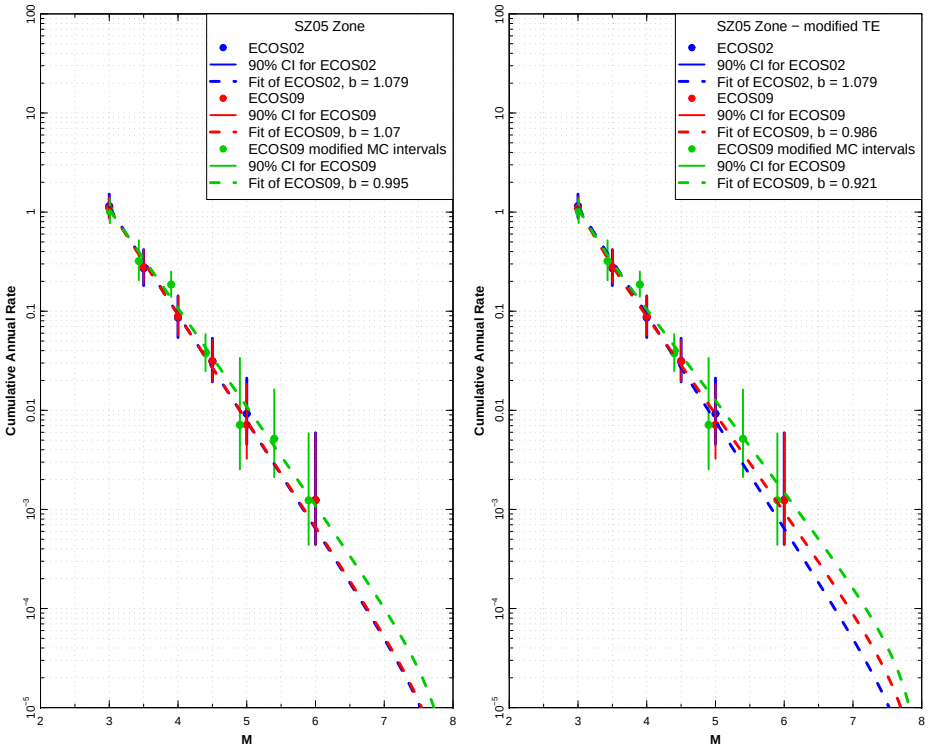

Figure 2.144: Seismicity data and earthquake recurrence rates for EG1c catalog completeness region SZ05. Left standard truncated exponential applied to ECOS-09 catalog, Right modified truncated exponential applied to ECOS-09 catalog.

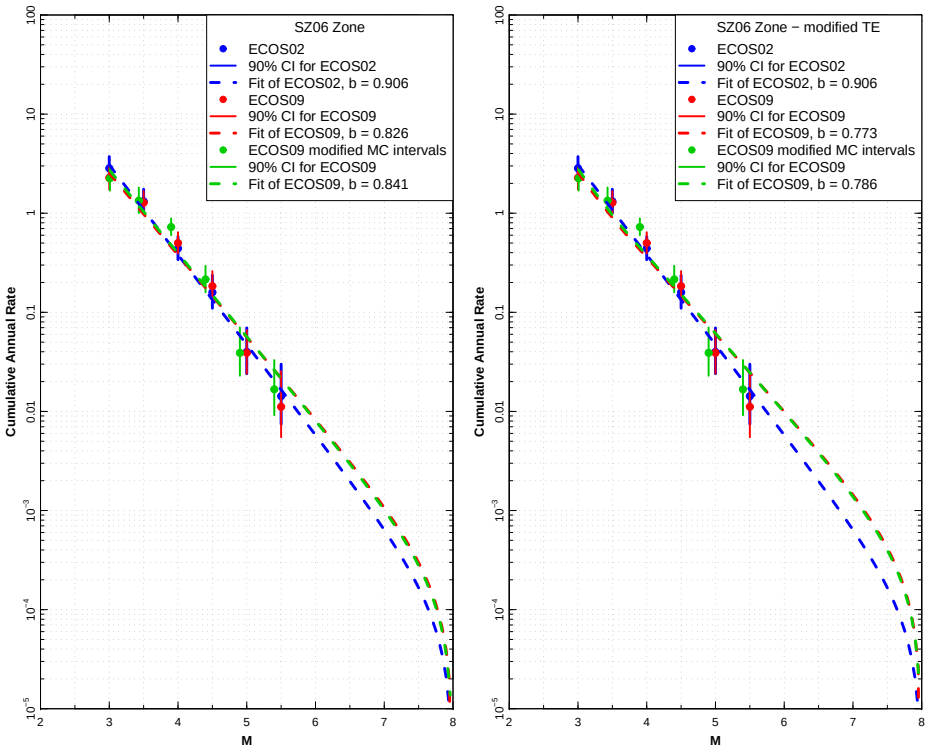

Figure 2.145: Seismicity data and earthquake recurrence rates for EG1c catalog completeness region SZ06. Left standard truncated exponential applied to ECOS-09 catalog, Right modified truncated exponential applied to ECOS-09 catalog.

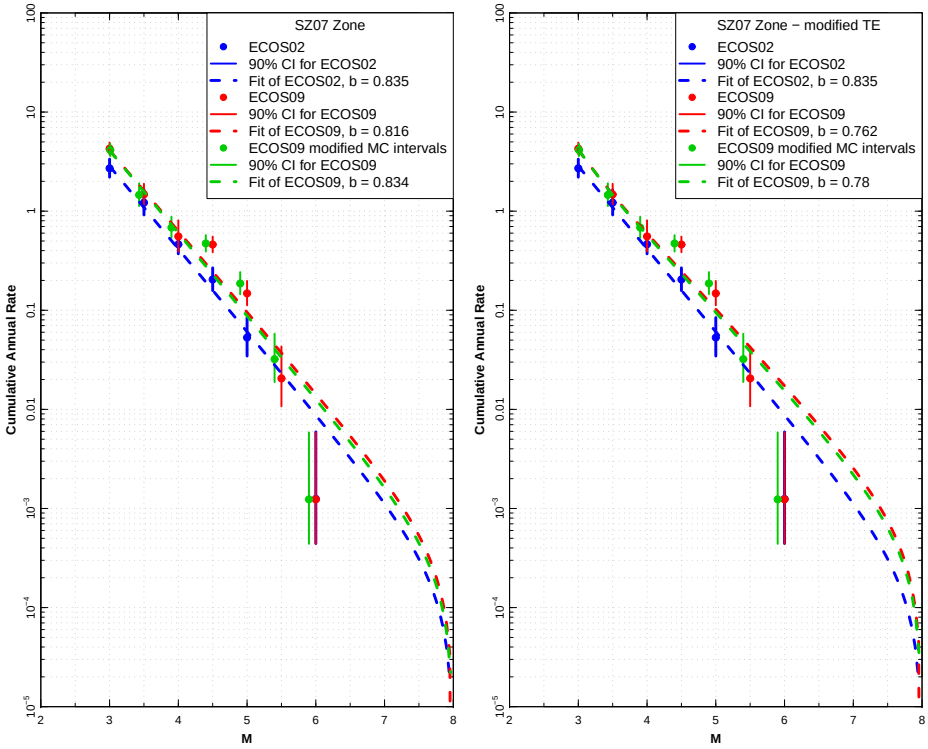

Figure 2.146: Seismicity data and earthquake recurrence rates for EG1c catalog completeness region SZ07. Left standard truncated exponential applied to ECOS-09 catalog, Right modified truncated exponential applied to ECOS-09 catalog.

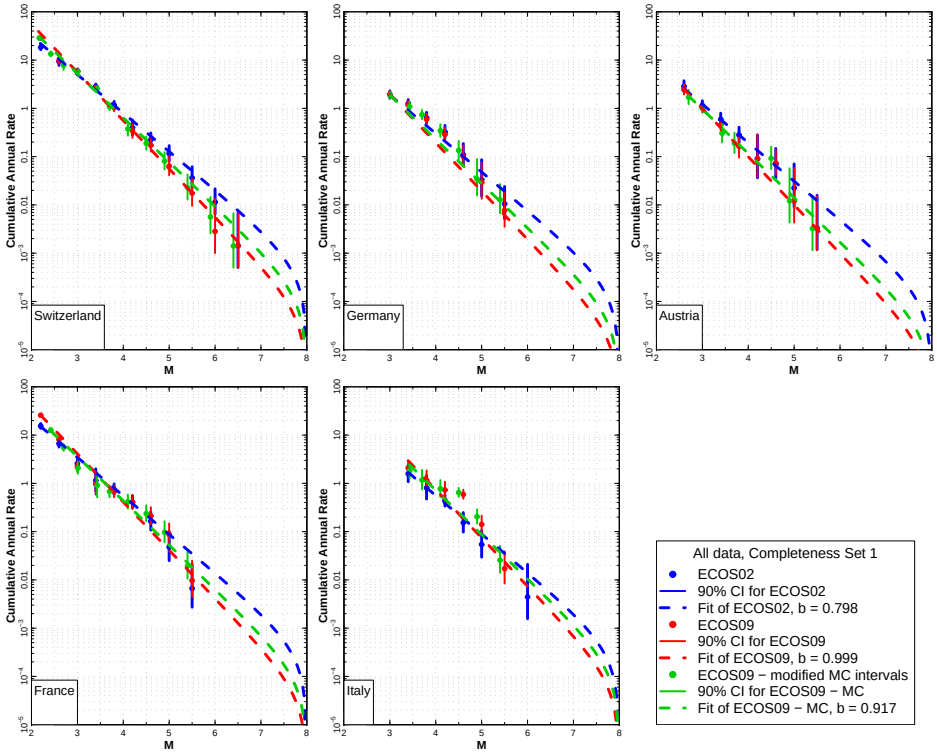

Figure 2.147: Seismicity data for EG1d five completeness regions and completeness Set 1 Curves show combined maximum likelihood fit with a common b-value.

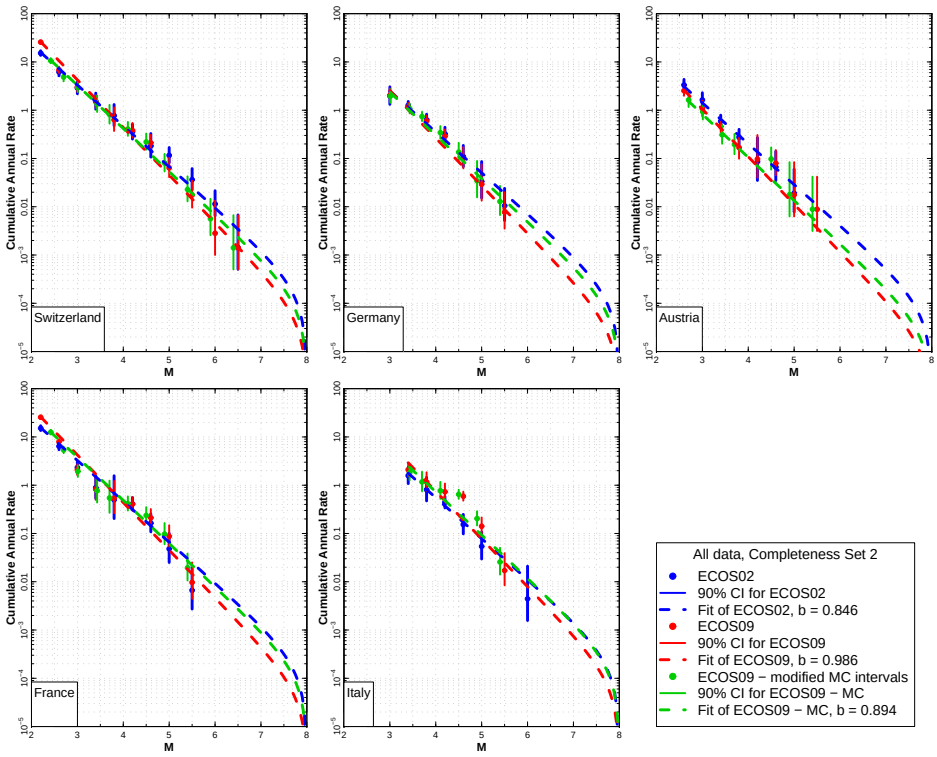

Figure 2.148: Seismicity data for EG1d five completeness regions and completeness Set 2 Curves show combined maximum likelihood fit with a common b-value.

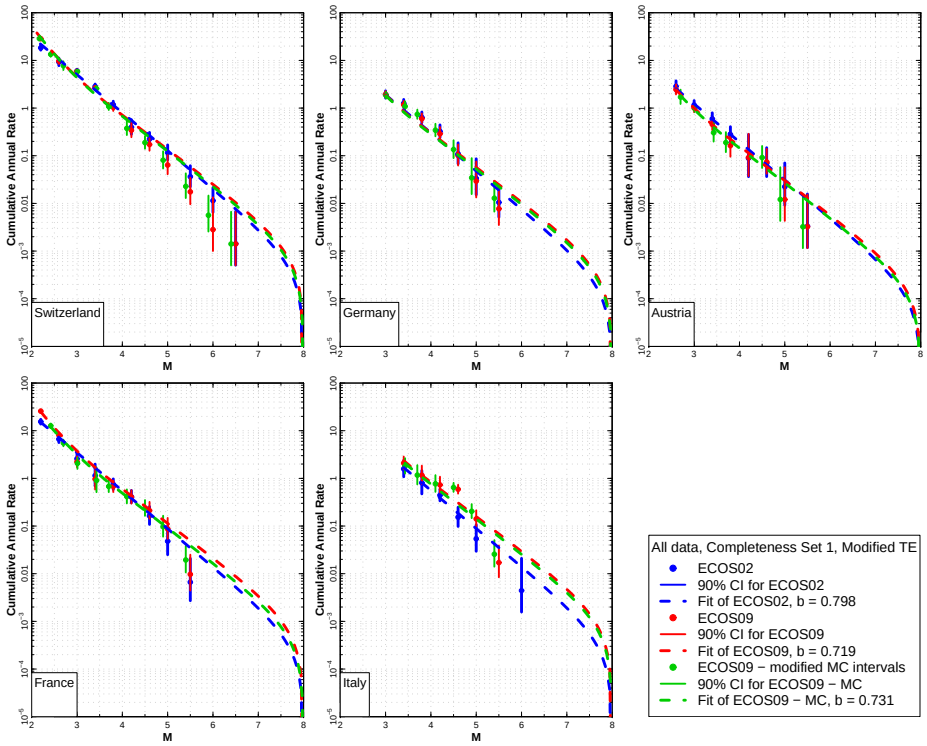

Figure 2.149: Seismicity data for EG1d five completeness regions and completeness Set 1 Curves show combined maximum likelihood fit with a common b-value using a modified truncated exponential distribution incorporating the magnitude scaling from Equation 2.11.

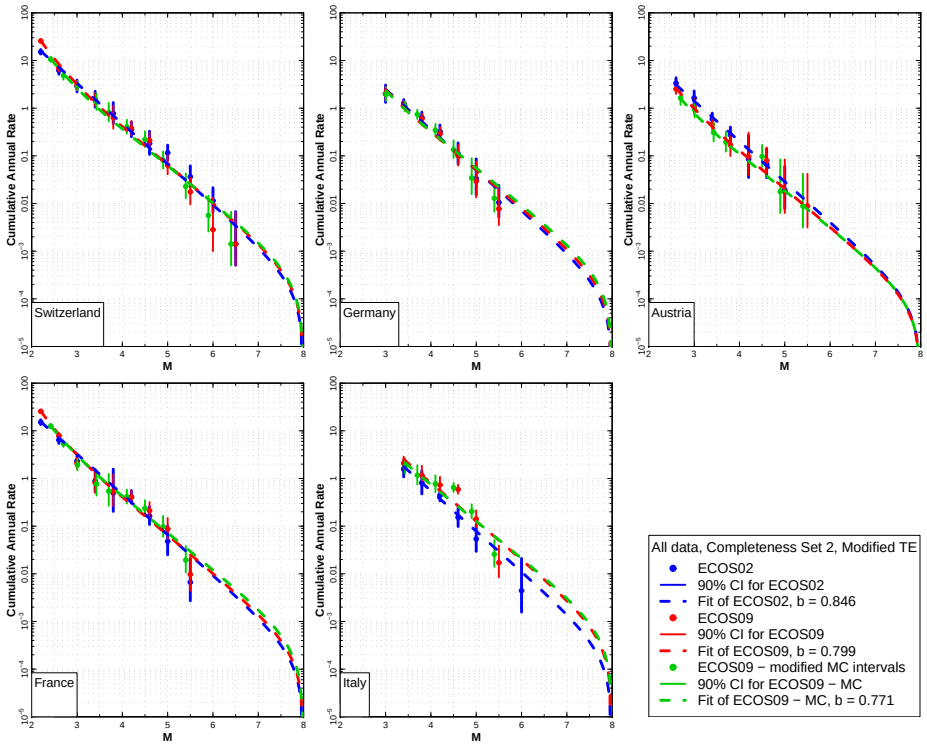

Figure 2.150: Seismicity data for EG1d five completeness regions and completeness Set 2 Curves show combined maximum likelihood fit with a common b-value using a modified truncated exponential distribution incorporating the magnitude scaling from Equation 2.11.

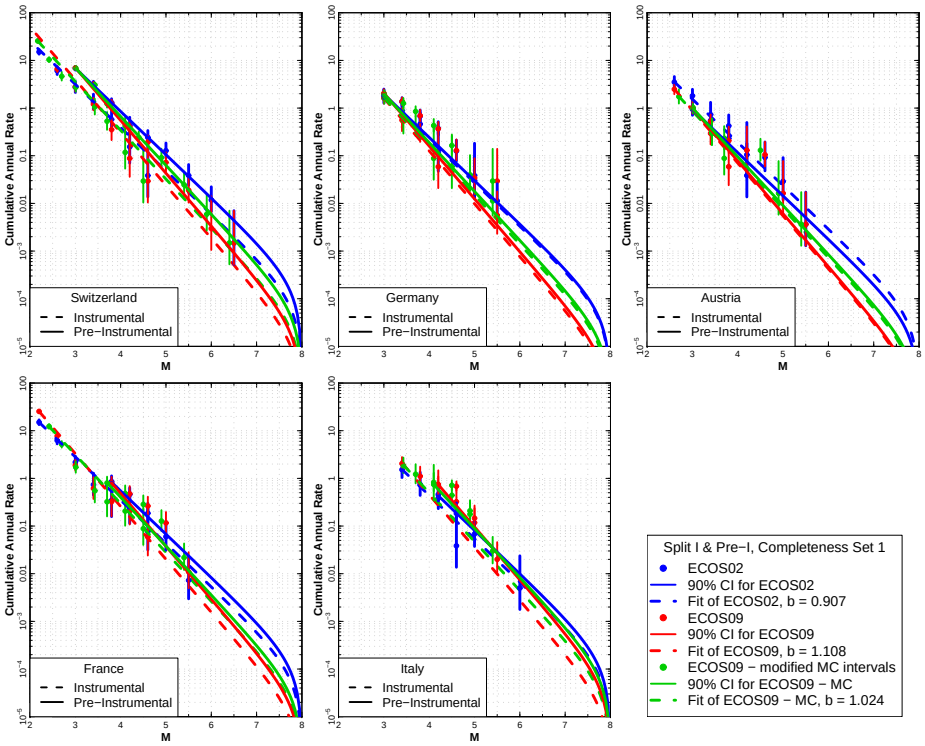

Figure 2.151: Seismicity data for EG1d five completeness regions and completeness Set 1 allowing for difference in seismicity rate in the instrumental (post 1975) and pre-instrumental (pre 1975) periods. Curves show combined maximum likelihood fit with a common b-value.

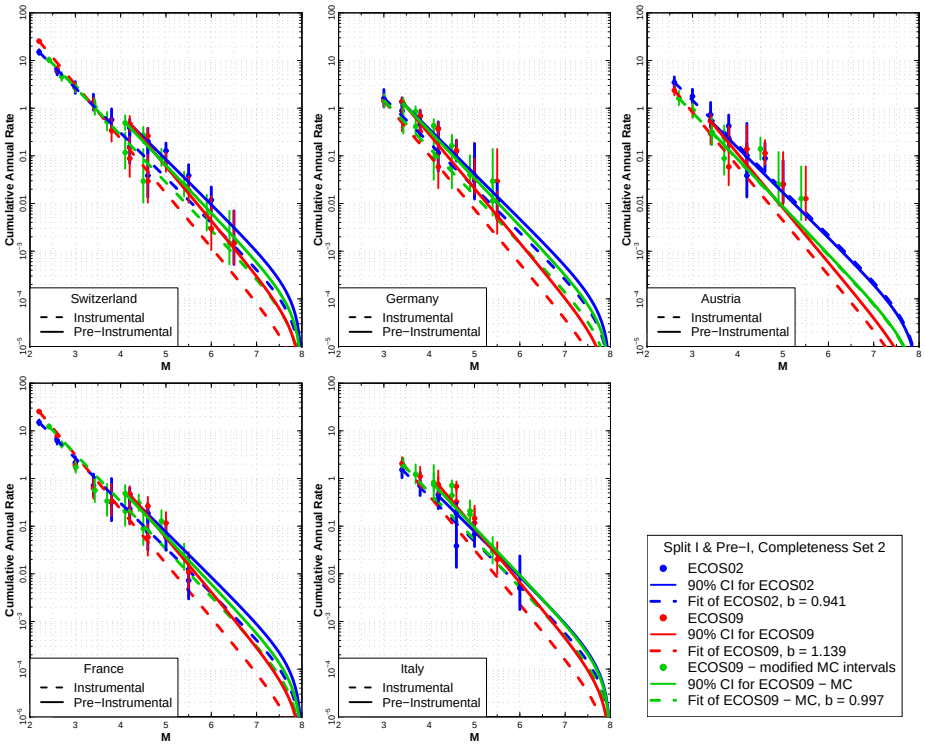

Figure 2.152: Seismicity data for EG1d five completeness regions and completeness Set 2 allowing for difference in seismicity rate in the instrumental (post 1975) and pre-instrumental (pre 1975) periods. Curves show combined maximum likelihood fit with a common b-value.

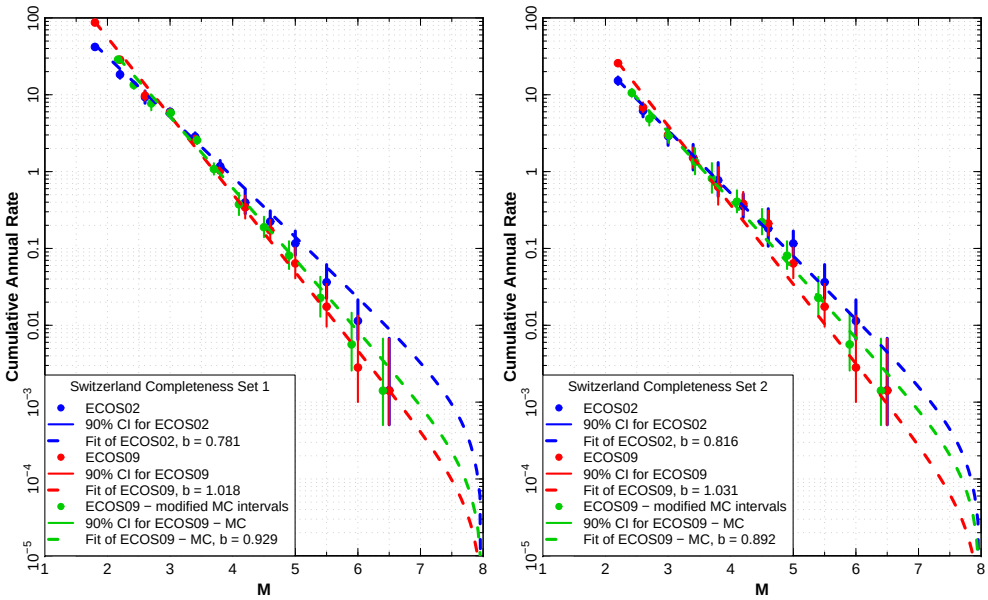

Figure 2.153: Seismicity data for EG1d Switzerland completeness region Curves show combined maximum likelihood fit using a standard truncated exponential distribution.

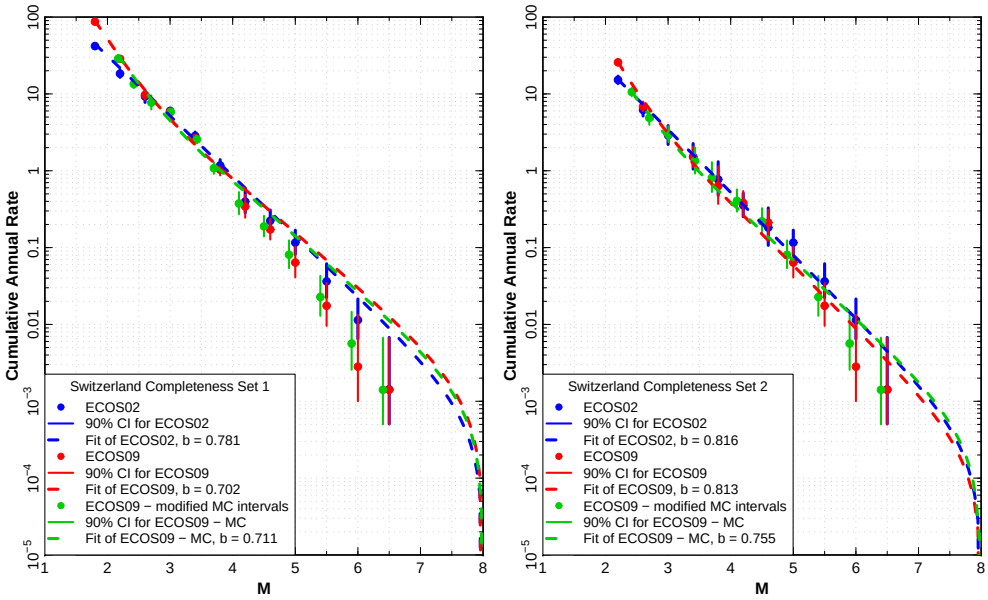

Figure 2.154: Seismicity data for EG1d Switzerland completeness region Curves show combined maximum likelihood fit using a modified truncated exponential distribution incorporating the magnitude scaling from Equation 2.11.

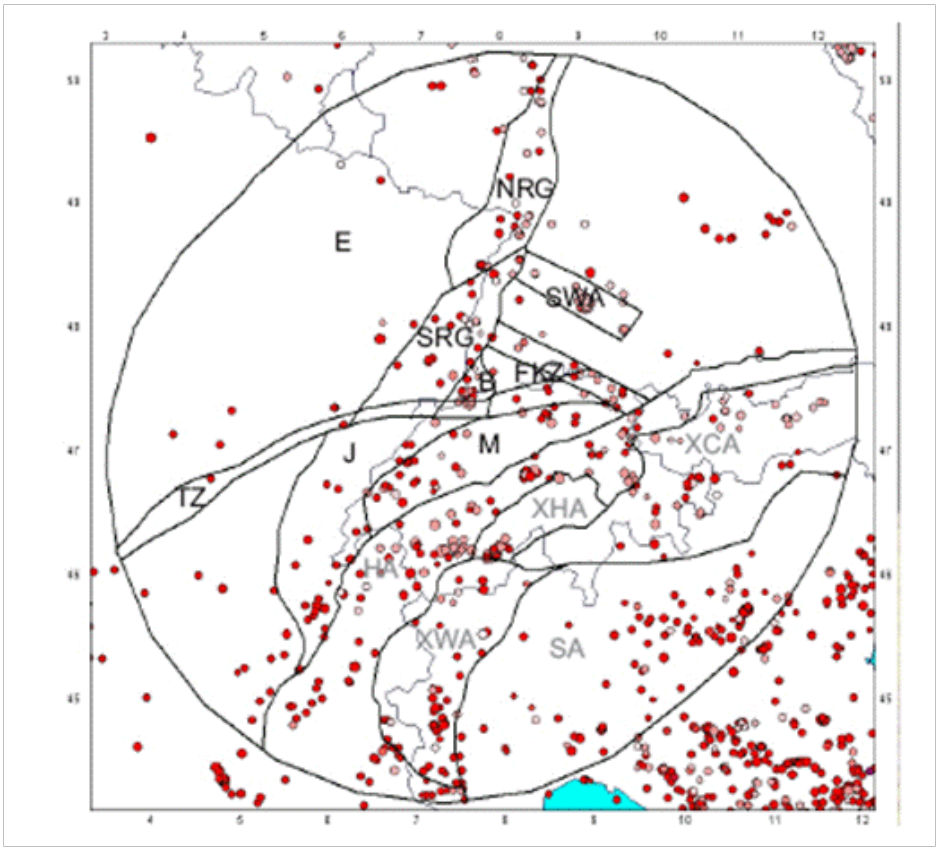

Figure 2.155: Seismic source zones defined by the EG1d Expert Team.

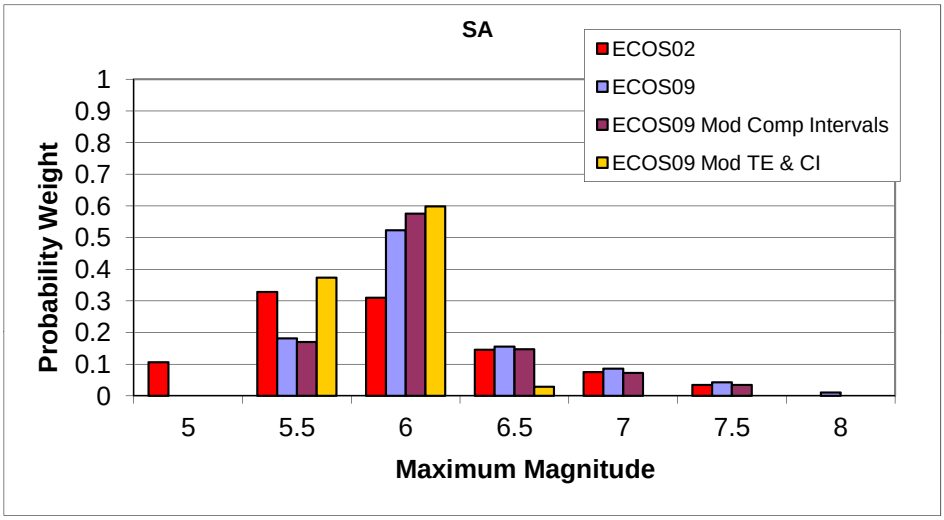

Figure 2.156: Maximum magnitude distributions for EG1d source SA.

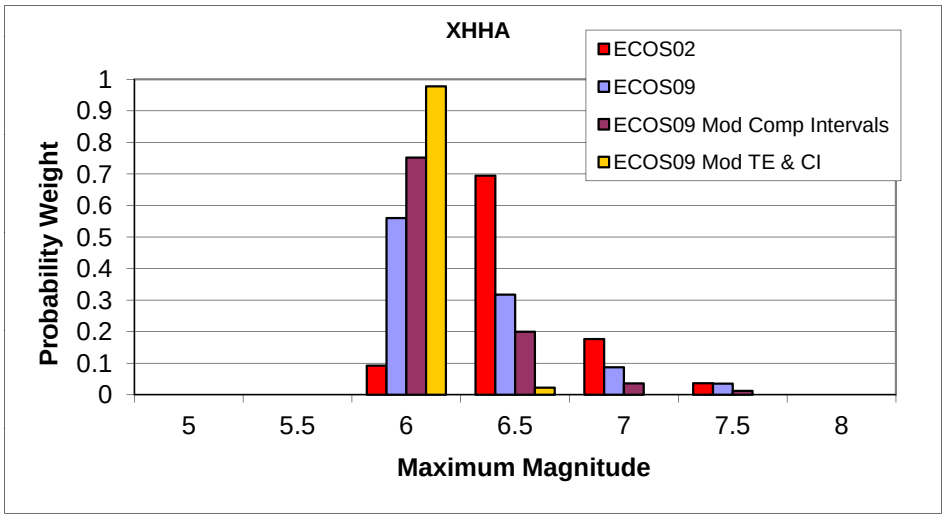

Figure 2.157: Maximum magnitude distributions for EG1d source XHHA.

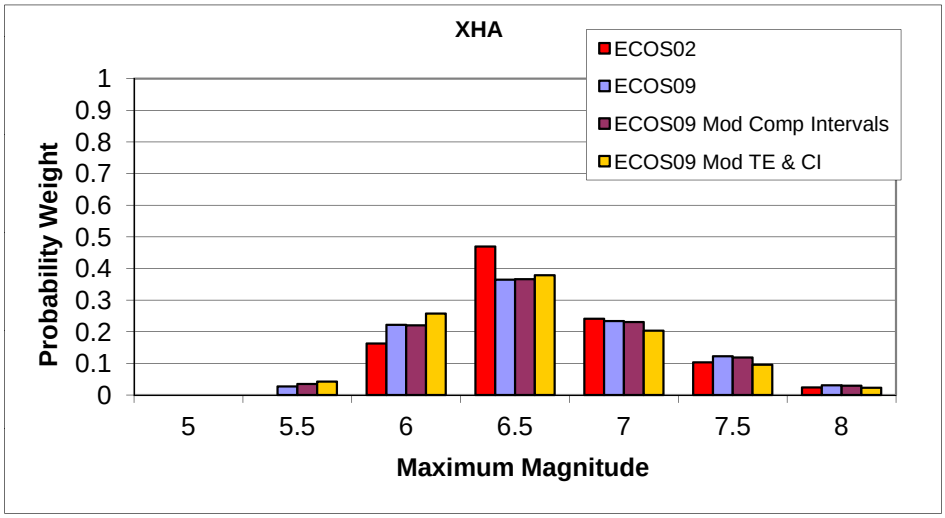

Figure 2.158: Maximum magnitude distributions for EG1d source XHA.

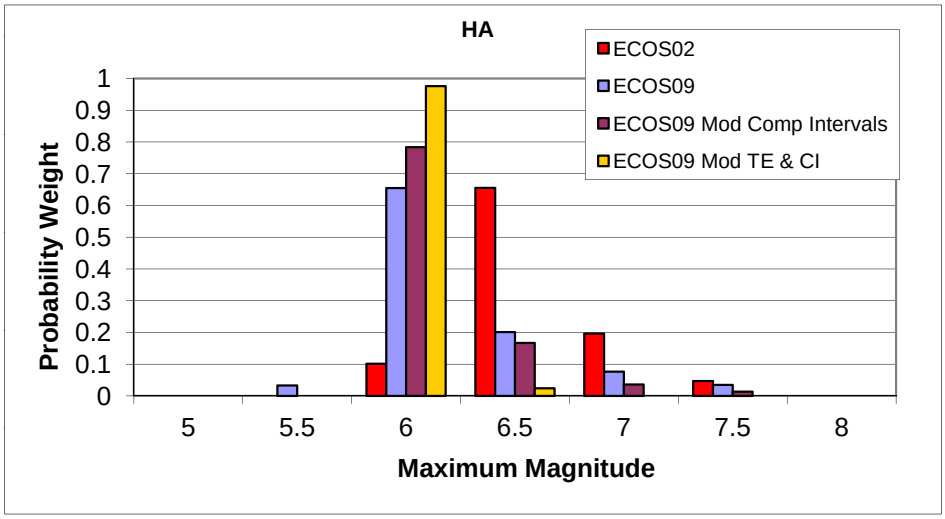

Figure 2.159: Maximum magnitude distributions for EG1d source HA.

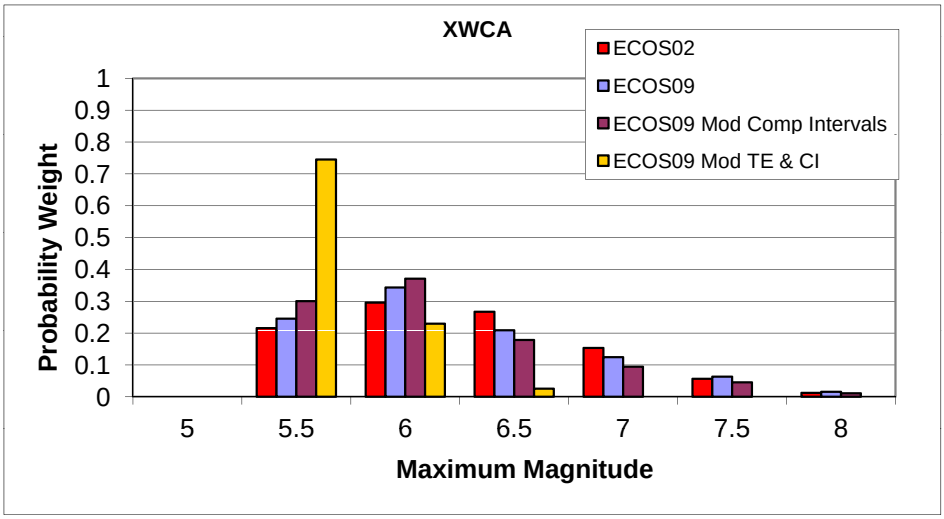

Figure 2.160: Maximum magnitude distributions for EG1d source XWCA.

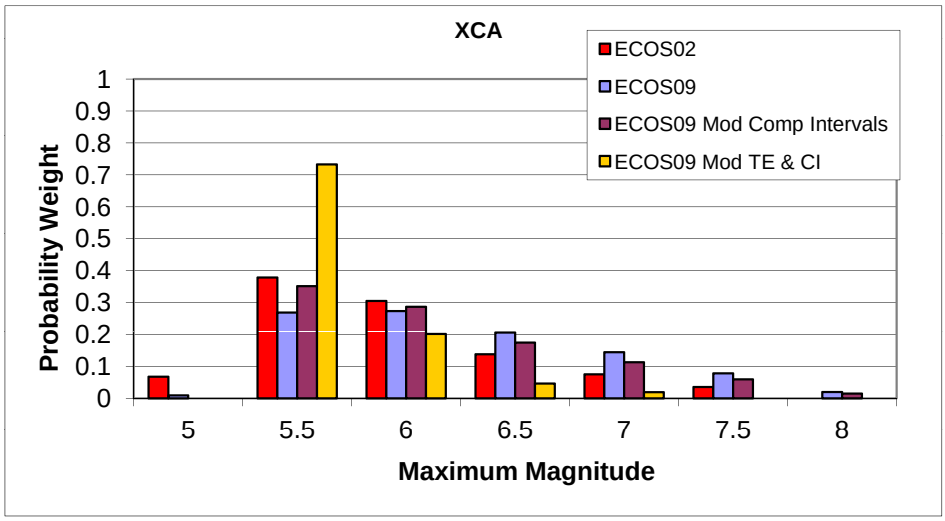

Figure 2.161: Maximum magnitude distributions for EG1d source XCA.

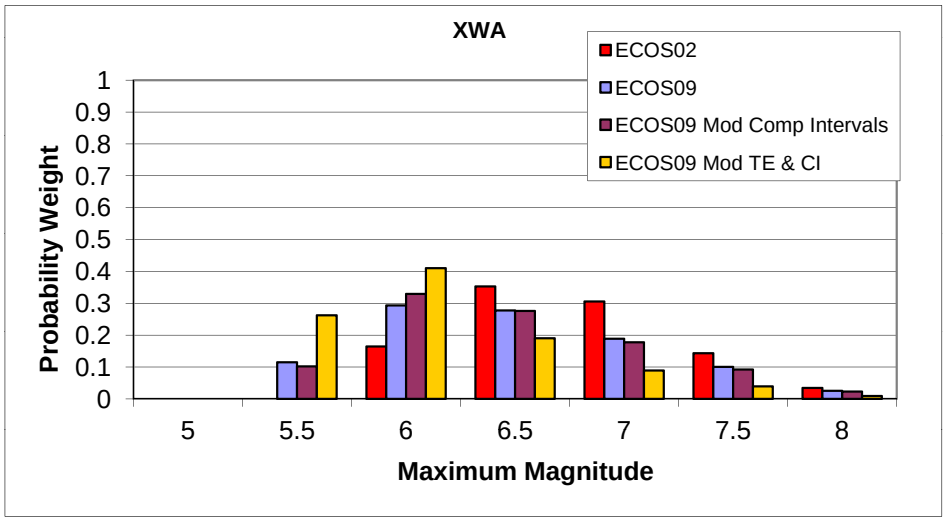

Figure 2.162: Maximum magnitude distributions for EG1d source XWA.

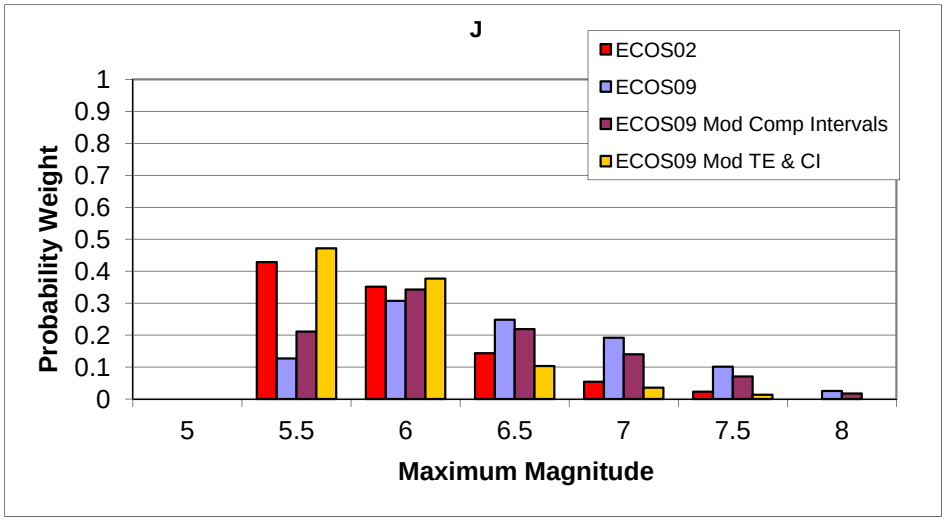

Figure 2.163: Maximum magnitude distributions for EG1d source J.

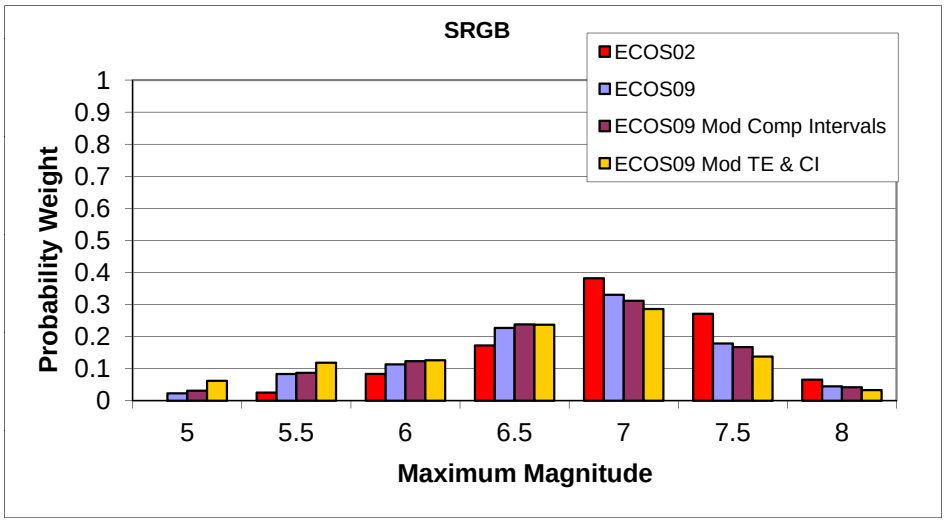

Figure 2.164: Maximum magnitude distributions for EG1d source SRGB.

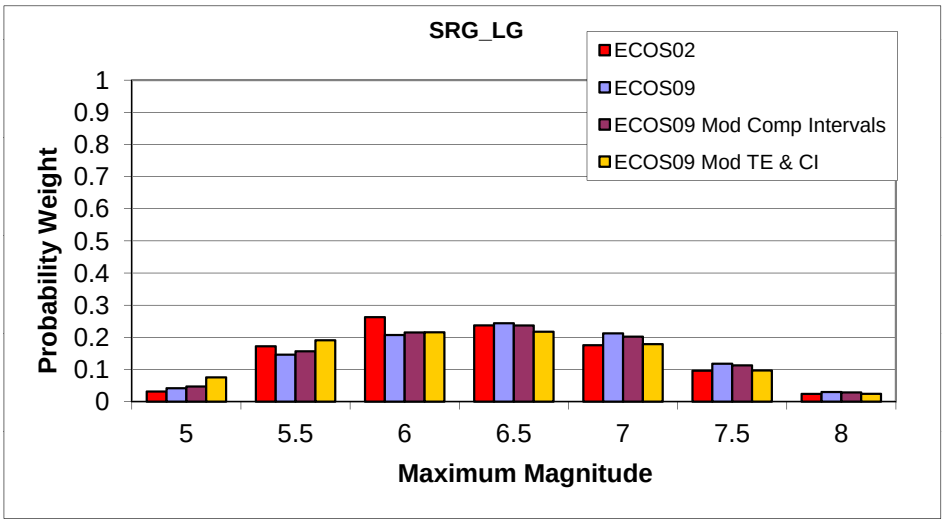

Figure 2.165: Maximum magnitude distributions for EG1d source SRG_LG.

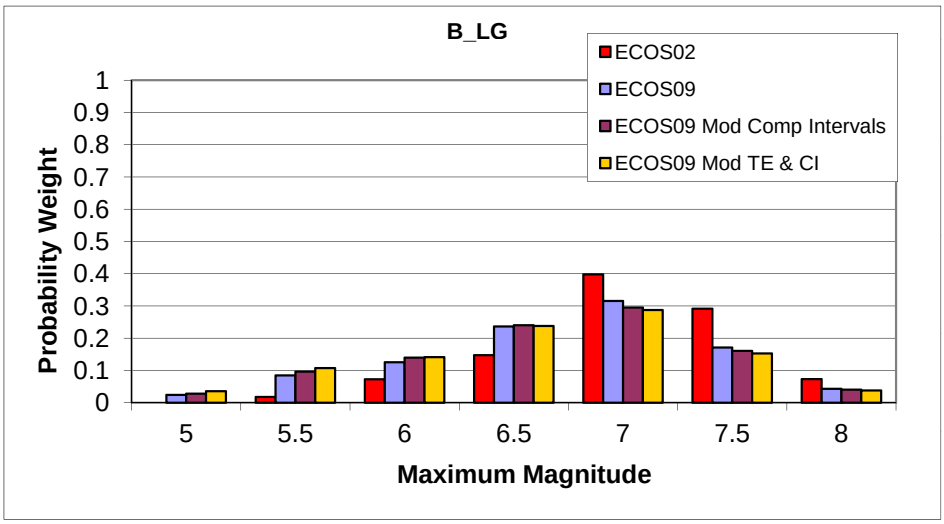

Figure 2.166: Maximum magnitude distributions for EG1d source B_LG.

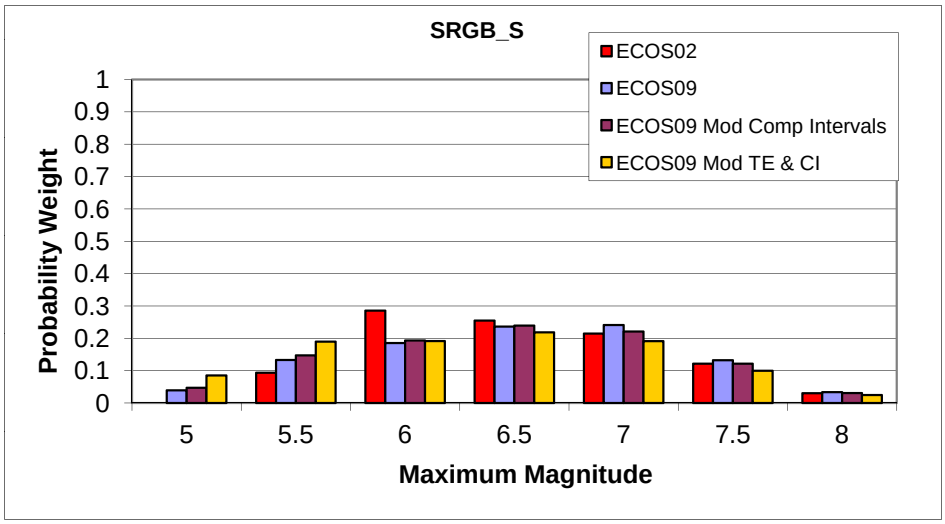

Figure 2.167: Maximum magnitude distributions for EG1d source SRGB_S.

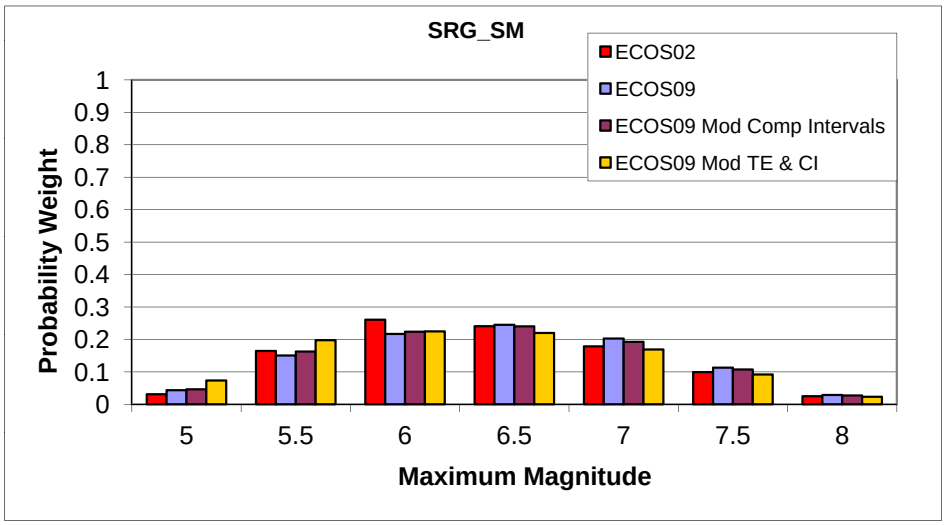

Figure 2.168: Maximum magnitude distributions for EG1d source SRG_SM.

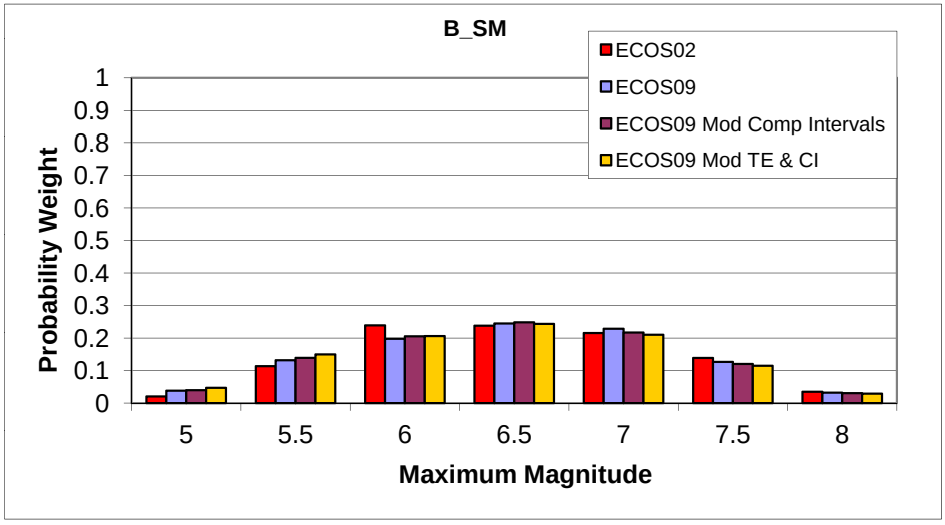

Figure 2.169: Maximum magnitude distributions for EG1d source B_SM.

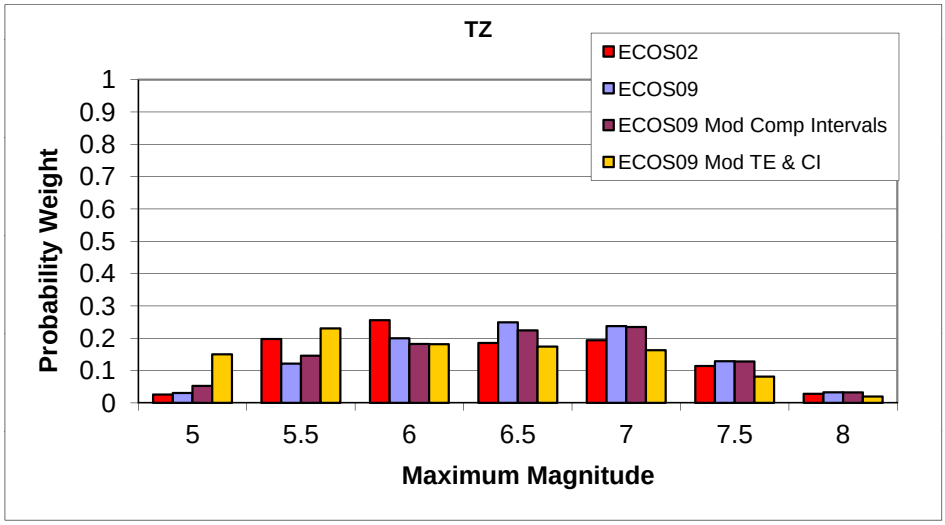

Figure 2.170: Maximum magnitude distributions for EG1d source TZ.

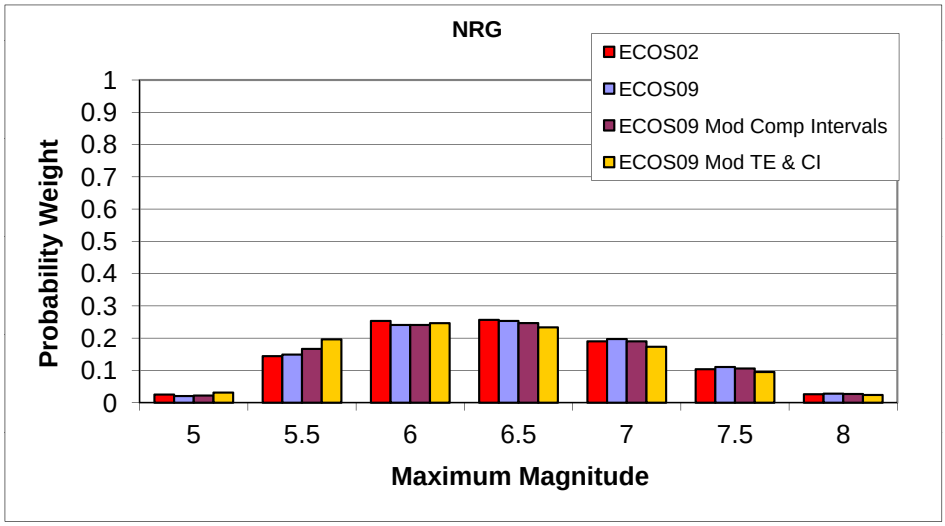

Figure 2.171: Maximum magnitude distributions for EG1d source NRG.

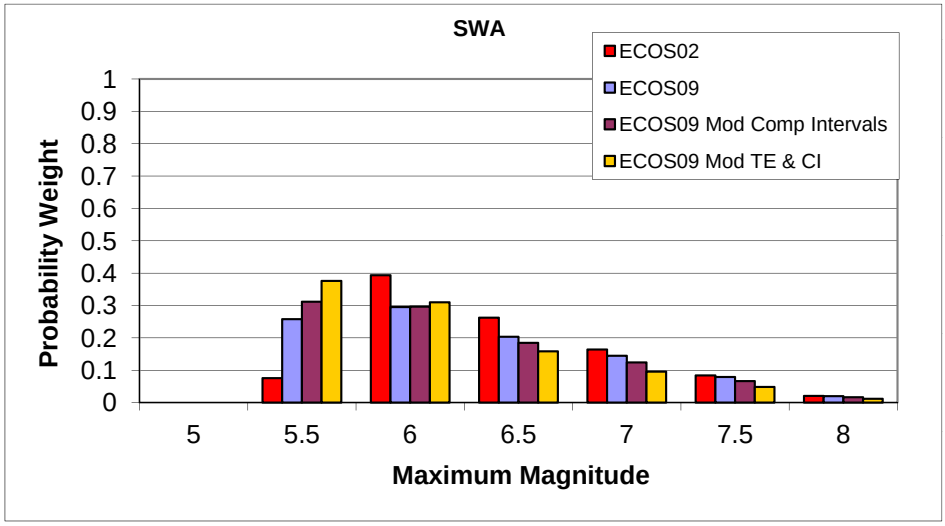

Figure 2.172: Maximum magnitude distributions for EG1d source SWA.

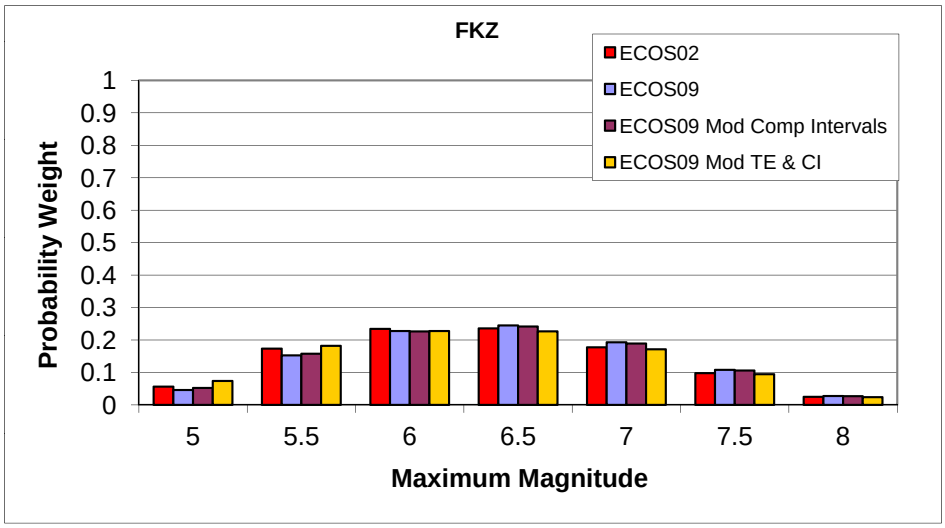

Figure 2.173: Maximum magnitude distributions for EG1d source FKZ.

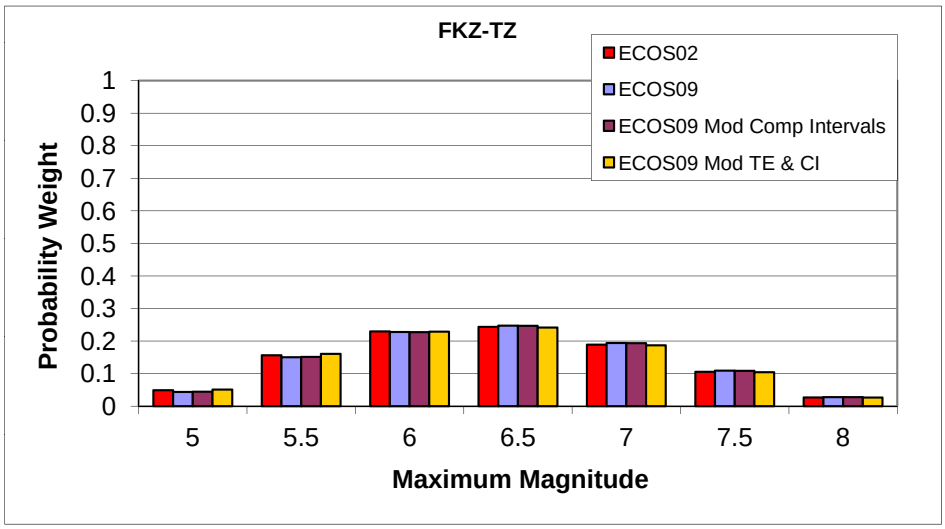

Figure 2.174: Maximum magnitude distributions for EG1d source FKZ-TZ.

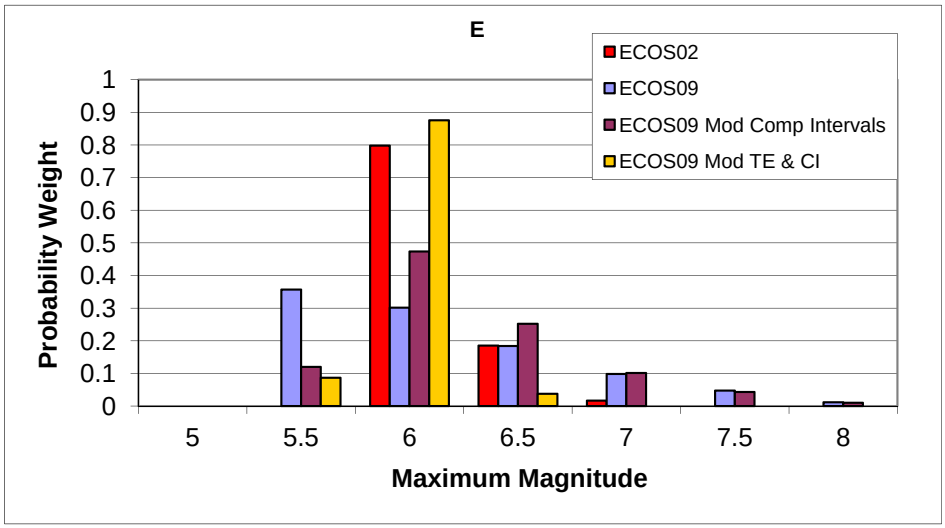

Figure 2.175: Maximum magnitude distributions for EG1d source E.

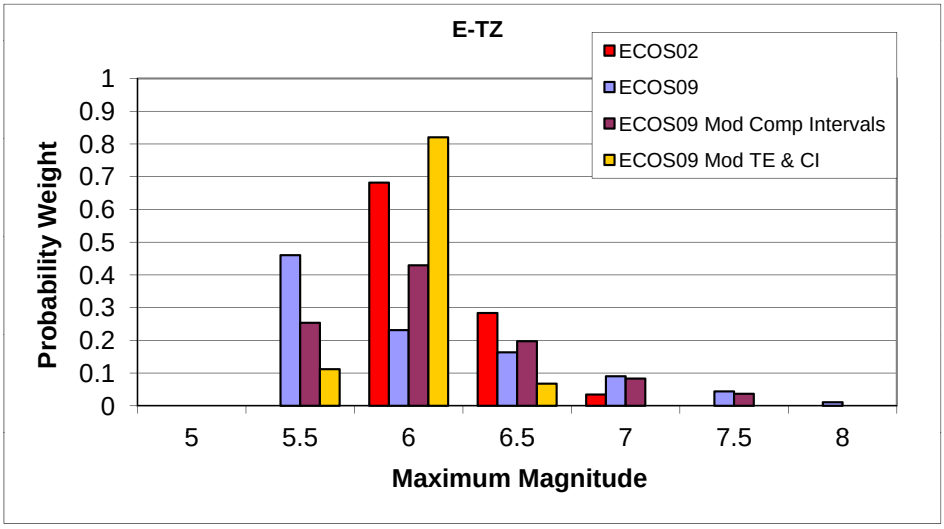

Figure 2.176: Maximum magnitude distributions for EG1d source E-TZ.

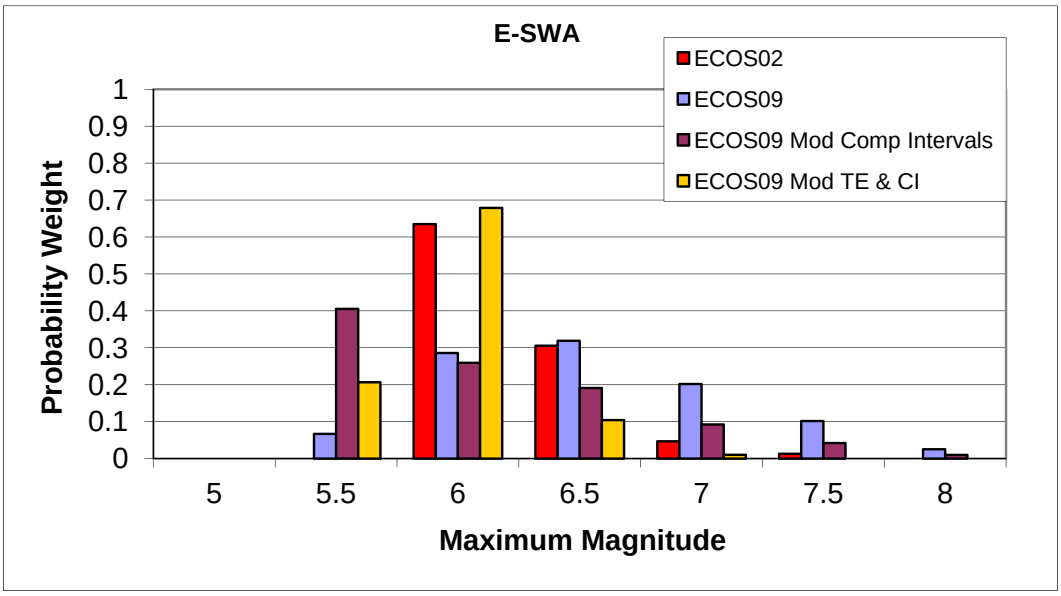

Figure 2.177: Maximum magnitude distributions for EG1d source E-SWA.

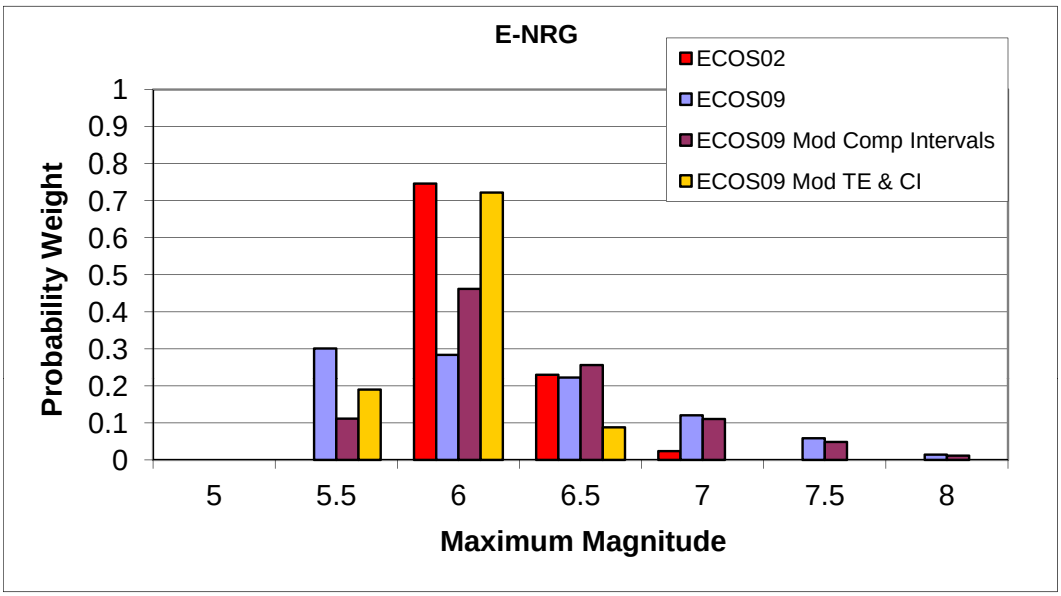

Figure 2.178: Maximum magnitude distributions for EG1d source E-NRG.

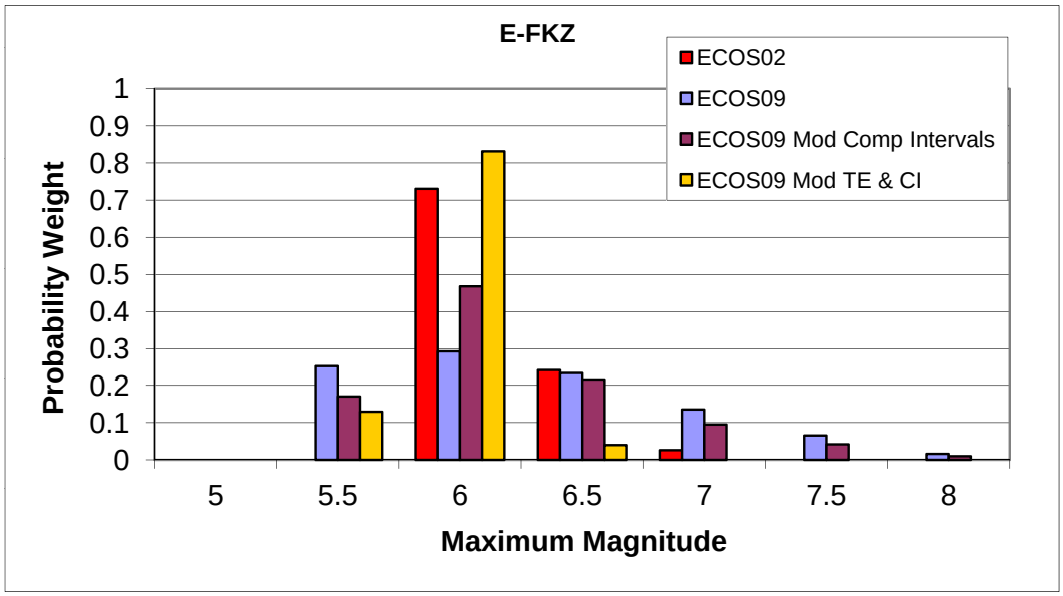

Figure 2.179: Maximum magnitude distributions for EG1d source E-FKZ.

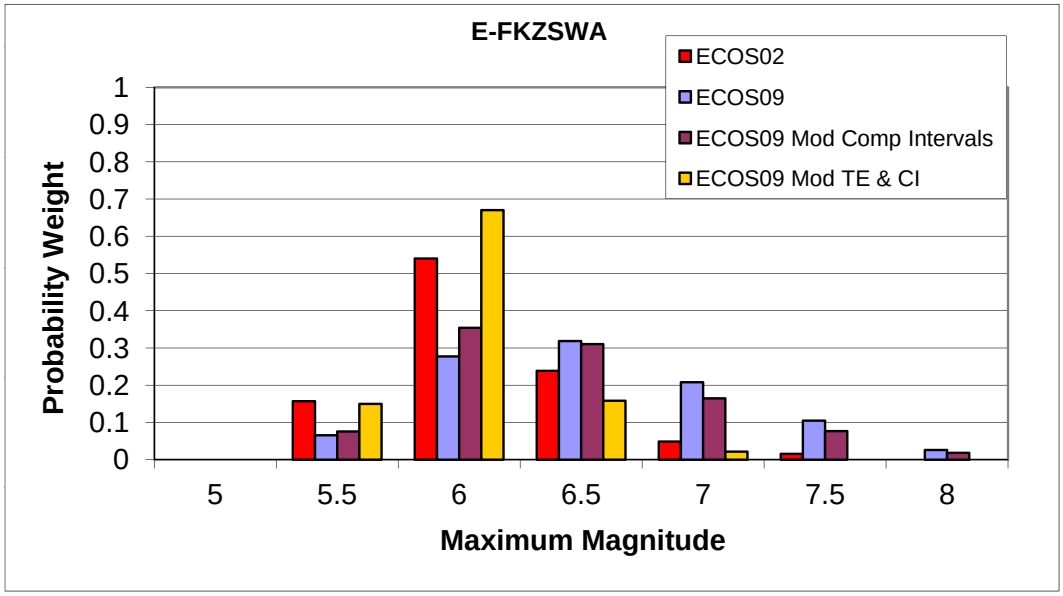

Figure 2.180: Maximum magnitude distributions for EG1d source E-FKZ& SWA.

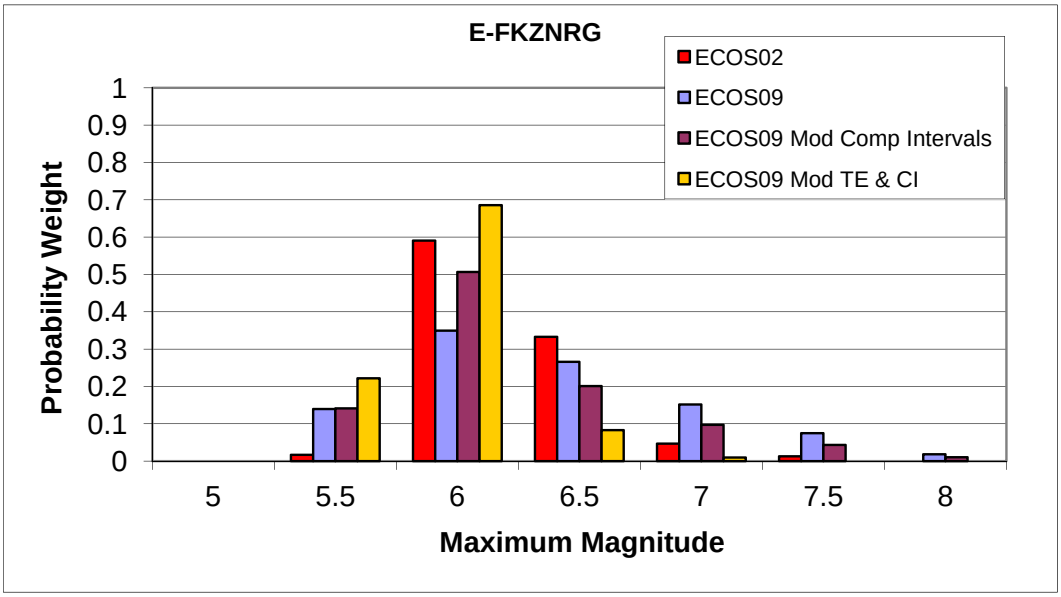

Figure 2.181: Maximum magnitude distributions for EG1d source E-FKZ& NRG.

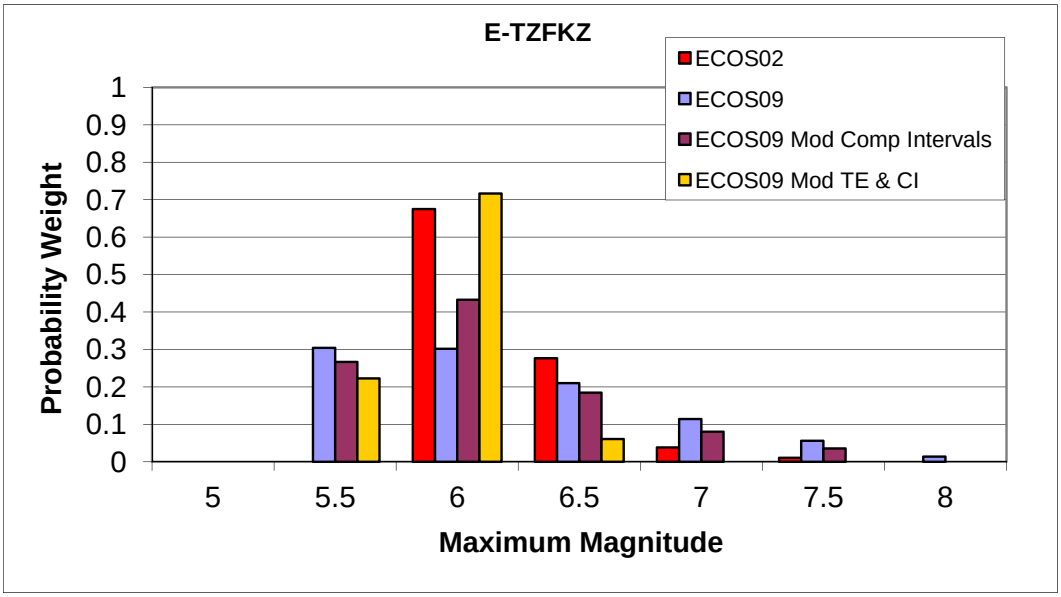

Figure 2.182: Maximum magnitude distributions for EG1d source E-TZ& FKZ.

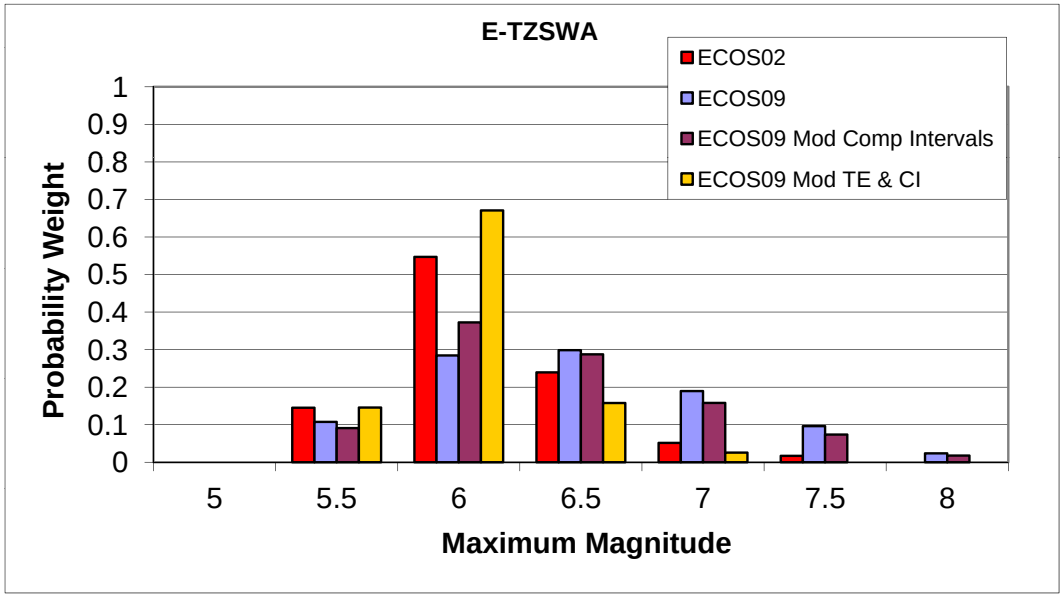

Figure 2.183: Maximum magnitude distributions for EG1d source E-TZ& SWA.

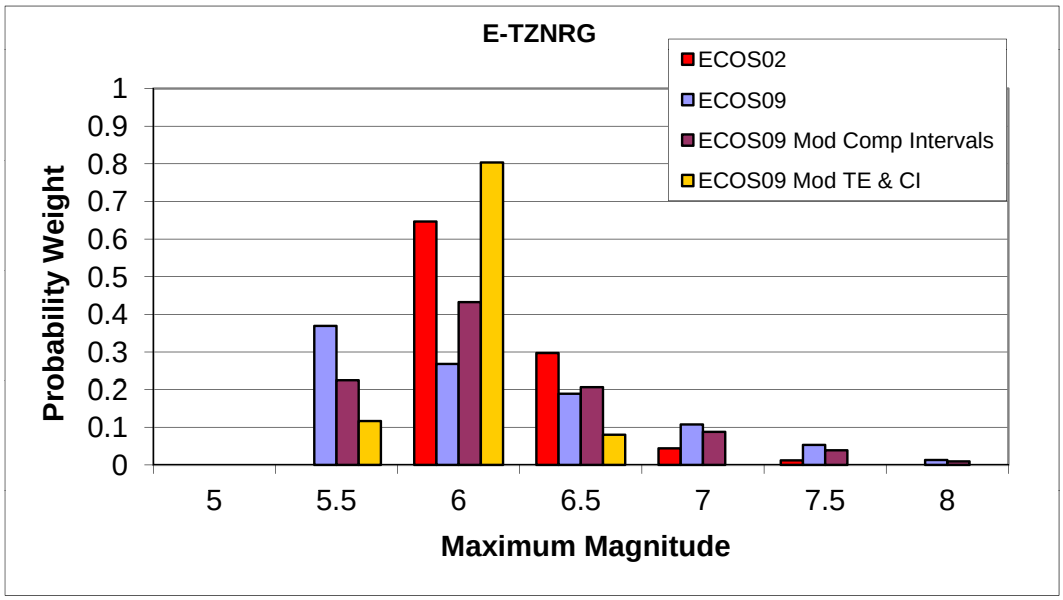

Figure 2.184: Maximum magnitude distributions for EG1d source E-TZ& NRG.

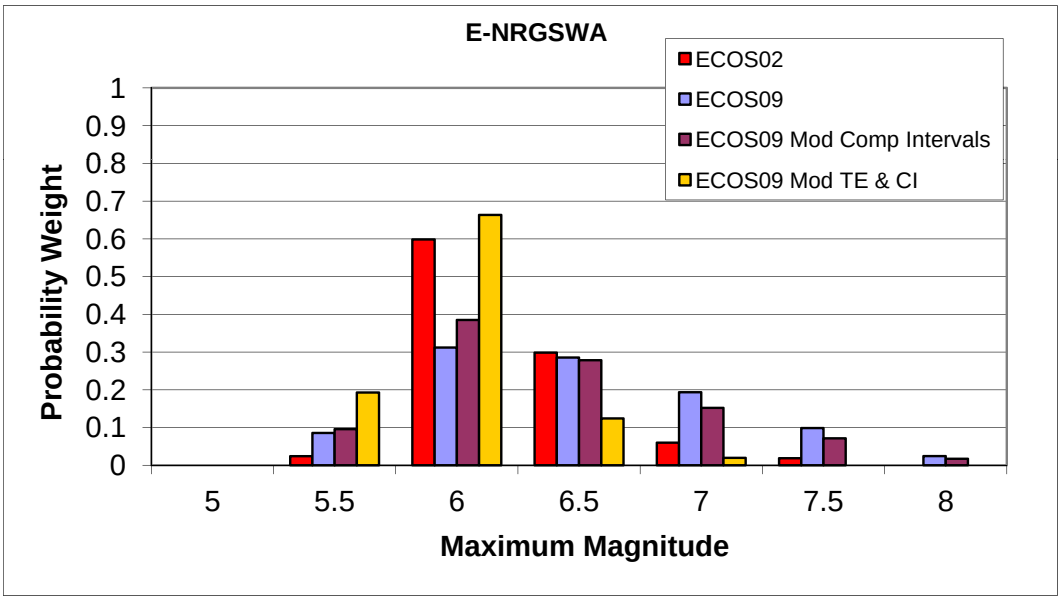

Figure 2.185: Maximum magnitude distributions for EG1d source E-NRG& SWA.

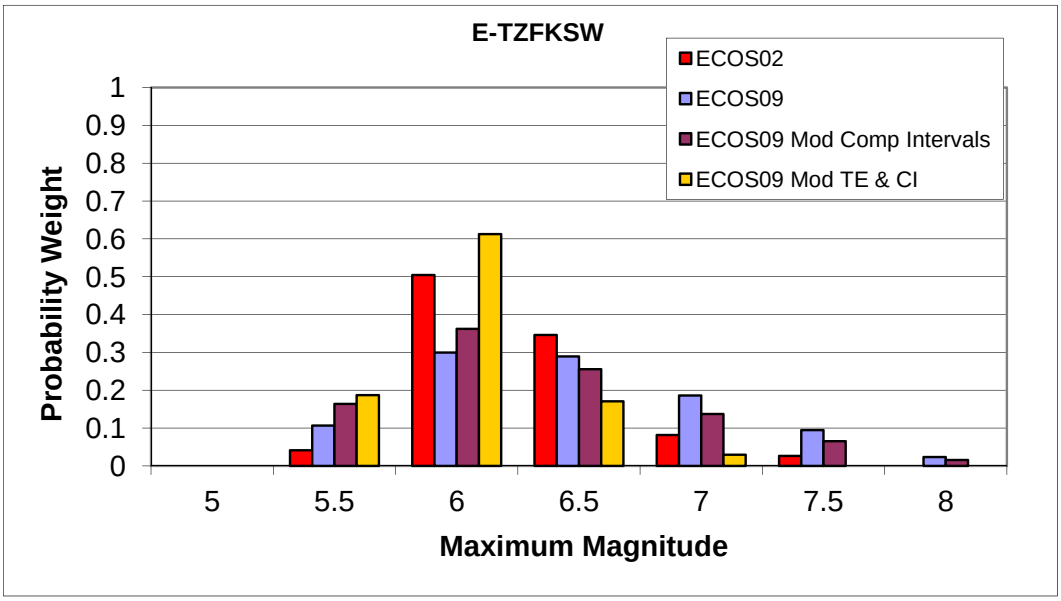

Figure 2.186: Maximum magnitude distributions for EG1d source E-TZ, FKZ, & SWA.

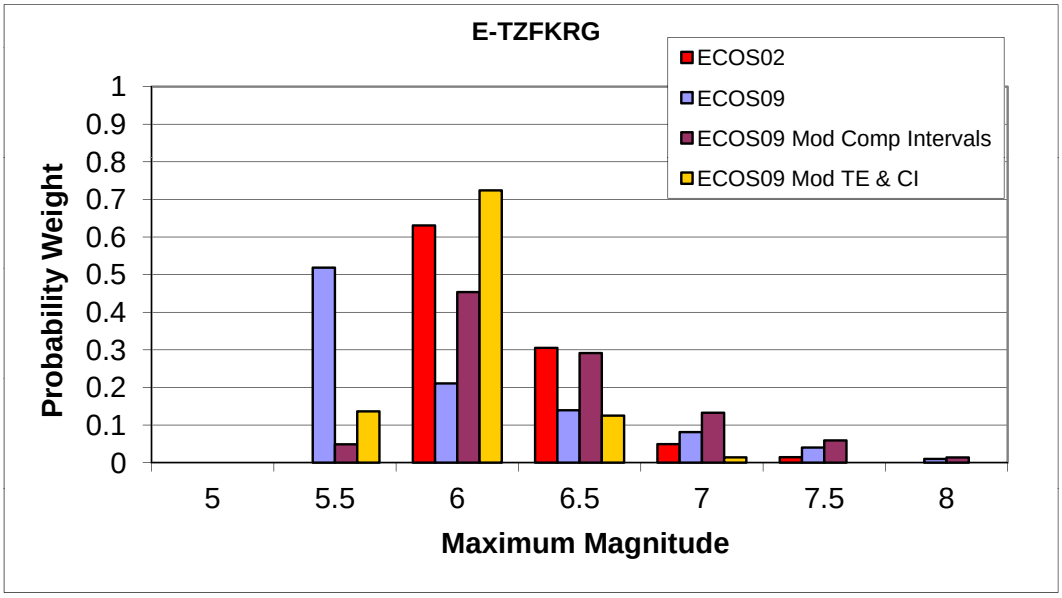

Figure 2.187: Maximum magnitude distributions for EG1d source E-TZ, FKZ, & NRG.

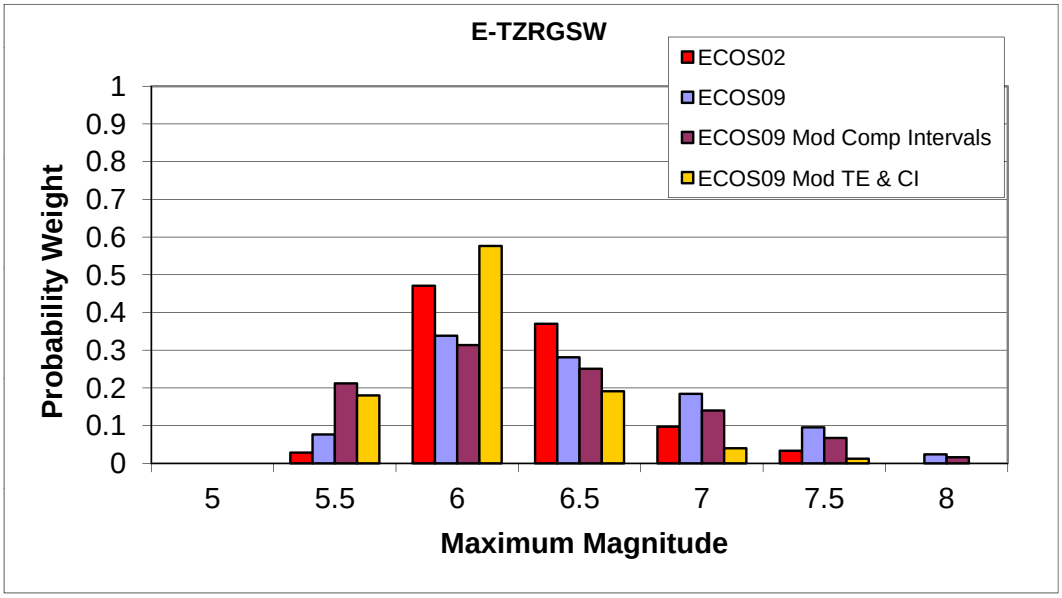

Figure 2.188: Maximum magnitude distributions for EG1d source E-TZ, NRG, & SWA.

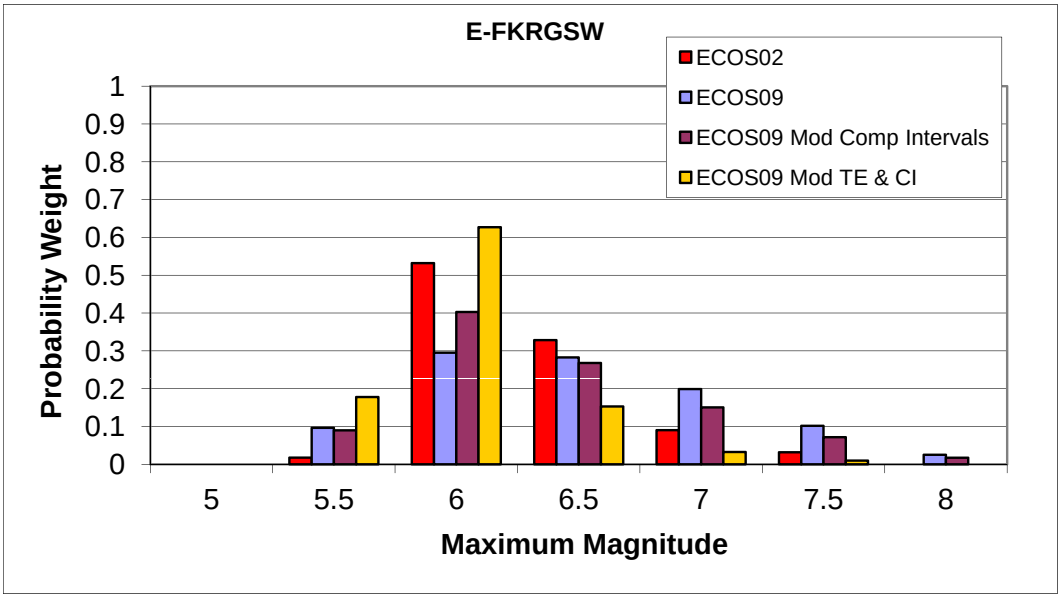

Figure 2.189: Maximum magnitude distributions for EG1d source E-FKZ, NRG, & SWA.

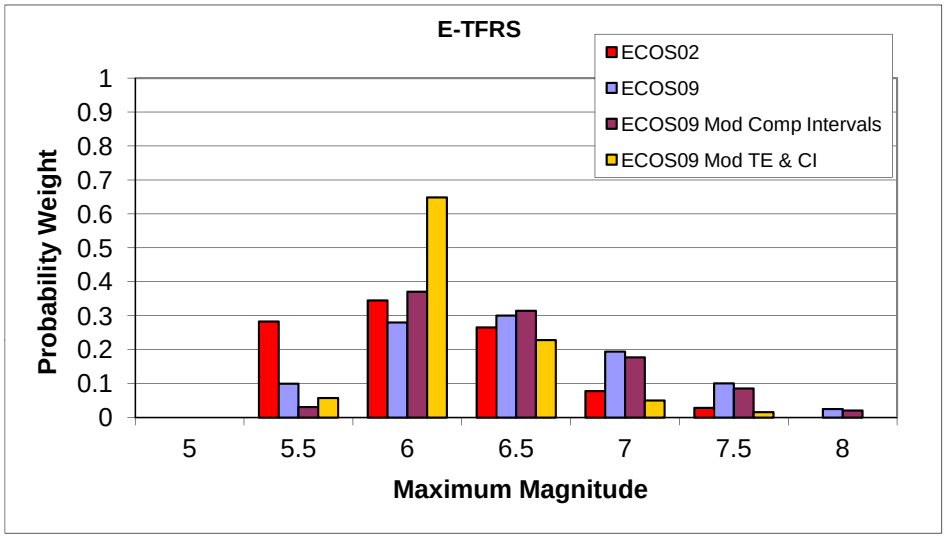

Figure 2.190: Maximum magnitude distributions for EG1d source E-TZ, FKZ, NRG, & SWA.

Part II

Assessments of EG1a

by N. Deichmann, S. Schmidt and D. Slejko

Chapter 1

EG1a Evaluation Summary (EG1-ES-1001)

After the workshop of 23. February 2010 the SP1a Experts considered modifications regarding the determination of activity rate, with respect to the previous assessment during the PEGASOS project. Such modifications result from the new scaling relation of M_W vs. M_L proposed for the Swiss earthquakes [Allmann et al. 2009]. A 3-step fit is proposed as a best fit of the data.

Fig. 4 in Allmann et al. [2009] shows that the dataset that deviates most from a constant shift of M_W with respect to M_L is that obtained with the Allmann method for determining M_W; in this case the deviation from a constant shift also applies for magnitudes larger than 4. The data obtained from the Edwards method rarely yield solutions of good quality for M_L smaller than 1.5. The results obtained with the Allmann method were calibrated based on the estimates provided by the Edwards method. Consequently, it seems reasonable to only consider results that refer to an M_L larger than 1.5 as reliable. Moreover, in the case of an improbable bias in the Edwards results, the same bias would have propagated to the Allmann results as well. Finally, from Fig. 4 of the Allmann et al. [2009] report it is not clear if the remaining data files considered (Clinton, Braunmiller, Bethmann, and Gruenthal) really show the same features of departure from a constant shift when converting to M_W. Based on these considerations the SP1a Experts decided to restrict their analysis of activity rate to M_W larger than 2.7, i.e. in an area where a constant shift of M_W from M_L can hold.

After considering the completeness periods, SP1a Experts propose to maintain those reported in their PEGASOS elicitation summary [Deichmann et al. 2003] by only introducing a correction to the magnitudes. To do this, scatter plots of identical events in ECOS-02 and ECOS-09 for each national catalogue were needed, similar to those reported in Figs. 13 to 15 of Wiemer and Wössner [2010]. These plots, moreover, need to separately refer to the historical (pre-1975) and instrumental periods. The average correction was identified for each M_W class directly from the plots and was compared for the low magnitudes with the evidence coming from the analysis of the Stepp plots already provided by R. Youngs. However, SP1a Experts needed a clarification by this author that the plots are based on the national

catalogues contributing to the ECOS-09 declustered catalogue with M_W properly updated. A preliminary comparison between the completeness periods of our elicitation summary (see page 77 and following of Deichmann et al. [2003]) and the evidence of the new Stepp plots is reported in table 1.1.

Table 1.1: Completeness periods for the national catalogues contributing to ECOS-09. Columns "old" refer to our elicitation summary (page 77 and following of Deichmann et al. [2003]), columns "new" refer to the Stepp plots provided by R. Youngs in January 2010.

M_W	D		F		I		A		W.Alps		CH	
	old	new	old	new	old	new	old	new	old	new	old	new
2.3											1975	
2.7		1975		1980		1980		1975		1975		1975
3.1		1900	1975	1975		1975		1900			1900	1900
3.2							1900					
3.3					1975							
3.5				1970								
3.9	1825	1825	1825	1820		1960			1900	1900	1879	1879
4.0					1900							
4.3						1900						
4.7	1775	1775				1800	1850		1820	1820	1750	1750
4.8					1800							
5.0								1890				
5.4	1500	1600	1825		1400	1400	1670				1680	1680
5.5									1750			
6.2	1250				1200		1550				1500	
7.0	1000		1000		1000		1200		1000			

1.1 Scaling Laws between M_W in the ECOS02 and ECOS09 Earthquake Catalogues

On July 16, 2010 the data supporting the plots received from R. Youngs on June, 2010 have been analyzed to identify the relations between the M_W values reported in the ECOS02 and ECOS09 earthquake catalogues. According to the notes sent by the EG1a team after the workshop of February 23, 2010, the attention has been focused to value larger than 2.7, because it does not seem reasonable to consider lower magnitude for seismic hazard assessment at this stage. In the following, countrywise evaluations are reported.

1.1.1 Austria

- Before 1975: Two trends are visible, one fits well with an M_W09=M_W02 line, while the second shows a clear shift downwards.
- After 1975: A great dispersion of points is visible considering all data, the situation is better but still not satisfactory considering only data with both M_W02 and M_W09 larger than, or equal to 2.5. A linear trend M_W02=M_W09 is visible, and it seems to be the best choice.
- Conclusions: For both periods a relation M_W09=M_W02 seems to be the most reasonable option.

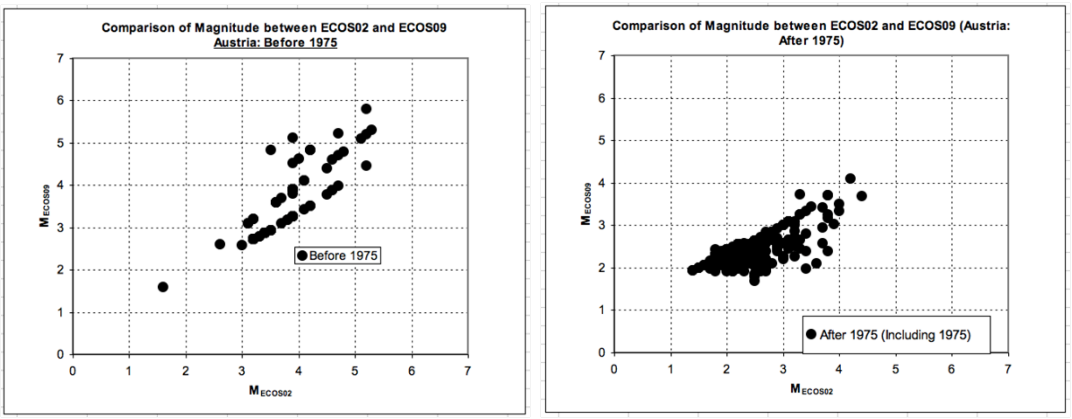

Figure 1.1: Comparison of magnitude between ECOS02 and ECOS09 - Austria.

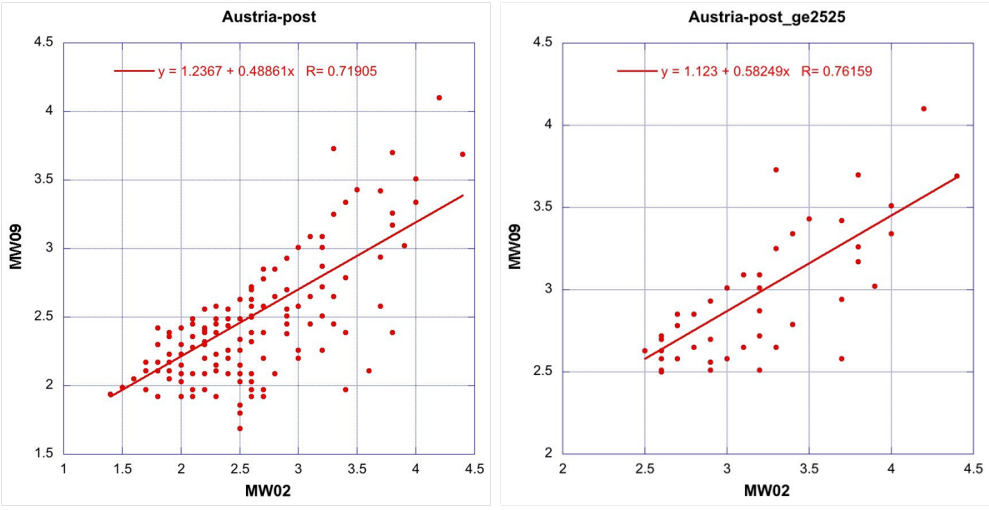

Figure 1.2: Comparison of magnitude between ECOS02 and ECOS09 - Austria.

1.1.2 France

- Before 1975: The relation M09=M02 holds almost perfectly.
- After 1975: The regression is not satisfactory using all data, while a good fit is obtained considering the data with both M_W02 and M_W09 larger than, or equal to, 2.5. In this case the linear fit $M_W09=0.36+0.89 \cdot M_W02$ seems to be acceptable.
- Conclusions: For the period pre-1975, a relation $M_W09=M_W02$ seems to be acceptable, while for the period post-1975, the relation $M_W09=0.36+0.89 \cdot M_W02$ is suggested.

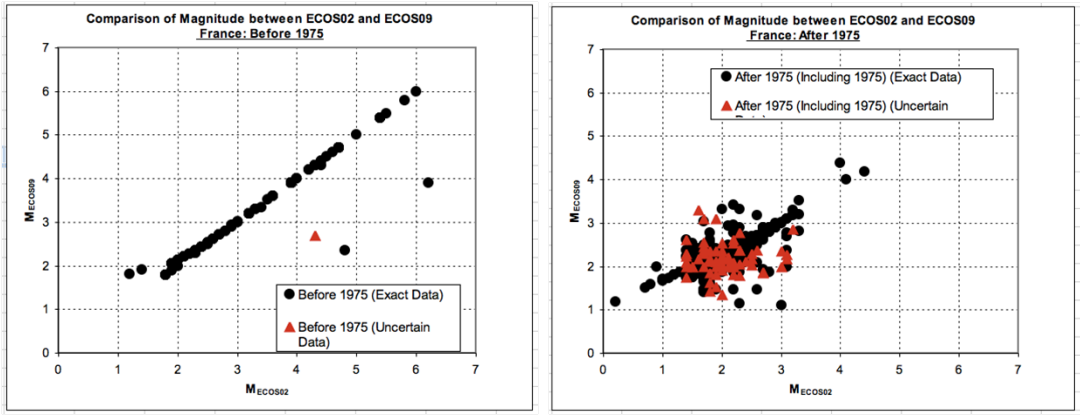

Figure 1.3: Comparison of magnitude between ECOS02 and ECOS09 - France.

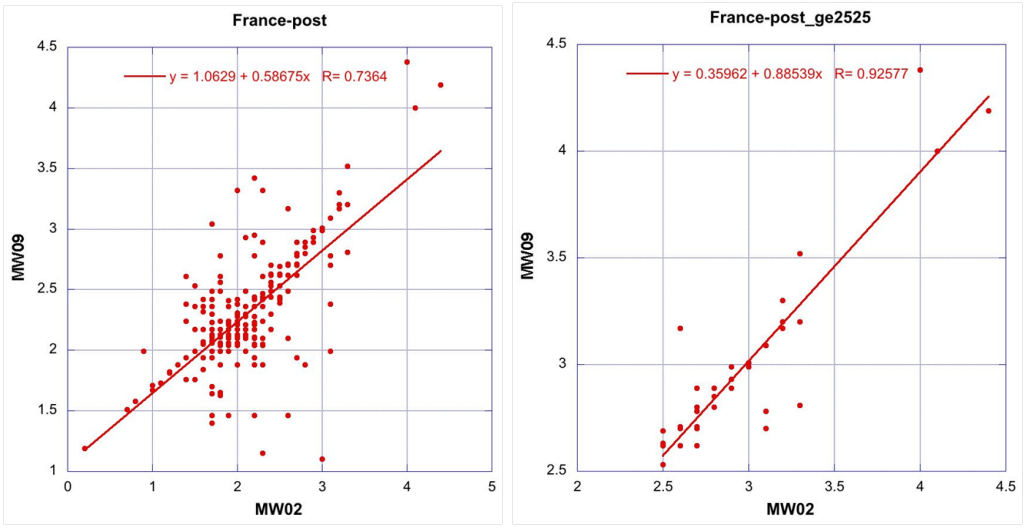

Figure 1.4: Comparison of magnitude between ECOS02 and ECOS09 - France.

1.1.3 Germany

- Before 1975: The relation M09=M02 holds almost perfectly for M_W02 larger than 2.0.
- After 1975: Considering all the data, a change in the slope can be seen, while considering only data with both M_W02 and M_W09 larger than, or equal to, 2.5, a quite good linear fit M09=0.408+0.878 · M02 is obtained.
- Conclusions: For the period pre-1975, a relation M_W09=M_W02 seems to be acceptable, while for the period post-1975, the relation M09=0.408+0.878 · M02 is suggested.

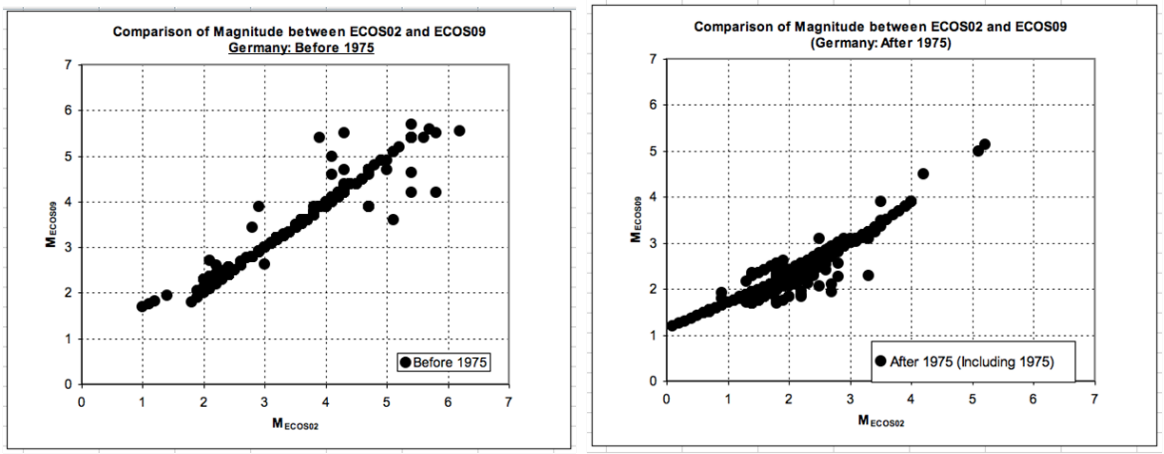

Figure 1.5: Comparison of magnitude between ECOS02 and ECOS09 - Germany.

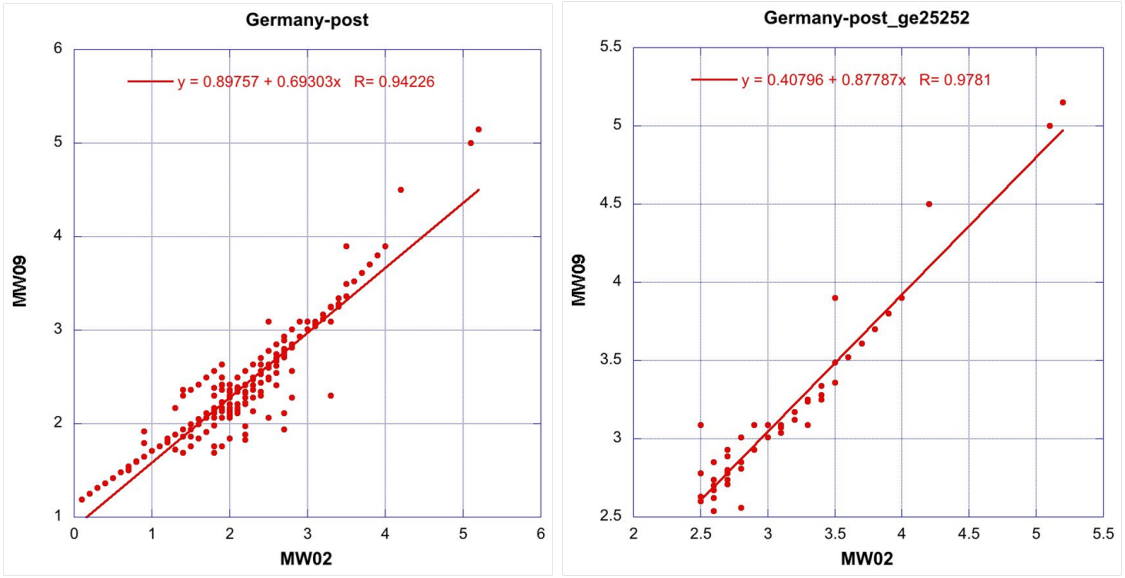

Figure 1.6: Comparison of magnitude between ECOS02 and ECOS09 - Germany.

1.1.4 Italy

- Before 1975: Although the situation is problematic because an additional trend is visible for events in the M_W range 4.5 to 6.0, the linear trend $M_W09{=}M_W02$ seems to be dominating.
- After 1975: Two linear trends are visible, one for M_W02 between 1.0 and 3.0 ($M_W09{=}1.093 \cdot M_W02{+}0.605$), and the second for M_W02 larger than 3.0 ($M_W09{=}0.412 \cdot M_W02{+}1.175$).
- Conclusions: For the period pre-1975, a relation $M_W09{=}M_W02$ seems to be proposed, while for the period post-1975, the relation $M_W09{=}1.093 \cdot M_W02{+}0.605$ is suggested for events with an M_W between 1.0 and 3.0, and the relation $M_W09{=}0.412 \cdot M_W02{+}1.175$ for those larger than 3.0.

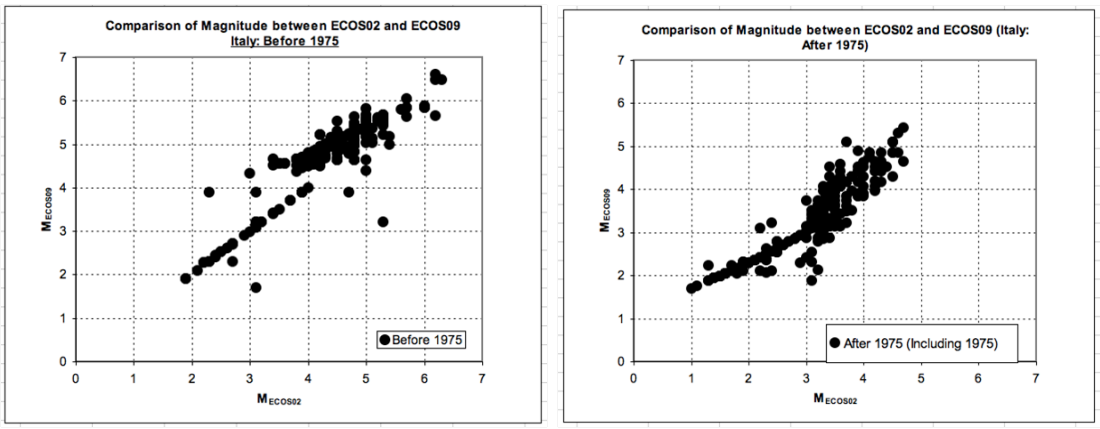

Figure 1.7: Comparison of magnitude between ECOS02 and ECOS09 - Italy.

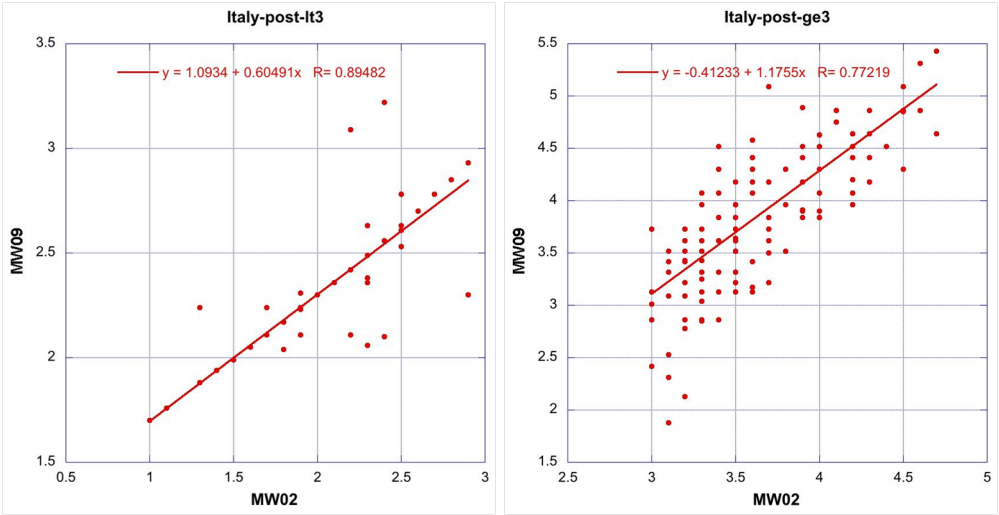

Figure 1.8: Comparison of magnitude between ECOS02 and ECOS09 - Italy.

1.1.5 Switzerland

- Before 1975: the relation M09=M02 holds almost perfectly for M_W02 larger than 2.0.
- After 1975: two linear trends are visible, one for M_W02 between 2.0 and 3.5, and the second for M_W02 larger than 3.5.
- Conclusions: For the period pre-1975, a relation M_W09=M_W02 seems to be acceptable, while for the period post-1975, the relation M09=0.113+0.955 · M02 is suggested for magnitudes 2.7 and over although it is calibrated on data exceeding 2.9.

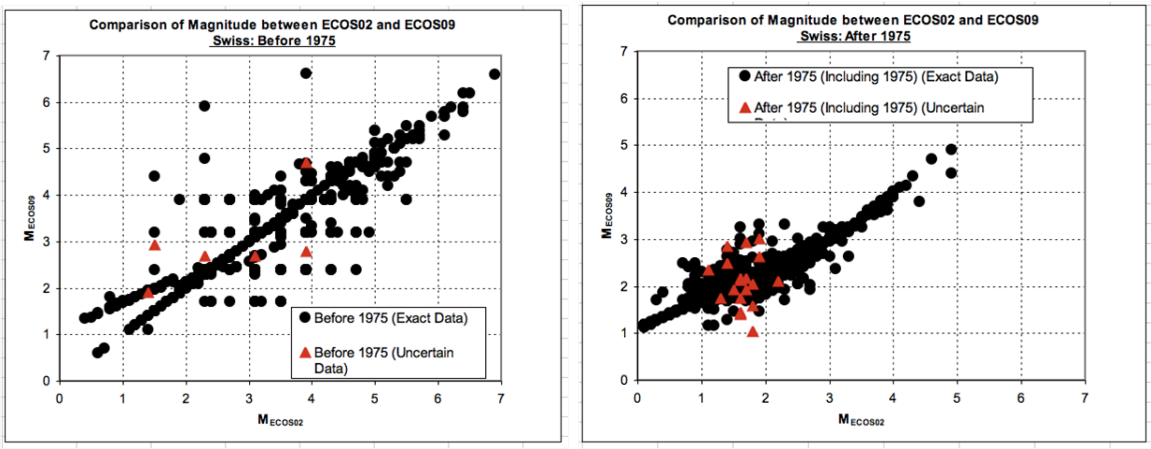

Figure 1.9: Comparison of magnitude between ECOS02 and ECOS09 - Switzerland.

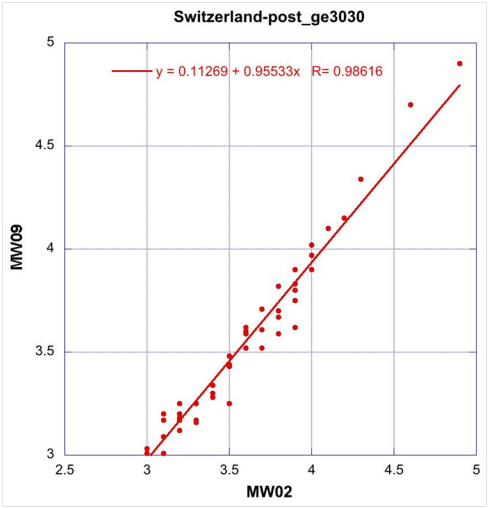

Figure 1.10: Comparison of magnitude between ECOS02 and ECOS09 - Switzerland.

1.1.6 Western Alps

- Before 1975: The relation M09=M02 holds almost perfectly for most of the events but, in addition, a quite large dispersion of data can be seen between M_W02 3.2 and 5.5.
- After 1975: The dispersion of data is quite large especially for M_W02 larger than 3. The linear trend M_W09=0.353+0.89 · M_W02 can be suggested for M_W02 larger than 2.0.
- Conclusions: For the period pre-1975, a relation M_W09=M_W02 seems to be acceptable, while for the period post-1975, the relation M_W09=0.353+0.89 · M_W02 is suggested.

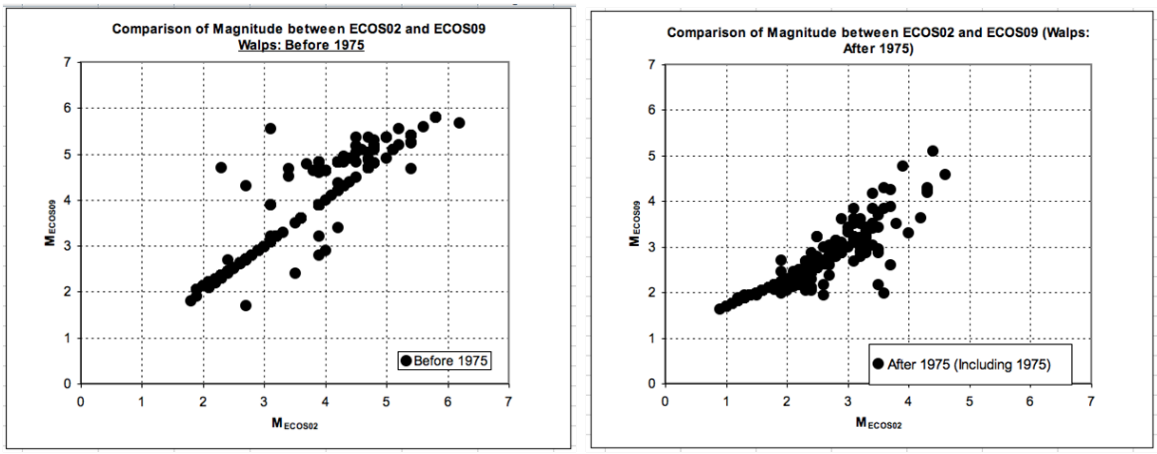

Figure 1.11: Comparison of magnitude between ECOS02 and ECOS09 - Western Alps.

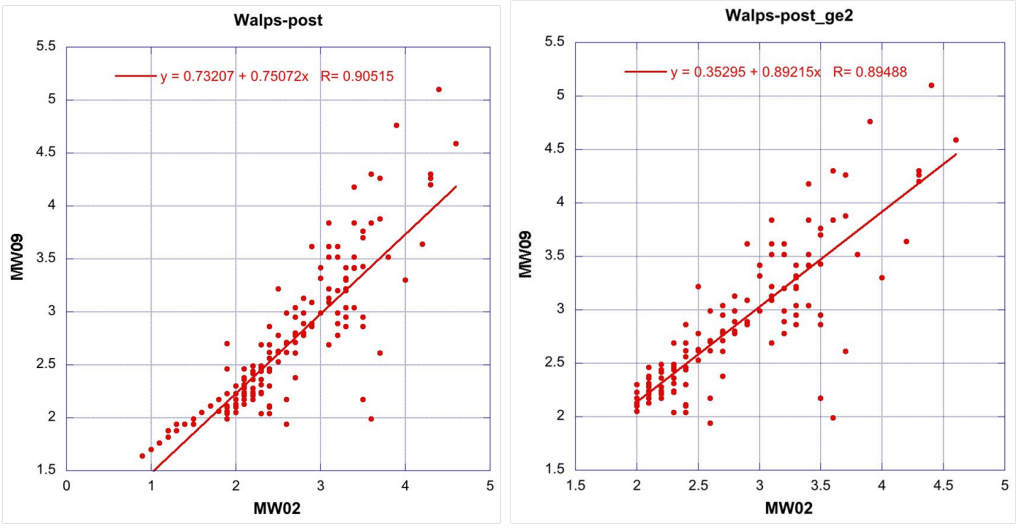

Figure 1.12: Comparison of magnitude between ECOS02 and ECOS09 - Western Alps.

From the analysis described before (no M_W shift needed for events in the pre-1975 period) it seems reasonable not to modify the completeness intervals of Deichmann et al. [2003] referring to M_W classes larger than 3.1, because they refer to periods longer than those starting from 1975 or after. For the low magnitudes, the analysis of the Stepp plots provided by R. Youngs in January 2010 and reported in the notes sent by the EG1a team after the workshop of February 23, 2010 can be considered valid. In conclusion, table 1.1 of the notes sent by the EG1a team after the workshop of February 23, 2010 is the basis for the final evaluation of completeness that is here reported in table 1.2.

Table 1.2: Completeness periods for the national catalogues contributing to ECOS-09. The bold values indicate new intervals coming from the analysis of the Stepp plots and not available in Deichmann et al. [2003].

M_W	D	F	I	A	W.Alps	CH
2.7	1975	1980	1980	1975	1975	1975
3.1	1900	1975	1975			1900
3.2				1900		
3.5		**1970**				
3.9	1825	1820	**1960**		1900	1879
4			1900			
4.7	1775			1850	1820	1750
4.8			1800			
5.4	**1600**		1400	1670		1680
5.5					1750	
6.2	1250		1200	1550		1500
7	1000	1000	1000	1200	1000	

1.2 Considerations on the new b-values

A comparison between the b-values calculated on the basis of the new catalogue and those of the EG1a elicitation summary is reported in the table 1.3, based on an evaluation of October 5, 2010.

This comparison points out the following considerations:

- Austria: Only the combined fit seems to be acceptable. The related b-value is in good agreement with that of the PEGASOS EG1a elicitation summary.
- France: Only the combined fit seems to be acceptable. The related b-value is significantly higher than that of the PEGASOS EG1a elicitation summary.
- Germany: The historical and the instrumental fits are in good agreement although the instrumental ones does not look good. They give a b-value not very different from that of the PEGASOS EG1a elicitation summary. The combined fit seems acceptable as well and it is better constrained by the data.
- Italy: All fits forecast for large events rates much higher than those observed. Consequently, the b-values are much lower than that of the PEGASOS EG1a elicitation summary.

Table 1.3: Considerations on the new b-values.

Region	Comb.	Hist.	Instr.	MZ	Cat.	Final
Zone A	0.768	0.733	0.645	0.92-1.00	1	0.96
Zone B	0.881	1.092	0.782	0.78-1.00	1	1
Zone C	0.805	0.991	0.981	0.72-0.82	1	0.92
Zone D1	0.797	0.926	1.049	0.74-0.86	1	0.93
Zone D23	0.898	0.934	1.052	0.85-0.90	1	0.94
Zone D4	0.758	0.655	0.762	0.99-1.03	1	1
Zone E1	0.616	0.767	0.95	0.68-0.90	0.94	0.95
Zone E23	0.801	1.014	1.205	0.80-0.90	0.89	0.89
Zone F1	1.184	1.615	1.472	0.84-1.04	0.94	0.95
Zone F2	0.874	1.067	1.219	0.89-0.93	0.88-0.94	0.9
Zone F3	0.856	1.076	1.019	0.79-0.85	0.94	0.88
Austria	0.944	0.631	1.185		0.981	
France	0.924	0.965	1.426		0.85	
Germany	0.847	1.172	1.103		0.94	
Italy	0.774	0.773	0.691		1.019	
Switzerland	0.866	0.978	1.069		0.97	
W. Alps	0.73	0.794	0.927		0.892	

- Switzerland: The historical and the instrumental fits are in good agreement and give b-values very similar to that of the PEGASOS EG1a elicitation summary. The combined fit overestimates largely the rates of the large events.

- Western Alps: The instrumental fit looks good and it is similar to that of the PEGASOS EG1a elicitation summary.

- Zone A: All combined, historical, and instrumental fits overestimate largely the rate of large magnitude events. The new results are remarkably lower than all those of the PEGASOS EG1a elicitation summary.

- Zone B: The combined fit looks good and it is reasonably close to those of the PEGASOS EG1a elicitation summary.

- Zone C: The historical and the instrumental fits are in good agreement although the historical one overestimates the rate of large events. Their agreement is not very bad also with all those of the PEGASOS EG1a elicitation summary.

- Zone D1: The historical and the instrumental fits are in a acceptable agreement although the historical one overestimates the rate of large events. Their agreement is not bad also with all those of the PEGASOS EG1a elicitation summary.

- Zone D23: The difference between the b-values from the combined, historical, and instrumental fits is about 0.1 and the estimate of the b-value agrees with all those of the PEGASOS EG1a elicitation summary.

- Zone D4: All fits are quite bad and giving b-values rather low with respect to those of the PEGASOS EG1a elicitation summary.

- Zone E1: All fits are not well constrained, the combined one is the lass bad but the related b-value is extremely lower with respect to that proposed in the PEGASOS EG1a elicitation summary. A large range of uncertainty was found in the elaboration for MZ of the EG1a team, pointing out also a possible low value.

- Zone E23: The historical fit seems to be the best and does not differ too much from those of the PEGASOS EG1a elicitation summary.

- Zone F1: The combined fit seems good and is higher, but not too much, than those of the PEGASOS EG1a elicitation summary. Conversely, very high b-values are related to the historical and instrumental fits.

- Zone F2: The combined fit can be preferred and it is in perfect agreement with those of the PEGASOS EG1a elicitation summary.

- Zone F3: Both the combined and the historical fits seems good: the combined one can be preferred because better constrained by the data and it is in perfect agreement with those of the PEGASOS EG1a elicitation summary.

As final remark, we can say that most of the new results in terms of Gutenberg-Richter fit and related b-value seem good. Furthermore, they "confirm" the conclusions reported in the PEGASOS EG1a elicitation summary for the results of the country catalogues. The agreement with the EG1a original results is fair for some zones but are quite different for others. This depends on the simplified approach applied now with respect to the articulated decisions taken by the EG1a. Accepting the present simplified approach, the following b-values can be preferred:

- Zone B: 0.88

- Zone C: 0.99

- Zone D1: 0.93

- Zone D23: 0.90

- Zone E23: 1.01

- Zone F1: 1.18

- Zone F2: 0.87

- Zone F3: 0.86

Simplifying the classes, the value 0.87 could be suggested for zones B, F2, and F3, the value 0.92 for zones D1 and D23, the value 1.00 for zones C and E23, and the value 1.18 for zone F1. A fixed standard deviation of 0.1 could represent the confidence in the results. The situation is more problematic for zones A, D4, and E1, where a b-value of 0.75 could be hypothesized with a large standard deviation, e.g.: 0.2.

1.3 Evaluation of the b-values Calculated for the Macro-Zones

On November 18, 2010 the EG1a experts define the b-values that should be assigned to the larger source zones as specified by EG1a in their original PEGASOS elicitation summary (the so-called macro-zones shown below in Figure 1.13)

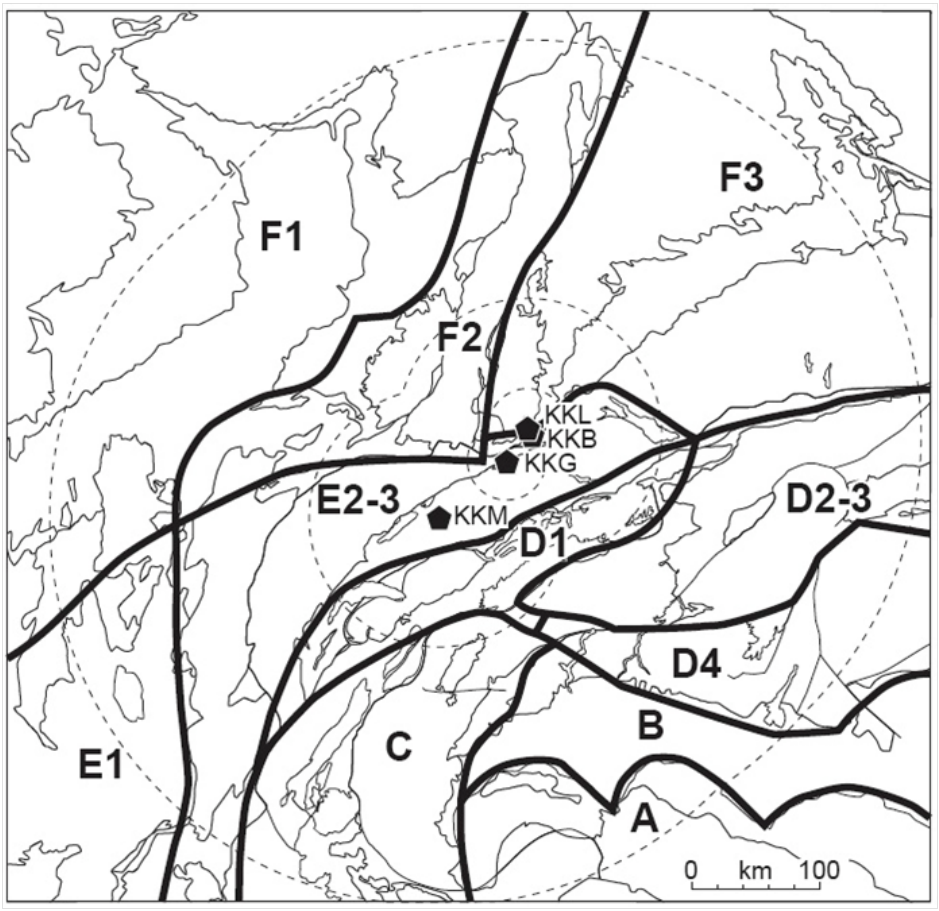

Figure 1.13: Map of the macro-zones as defined in the original PEGASOS EG1a Elicitation Summary.

The basis for the present evaluation are the following three tables (tables 1.4, 1.5, 1.6) and the corresponding Gutenberg-Richter (GR) plots and regressions. We also refer to the final version of the ECOS-09 report [SED 2010].

Table 1.4: Summary b-value table of the PEGASOS EG1a elicitation summary (Table 8) Comparison between the different b-values calculated and final b-values proposed.

MZ	CAT	b-CAT	sb-CAT	b-MZ	b-MZ range	b	$\sigma(b)$
A	I	1	0.1	0.96	0.92-1.00	0.96	0.1
B	I	1	0.1	1	0.78-1.00	1	0.1
C	F,I,CH	1	0.1	0.78	0.72-0.82	0.92	0.1
D1	CH,F	1	0.1	0.85	0.74-0.86	0.93	0.1
D2-3	CH,A	1	0.1	0.88	0.85-0.90	0.94	0.1
D4	I,CH	1	0.1	1	0.99-1.03	1	0.1
E1	F	0.94	0.1		0.68-0.90	0.95	0.1
E2-3	CH,F	0.89	0.1	0.85	0.80-0.90	0.89	0.1
F1	F	0.94	0.1	0.95	0.84-1.04	0.95	0.1
F2	D,CH,F	0.88-0.94	0.1	0.91	0.89-0.93	0.9	0.1
F3	D	0.94	0.1	0.81	0.79-0.85	0.88	0.1

MZ: macro zone;
CAT: dominating catalog(s) for the MZ;
b-CAT: b-values for CAT. A direct association of CAT to MZ is problematic but can drive the choice;
b-MZ: b-values for MZ;
b-MZ range: range of possible b-values for MZ;
b: final b-values proposed;
$\sigma(b)$: b-value standard deviation.

Table 1.5: Summary of first version b-values by R. Youngs (Sept. 4, 2010) with b-values computed for the combined historical and instrumental data and for the data split into historical and instrumental periods but constrained to give a single b-value.

Region	Combined		Split Instr. & Historical	
	b-value	$\sigma(b)$	b-value	$\sigma(b)$
Zone A	0.768	0.024	0.7	0.089
Zone B	0.881	0.072	0.763	0.194
Zone C	0.805	0.032	0.988	0.062
Zone D1	0.797	0.035	0.941	0.041
Zone D23	0.898	0.041	0.962	0.045
Zone D4	0.758	0.041	0.695	0.066
Zone E1	0.616	0.105	0.939	0.379
Zone E23	0.801	0.041	1.041	0.056
Zone F1	1.184	0.087	1.498	0.382
Zone F2	0.874	0.054	1.115	0.137
Zone F3	0.856	0.044	1.058	0.21
Austria	0.944	0.08	0.82	0.072
France	0.924	0.058	1.211	0.23
Germany	0.847	0.035	1.143	0.148
Italy	0.774	0.019	0.729	0.071
Switzerland	0.866	0.024	0.992	0.027
W. Alps	0.73	0.029	0.85	0.127

Table 1.6: Summary of the second version b-values by Bob Youngs (Sept. 29, 2010) with b-values from the combined historical and instrumental data (as above) and for the data split into historical and instrumental periods, computed separately without constraint.

Region	Combined		Split Instrumental and Historical			
			Historical		Instrumental	
	b-value	$\sigma(b)$	b-value	$\sigma(b)$	b-value	$\sigma(b)$
Zone A	0.768	0.024	0.733	0.058	0.645	0.038
Zone B	0.881	0.072	1.092	0.268	0.782	0.144
Zone C	0.805	0.032	0.991	0.108	0.981	0.075
Zone D1	0.797	0.035	0.926	0.043	1.049	0.12
Zone D23	0.898	0.041	0.934	0.05	1.052	0.095
Zone D4	0.758	0.041	0.655	0.176	0.762	0.076
Zone E1	0.616	0.105	0.767	0.147	0.95	0.33
Zone E23	0.801	0.041	1.014	0.062	1.205	0.143
Zone F1	1.184	0.087	1.615	0.387	1.472	0.172
Zone F2	0.874	0.054	1.067	0.257	1.219	0.135
Zone F3	0.856	0.044	1.076	0.212	1.019	0.12
Austria	0.944	0.08	0.631	0.077	1.185	0.146
France	0.924	0.058	0.965	0.228	1.426	0.146
Germany	0.847	0.035	1.172	0.149	1.103	0.1
Italy	0.774	0.019	0.773	0.073	0.691	0.032
Switzerland	0.866	0.024	0.978	0.03	1.069	0.071
W. Alps	0.73	0.029	0.794	0.122	0.927	0.069

A first conclusion from inspection of the GR-plots provided by R. Youngs is that the apparent differences in activity rates between the instrumental and historical periods already noticed in the ECOS-02 catalog have not disappeared from the ECOS-09 catalog, despite the revision. To attempt to find a reason for the differences in apparent activity rates is beyond the scope of this document. However, it is clear that calculating a single b-value from two datasets with different activity rates that have been merged into a single GR-plot (the values labled "Combined" in tables 1.5 and 1.6) does not make sense. Nevertheless, it is reasonable to assume that b-values should not be different for the two periods. Therefore the b-values derived from the datasets split into historical and instrumental periods, but with the constraint that the b-values should be the same for both periods, are the preferred values (listed above in table 1.5 under the heading "Split instrumental and historical"). However, the additional calculations performed without this constraint constitute a valuable help for judging the reliability of the results. Moreover, the computations of b-values for the individual national catalogs serve as a consistency check and to assess possible reasons for unexpected results.

In the following, we first evaluate the five macro-zones that are closest to or actually contain the sites of the four nuclear power plants (D1, D23, E23, F2 and F3). Based on the sensitivity studies performed under the original PEGASOS project, they are the most important for characterizing the seismic hazard. In a second step we then evaluate the other six more distant zones (A, B, C, D4, E1 and F1). For understanding the b-values obtained for the macro-zones it is in addition useful to examine the b-values obtained separately for the individual national catalogs.

1.3.1 Evaluation of the Closer Macro-Zones D1, D23, E23, F2, and F3

- Zone D1 (Haute Savoye, Central and Northern Alps of Switzerland): 0.94 ±0.04 The difference between the separately calculated b-values is 0.12. Most of the data in this zone comes from the Swiss catalog; the contribution of the French catalog is minor. The regressions fit the data over the entire magnitude range for both time periods.

- Zone D23 (Eastern Alps): 0.96 ±0.05 The difference between the separately calculated b-values is 0.12. Most of the data in this zone comes from the Swiss catalog, with some contribution from the Austrian catalog. The regressions fit the data over the entire magnitude range for both time periods.

- Zone E23 (Molasse Basin and Jura): 1.04 ±0.06 The difference between the separately calculated b-values is 0.19. Most of the data in this zone comes from the Swiss catalog; the contribution of the French catalog is minor. The regressions fit the data over the entire magnitude range for both time periods.

- Zone F2 (Rhine Graben and Bresse Transfer Zone): 1.12 ±0.14 The difference between the separately calculated b-values is 0.15. The data of this zone is based a conglomerate of French, German and Swiss catalogs. The slightly elevated b-value of this zone possibly reflects the elevated b-values of the former two catalogs relative to the latter catalog. The regressions fit the data over the entire magnitude range for both time periods, except for the largest magnitude bin of the historical data, which corresponds to the 1356 Basel event.

- Zone F3 (SW Germany): 1.06 ±0.21 The difference between the separately calculated b-values is 0.06. The data of this zone relies almost entirely on the German catalog. The regression fits the historical data over the entire magnitude range, while the fit of the larger-magnitude bins of the instrumental period is poor.

We note that in general the new b-values for these five macro-zones are either almost identical to those proposed in the original PEGASOS elicitation summary (zones D1 and D23, difference < 0.3) or slightly higher (E23, F2 and F3, differences 0.15-0.22) than the old ones. At least for the instrumental period, an increase of the b-values is in a qualitative agreement with the new M_L to M_W scaling derived for ECOS-09.

1.3.2 Evaluation of the More Distant Macro-Zones A, B, C, D4, E1 and F1

- Zone A (Appenines): 0.70 ±0.09 The data of zone A are based entirely on the Italian catalog (original M_L values converted to Swiss M_L and then converted to M_W). The instrumental data follow a linear relation with an unusually low b-value (b = 0.645). The historical data deviate strongly from a linear GR relation (frequency of large magnitude events is poorly predicted).

- Zone B (Po Plain): 0.76 ±0.19 The data of zone B are based entirely on the Italian catalog (original M_L values converted to Swiss M_L and then converted to M_W). The instrumental period has a low b-value of 0.78 and the historical period a higher b-value of 1.09. However, the cumulative number of events in the M = 4.3 bin are almost identical, so that in this case the cumulative b-value of 0.88 appears to be more reliable than the single value derived from the split data.

- Zone C (Western Alps and southern Valais): 0.99 ±0.06 Although the data for this zone is a conglomerate of the Swiss, French and Italian catalogs, the Valais and thus the Swiss catalog is a major part of it. The b-value for the split periods with the single-value constraint in table 1.5 matches the average b-value of the Swiss catalog. Moreover the difference between the b-values calculated separately for the historical and instrumental period is small (0.01). With 0.99 it is slightly higher than the old (ECOS-02) value of 0.92.

- Zone D4 (Southern Alps): 0.70 ±0.07 The data of zone D4 are based mostly on the Italian catalog (original M_L values converted to Swiss M_L and then converted to M_w) with a minor contribution from the Swiss catalog. The cumulative-frequency data for the historical period is highly nonlinear and the corresponding b-value of 0.655 is unusually low. The fit to the instrumental data is a little better, but the corresponding b-value of 0.76 is also unusually low.

- Zone E1 (SE France): 0.94 ±0.38 The data of zone E1 are based entirely on the French catalog (original M_L values converted to Swiss M_L and then converted to M_W). The regression through the historical data alone gives a b-value of 0.77 ±0.33. The instrumental data consists of a single bin at $M_W = 2.7$ and it is unclear how the corresponding b-value of 0.95 was derived. How the joint b-value of 0.94 was derived in this case is similarly unclear. Thus the b-value for this zone is effectively undetermined. A similar problem was already encountered in the original elicitation summery.

- Zone F1 (NE France): 1.50 ±0.38 The data of zone F1 are based entirely on the French catalog (original M_L values converted to Swiss M_L and then converted to M_W). The b-values determined separately for the historical and instrumental periods are 1.62 ±0.39 and 1.47 ±0.17. The single value of 1.50 is in between, but unusually large and, with a sigma of 0.38, it is obviously not very reliable.

We note that the difference between the new and the old value is small for zone C (0.99 instead of 0.92). For zones A, B and D4 the new b-values are substantially lower than the old ones (0.70, 0.76 and 0.70 instead of 0.96, 1.00 and 1.00) and for zone F1 the new b-value is substantially higher (1.50 instead of 0.95). Since for zone E1 the new b-value is essentially undetermined, a comparison with the old one is meaningless.

1.3.3 Evaluation of the b-values of the National Catalogs

In order to assess the reliability of the macro-zone b-values, it is useful to evaluate the b-values obtained for the national catalogs. Here the different b-values computed from separate regressions for the historical and instrumental periods (table 1.6) can serve as a check on the consistency of the individual catalogs with their corresponding magnitude conversions. So in the following we summarize the b-values for the historical and instrumental periods for each catalog with a qualitative evaluation of the goodness of fit of the corresponding regression, and for each catalog we evaluate the consistency between the historical and instrumental periods, We also recall the difficulties associated with the derivation of conversion from the original M_L values to the Swiss M_L values, as documented in Appendix K to the ECOS-09 report [SED 2010].

- Austria
  Historical: 0.63 ± 0.08 good fit for all magnitude bins, unusually low value
  Instrumental: 1.18 ± 0.15 poor fit of largest magnitude bin
  inconsistent historical/instrumental values
  instrumental magnitude (M_L/M_L) conversion moderately reliable

- France
  Historical: 0.96 ± 0.23 good fit for all magnitude bins but large sigma
  Instrumental: 1.43 ± 0.15 poor fit of the three largest magnitude bins, unusually high value
  inconsistent historical/instrumental values
  instrumental magnitude (M_L/M_L) conversion unreliable

- Germany
  Historical: 1.17 ± 0.15 good fit for all magnitude bins
  Instrumental: 1.10 ± 0.10 poor fit of the largest magnitude bin
  consistent historical/instrumental values
  instrumental magnitude (M_L/M_L) conversion reliable

- Italy
  Historical: 0.77 ± 0.07 non-linear Gutenberg-Richter plot and poor fit of all magnitude bins
  Instrumental: 0.69 ± 0.03 poor fit of the largest magnitude bin, unusually low value
  consistent historical/instrumental values instrumental magnitude (M_L/M_L) conversion unreliable

- Switzerland
  Historical: 0.98 ± 0.03 good fit for all magnitude bins
  Instrumental: 1.07 ± 0.07 good fit for all magnitude bins
  consistent historical/instrumental values no instrumental magnitude (M_L/M_L) conversion necessary

1.3.4 Discussion

Differences between b-values derived from the ECOS-02 and the ECOS-09 catalog can be due to a combination of several reasons:

1. The reevaluation of intensities and magnitudes of the historical data;
2. Revised conversion relations between foreign and Swiss local magnitudes;
3. The new conversion relation between Swiss M_L and M_W;
4. The chosen minimum magnitude of M_W 2.7 as a consequence of the non-linear scaling between M_L and M_W at lower magnitudes.

From inspection of the GR-plots it is clear that the data quality and consistency is good for some of the macro-zones, whereas it is poor for others. "Good" here means that calculated sigma-values are low (< 0.1) and, more importantly, that b-values calculated separately for the historical and instrumental periods are comparable. In addition, a good GR relation should predict the observations over the entire range of observed magnitudes - substantial deviations of the observations from a linear relation are taken as a sign that both the data and the calculated b-values are unreliable. In this sense, the GR-plots for macro-zones C, D1, D23, E23, F2, and F3 can be considered good, while for macro-zones A, B, D4, E1 and F1 they are poor. In addition, the new b-values obtained for zones A, B and D4 are unusually low and differ strongly from the old values. This is consistent with the fact that the data for these three zones relies either entirely or to a large part on the Italian catalog, for which the new b-value is similarly low. Considering the heterogeneity of the Italian catalog and the difficulties encountered in the attempt of deriving consistent and reliable conversion relations for converting the Italian magnitudes to Swiss magnitudes (see Appendix K of the ECOS-09 report) these results are not entirely surprising. Exactly the same can be said for the French catalog, which supplies the entire data for zones E1 and F1, except that in the case of zone F1 the new b-value is unusually high, which is consistent with the high instrumental b-value of the French catalog. We therefore suspect that at least part of the problem with the poorly determined b-values for zones A, B, D4, E1 and F1 could be due to a bias introduced by the

chain of magnitude conversions that were necessary to obtain a unified moment magnitude for the entire catalog.

1.3.5 Conclusions

The b-values proposed below for the six well-determined macro-zones C, D1, D23, E23, F2, and F3 correspond to the values in table 1.5 (single value determined simultaneously from the separate historical and instrumental datasets). In the original PEGASOS elicitation summary, all macro-zone b-values were assigned a one-sigma uncertainty of 0.1. Following the arguments in the original report and assuming that 0.1 is the lower bound for a realistic estimate of the uncertainty, we adopt either 0.1 or the uncertainty derived from the GR-regression in table 1.5, if the latter is larger.

Zone C	(Western Alps and southern Valais):	0.99 ± 0.1
Zone D1	(Haute Savoye, Central and Northern Alps of Switzerland):	0.94 ± 0.1
Zone D23	(Eastern Alps):	0.96 ± 0.1
Zone E23	(Molasse Basin and Jura):	1.04 ± 0.1
Zone F2	(Rhine Graben and Bresse Transfer Zone):	1.12 ± 0.14
Zone F3	(SW Germany):	1.06 ± 0.21

As already noted, the data comprising zones A, B and D4 are almost entirely subsets of the Italian catalog. Except for the regression through the GR-plot of the historical period in zone B, which results in a b-value of 1.09 $\pm$0.27, all b-values calculated for datasets based on the contribution of the Italian catalog to ECOS09 result in b-values between 0.65 and 0.77. Although the data in most of the GR-plots for these zones deviate from a linear relation and the corresponding regressions often do not fit the entire magnitude range, the resulting low b-values for both the historical and instrumental periods are surprisingly consistent. Thus an explanation for these low b-values in terms of systematic errors in the conversion of the original instrumental magnitudes into Swiss M_L is not plausible. These values are unusually low not only when compared to the b-values obtained for all other macro-zones and catalogs, but also when compared to the values around 1.0 obtained for the same zones from ECOS-02 (see above in table 1.4). They are even lower when compared with the values used for the Italian national hazard assessments in the same general regions, where values between 1.30 and 1.54 are used [Gruppo di Lavoro 2004]. Therefore, given the diverging estimates for the b-values in these zones that we can not resolve at this time, we follow the reasoning adopted in the original elicitation summary and assign a common b-value of 1.0 to these three macro-zones.

The data comprising zones E1 and F1 are small subsets of the French catalog alone. Because of the small number of events in these zones, the same difficulties in defining robust b-values for these two zones were encountered also in the course of the original elicitation summary based on ECOS-02. Here we note that the most reliable regression through the various GR-plots of zones E1, F1 and the French catalog appears to be the one for the historical data of the French catalog, which results in a b-value of 0.96 $\pm$0.23. We therefore assign this value to both the E1 and the F1 macro-zone. This avoids a possible bias due to systematic errors in the M_L conversion from the heterogeneous magnitudes in the French instrumental data and it is also consistent with the procedure adopted in the original PEGASOS elicitation summary.

To the poorly determined b-values of the five macro-zones A, B, D4, E1 and F1 we assign an uncertainty of ±0.3. This value is more or less consistent with the corresponding uncertainties listed above in table 1.5.

Zone A (Appenines):	1.0 ± 0.3
Zone B (Po Plain):	1.0 ± 0.3
Zone D4 (Southern Alps):	1.0 ± 0.3
Zone E1 (SE France):	0.96 ± 0.3
Zone F1 (NE France):	0.96 ± 0.3

Considering that all five of these macro-zones are distant from the nuclear power plant sites, the somewhat arbitrary nature of the assigned b-values and the associated large uncertainty will not have a serious effect on the computed hazard.

1.4 Re-evaluation of Recurrence Rates

On March 30, 2011 the EG1a experts performed a re-evaluation of the a-values. Plots provided by R. Youngs pinpoint some situations where the decisions taken earlier seem questionable. Nevertheless, in most cases, conversely, the situation is reasonable. The questionable cases all relate to the zones where a large uncertainty (0.2 to 0.3) was proposed for the b-value (macrozones A, B, D4, E1, F1, F3). The idea of R. Youngs to reduce the percentiles is interesting but sometimes it does not allow us to capture the real uncertainty. A 3-point approximation to a uniform distribution, also suggested by R. Youngs, seems to spread the results in a too large range. Consequently, we should remain anchored to the original PEGASOS choices.

For the macrozones A and B, although the extreme percentiles lead to very different estimates of a-values, that they represent the real uncertainty of the magnitude distribution. The zones in the macrozone D4 are characterized either by very poor data (D4a and D4c) or by an odd distribution (D4b): perhaps the proposed b-value of 1.0 could be re-modulated to a lower value but in this case the only 2 magnitude classes larger than 5 would be missed. The lower b-value of 0.7 (±0.2) seems more appropriate for macrozone E1, and would not contradict our evaluation of section 1.3 where it is written "the b-value for this zone is effectively undetermined". As the value 0.77 (±0.33) was obtained with the historical data alone, and it does not differ too much from the value suggested by the new plots. Three zones of macrozone E2-3 show an unsatisfactory situation because they are characterized either by very poor (E2b and E2c) or odd (E2a) magnitude distributions. As the situation is reasonable for all the other zones of the macrozone, we have to live with those three unsatisfactory situations.

The higher b-value of 1.0 (±0.2) seems more appropriate for macrozone F1, and would not contradict our evaluation of section 1.3 where it is written "for zone E1 the new b-value is essentially undetermined" as the single value of 1.50 is the average of the different estimates obtained, but it is unusually large and, with a sigma of 0.38, it is obviously not very reliable. The bad situation of several zones in macrozone F3 is justified by the contradictory magnitude distributions of instrumental and historical events and it is represented by the present large uncertainty of the b-value.

As final remark, it is worth noting that the Basel earthquake remains apart of all the magnitude distributions in zones RF, F2d, and F2e. In conclusion, almost all magnitude distributions

seems reasonable with the exception of those referring to macrozones E1 and F1. For these macrozones the b-value of the French catalogue (0.96 ±0.3) was originally proposed. Although that suggestion sounds still valid, the new individual plots point out large differences between the 2 macrozones. Consequently, the individual b-values of 0.77 ±0.33 (or alternatively of 0.7 ±0.2) and 1.0 ±0.2 could be proposed for macrozone E1 and F1, respectively. The fact that the Basel earthquake does not agree with most of the distributions, and presents a rate notably higher than that suggested by the distributions, should be considered with more attention.

1.5 Re-evaluation of the Recurrence Rates for each Source Zone

On May 9, 2011 the EG1a experts finally evaluated the recurrence rates for each source zone calculated by R. Youngs and documented in his technical note of March 24, 2011. As reference we include herein the table with the b-values and weights proposed by R. Youngs from his document (see below). The b-value for each source zone is derived from the corresponding macro-zone (as documented in section 1.3 of Nov. 18, 2010). The recurrence rates were calculated using these b-values and their estimated errors, matched to the frequency-magnitude plots for each source zone. Following the strategy used in the original PEGASOS EG1a Elicitation Summary, the macro-zone b-values were anchored at different subsets of the frequency-magnitude data, depending on the peculiarities of the respective source zones (instrumental, historical, historical large magnitudes, etc. - see the table 1.6). As stated by R. Youngs in his documentation:

> *The methodology used in PEGASOS was to represent the uncertainty in b-value with a three point distribution specified as the best estimate value with weight 0.63, and the 5th and 95th percentiles, each with a weight 0.185. The 5th and 95th percentiles occur at* (±1.645) *standard deviations. For those sources with a large specified standard deviation in b-value, that represents a large change in b-value.*

The large uncertainty in b-values (±0.3) applies to source zones A, B, D4x, E1 and F1x. This large uncertainty reflects the magnitude inconsistencies of the original French and Italian catalogs and the consequent difficulties encountered in the conversion to a homogenous ECOS-09 magnitude. Interpreting the b-value uncertainty of ±0.3 as a single standard deviation of a normal distribution leads to unrealistic b-values (on the order of 0.5 and 1.5) at the 5th and 95th percentiles and to a large spread in the resulting recurrence rates (clearly visible in the plots provided by R. Youngs). In his accompanying e-mail of March 30, 2011, R. Youngs suggests interpreting the uncertainty of the b-values of these source zones as a uniform distribution between ±0.3 and discretizing this distribution with a three-point distribution with weights of 0.444 at the central value and of 0.278 at ±0.233 on each side of the central value. Considering the fact that the b-value of 1.0 assigned to most of these problematic source zones is somewhat arbitrary and does not deserve the relatively large weight it would receive in a normal distribution, and that the b-values at the tail of a normal distribution with a sigma of 0.3 are very unlikely, we concur with R. Youngs that treating the estimated errors as uniformly rather than as normally distributed is justifiable in these cases.

For all other source zones, the b-value uncertainty of ±0.1 (or ±0.21 for zones F3x) can be interpreted as one sigma of a normal distribution, discretized with weights of 0.63 at the central value and 0.185 at ±1.645 sigma.

In the plots for source zone E2b we note that the GR-regressions are anchored at the low-magnitude data point for both the "all magnitudes" and the "large magnitudes" plot - is this correct? In the original PEGASOS EG1a Elicitation Summary, the recurrence rate for this source zone was based solely on the "large magnitude" data point. In fact, considering the paucity of the instrumental data for the two source zones E2a and E2b, we propose to give the "large magnitude" recurrence rates a weight of 0.8 and the "low-magnitude" recurrence rates a weight of only 0.2 for these two zones (rather than 0.5 and 0.5 as listed in the table 1.7).

We also note that the Basel event of 1356 is not matched by any of the frequency-magnitude regressions shown for sources RF, F2d and F2e. This could be a consequence of the small size of the source zones (lack of stationarity). On the other hand, this mismatch is also visible in the regressions for macro-zone F2 (see technical note of Sept. 30, 2010 by R. Youngs) and could be an indication that this data point is not representative of the true recurrence rate for an event of this magnitude.

Table 1.7: Table of EG1a source zones with adopted b-values and weights for different data subsets (from technical note of March 24, 2011 by R. Youngs).

Sources with correlated b-values	*b*-value	Seismicity rate alternatives	Weight
A	1.00 ± 0.3	All data	(0.5)
		All data, larger mag	(0.5)
B	1.00 ± 0.3	All data	(0.5)
		All data, larger mag	(0.5)
C1, C2, C3	0.99 ± 0.1	All data	(0.5)
		All data, larger mag	(0.5)
D1a, D1b, D1c, D1e,	0.94 ± 0.1	Instrumental data	(0.333)
D1f, D1bcd, D1bcde, D1de		Historical data	(0.334)
		Historical data, larger mag	(0.333)
D2, D3a, D3b	0.96 ± 0.1	Instrumental data	(0.333)
		Historical data	(0.334)
		Historical data, larger mag	(0.333)
D4a, D4b, D4c	1.00 ± 0.3	All data	(0.5)
		All data, larger mag	(0.5)
E1	0.96 ± 0.3	All data	(0.5)
		All data, larger mag	(0.5)
E2a, E2b, E2c, E2d,	1.04 ± 0.1	For E2a, E2b:	
E2e, E2cde, FF,		All data	(0.5)
E2dF2f, E2eF2f, E2cdeF2f,		All data, larger mag	(0.5)
E2n, E2s, E2f, E3a, E3aF2f, E3b		For rest of sources:	
		Instrumental data	(0.333)
		Historical data	(0.334)
		Historical data, larger mag	(0.333)
F1a, F1b	0.96 ± 0.3	All data	(0.5)
		All data, larger mag	(0.5)
F2a, F2b, F2b_RF,	1.12 ± 0.1	For F2c:	
RF, F2bpcy, F2bF2f, F2c,		All data	(0.5)
F2d, F2e, F2f		All data, larger mag	(0.5)
		For rest of sources:	
		Instrumental data	(0.333)
		Historical data	(0.334)
		Historical data, larger mag	(0.333)
F3a, F3aF2f, F3b, F3c	1.06 ± 0.21	Instrumental data	(0.333)
		Historical data	(0.334)
		Historical data, larger mag	(0.333)

1.6 Kijko and Graham M_{max} Assessments

On February 4, 2011 the project received the final M_{max} assessment of the EG1a experts. As in the original PEGASOS elicitation summary, the maximum magnitude has been computed for the macro-zones (MZs) according to the Kijko and Graham [1998] approach. Table 1.8 summarizes the estimates obtained using the new catalogue (denoted PRP in table 1.8), and quoted in the original elicitation summary (PEGASOS) for comparison. In both cases, the exact formulation proposed by A. Cisternas (personal communication) was used and this modification replaces the original approximation used by Kijko & Graham.

For a given MZ the Kijko & Graham approach uses the maximum observed magnitude (Mx), the minimum magnitude which is considered to be complete in the catalogue (a value of 2.7 was taken for all MZs), and the seismicity parameters a and b. The chosen b-values and their errors are the results of the calculations reported in the document "PRP EG1a: Evaluation of the b-values calculated for the macro-zones" distributed on November 19, 2010. The a-values are those reported in the column referring to the mean b-value in the table "Fit all data" of the document "Fit to Seismicity in Macro Zones Using Specified b-values " distributed by R. Youngs on December 9, 2010. The catalogue of each MZ was taken as being complete over its whole period of time, because the way the seismicity parameters were assessed justifies this choice. This time interval is reported in column "T" of table 1.8.

As can be seen in table 1.8 some Mx are remarkably different when using the new version of the ECOS catalogue compared to those derived from to the previous version. Hence the new catalogue notably changes a part of the M_{max} estimates. In fact, the significantly higher M_{max} for SZs B and D4 derived from the new catalogue are primarily due to the increase in the values of Mx within these particular SZs (by 1.2 and 0.4 in terms of magnitude, in SZ B and SZ D4, respectively). Conversely, there is another cause that determines the new M_{max} estimate for SZ F2: in this case it is the new and higher b-value (1.12) that conditions the new M_{max} estimate. Finally, we note that a larger uncertainty is associated with some of the new M_{max} estimates when compared to those obtained in the previous elaboration.

Table 1.8: Statistical M_{max} for the makrozones (MZ). Mo and T indicate the magnitude and the period of completeness (see the text for the explanation). a, b, and $\sigma(b)$ are the parameters and uncertainty of the Gutenberg-Richter relation. Mx indicates the maximum observed magnitude, M_{max} the maximum calculated magnitude and σ its standard deviation.

MZ	PRP (new)								PEGASOS (original)							
	M0	Mx	T	a	b	$\sigma(b)$	M_{max}	$\sigma(M_{max})$	M0	Mx	T	a	b	$\sigma(b)$	M_{max}	$\sigma(M_{max})$
A	2.7	6.48	827	3.75	1	0.3	6.5	0.2	3.8	6.3	900	3.8	0.96	0.1	6.3	0.2
B	2.7	6.49	892	2.89	1	0.3	7	0.5	3.2	5.3	800	2.9	1	0.1	5.3	0.2
C	2.7	6.2	698	3.55	0.99	0.1	6.2	0.2	3.2	6.4	700	2.97	0.92	0.1	6.5	0.2
D1	2.7	5.9	505	3.24	0.94	0.1	5.9	0.2	2.9	6.4	700	2.9	0.93	0.1	6.6	0.3
D23	2.7	6.2	714	3.29	0.96	0.1	6.2	0.2	2.9	6.5	800	3.27	0.94	0.1	6.6	0.2
D4	2.7	6.61	944	3.26	1	0.3	6.9	0.4	4.1	6.2	1000	3.56	1	0.1	6.2	0.2
E1	2.7	5.8	559	2.4	0.96	0.3	6.2	0.4	3.8	5.8	600	2.76	0.95	0.1	6.1	0.3
E23	2.7	5.8	652	3.5	1.04	0.1	5.8	0.2	2.3	5.8	700	2.73	0.89	0.1	5.8	0.2
F1	2.7	5.4	854	2.93	0.96	0.3	5.4	0.2	3.8	6.2	900	2.78	0.95	0.1	6.5	0.3
F2	2.7	6.6	1151	3.51	1.12	0.14	7.2	0.6	3.5	6.9	1200	3.01	0.9	0.1	7.1	0.3
F3	2.7	5.6	896	3.45	1.06	0.21	5.6	0.2	3.2	5.8	1000	3.22	0.88	0.1	5.8	0.2

The Figures 1.14, 1.15 and 1.16 depict the histograms of the EPRI M_{max} estimates. These are based on the revised calculations reported in document "EPRI (Bayesian) M_{max} Assessments, Updated" received from R. Youngs on January 26, 2011 as well as on the the new values for

Mx (with x) and the Kijko & Graham M_{max} (with o). The histogram bins are M_W = 5.3, 5.7, 6.1, 6.5, 6.9, 7.2, 7.6.

A comparison between these EPRI M_{max} estimates with those obtained from the Kijko & Graham approach generally shows a good agreement. No notable differences are found and the Kijko & Graham M_{max} estimates are found to exactly correspond to the peak of the EPRI distribution in 6 out 11 MZs and are very close to the peak in all other cases.

In conclusion, the EPRI M_{max} distributions calculated in the previously cited document are satisfactory. The Kijko & Graham M_{max} distributions can be calculated from the values of the last two columns (M_{max} and σ) of the PRP part of table 1.8.

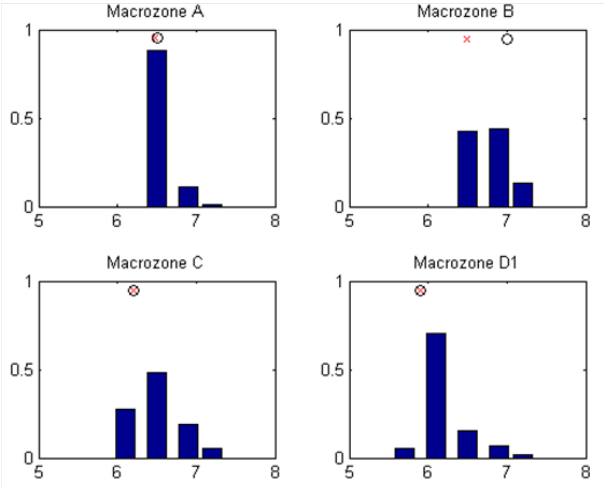

Figure 1.14: M_{max} plots for the makrozones A, B, C, D1.

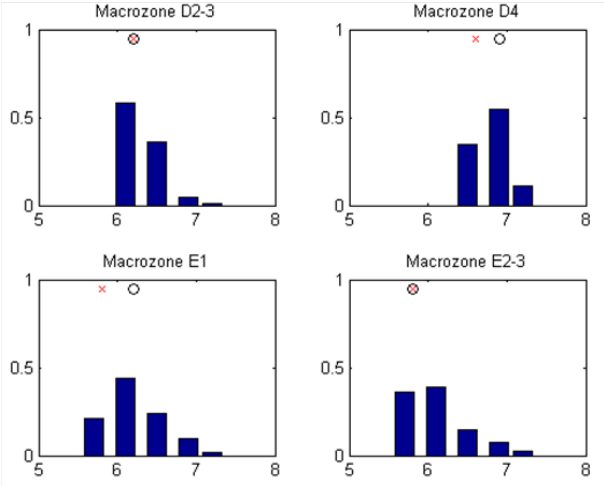

Figure 1.15: M_{max} plots for the makrozones D2-3, D4, E1, E2-3.

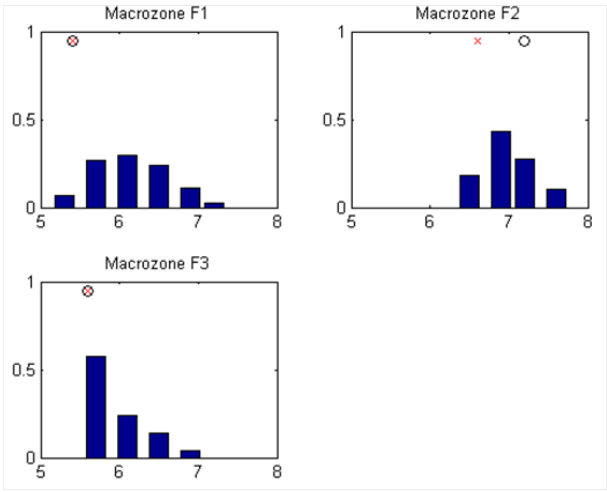

Figure 1.16: M_{max} plots for the makrozones F1, F2, F3.

Chapter 2

Supporting Calculations for EG1a by R. Youngs

2.1 Calculations for Expert Team EG1a

This section documents the calculations performed to support the EG1a Expert Team's review and finalization of the updated seismicity parameters based on the ECOS-09 catalog. These calculations are all performed using the final ECOS-09 catalog [SED 2010] and the final ECOS-09 catalog declustered by Dr. Stefan Wiemer utilizing Gardner and Knopoff [1974] approach with the time and distance widows developed by Grünthal [1985] as published in Burkhard and Grünthal [2009].

2.2 Comparisons of Magnitudes in ECOS-02 and ECOS-09

The first set of calculations was the development of plots comparing the magnitudes of individual earthquakes reported in the ECOS-02 and ECOS-09 catalogs. The two catalogs were sorted into individual catalogs for the six catalog completeness regions defined by EG1a (Figure 2.1). The earthquakes were then sorted by date, time, and location in order to identify the same earthquake in both catalogs. Compilations of earthquakes common to both catalogs were then developed from these lists for the purpose of comparing the moment magnitude assignments. Figures 2.1 through 2.6 show plots that compare the magnitudes for individual earthquakes in the two catalogs for the six catalog completeness regions. The data are plotted separately for the "historical period" prior to 1975) and the "instrumental period" (1975 through 2000, the end of the ECOS02 catalog). For a few earthquakes in Switzerland and a number of earthquakes in France, questionable correlations were established between the same event in both catalogs. These data points are denoted by the red symbols denoted as "uncertain data" in the legends.

2.3 Regional b-value Calculations

The maximum likelihood method described in section 2.2.3 was used to compute seismicity parameters for the EG1a macro zones (Figure 2.8) and for the EG1a completeness regions (Figure 2.1). The purpose of these calculations was to provide assessments of b-values for various portions of the study region. The calculations were performed using the catalog completeness periods extended through the end of 2008 and the original magnitude intervals defined in the PEGASOS project. Table 2.1 lists the catalog completeness periods used. Calculations were performed for the entire catalog and for the instrumental period (1975 through 2008) and historical period (pre 1975) separately. Table 2.2 lists the computed b-values and Figures 2.7 through 2.23 show the seismicity data and fitted recurrence relationships.

2.4 Maximum Magnitude Distributions

Maximum magnitude distributions were computed for the EG1a macro-zones (Figure 2.8) using the Bayesian (EPRI) approach described in section 2.2.4. The parameters used for these calculations are presented in table 2.3.

Table 2.4 summarizes the maximum observed magnitudes in each macro-zone. Values are presented for the assessed complete period of earthquake reporting and for the entire period covered by the ECOS-09 catalog. For macro-zones B, D1, and F1, the maximum earthquake observed in the catalog occurs prior to the period considered complete for that magnitude interval. For all of the other zones the maximum observed occurs in the first magnitude increment.

The data in tables 2.3 and 2.4 were used to compute maximum magnitude distributions for the EG1a macro-zones using the Bayesian methodology. The maximum observe magnitude used is the maximum observed, regardless of whether or not it occurs in the period of complete catalog reporting. Table 2.5 lists the resulting maximum magnitude distributions in which the Bayesian posterior distribution is discretized using the magnitude binning intervals employed by EG1a in the PEGASOS Project. Table 2.6 lists the resulting maximum magnitude distributions using an alternative discretization magnitude interval of 1/4 magnitude units.

The final maximum magnitude distributions consist of the Bayesian estimates listed in table 2.5 and values based on the Kijko & Graham approach (chapter 1.6) provided by EG1a. The last two columns of table 2.7 list the values of M_{max} and its standard deviation provided by EG1a. These were used to compute distributions for maximum magnitude following the approach used in PEGASOS. Because of the nature of the Kijko & Graham formulation, it was assumed that the resulting distribution for M_{max} could be approximated by an exponential distribution with parameter $1/\sigma(M_{max})$. Using this assumption, the probability density function for M_{max} within the limits defined by the maximum observed earthquake and the upper limit imposed by EG1a is proportional to the density function for an exponential distribution, specifically

$$P(M_{max}) \propto \left(\frac{\exp^{(-M_{max}/\sigma(M_{max})}}{\sigma(M_{max})} \right) \tag{2.1}$$

2.1 was used to compute probability density values for M_{max} within the specified limits. These values were then normalized to produce a probability mass function, which was then

Table 2.1: EG1a Earthquake Catalog Completeness Periods.

Completeness Region	Magnitude	Beginning Year
Austria	2.7	1975
	3.1	1900
	4.7	1850
	5.4	1670
	6.2	1550
	7	1200
France	2.7	1980
	3.1	1975
	3.5	1970
	3.9	1820
	7	1000
Germany	2.7	1975
	3.1	1900
	3.9	1825
	4.7	1775
	5.4	1600
	6.2	1250
	7	1000
Italy	2.7	1980
	3.1	1975
	3.9	1960
	4.1	1900
	4.7	1800
	5.4	1400
	6.2	1200
	7	1000
Switzerland	2.7	1975
	3.1	1900
	3.9	1879
	4.7	1750
	5.4	1680
	6.2	1500
	6.6	1200
Western Alps	2.7	1975
	3.9	1900
	4.7	1820
	5.4	1750
	7	1000

Table 2.2: Regional b-values for EG1a Macro-zones and Completeness Regions.

Region	Combined		Split Instrumental and Historical			
			Historical		Instrumental	
	b-value	$\sigma(b)$	b-value	$\sigma(b)$	b-value	$\sigma(b)$
Zone A	0.768	0.024	0.733	0.058	0.645	0.038
Zone B	0.881	0.072	1.092	0.268	0.782	0.144
Zone C	0.805	0.032	0.991	0.108	0.981	0.075
Zone D1	0.797	0.035	0.926	0.043	1.049	0.12
Zone D23	0.898	0.041	0.934	0.05	1.052	0.095
Zone D4	0.758	0.041	0.655	0.176	0.762	0.076
Zone E1	0.616	0.105	0.767	0.147	0.95	0.33
Zone E23	0.801	0.041	1.014	0.062	1.205	0.143
Zone F1	1.184	0.087	1.615	0.387	1.472	0.172
Zone F2	0.874	0.054	1.067	0.257	1.219	0.135
Zone F3	0.856	0.044	1.076	0.212	1.019	0.12
Austria	0.944	0.08	0.631	0.077	1.185	0.146
France	0.924	0.058	0.965	0.228	1.426	0.146
Germany	0.847	0.035	1.172	0.149	1.103	0.1
Italy	0.774	0.019	0.773	0.073	0.691	0.032
Switzerland	0.866	0.024	0.978	0.03	1.069	0.071
W. Alps	0.73	0.029	0.794	0.122	0.927	0.069

Table 2.3: Parameters Used for EPRI M_{max} Assessment for EG1a Macro Zones.

Macro Zone	b-value	Prior Mean	Prior σ	Geologic Upper Limit
A	1	6.4	0.84	7.2
B	1	6.4	0.84	7.2
C	0.99	6.4	0.84	7.2
D1	0.94	6.4	0.84	7.2
D2_3	0.96	6.4	0.84	7.2
D4	1	6.4	0.84	7.2
E1	0.96	6.3	0.5	7.2
E2_3	1.04	6.4	0.84	7.2
F1	0.96	6.3	0.5	7.2
F2	1.12	6.4	0.84	7.6
F2	1.06	6.4	0.5	6.9

Table 2.4: Maximum Observed Magnitudes in EG1a Macro-Zones.

Macro Zone	Maximum Observed In Complete Period	Maximum Observed	Year of Maximum Observes	Year Maximum Observed Considered Complete in Catalog
A	6.48	6.48		
B	5.67	6.49	1117	1200
C	6.2	6.2		
D1	5.8	5.9	1584, 1601	1680
D2_3	6.2	6.2		
D4	6.61	6.61		
E1	5.8	5.8		
E2_3	5.8	5.8		
F1	4.4	5.4	1595	1820
F2	6.6	6.6		
F3	5.6	5.6		

Table 2.5: Bayesian Approach M_{max} Distributions for EG1a Macro Zones Using PEGASOS M_{max} Bins. With Completeness Modified in Zones B, D1, and F1 to include maximum historic.

Macro Zone	Maximum Observed	Weight Assigned to M_{max} Value of:						
		5.3	5.7	6.1	6.5	6.9	7.2	7.6
A	6.48				0.87906	0.11048	0.01046	
B	6.49				0.42338	0.44116	0.13547	
C	6.2			0.27513	0.47917	0.19151	0.05419	
D1	5.9		0.05383	0.70437	0.15405	0.06793	0.01982	
D2_3	6.2			0.58371	0.36264	0.04491	0.00873	
D4	6.61				0.34481	0.54573	0.10946	
E1	5.8		0.20962	0.44059	0.2367	0.09456	0.01853	
E2_3	5.8		0.36313	0.38982	0.14476	0.07788	0.02441	
F1	5.4	0.06899	0.26846	0.29521	0.23685	0.10829	0.0222	
F2	6.6				0.18375	0.43399	0.2777	0.10455
F3	5.6		0.57741	0.24255	0.14039	0.03965		

Table 2.6: Bayesian Approach M_{max} Distributions for EG1a Macro Zones Using 1/4 Magnitude M_{max} Bins with Completeness Modified in Zones B, D1, and F1 to Include Maximum Historic.

Macro Zone	Maximum Observed	Weight Assigned to M_{max} Value of:								
		5.5	5.75	6	6.25	6.5	7.75	7	7.25	7.5
A	6.48					0.79551	0.1723	0.03219		
B	6.49					0.30649	0.36878	0.2649	0.05983	
C	6.2				0.41628	0.28333	0.16699	0.10971	0.0237	
D1	5.9			0.61721	0.18421	0.09211	0.05812	0.03965	0.00869	
D2_3	6.2				0.75358	0.17738	0.04846	0.02057		
D4	6.61					0.12077	0.57984	0.25327	0.04612	
E1	5.8		0.17689	0.32059	0.21288	0.14618	0.08976	0.04627	0.00744	
E2_3	5.8		0.31761	0.33227	0.13967	0.0883	0.06394	0.04742	0.0108	
F1	5.4	0.15181	0.1712	0.18508	0.17994	0.14833	0.10023	0.05445	0.00896	
F2	6.6					0.07048	0.3598	0.26293	0.18982	0.11698
F3	5.6	0.16502	0.39699	0.1736	0.12201	0.08725	0.05513			

descritized in the same manner as the posterior probability from the Bayesian approach. Figures 2.24 through 2.34 compare the resulting maximum magnitude distributions.

Table 2.7: Maximum Magnitude Parameters from the Kijko & Graham Approach (see chapter 1.6).

Macro Zone	PRP (new)							
	M_0	M_X	T	a	b	$\sigma(b)$	M_{max}	$\sigma(M_{max})$
A	2.7	6.48	827	3.75	1	0.3	6.5	0.2
B	2.7	6.49	892	2.89	1	0.3	7.0	0.5
C	2.7	6.2	698	3.55	0.99	0.1	6.2	0.2
D1	2.7	5.9	505	3.24	0.94	0.1	5.9	0.2
D23	2.7	6.2	714	3.29	0.96	0.1	6.2	0.2
D4	2.7	6.61	944	3.26	1	0.3	6.9	0.4
E1	2.7	5.8	559	2.4	0.96	0.3	6.2	0.4
E23	2.7	5.8	652	3.5	1.04	0.1	5.8	0.2
F1	2.7	5.4	854	2.93	0.96	0.3	5.4	0.2
F2	2.7	6.6	1151	3.51	1.12	0.14	7.2	0.6
F3	2.7	5.6	896	3.45	1.06	0.21	5.6	0.2

2.5 Earthquake Recurrence Relationships

Maximum magnitude distributions were computed for the EG1a macro-zones (Figure 2.8) using the Bayesian (EPRI) approach described in section 2.2.4. The parameters used for these calculations are presented in table 2.8. The recurrence relationships were computed from the ECOS-09 catalog using the maximum likelihood formulation presented in section 2.2.3 with the b-values fixed at the values given in table 2.8. Figures 2.35 through 2.86 show the resulting earthquake recurrence relationships for each source zone. The magnitude intervals used for the recurrence calculations based on "large magnitudes" was nominally set at magnitudes of M 4.3 and larger. For some sources, this magnitude range was adjusted to account for the lack of data in the larger magnitude intervals.

The specific adjustments were as follows:

- Zone D1f - larger magnitudes was set at $M \geq 3.1$
- Zone D4a - larger magnitudes was set at $M \geq 3.5$
- Zone E2b - larger magnitudes was set at $M \geq 5.4$
- Zone E2e - larger magnitudes was set at $M \geq 3.5$
- Zone E3b - larger magnitudes was set at $M \geq 3.9$
- Zone F2a - larger magnitude was set at $M \geq 4.7$

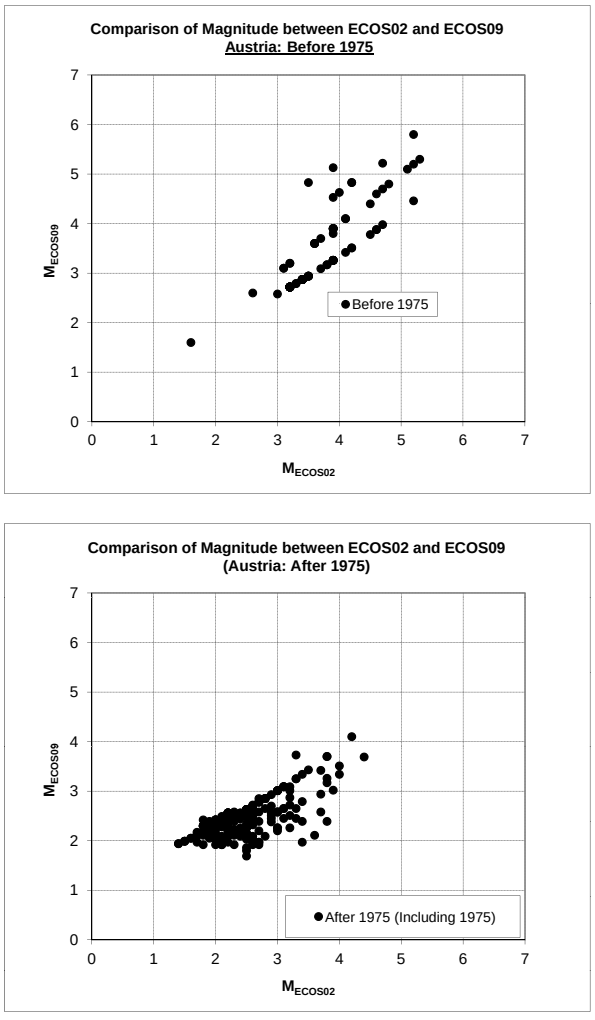

Figure 2.1: Comparison of assigned moment magnitudes for earthquakes common to the ECOS-02 and ECOS-09 earthquake catalogs in the EG1a Austria completeness region.

Table 2.8: Parameter Specifications for Developing EG1a Earthquake Recurrence Relationships.

Sources with correlated *b*-values	*b*-value	Weight	Seismicity Rate Alternatives	Weight
A	0.767	(0.278)	All data	(0.5)
	1.0	(0.444)	All data, larger mag	(0.5)
	1.233	(0.278)		
B	0.767	(0.278)	All data	(0.5)
	1.0	(0.444)	All data, larger mag	(0.5)
	1.233	(0.278)		
C1, C2, C3	0.826	(0.185)	All data	(0.5)
	0.99	(0.63)	All data, larger mag	(0.5)
	1.155	(0.185)		
D1a, D1b, D1c,	0.775	(0.185)	Instrumental data	(0.333)
D1e, D1f,	0.94	(0.63)	Historical data	(0.334)
D1bcd, D1bcde, D1de	1.105	(0.185)	Historical data, larger mag	(0.333)
D2, D3a, D3b	0.795	(0.185)	Instrumental data	(0.333)
	0.96	(0.63)	Historical data	(0.334)
	1.125	(0.185)	Historical data, larger mag	(0.333)
D4a, D4b, D4c	0.767	(0.278)	All data	(0.5)
	1.0	(0.444)	All data, larger mag	(0.5)
	1.233	(0.278)		
E1	0.727	(0.278)	All data	(0.5)
	0.96	(0.444)	All data, larger mag	(0.5)
	1.193	(0.278)		
E2a, E2b, E2c, E2d,	0.875	(0.185)	For E2a, E2b:	
E2e, E2cde, FF, E2dF2f,	1.04	(0.63)	All data	(0.2)
E2eF2f, E2cdeF2f,	1.204	(0.185)	All data, larger mag	(0.8)
E2n, E2s, E2f, E3a,			For rest of sources:	
E3aF2f, E3b			Instrumental data	(0.333)
			Historical data	(0.334)
			Historical data, larger mag	(0.333)
F1a, F1b	0.727	(0.278)	All data	(0.5)
	0.96	(0.444)	All data, larger mag	(0.5)
	1.193	(0.278)		
F2a, F2b, F2b_RF,	0.89	(0.185)	For F2c:	
RF, F2bpcy, F2bF2f,	1.12	(0.63)	All data	(0.5)
F2c, F2d, F2e, F2f	1.35	(0.185)	All data, larger mag	(0.5)
			For rest of sources:	
			Instrumental data	(0.333)
			Historical data	(0.334)
			Historical data, larger mag	(0.333)
F3a, F3aF2f,	0.715	(0.185)	Instrumental data	(0.333)
F3b, F3c	1.06	(0.63)	Historical data	(0.334)
	1.405	(0.185)	Historical data, larger mag	(0.333)

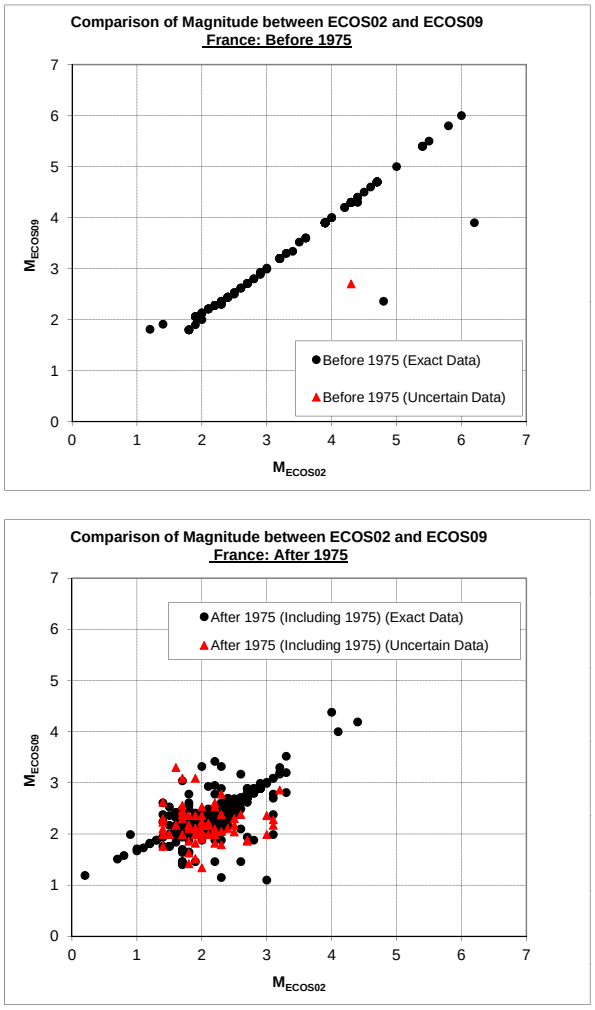

Figure 2.2: Comparison of assigned moment magnitudes for earthquakes common to the ECOS-02 and ECOS-09 earthquake catalogs in the EG1a France completeness region.

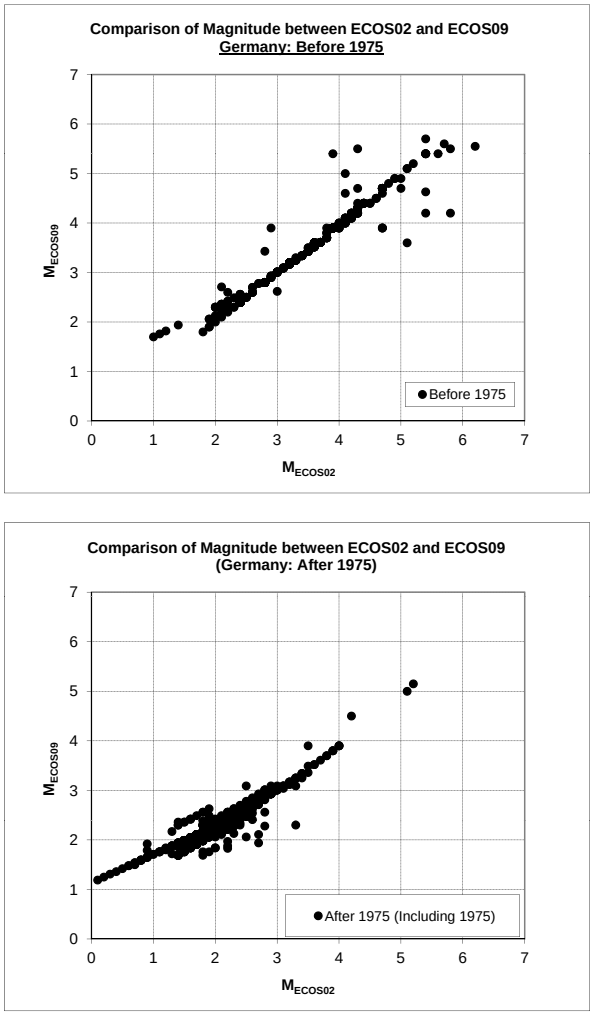

Figure 2.3: Comparison of assigned moment magnitudes for earthquakes common to the ECOS-02 and ECOS-09 earthquake catalogs in the EG1a Germany completeness region.

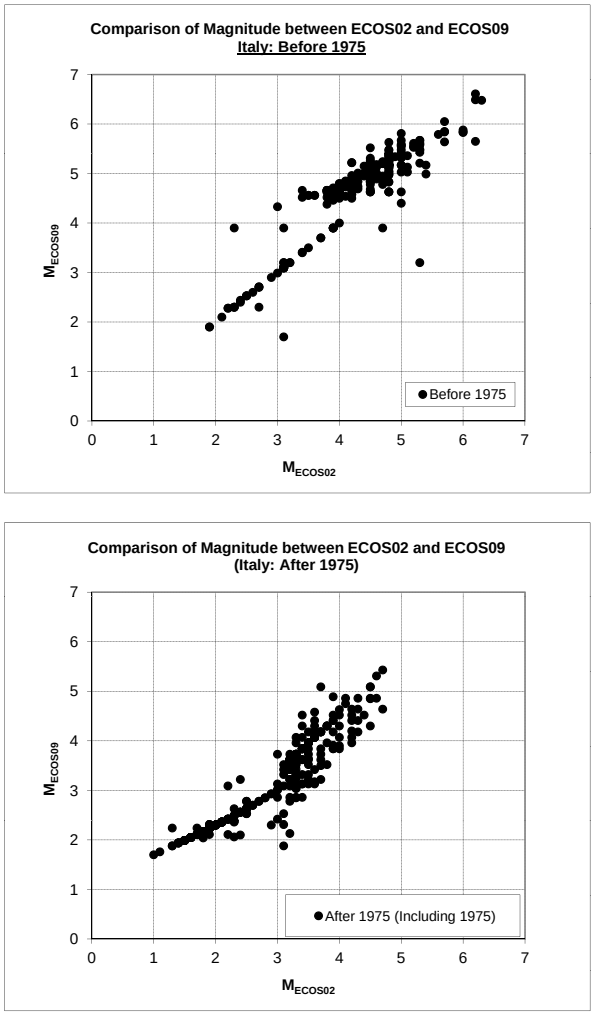

Figure 2.4: Comparison of assigned moment magnitudes for earthquakes common to the ECOS-02 and ECOS-09 earthquake catalogs in the EG1a Italy completeness region.

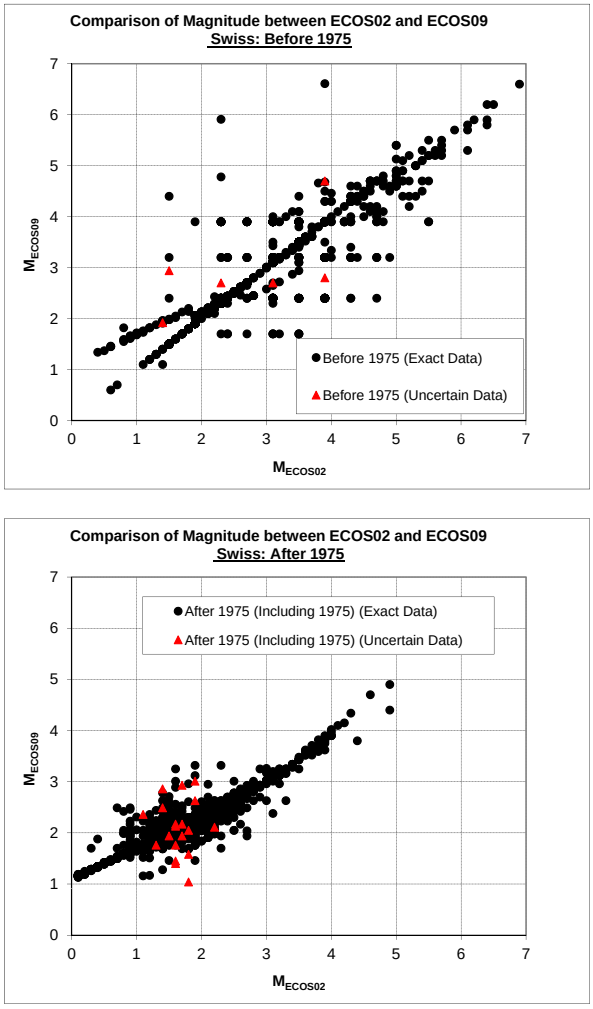

Figure 2.5: Comparison of assigned moment magnitudes for earthquakes common to the ECOS-02 and ECOS-09 earthquake catalogs in the EG1a Switzerland completeness region.

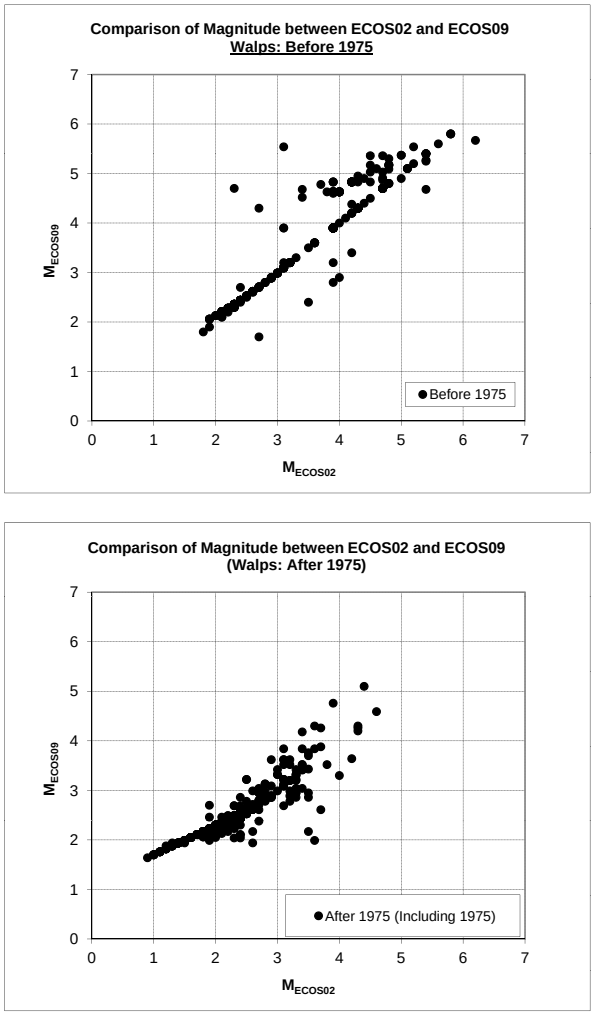

Figure 2.6: Comparison of assigned moment magnitudes for earthquakes common to the ECOS-02 and ECOS-09 earthquake catalogs in the EG1a Western Alps completeness region.

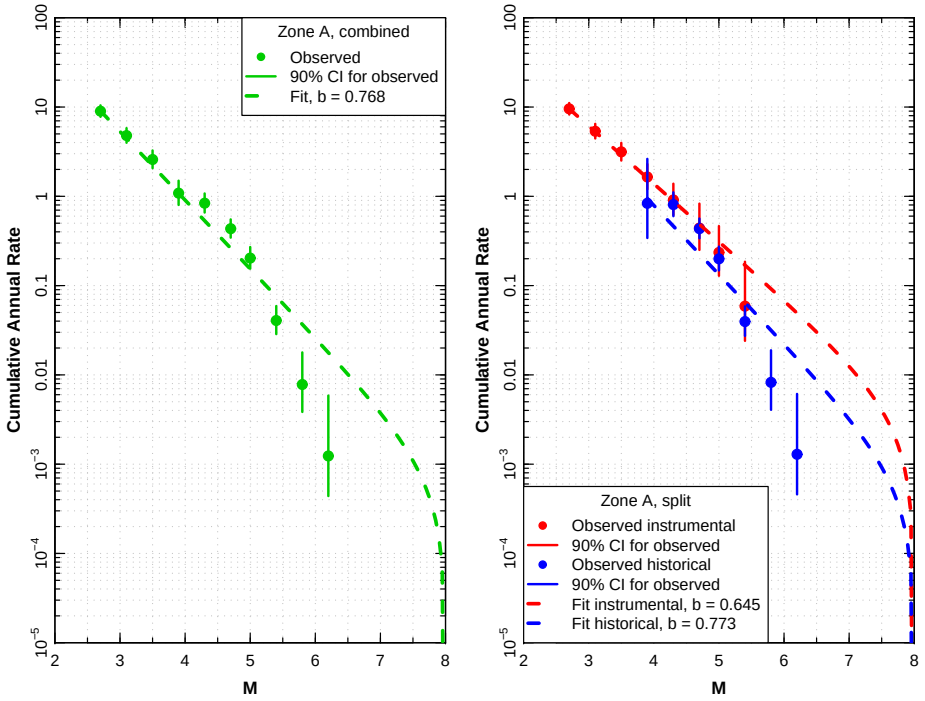

Figure 2.7: Seismicity data and fitted recurrence relationships for EG1a Zone A – Left, fit to all data, Right, fit to instrumental and historical data separately.

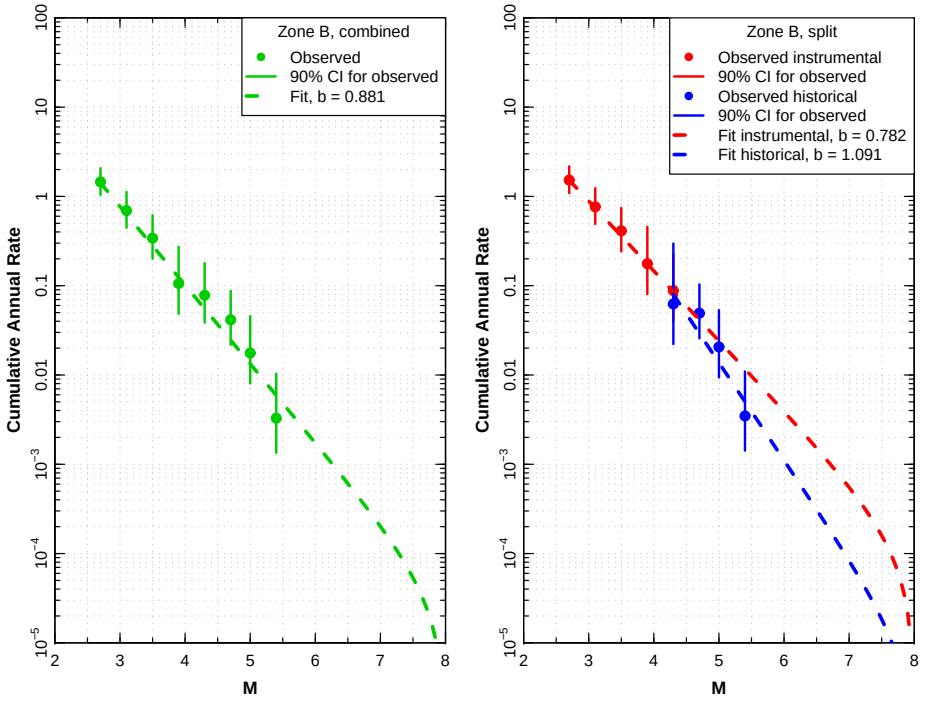

Figure 2.8: Seismicity data and fitted recurrence relationships for EG1a Zone B – Left, fit to all data, Right, fit to instrumental and historical data separately.

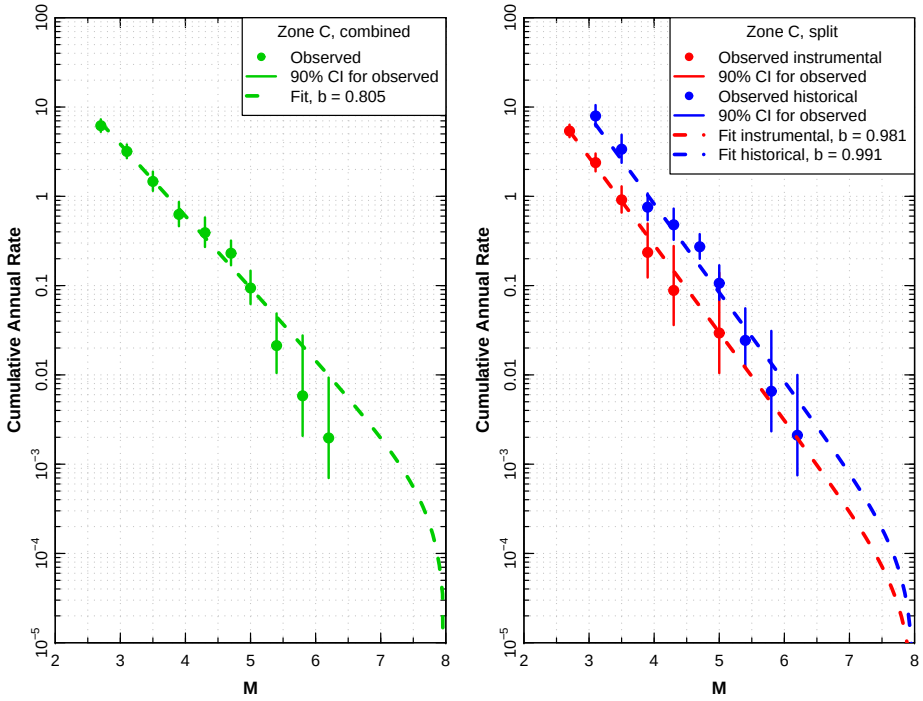

Figure 2.9: Seismicity data and fitted recurrence relationships for EG1a Zone C– Left, fit to all data, Right, fit to instrumental and historical data separately.

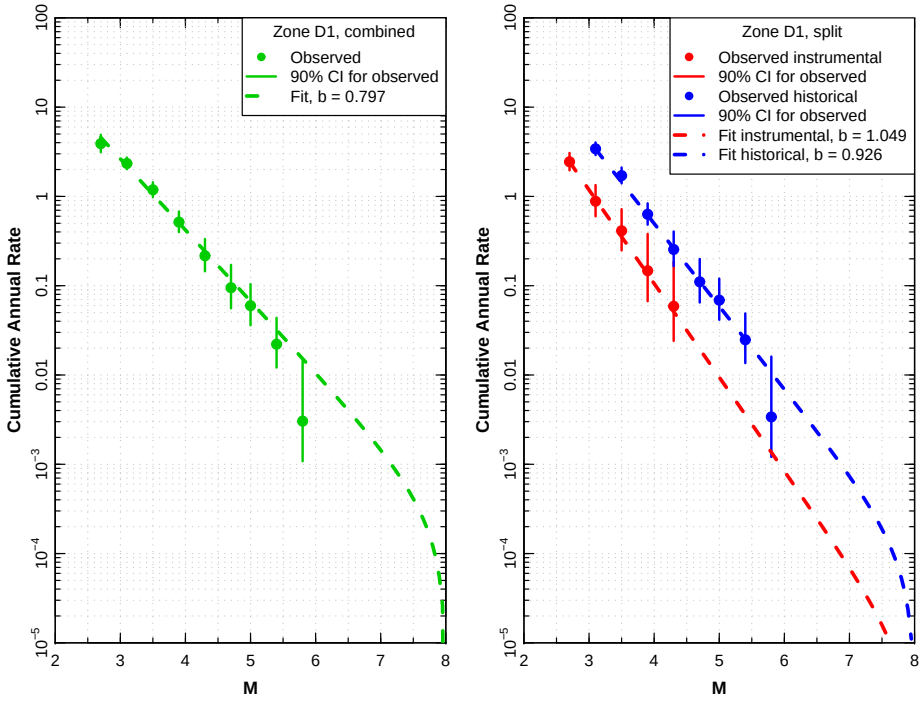

Figure 2.10: Seismicity data and fitted recurrence relationships for EG1a Zone D1 – Left, fit to all data, Right, fit to instrumental and historical data separately.

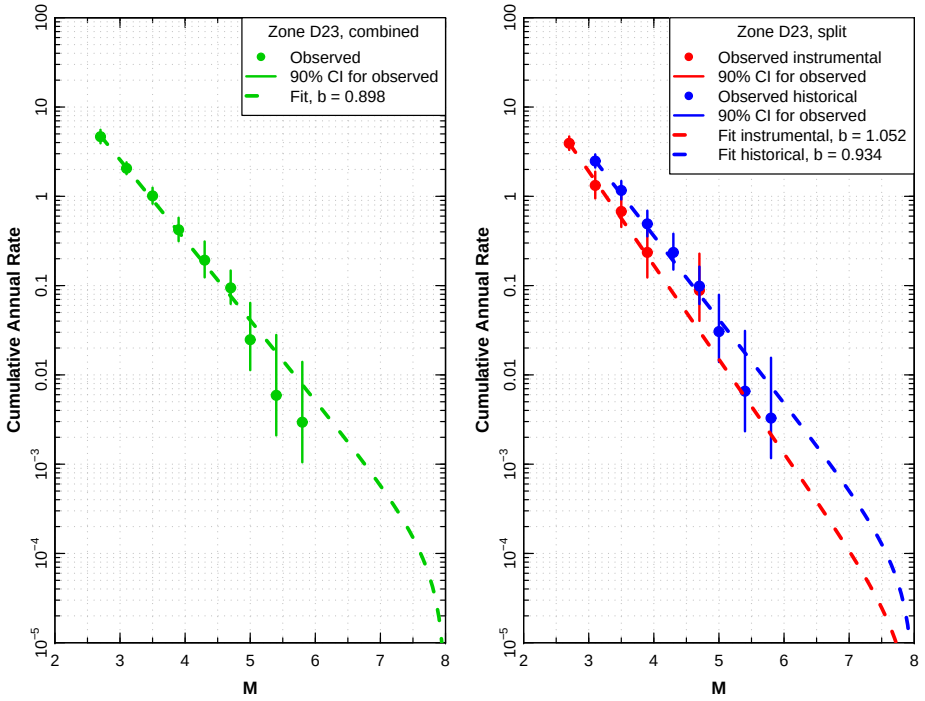

Figure 2.11: Seismicity data and fitted recurrence relationships for EG1a Zone D23 - Left, fit to all data, Right, fit to instrumental and historical data separately.

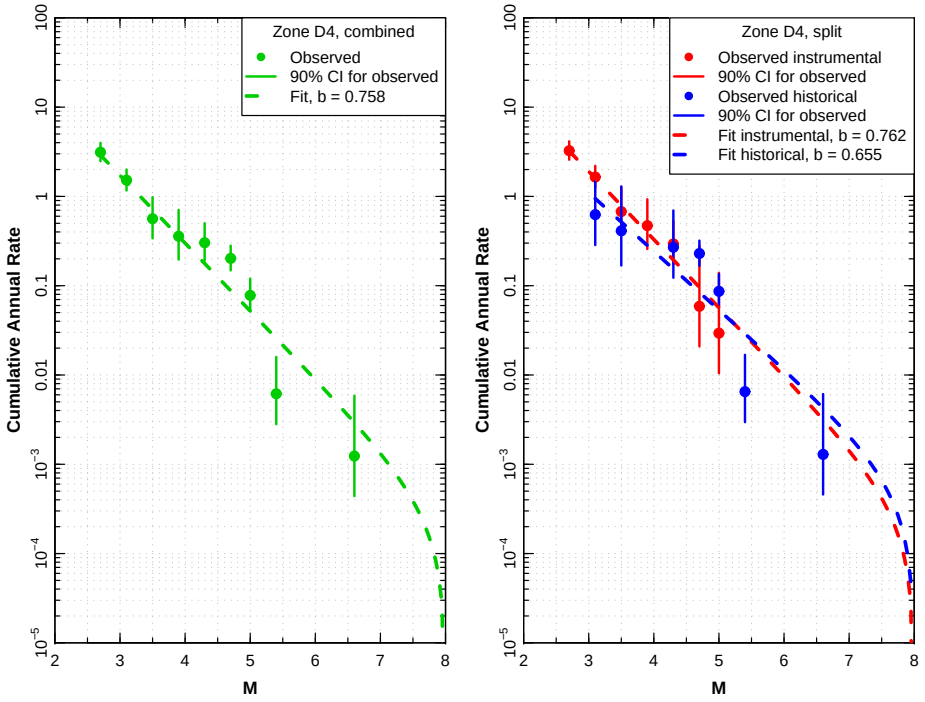

Figure 2.12: Seismicity data and fitted recurrence relationships for EG1a Zone D4 – Left, fit to all data, Right, fit to instrumental and historical data separately.

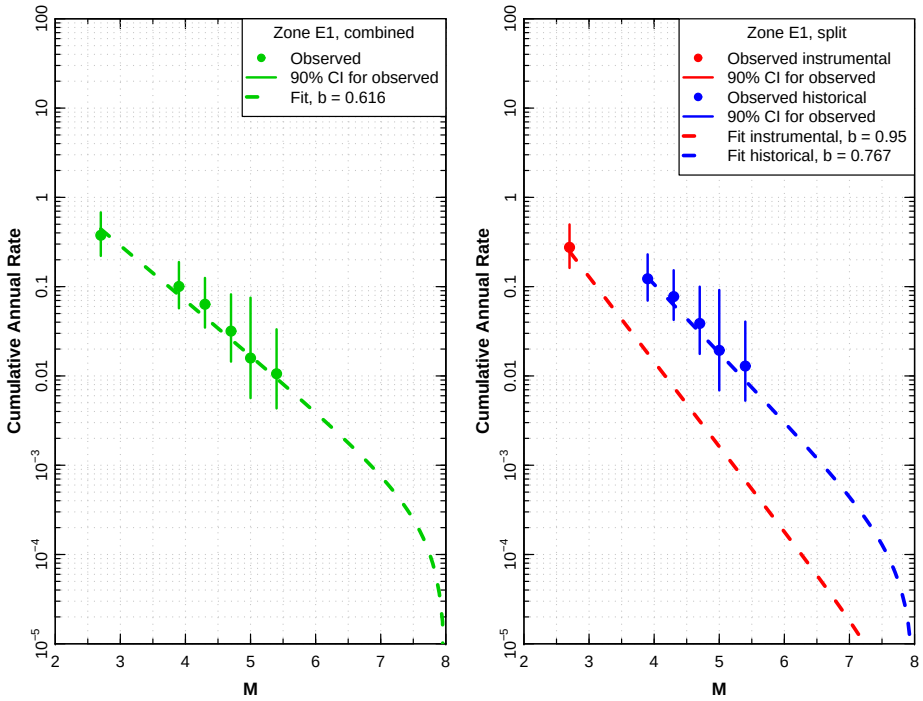

Figure 2.13: Seismicity data and fitted recurrence relationships for EG1a Zone E1 – Left, fit to all data, Right, fit to instrumental and historical data separately.

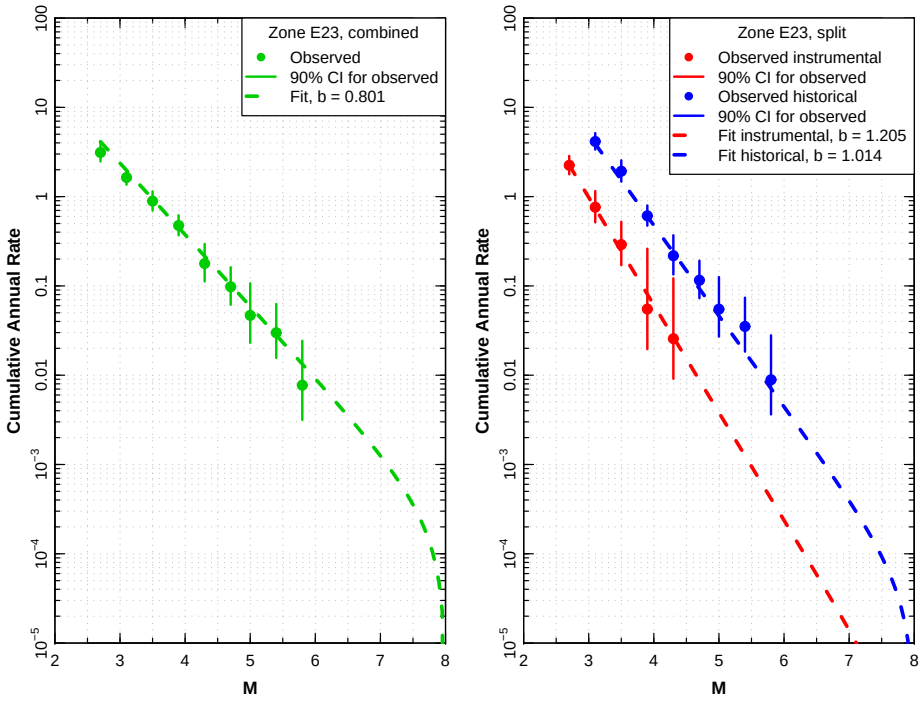

Figure 2.14: Seismicity data and fitted recurrence relationships for EG1a Zone E23 – Left, fit to all data, Right, fit to instrumental and historical data separately.

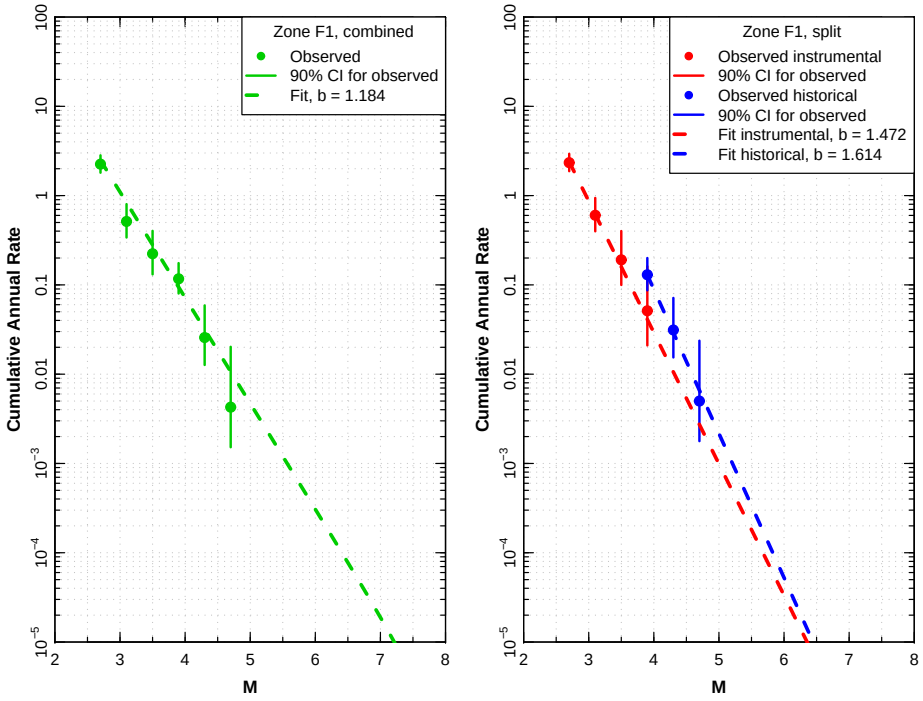

Figure 2.15: Seismicity data and fitted recurrence relationships for EG1a Zone F1 – Left, fit to all data, Right, fit to instrumental and historical data separately.

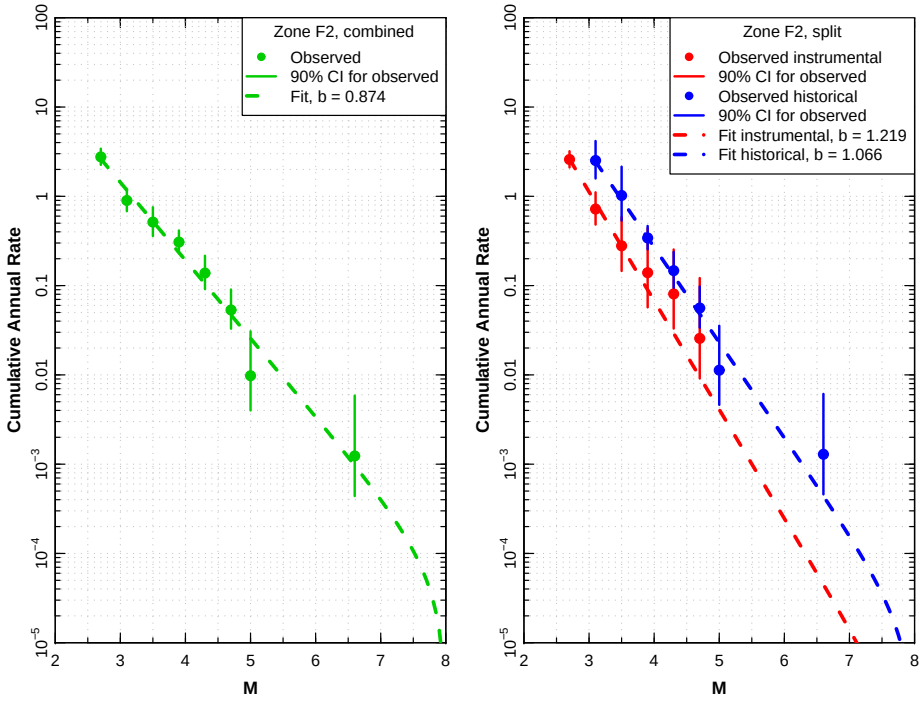

Figure 2.16: Seismicity data and fitted recurrence relationships for EG1a Zone F2 – Left, fit to all data, Right, fit to instrumental and historical data separately.

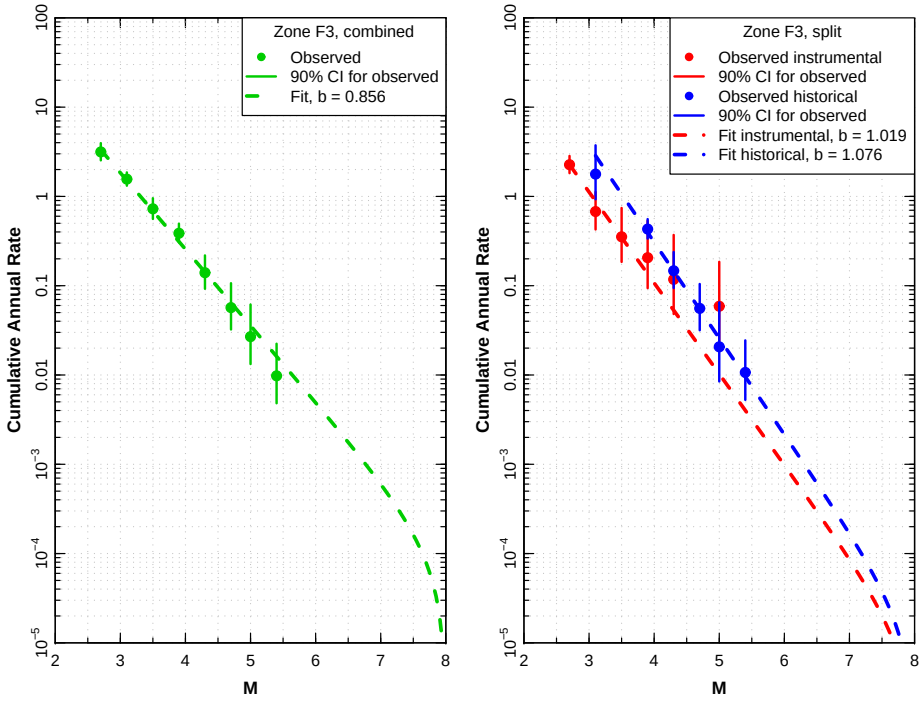

Figure 2.17: Seismicity data and fitted recurrence relationships for EG1a Zone F3 – Left, fit to all data, Right, fit to instrumental and historical data separately.

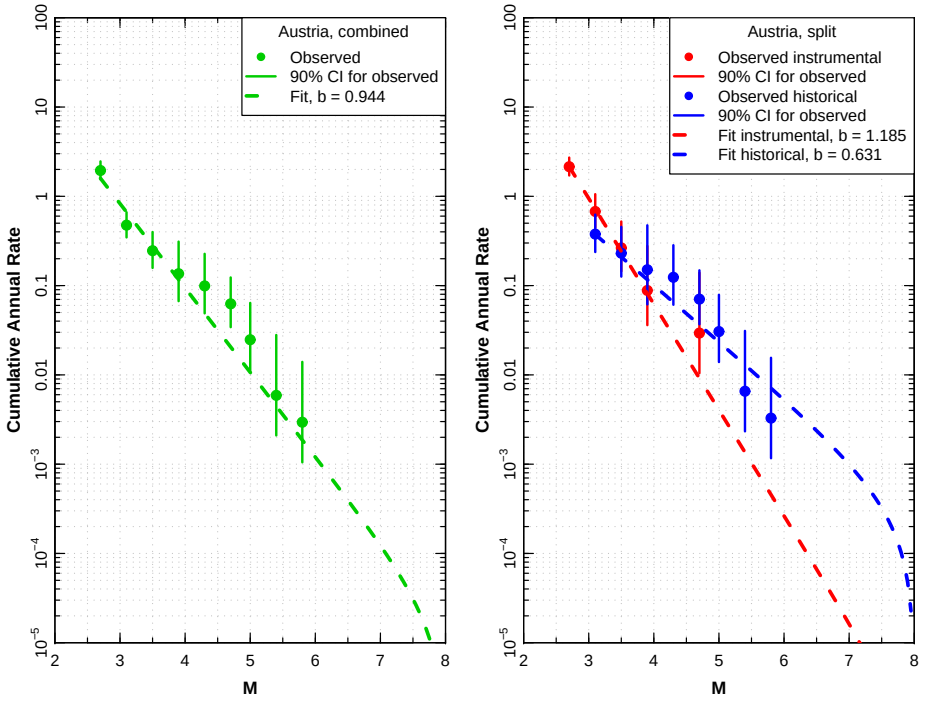

Figure 2.18: Seismicity data and fitted recurrence relationships for EG1a Austria completeness region Left, fit to all data, Right, fit to instrumental and historical data separately.

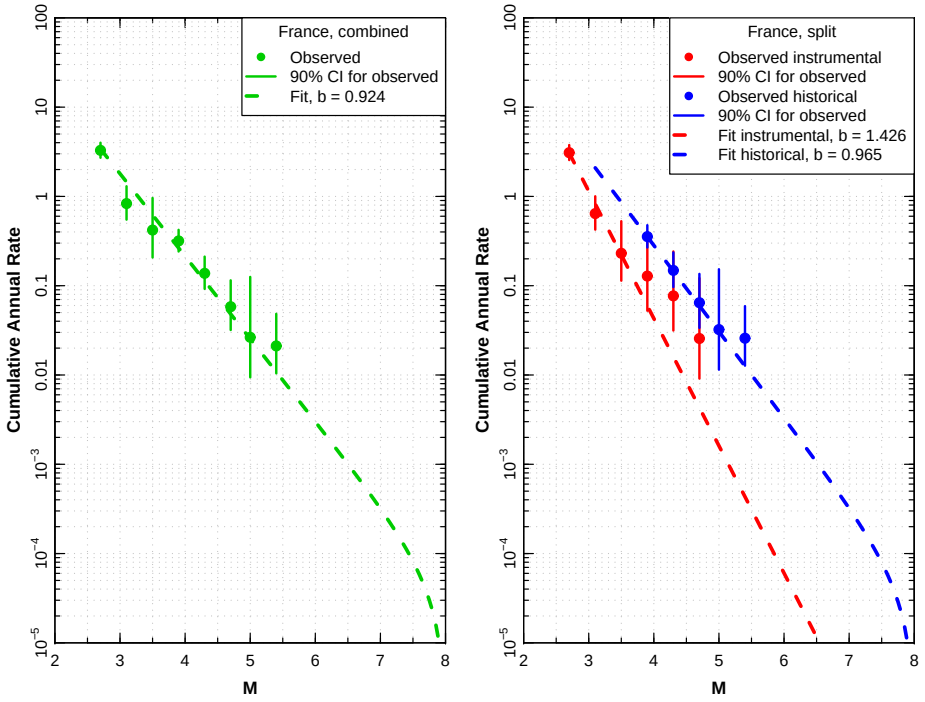

Figure 2.19: Seismicity data and fitted recurrence relationships for EG1a France completeness region Left, fit to all data, Right, fit to instrumental and historical data separately.

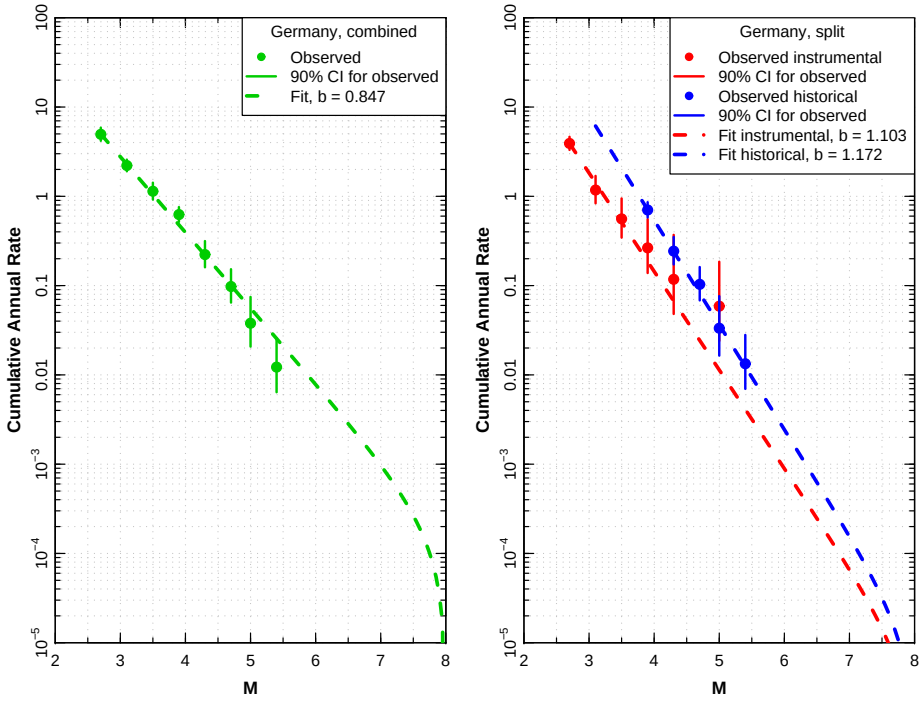

Figure 2.20: Seismicity data and fitted recurrence relationships for EG1a Germany completeness region Left, fit to all data, Right, fit to instrumental and historical data separately.

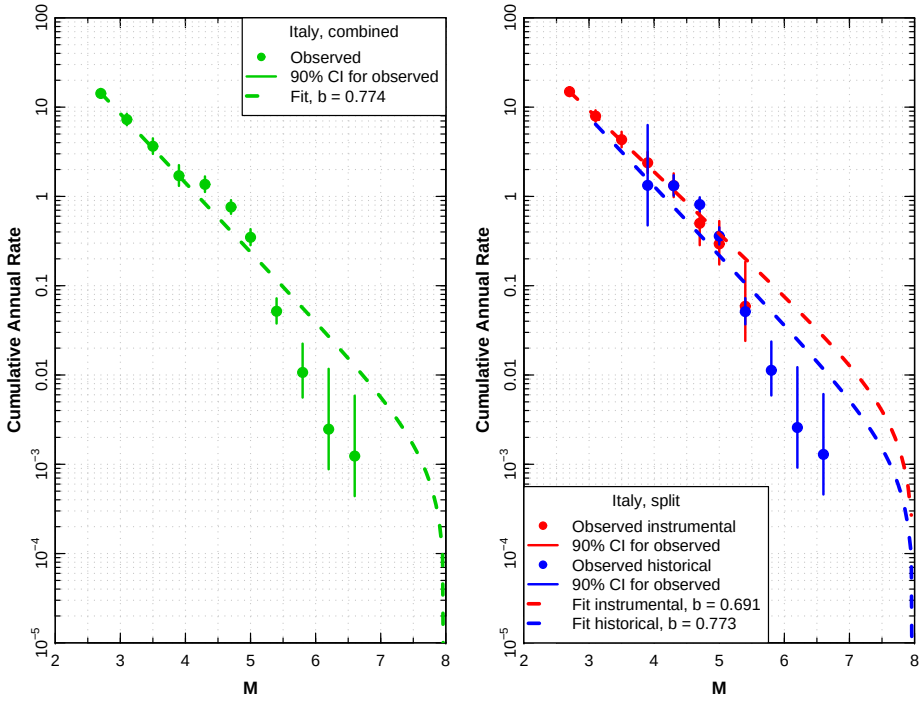

Figure 2.21: Seismicity data and fitted recurrence relationships for EG1a Italy completeness region Left, fit to all data, Right, fit to instrumental and historical data separately.

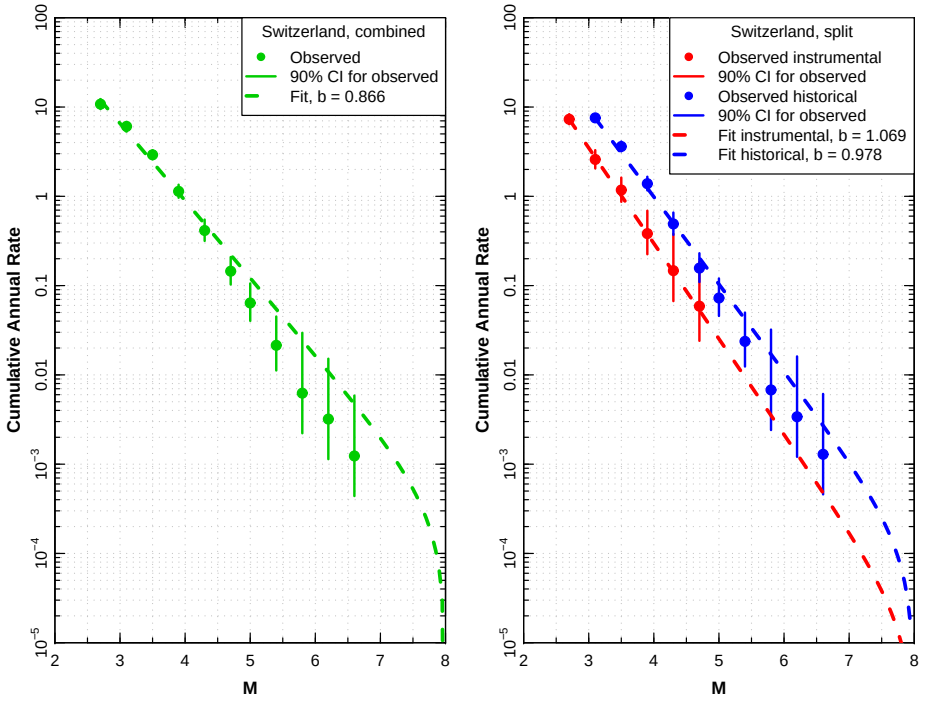

Figure 2.22: Seismicity data and fitted recurrence relationships for EG1a Switzerland completeness region Left, fit to all data, Right, fit to instrumental and historical data separately.

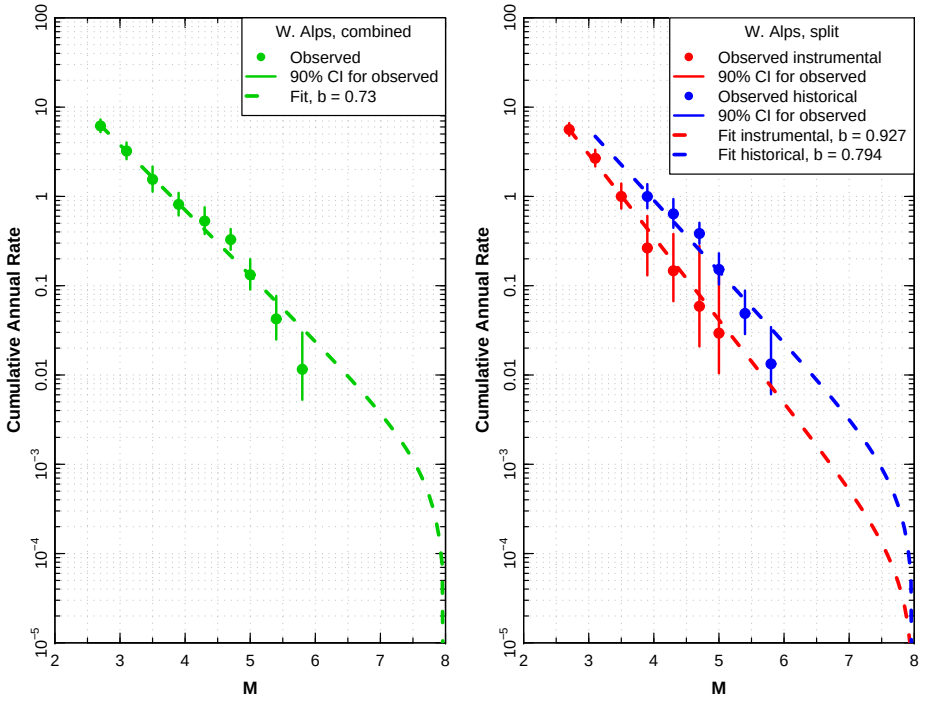

Figure 2.23: Seismicity data and fitted recurrence relationships for EG1a Western Alps completeness region Left, fit to all data, Right, fit to instrumental and historical data separately.

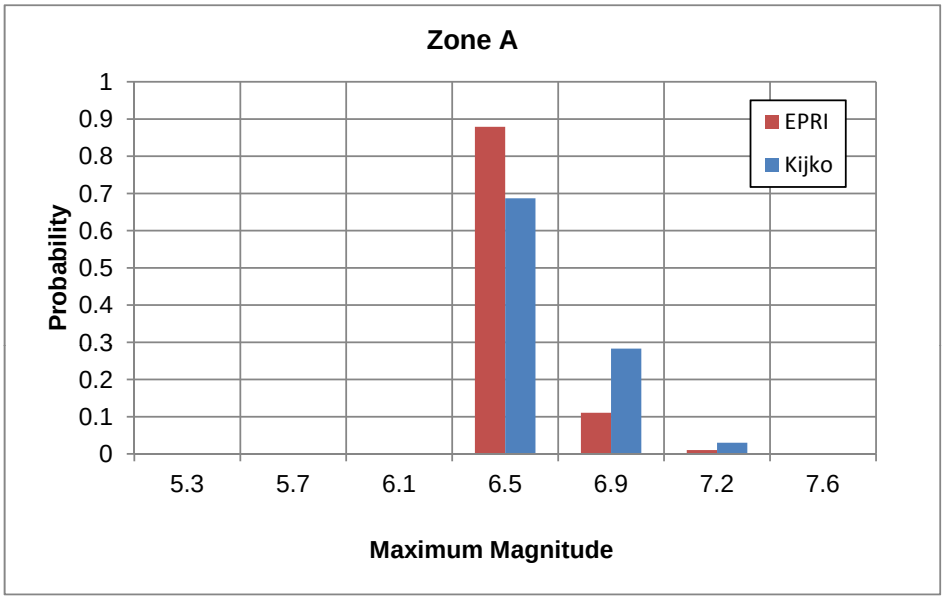

Figure 2.24: Maximum magnitude distributions for EG1a macro-zone A computed using the Bayesian (EPRI) and Kijko and Graham (Kijko) methods.

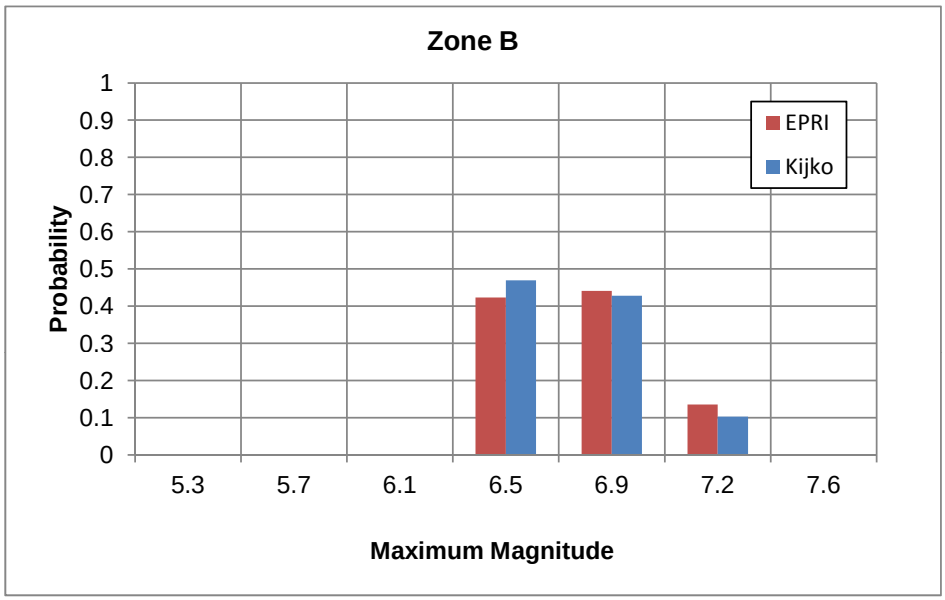

Figure 2.25: Maximum magnitude distributions for EG1a macro-zone B computed using the Bayesian (EPRI) and Kijko and Graham (Kijko) methods.

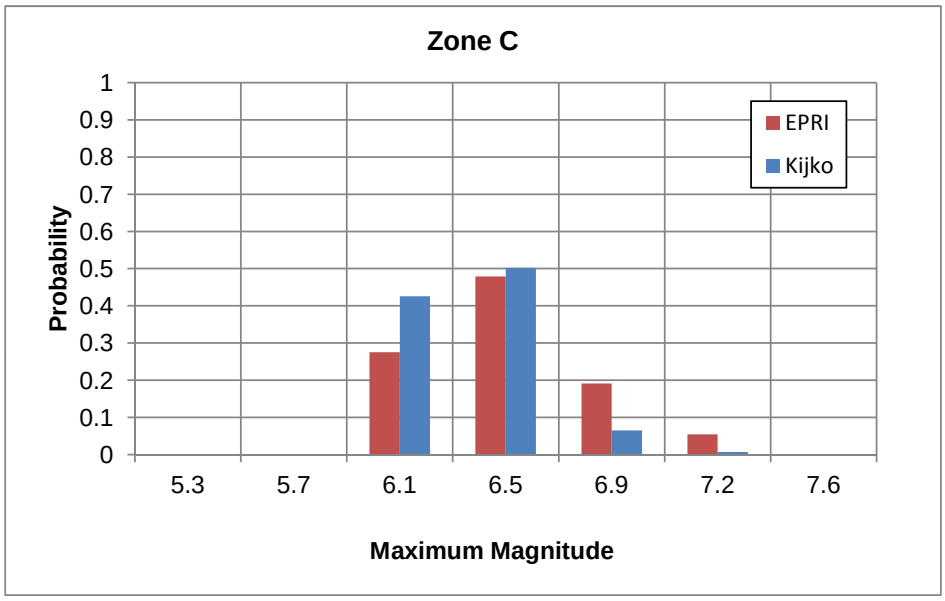

Figure 2.26: Maximum magnitude distributions for EG1a macro-zone C computed using the Bayesian (EPRI) and Kijko and Graham (Kijko) methods.

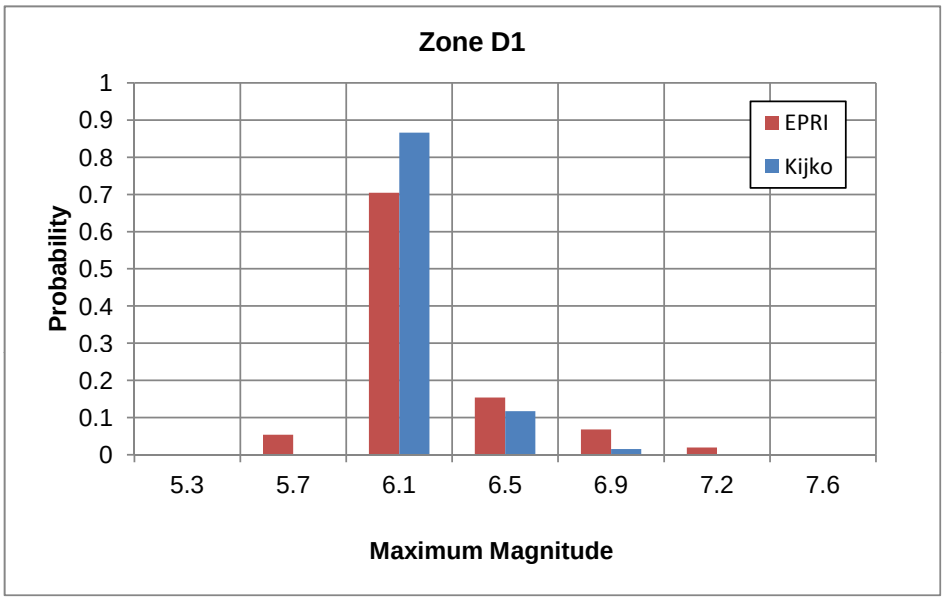

Figure 2.27: Maximum magnitude distributions for EG1a macro-zone D1 computed using the Bayesian (EPRI) and Kijko and Graham (Kijko) methods.

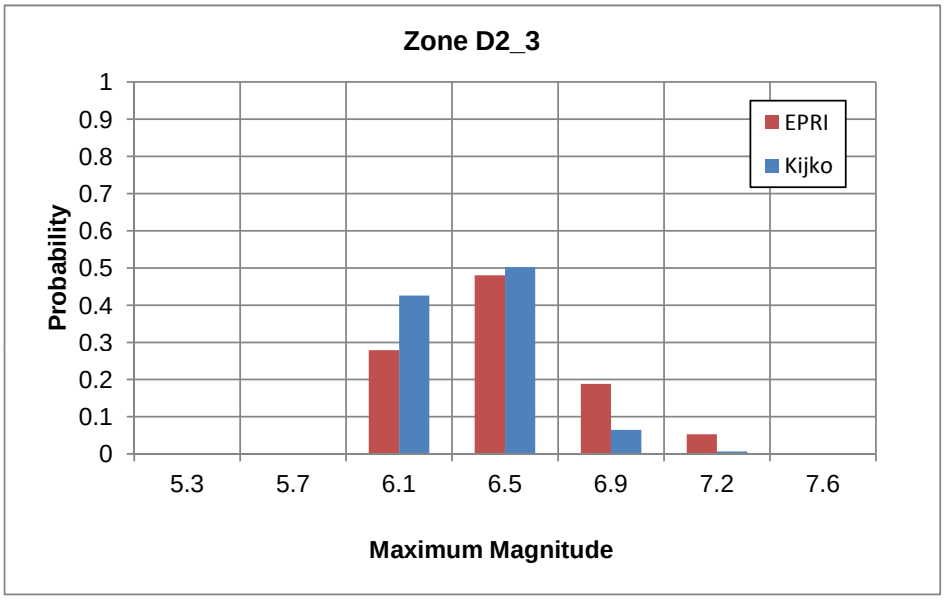

Figure 2.28: Maximum magnitude distributions for EG1a macro-zone D23 computed using the Bayesian (EPRI) and Kijko and Graham (Kijko) methods.

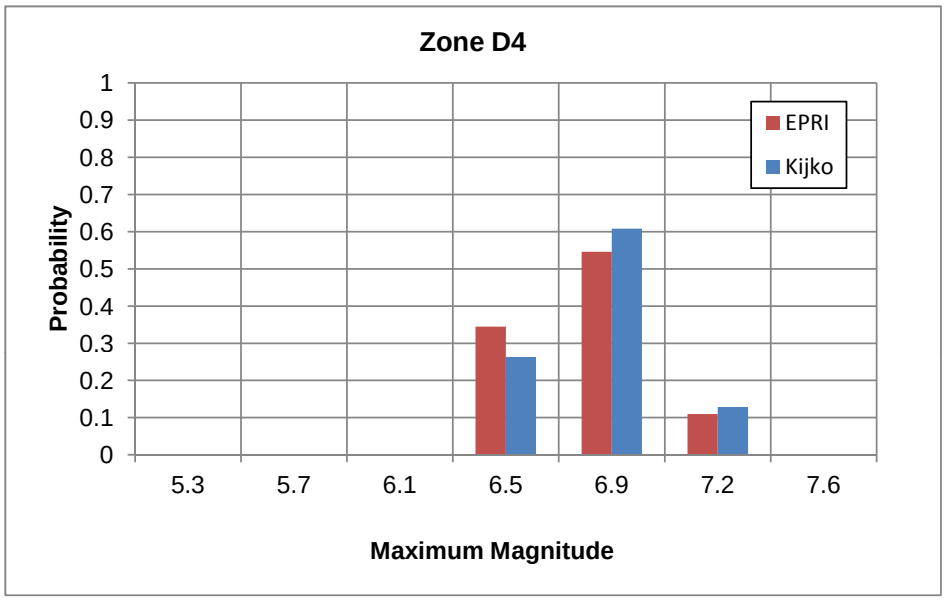

Figure 2.29: Maximum magnitude distributions for EG1a macro-zone D4 computed using the Bayesian (EPRI) and Kijko and Graham (Kijko) methods.

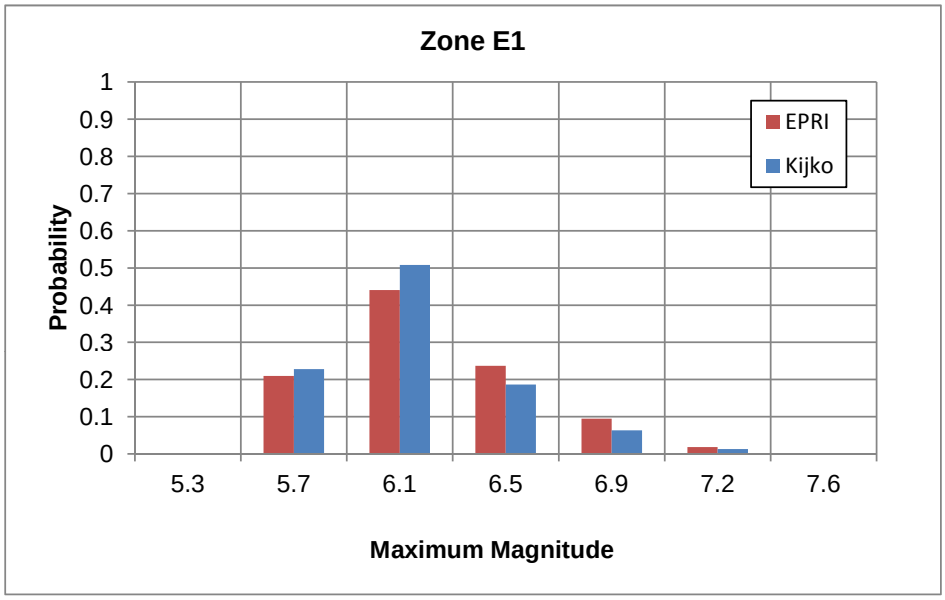

Figure 2.30: Maximum magnitude distributions for EG1a macro-zone E1 computed using the Bayesian (EPRI) and Kijko and Graham (Kijko) methods.

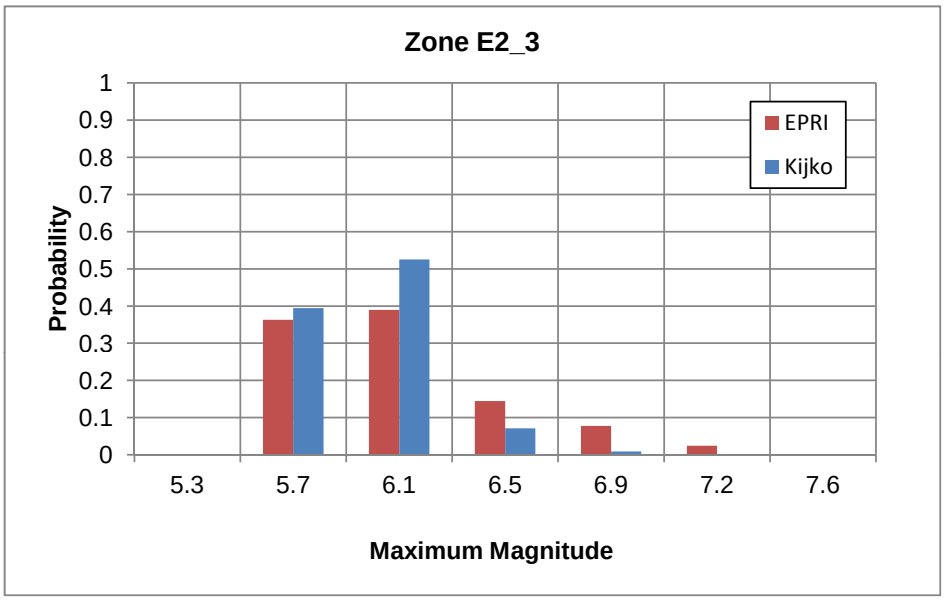

Figure 2.31: Maximum magnitude distributions for EG1a macro-zone E23 computed using the Bayesian (EPRI) and Kijko and Graham (Kijko) methods.

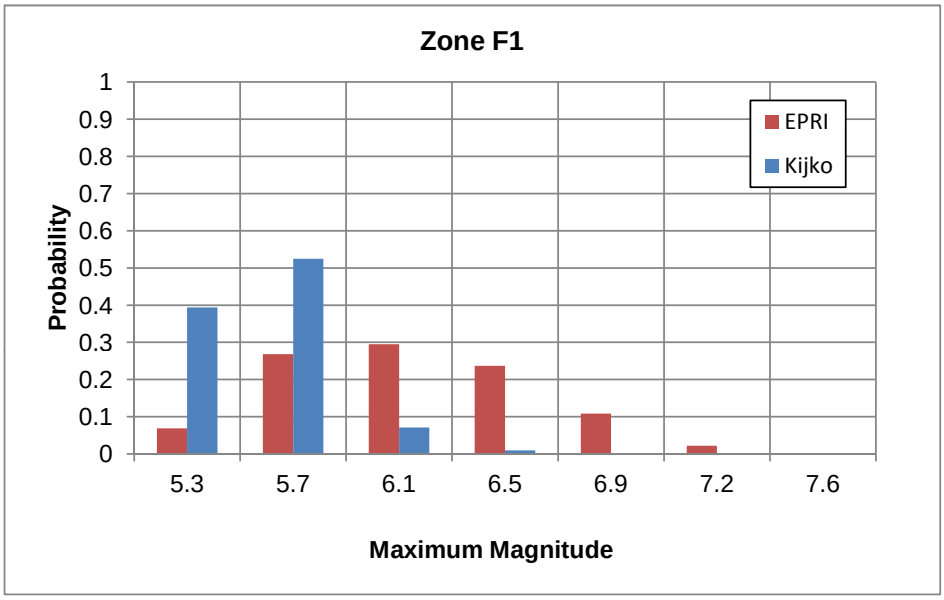

Figure 2.32: Maximum magnitude distributions for EG1a macro-zone F1 computed using the Bayesian (EPRI) and Kijko and Graham (Kijko) methods.

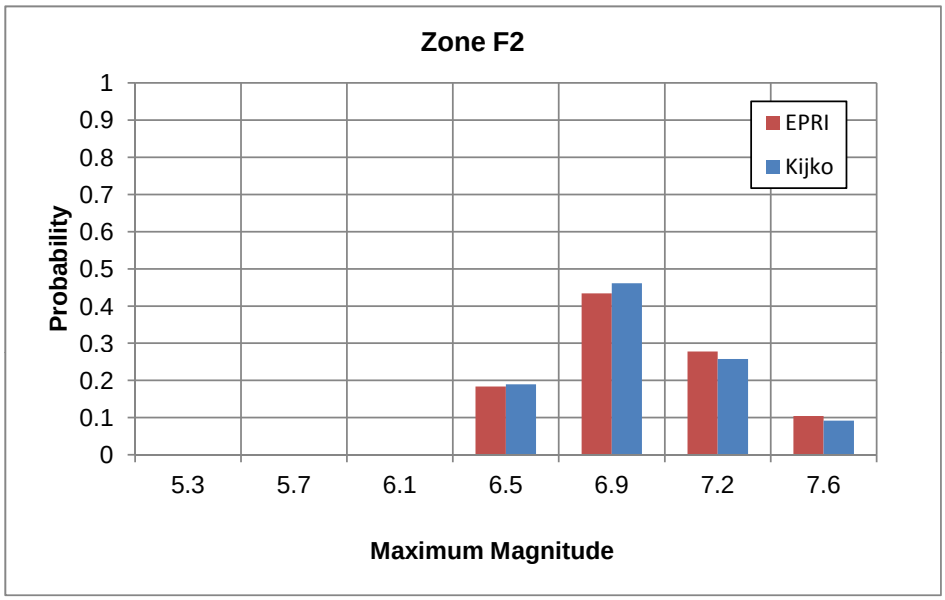

Figure 2.33: Maximum magnitude distributions for EG1a macro-zone F2 computed using the Bayesian (EPRI) and Kijko and Graham (Kijko) methods.

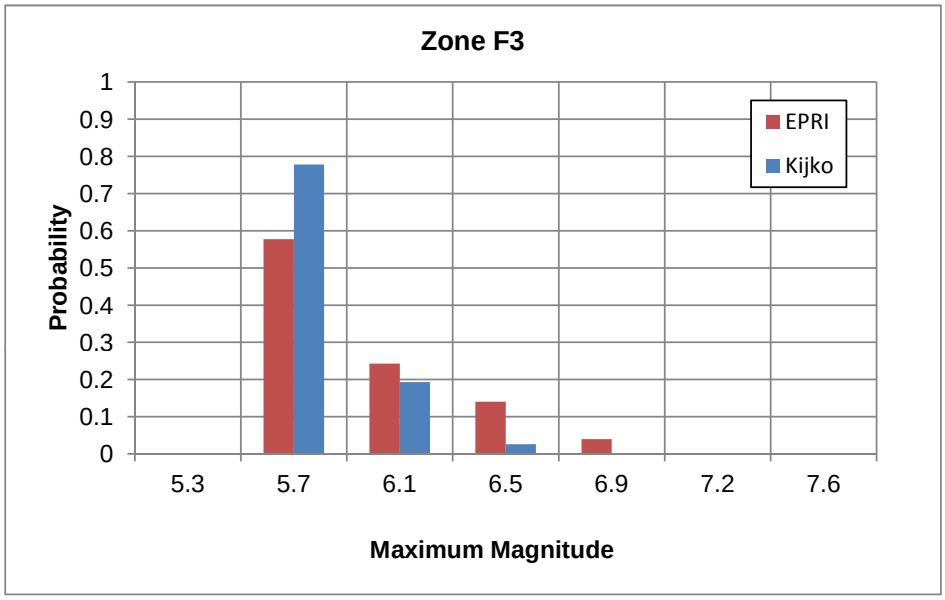

Figure 2.34: Maximum magnitude distributions for EG1a macro-zone F3 computed using the Bayesian (EPRI) and Kijko and Graham (Kijko) methods.

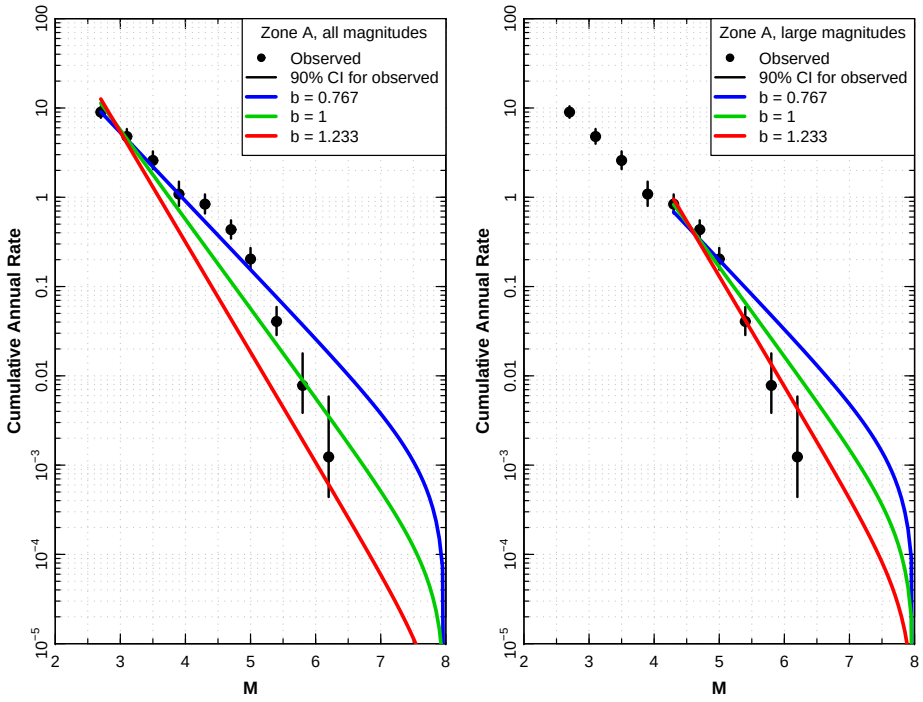

Figure 2.35: Earthquake recurrence relationships for Source Zone A.

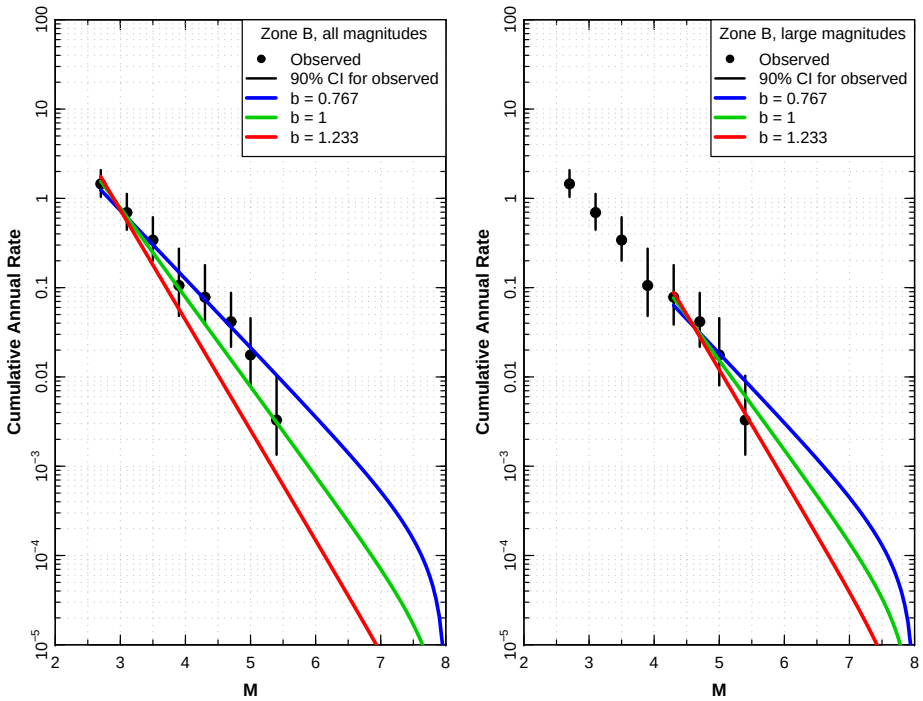

Figure 2.36: Earthquake recurrence relationships for Source Zone B.

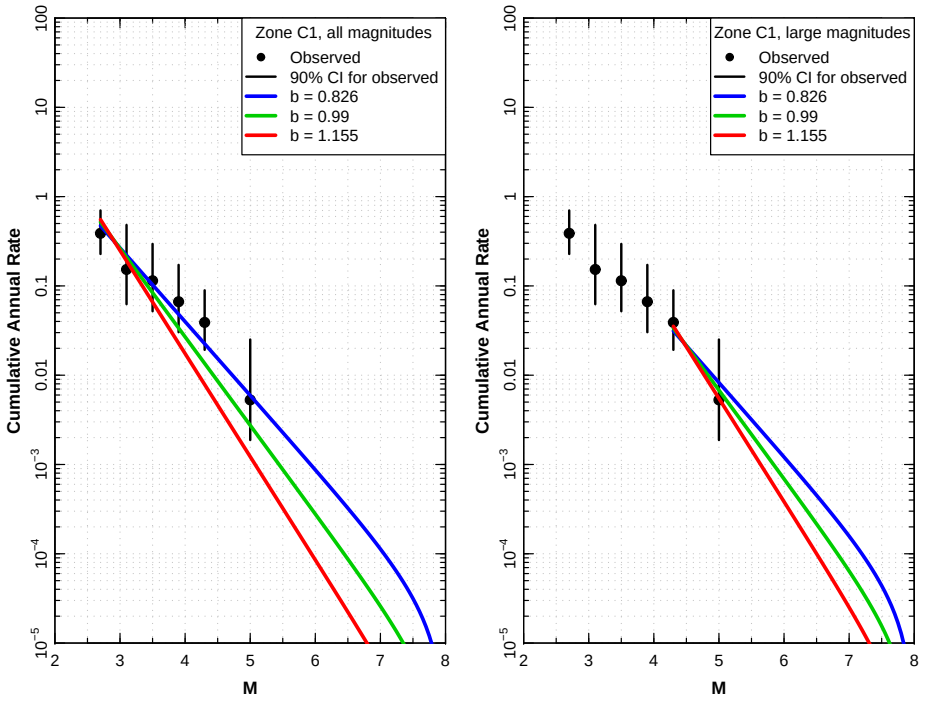

Figure 2.37: Earthquake recurrence relationships for Source Zone C1.

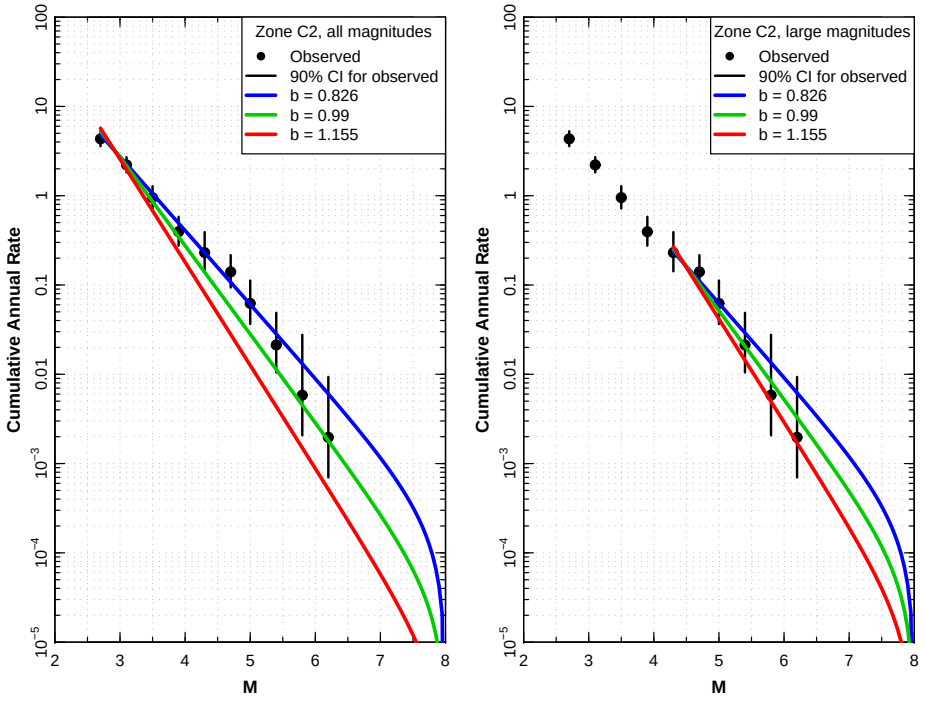

Figure 2.38: Earthquake recurrence relationships for Source Zone C2.

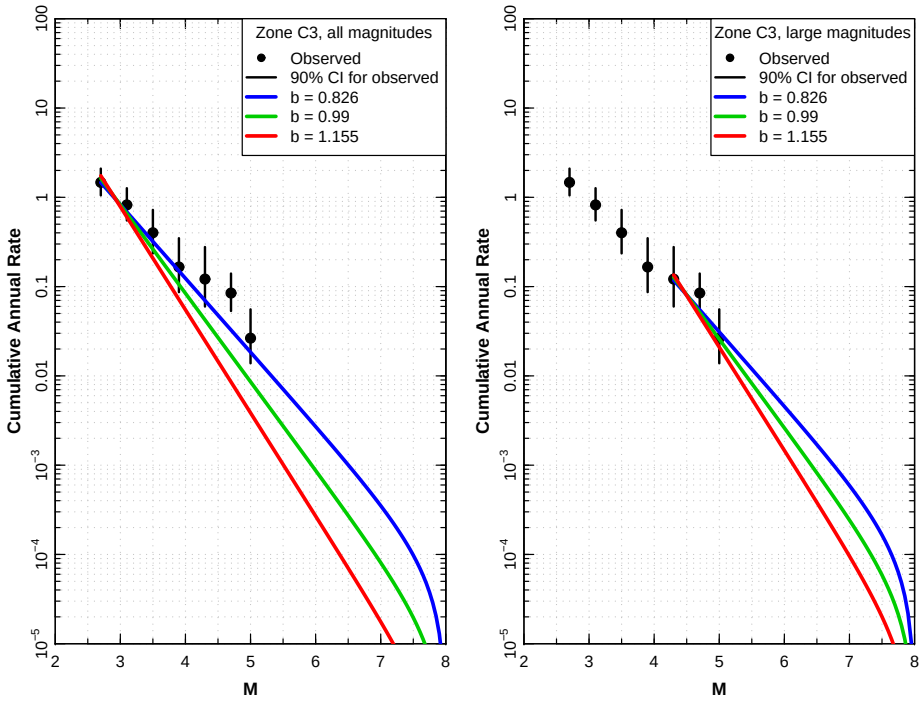

Figure 2.39: Earthquake recurrence relationships for Source Zone C3.

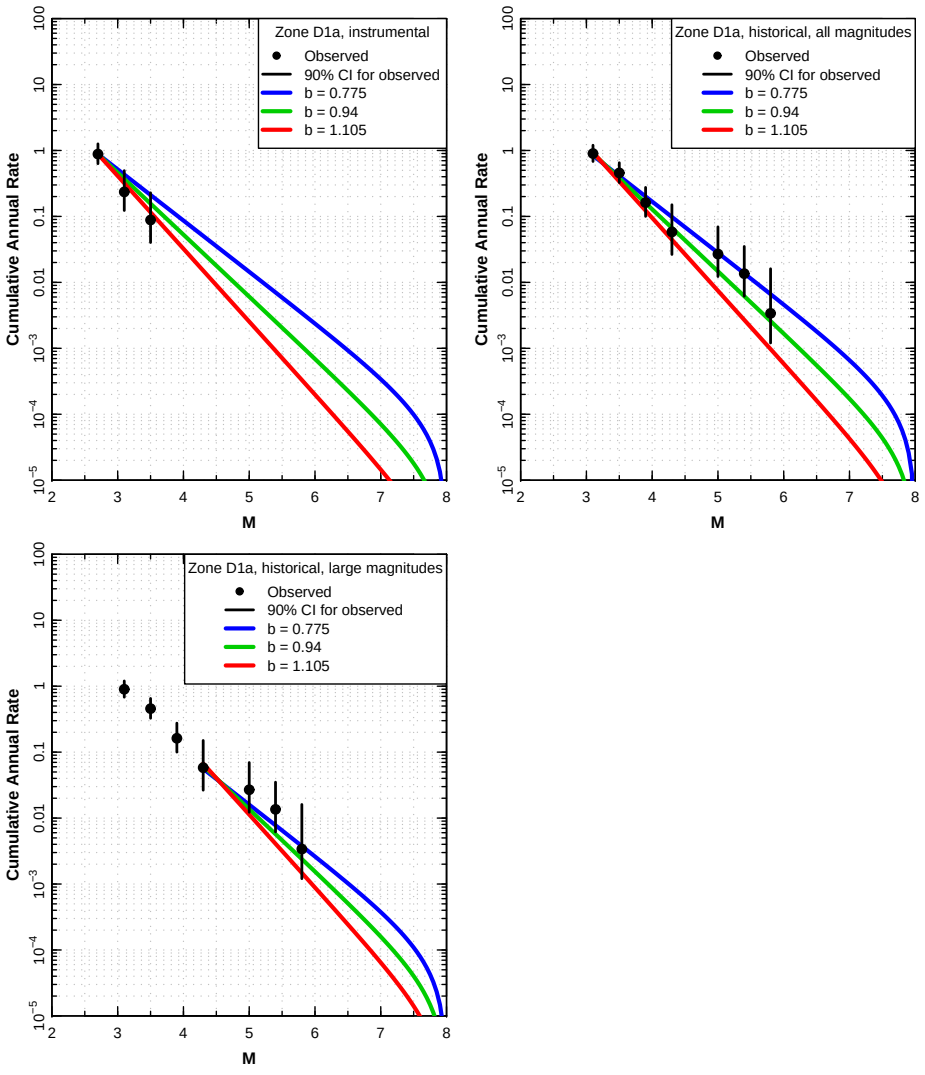

Figure 2.40: Earthquake recurrence relationships for Source Zone D1a.

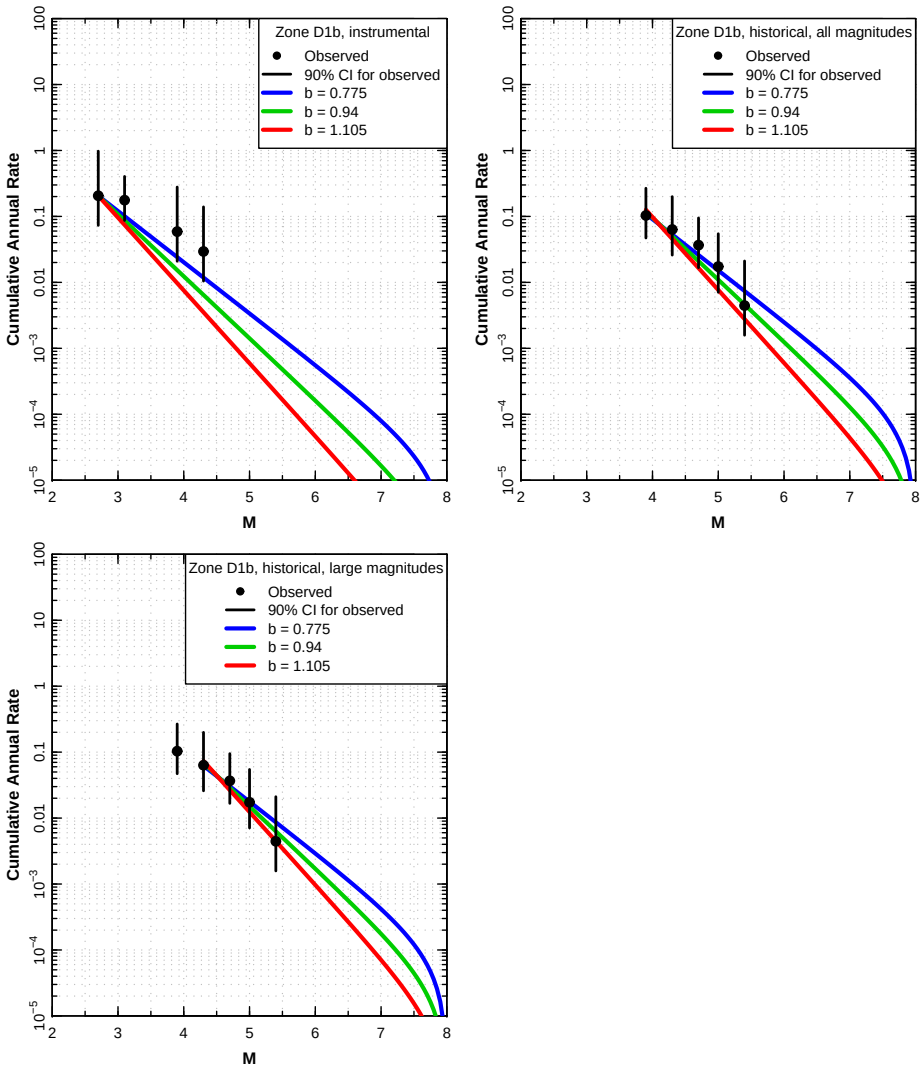

Figure 2.41: Earthquake recurrence relationships for Source Zone D1b.

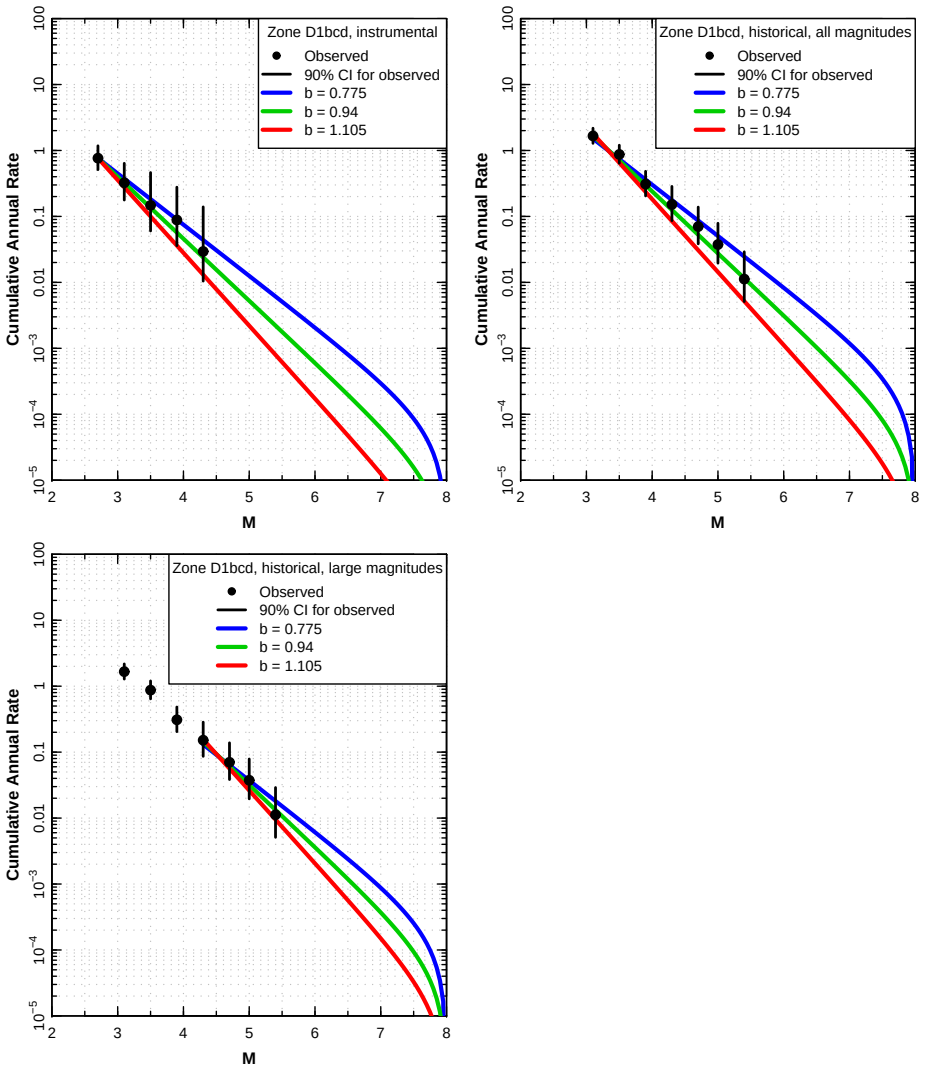

Figure 2.42: Earthquake recurrence relationships for Source Zone D1bcd.

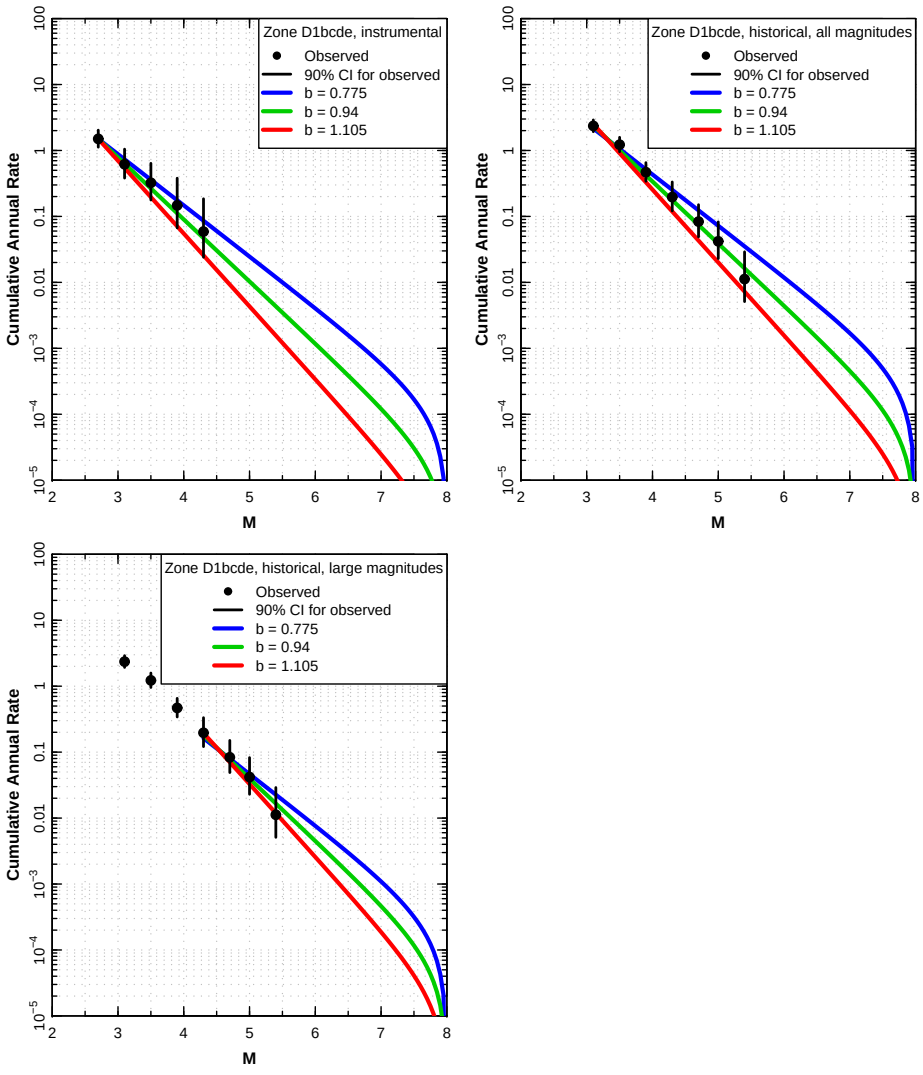

Figure 2.43: Earthquake recurrence relationships for Source Zone D1bcde.

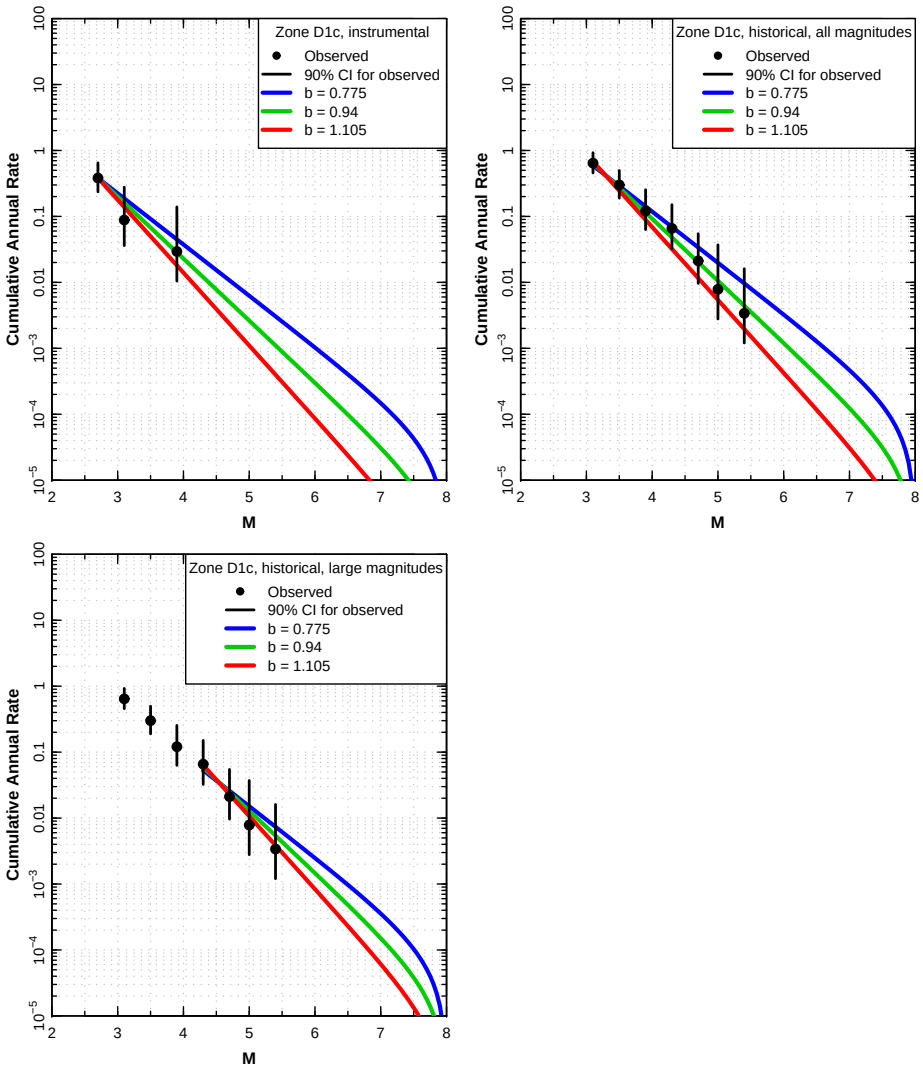

Figure 2.44: Earthquake recurrence relationships for Source Zone D1c.

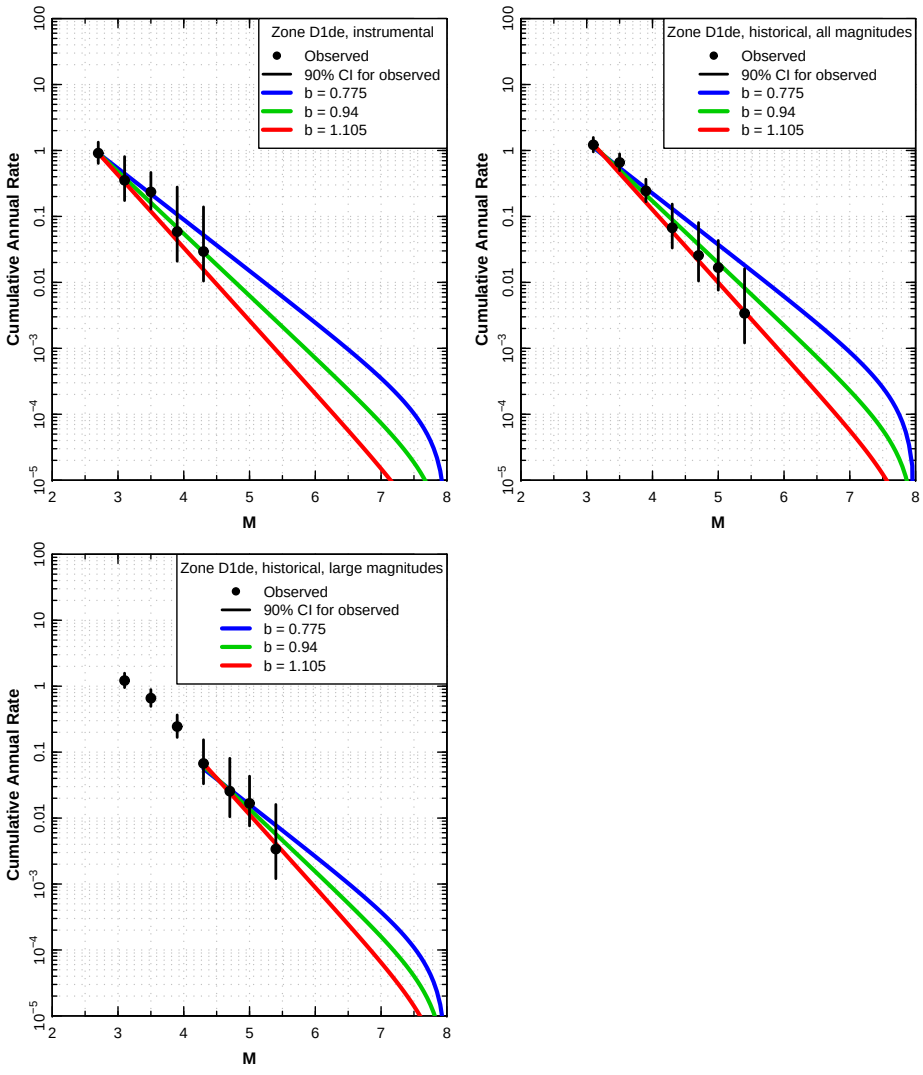

Figure 2.45: Earthquake recurrence relationships for Source Zone D1de.

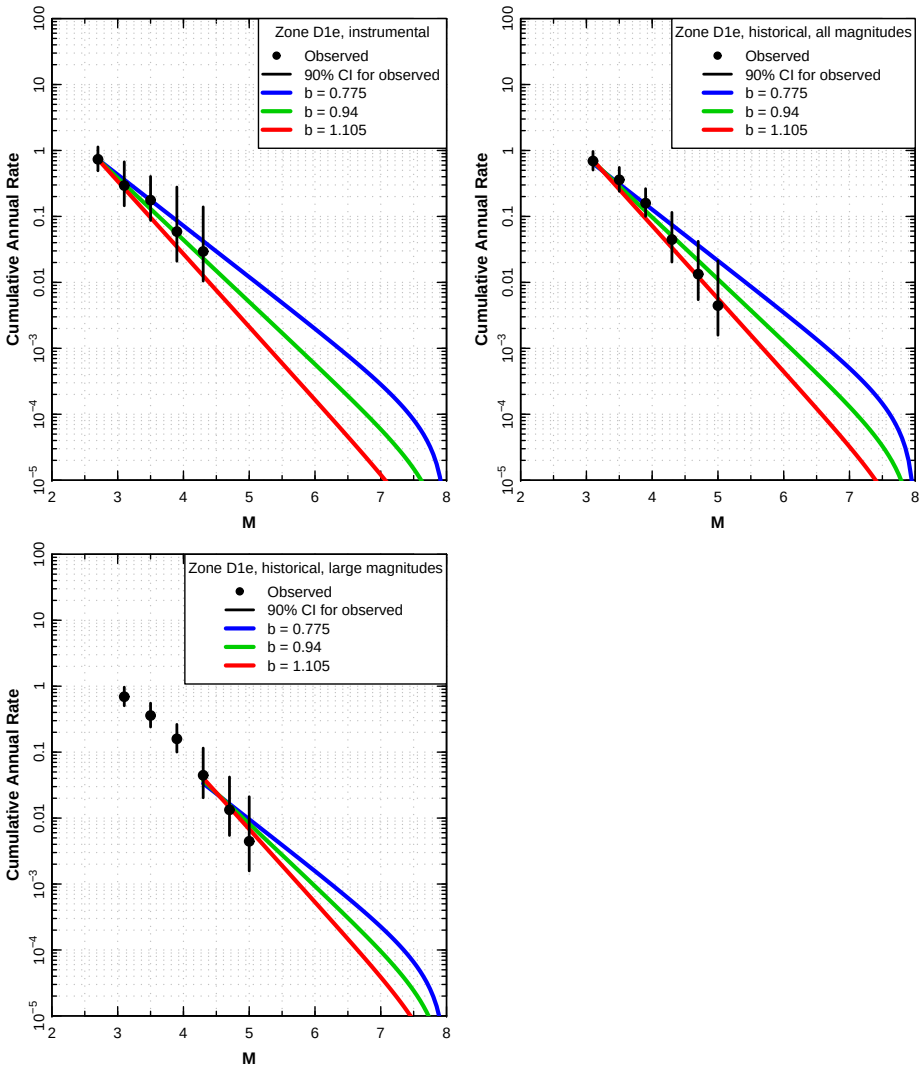

Figure 2.46: Earthquake recurrence relationships for Source Zone D1e.

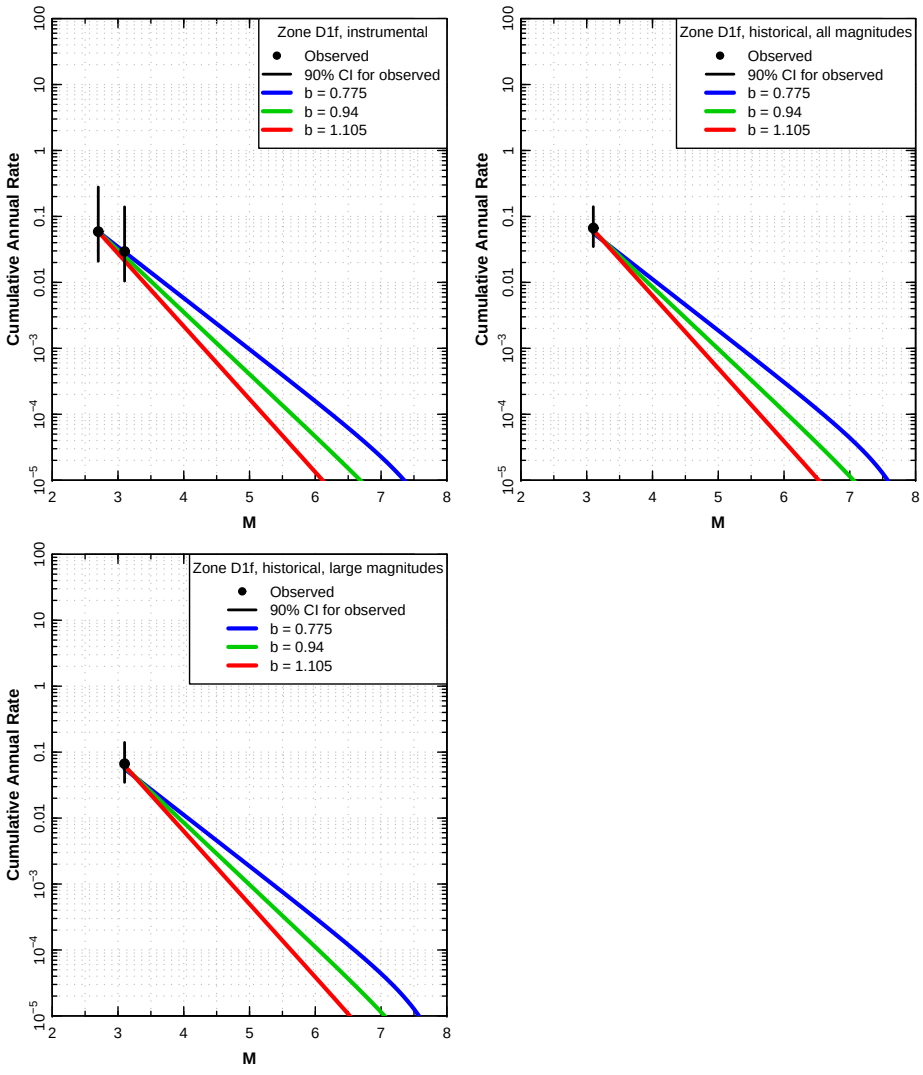

Figure 2.47: Earthquake recurrence relationships for Source Zone D1f.

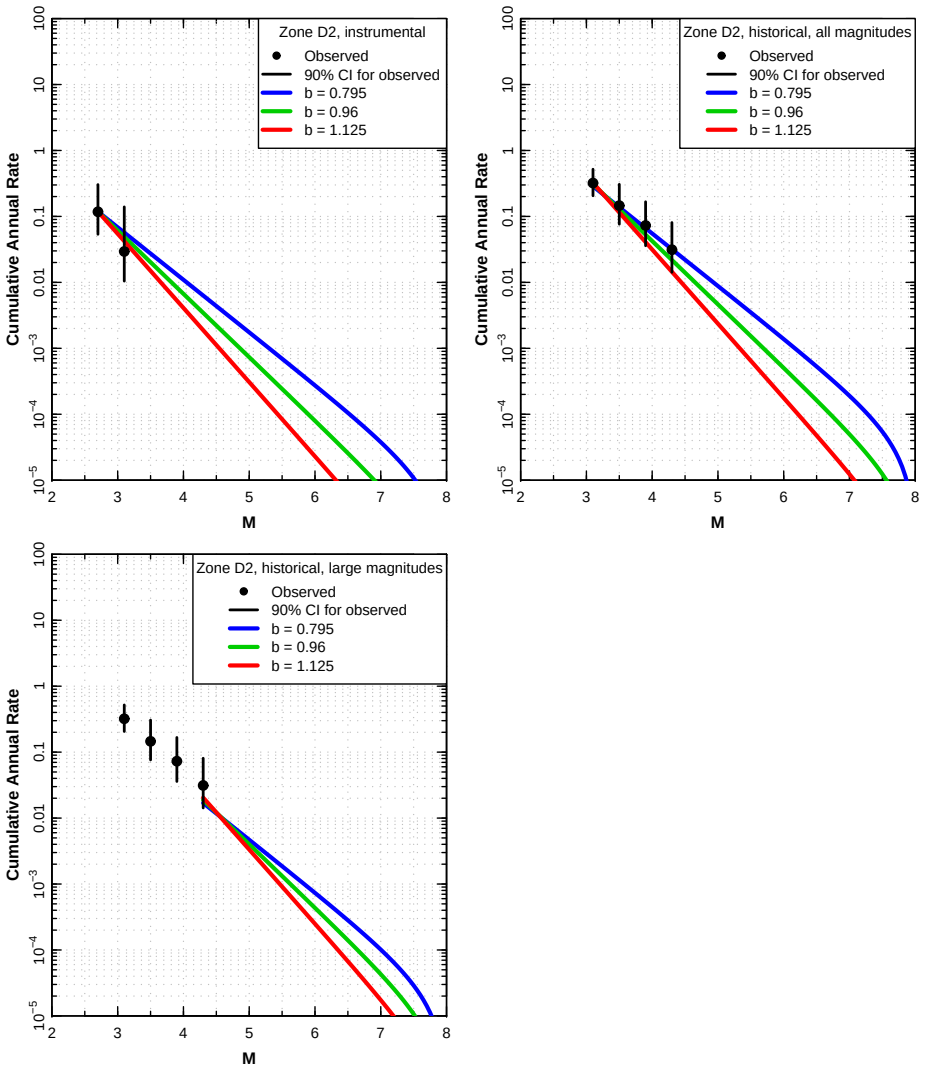

Figure 2.48: Earthquake recurrence relationships for Source Zone D2.

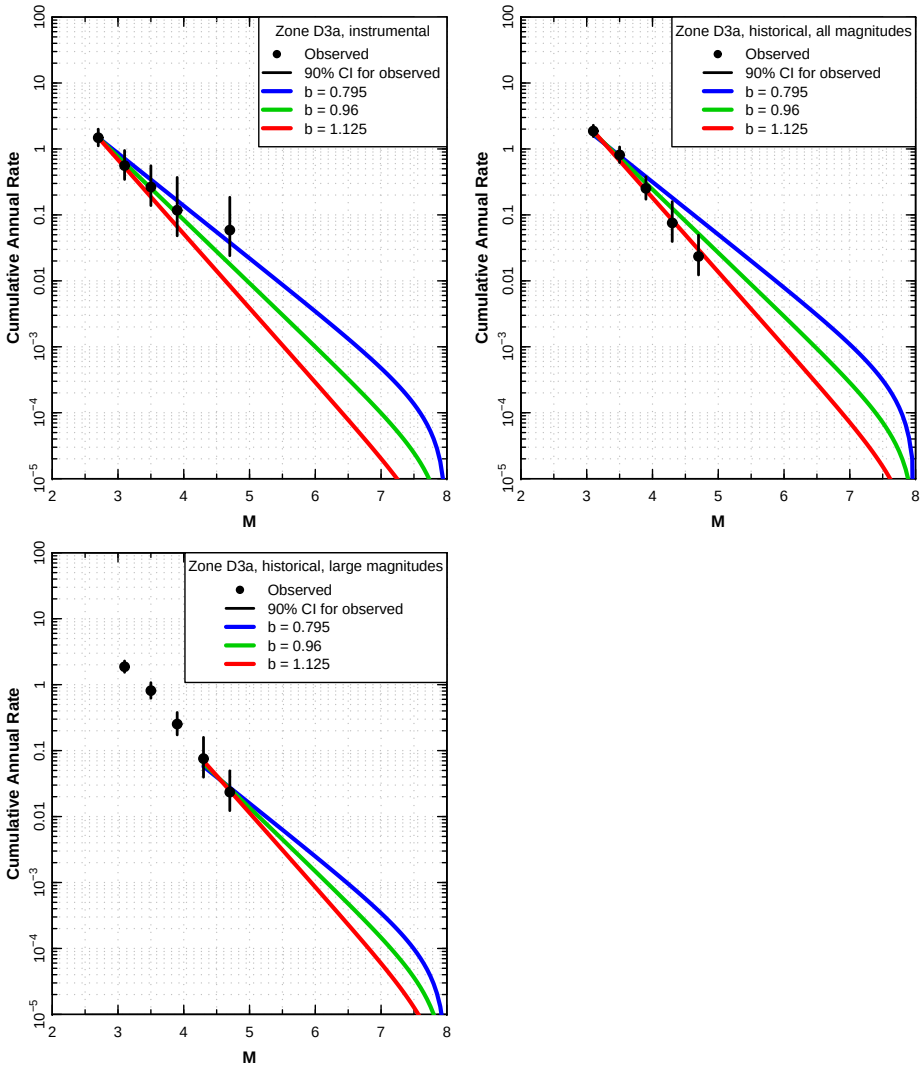

Figure 2.49: Earthquake recurrence relationships for Source Zone D3a.

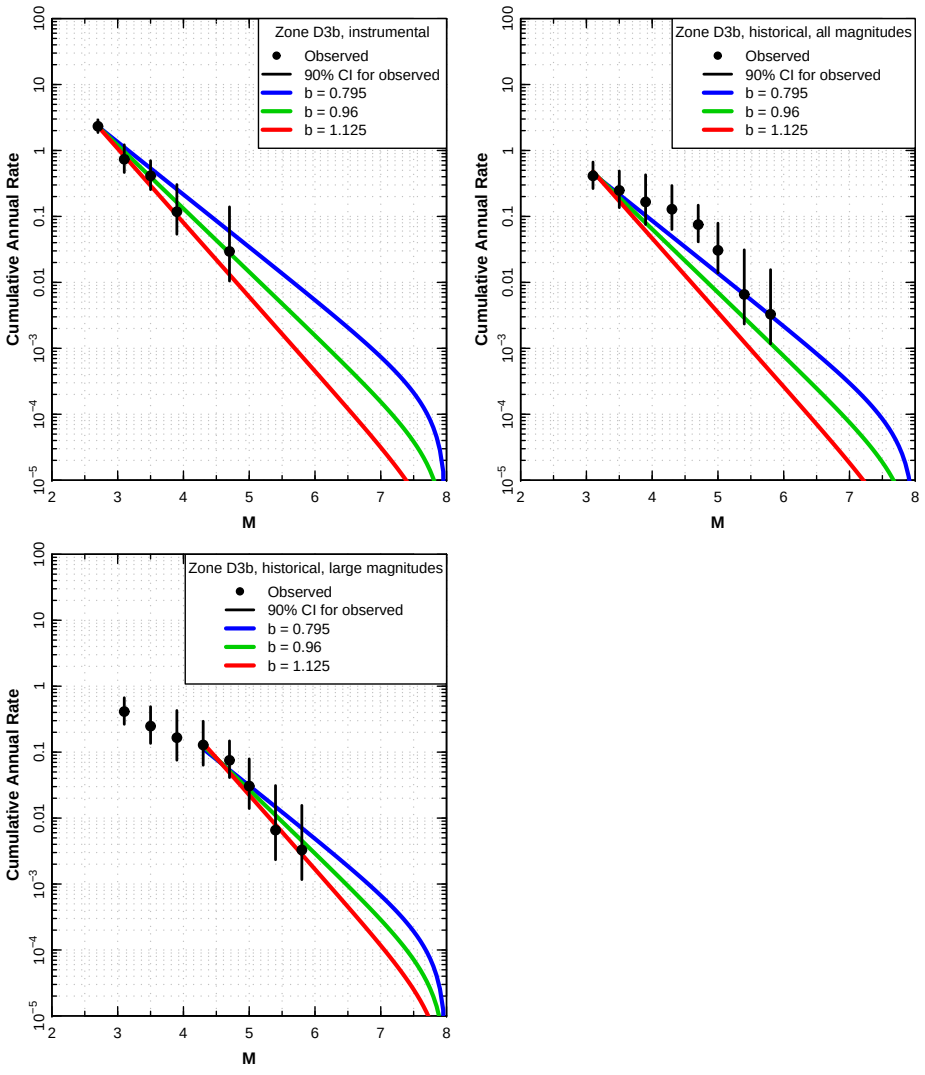

Figure 2.50: Earthquake recurrence relationships for Source Zone D3b.

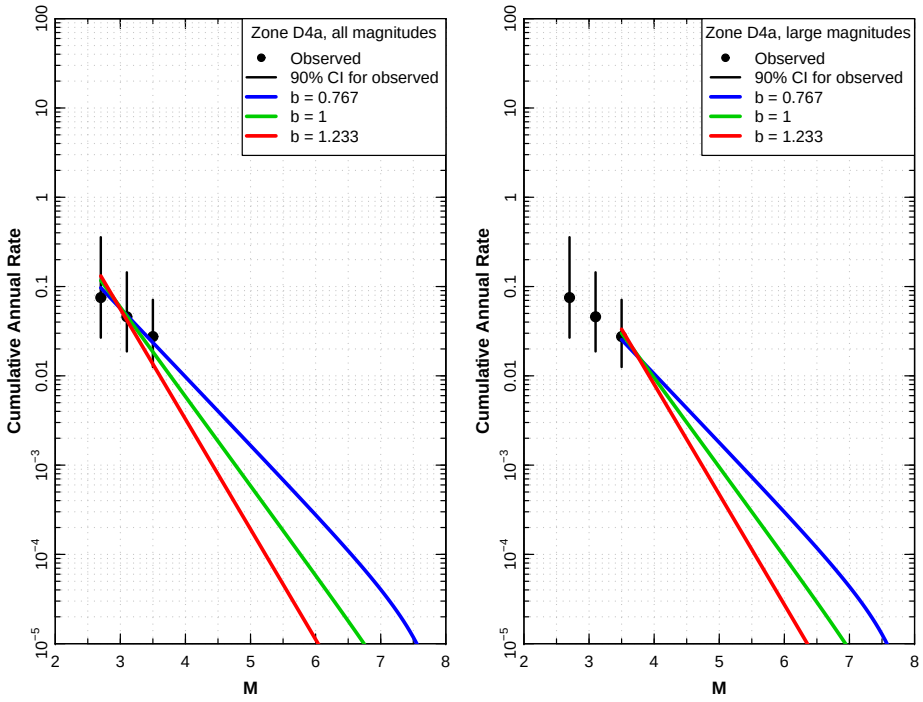

Figure 2.51: Earthquake recurrence relationships for Source Zone D4a.

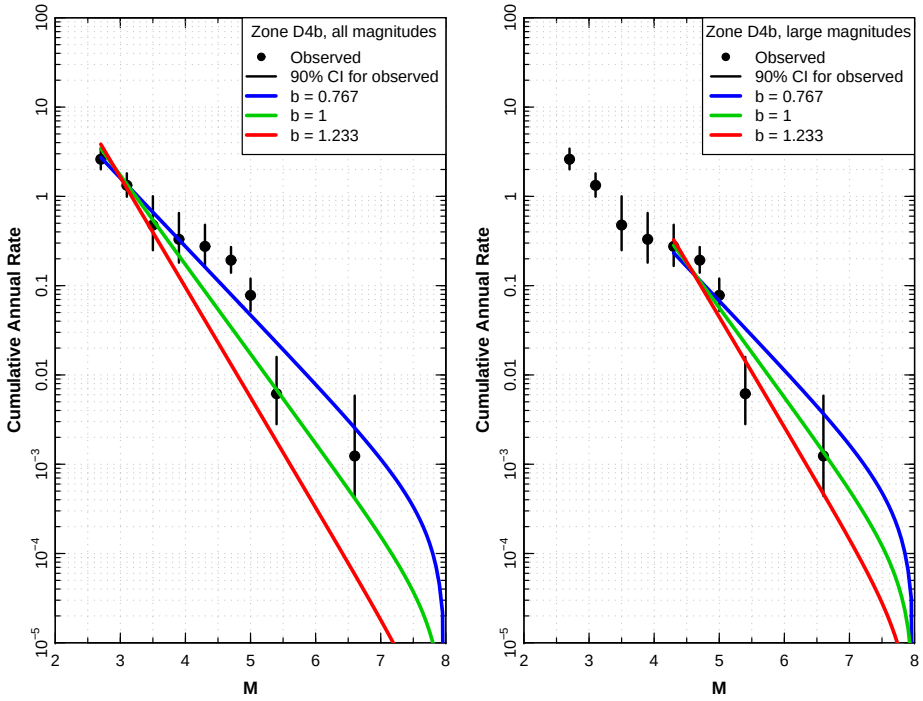

Figure 2.52: Earthquake recurrence relationships for Source Zone D4b.

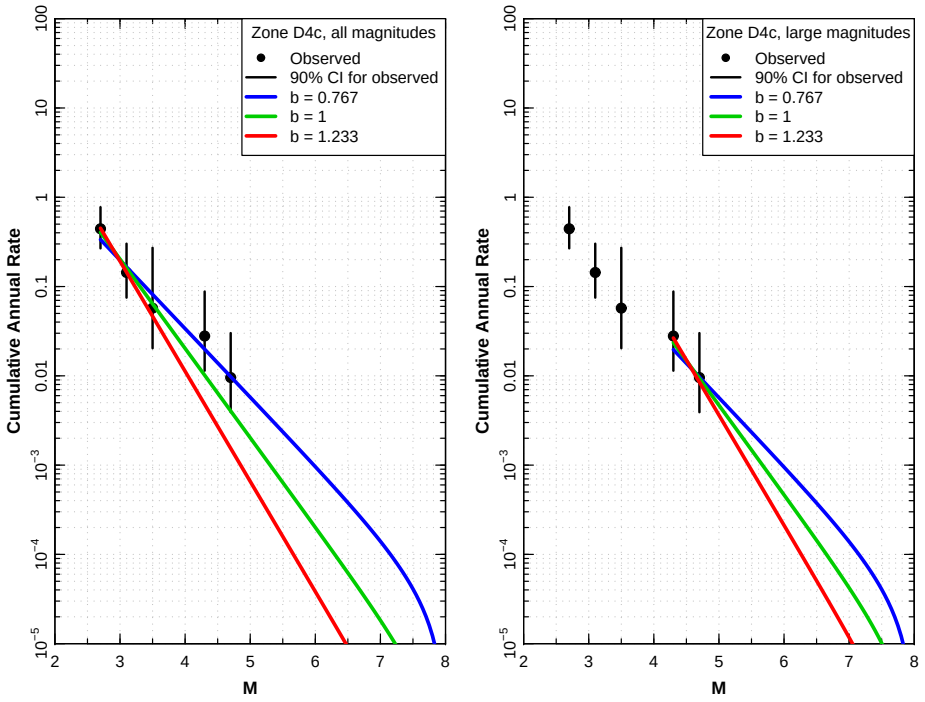

Figure 2.53: Earthquake recurrence relationships for Source Zone D4c.

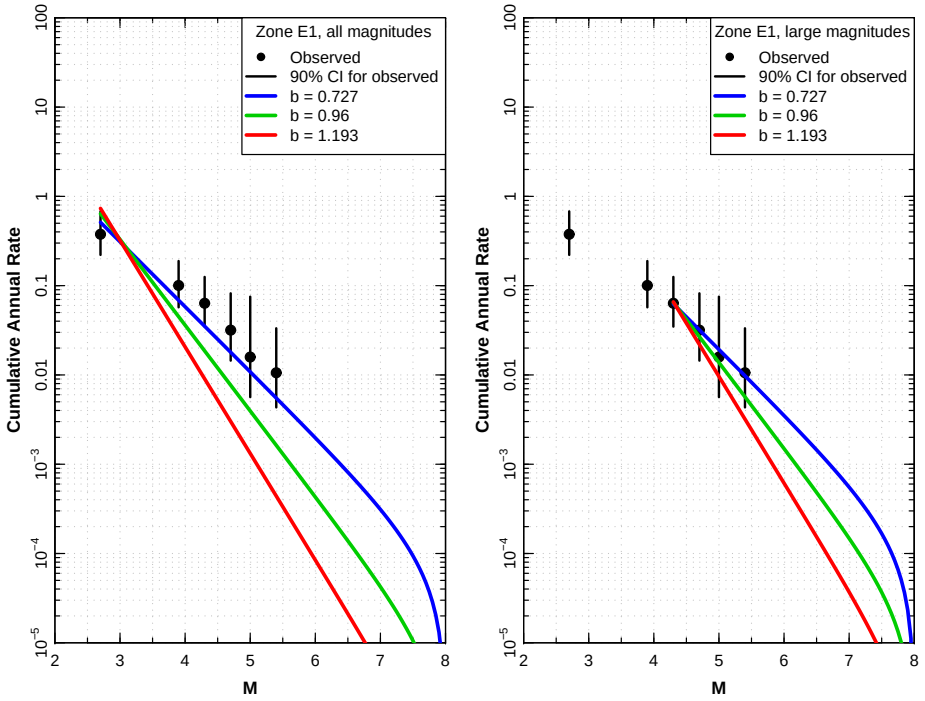

Figure 2.54: Earthquake recurrence relationships for Source Zone E1.

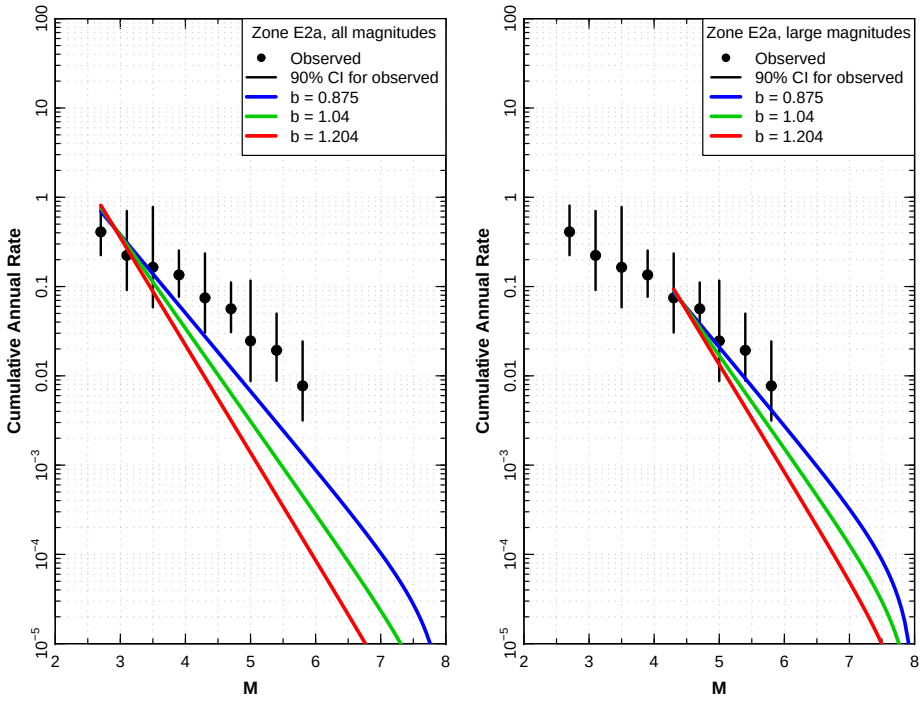

Figure 2.55: Earthquake recurrence relationships for Source Zone E2a.

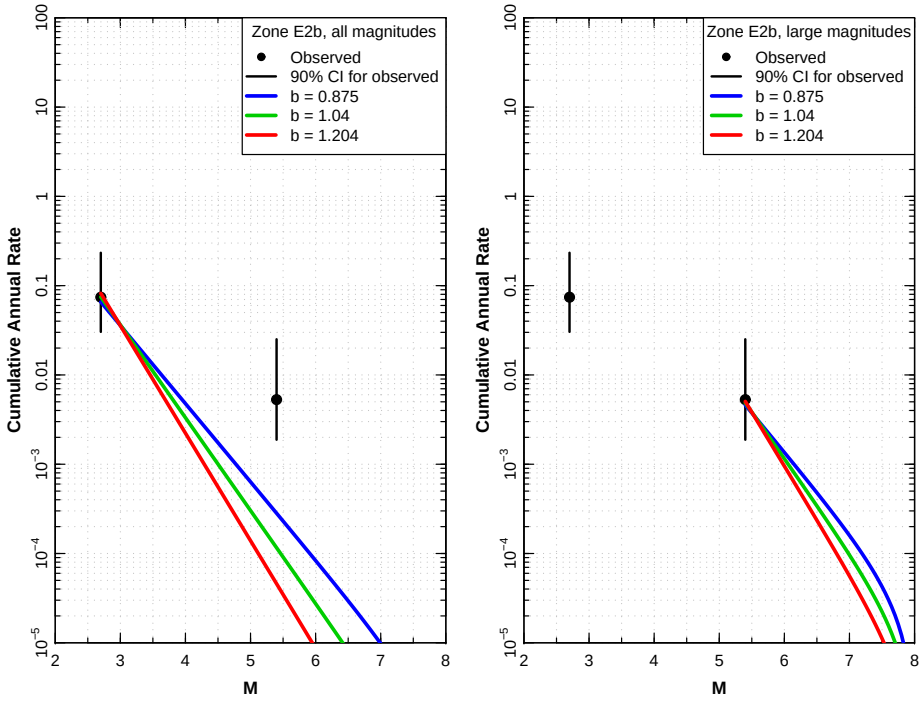

Figure 2.56: Earthquake recurrence relationships for Source Zone E2b.

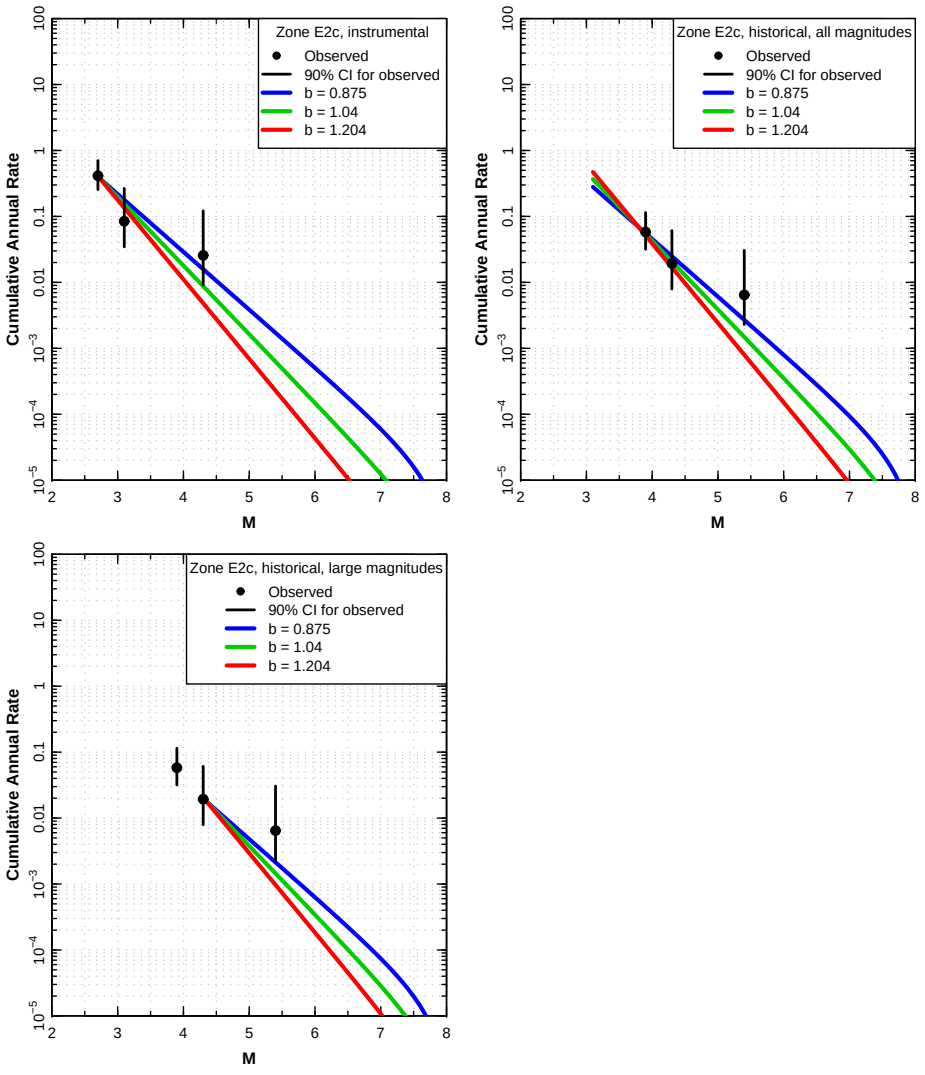

Figure 2.57: Earthquake recurrence relationships for Source Zone E2c.

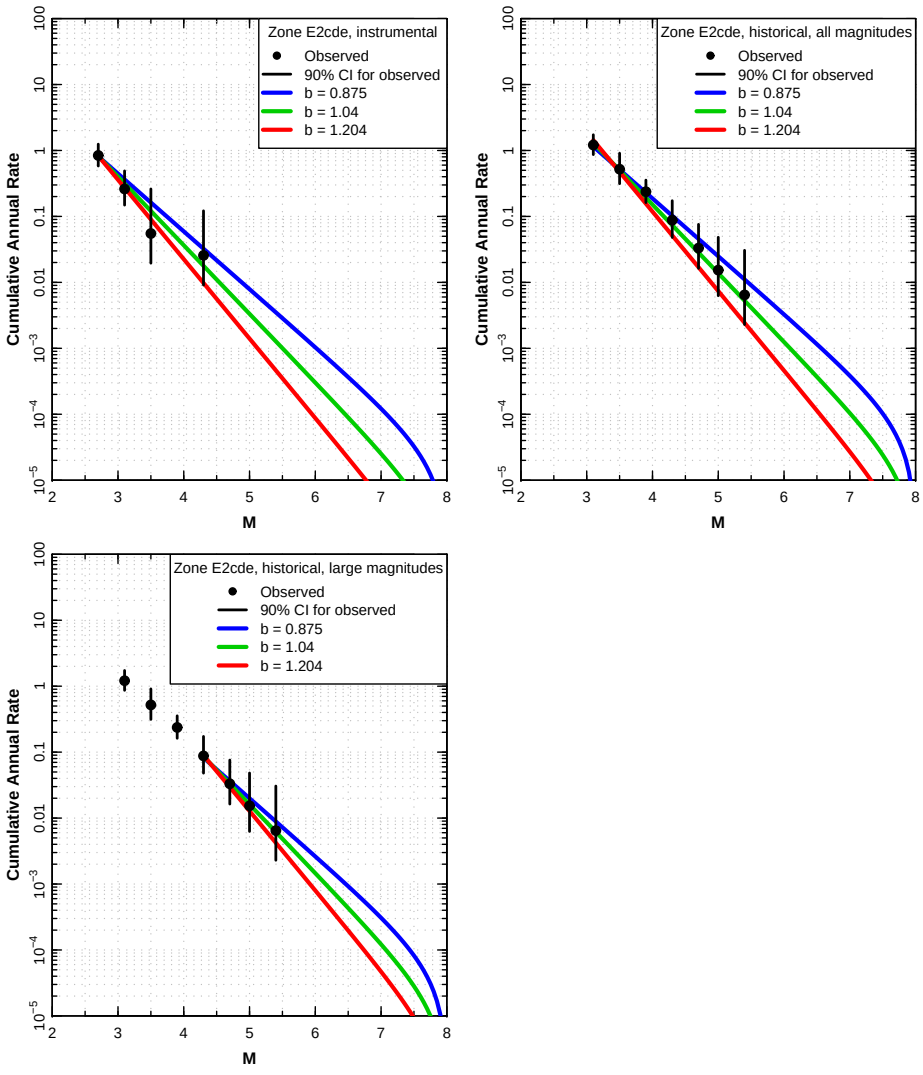

Figure 2.58: Earthquake recurrence relationships for Source Zone E2cde.

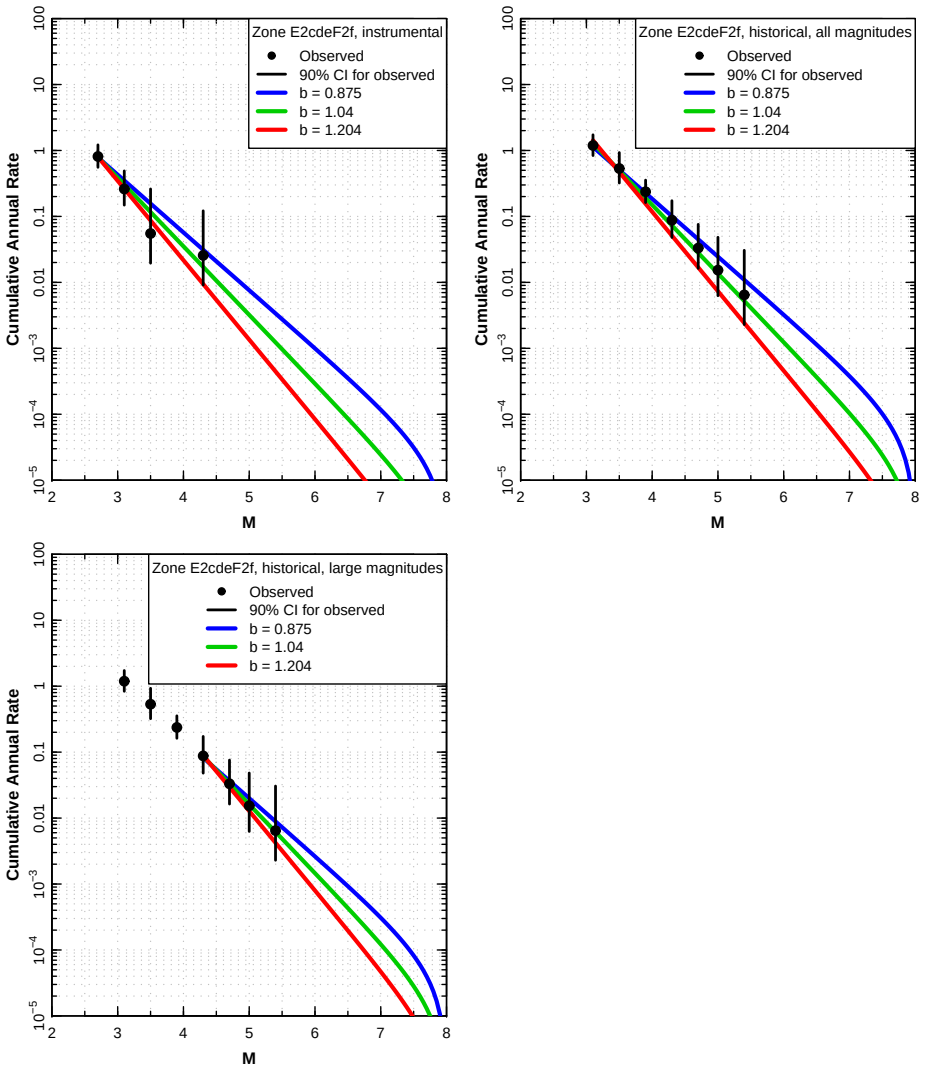

Figure 2.59: Earthquake recurrence relationships for Source Zone E2cdeF2f.

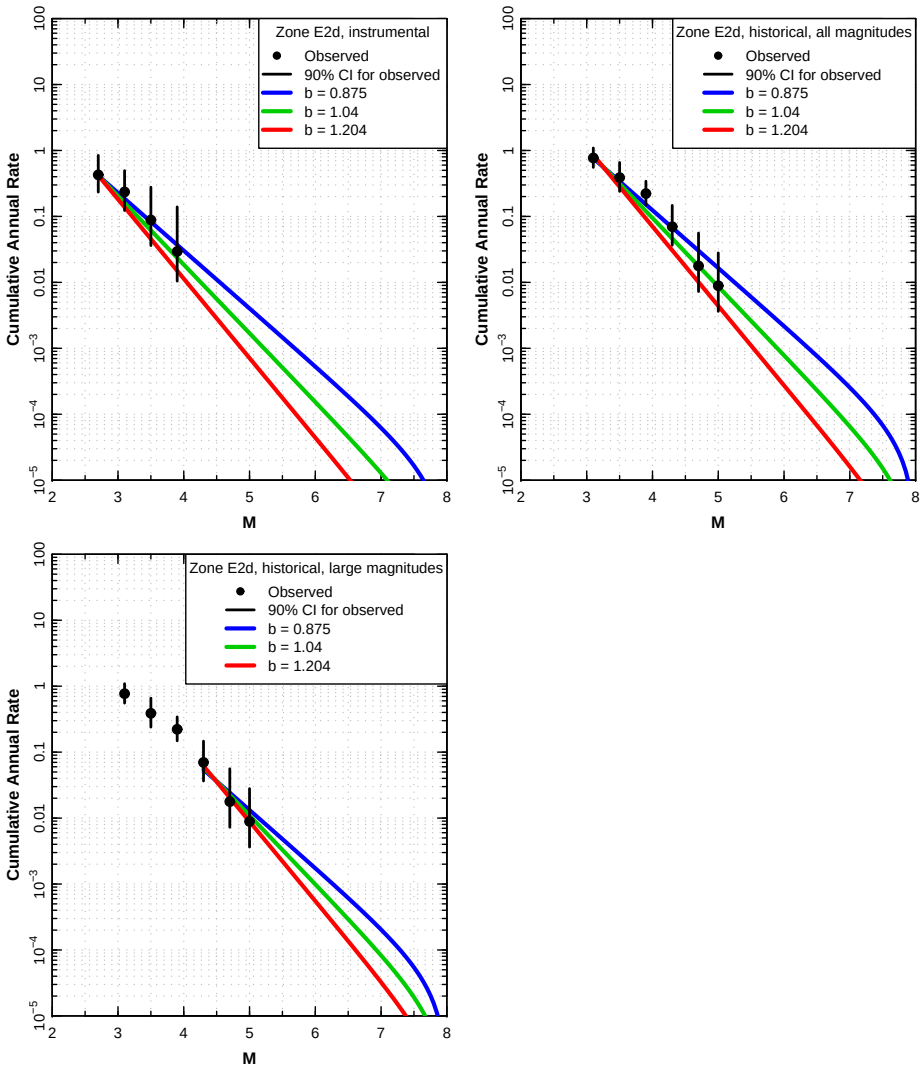

Figure 2.60: Earthquake recurrence relationships for Source Zone E2d.

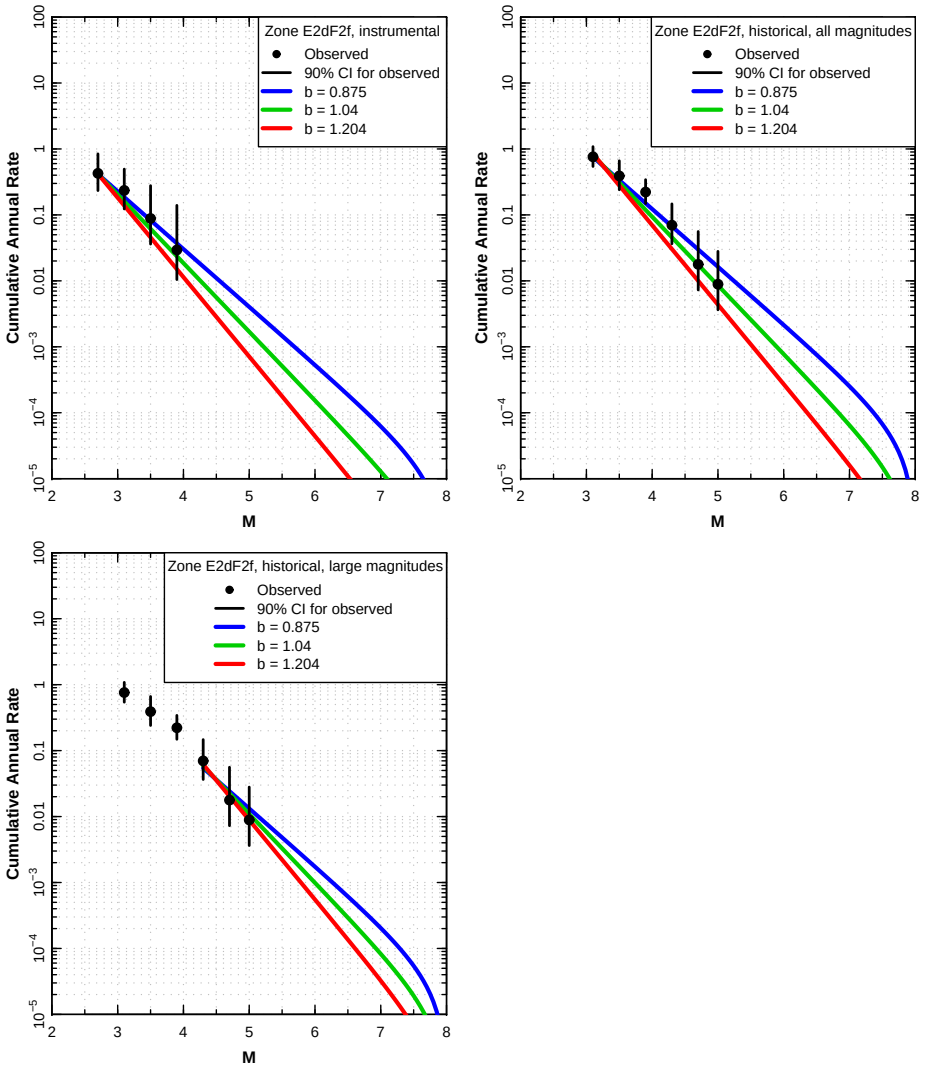

Figure 2.61: Earthquake recurrence relationships for Source Zone E2dF2f.

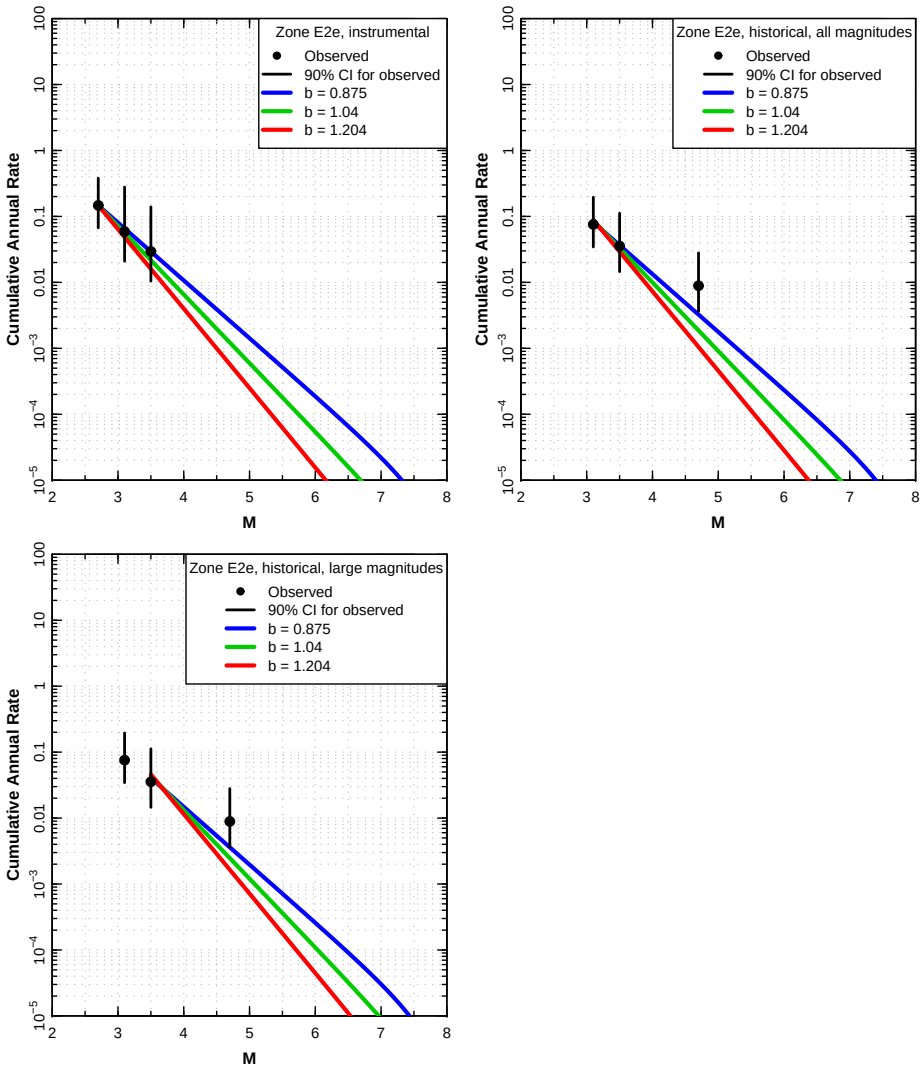

Figure 2.62: Earthquake recurrence relationships for Source Zone E2e.

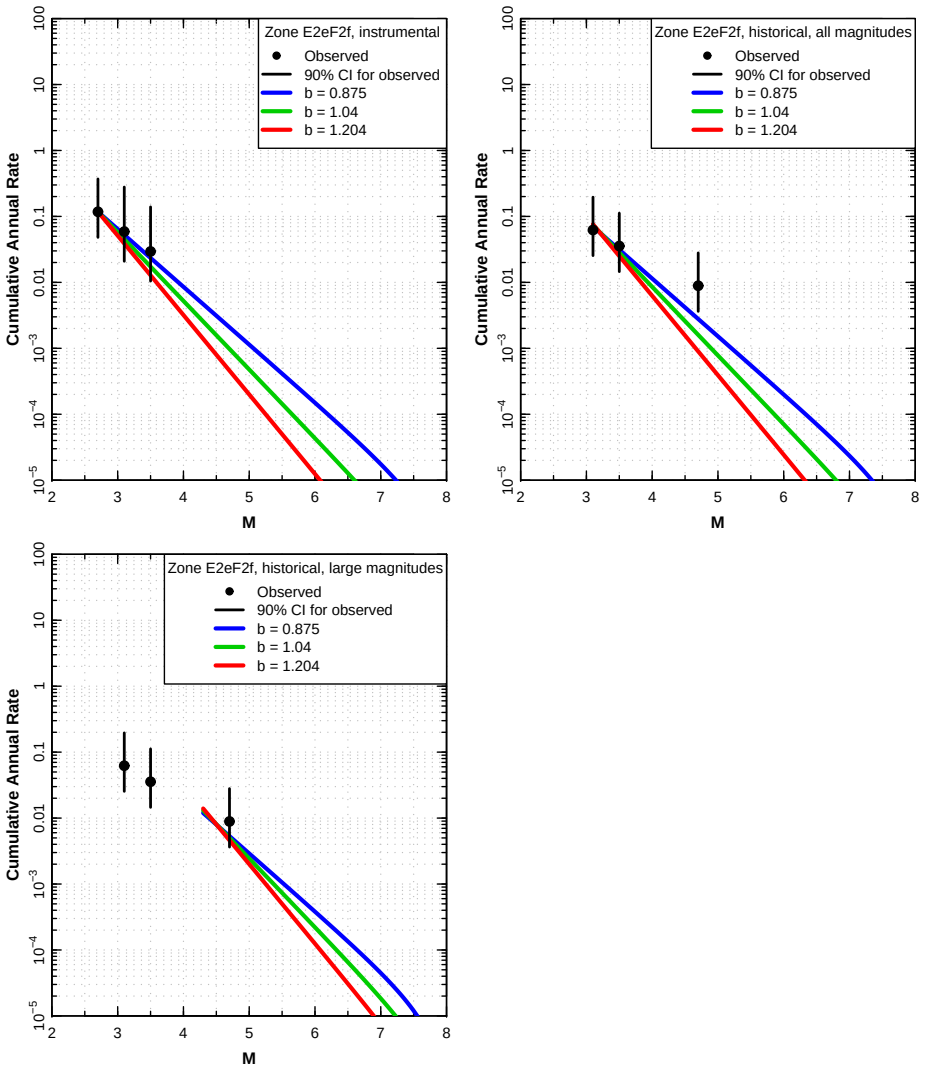

Figure 2.63: Earthquake recurrence relationships for Source Zone E2eF2f.

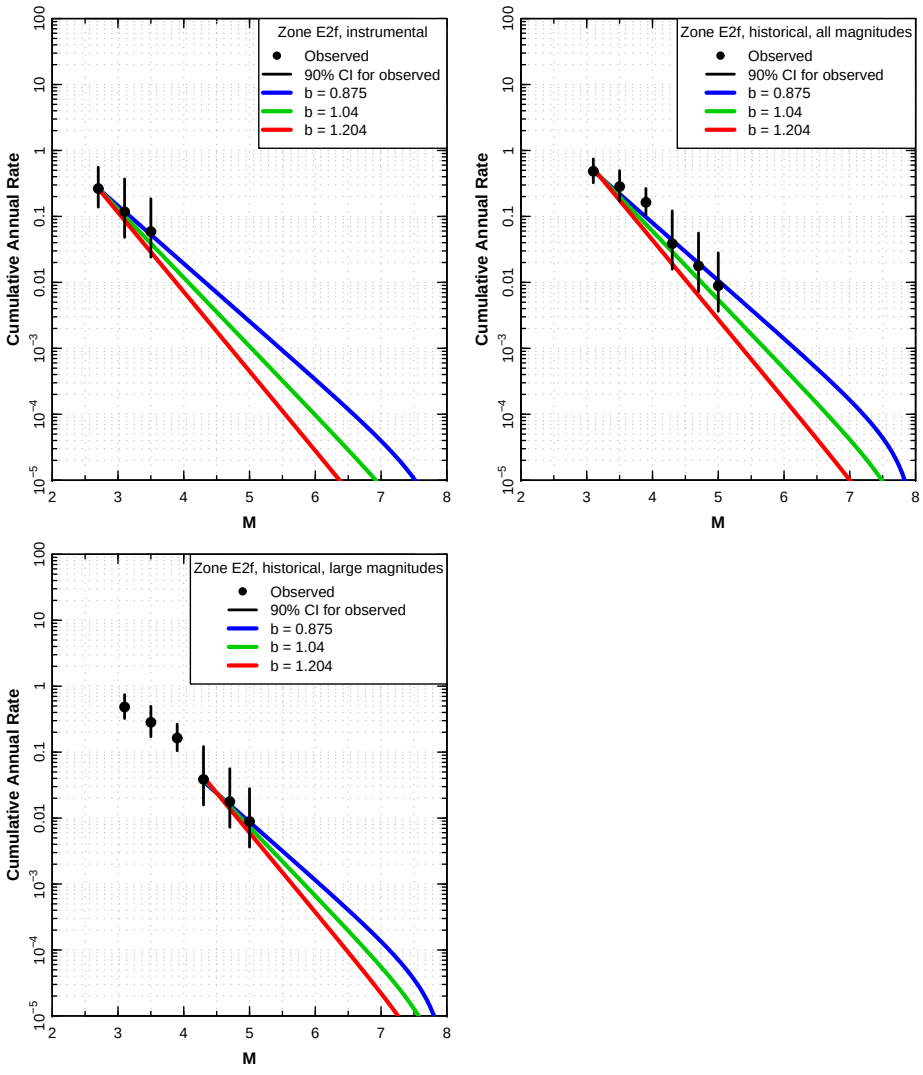

Figure 2.64: Earthquake recurrence relationships for Source Zone E2f.

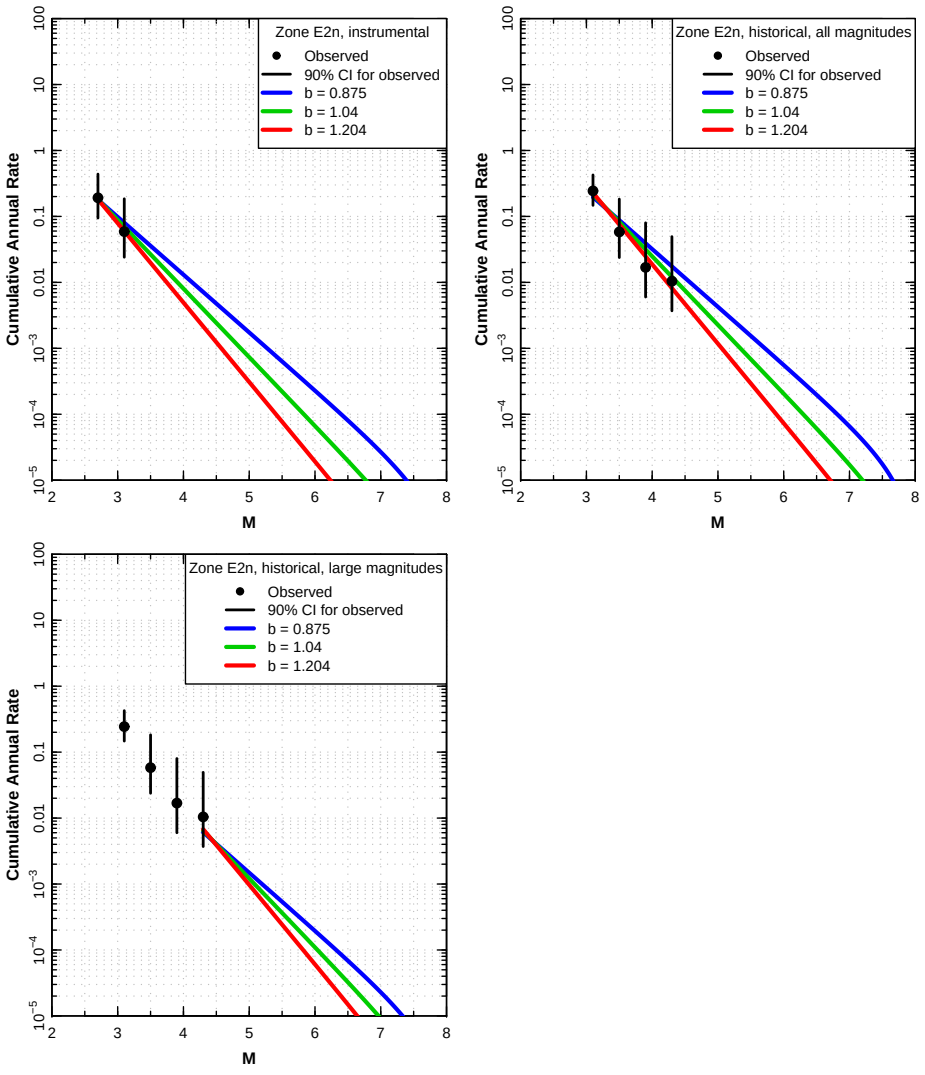

Figure 2.65: Earthquake recurrence relationships for Source Zone E2n.

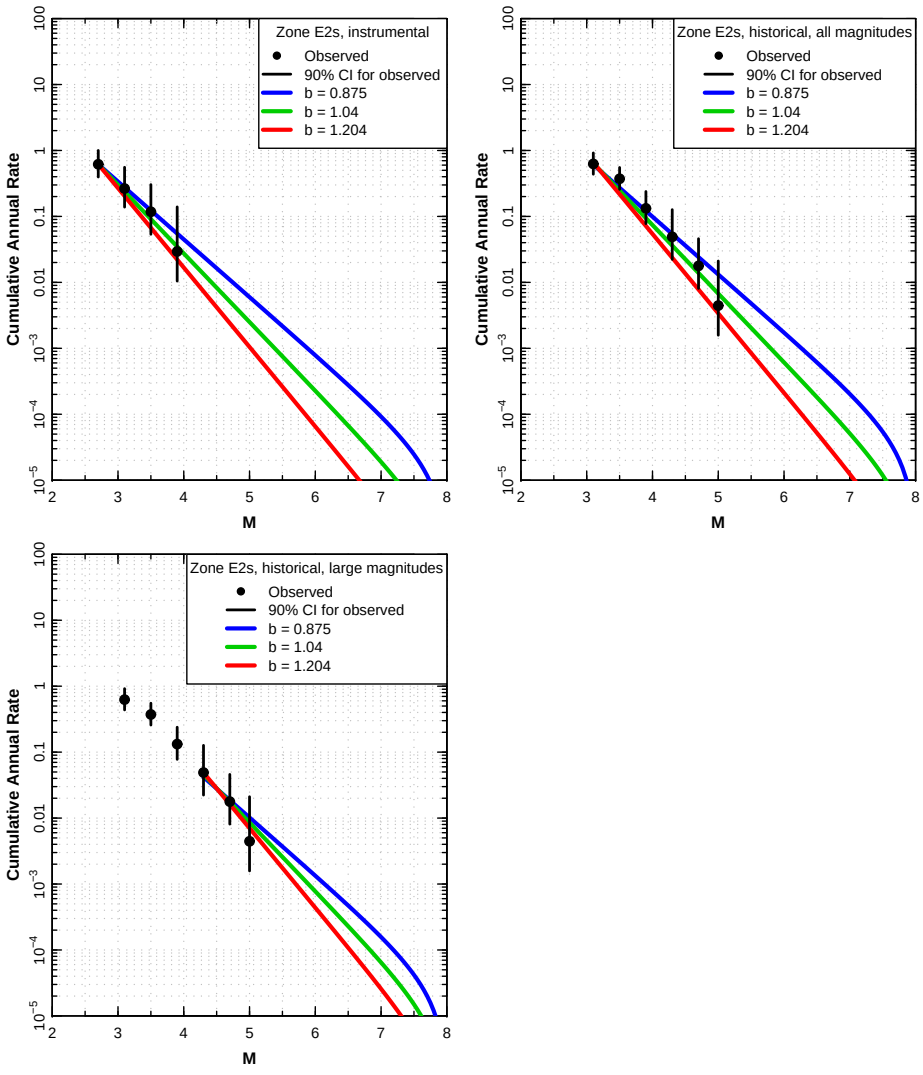

Figure 2.66: Earthquake recurrence relationships for Source Zone E2s.

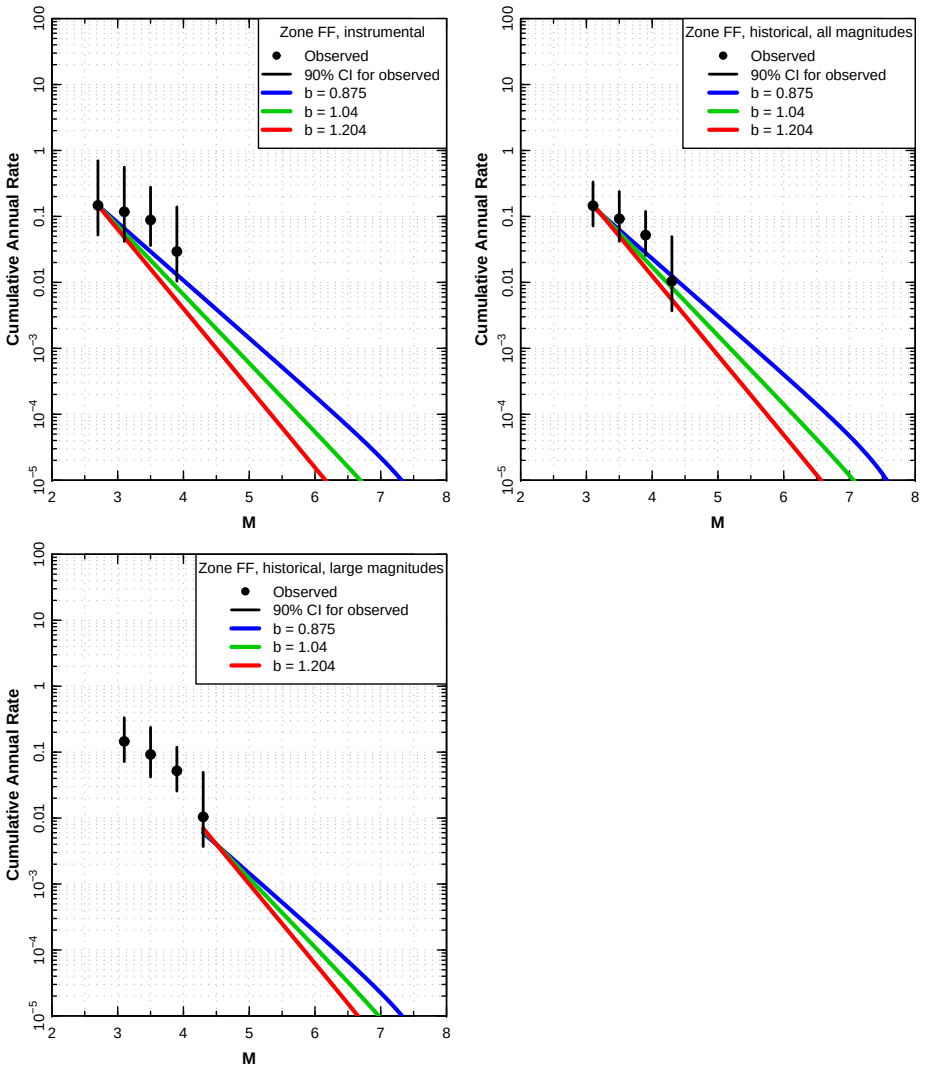

Figure 2.67: Earthquake recurrence relationships for Source Zone FF.

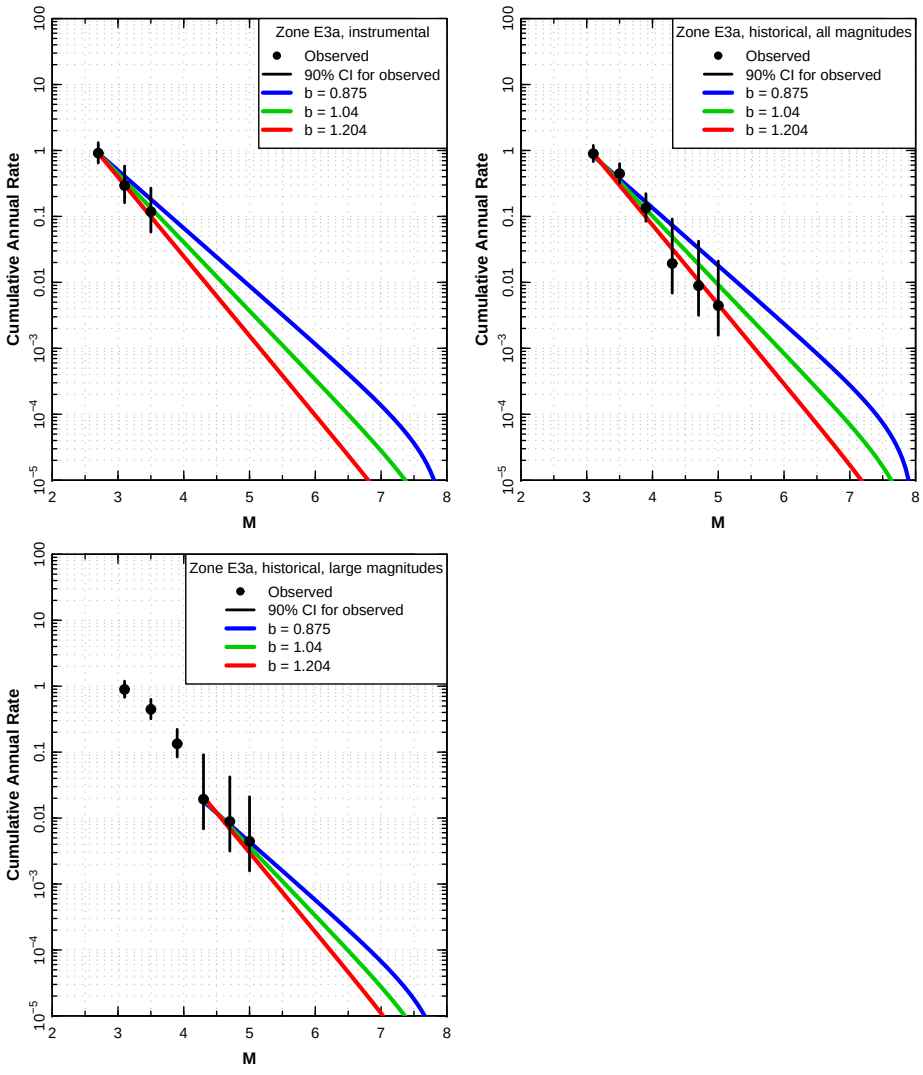

Figure 2.68: Earthquake recurrence relationships for Source Zone E3a.

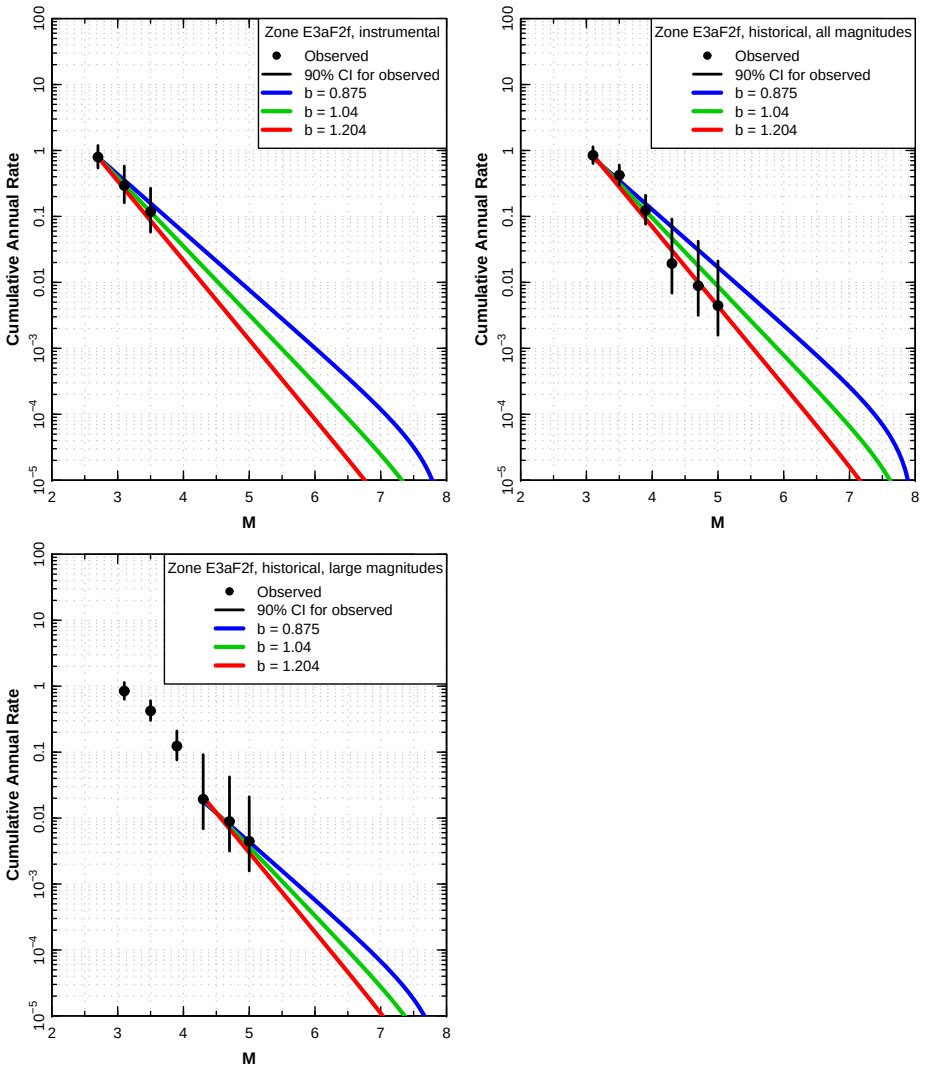

Figure 2.69: Earthquake recurrence relationships for Source Zone E3aF2f.

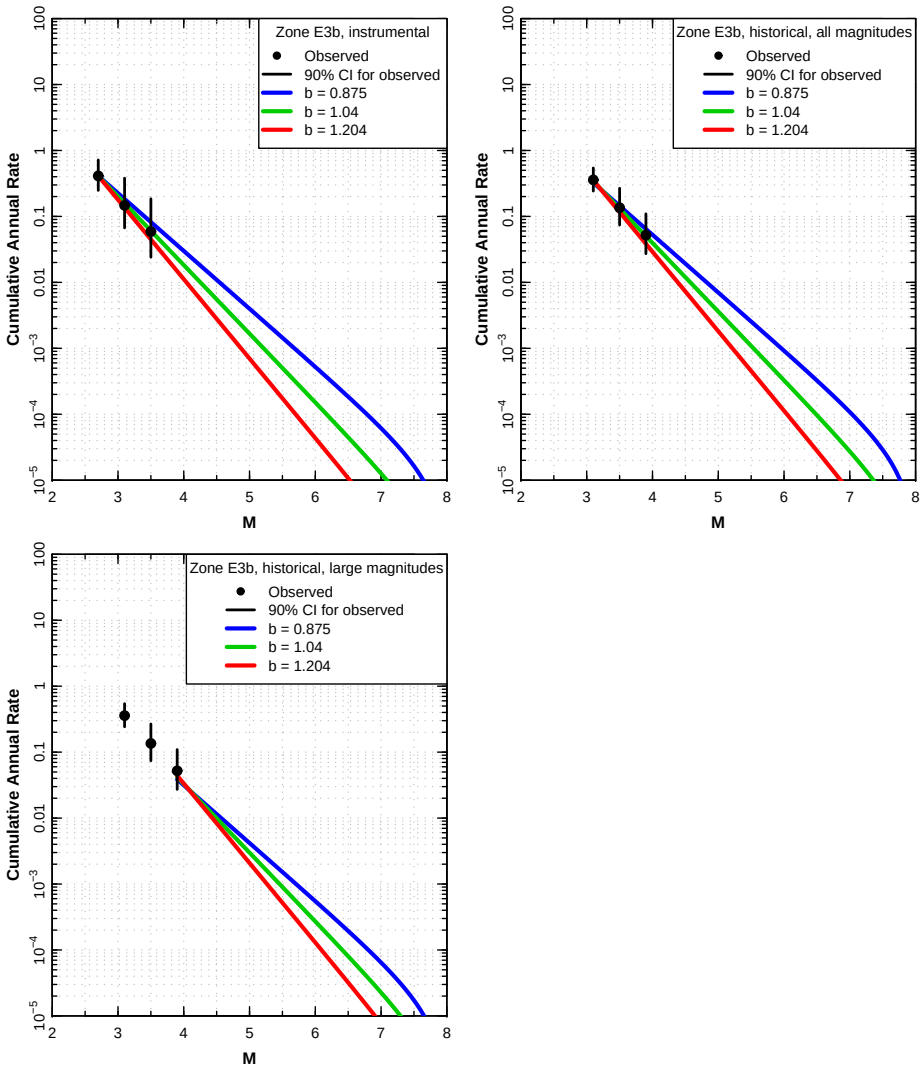

Figure 2.70: Earthquake recurrence relationships for Source Zone E3b.

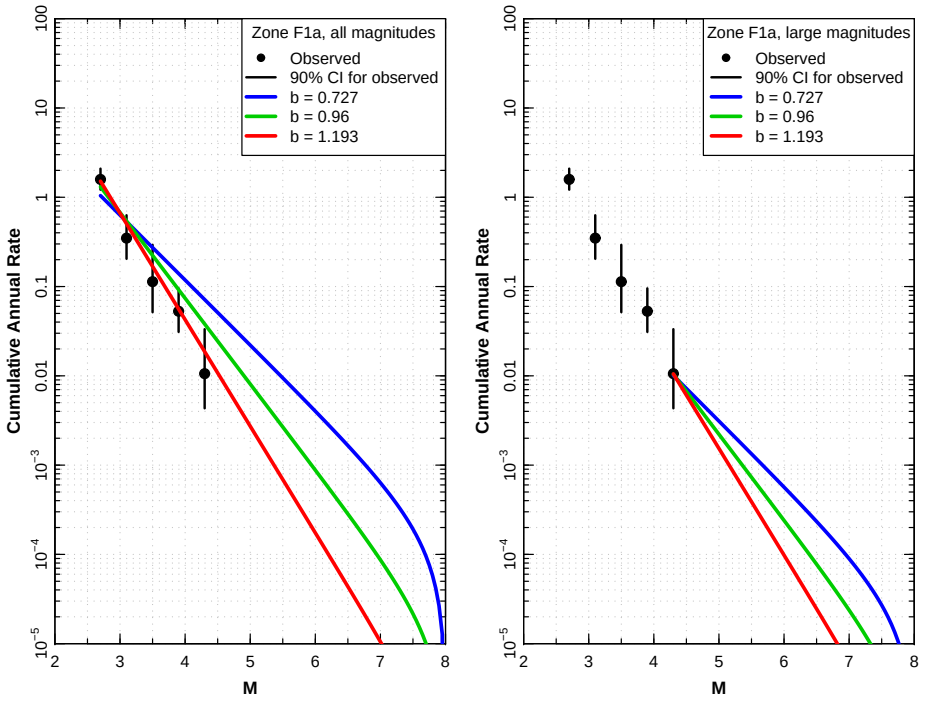

Figure 2.71: Earthquake recurrence relationships for Source Zone F1a.

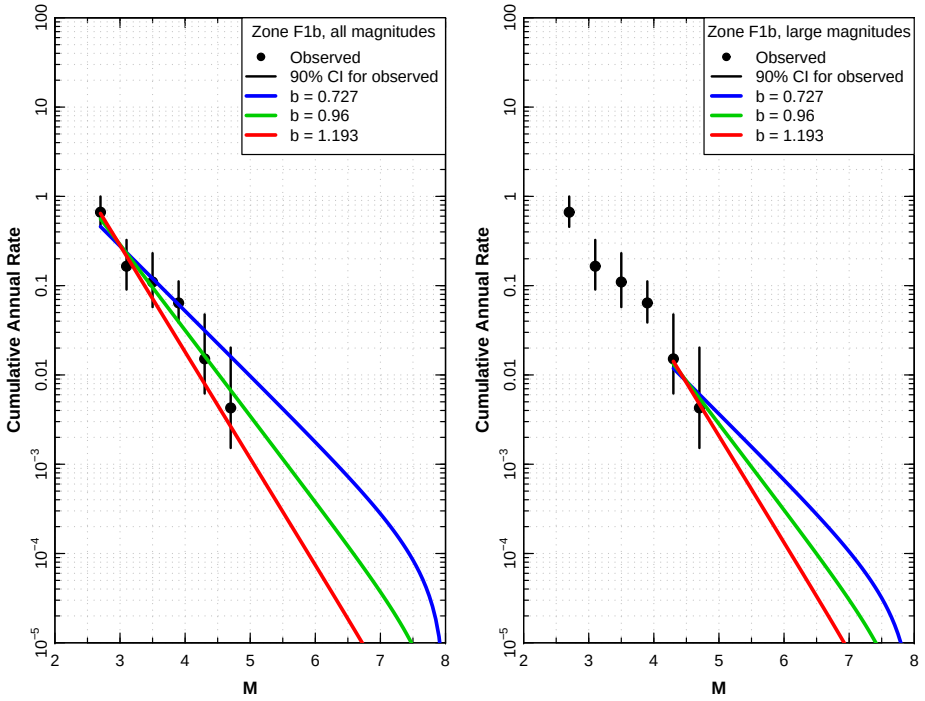

Figure 2.72: Earthquake recurrence relationships for Source Zone F1b.

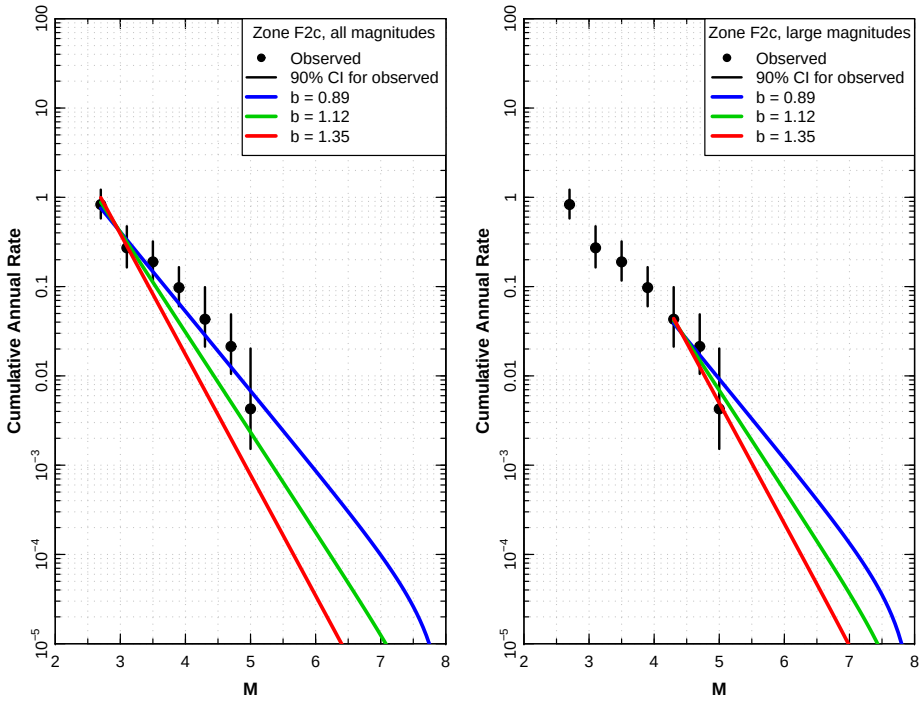

Figure 2.73: Earthquake recurrence relationships for Source Zone F2c.

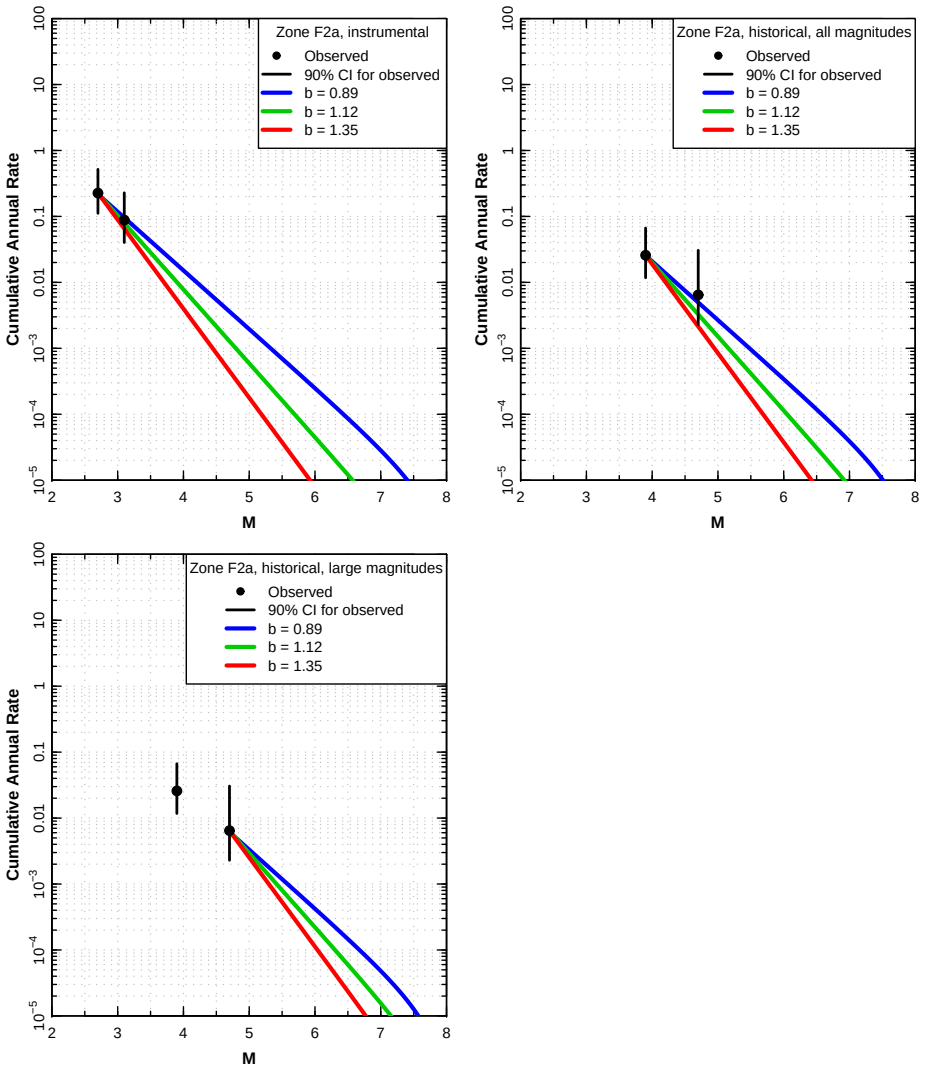

Figure 2.74: Earthquake recurrence relationships for Source Zone F2a.

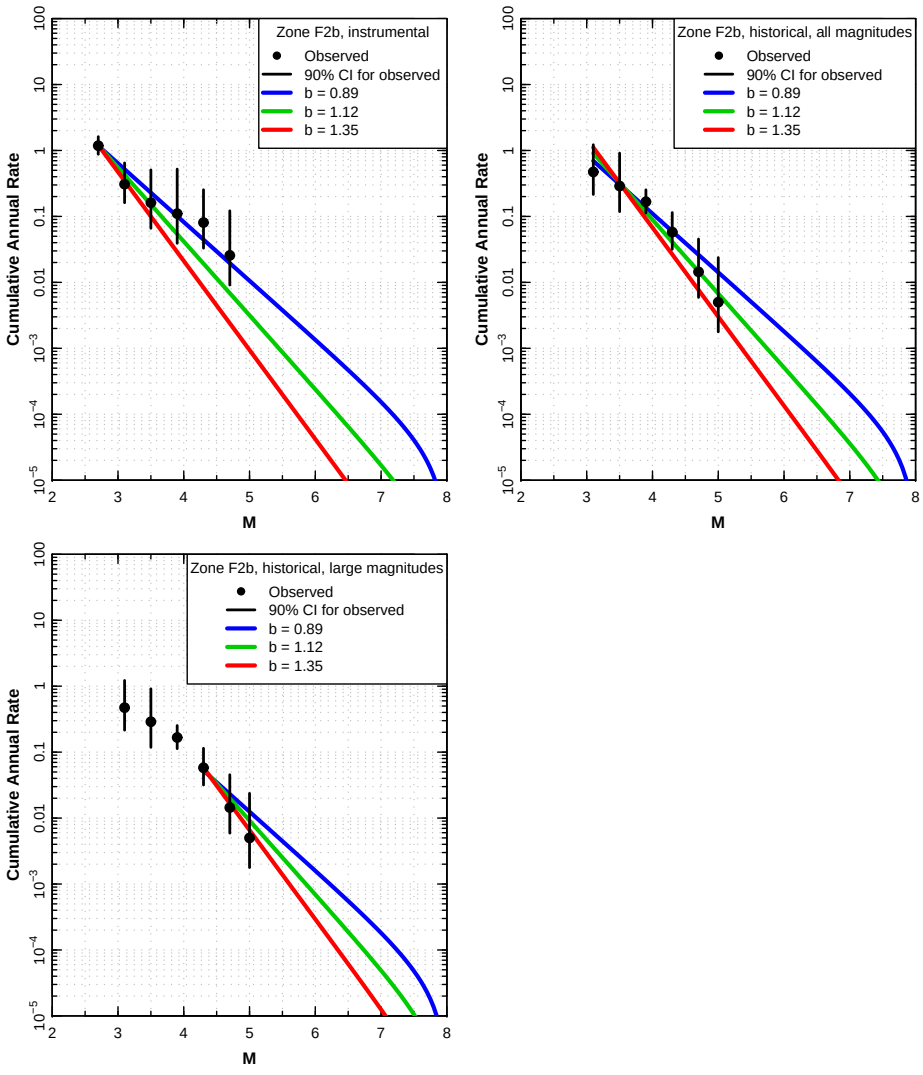

Figure 2.75: Earthquake recurrence relationships for Source Zone F2b.

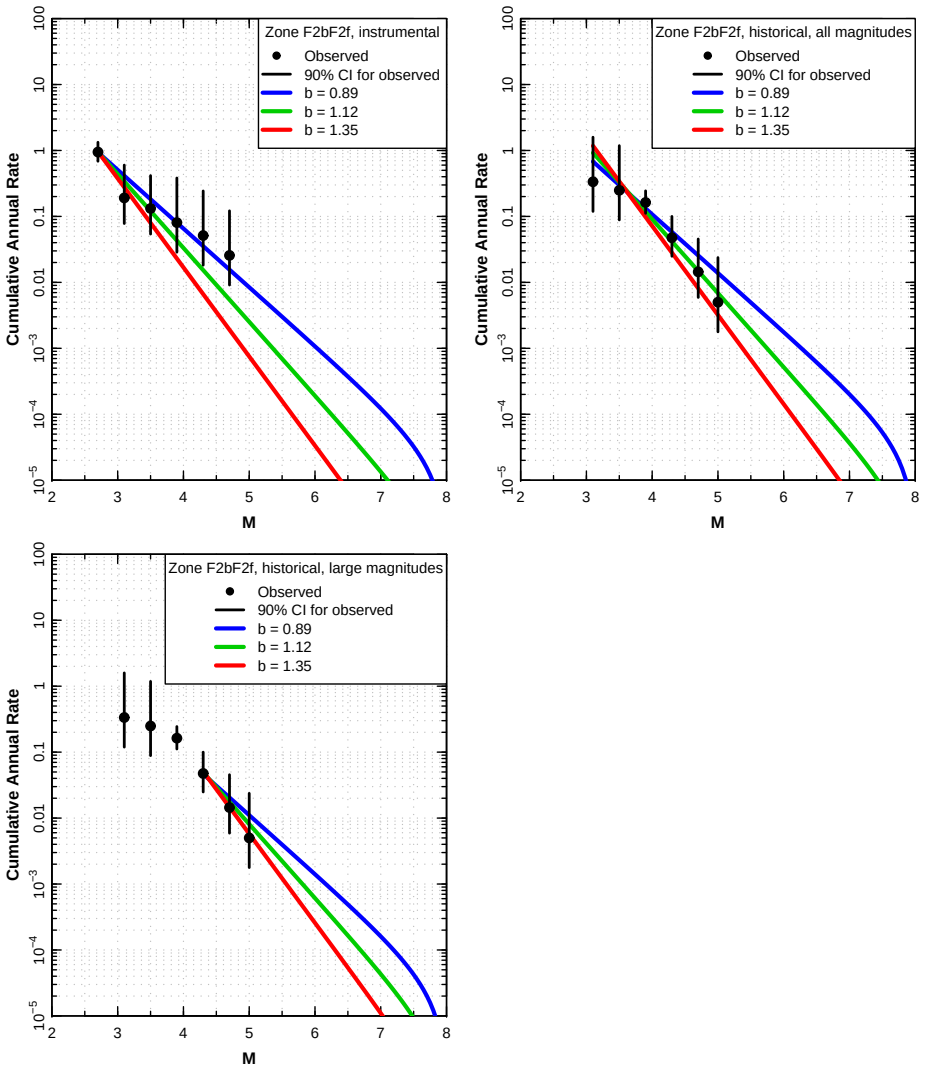

Figure 2.76: Earthquake recurrence relationships for Source Zone F2bF2f.

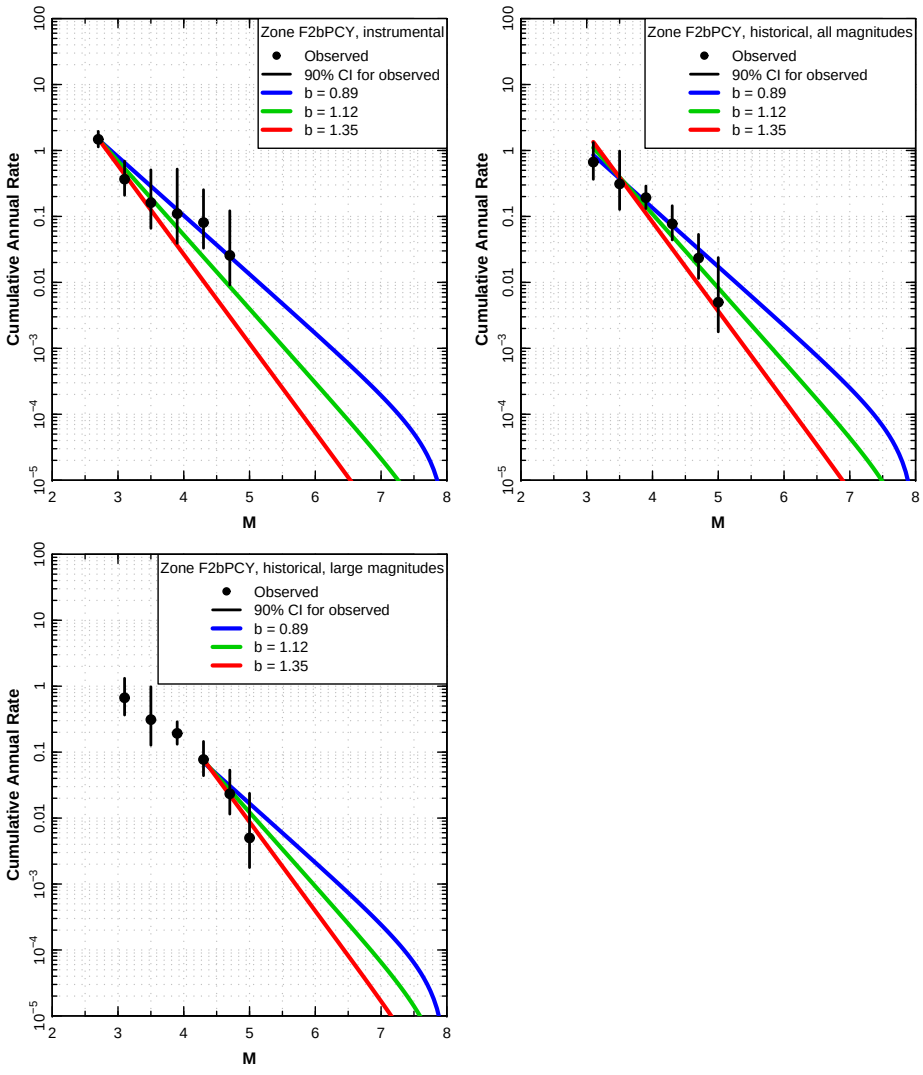

Figure 2.77: Earthquake recurrence relationships for Source Zone F2fPCY.

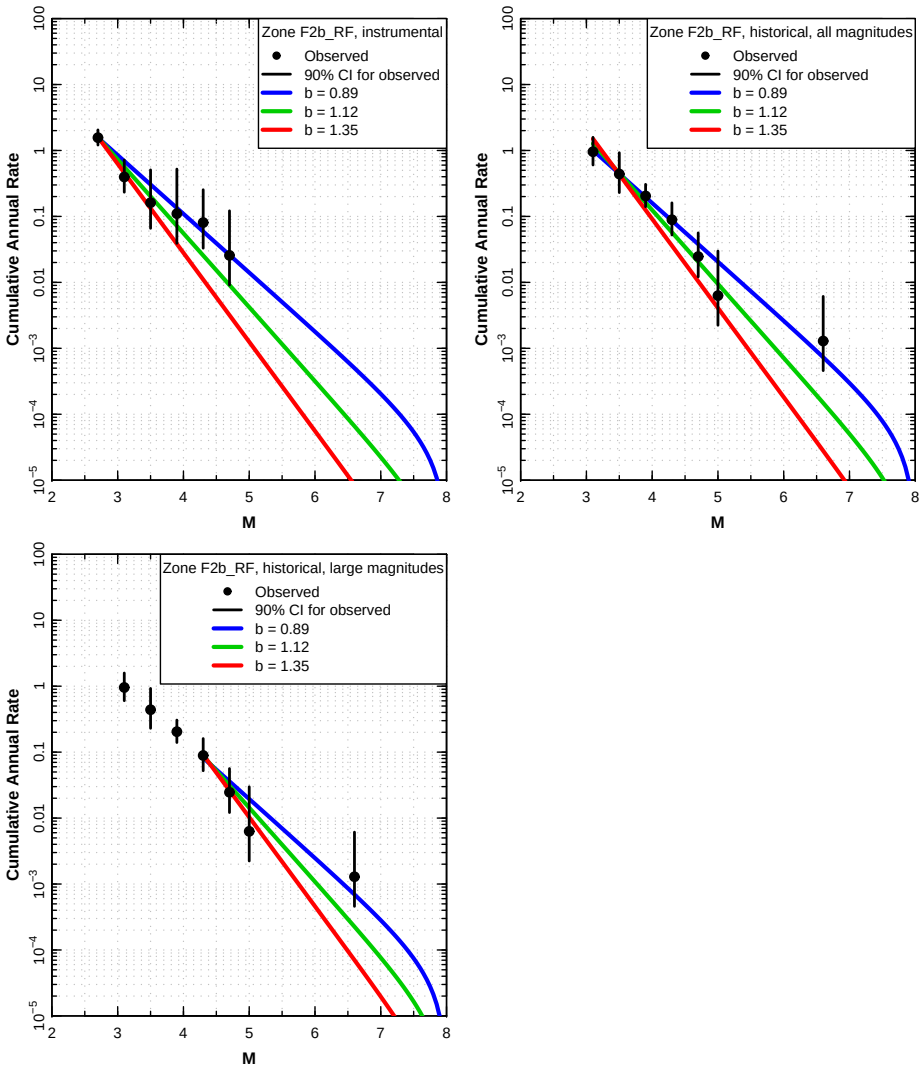

Figure 2.78: Earthquake recurrence relationships for Source Zone F2b_RF.

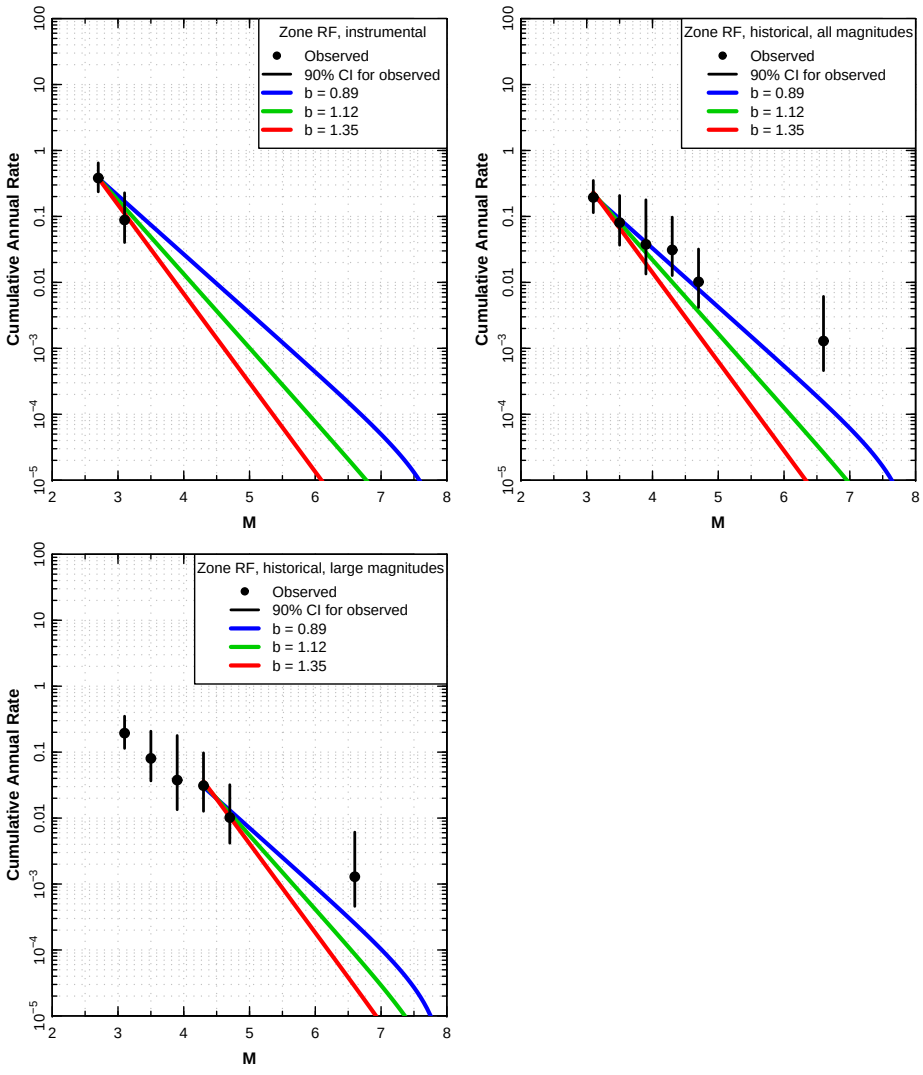

Figure 2.79: Earthquake recurrence relationships for Source Zone RF.

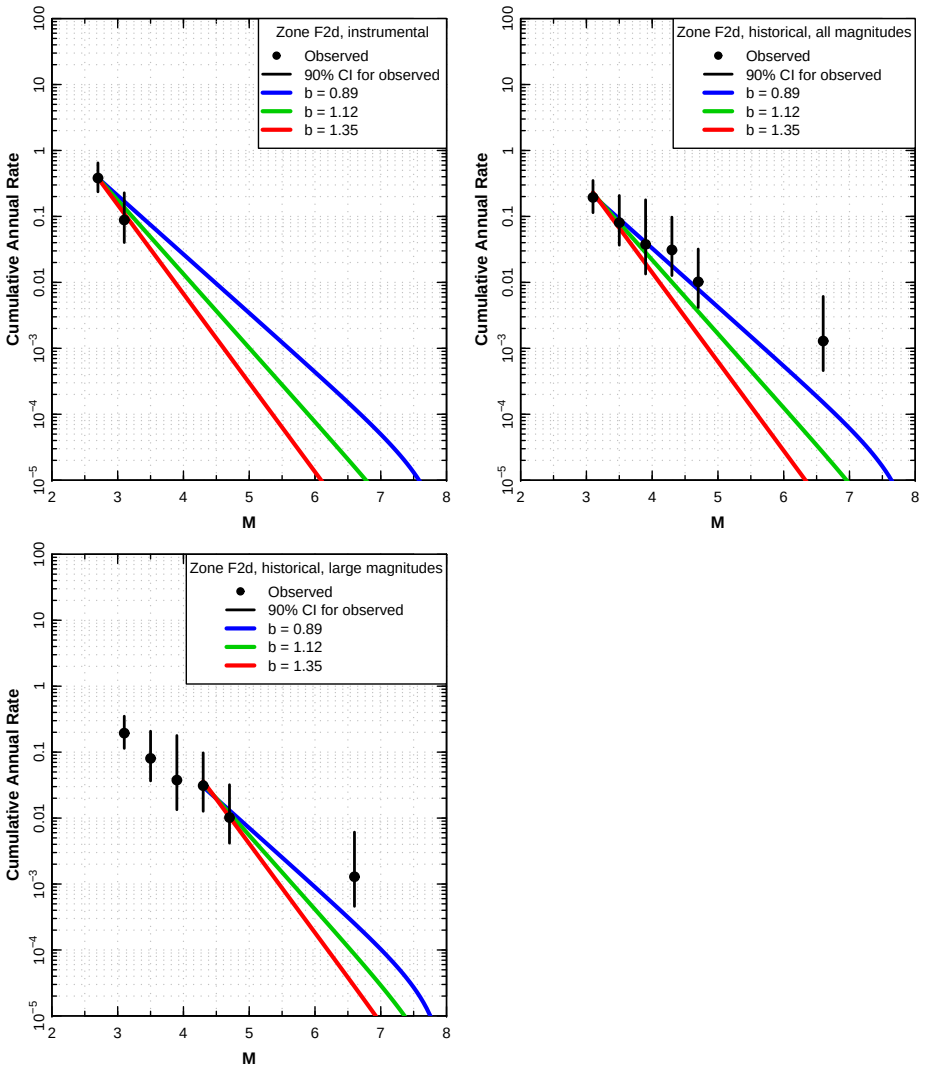

Figure 2.80: Earthquake recurrence relationships for Source Zone F2d.

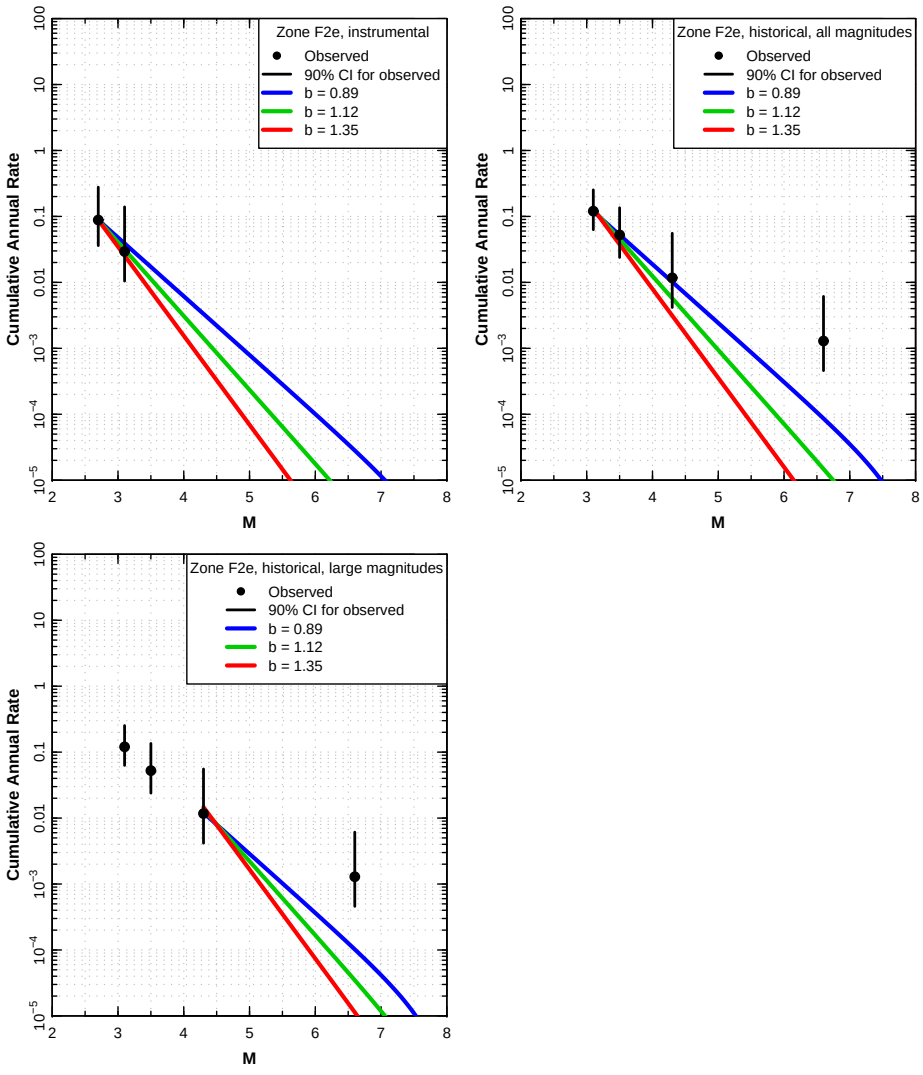

Figure 2.81: Earthquake recurrence relationships for Source Zone F2e.

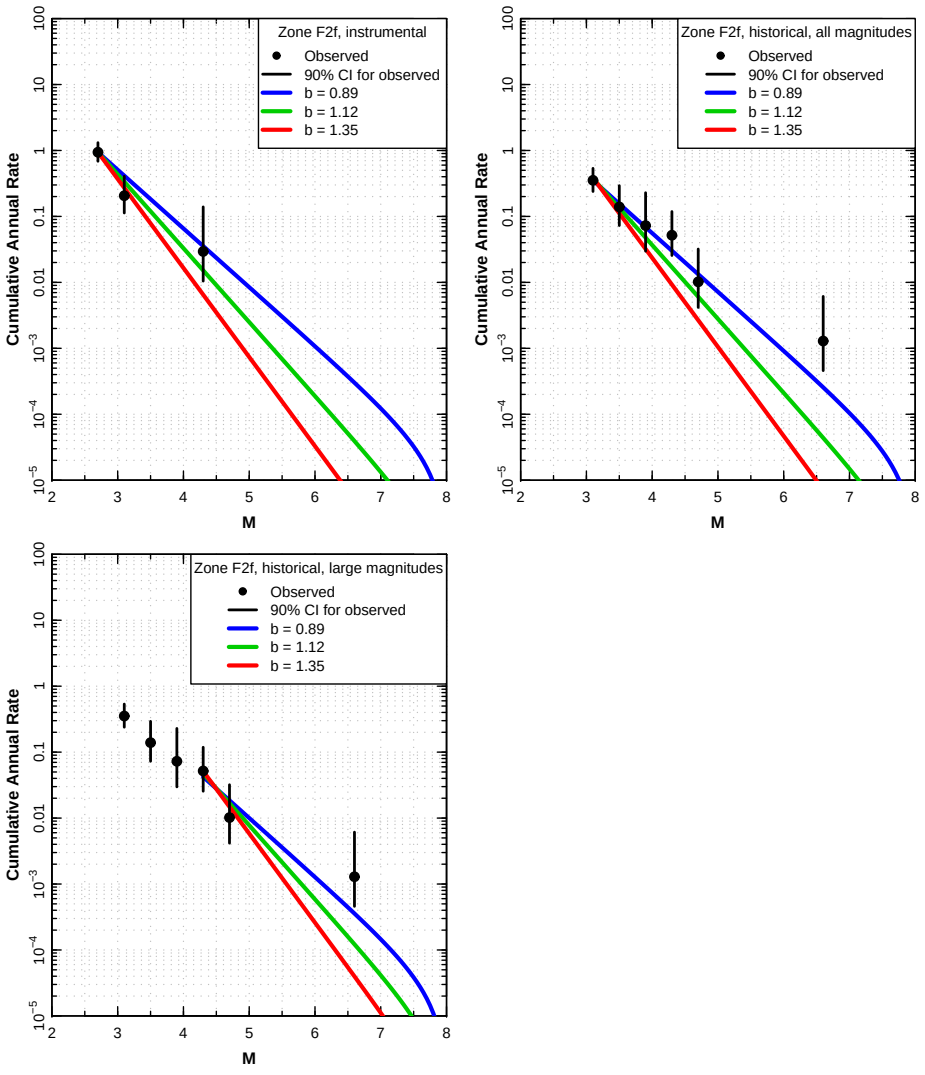

Figure 2.82: Earthquake recurrence relationships for Source Zone F2f.

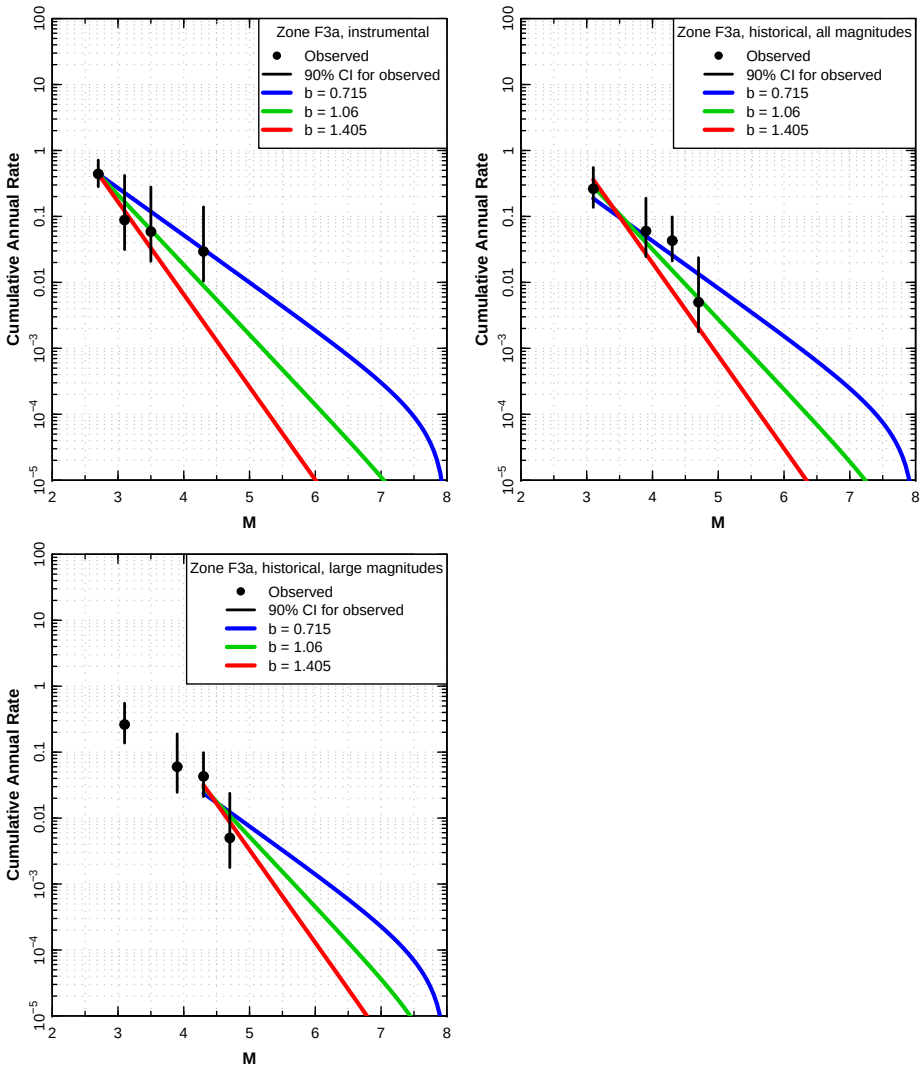

Figure 2.83: Earthquake recurrence relationships for Source Zone F3a.

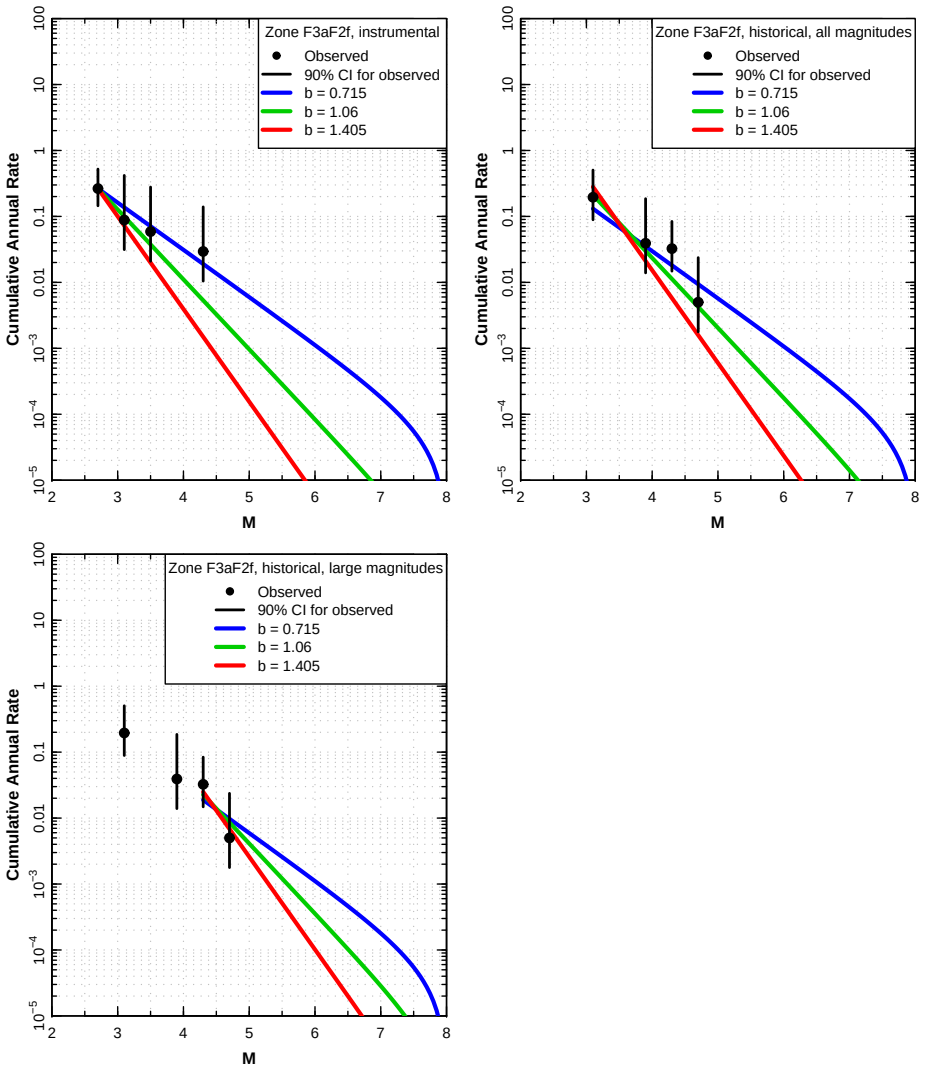

Figure 2.84: Earthquake recurrence relationships for Source Zone F3aF2f.

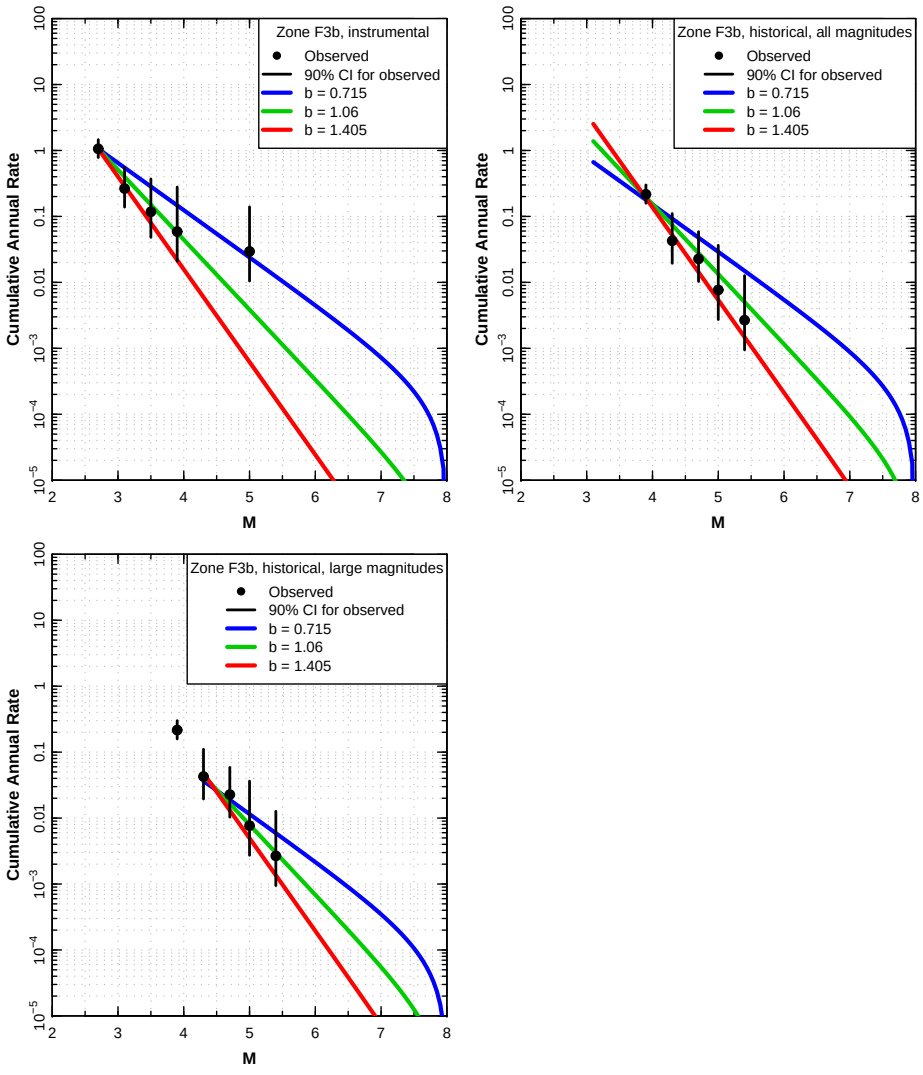

Figure 2.85: Earthquake recurrence relationships for Source Zone F3b.

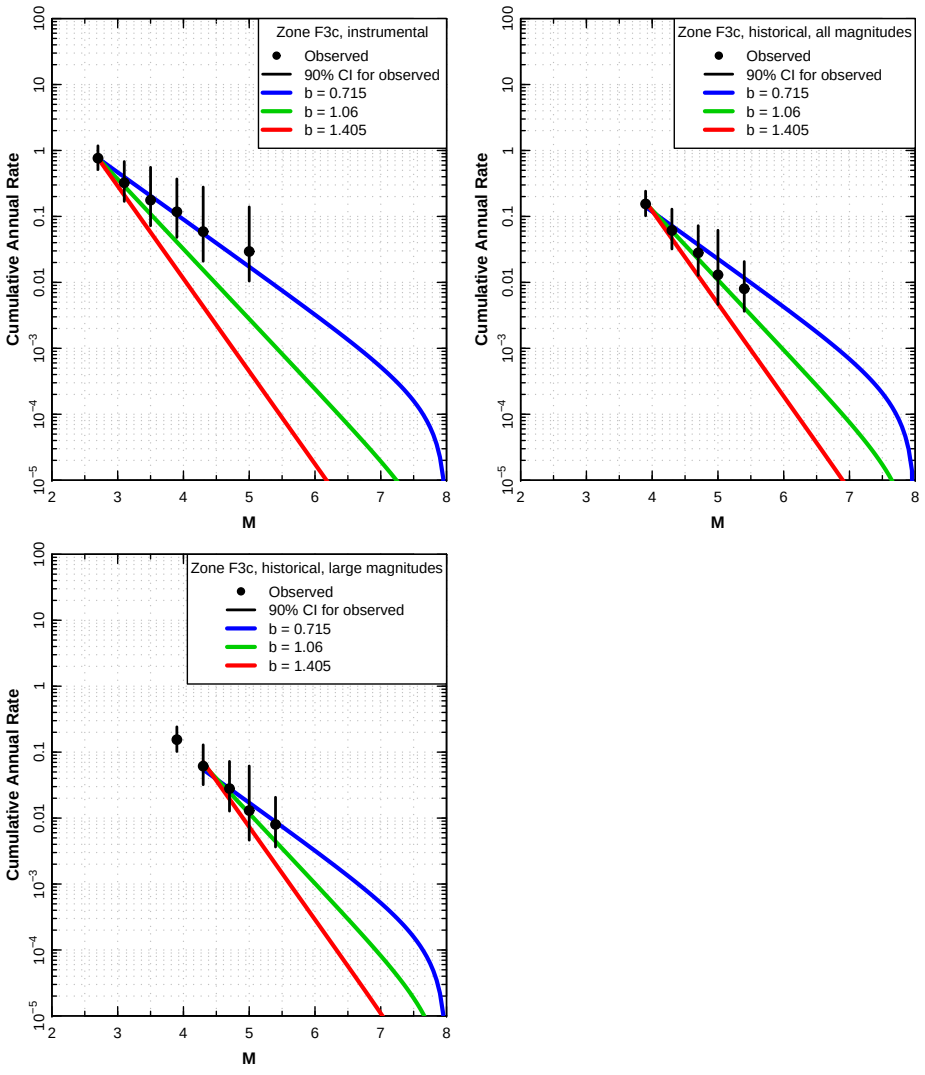

Figure 2.86: Earthquake recurrence relationships for Source Zone F3c.

Chapter 3

Hazard Input Document for EG1a (EG1-HID-1001) of June 12, 2011

Written by the PMT, SP4 and TFI

This document describes the final seismic source model developed by Expert Team EG1a in the PRP project. The data files associated with this seismic source model are located in the zip file EG1-HID-1001_EG1a_data.zip. This document is based on the PEGASOS Hazard Input Document EG1-HID-0032. Based on the new earthquake ECOS09 catalog published in March 2010 the EG1a team revised its model, updating the seismicity parameters that go with that seismic source model and revising a few weights for the *b*-values and seismicity rate alternatives. This document repeats for the most part the content of the PEGASOS Hazard Input Document EG1-HID-0032. The modifications caused by the model revision are highlighted in blue.

3.1 Seismic Zonation

The master logic tree that defines the alternative seismic source zonations is shown on Figure 3.1. The first node addresses whether or not the Permo-Carboniferous troughs are an active source. Figure 3.2 shows the seismic source zonation of the Alpine foreland for the case when the Permo-Carboniferous troughs are an active source ("PC YES" case). If the Permo-Carboniferous troughs are not active ("PC NO" case), a number of alternatives for Basel and the Alpine foreland are included.

The second node address whether or not the Reinach fault is modeled as active fault-specific source localizing seismicity and the third node addresses the source . For the PC YES case, the fault is not considered to be a localizer of seismicity, and the Basel source is an east-west trending zone F2e (Figure 3.2). For the PC NO case, Figure 3.3 shows the alternative seismic sources. If the Reinach fault (RF) is considered a line source, then it lies within a larger zone, source F2b_RF. If not, then the Basel region is modeled as a narrow, north-south trending zone (F2d), or as a large zone representing the intersection of north-south and east-west

structures (F2f). In the case that source F2f is use, the surrounding source zones have modified boundaries (e.g. zone F3a is changed to zone F3aF2f).

The next node of the logic tree addresses the source zonation in the Alpine foreland and the Fribourg area. The alternative source models are shown on Figure 3.4 for the PC NO case. If the Fribourg fault (FF) is considered to be an active fault localizing seismicity, it is modeled as a line source within a large Alpine foreland source E2cde (lower left plot of Figure 3.4). If not, then the Alpine foreland is modeled by the three zones E2c, E2d, and E2e (upper left plot of Figure 3.4). The right-hand plots on Figure 3.4 show the modifications to the Alpine foreland zones in the case that the Basel source is represented by zone F2f.

The final node of the logic tree (Figure 3.1) shows the source zonation for the Alps (regional zone D1). Three alternatives are considered, as shown on Figure 3.5.

The remaining portion of the study region is modeled by a number of source zones whose geometry does not change with the alternative zonations described above. Figure 3.6 shows these source zones.

The right-hand column in Figure 3.1 indicates the various source sets produced by the logic tree. The source zones comprising these source sets are listed in table 3.1 Source Sets for EG1a.

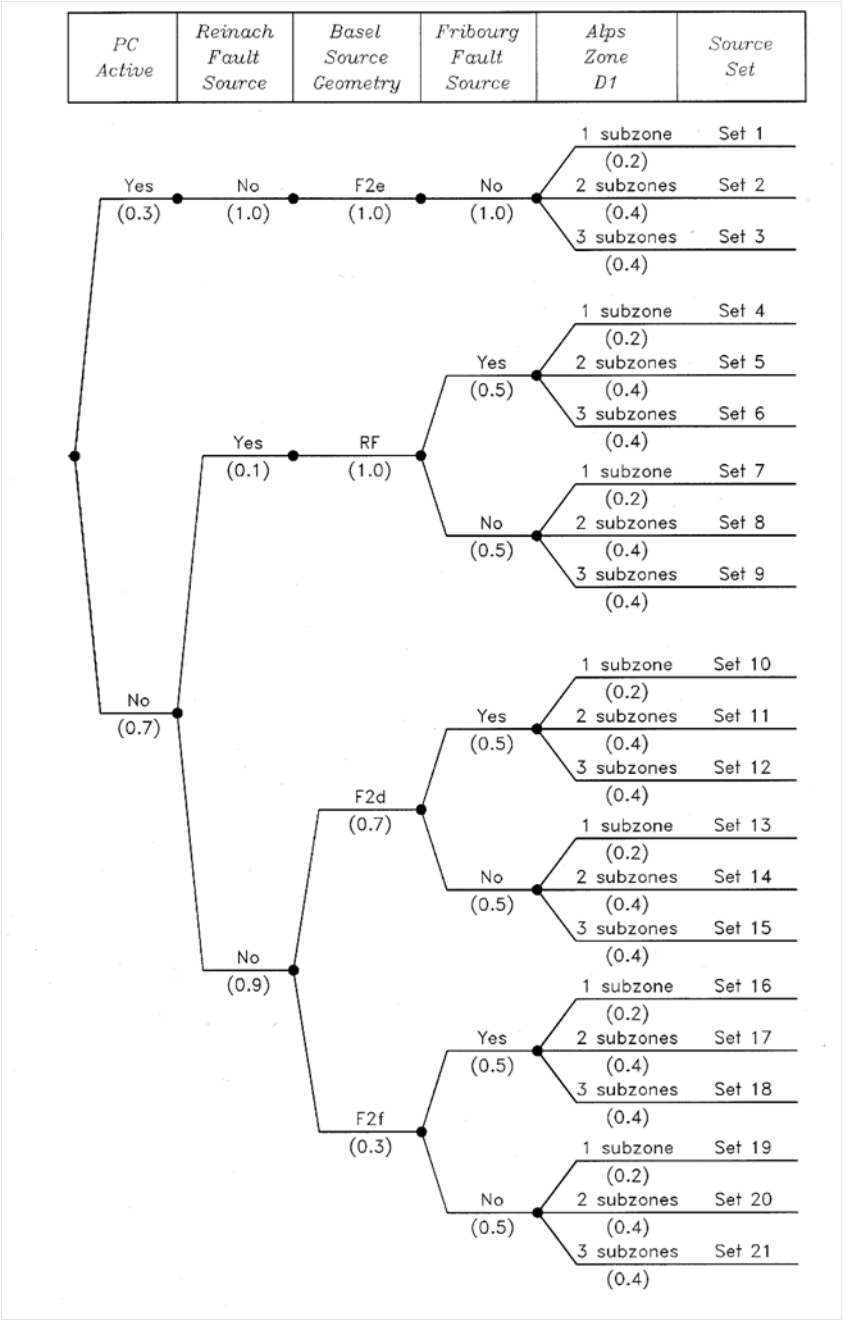

Figure 3.1: Logic tree for EG1a seismic source zonation.

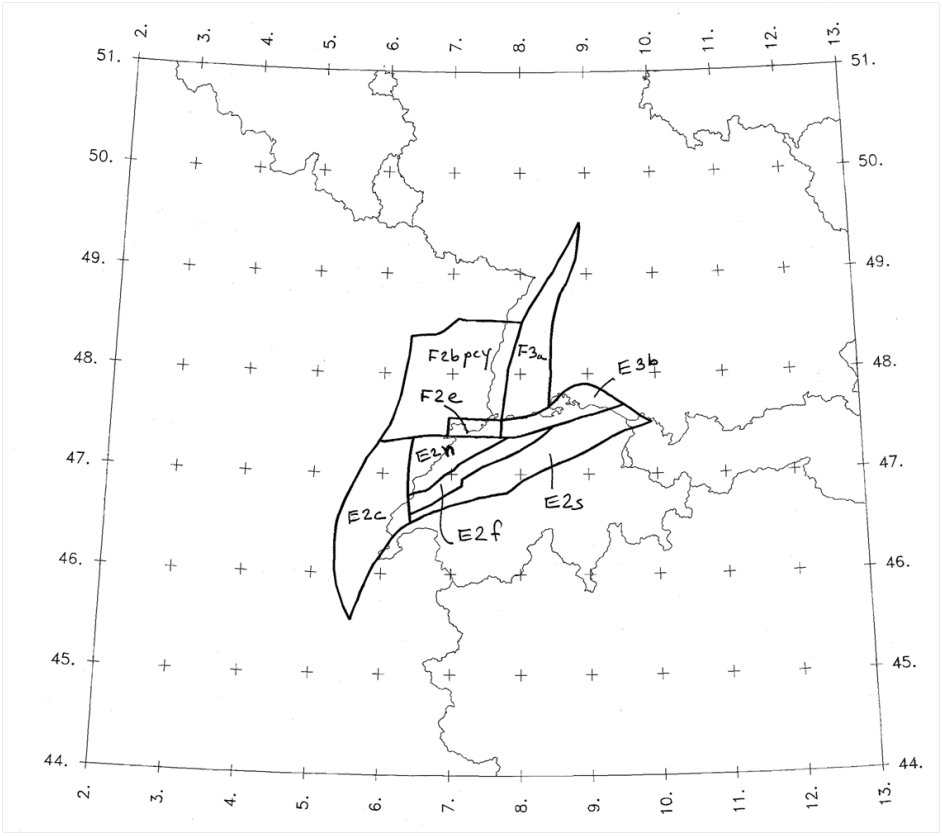

Figure 3.2: The Alpine foreland zones for the "PC YES" case (Permo-Carboniferous troughs are an active source).

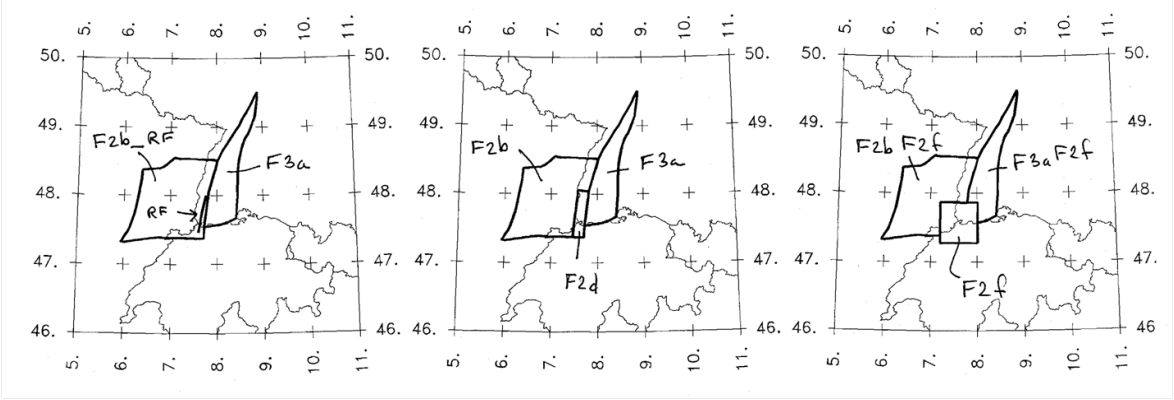

Figure 3.3: Alternative source zonations for Basel area for the "PC NO" case (permocarboniferous troughs not an active source).

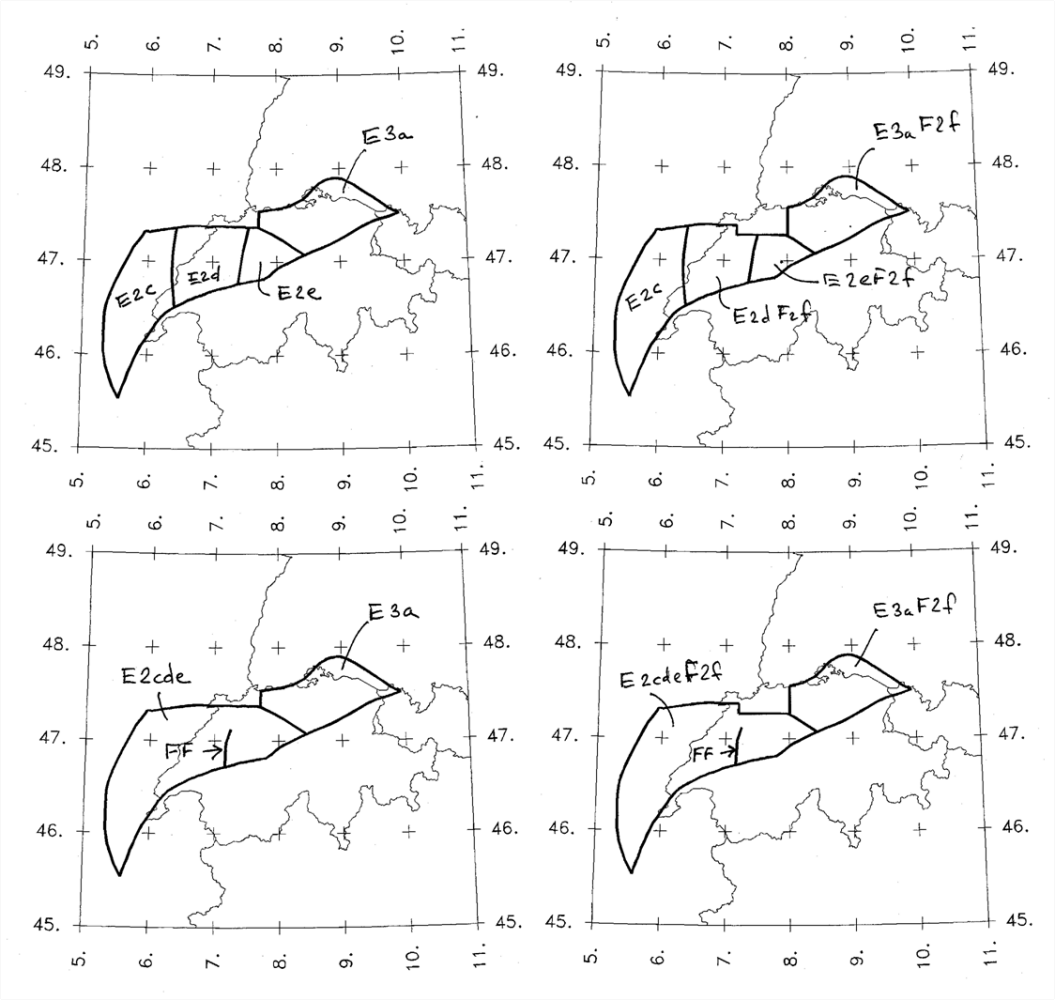

Figure 3.4: Alternative source zonations for Alpine foreland for the "PC NO" case (Permo-Carboniferous troughs are not an active source).

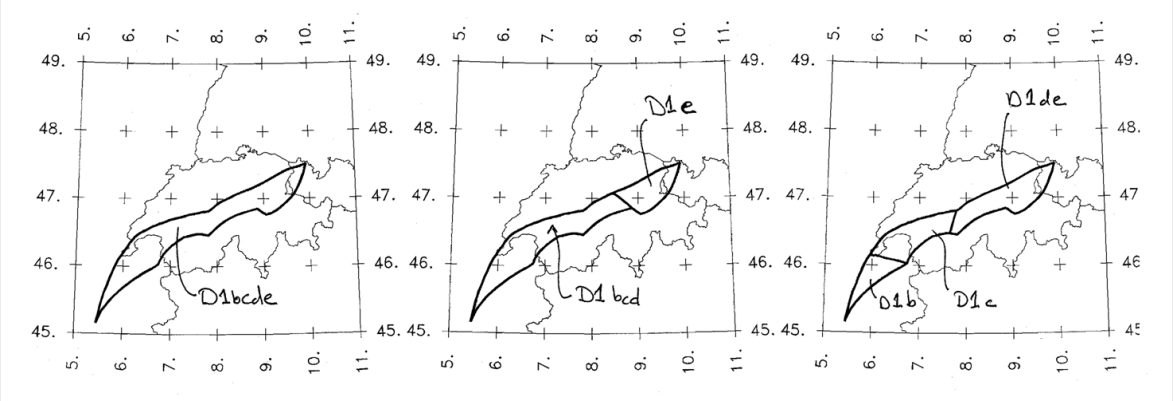

Figure 3.5: Alternative source zonations for the Alps.

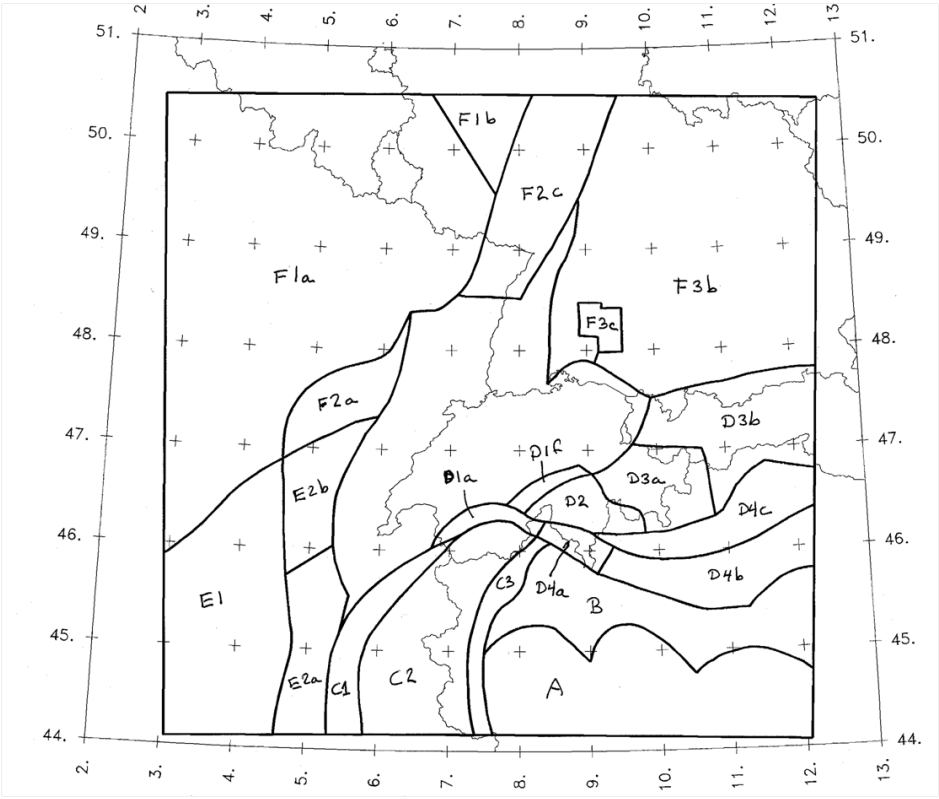

Figure 3.6: Source zones whose boundaries do not change as a function of alternative zonations.

The zone boundary files are located in directory `./ZONES` with the extension `*.zon`. The FF and RF fault traces are located in the same directory with the extension `*.flt`. Note that the RF source dips to the east.

Table 3.1: Source Sets for EG1a.

Source Set	Sources
Set 1	F2bpcy, F2e, F3a, E2c, E2n, E2f, E2s, E3b, D1bcde + UC*
Set 2	F2bpcy, F2e, F3a, E2c, E2n, E2f, E2s, E3b, D1bcd, D1e + UC
Set 3	F2bpcy, F2e, F3a, E2c, E2n, E2f, E2s, E3b, D1b, D1c, D1de + UC
Set 4	F2b_RF, RF, F3a, E2cde, FF, E3a, D1bcde + UC
Set 5	F2b_RF, RF, F3a, E2cde, FF, E3a, D1bcd, D1e + UC
Set 6	F2b_RF, RF, F3a, E2cde, FF, E3a, D1b, D1c, D1de + UC
Set 7	F2b_RF, RF, F3a, E2c, E2d, E2e, E3a, D1bcde + UC
Set 8	F2b_RF, RF, F3a, E2c, E2d, E2e, E3a, D1bcd, D1e + UC
Set 9	F2b_RF, RF, F3a, E2c, E2d, E2e, E3a, D1b, D1c, D1de + UC
Set 10	F2b, F2d, F3a, E2cde, FF, E3a, D1bcde + UC
Set 11	F2b, F2d, F3a, E2cde, FF, E3a, D1bcd, D1e + UC
Set 12	F2b, F2d, F3a, E2cde, FF, E3a, D1b, D1c, D1de + UC
Set 13	F2b, F2d, F3a, E2c, E2d, E2e, E3a, D1bcde + UC
Set 14	F2b, F2d, F3a, E2c, E2d, E2e, E3a, D1bcd, D1e + UC
Set 15	F2b, F2d, F3a, E2c, E2d, E2e, E3a, D1b, D1c, D1de + UC
Set 16	F2bF2f, F2f, F3aF2f, E2cdeF2f, FF, E3aF2f, D1bcde + UC
Set 17	F2bF2f, F2f, F3aF2f, E2cdeF2f, FF, E3aF2f, D1bcd, D1e + UC
Set 18	F2bF2f, F2f, F3aF2f, E2cdeF2f, FF, E3aF2f, D1b, D1c, D1de + UC
Set 19	F2bF2f, F2f, F3aF2f, E2c, E2dF2f, E2eF2f, E3aF2f, D1bcde + UC
Set 20	F2bF2f, F2f, F3aF2f, E2c, E2dF2f, E2eF2f, E3aF2f, D1bcd, D1e + UC
Set 21	F2bF2f, F2f, F3aF2f, E2c, E2dF2f, E2eF2f, E3aF2f, D1b, D1c, D1de + UC

*Set UC	A, B, C1, C2, C3, D1a, D1f, D2, D3a, D3b, D4a, D4b, D4c, E1, E2a, E2b, F1a, F1b, F2a, F2c, F3b, F3c

3.2 Earthquake Rupture Geometry

The size of earthquake ruptures is defined by the relationship:

$$\text{Mean}\log_{10}(\text{rupture area}) = M - 4 \tag{3.1}$$

$$\sigma\log_{10}(\text{rupture area}) = 0.24 \tag{3.2}$$

Using the relationship for the expectation of a lognormal distribution, the mean (expected) rupture area is given by the relationship:

$$\text{mean rupture area} = 10^{(M-3.934)} \tag{3.3}$$

The relationship for the mean rupture area will be used in the hazard computations. The rupture length and width have an aspect ratio of 1:1 until the maximum rupture width for a source is reached. The maximum rupture width is determined on the basis of the maximum

depth and fault dip, as define below. For larger ruptures, the width is held constant at the maximum width and the length is obtained by dividing the rupture area by this width.

Earthquake epicenters are uniformly distributed within the source. Earthquake ruptures are located symmetrically on the epicenters (the epicenter is at the midpoint of the rupture). For those epicenters located closer than 1/2 rupture length to the source zone boundary, the ruptures are allows to extend beyond the source boundary.

Table 3.2 defines the relative frequency of the style-of-faulting and rupture orientations for the individual sources. Three specific styles-of-faulting are considered, normal, strike-slip and reverse. For each style-of-faulting, there is a preferred fault dip that should be used to model ruptures.

The depth distribution of hypocenters for small magnitude earthquakes within the sources is defined by the following three distributions. For the northern Alpine foreland sources (FF, E2d, E2dF2f, E2e, E2eF2f, E2cde, E2cdeF2f, E2n, E2f, E2s, E3a, E3aF2f, E3b) the distribution is triangular over the depth range of 1 to 30 km, with the mode at a depth of 10 km (Figure 3.7). For the southern Alpine foreland and southern Germany sources (C3, D4a, D4b, D4c, F3a, F3aF2f, F3b, F3c) the depth distribution is triangular over the depth range of 1 to 25 km, with the mode at a depth of 10 km (Figure 3.8). For the remaining zones and RF, the distribution is trapezoidal over the depth range of 1 to 20 km, with the upper uniform region extending over the depth range of 1 to 10 km (Figure 3.9). For larger earthquakes, a magnitude-dependent depth distribution is to be developed using the weighted approach outlined in Toro [2003] (TP1-TN-0373) with T = 0.5 (hypocenter in lower half of rupture). Earthquake ruptures on the Reinach (RF) and Fribourg (FF) fault sources may extend all the way to the surface.

Table 3.2: Style of Faulting and Rupture Orientation for EG1a Sources.

Sources	Relative Frequency for for Style of faulting			Orientation of Ruptures		
	SS*	NF*	TF*	SS*	NF*	TF*
A, B, D1f, D2, D4a, D4c, E1, E2e, E2eF2f, F3c	0.33	0.33	0.33	Random	Random	Random
C1, C3	0.75		0.25	N20E		N20E
C2		1			N20E	
D1a	1			N90E		
D1b, D1d, D1e, D1bcde, D1bcd, D1de,	0.75		0.25	Random		Random
D1c	0.8	0.1	0.1	Random	Random	Random
D3a	0.25	0.75		Random	Random	
D3b	1			N70E		
D4b, E2f			1			N70E
E2a, E2b, E2c, E2d, E2dF2f, E2n, E2cde, E2cdeF2f, F2c	1			N15E		
E3a, E3aF2f, F1b	0.5.	0.5		N45W	N45W	
F2a	0.75	0.25		N15E	N15E	
F2b, F2bpcy, F2b_RF, F2bF2f	0.5	0.5		N15E	N15E	
F1a	0.5	0.5		Random	Random	
E2s	0.7	0.2	0.1	Random	Random	Random
E3b			1			N80E
F2d	0.3	0.7		N15E	N15E	
F2e	0.3		0.7	N90E		N90E
F2f	0.4	0.4	0.2	Random	Random	Random
F3a, F3aF2f	0.25	0.75		N15E & N45W	N15E & N45W	
F3b		1			N45E	
RF	0.3	0.7				
FF	1					

* SS – strike slip, dip 90°, NF normal slip, dip 60°, TF thrust, dip 30°

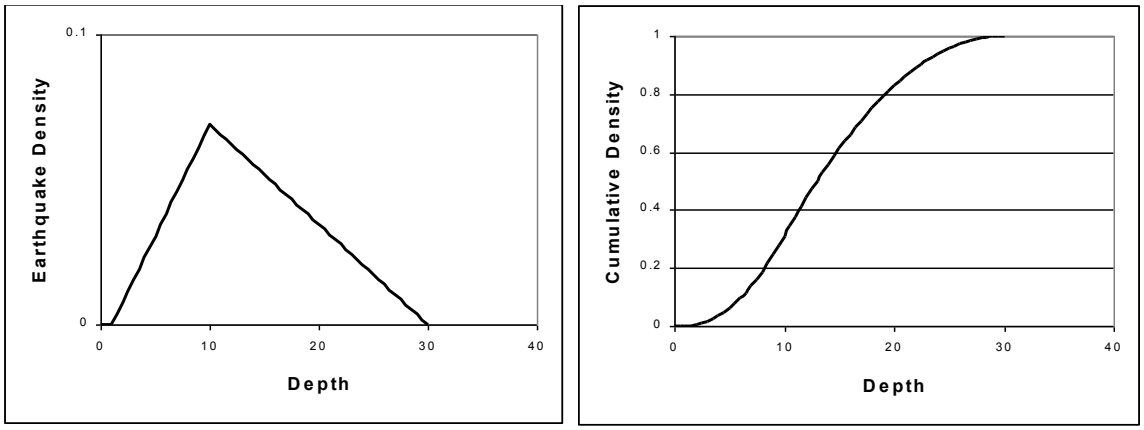

Figure 3.7: Earthquake depth distribution for sources FF, E2d, E2dF2f, E2e, E2eF2f, E2cde, E2cdeF2f, E2n, E2f, E2s, E3a, E3aF2f, and E3b.

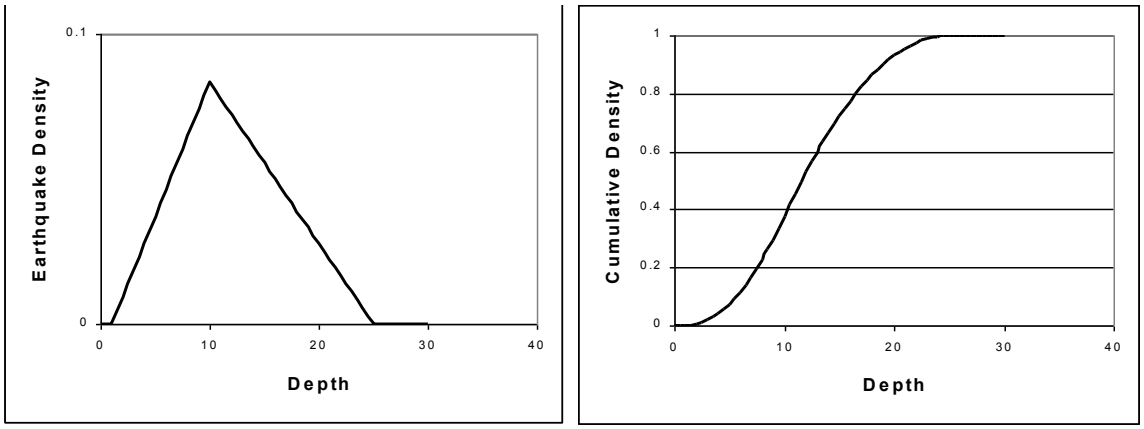

Figure 3.8: Earthquake depth distribution for sources C3, D4a, D4b, D4c, F3a, F3aF2f, F3b, and F3c.

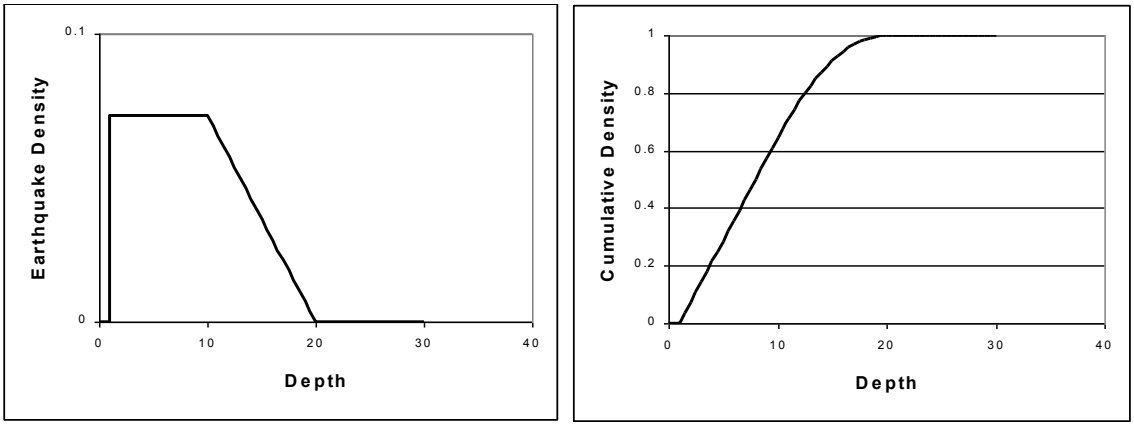

Figure 3.9: Earthquake depth distribution for all other sources except those listed for Figures 3.7 and 3.8.

3.3 Earthquake Recurrence Parameters

3.3.1 Maximum Magnitude

Two global options are used for the maximum magnitude assessment. The first is the Kijko approach and the second is the EPRI approach. These alternative branches are dependent across all sources. Equal weight is given to the two approaches. These two alternatives are correlated over all sources. The maximum magnitude distributions were developed for larger regional zones and then applied to the source zones within each regional source zone. The files are located in directory `./`M_{MAX}. Files with the extension `*.KMX` contain the results for the Kijko approach and files with the extension `*.EMX` contain the results for the EPRI approach.

3.3.2 Seismicity Rates

The earthquake recurrence parameters for the sources are modeled by the truncated exponential recurrence relationship. The recurrence parameters were defined by first establishing the b-value for a "macrozone" and then using this fixed b-value to calculate the seismicity rate for each source within the macrozone. The b-value is assumed to be correlated among all sources that make up the macrozone . A three-point discrete distribution is used to represent the uncertainty in the regional b-value and 5-point distributions are used to model the uncertainty in $N(m \geq 5)$ for each source, conditional on a given b-value. The zones that make up each marcozone with correlated b-values are listed in table 3.3. The weights assigned to the three b-values depend upon the macrozone, as indicated in table 3.3. They either represent a three-point approximation to a normal distribution or a three-point approximation to a uniform distribution.

In addition, there are two or three alternatives for defining the seismicity rate that apply to all zones that make up a macrozone. These occur in one of two cases, as indicated in table 3.3. Note that each source zone uses either Case 1 or Case 2, no source zone has both applied to it.

- Case 1: Two alternatives, one based on all data and one based on larger magnitude data (nominally above minimum magnitude $m_0 = 4.3$). The weights applied to these two alternatives are given in table 3.3. These are equal weights except for source E2a and E2b.

- Case 2: Three alternatives, one based on the instrumental (post-1975) data, one based on the historical (pre-1975) data, and one based on the historical (pre-1975) data for larger magnitudes (again nominally above minimum magnitude $m_0 = 4.3$). The weights applied to these three alternatives are given in table 3.3. These are equal weights adjusted to sum to 1.0.

The data files are contained within directory `./REC`. The file extension indicates the particular branch defined in table 3.3. The results for the three b-values are indicated by `*.?b0` for the central estimate of b-value value, `*.?bm` for the lower b-value, and `*.?bp` for the upper b-value. The first character of the extension is "a" for the rates based on all data; "i" for the rates based on instrumental data; "h" for the rates based on historical data; and "l" for the rates

based on larger magnitude data, either all large magnitude data for Case 1 or large magnitude data pre 1975 for Case 2.

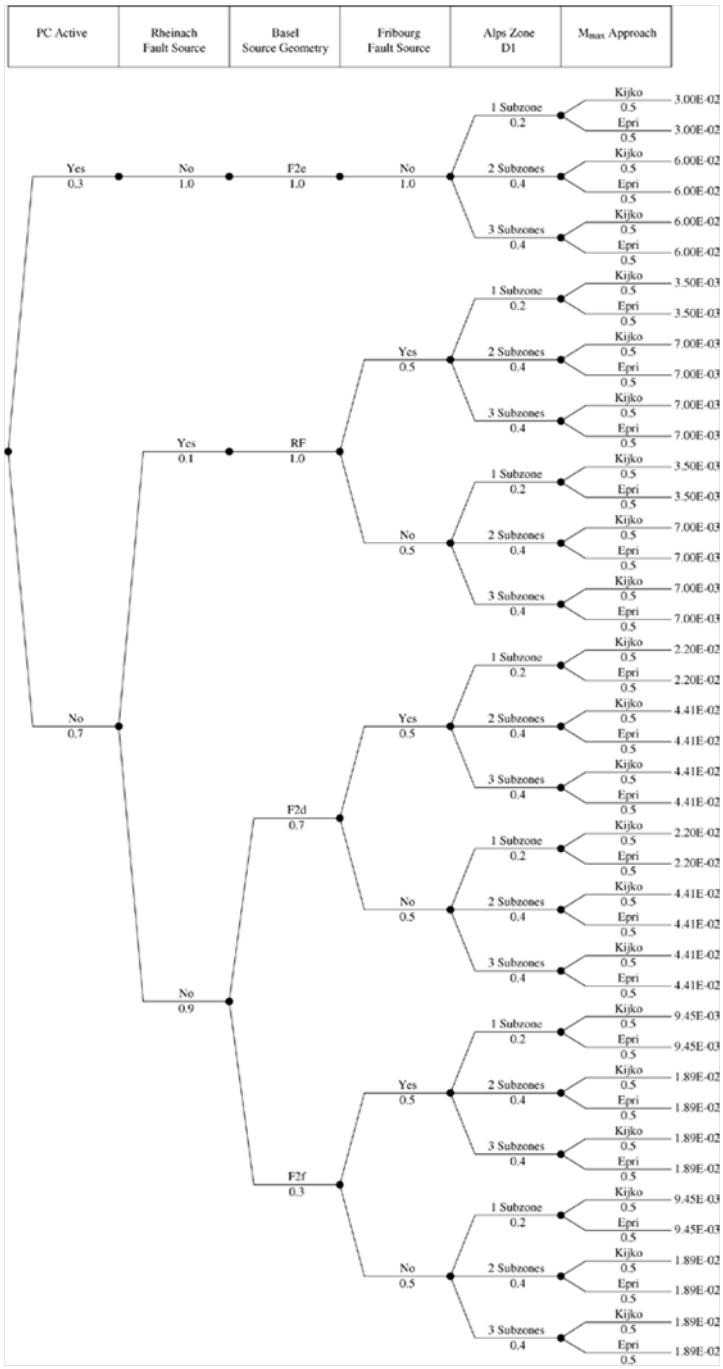

Figure 3.10: Logic tree for EG1a. The 23 tree variables that handle the correlation of the b-value and of the seismicity rate among all sources that make up the individual macrozones are not shown.

Table 3.3: Seismic Source Sets for Recurrence Parameters.

Sources with correlated *b*-values	*b*-value	Weight	Seismicity Rate Alternatives	Weight
A	0.767	(0.278)	All data	(0.5)
	1.000	(0.444)	All data, larger mag	(0.5)
	1.233	(0.278)		
B	0.767	(0.278)	All data (0.5)	
	1.000	(0.444)	All data, larger mag	(0.5)
	1.233	(0.278)		
C1, C2, C3	0.826	(0.185)	All data	(0.5)
	0.990	(0.630)	All data, larger mag	(0.5)
	1.155	(0.185)		
D1a, D1b, D1c,	0.775	(0.185)	Instrumental data	(0.333)
D1e, D1f, D1bcd,	0.940	(0.630)	Historical data	(0.334)
D1bcde, D1de	1.105	(0.185)	Historical data,	
			larger mag	(0.333)
D2, D3a, D3b	0.795	(0.185)	Instrumental data	(0.333)
	0.960	(0.630)	Historical data	(0.334)
	1.125	(0.185)	Historical data,	
			larger mag	(0.333)
D4a, D4b, D4c	0.767	(0.278)	All data	(0.5)
	1.000	(0.444)	All data, larger mag	(0.5)
	1.233	(0.278)		
E1	0.727	(0.278)	All data	(0.5)
	0.960	(0.444)	All data, larger mag	(0.5)
	1.193	(0.278)		
E2a, E2b, E2c, E2d,	0.875	(0.185)	For E2a, E2b:	
E2e, E2cde, FF, E2dF2f,	1.040	(0.630)	All data	(0.2)
E2eF2f, E2cdeF2f,	1.204	(0.185)	All data, larger mag	(0.8)
E2n, E2s, E2f, E3a,			For rest of sources:	
E3aF2f, E3b			Instrumental data	(0.333)
			Historical data	(0.334)
			Historical data,	
			larger mag	(0.333)
F1a, F1b	0.727	(0.278)	All data	(0.5)
	0.960	(0.444)	All data, larger mag	(0.5)
	1.193	(0.278)		
F2a, F2b,	0.890	(0.185)	For F2c:	
F2b_RF, RF,	1.120	(0.630)	All data	(0.5)
F2bpcy, F2bF2f,	1.350	(0.185)	All data, larger mag	(0.5)
F2c, F2d, F2e, F2f			For rest of sources:	
			Instrumental data	(0.333)
			Historical data	(0.334)
			Historical data,	
			larger mag	(0.333)
F3a, F3aF2f,	0.715	(0.185)	Instrumental data	(0.333)
F3b, F3c	1.060	(0.630)	Historical data	(0.334)
	1.405	(0.185)	Historical data,	
			larger mag	(0.333)

Chapter 4

QA-Certificate EG1-QC-1022

QA Certificate	PEGASOS REFINEMENT PROJECT
EG1-QC-1022	

Hazard Input Document (HID)

Expert group:	**EG1a**	***HID designation:***	**EG1-HID-1001**
Expert:	N. Deichmann, S. Schmid, D. Slejko	***Expert Model (EXM)***	EG1-EXM-1001

HID parameterisation of Expert Model:

TFI: N. A. Abrahamson ***Hazard Input Specialist of TFI-team:*** Ph. Roth

HID based on Elicitation Documents: ☒ EG1-ES-1001

HID based on Exp. Assessments (EXA): ☐

Remarks on the HID model parameterisation in terms of hazard computation input:

The undersigned Hazard Input Specialist confirms that this HID includes all required (subproject specific) input information for hazard computations. No further interpretations of this input will be required and no simplifications except Algorithmic Pinching according to paragraph 2.9 of the QA-Guidelines will be applied to convert this HID into hazard software Input Files.

Signature:

HID acceptance by the Expert / Expert Group:

Date of HID review by the Expert / Expert group: 02.11.2011

HID accepted: ☒ ***HID not accepted:*** ☐

Reasons for non-acceptance of HID / Recommendations:

The undersigned Expert(s) accept(s) the parameterisation proposed in this HID as a faithful and adequate representation of his/their Expert Model. He/they confirm(s) that this HID is free of errors and agree(s) to its use as hazard computation input.

Signature Expert 1 / Expert:

Signature Expert 2:

Signature Expert 3:

Part III

Assessments of EG1b

by A. Cisternas and G. Grünthal

Chapter 1

EG1b Evaluation Summary (EG1-ES-1002)

1.1 Applicability of the SP1 EG1b Model for PRP Considering ECOS09

On March 27, 2010 the SP1 EG1b expert team provided its conclusions on the applicability of the SP1 EG1b PEGASOS model, which is based on the seismicity data file ECOS02, also for the new catalogue ECOS09 for the PEGASOS Refinement Project PRP. These statements on the EG1b source zone characterization update for the usage of ECOS09 refer to the following parameters: Zone boundaries, declustering and seismicity data completeness, calculation of the frequency-magnitude parameter, M_{max} distributions, and depth distributions. As it will be shown, some of the elements of the model need not to be changed, while others need a modification.

The EG1b team appreciates the replacement of ECOS02 by ECOS09. The fact that ECOS02 had tendentially overestimated the M_W of historical earthquakes was obvious and has been expressed in the materials by the team. Quantitatively the degree of overestimation in M_W has been given in Grünthal et al. [2009b].

1.1.1 Zone Boundaries

There is no need to change the zone boundaries. The large scale seismic source zone (SSZ) model (fig. 1.1) is solely based on the large scale tectonic architecture and is not affected by seismicity characteristics. Also the small scale SSZ model (fig.1.2) does not need to be changed, since the modified parameters in ECOS09 do not require this. There exists one exception only, which concerns the small scale N-S elongated SSZ Fribourg AE-7, whose originally soft eastern boundary can be waived entirely due to the new findings by Kastrup et al. [2007]. This has been described in detail in Burkhard and Grünthal [2009].

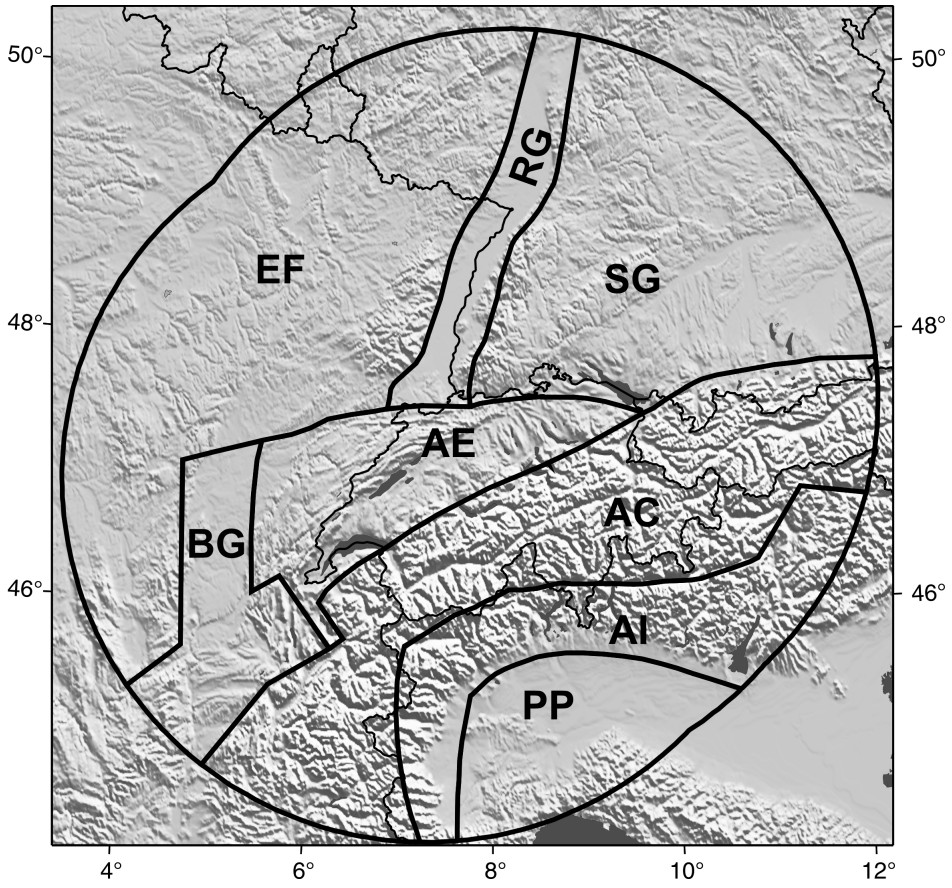

Figure 1.1: The EG1b large scale seismic source zone (SSZ) model.

1.1.2 Declustering and Completeness of Seismic Data

What concerns the declustering, it has been verified by the team that there is no need for a change in the method used for declustering. The EG1b method for declustering has been described in the PEGASOS materials.

The completeness analysis has been performed separately for the five sub-regions of national earthquake cataloging areas from which ECOS has been assembled Figure 1.3. It is recommended to apply the same methodology as it has been used in PEGASOS.

1.1.3 Frequency-Magnitude Parameter

The conversion from M_L to M_W adopted for ECOS09 is now quadratic and very similar to the one developed by Stromeyer et al. [2004] which had already been applied for the M_W-based central and northern European earthquake catalogue [Grünthal and Wahlström 2003] as well as in its updated form for the CENEC catalogue [Grünthal et al. 2009c]. The quadratic M_L-M_W relation requires to consider that the Gutenberg-Richter relation can be applied in its classical linear form only above a certain M_W. According to figure 8 in Wiemer and Wössner [2010], stable b-values can be expected for $M_W \geq 2.7$. Therefore, it has been concluded for EG1b to limit the ECOS09-M_W data to $M_W \geq 2.7$ for the MLE of the frequency-magnitude parameter.

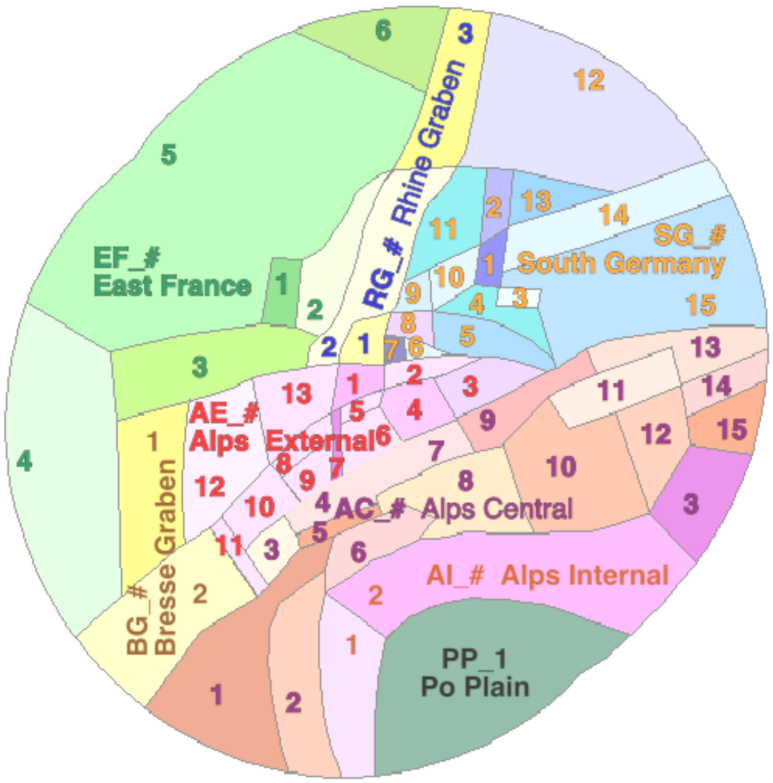

Figure 1.2: The EG1b small scale SSZ model.

1.1.4 M_{max} Distributions

The EG1b team decided to apply again the Bayesian EPRI approach for determining M_{max}. But there is the need for a change in the discretization procedure and in the truncation of the EPRI a-posteriori distribution functions.

Discretization of the EPRI-M_{max} Distribution using Equal Weights of the Magnitude Bins m_u

To avoid a not well constraint homogeneous discretization of the a posteriori distribution we suggest the following approach for the discretization as it has been applied by one of the expert team members since more than ten years (e.g. Grünthal and Wahlström [2006], Grünthal et al. [2009a]):

Discretization by using N values of magnitude bins mu with normalized equal weights $W_i = 1/N$, from W_1 to W_N. This is performed by a division of the area under the probability curve, i.e. within the range of the magnitudes $[M_{max,obs}, M_{max,cut}]$, in N equally large areas defined on the abscissa by $[Q_0, Q_1] \ldots [Q_{n-1}, Q_n]$. Then, the N discretizations m_u are defined as the arithmetic means (or centres of gravity) of the areas corresponding to the intervals $[Q_0, Q_1] \ldots [Q_{n-1}, Q_n]$. Figure 1.4 illustrates this according to two the SSZs (Cheb and Lower Rhine Embayment), both corresponding to cases of extended crust.

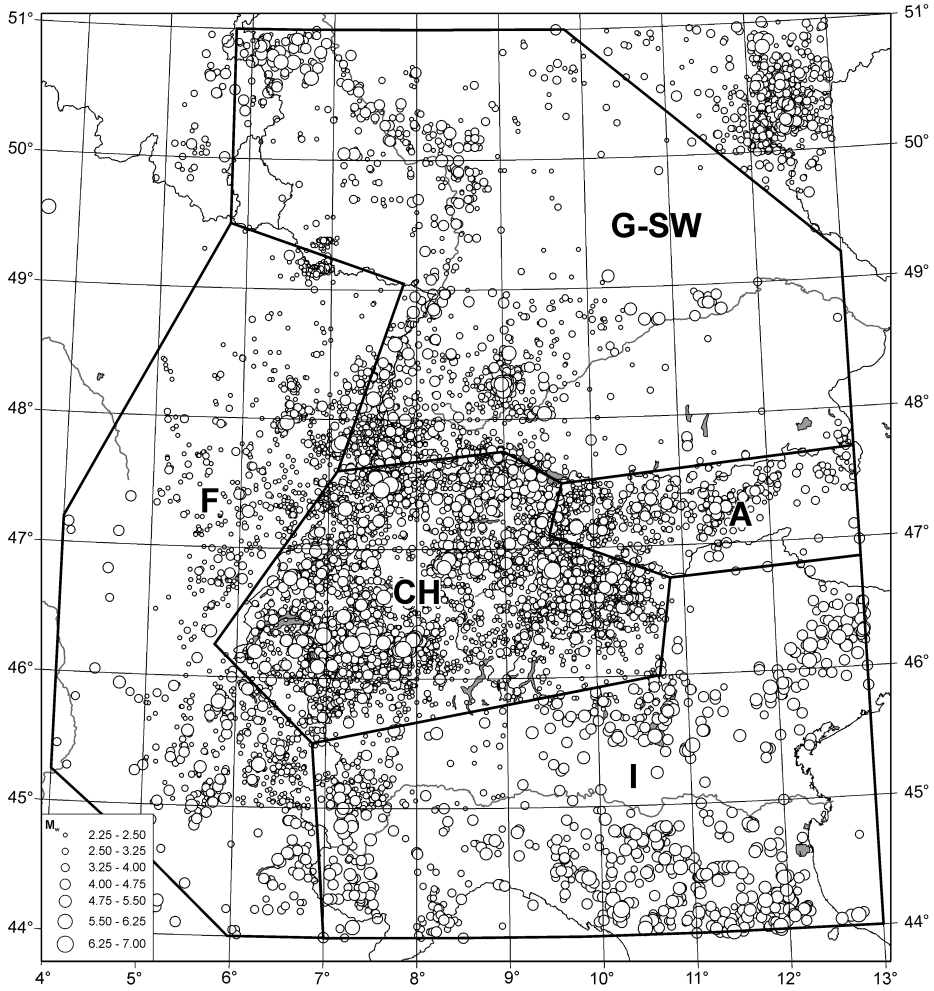

Figure 1.3: Subdivision of the study area into sub-regions for analyzing catalogue completeness.

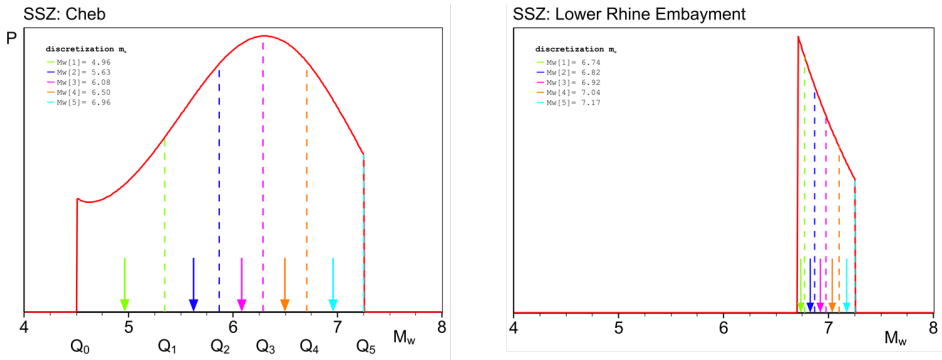

Figure 1.4: Examples of the application of the discretization using equal weights of the magnitude bins after Grünthal et al. [2009a].

New Considerations on the Geological Truncation of the EPRI a Posteriori Distribution Functions

No change should be applied to the 95% cumulative truncation, introduced in the frame of PEGASOS, nor in the largest size of faults within small SSZs based on the Wells and Coppersmith [1994] relation.

New findings on geological constraints for the truncation of M_{max} ($M_{max,cut}$) for central European conditions, described in Grünthal et al. [2009a], led to the following new truncation magnitudes $M_{max,cut}$:

1. for the SSZ covering mostly non-extended crust: $M_{max,cut} = 6.8$,
2. for the SSZ covering mostly extended crust: $M_{max,cut} = 7.25$.

These new values for $M_{max,cut}$ follow considerations in Grünthal et al. [2009a] on expected maximum fault lengths for:

- non-extended crust: 24 km
- extended crust: 70 km
- maximum seismogenic depth range: 25 km

By applying the appropriate relation in Wells and Coppersmith [1994] these maximum fault lengths have been expressed as respective values of $M_{max,cut}$. The association of SSZ to one of these two crustal types should not change with respect to the results developed for PEGASOS.

1.1.5 Depth Distributions

The changes in depth values in ECOS09 with respect to ECOS02 are marginally only. Therefore, no change in the depth distributions is needed for the application of ECOS09 in PRP.

1.2 Groups of Small Zones to Determine M_{max} Distributions

Table 1.1: Groups of small zones to determine M_{max} distributions.

Within large Zone RG	
RG01 + RG02 + RG03	within all of them
RG1_AE1 should remain as it is.	
Within Large Zone EF	
EF02 + EF03 + EF04 + EF05 + EF06	within all of them
Within Large Zone SG	
SG01 + SG02	within SG01, SG02, SG1_2
SG01 + SG03 + SG04	within SG03, SG04
SG01 + SG05 + SG06 + SG07 + SG08 +	within SG05, SG06, SG07, SG08,
SG09 + SG10 + SG14	SG09, SG10, SG14
	SG5678, SG5_6_8, SG5_8, SG6_7
SG01 + SG02 + SG11 + SG12 +	within SG11, SG12, SG13, SG15
SG13 + SG15	
Within Large Zone BG	
BG01 + BG02	within BG01, BG02
Within Large Zone AI	
AI01 + AI02	within AI01, AI02
AI01 + AI02 + AI03	within AI03
Within Large Zone AE	
No groups of small zones needed.	
All can remain as initially calculated.	
Within Large Zone AC	
AC04 + AC05	within AC04, AC05
AC08 + AC10 + AC12	within AC08, AC10, AC12
AC09 + AC11 + AC13 + AC15	within AC09, AC11, AC13, AC15
separate small zones:	
AC01, AC02, AC03, AC06, AC07, AC14	

Chapter 2

Supporting Calculations for EG1b by R. Youngs

2.1 Calculations for Expert Team EG1b

This section documents the calculations performed to support the EG1b Expert Team's review and finalization of the updated seismicity parameters based on the ECOS-09 catalog. These calculations are all performed using the final ECOS-09 catalog SED [2011] and the final ECOS-09 catalog declustered by Dr. Stefan Wiemer utilizing the [Gardner and Knopoff 1974] approach with the time and distance widows developed by Grünthal [1985] as published in Burkhard and Grünthal [2009].

2.2 Large Zone Earthquake Recurrence Relationships

The maximum likelihood method described in section 2.2.3 was used to compute seismicity parameters for the EG1b large zones (Figure 2.27). The calculations were performed using the catalog completeness periods extended through the end of 2008. EG1b specified completeness for magnitude intervals of 0.5 units in width starting at M 2.3. To satisfy the request by EG1b to use only $M \geq 2.7$, the earthquake data and completeness intervals were limited to the intervals starting at M 2.8. For purposes of evaluating differences in magnitude scaling two sets of earthquake recurrence relationships were develop, on using the original magnitude intervals specified in PEGASOS and the a second set using magnitude intervals modified using equation 2.11. Table 2.1 lists magnitude intervals and catalog completeness periods used. Figures 2.1 through 2.8 show the seismicity data and fitted earthquake recurrence relationships.

Table 2.1: Magnitude Intervals and Completeness Periods Used in Earthquake Recurrence Calculations for EG1b Large Source Zones.

Magnitude Interval	Original Mag. interval used in PEGASOS	Mag. interval modified by equation 2.11	Beginning year for complete reporting				
			Austria	France	Germany	Italy	Switzerland
1	2.8 to 3.3	2.851 to 3.254	1975	1970	1965	1975	1880
2	3.3 to 3.8	3.254 to 3.7	1900	1965	1870	1975	1880
3	3.8 to 4.3	3.7 to 4.2	1875	1810	1865	1875	1860
4	4.3 to 4.8	4.2 to 4.7	1875	1810	1865	1850	1825
5	4.8 to 5.3	4.7 to 5.2	1550	1750	1860	1750	1770
6	5.3 to 5.8	5.2 to 5.7	1550	1650	1200	1750	1650
7	5.8 to 6.3	5.7 to 6.2	1550	1650	1200	1600	1575
8	6.3 to 6.8	6.3 to 6.7	1550	1650	1200	1600	1250
9	> 6.8	> 6.7	1550	1650	1200	1600	1250

2.3 Small Zone Earthquake Recurrence Relationships

The maximum likelihood method described in section 2.2.3 was used to compute seismicity parameters for the EG1b small zones. The calculations were performed using the catalog completeness periods extended through the end of 2008 and the original magnitude intervals specified in the PEGASOS Project starting at M 2.8. The data for each zone was fit in two ways. The first was a maximum likelihood fit to the data without constraint on the b-value. The second was a maximum likelihood fit using a prior for the b-value consisting of the b-value obtained for the corresponding large zone with a weight of 100%, which is equivalent to a sigma on b of 0.1. Modifications to the general approach were made for small sources BG01, SG06, SG11, and SG12 in which the first one or two magnitude intervals with zero counts were not used. For small source SG06W the magnitude interval starting at M 2.3 was used because it is the only interval with non-zero earthquake counts. Figures 2.9 through 2.58 show the seismicity data and fitted recurrence relationships for the small source zones.

2.4 Maximum Magnitude Distributions

Maximum magnitude distributions were computed for the EG1b seismic sources using the Bayesian (EPRI) approach described in section 2.2.4. The Johnston et al. [1994] Non-Extended Crust prior was applied to the EF and SG zones and the Extended Crust prior was applied to all others. The likelihood function for each source was computed using the earthquake counts for M4.8 and larger earthquakes and the b-value computed for each source. Upper bound truncations were applied to be the lower of the 95th percentile value of the posterior distribution or the geologic maximum. The specified values of M6.8 for non-extended crust and M7.25 for extended crust were used for the geologic maximums as these values are generally equal to or lower than the zone-specific values specified in the PEGASOS project. The final truncated posterior distributions were represented by a five-point discrete approximation based on Miller and Rice [1983] approach to representing an arbitrary cumulative distribution. This representation uses five points with assigned weights at specific values of the M_{max} cumulative distribution function (CDF). Table 2.2 lists the cumulative probability levels selected as the five discrete points and the associated probability weight assigned to each.

Table 2.2: Miller and Rice (1983) Discrete 5-point Approximation to a Continuous Probability Distribution.

Cumulative Probability Level of Continuous Distribution	Assigned Probability Weight
0.034893	0.10108
0.211702	0.24429
0.5	0.30926
0.788298	0.24429
0.965107	0.10108

2.4.1 Initial Maximum Magnitude Distributions

The initial Bayesian maximum magnitude distributions computed for the EG1b source zones are shown on Figures 2.59 through 2.80. Each figure contains the maximum magnitude distributions for one of the eight large source zones and the maximum magnitude distributions for the associated small source zones. Both the untruncated and the truncated posteriors are shown on each plot. It should be noted that the 1368 Basel earthquake is located in the AE large source rather than the RG large source.

2.4.2 Final Maximum Magnitude Distributions

Review of the initial maximum magnitude distributions indicated that in a number of cases the maximum magnitude distributions for the small zones were broader than that for the corresponding large zone. This was due to the larger zone having a greater number of earthquakes, and thus a more peaked likelihood function that more strongly modifies the prior. In many of the small zones there are no events larger than M 4.8, resulting in a posterior equal to the prior. Accordingly EG1b review the data and in a number of cases grouped small zones to produce a composite dataset for the assessment of maximum magnitude. Figures 2.81 through 2.95 present the final maximum magnitude distributions. The truncated posterior distributions shown in these figures were used to create the five-point discrete maximum magnitude distributions for use in the PSHA. These distributions are listed in tables 2.3 through 2.10. The small zone groupings used to develop the final maximum magnitude distributions are indicated in the tables.

Note that for some cases, the first M_{max} value has a large enough probability that the CDF value is equal or grater than the Miller & Rice values for the first two discrete points. For example in Table 2.3, the first M_{max} value of 6.20 has a probability of 0.2358. The Miller & Rice CDF points are at 0.034893, 0.211702, 0.5, 0.788298, and 0.965107. Thus, the first two probability weights are assigned to it.

Table 2.3: Maximum Magnitude Distributions for EG1b AC Zones.

Weight	Maximum Magnitudes for Zone:				
	AC	AC01	AC02	AC03	AC04 and AC05[1]
0.10108	6.2	5.8	5.55	5.5	5.9
0.24429	6.2	5.9	5.6	5.75	5.95
0.30926	6.3	6.2	5.75	6.25	6.05
0.24429	6.45	6.65	6.3	6.75	6.5
0.10108	6.85	7.15	7.05	7.15	7.1

Weight	Maximum Magnitudes for Zone:				
	AC06	AC07	AC08, AC10, and AC12[2]	AC09, AC11, AC13, and AC15[3]	AC14
0.10108	6.2	5.9	5.5	5.5	5.85
0.24429	6.3	6	5.8	5.6	6.05
0.30926	6.55	6.3	6.25	5.8	6.45
0.24429	6.9	6.75	6.75	6.4	6.85
0.10108	7.2	7.15	7.15	7.05	7.2

[1] Based on combination of AC04 and AC05
[2] Based on combination of AC08, AC10, and AC12
[3] Based on combination of AC09, AC11, AC13, and AC15

Table 2.4: Maximum Magnitude Distributions for EG1b AE Zones.

Weight	Maximum Magnitudes for Zone:							
	AE	AE01	AE02	AE03	AE04	AE05	AE06	AE07
0.10108	6.6	6.6	5.55	5.55	5.55	5.55	5.55	5.55
0.24429	6.7	6.65	5.9	5.9	5.9	5.9	5.85	5.9
0.30926	6.85	6.85	6.4	6.4	6.4	6.4	6.35	6.4
0.24429	7.05	7.05	6.85	6.85	6.85	6.85	6.8	6.85
0.10108	7.25	7.25	7.2	7.2	7.2	7.2	7.2	7.2
Weight	Maximum Magnitudes for Zone:							
	AE08	AE09	AE10	AE11	AE12	AE13	AE1_13	AE1_2
0.10108	5.5	5.55	5.55	5.5	5.5	5.55	6.6	6.6
0.24429	5.8	5.9	5.9	5.8	5.75	5.85	6.7	6.7
0.30926	6.25	6.4	6.4	6.3	6.2	6.35	6.85	6.85
0.24429	6.75	6.85	6.85	6.8	6.75	6.8	7.05	7.05
0.10108	7.15	7.2	7.2	7.15	7.15	7.2	7.25	7.25
Weight	Maximum Magnitudes for Zone:							
	AE1_2_13							
0.10108	6.6							
0.24429	6.7							
0.30926	6.85							
0.24429	7.05							
0.10108	7.25							

Table 2.5: Maximum Magnitude Distributions for EG1b AI Zones.

Weight			
	AI	AI01 and AI02[1]	AI03[2]
0.10108	5.65	5.65	5.65
0.24429	5.65	5.65	5.65
0.30926	5.7	5.7	5.7
0.24429	5.75	5.75	5.75
0.10108	5.8	5.8	5.8

[1] Based on combination of AI01 and AI02
[2] Based on combination of AI01, AI02, and AI03

Table 2.6: Maximum Magnitude Distributions for EG1b BG Zones.

Weight	Maximum Magnitudes for Zone:	
	BG	BG01 and BG02[1]
0.10108	5.6	5.6
0.24429	5.75	5.75
0.30926	6.1	6.1
0.24429	6.65	6.65
0.10108	7.15	7.15

[1] Based on combination of BG01 and BG02

Table 2.7: Maximum Magnitude Distributions for EG1b EF Zones.

Weight	Maximum Magnitudes for Zone:		
	EF	EF01	EF02, EF03, EF04, EF05 and EF06[1]
0.10108	6	6	5.6
0.24429	6.15	6.15	5.9
0.30926	6.35	6.35	6.25
0.24429	6.6	6.6	6.55
0.10108	6.8	6.8	6.75

[1] Based on combination of EF01, EF02, EF03, EF04, EF05, and EF06

Table 2.8: Maximum Magnitude Distributions for EG1b PP Zone.

Weight	Maximum Magnitudes for Zone:
	PP
0.10108	5.65
0.24429	5.7
0.30926	5.85
0.24429	6.25
0.10108	6.95

Table 2.9: Maximum Magnitude Distributions for EG1b RG Zones.

Weight	Maximum Magnitudes for Zone:		
	RG	RG01, RG02 and RG03[1]	RG1_AE1
0.10108	5.5	5.5	6.6
0.24429	5.5	5.5	6.7
0.30926	5.6	5.6	6.9
0.24429	5.95	5.95	7.1
0.10108	6.65	6.65	7.25

[1] Based on combination of RG01, RG02, and RG03

Table 2.10: Maximum Magnitude Distributions for EG1b SG Zones.

Weight	Maximum Magnitudes for Zone:				
	SG	SG01, SG02, and SG1_2[1]	SG03 and SG04[2]	SG05, SG06, SG07, SG08, SG09, SG10, SG14, SG5_8, SG6_7, SG5_6_8, SG5678[3]	SG11, SG12, SG13, and SG15[4]
0.10108	5.6	5.5	5.6	5.5	5.5
0.24429	5.6	5.55	5.6	5.55	5.55
0.30926	5.7	5.65	5.7	5.65	5.65
0.24429	5.9	5.9	5.8	5.9	5.9
0.10108	6.3	6.35	6.1	6.35	6.4

[1] Based on combination of SG01 and SG02
[2] Based on combination of SG01, SG03, and SG04
[3] Based on combination of SG01, SG05, SG06, SG07, SG08, SG09, SG10, and SG14
[4] Based on combination of SG01, SG02, SG11, SG12, SG13, and SG15

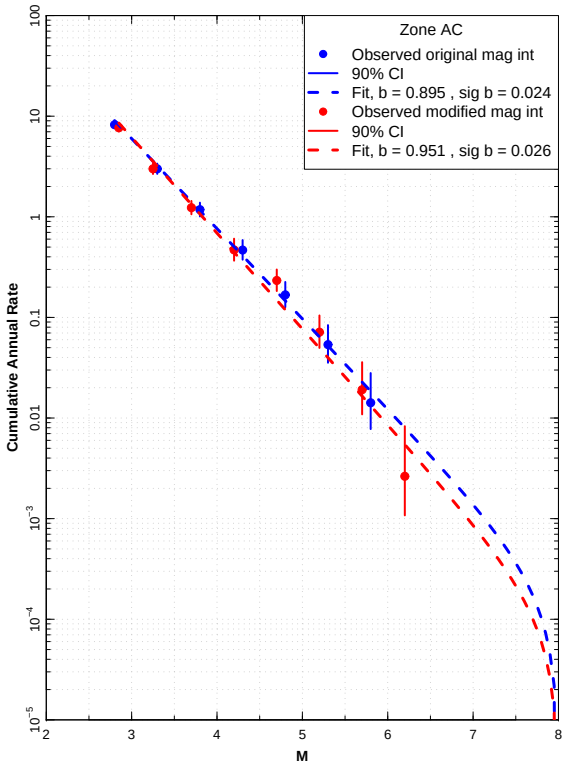

Figure 2.1: Earthquake Recurrence Relationships for EG1b AC Zone.

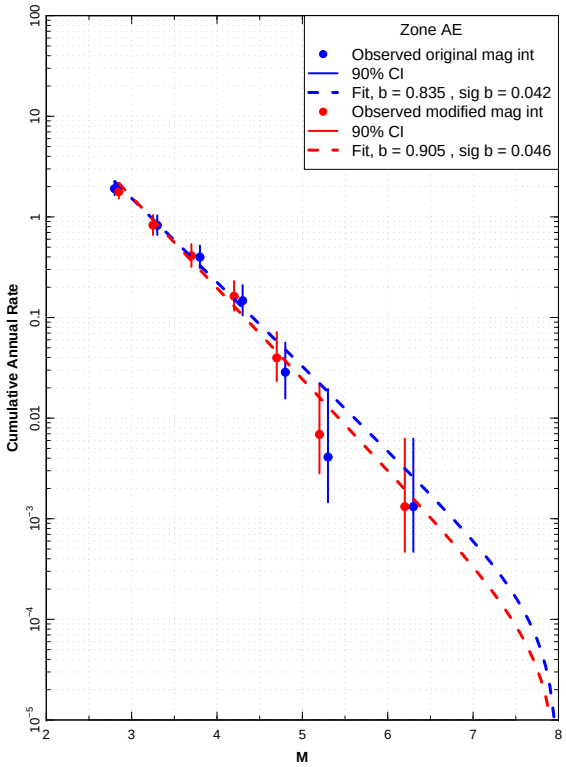

Figure 2.2: Earthquake Recurrence Relationships for EG1b AE Zone.

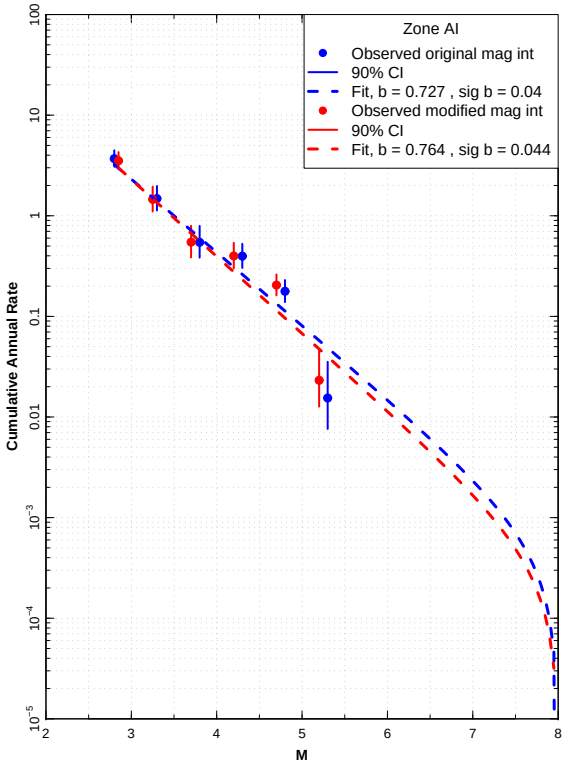

Figure 2.3: Earthquake Recurrence Relationships for EG1b AI Zone.

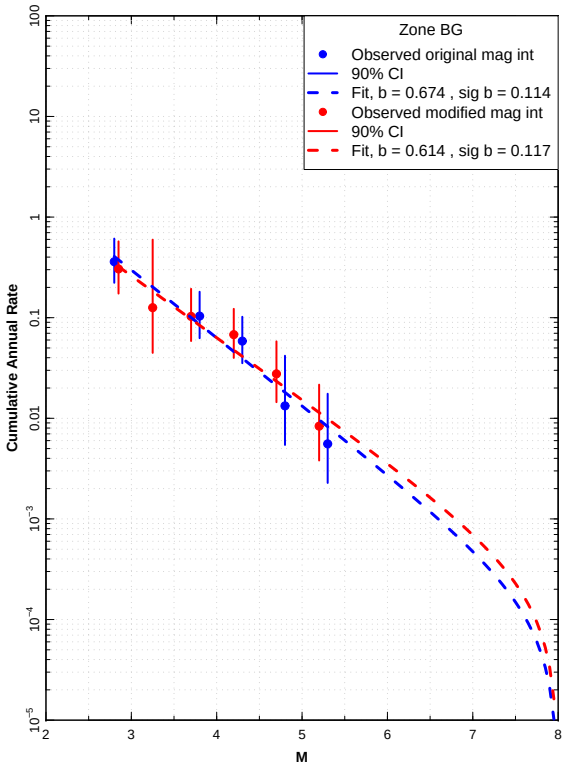

Figure 2.4: Earthquake Recurrence Relationships for EG1b BG Zone.

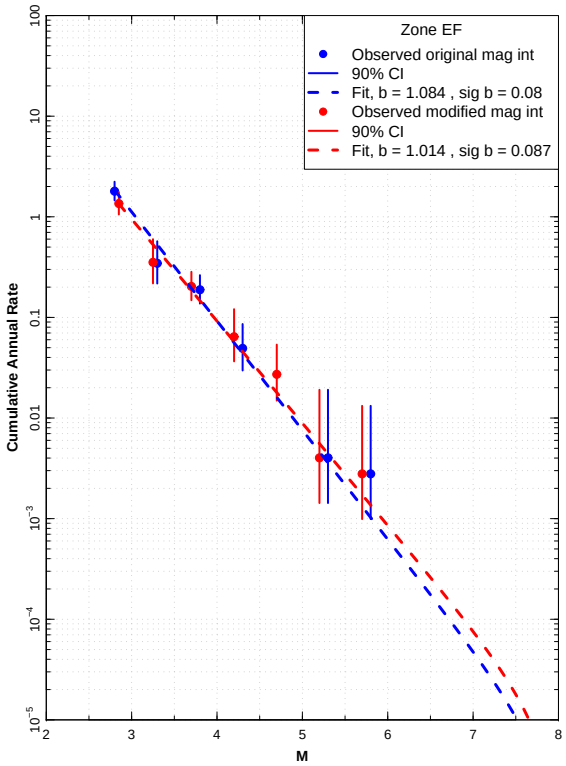

Figure 2.5: Earthquake Recurrence Relationships for EG1b EF Zone.

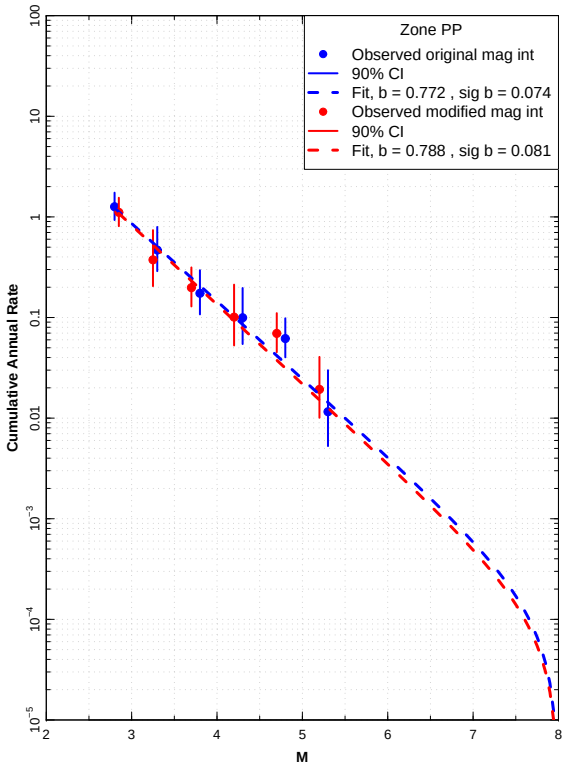

Figure 2.6: Earthquake Recurrence Relationships for EG1b PP Zone.

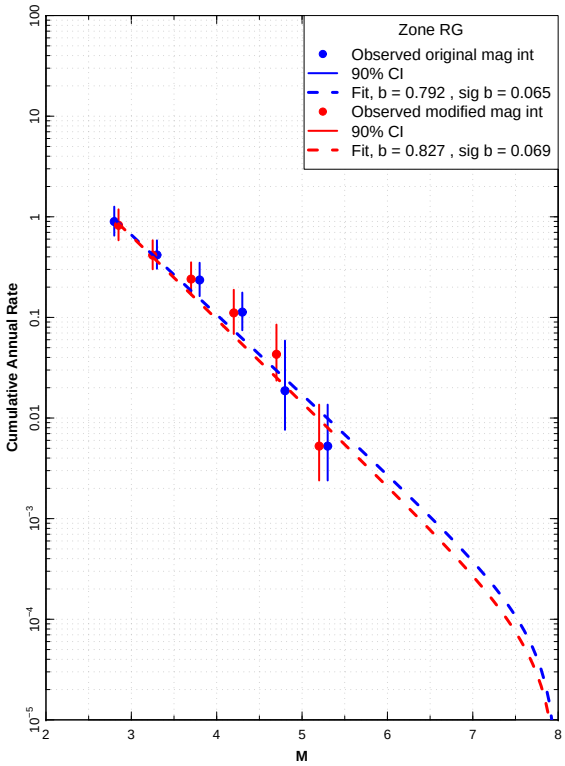

Figure 2.7: Earthquake Recurrence Relationships for EG1b RG Zone.

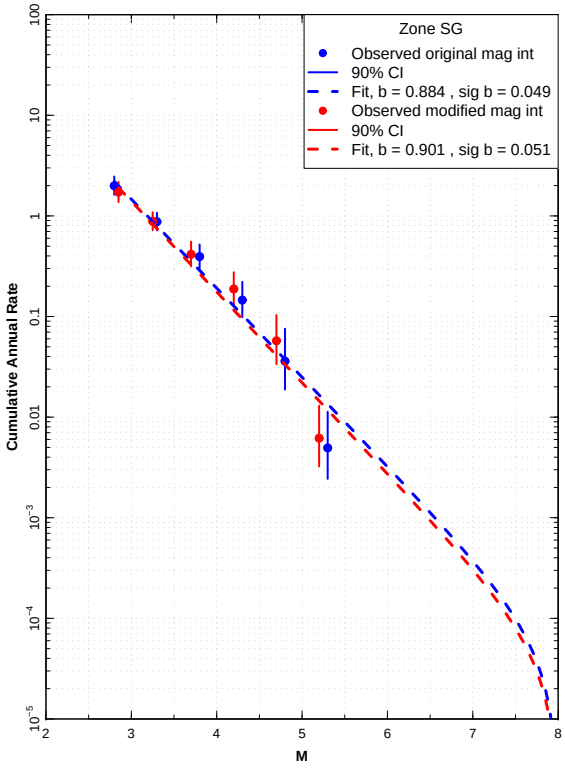

Figure 2.8: Earthquake Recurrence Relationships for EG1b SG Zone.

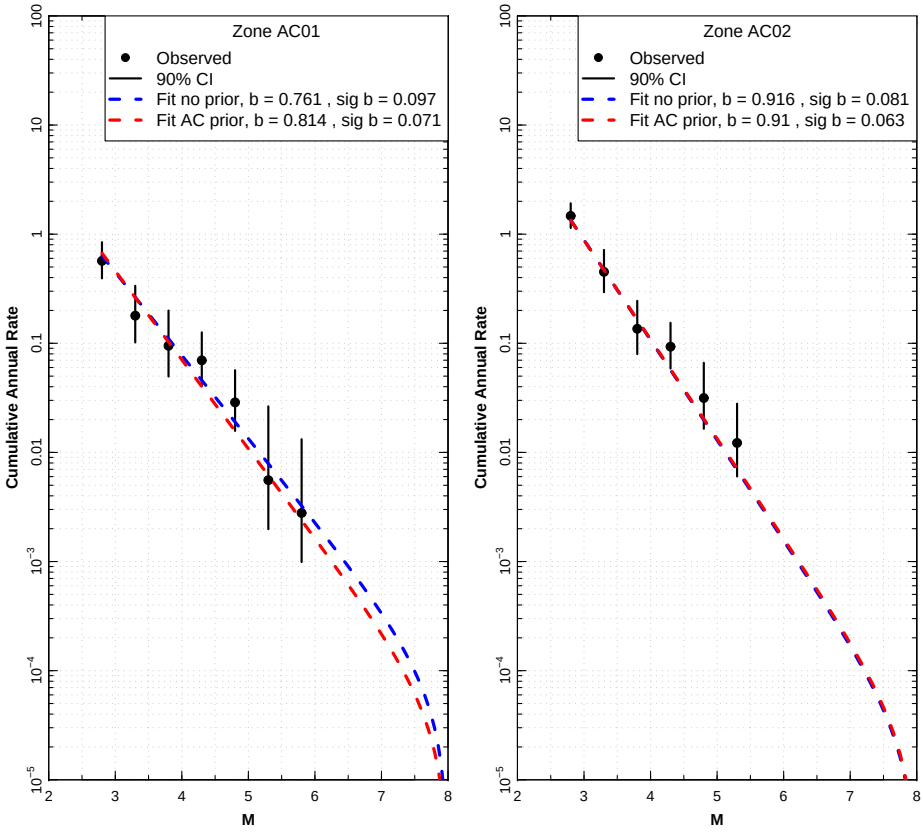

Figure 2.9: Earthquake recurrence relationships for EG1b small zones AC01 and AC02.

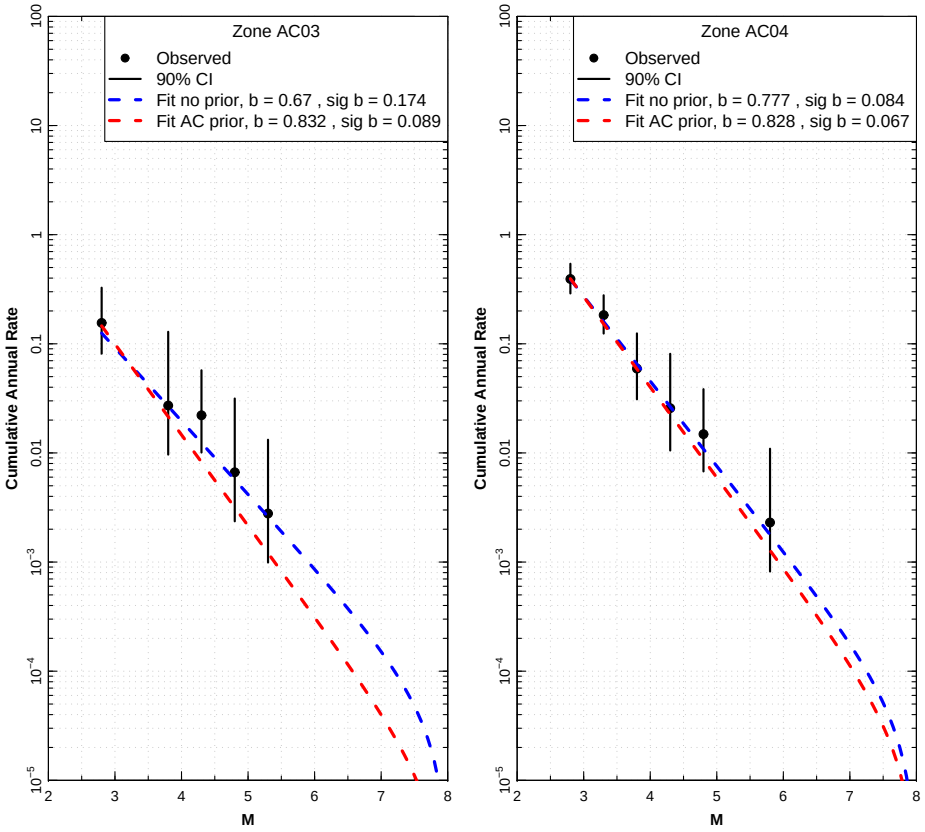

Figure 2.10: Earthquake recurrence relationships for EG1b small zones AC03 and AC04.

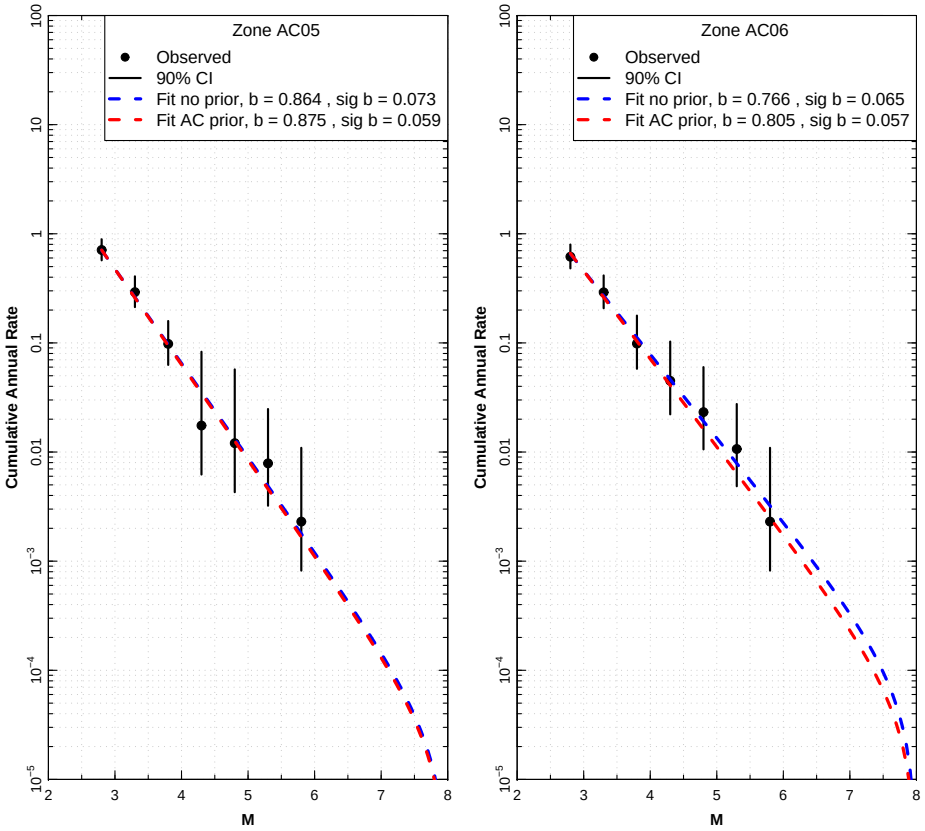

Figure 2.11: Earthquake recurrence relationships for EG1b small zones AC05 and AC06.

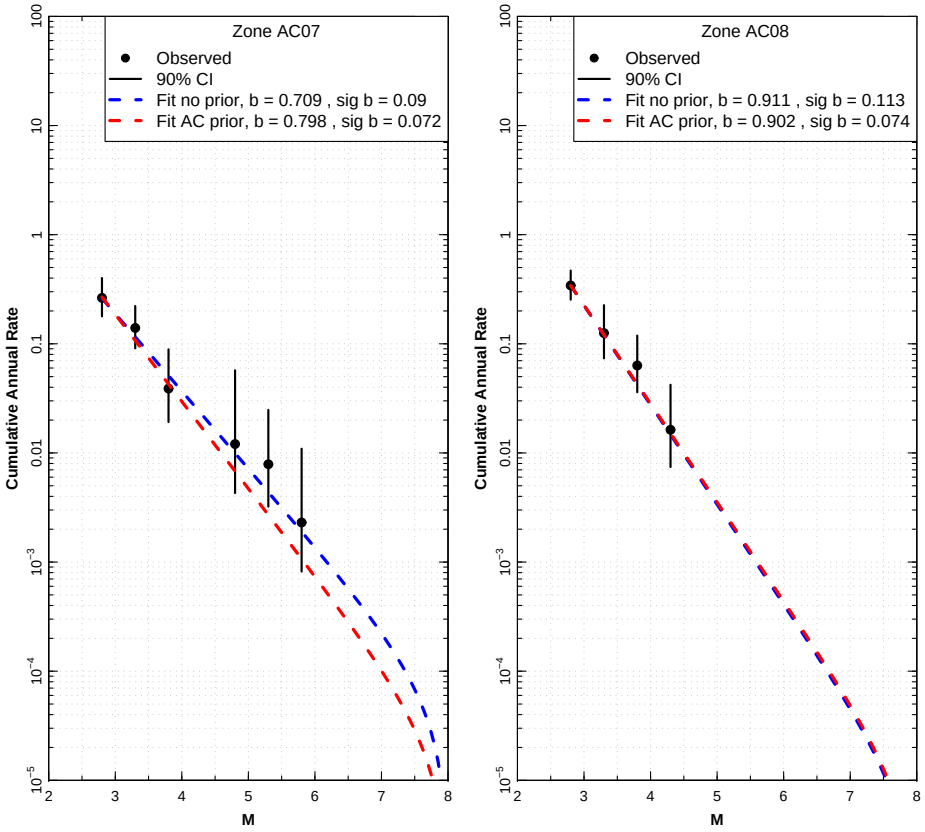

Figure 2.12: Earthquake recurrence relationships for EG1b small zones AC07 and AC08.

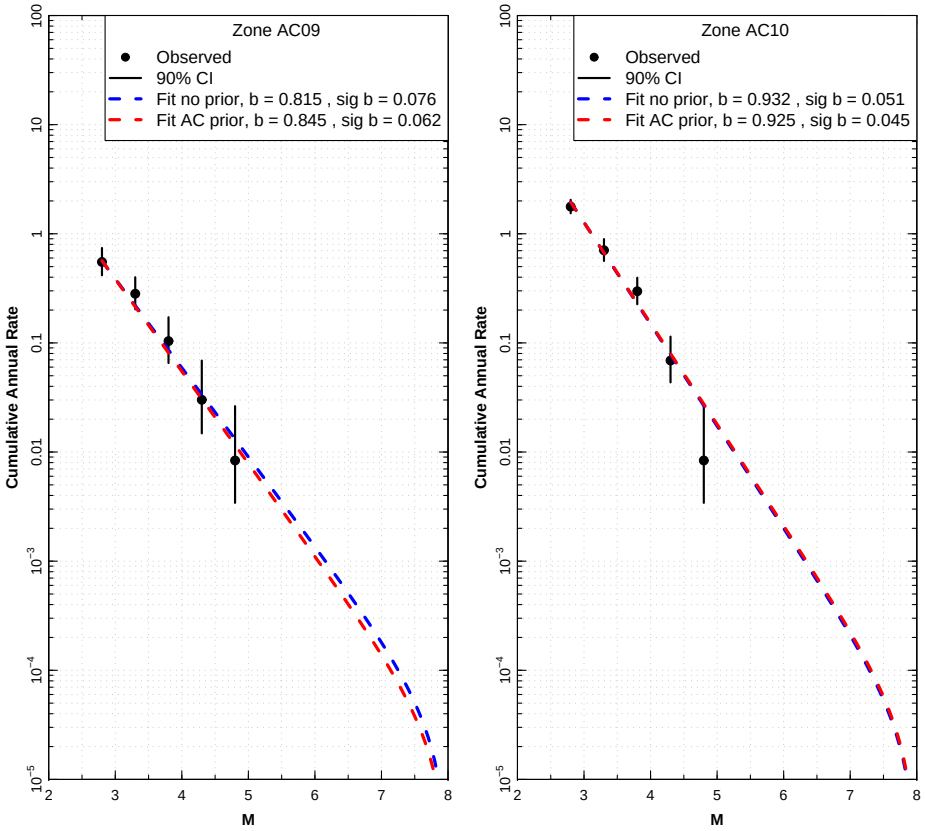

Figure 2.13: Earthquake recurrence relationships for EG1b small zones AC09 and AC10.

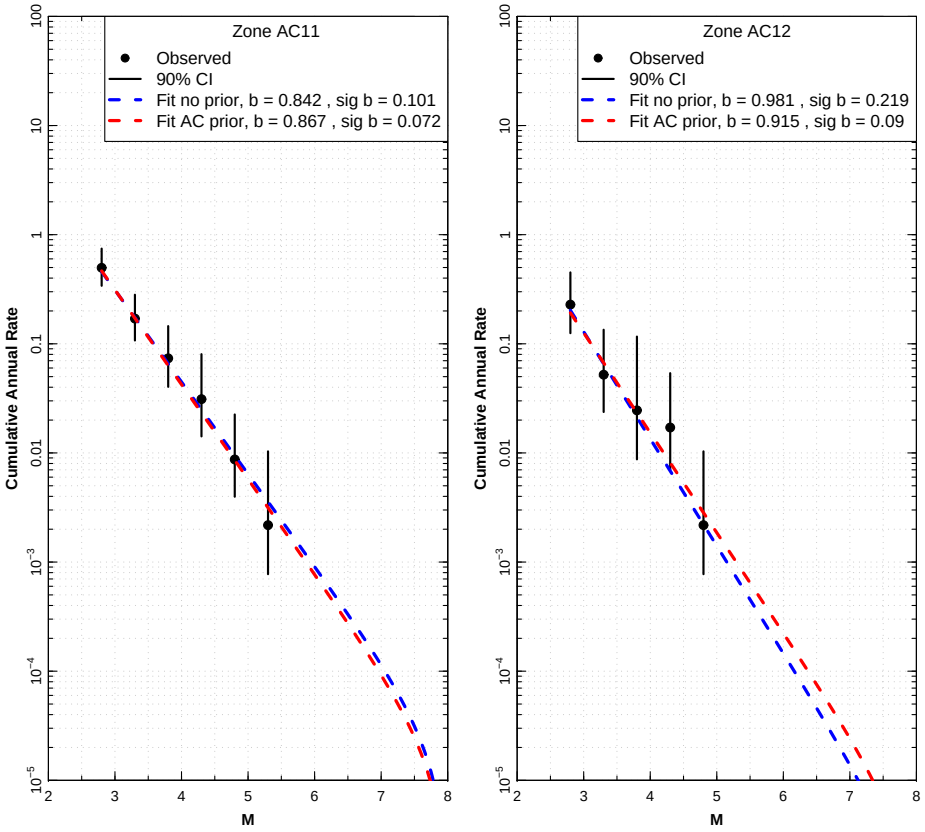

Figure 2.14: Earthquake recurrence relationships for EG1b small zones AC11 and AC12.

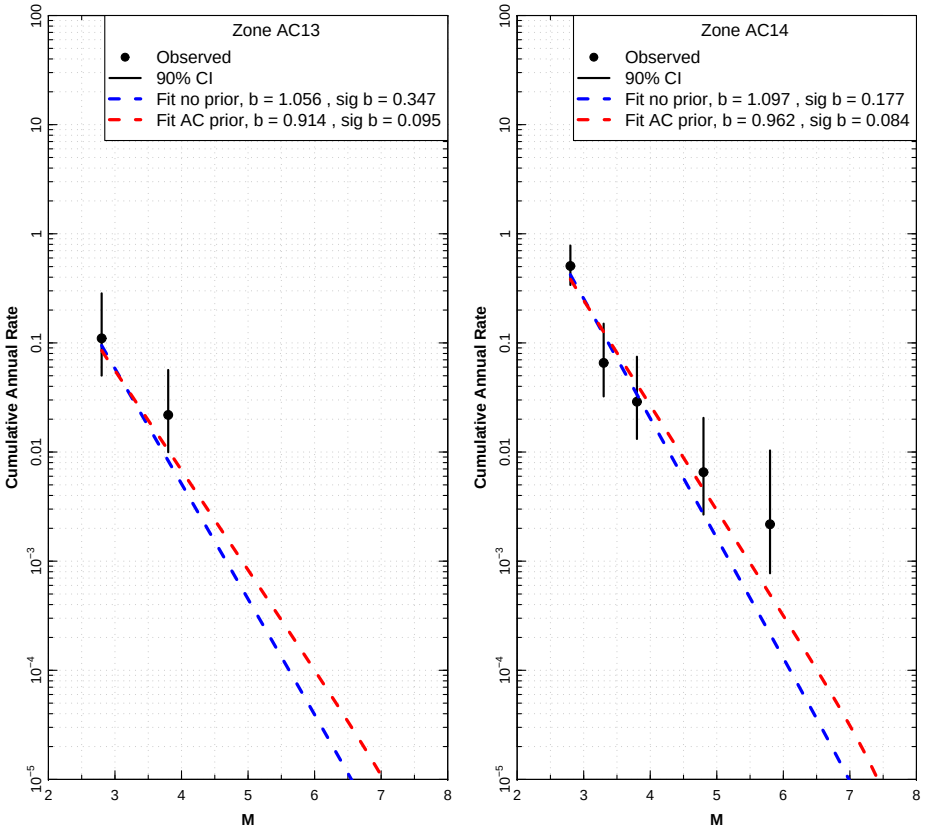

Figure 2.15: Earthquake recurrence relationships for EG1b small zones AC13 and AC14.

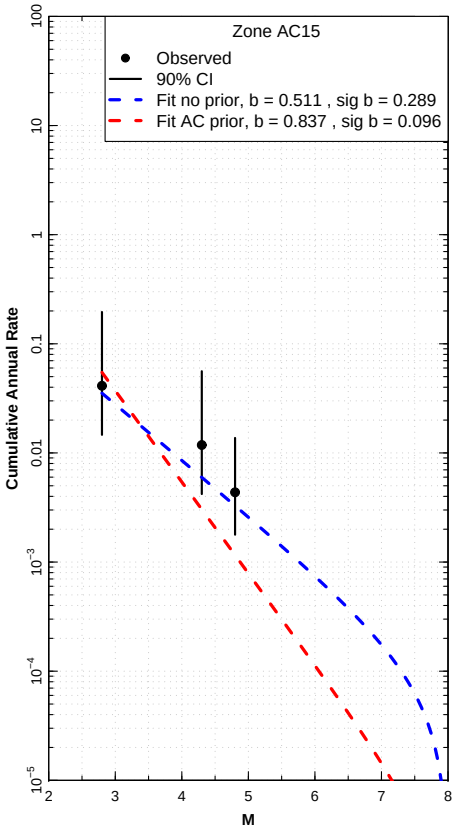

Figure 2.16: Earthquake recurrence relationships for EG1b small zone AC15.

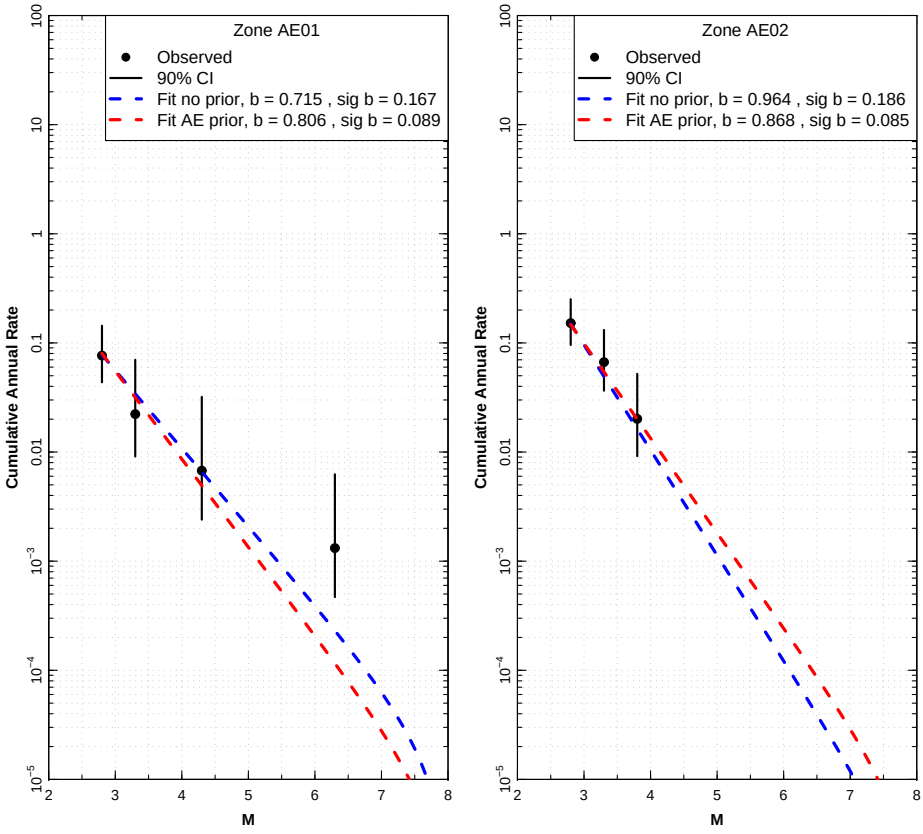

Figure 2.17: Earthquake recurrence relationships for EG1b small zones AE01 and AE02.

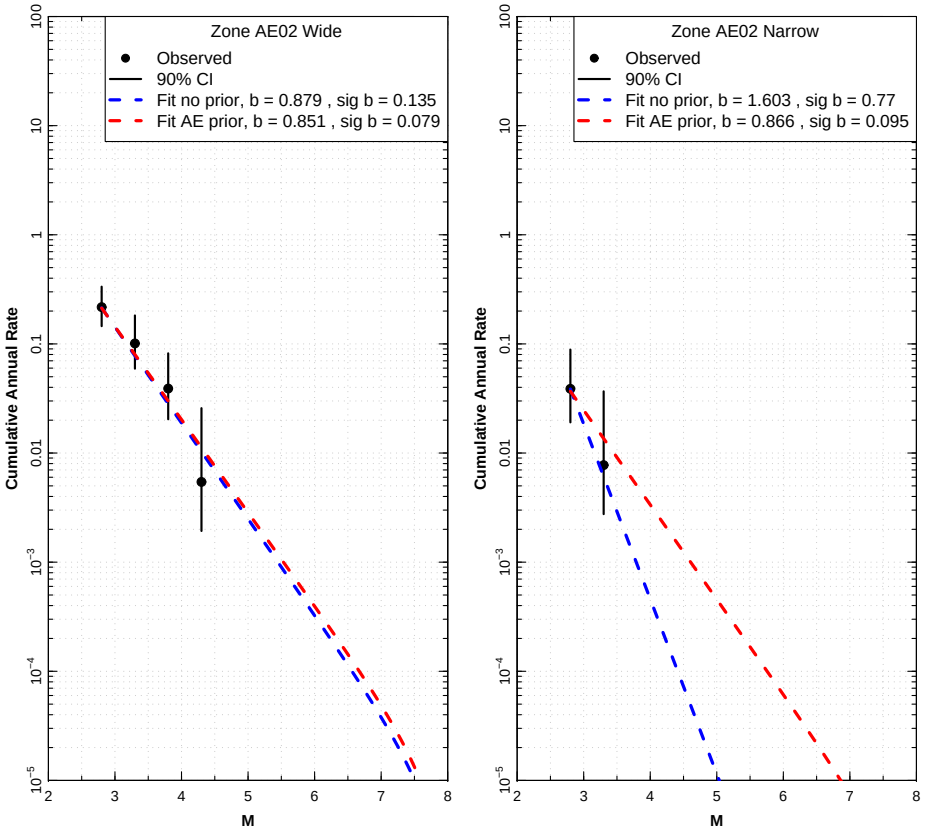

Figure 2.18: Earthquake recurrence relationships for EG1b small zones AE02 Wide and AE02 Narrow.

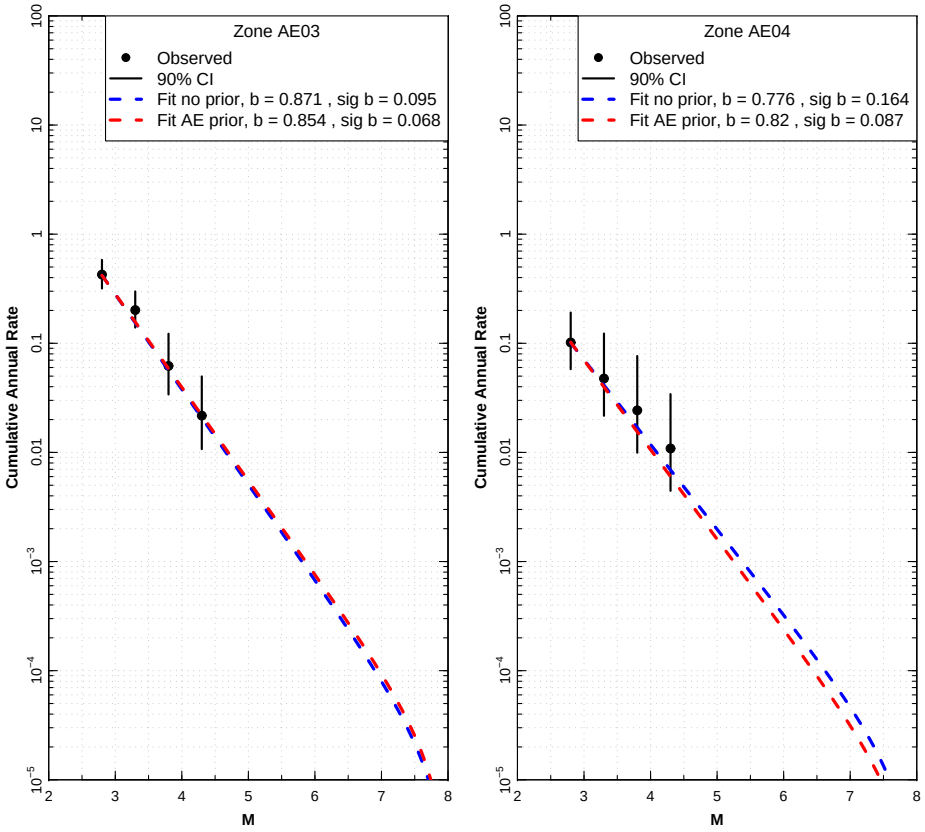

Figure 2.19: Earthquake recurrence relationships for EG1b small zones AE03 and AE04.

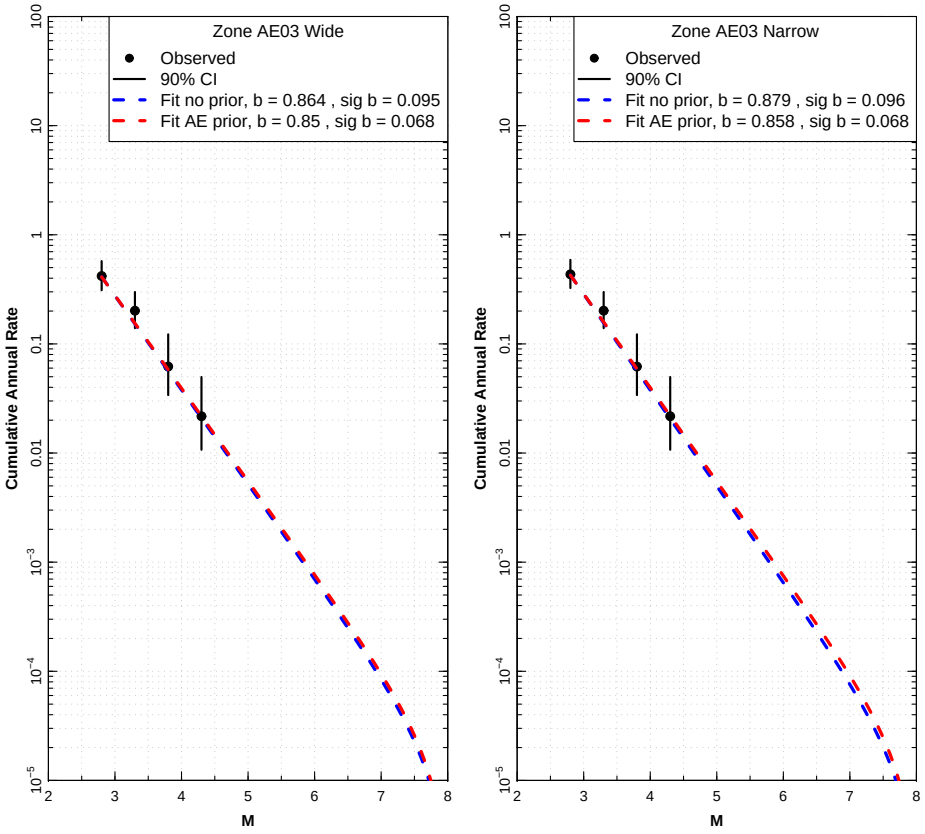

Figure 2.20: Earthquake recurrence relationships for EG1b small zones AE03 Wide and AE03 Narrow.

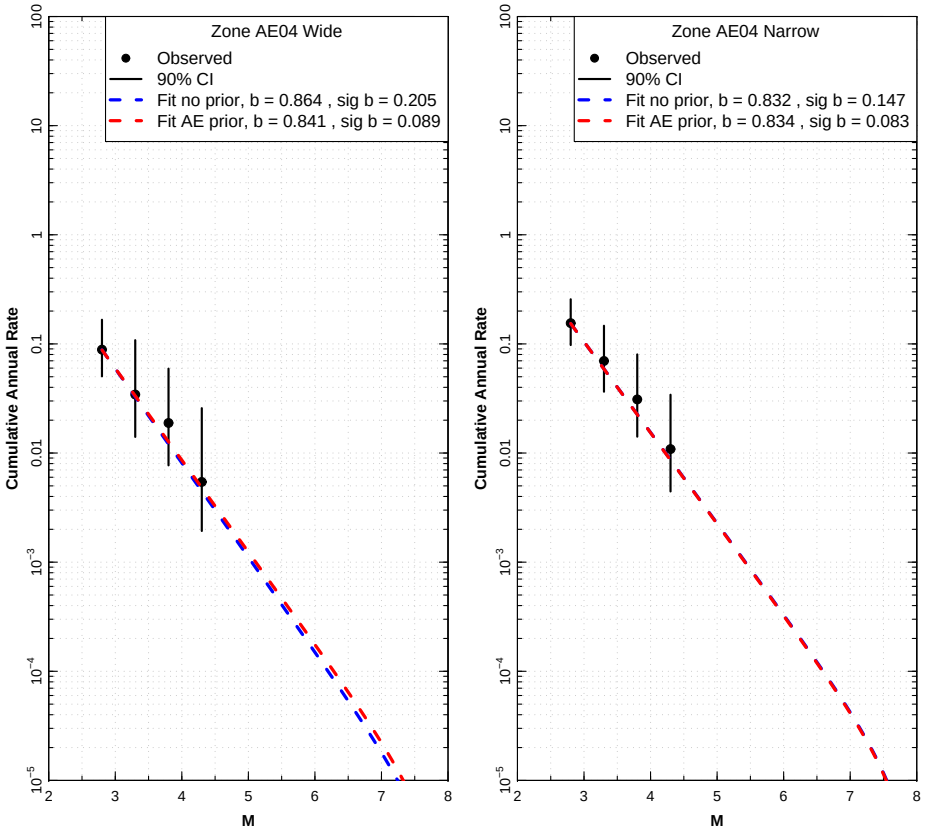

Figure 2.21: Earthquake recurrence relationships for EG1b small zones AE04 Wide and AE04 Narrow.

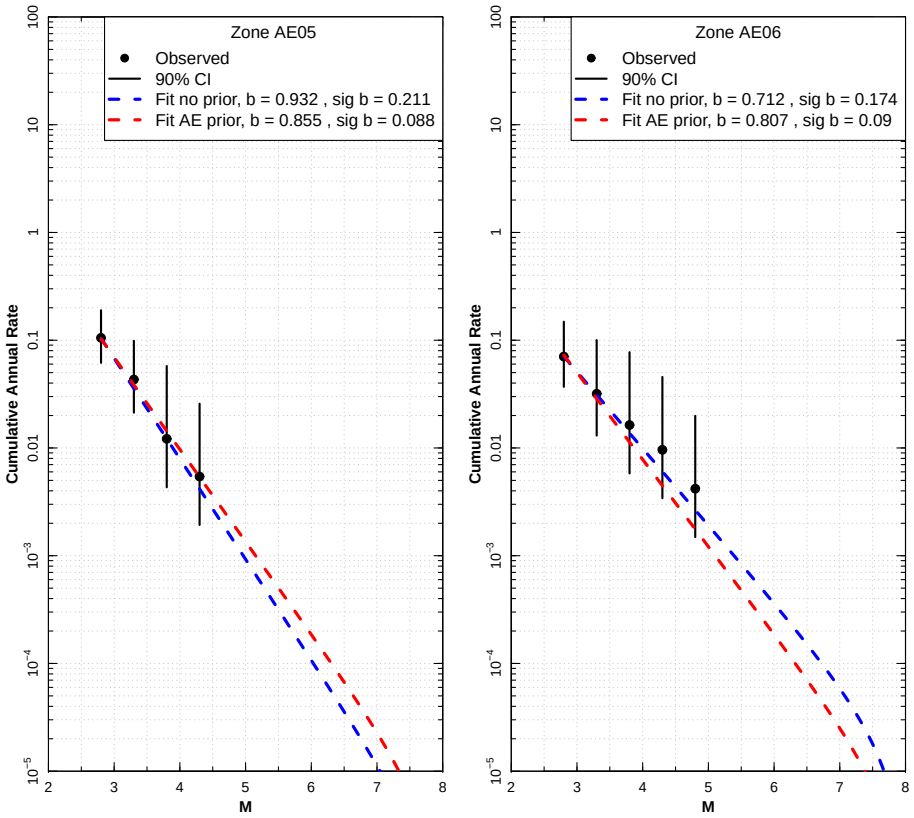

Figure 2.22: Earthquake recurrence relationships for EG1b small zones AE05 and AE06.

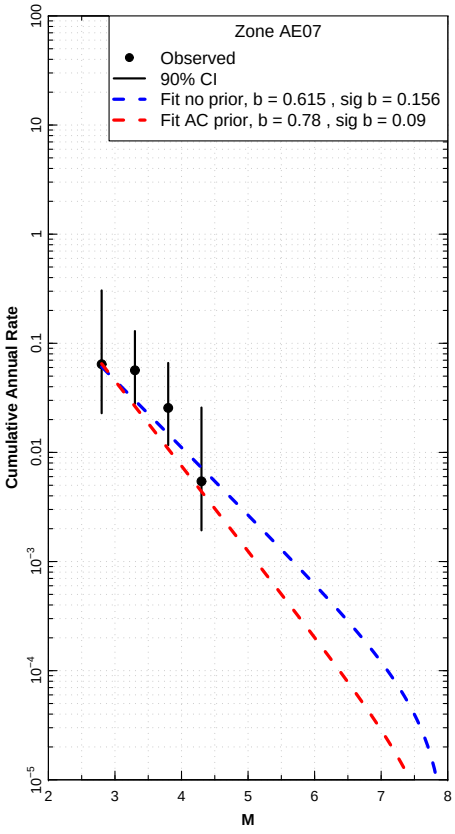

Figure 2.23: Earthquake recurrence relationships for EG1b small zone AE07.

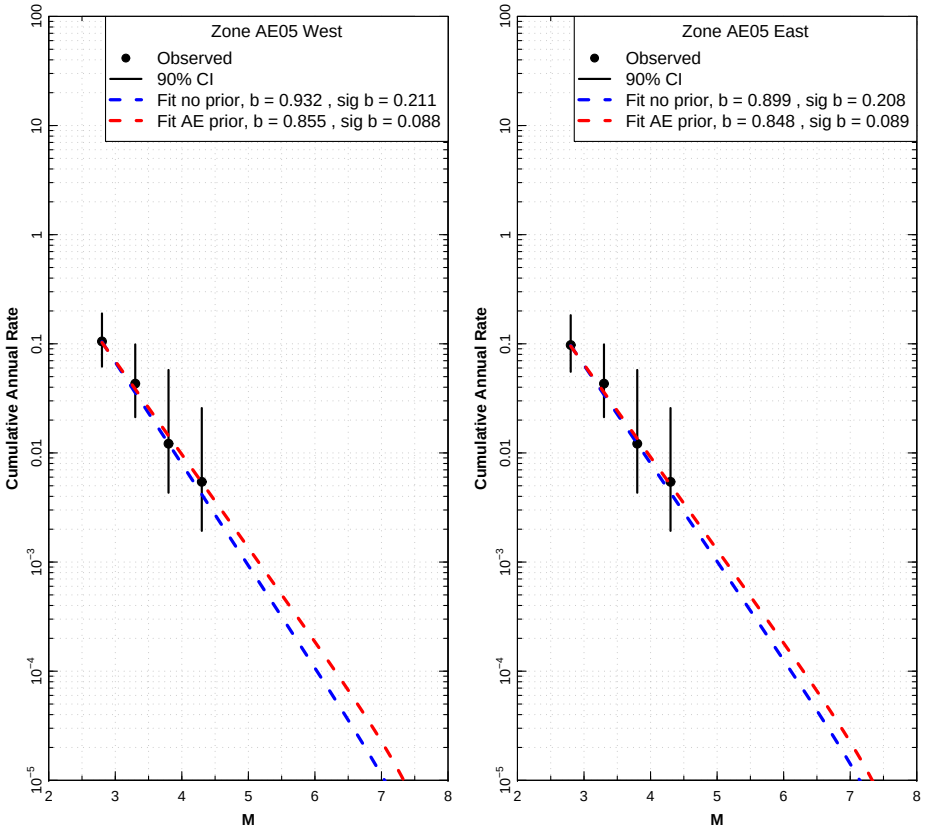

Figure 2.24: Earthquake recurrence relationships for EG1b small zones AE05 West and AE05 East.

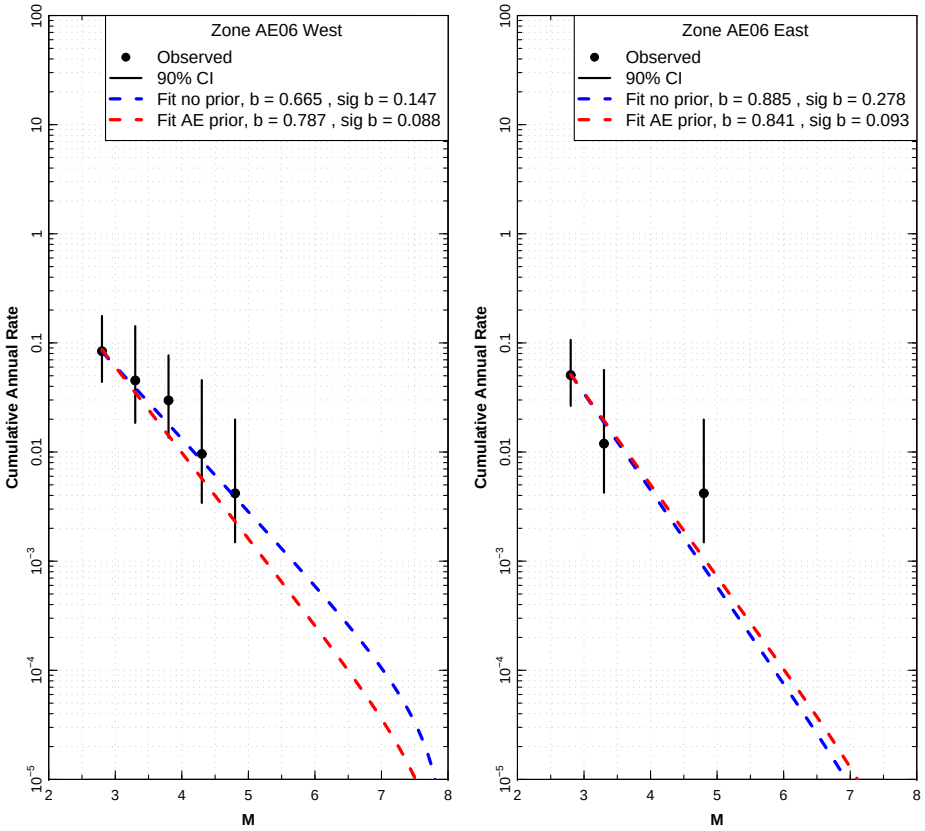

Figure 2.25: Earthquake recurrence relationships for EG1b small zones AE06 West and AE06 East.

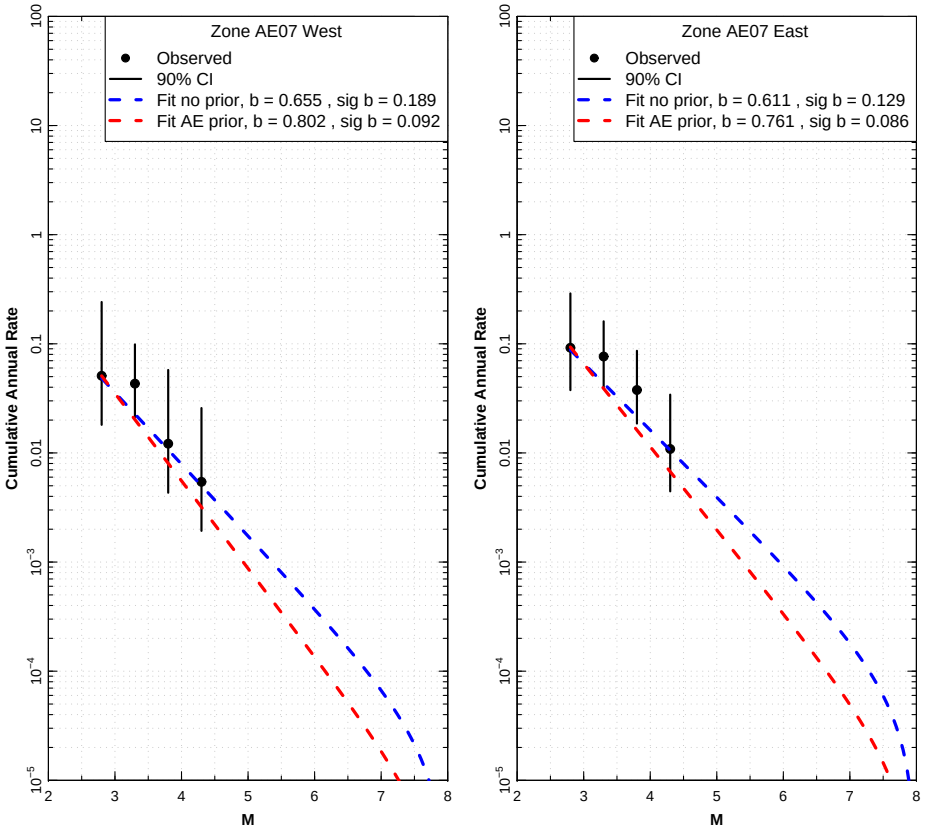

Figure 2.26: Earthquake recurrence relationships for EG1b small zones AE07 West and AE07 East.

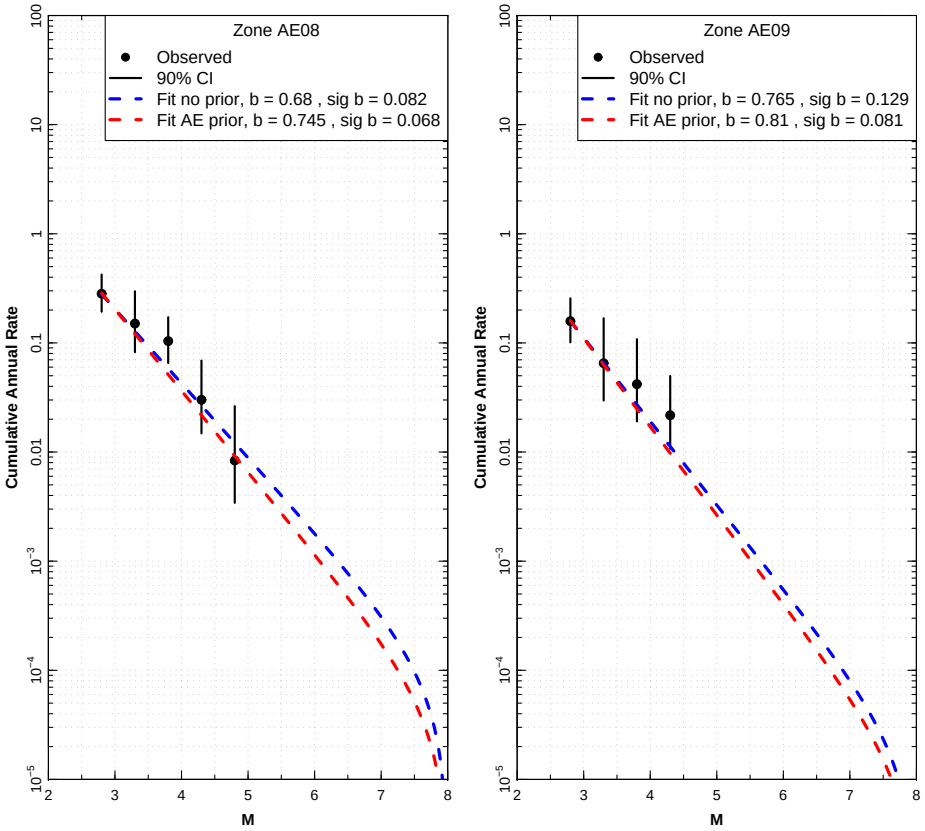

Figure 2.27: Earthquake recurrence relationships for EG1b small zones AE08 and AE09.

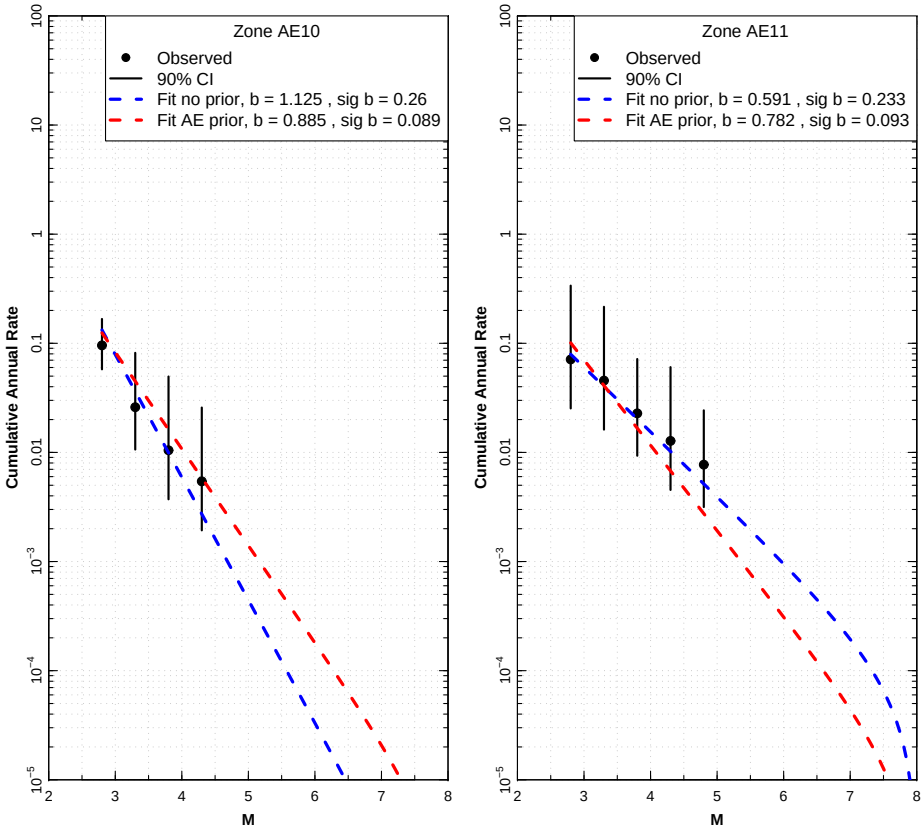

Figure 2.28: Earthquake recurrence relationships for EG1b small zones AE10 and AE11.

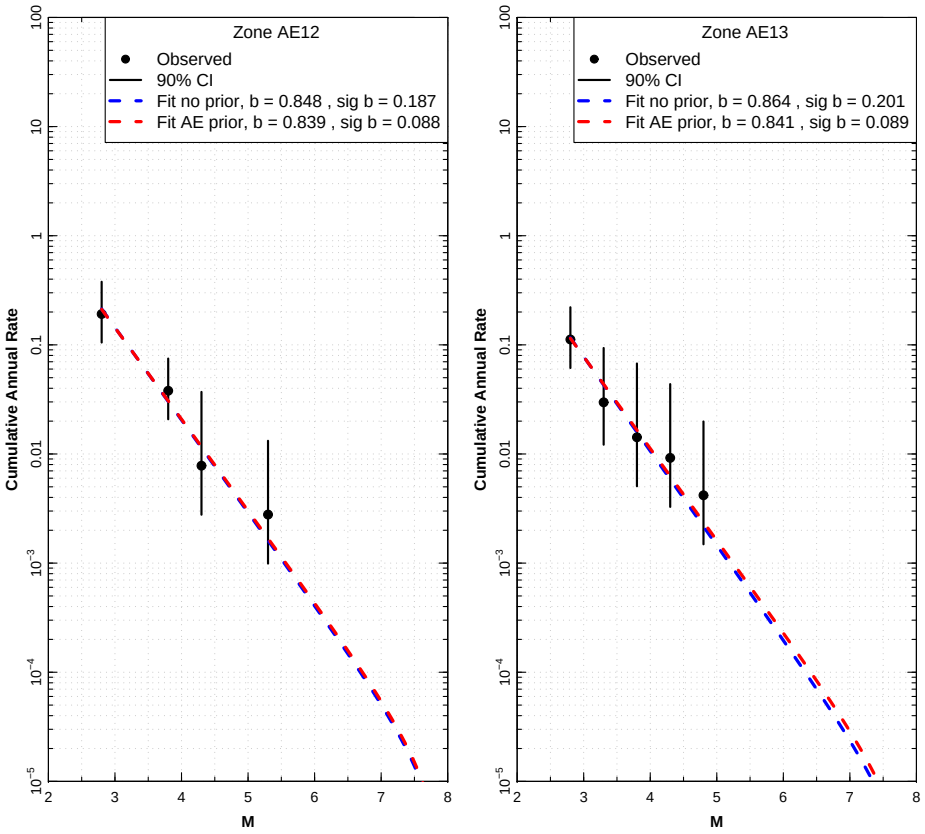

Figure 2.29: Earthquake recurrence relationships for EG1b small zones AE12 and AE13.

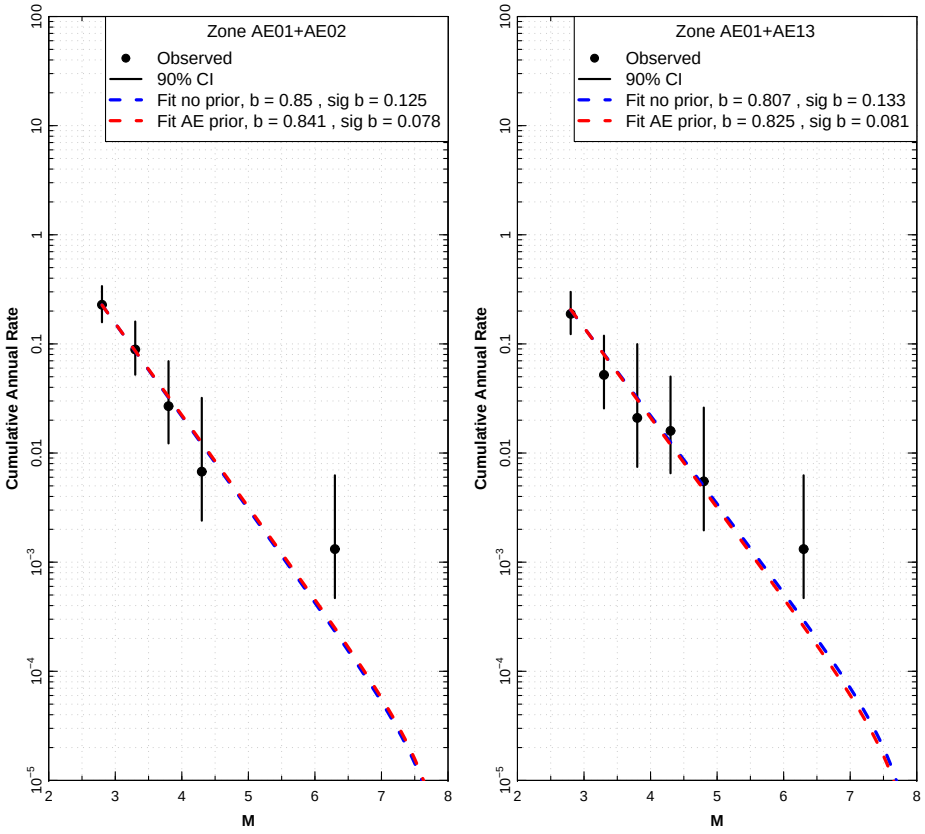

Figure 2.30: Earthquake recurrence relationships for EG1b combined small zones AE01+AE02 and AE01+AE13.

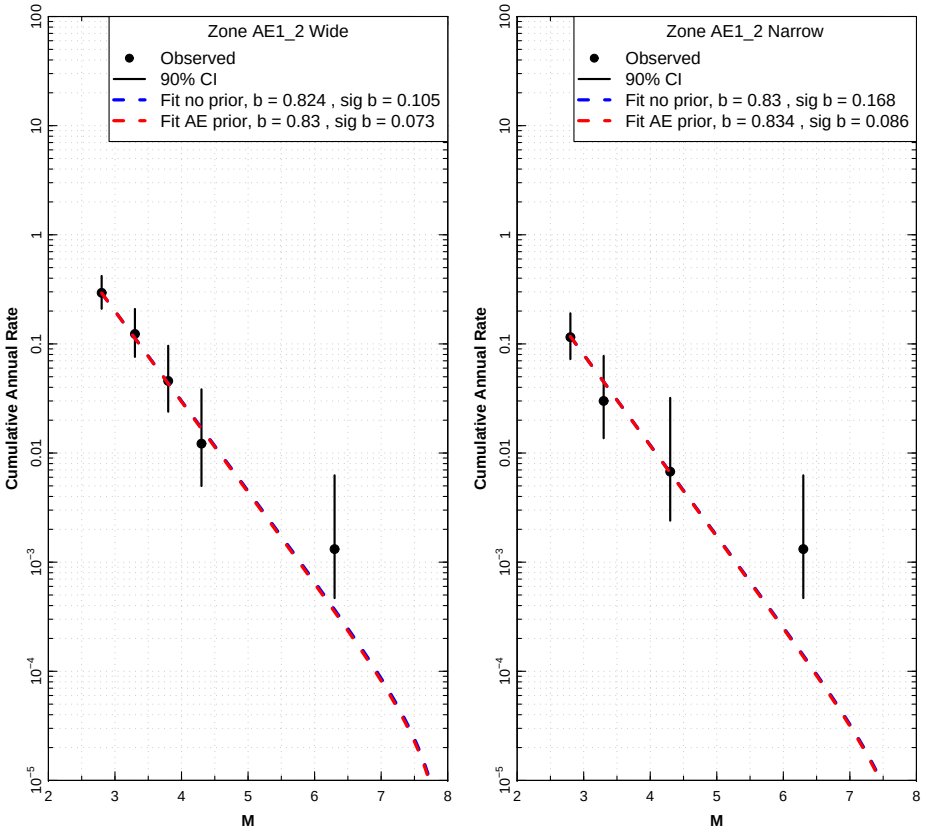

Figure 2.31: Earthquake recurrence relationships for EG1b combined small zones AE01+AE02 Wide and AE01+AE02 Narrow.

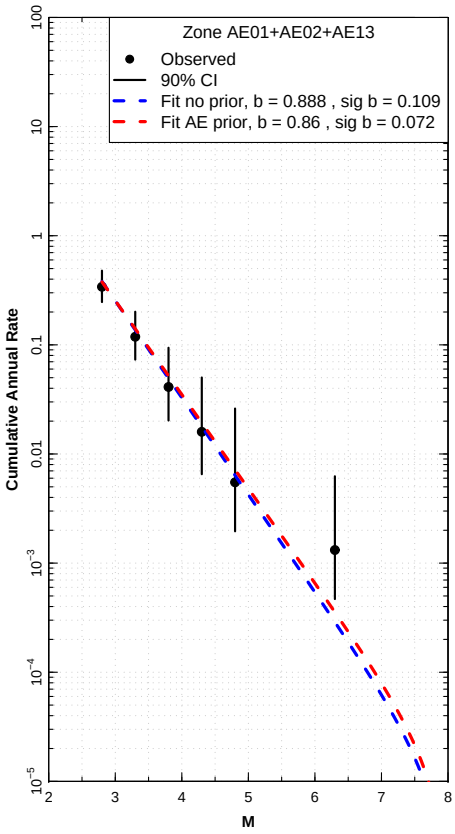

Figure 2.32: Earthquake recurrence relationships for EG1b combined small zone AE01+AE02+AE13.

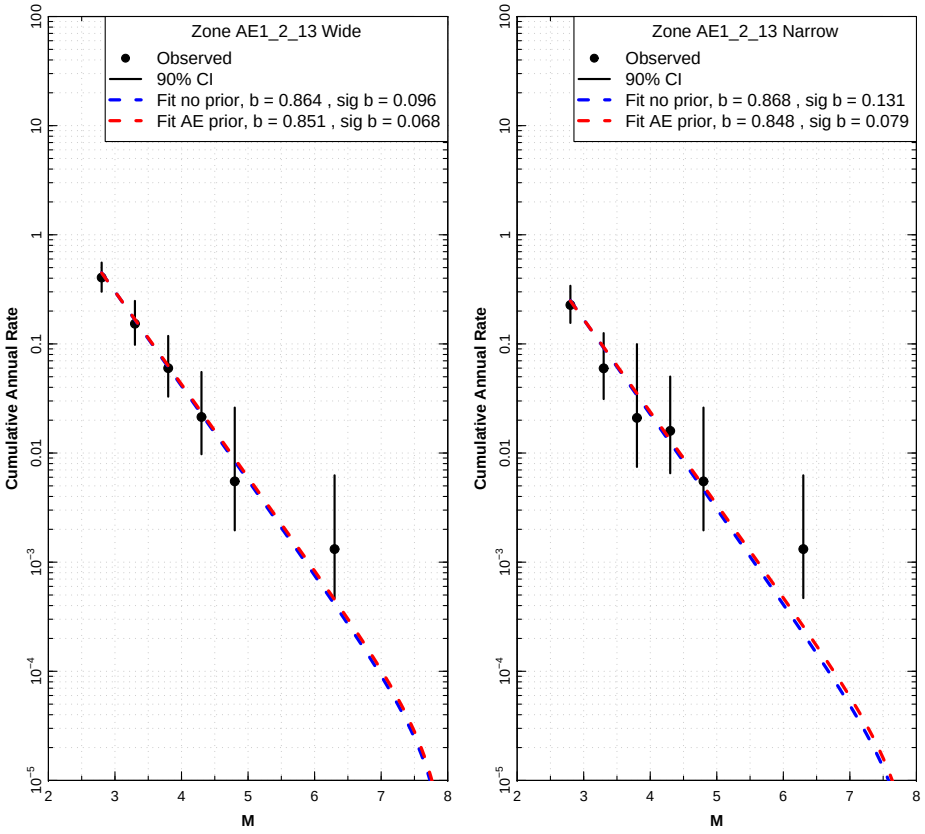

Figure 2.33: Earthquake recurrence relationships for EG1b combined small zones AE01+AE02+AE13 Wide and AE01+AE02+AE13 Narrow.

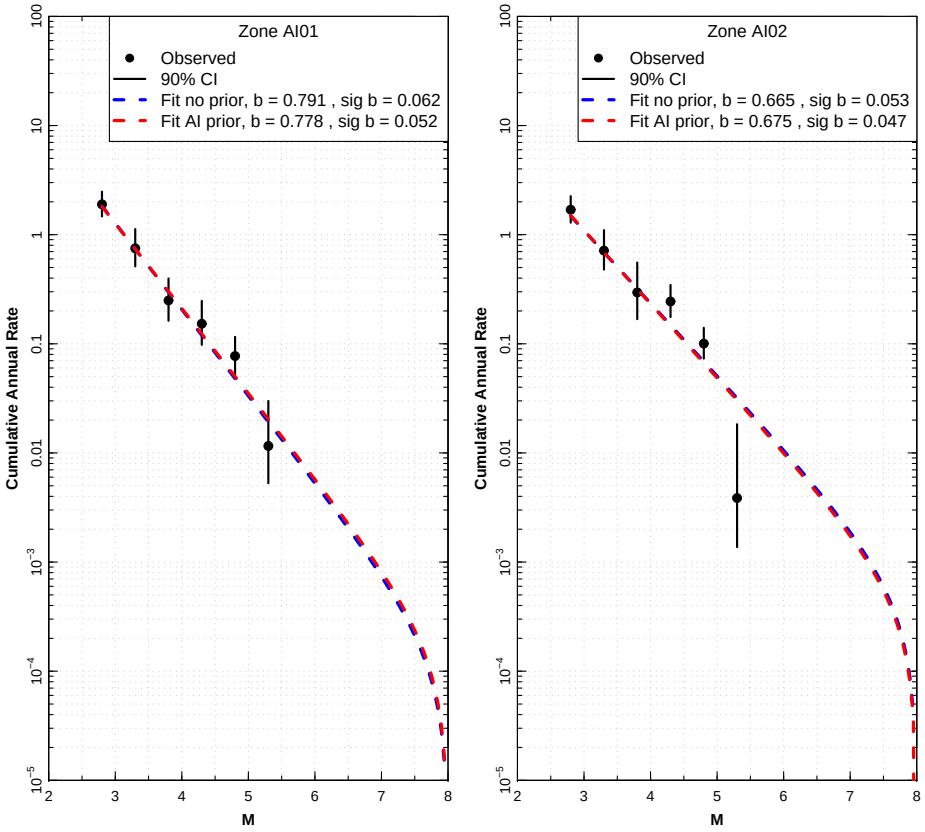

Figure 2.34: Earthquake recurrence relationships for EG1b small zones AI01 and AI02.

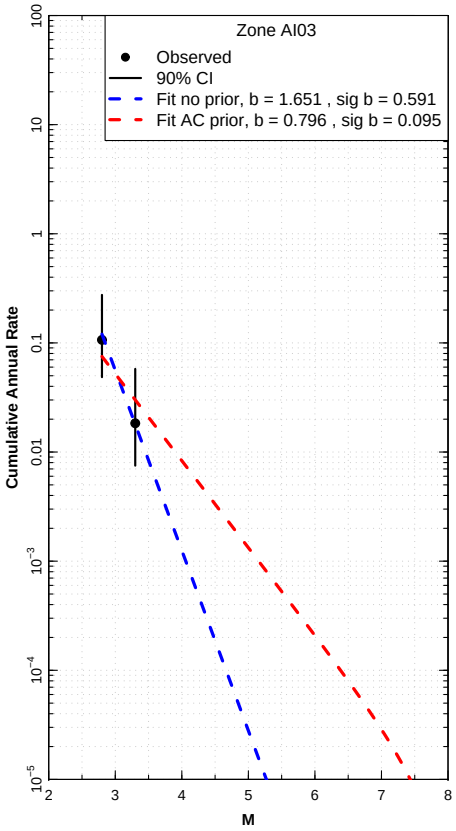

Figure 2.35: Earthquake recurrence relationships for EG1b small zone AI03.

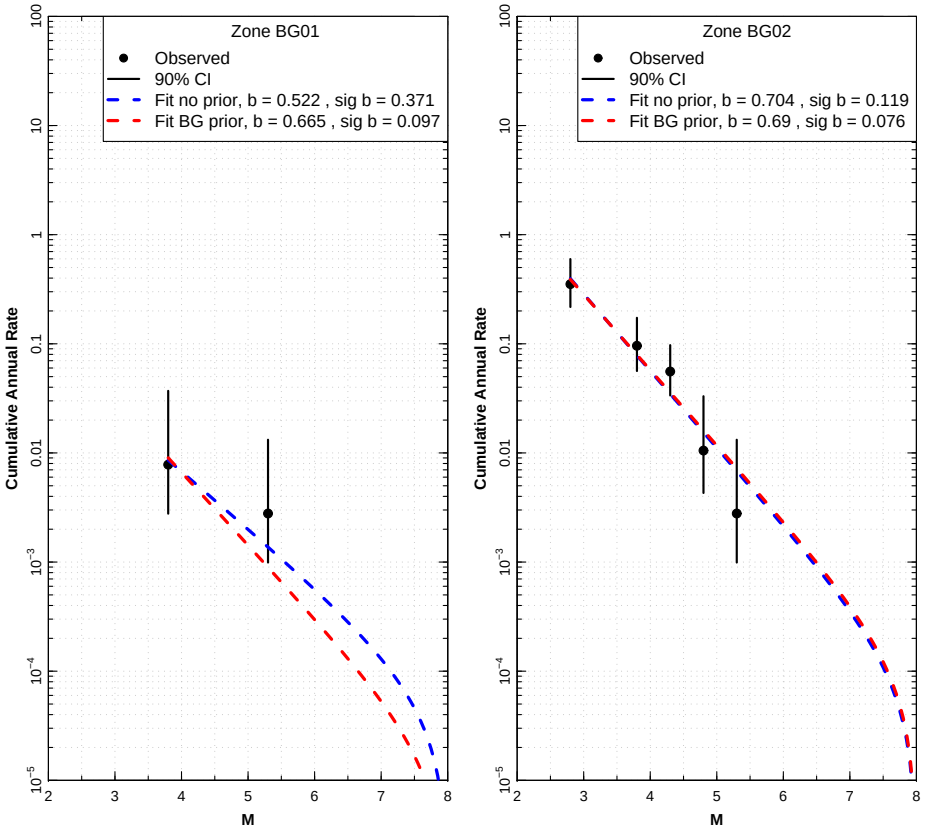

Figure 2.36: Earthquake recurrence relationships for EG1b small zones BG01 and BG02.

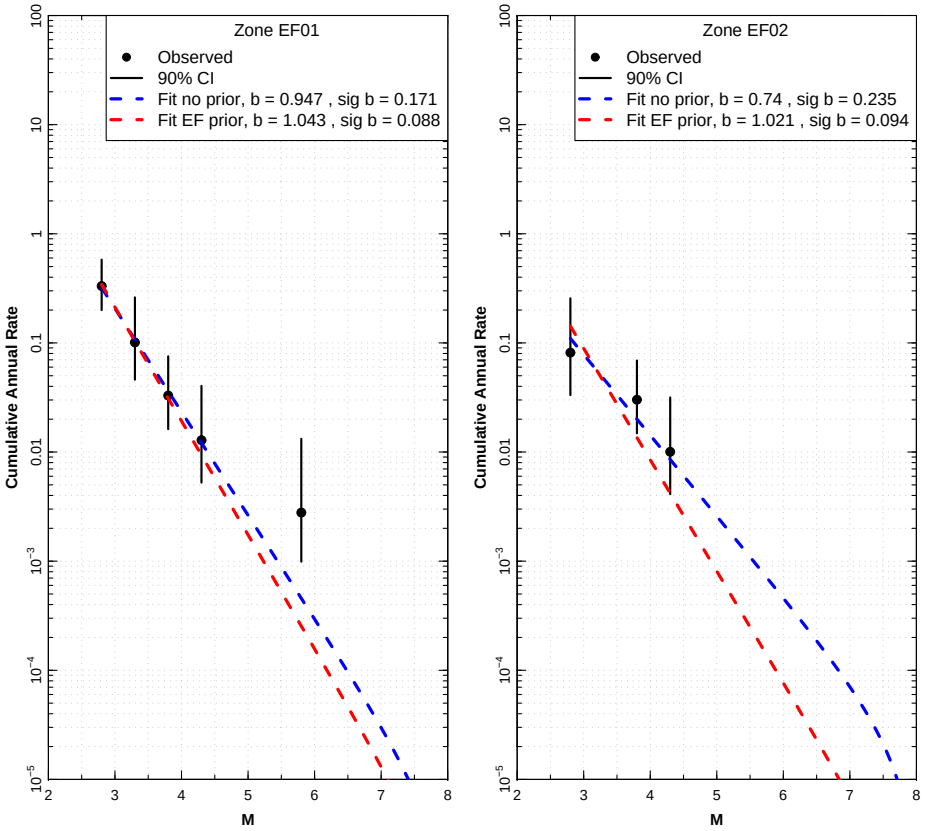

Figure 2.37: Earthquake recurrence relationships for EG1b small zones EF01 and EF02.

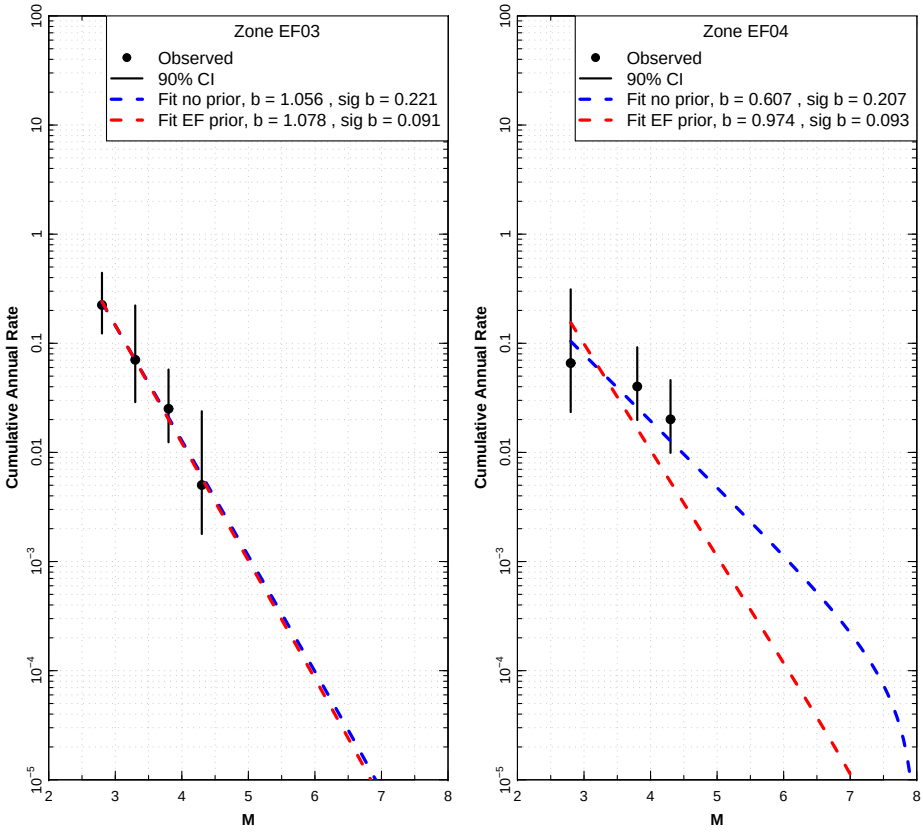

Figure 2.38: Earthquake recurrence relationships for EG1b small zones EF03 and EF04.

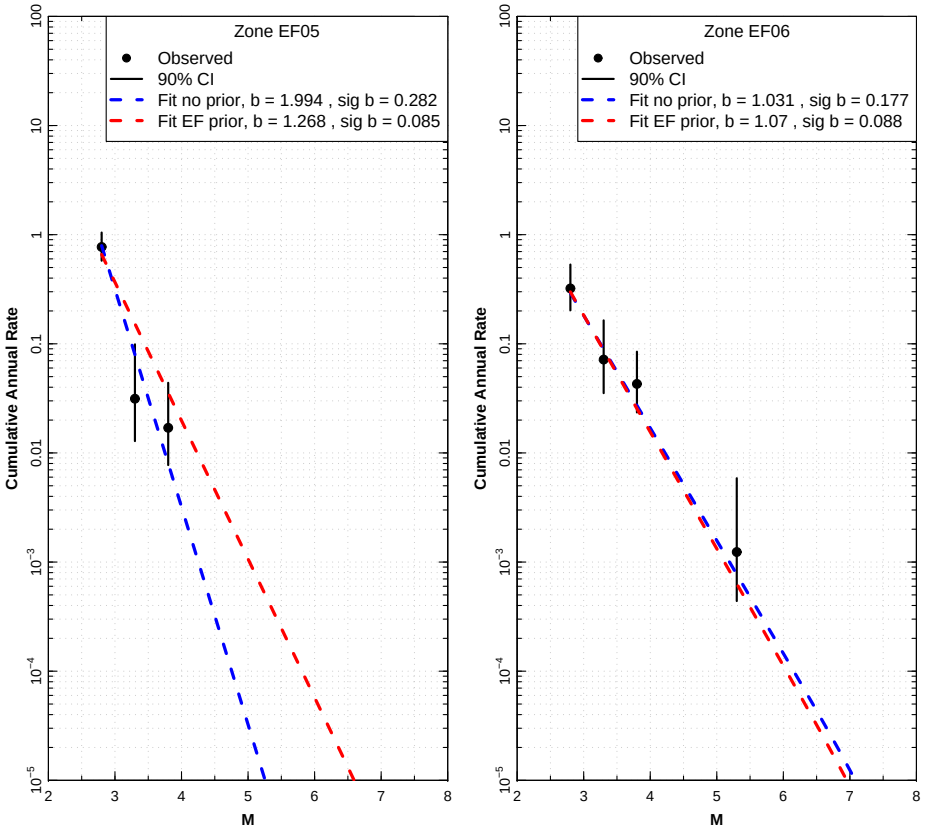

Figure 2.39: Earthquake recurrence relationships for EG1b small zones EF05 and EF06.

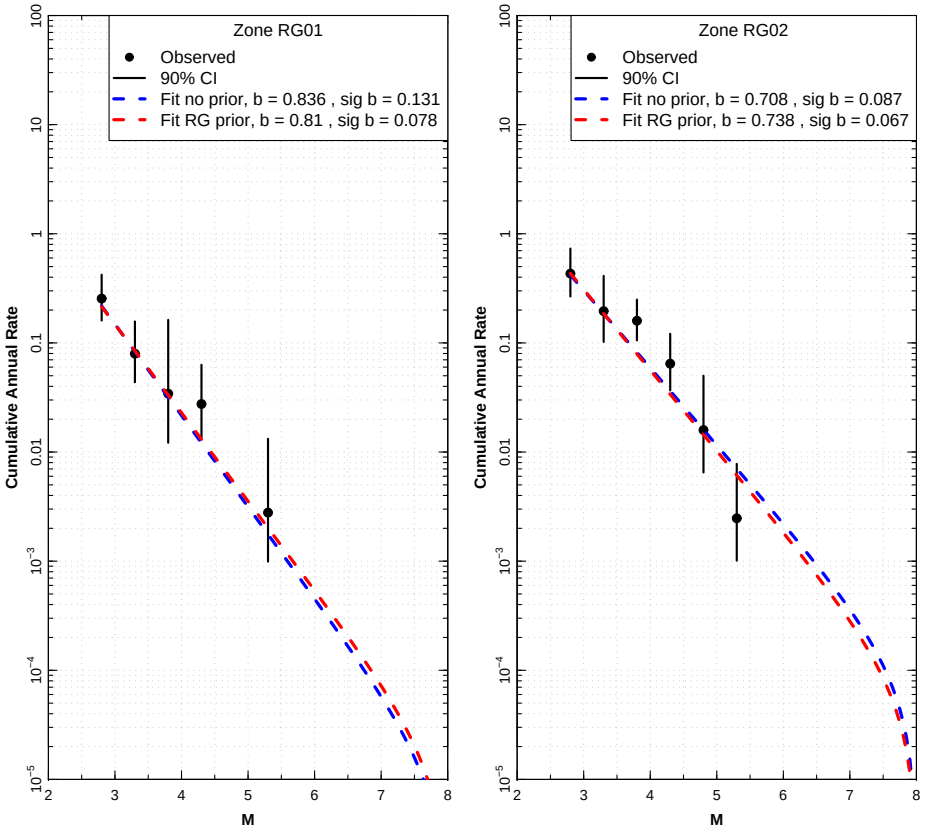

Figure 2.40: Earthquake recurrence relationships for EG1b small zones RG01 and RG02.

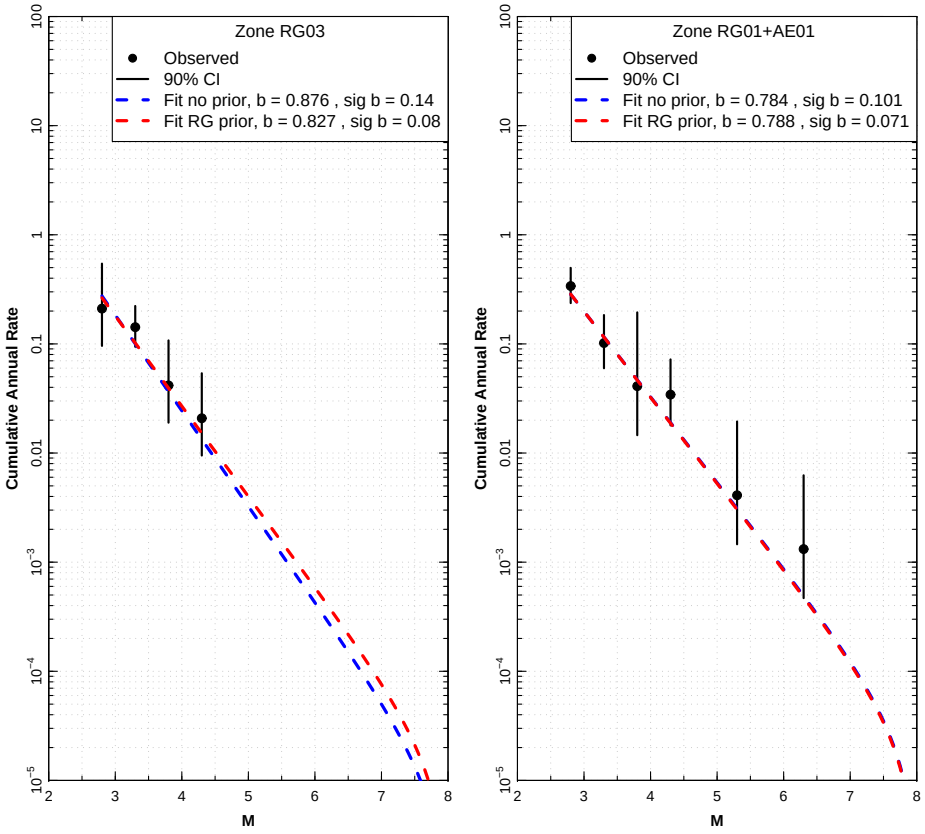

Figure 2.41: Earthquake recurrence relationships for EG1b small zone RG013 and combined small zone RG01+AE01.

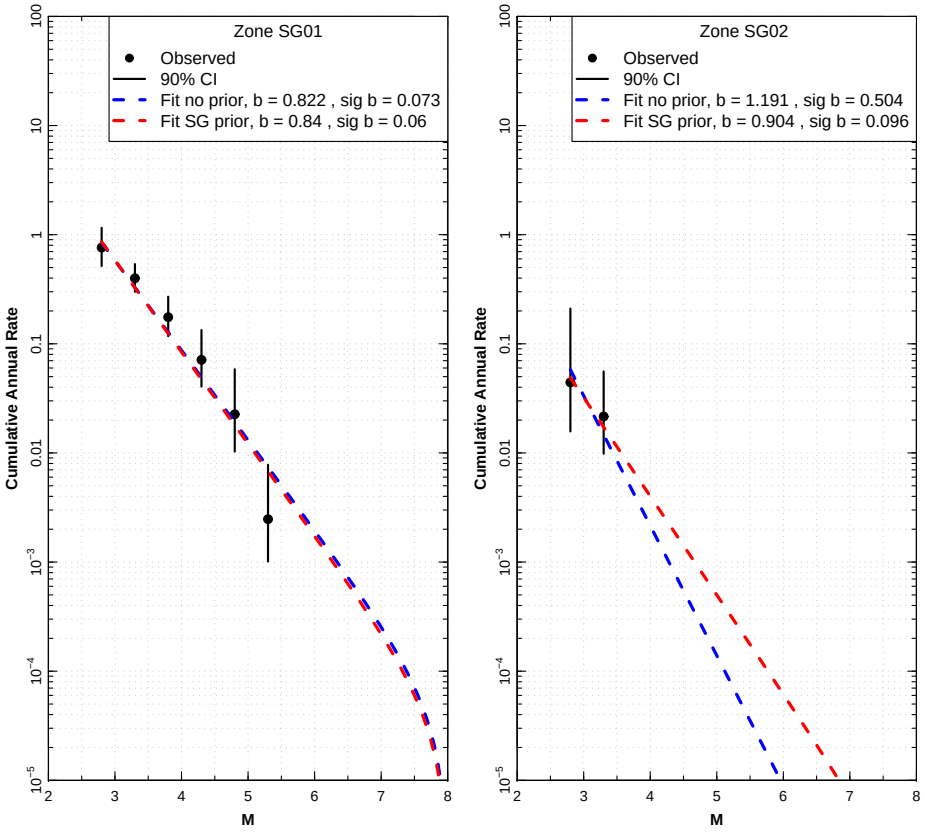

Figure 2.42: Earthquake recurrence relationships for EG1b small zones SG01 and SG02.

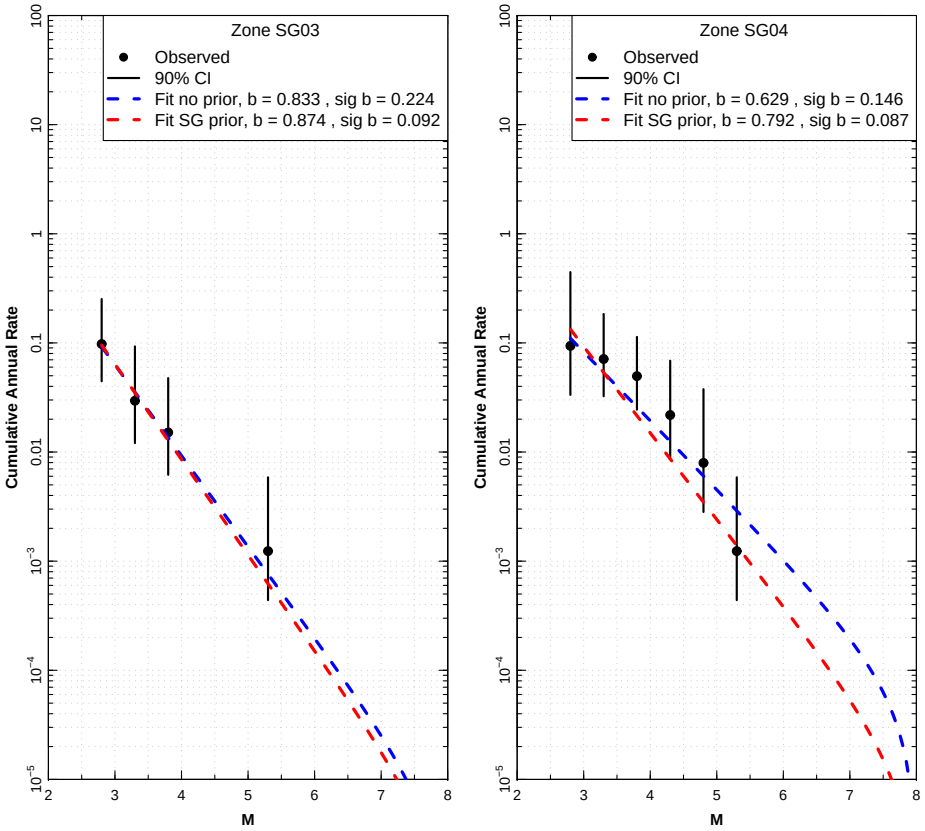

Figure 2.43: Earthquake recurrence relationships for EG1b small zones SG03 and SG04.

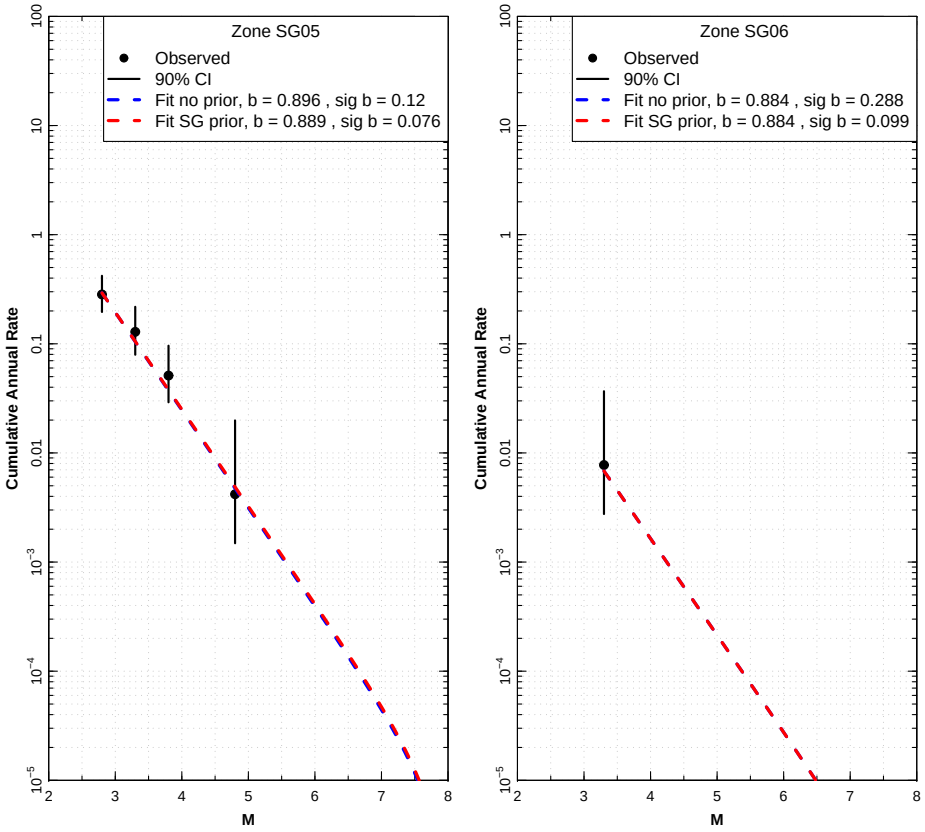

Figure 2.44: Earthquake recurrence relationships for EG1b small zones SG05 and SG06.

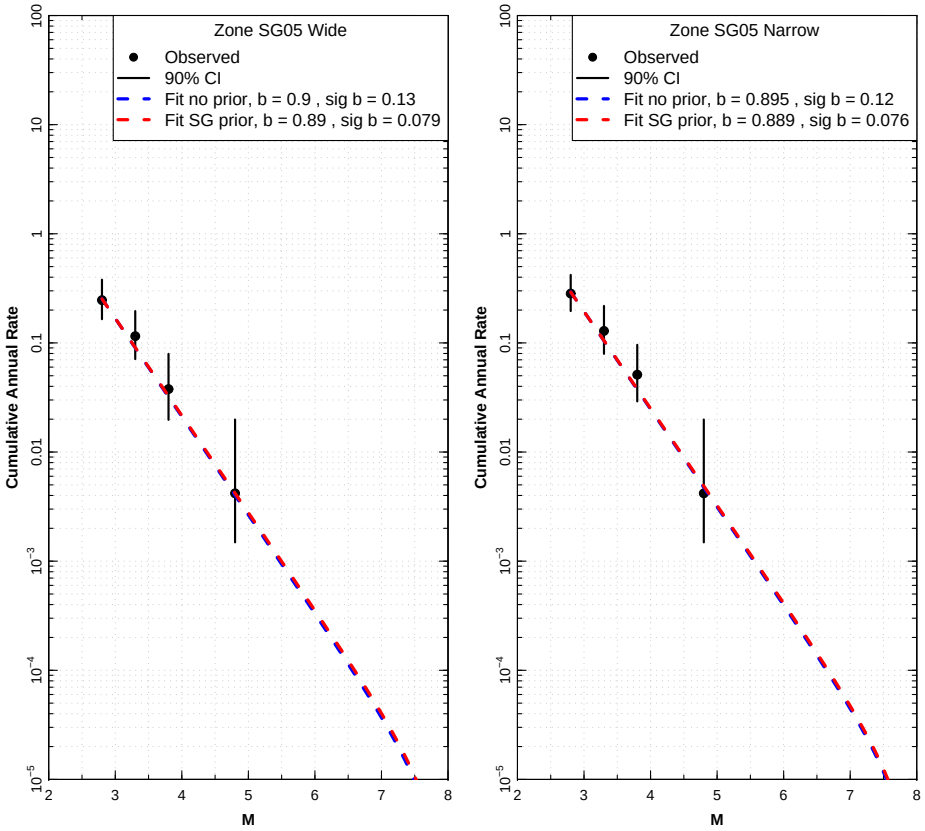

Figure 2.45: Earthquake recurrence relationships for EG1b small zones SG05 Wide and SG05 narrow.

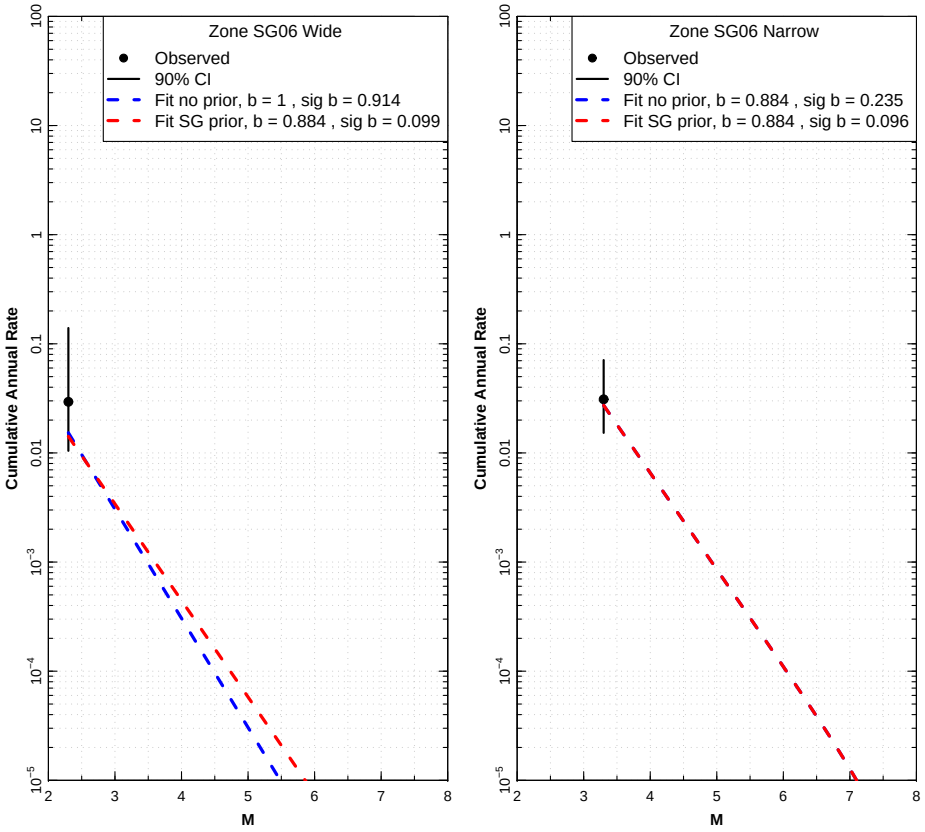

Figure 2.46: Earthquake recurrence relationships for EG1b small zones SG06 Wide and SG06 Narrow.

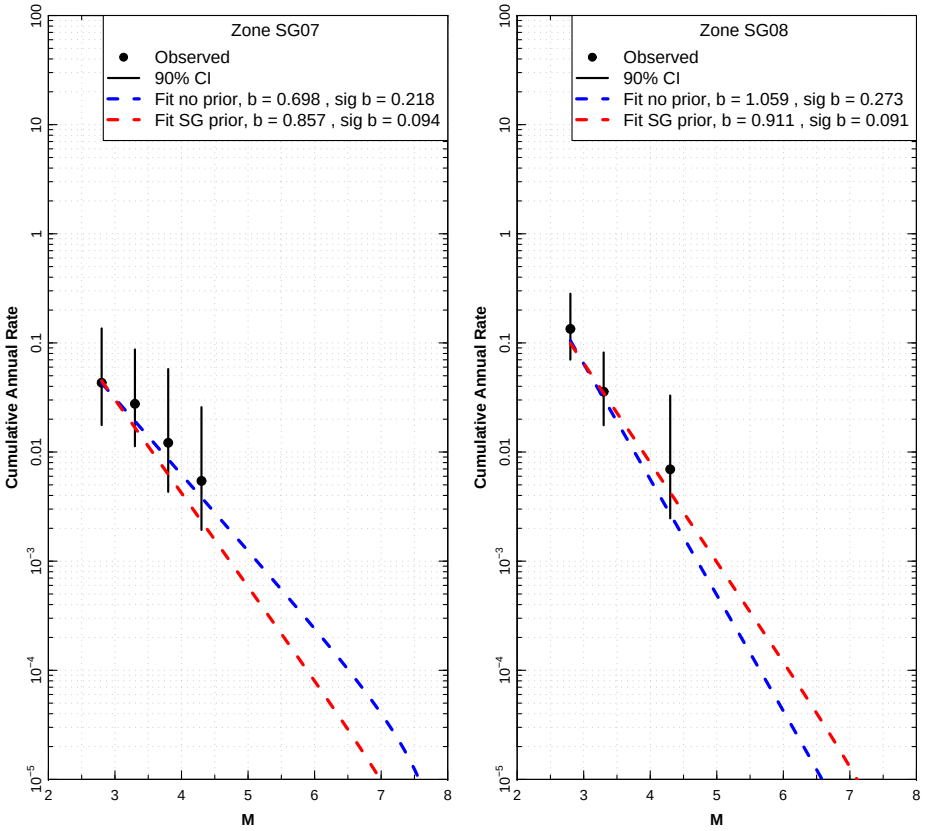

Figure 2.47: Earthquake recurrence relationships for EG1b small zones SG07 and SG08.

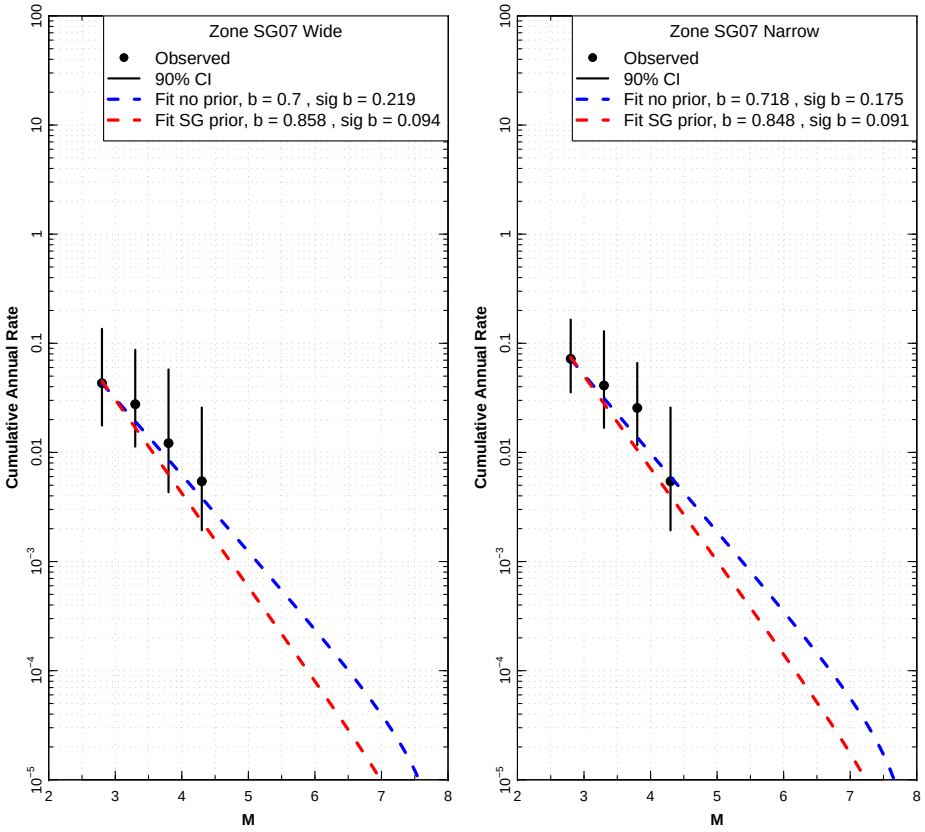

Figure 2.48: Earthquake recurrence relationships for EG1b small zones SG07 Wide and SG07 Narrow.

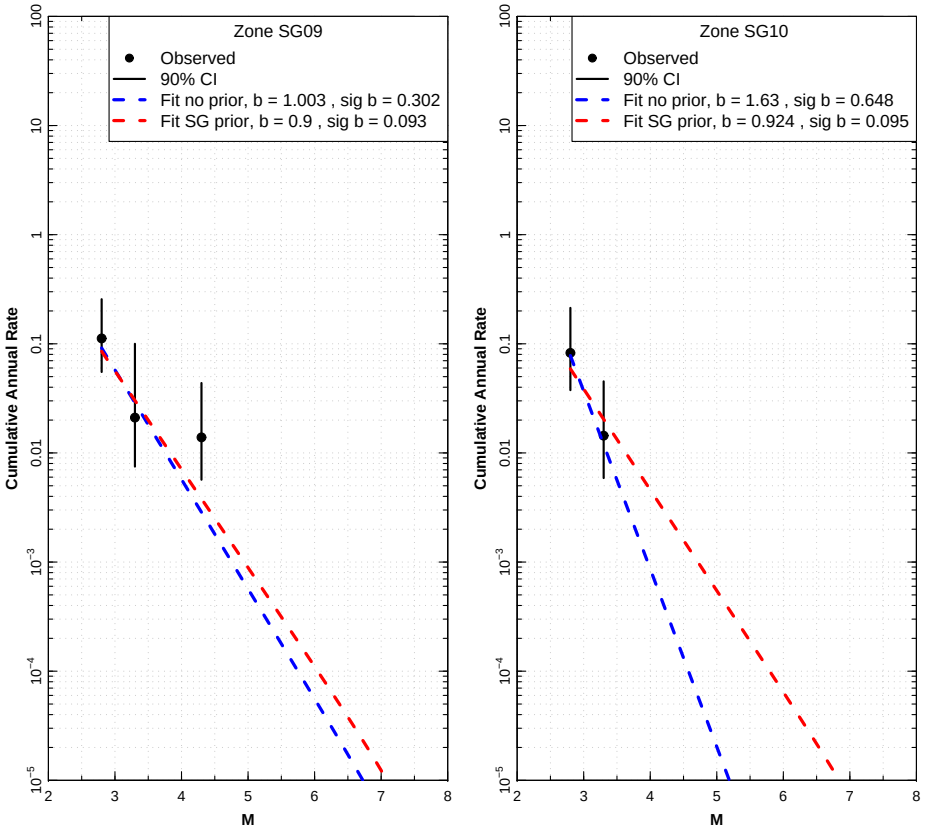

Figure 2.49: Earthquake recurrence relationships for EG1b small zones SG09 and SG10.

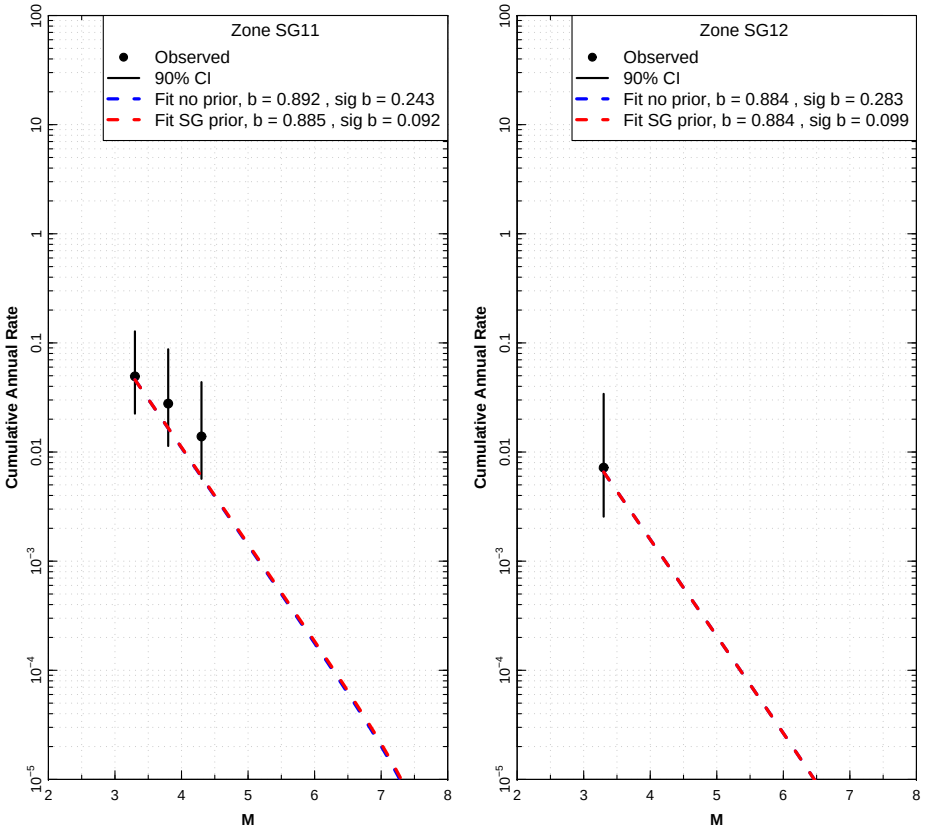

Figure 2.50: Earthquake recurrence relationships for EG1b small zones SG11 and SG12.

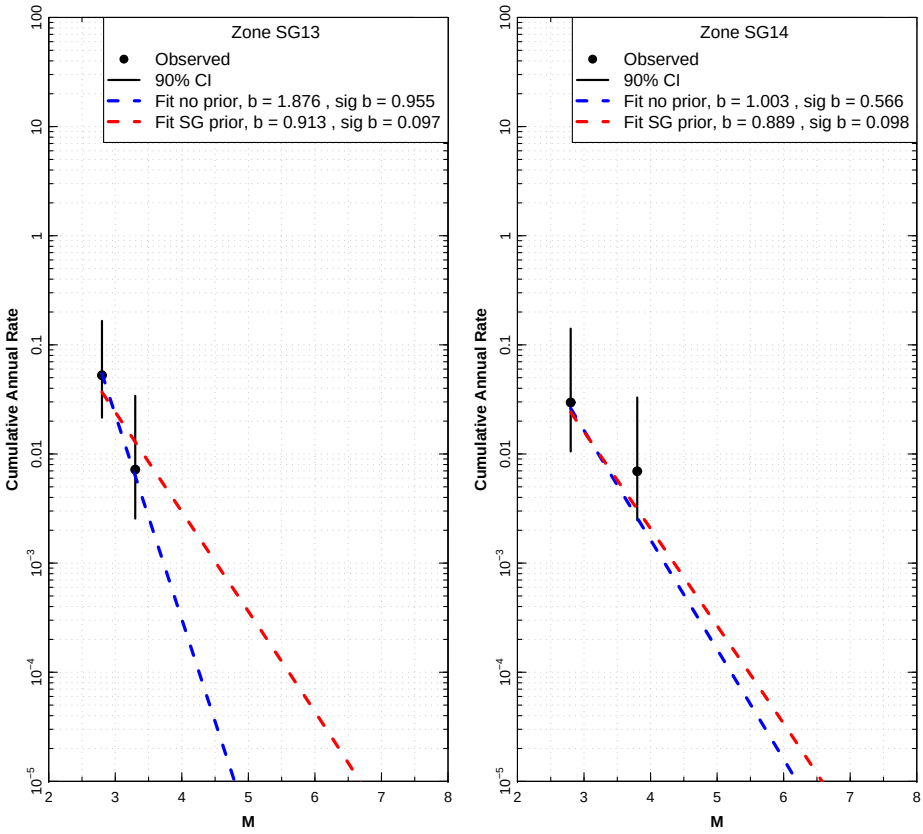

Figure 2.51: Earthquake recurrence relationships for EG1b small zones SG13 and SG14.

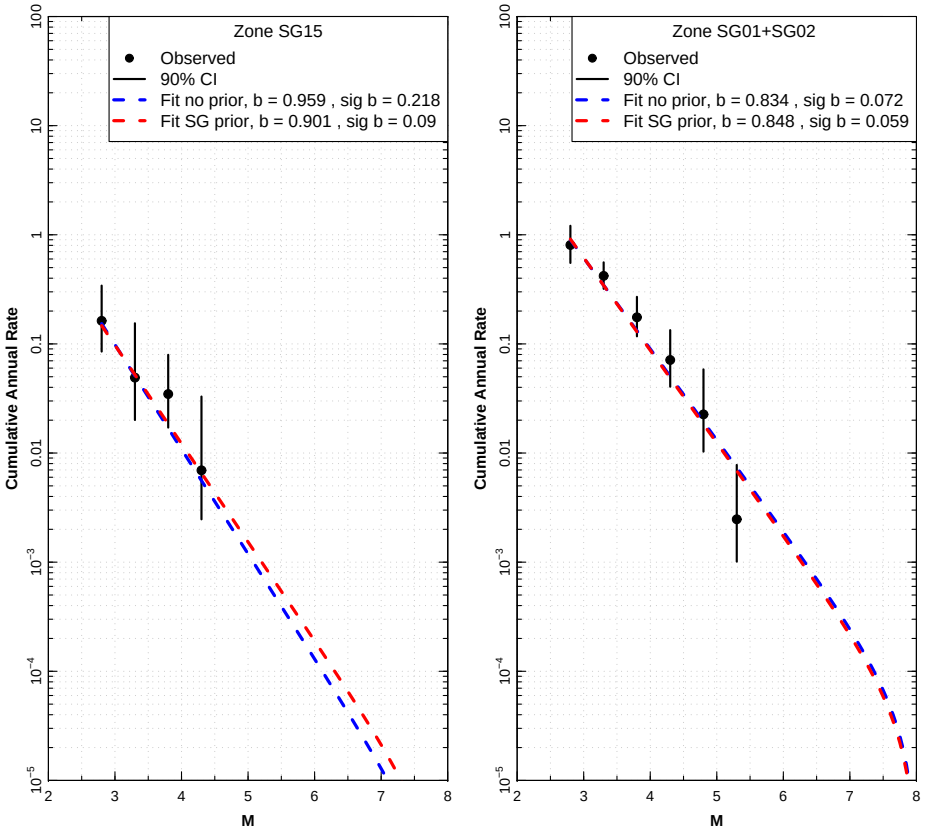

Figure 2.52: Earthquake recurrence relationships for EG1b small zone SG15 and combined small zone SG01+SG02.

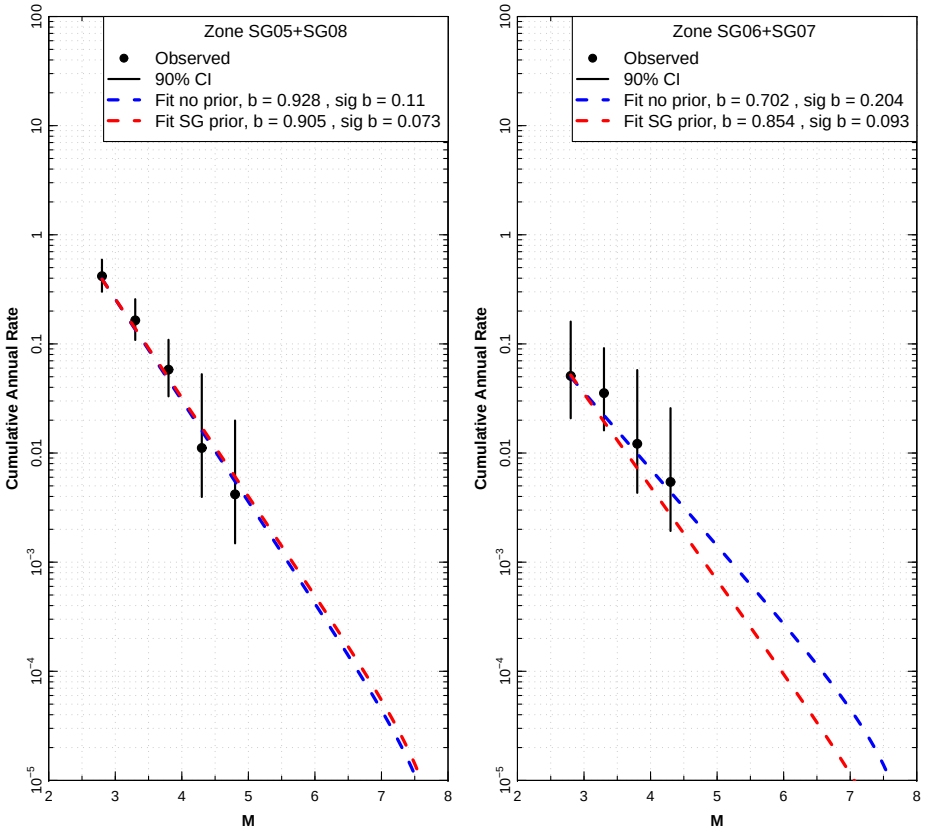

Figure 2.53: Earthquake recurrence relationships for EG1b combined small zones SG05+SG08 and SG06+SG07.

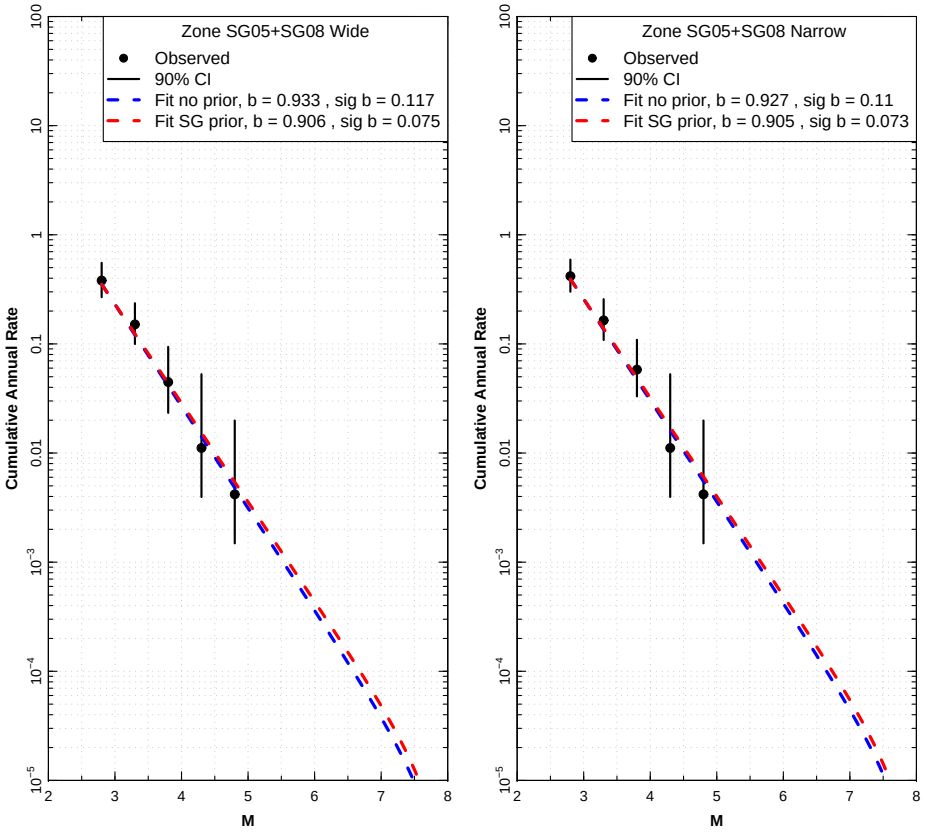

Figure 2.54: Earthquake recurrence relationships for EG1b combined small zones SG05+SG08 Wide and SG05+SG08 Narrow.

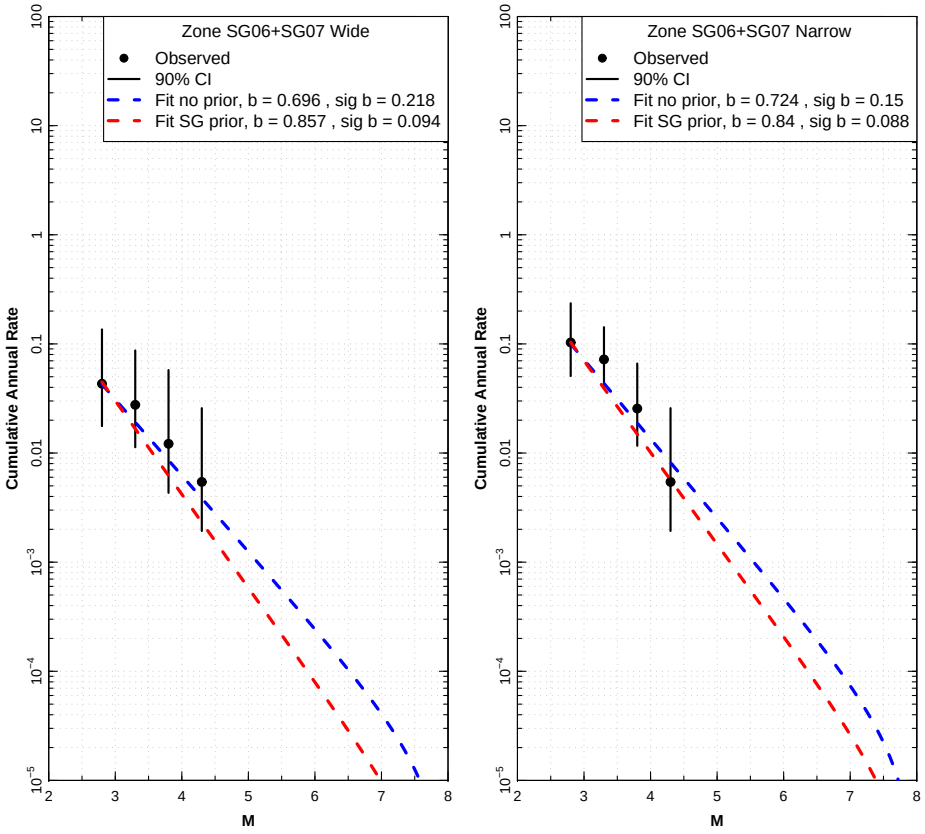

Figure 2.55: Earthquake recurrence relationships for EG1b combined small zones SG06+SG07 Wide and SG06+SG07 Narrow.

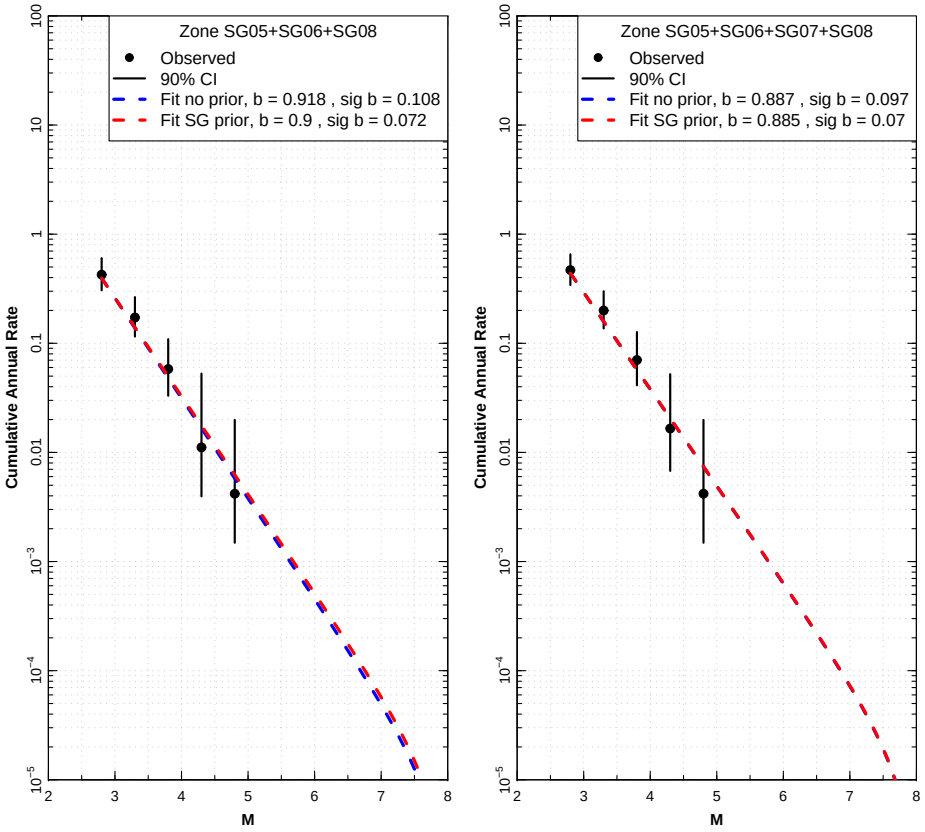

Figure 2.56: Earthquake recurrence relationships for EG1b combined small zones SG05+SG06+SG08 and SG05+SG06+SG07+SG08.

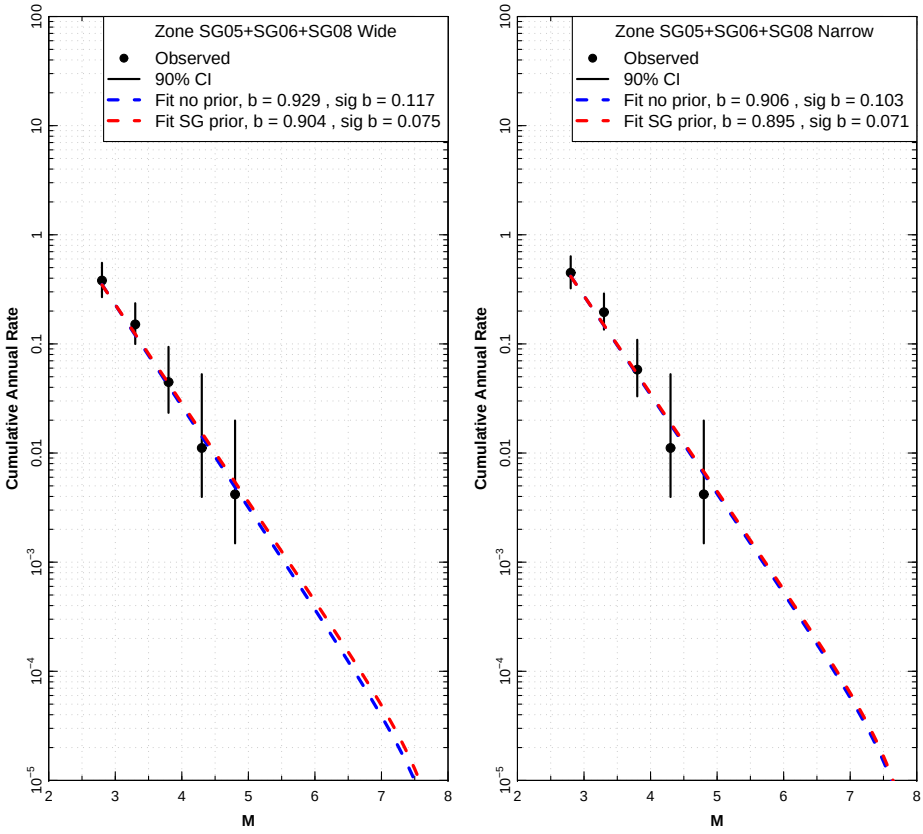

Figure 2.57: Earthquake recurrence relationships for EG1b combined small zones SG05+SG06+SG08 Wide and SG05+SG06+SG08 Narrow.

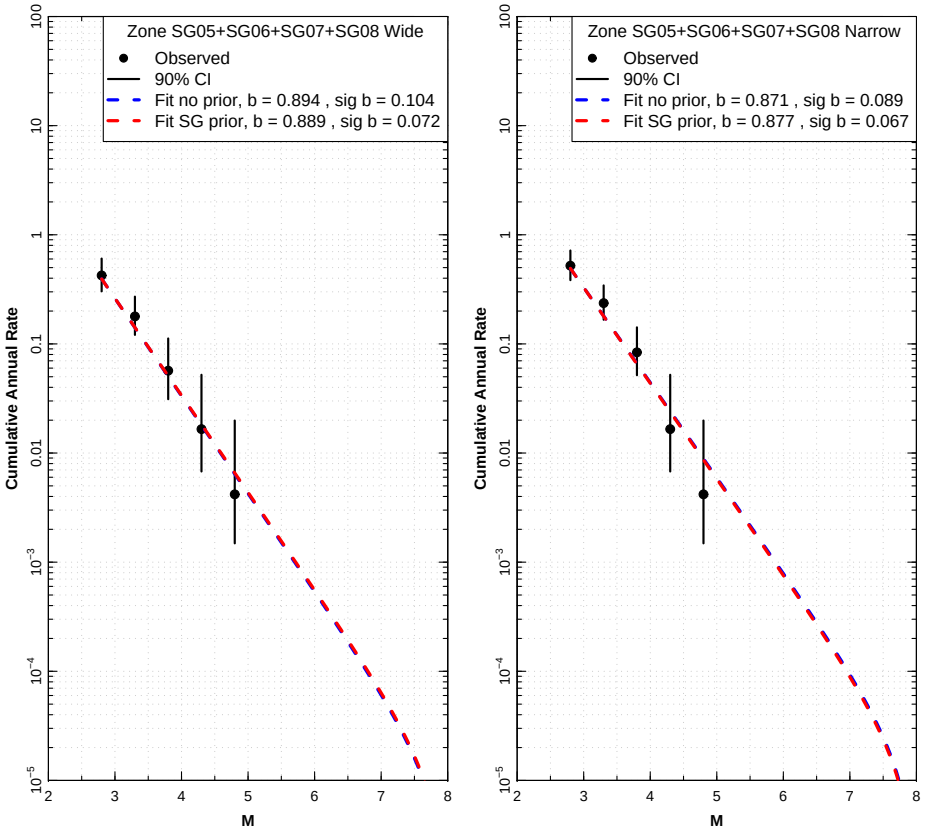

Figure 2.58: Earthquake recurrence relationships for EG1b combined small zones SG05+SG06+SG07+SG08 Wide and SG05+SG06+SG07+SG08 Narrow.

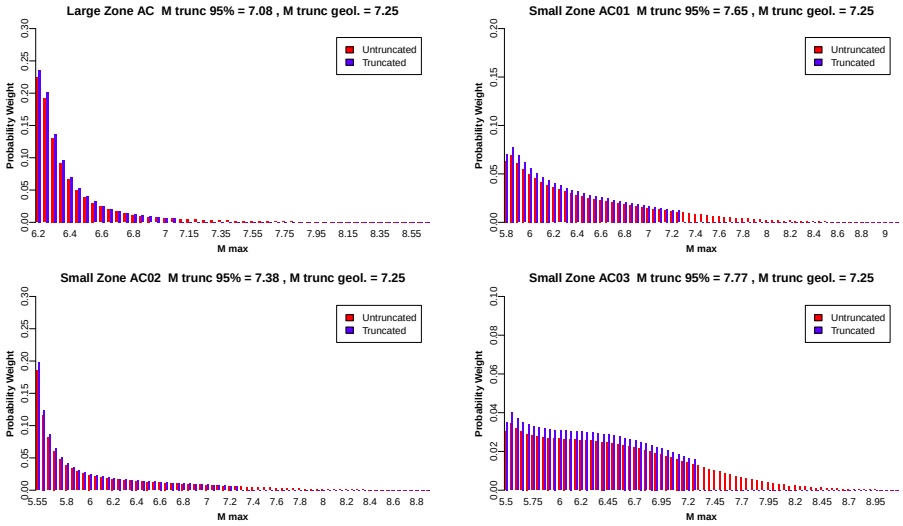

Figure 2.59: Initial maximum magnitude distributions for EG1b AC zones (1 of 4).

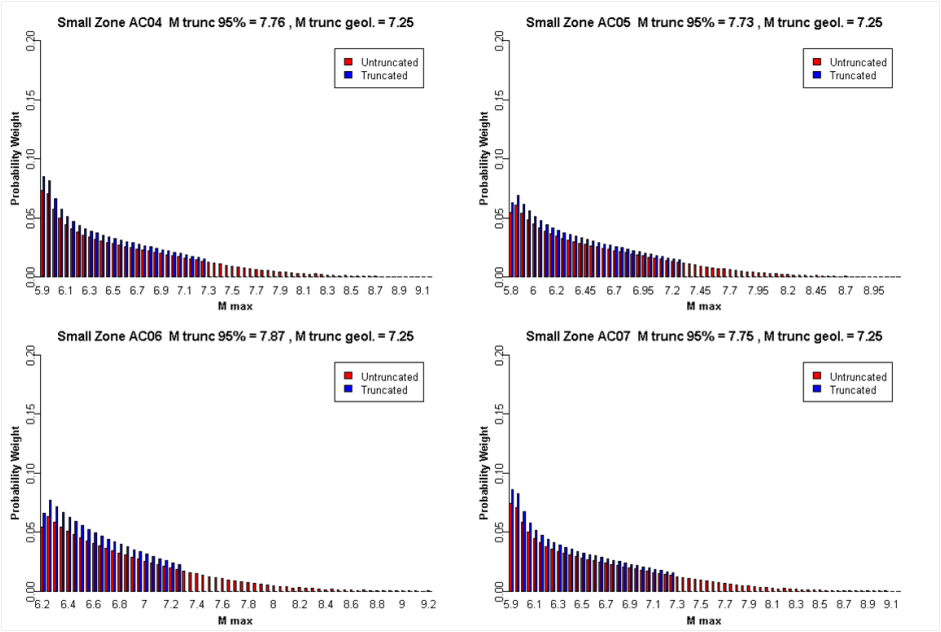

Figure 2.60: Initial maximum magnitude distributions for EG1b AC zones (2 of 4).

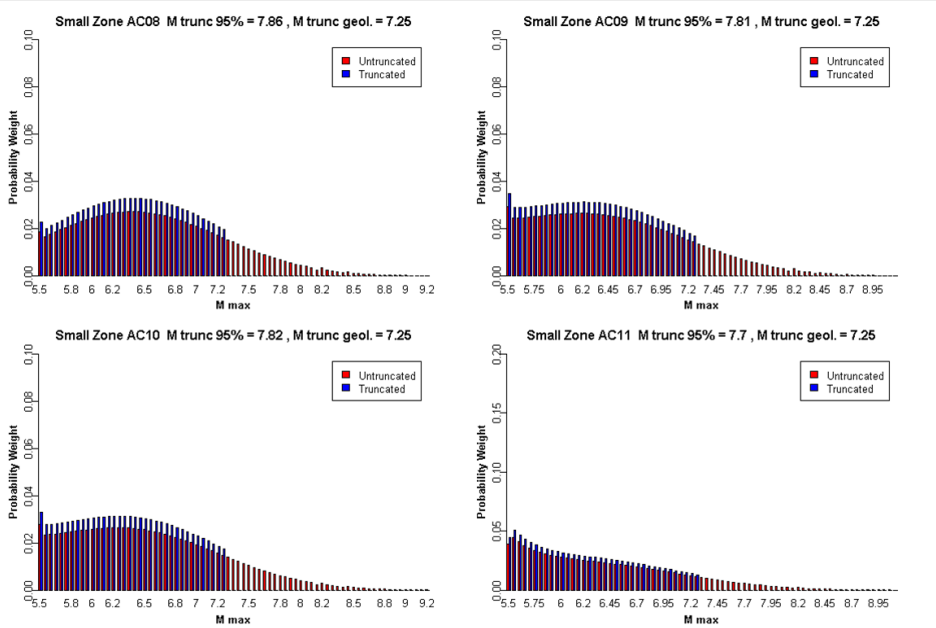

Figure 2.61: Initial maximum magnitude distributions for EG1b AC zones (3 of 4).

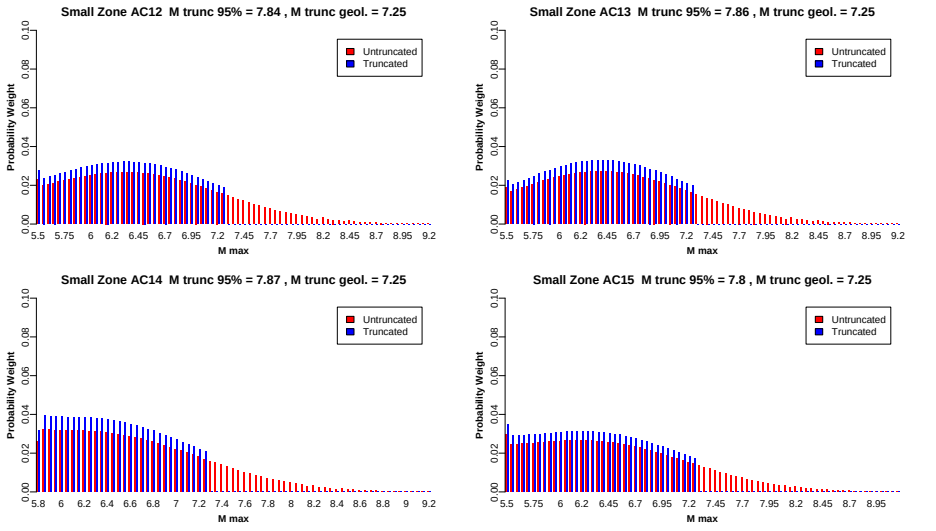

Figure 2.62: Initial maximum magnitude distributions for EG1b AC zones (4 of 4).

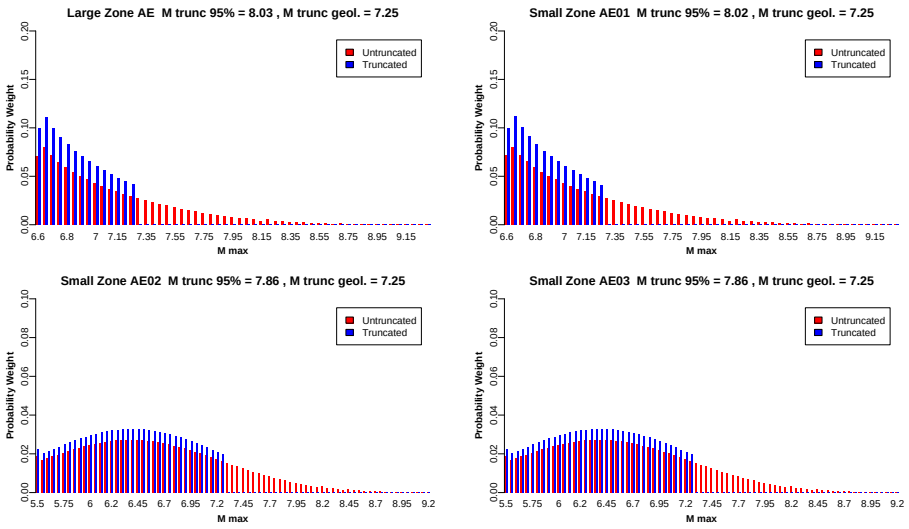

Figure 2.63: Initial maximum magnitude distributions for EG1b AE zones (1 of 5).

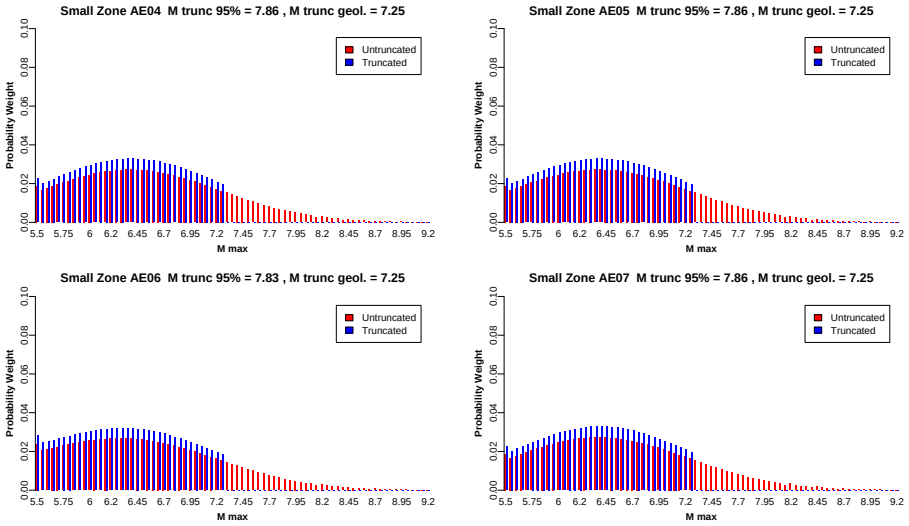

Figure 2.64: Initial maximum magnitude distributions for EG1b AE zones (2 of 5).

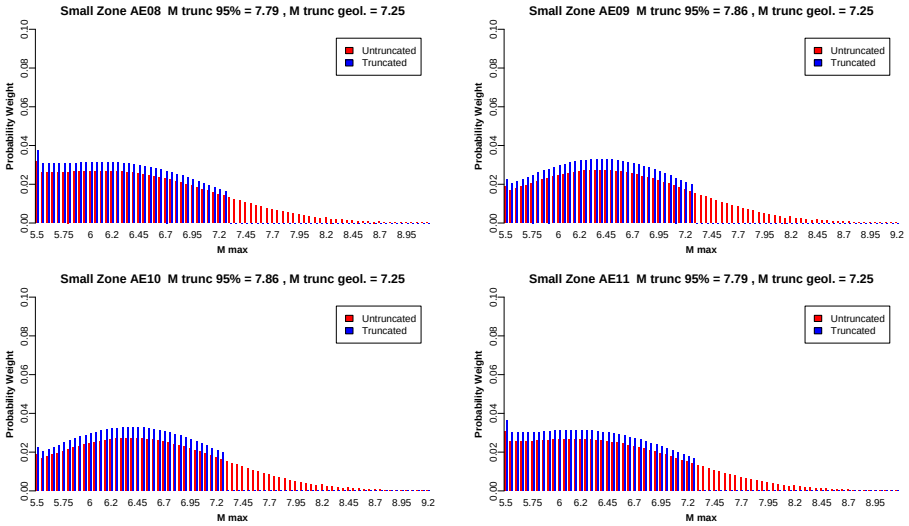

Figure 2.65: Initial maximum magnitude distributions for EG1b AE zones (3 of 5).

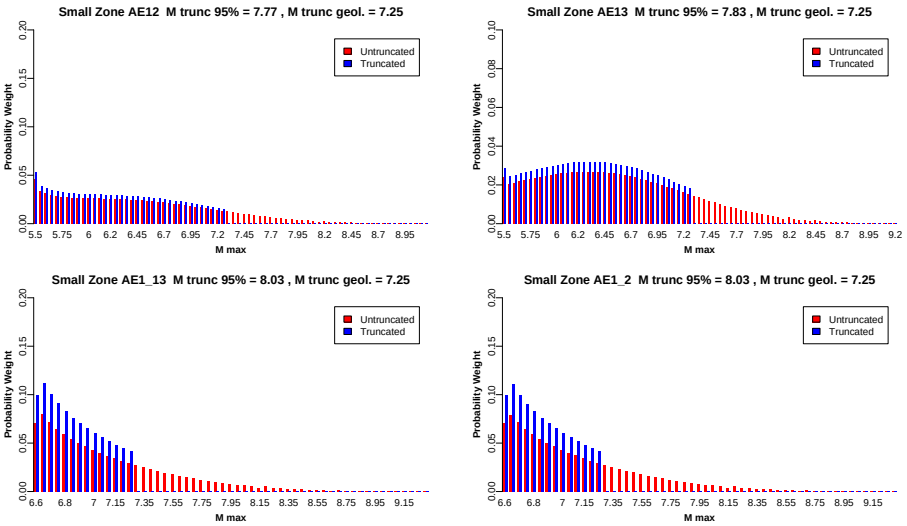

Figure 2.66: Initial maximum magnitude distributions for EG1b AE zones (4 of 5).

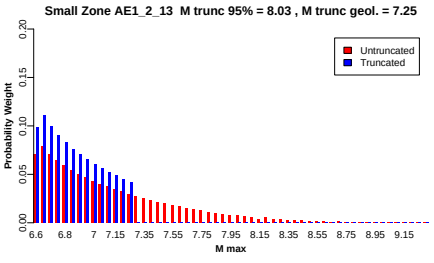

Figure 2.67: Initial maximum magnitude distributions for EG1b AE zones (5 of 5).

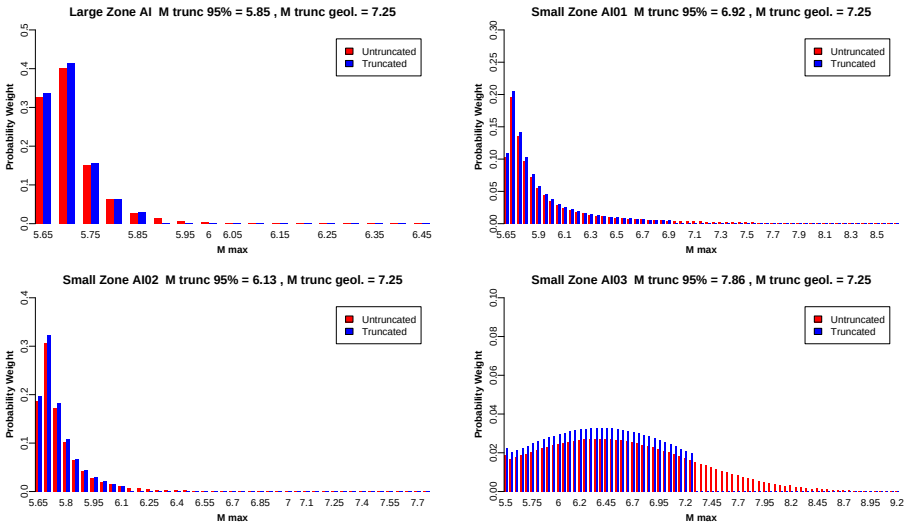

Figure 2.68: Initial maximum magnitude distributions for EG1b AI zones.

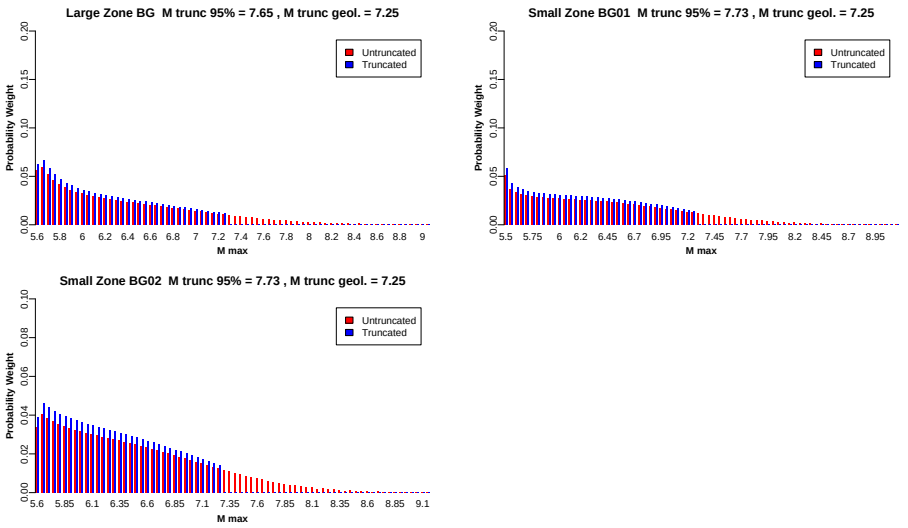

Figure 2.69: Initial maximum magnitude distributions for EG1b BG Zones.

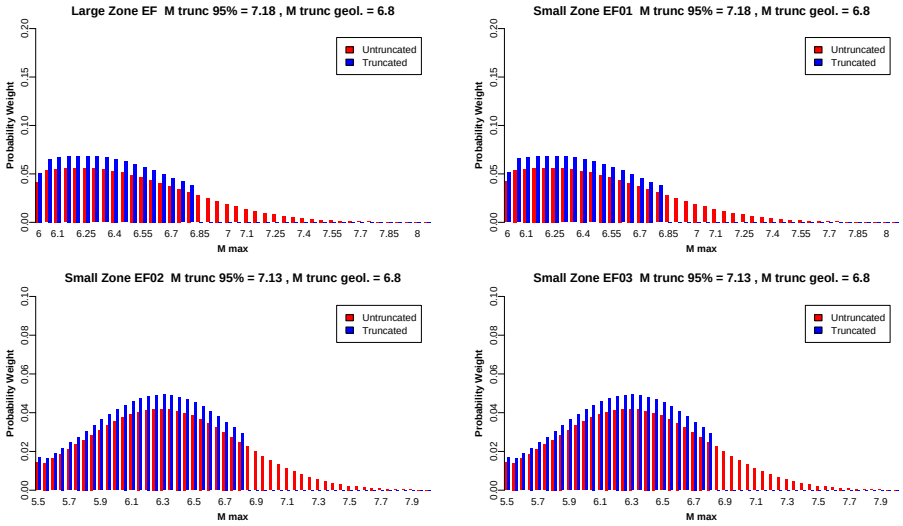

Figure 2.70: Initial maximum magnitude distributions for EG1b EF Zones (1 of 2).

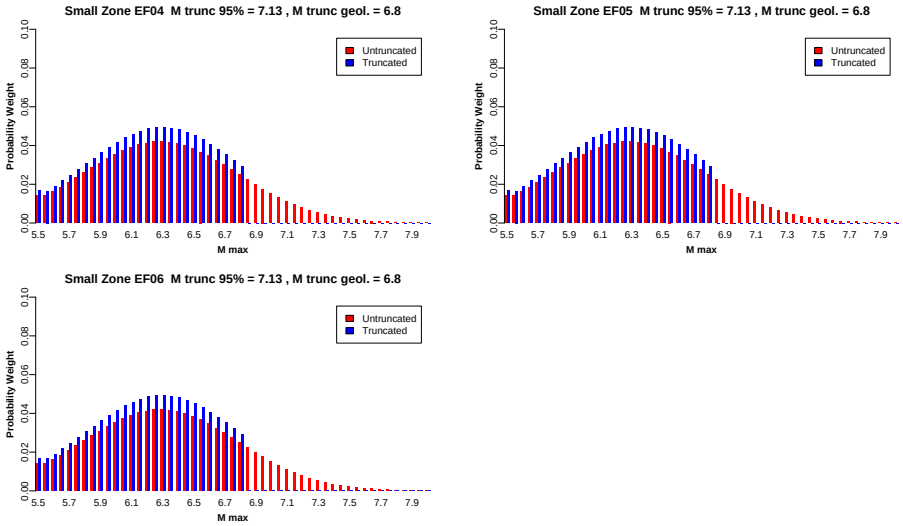

Figure 2.71: Initial maximum magnitude distributions for EG1b EF Zones (2 of 2).

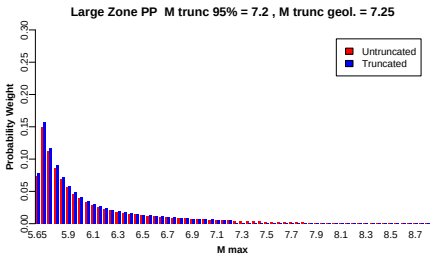

Figure 2.72: Initial maximum magnitude distributions for EG1b PP Zone.

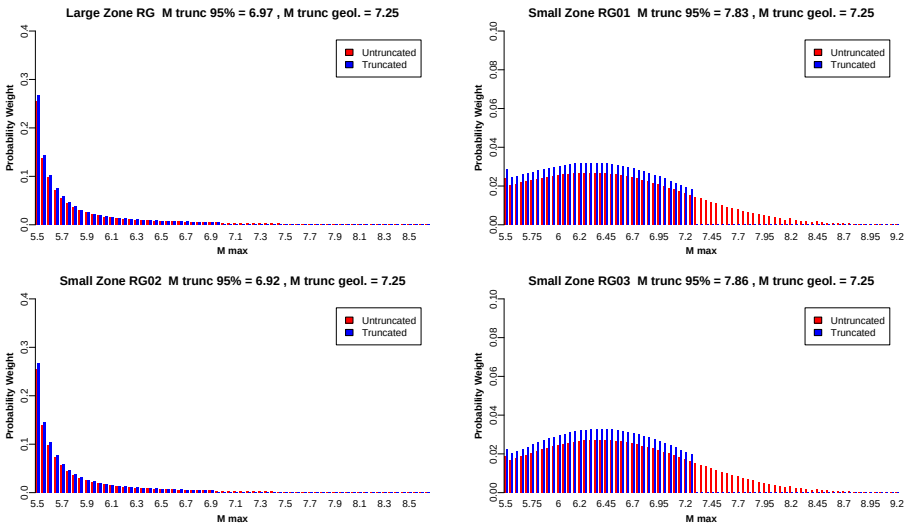

Figure 2.73: Initial maximum magnitude distributions for EG1b RG Zones (1 of 2).

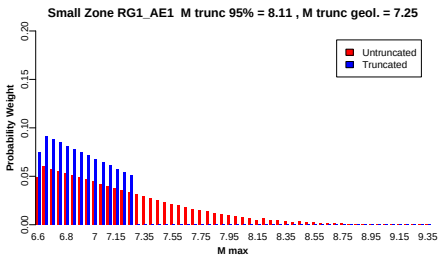

Figure 2.74: Initial maximum magnitude distributions for EG1b RG Zones (2 of 2).

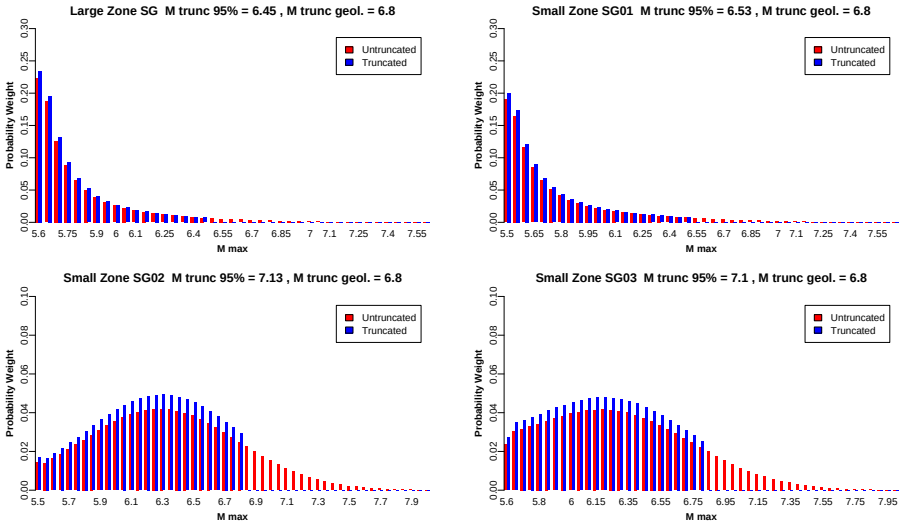

Figure 2.75: Initial maximum magnitude distributions for EG1b SG Zones (1 of 6).

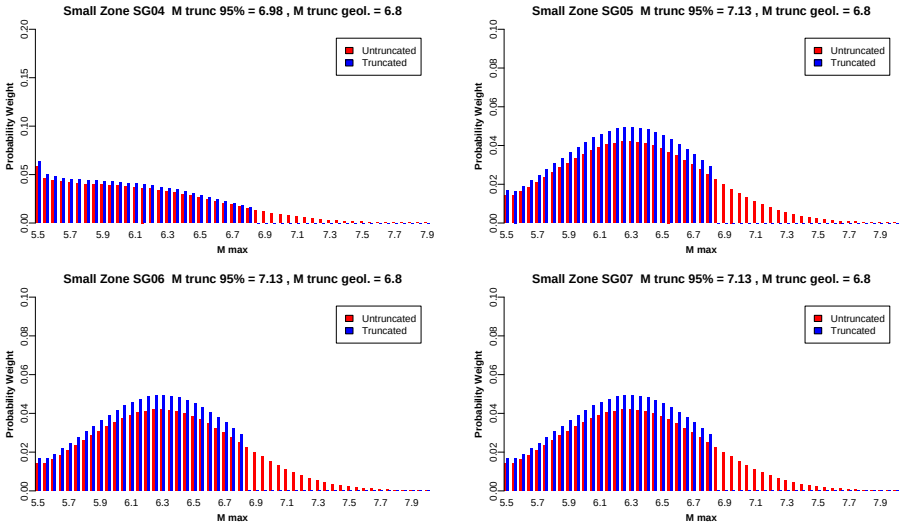

Figure 2.76: Initial maximum magnitude distributions for EG1b SG Zones (2 of 6).

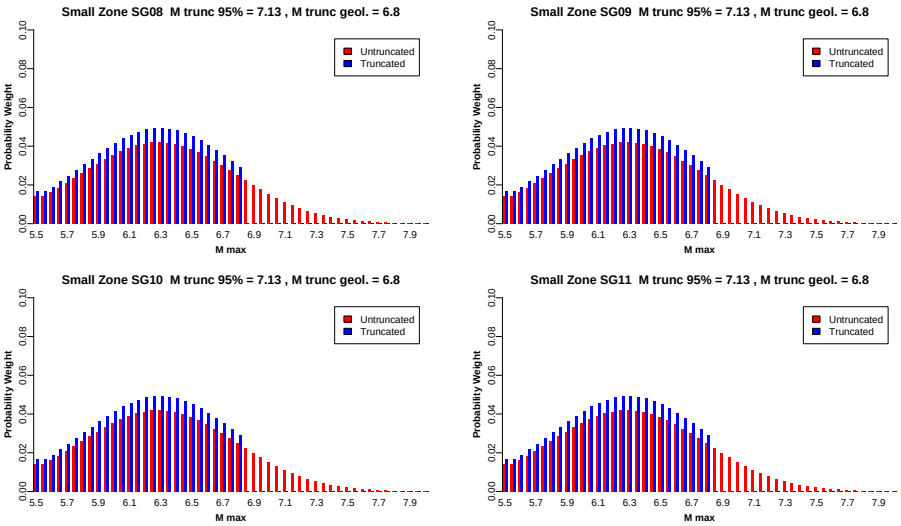

Figure 2.77: Initial maximum magnitude distributions for EG1b SG Zones (3 of 6).

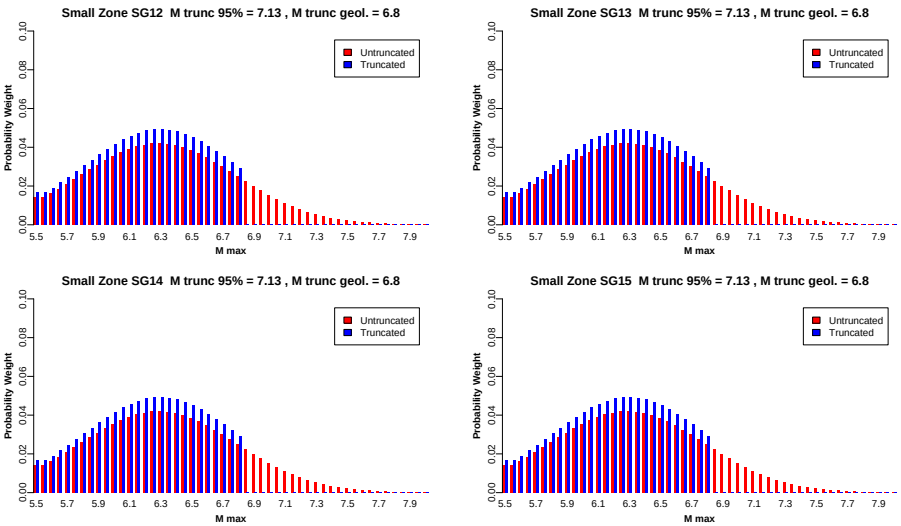

Figure 2.78: Initial maximum magnitude distributions for EG1b SG Zones (4 of 6).

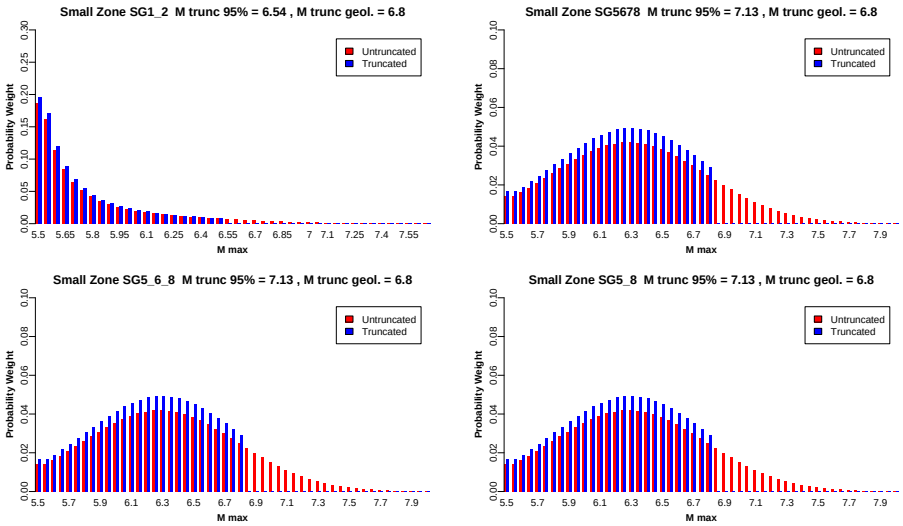

Figure 2.79: Initial maximum magnitude distributions for EG1b SG Zones (5 of 6).

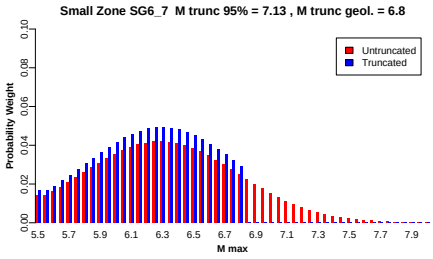

Figure 2.80: Initial maximum magnitude distributions for EG1b SG Zones (6 of 6).

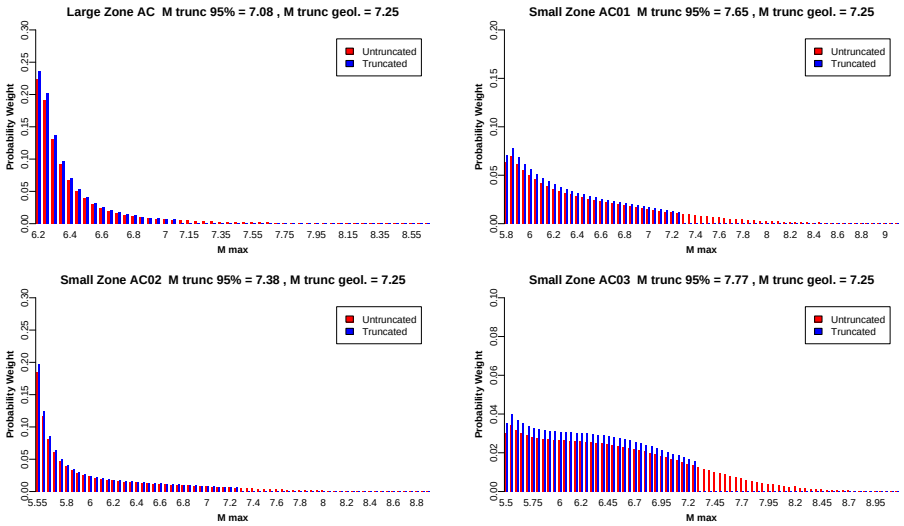

Figure 2.81: Final maximum magnitude distributions for EG1b AC zones (1 of 3).

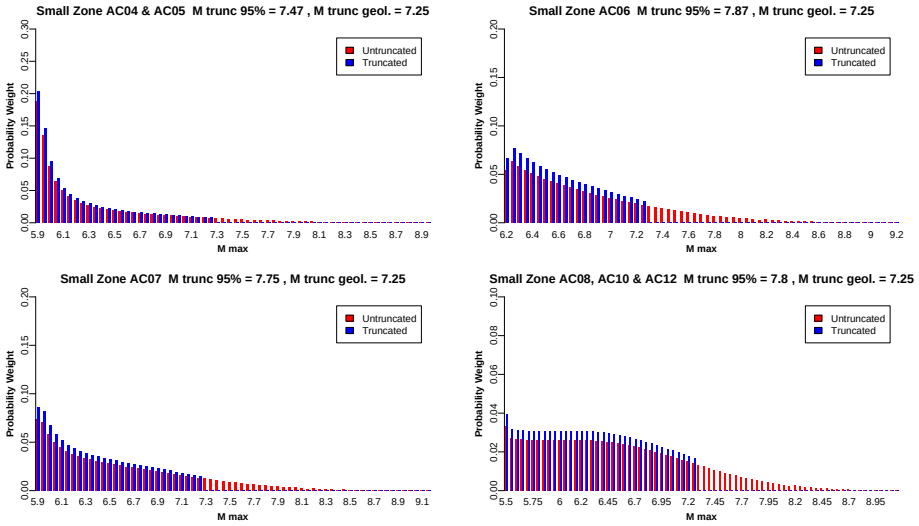

Figure 2.82: Final maximum magnitude distributions for EG1b AC zones (2 of 3).

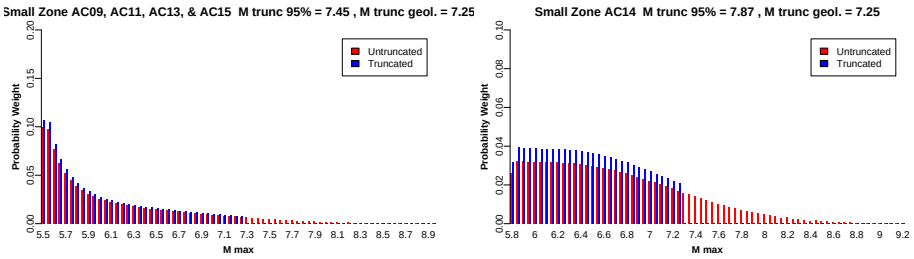

Figure 2.83: Final maximum magnitude distributions for EG1b AC zones (3 of 3).

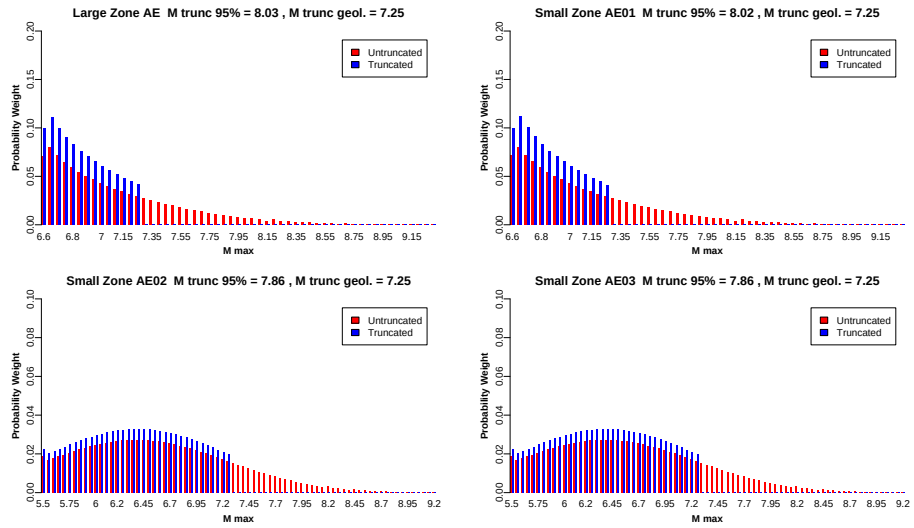

Figure 2.84: Final maximum magnitude distributions for EG1b AE zones (1 of 5).

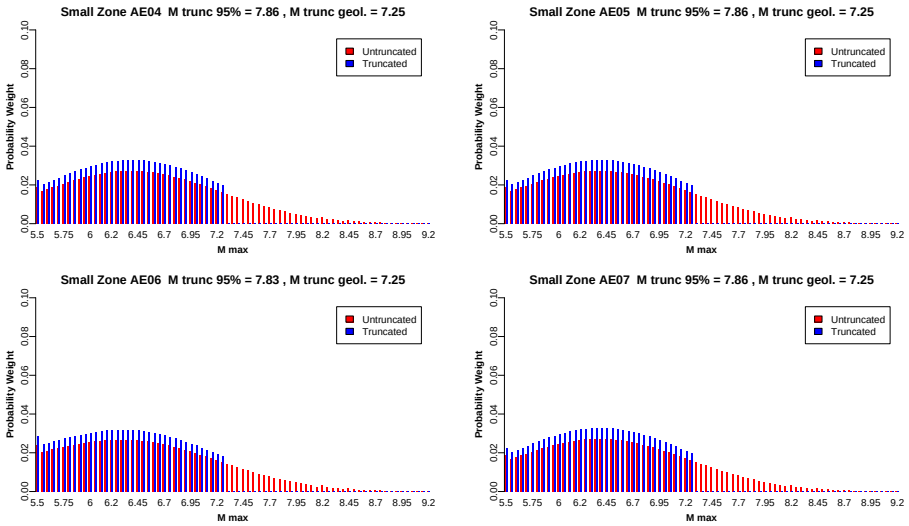

Figure 2.85: Final maximum magnitude distributions for EG1b AE zones (2 of 5).

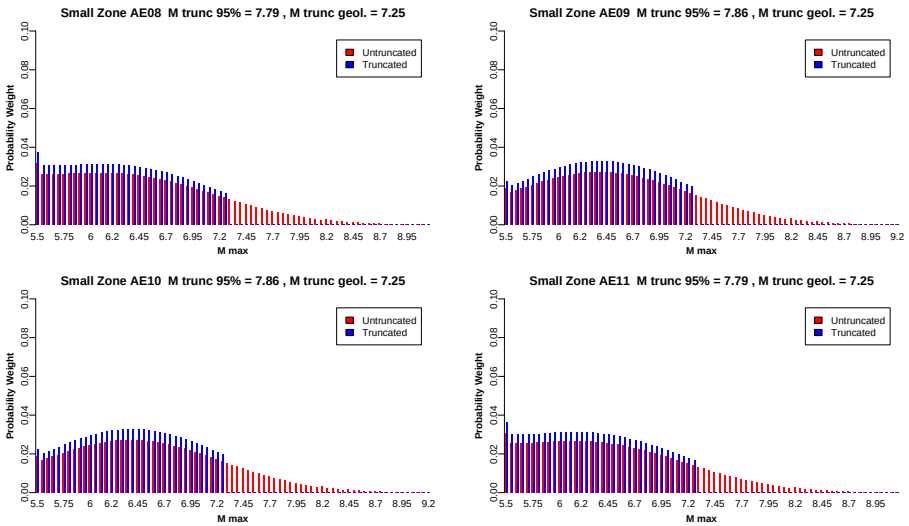

Figure 2.86: Final maximum magnitude distributions for EG1b AE zones (3 of 5).

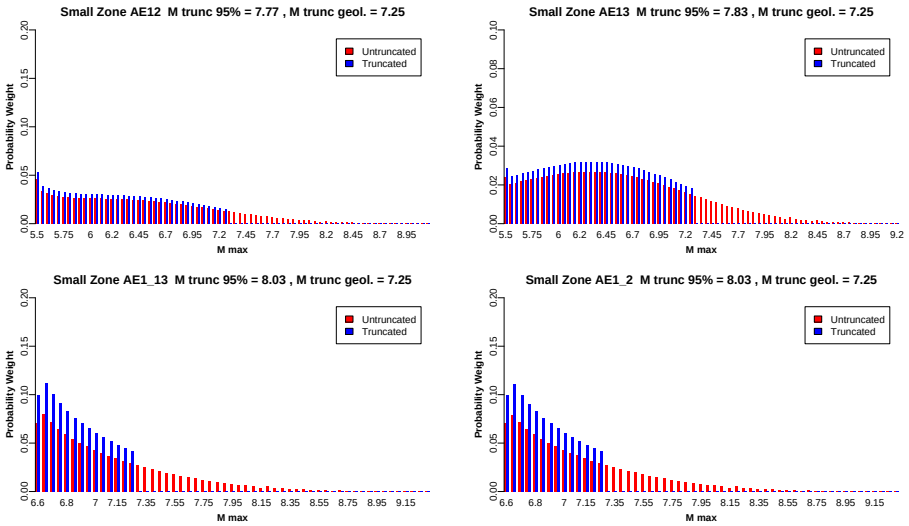

Figure 2.87: Final maximum magnitude distributions for EG1b AE zones (4 of 5).

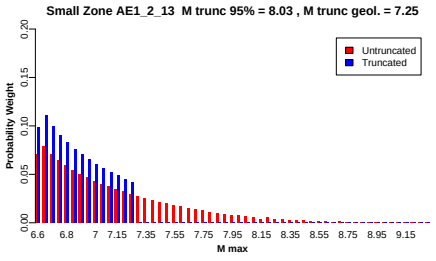

Figure 2.88: Final maximum magnitude distributions for EG1b AE zones (5 of 5).

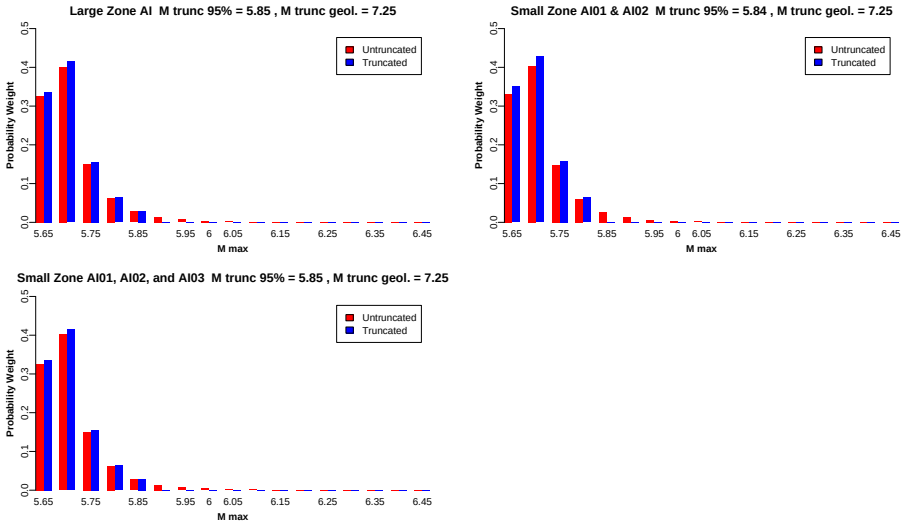

Figure 2.89: Final maximum magnitude distributions for EG1b for AI zones.

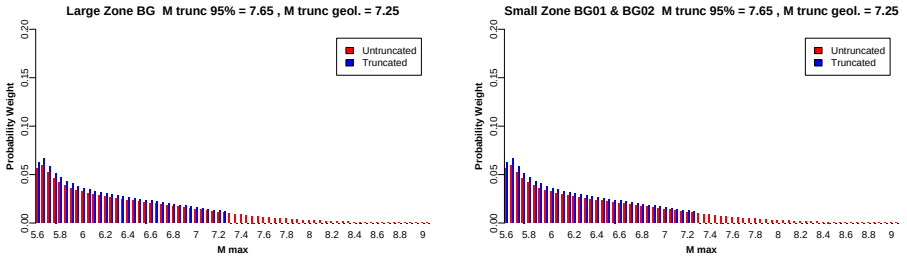

Figure 2.90: Final maximum magnitude distributions for EG1b BG Zones.

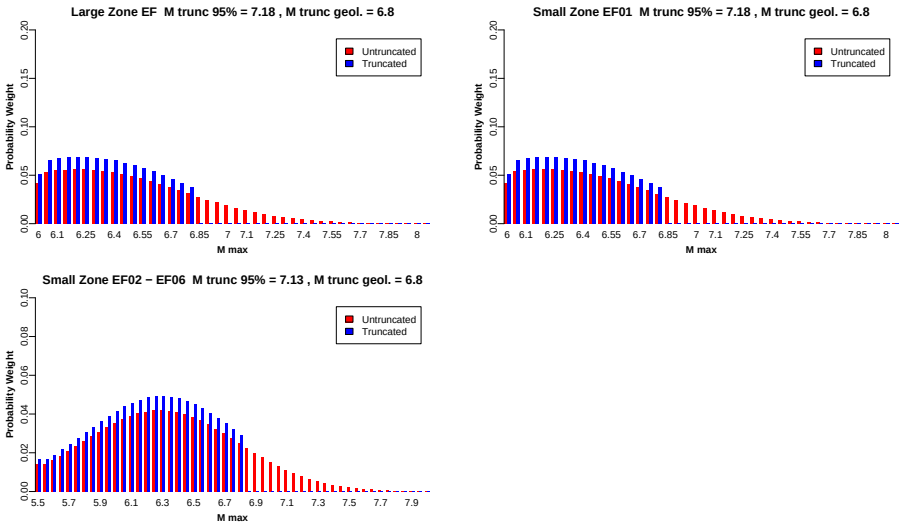

Figure 2.91: Final maximum magnitude distributions for EG1b EF Zones.

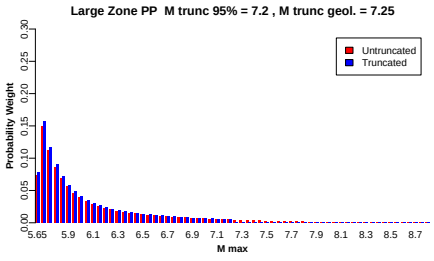

Figure 2.92: Final maximum magnitude distributions for EG1b PP Zone.

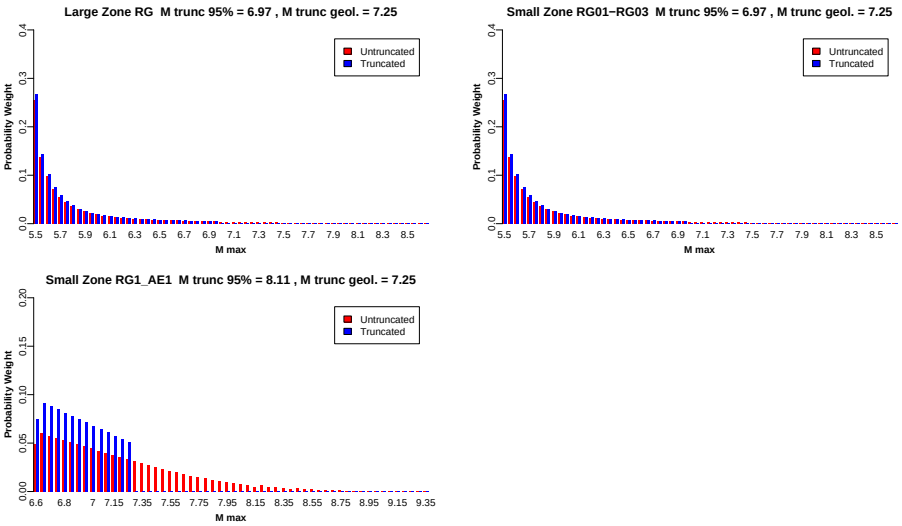

Figure 2.93: Final maximum magnitude distributions for EG1b RG Zones.

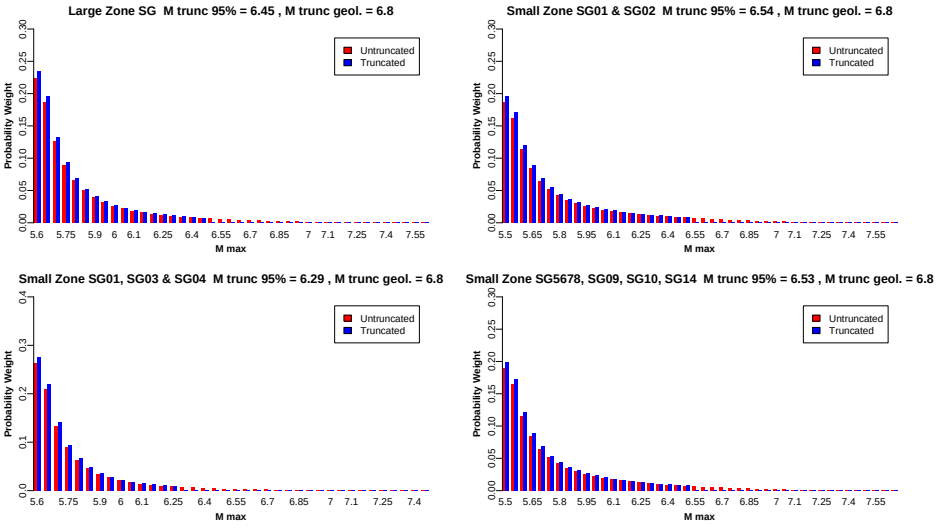

Figure 2.94: Final maximum magnitude distributions for EG1b SG Zones (1 of 2).

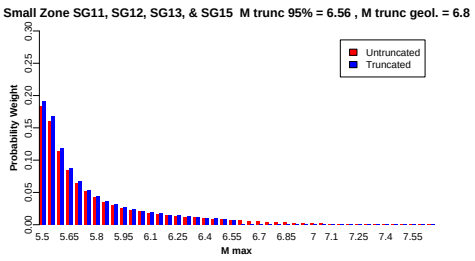

Figure 2.95: Final maximum magnitude distributions for EG1b SG Zones (2 of 2).

Chapter 3

Hazard Input Document for EG1b (EG1-HID-1002) of March 14, 2011

Written by the PMT, SP4 and TFI

This document describes the final seismic source model developed by Expert Team EG1b in the PRP project. The data files associated with this seismic source model are located in the zip file EG1-HID-1002_EG1b_data.zip. This document is based on the PEGASOS Hazard Input Document EG1-HID-0033. Based on the new earthquake ECOS09 catalog published in March 2010 the EG1b team revised its model, updating the seismicity parameters that go with that seismic source model and making one small modification to the zonation (removing 'soft' boundaries for the Fribourg zone). This document repeats for the most part the content of the PEGASOS Hazard Input Document EG1-HID-0033. The modifications caused by the model revision are highlighted in blue.

3.1 Seismic Source Zonation

Figure 3.1 shows the overall logic tree for seismic source zonation. Two alternative zonations are considered.

The first is termed "large scale" and consists of 8 large regional zones, shown on Figure 3.1. The zone polygon files are located in directory `./ZONES.LRG`. Within each zone, seismicity is modeled by kernel smoothing with three alternative values of the kernel smoothing parameter h. The values are h = 5 km (weight 0.2), h = 7.5 km (weight 0.6), and h = 10 km (weight 0.2). The corresponding spatial seismicity grid files are designated by zone name and h value and are also located in directory `./ZONES.LRG`.

The alternative approach is "small scale" zonation in which the regional zones shown on Figure 3.2 are subdivided. Figures 3.3, 3.4 , 3.5 , 3.6 and 3.7 show the "small scale" source zones. Seismicity within each "small scale" zone is assumed to be spatially homogeneous. The zone polygon files for these zones are located in directory `./ZONES.SML`.

As indicated on the master logic tree (Figure 3.1), there are a number of alternative "small scale" zone combinations and alternative boundaries. These are described in the following

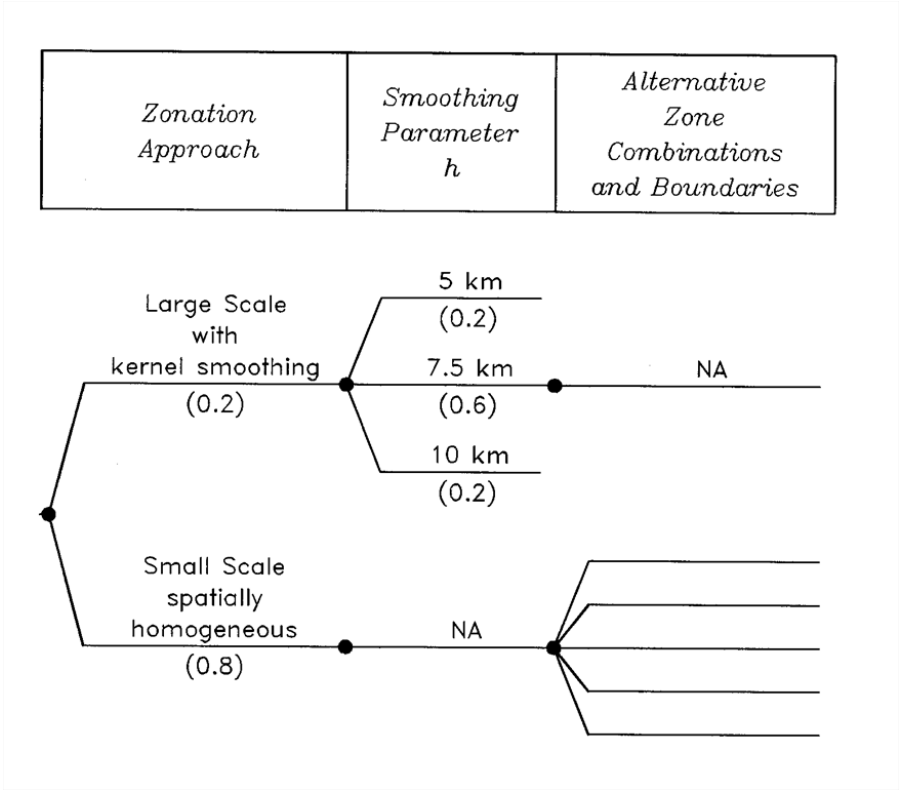

Figure 3.1: Master logic tree for EG1b seismic source zonation.

sections.

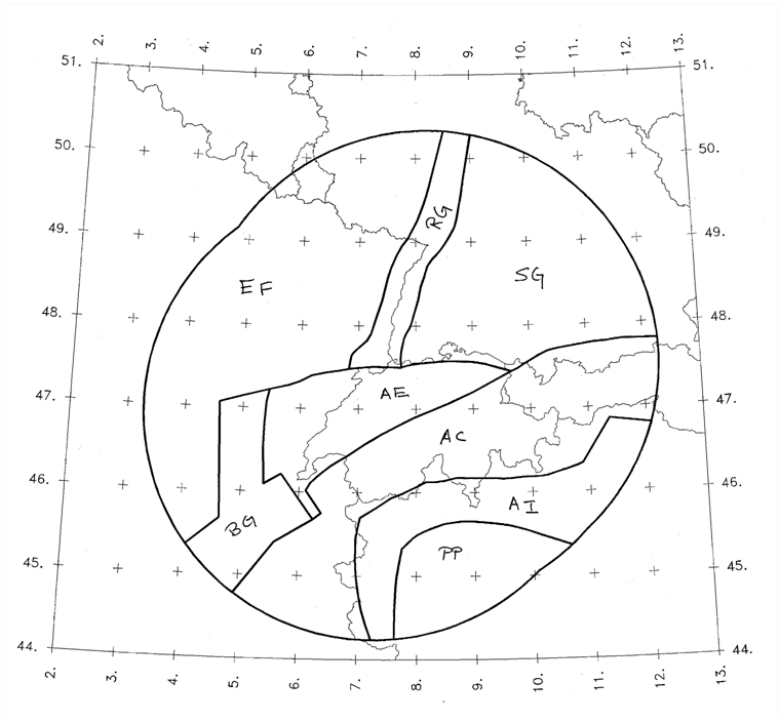

Figure 3.2: Regional source zones in "large scale" seismic source zonation.

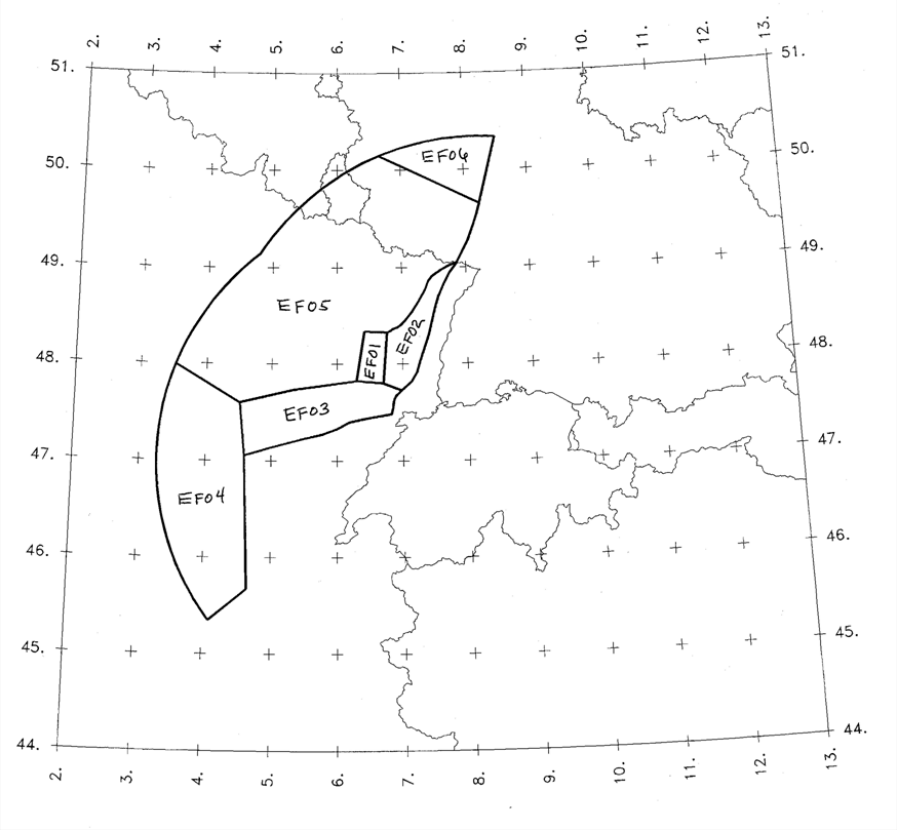

Figure 3.3: Zonation of Eastern France (EF) in "small scale" seismic source zonation.

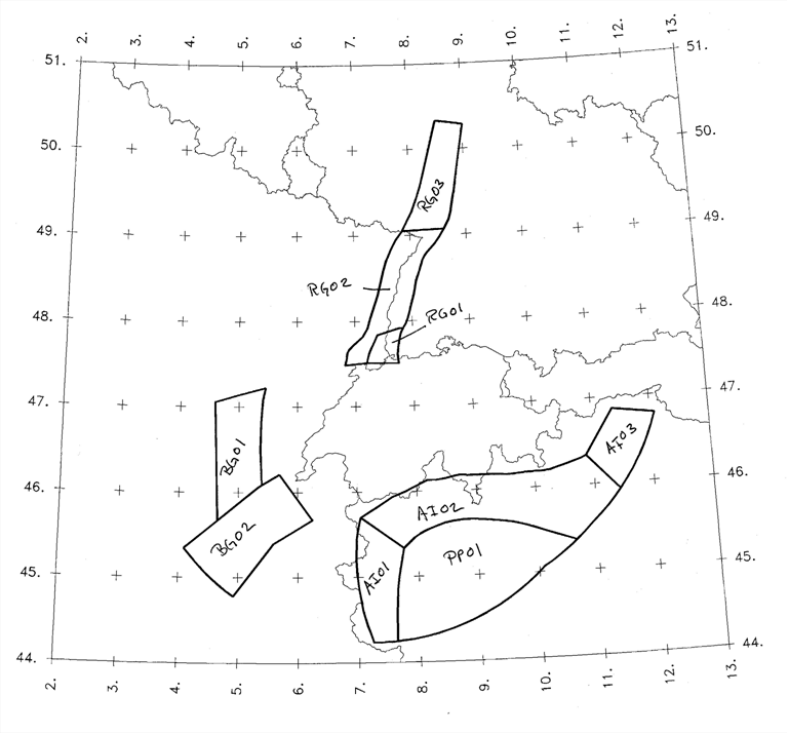

Figure 3.4: Zonation of Bresse Graben (BG), Rhine Graben (RG), Alps Internal (AI), and Po Plain (PP) in "small scale" seismic source zonation.

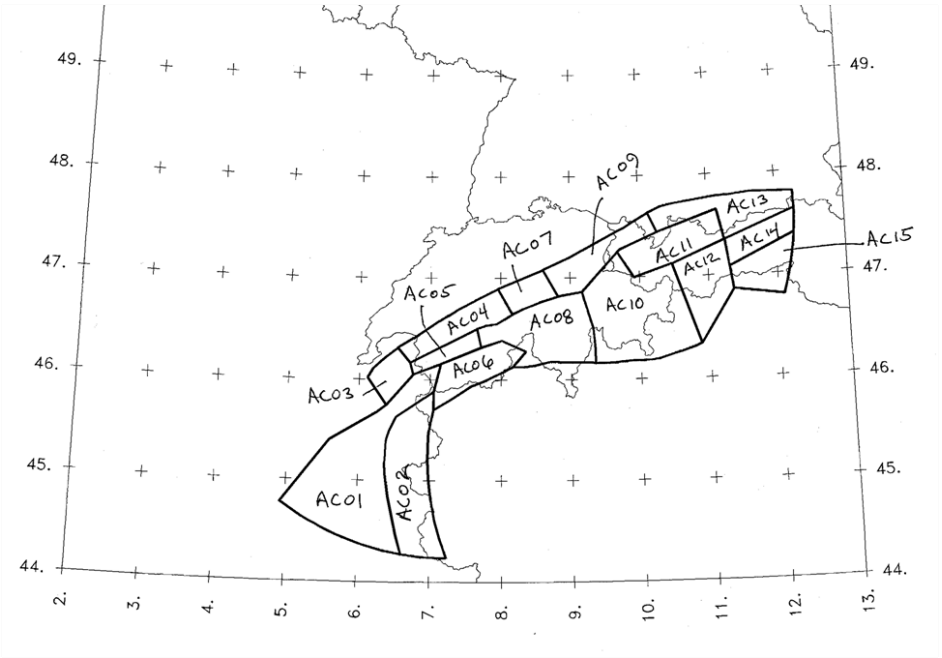

Figure 3.5: Zonation of Alps Central (AC) in "small scale" seismic source zonation.

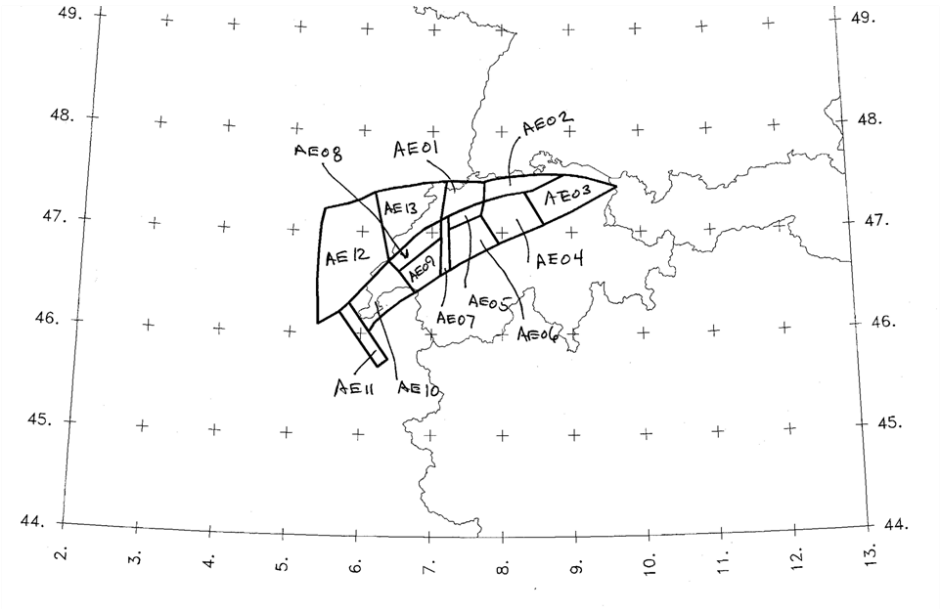

Figure 3.6: Zonation of Alps External (AE) in "small zones" seismic source zonation.

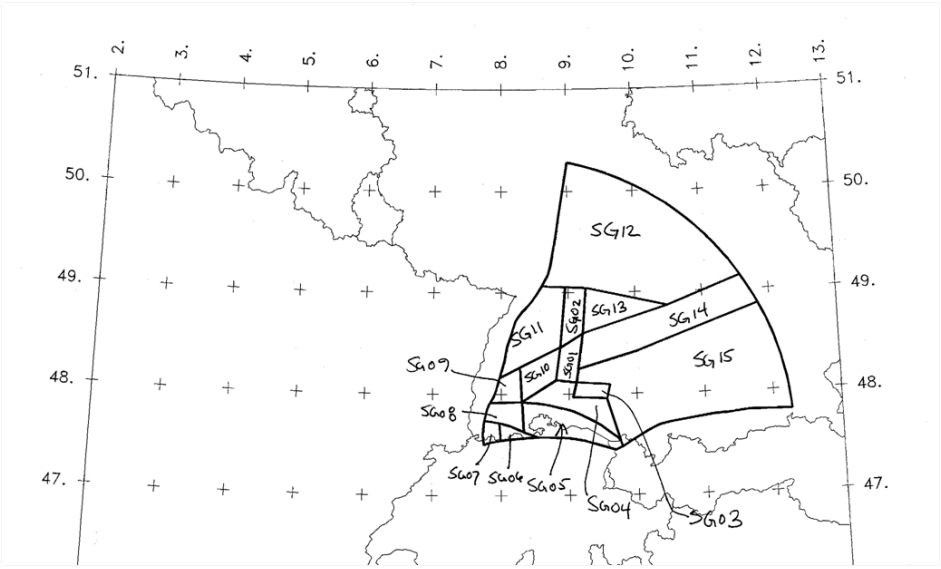

Figure 3.7: Zonation of South Germany (SG) in "small scale" seismic source zonation.

3.2 Zone Combinations within the "Small Scale" Model

There are three sets of alternative "small scale" zone combinations that affect different areas. The first is the treatment of the Swabian Alps region. 3.8 shows the logic tree for these zones. Zones SG01 and SG02 are either considered to be separate, or are combined into a single zone SG1_2 (see 3.9).

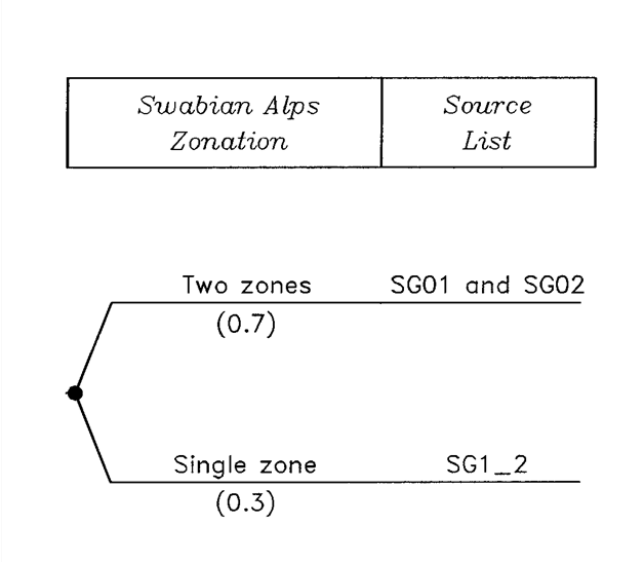

Figure 3.8: Logic tree for Swabian Alps "small scale" zonation.

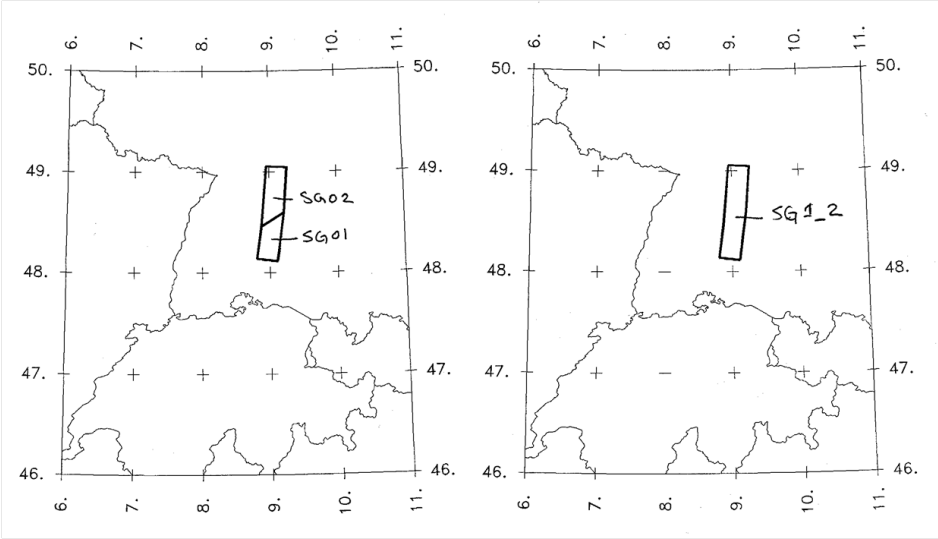

Figure 3.9: Alternative zone combinations for the Swabian Alps in the "small scale" seismic source zonation.

Figure 3.10 shows the logic tree for "small scale" zonation in the Basel-Jura area. The first level addresses whether or not the Basel source extends into the Jura. If it does, then zones RG01 and AE01 are combined into zone RG1_AE1 (see Figure 3.11). If the Basel source is separate from the Jura, then there are 4 alternative combinations of the Jura zones AE01, AE02, and AE13, as shown on Figures 3.10 and 3.11

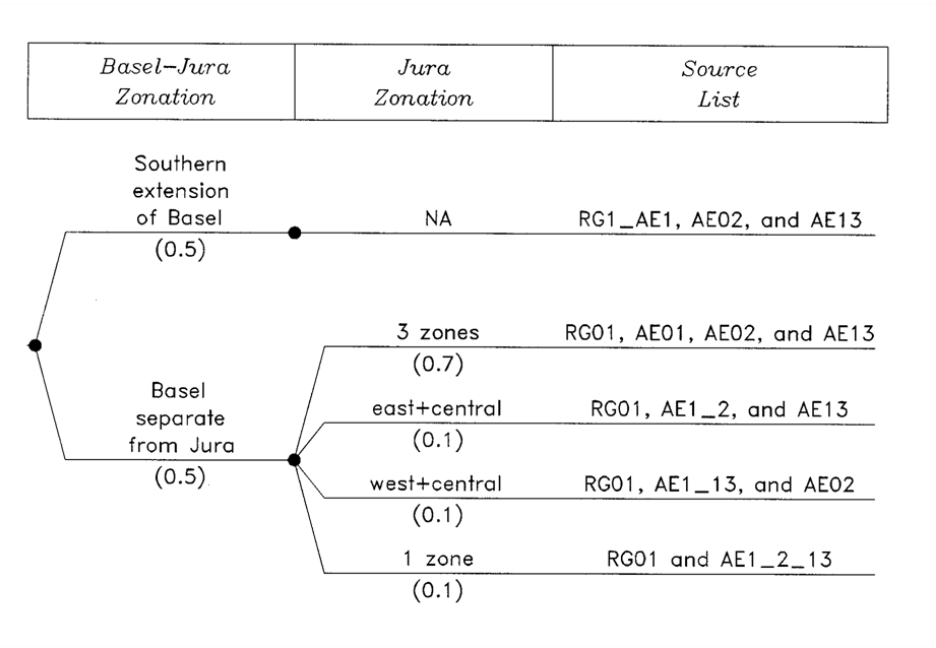

Figure 3.10: Logic tree for Basel-Jura "small scale" zonation.

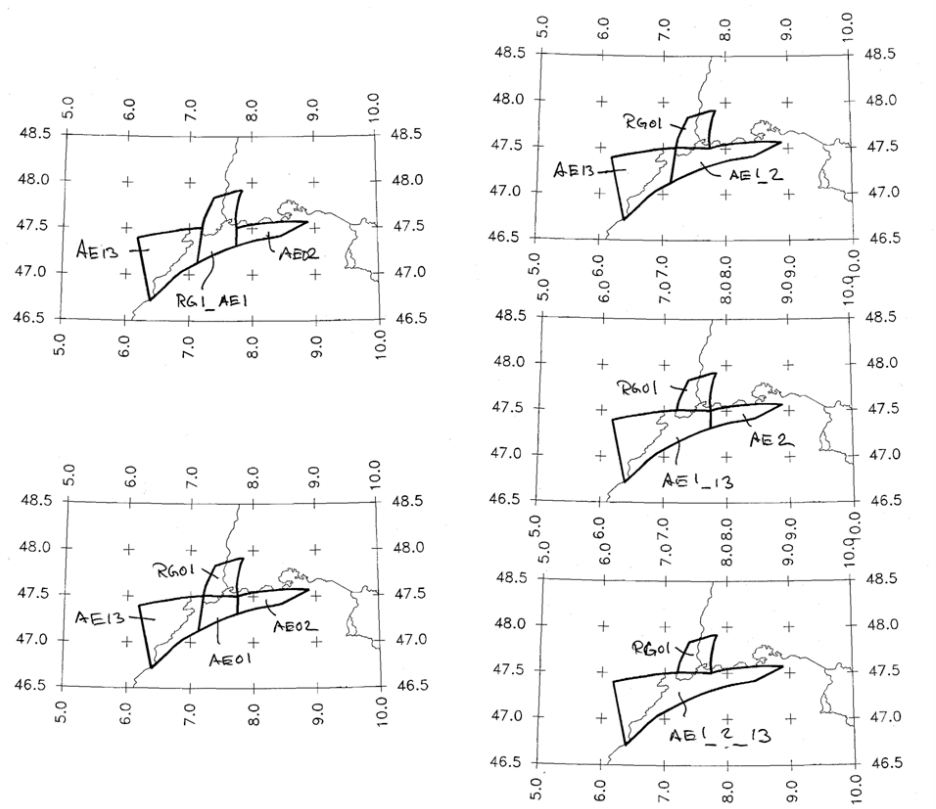

Figure 3.11: Alternative zone combinations for Basel-Jura in the "small scale" seismic source zonation.

Figure 3.12 shows the logic tree for "small scale" zonation in the Dinkelberg-Bodensee area. The level addresses whether or not the Dinkelberg source (SG07) is separate from the rest of the area or is combined with zone SG06. The second level addresses the three alternative zone combinations conditional on the first branch. The resulting six sets of zones are listed on Figure 3.12 and are shown on Figure 3.13.

Polygons for all of the combined zones shown on the above figures are in directory `./ZONES.SML`.

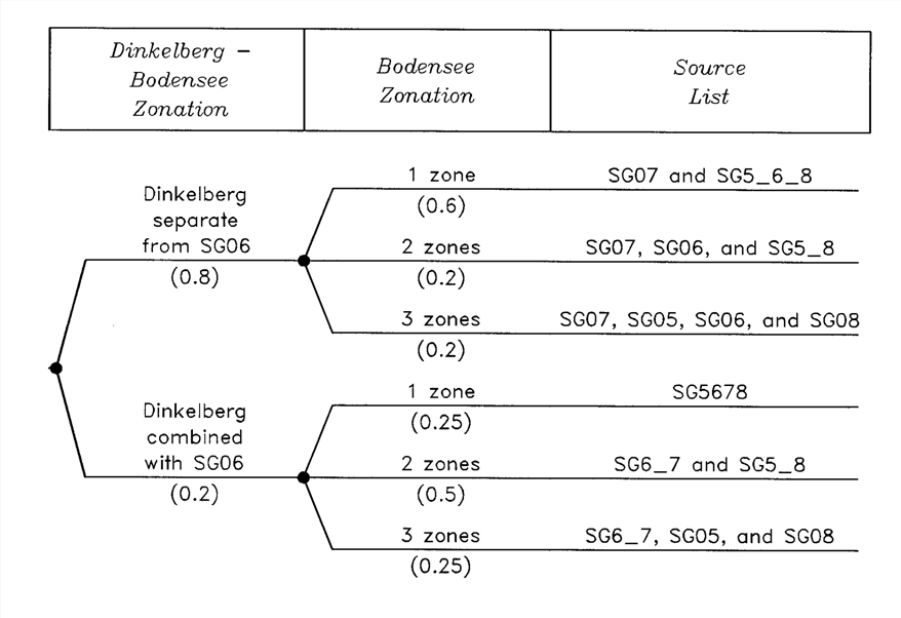

Figure 3.12: Logic tree for Dinkelberg-Bodensee "small scale" zonation.

3.3 Uncertain Zone Boundaries within the "Small Scale" Model

There is one case where the zone boundaries are considered to be uncertain in location ("soft"). It affects the location of the northern and southern boundaries for the eastern Jura source AE02. As shown on Figure 3.14, there are narrower and wider alternatives for this zone. The central estimate is given the highest weight of 0.5. The two alternative locations are each given a weight of 0.25. These alternative boundaries affect a number of the surrounding zones, as shown on Figures 3.14 and 3.15. The alternative zone polygon files are located in directory `./ZONES.SML`. The zone boundary files for the preferred location have the extension `*.ZON`. The zone boundary files for the wide eastern Jura have the extension `*.WZO` and those for the narrow eastern Jura have the extension `*.NZO`. These boundaries are completely dependent, all `*.WZO` files are to be used together as one alternative and all `*.NZO` files are to be used together as another alternative. Again, note that these alternative zonation boundaries are used only for the hazard computation. The zone seismicity parameters are obtained using the central location and are to be applied to all three geometries. Please also note that this alternative width of the eastern Jura zone AE02 also interacts with the logic trees for the Basel-Jura area (Figures 3.10 and 3.11) and with the Dinkelberg-Bodensee area (Figures 3.12 and 3.13) to produce three alternatives for each.

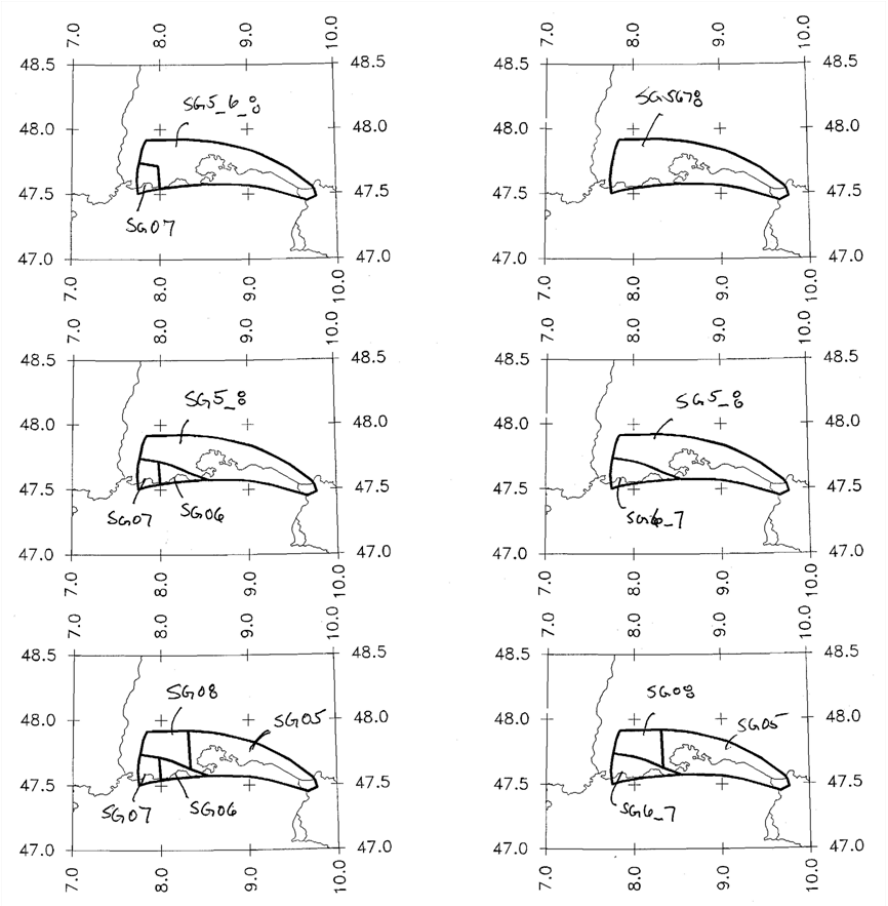

Figure 3.13: Alternative zone combinations for the Dinkelberg-Bodensee area in the "small scale" seismic source zonation.

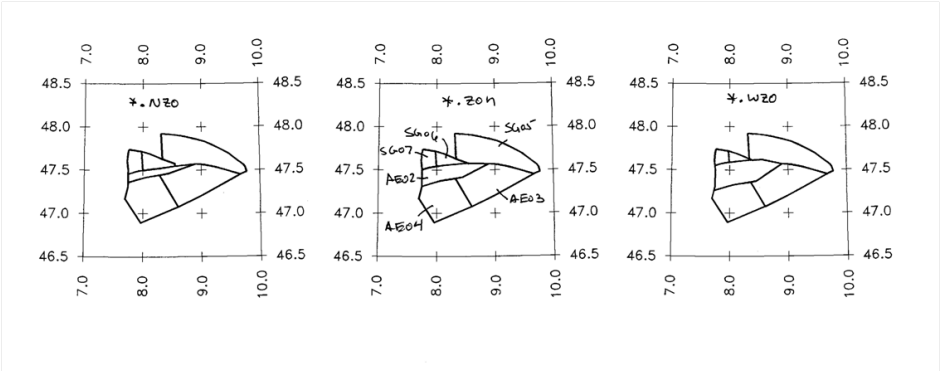

Figure 3.14: Alternative "soft" boundaries for the eastern Jura zone AE02 and its neighboring zones in the "small zones" seismic source zonation.

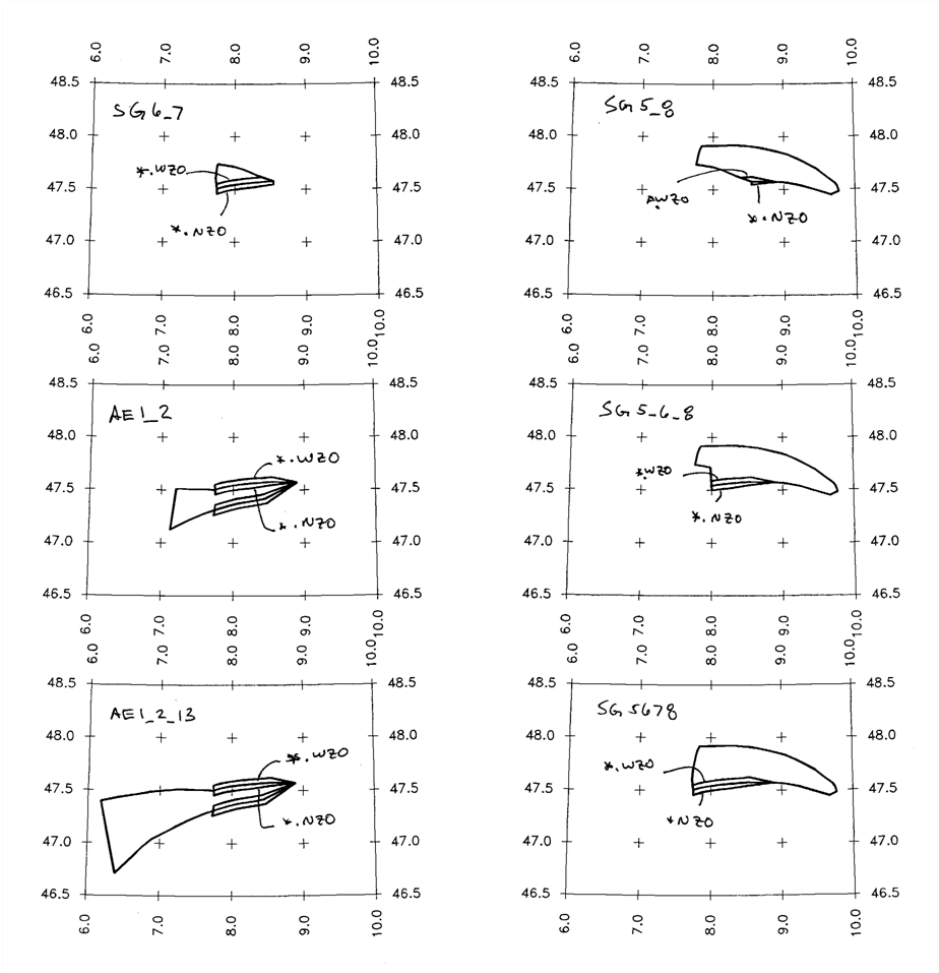

Figure 3.15: Alternative combined zone boundaries produced by the "soft" boundaries for the eastern Jura zone AE02.

3.4 Earthquake Rupture Geometry

The size of earthquake ruptures is defined by the relationship:

$$\text{Mean}\log_{10}(\text{rupture area}) = 1.02M - 4.15 \quad (3.1)$$

$$\sigma\log_{10}(\text{rupture area}) = 0.24 \quad (3.2)$$

Using the relationship for the expectation of a lognormal distribution, the mean (expected) rupture area is given by the relationship:

$$\text{mean rupture area} = 10^{(1.02M-4.084)} \quad (3.3)$$

The relationship for the mean rupture area will be used in the hazard computations. The rupture length and width have an aspect ratio of 1:1 until the maximum rupture width for a source is reached. For larger earthquakes, the aspect ratio should change in order to preserve the rupture area. For the "large scale" zones, earthquake epicenters are distributed according to the kernel density grids defined above. For the "small scale zones" earthquake epicenters are uniformly distributed.

Earthquake ruptures are located symmetrically on the epicenters (the epicenter is at the midpoint of the rupture). For those epicenters located closer than 1/2 rupture length to the source zone boundary, the ruptures are truncated at the source boundary, preventing them from coming closer to the site than the source boundary.

Table 3.1 and 3.2 defines the relative frequency of the style-of-faulting for the individual sources. Three specific styles-of-faulting are considered, normal, strike-slip and reverse. For each style-of-faulting, there is a preferred direction of rupture and a preferred fault dip that should be used to model ruptures. The dip direction(s) are also given.

The depth distribution for small earthquakes for each zone is defined by a truncated normal distribution. The last three columns of table 3.1 and 3.2 list the peak of the distribution (the mean for an un-truncated distribution), the standard deviation (again for the un-truncated distribution) and the maximum depth that defines the lower limit of the distribution. The upper truncation point is zero depth. For larger earthquakes, a magnitude-dependent depth distribution is to be developed using the weighted approach outlined in Toro [2003] (TP1-TN-0373) with T = 0.5 (hypocenter in lower half of rupture).

3.5 Earthquake Recurrence Parameters

Each source has a single distribution for maximum magnitude and a single distribution for earthquake recurrence parameters. Individual M_{max} distribution files for each source zone are contained in subdirectories `./MMAX.LRG` and `./MMAX.SML`. These distributions are limited to a minimum value of M_{max} of 5.5. These distributions are defined in terms of five weighted alternative values of M_{max}.

The joint distributions for beta [b-value $\times \ln(10)$] and $N(m \geq 5)$ are contained in subdirectories `./REC.LRG` and `./REC.SML`. A truncated exponential earthquake recurrence relationship is used to define the relative frequency of earthquakes of different magnitudes.

Table 3.1: Earthquake Rupture Parameters for EG1b Part 1.

		"Large Scale" Zones															
		style-of-faulting			Fault orientation										Depth (km)		
		%	%	%	Normal Fault			Strike Slip Fault			Thrust Fault					
label	Name	Nor-	Strike	Thrust	Strike	dip	dip dir	Strike	dip	dip dir	Strike	dip	dip dir		max	peak	σ
		mal	Slip														
EF	Eastern France	0.15	0.8	0.05	150	60	NE,SW	0	90	-	60	45	NW,SE		15	10	3
RG	Rhine Graben	0.25	0.75	0	145	60	E,W	5	90	-	65	45	SE,NW		26	13	5
SG	South Germany	0.15	0.8	0.05	160	60	E,W	10	90	-	70	45	S,N		20	9	3
BG	Bresse Graben	0.4	0.6	0	160	60	E,W	10	90	-	70	45	S,N		30	15	15
AE	Alps external	0.1	0.8	0.1	150	60	NE,SW	0	90	-	60	30	SE		30	12	10
AC	Alps central	0.5	0.3	0.2	150	60	E,W	0	90	-	60	30	SE		15	9	4
AI	Alps internal	0	0.8	0.2	180	60	E,W	30	90	-	90	30	SE		37	18	10
PP	Po plain	0.333	0.334	0.333	rand	60	-	rand	90	-	rand	45	-		20	10	8
		"Small Scale" Zones															
EF01	Remiremont	0.15	0.8	0.05	150	60	NE,SW	0	90	-	60	45	NW,SE		15	10	3
EF02	Vosges	0.15	0.8	0.05	150	60	NE,SW	0	90	-	60	45	NW,SE		15	10	3
EF03	Dijon-Saône	0.15	0.8	0.05	150	60	NE,SW	0	90	-	60	45	NW,SE		15	10	3
EF04	Massif Central	0.15	0.8	0.05	150	60	NE,SW	0	90	-	60	45	NW,SE		15	10	3
EF05	Lorraine	0.15	0.8	0.05	150	60	NE,SW	0	90	-	60	45	NW,SE		15	10	3
EF06	Mainz	0.15	0.8	0.05	150	60	NE,SW	0	90	-	60	45	NW,SE		15	10	3
RG01	Basel	0.25	0.75	0	145	60	E,W	5	90	-	65	45	SE,NW		26	13	5
RG02	South Rhine Graben	0.25	0.75	0	145	60	E,W	5	90	-	65	45	SE,NW		26	13	5
RG03	North Rhine Graben	0.25	0.75	0	145	60	E,W	5	90	-	65	45	SE,NW		26	13	5
SG01	Schwäbische Alb	0.15	0.8	0.05	160	60	E,W	10	90	-	70	45	S,N		20	9	3
SG02	Stuttgart	0.15	0.8	0.05	160	60	E,W	10	90	-	70	45	S,N		20	9	3
SG03	Saulgau	0.15	0.8	0.05	160	60	E,W	10	90	-	70	45	S,N		20	9	3
SG04	Linzgau	0.15	0.8	0.05	160	60	E,W	10	90	-	70	45	S,N		20	9	3
SG05	Singen-Bodensee	0.15	0.8	0.05	160	60	E,W	10	90	-	70	45	S,N		20	9	3
SG06	Leibstadt	0.15	0.8	0.05	160	60	E,W	10	90	-	70	45	S,N		20	9	3
SG07	Dinkelberg	0.15	0.8	0.05	160	60	E,W	10	90	-	70	45	S,N		20	9	3
SG08	S Schwarzwald	0.15	0.8	0.05	160	60	E,W	10	90	-	70	45	S,N		20	9	3
SG09	W Schwarzwald	0.15	0.8	0.05	160	60	E,W	10	90	-	70	45	S,N		20	9	3
SG10	Rottweil	0.15	0.8	0.05	160	60	E,W	10	90	-	70	45	S,N		20	9	3
SG11	N Schwarzwald	0.15	0.8	0.05	160	60	E,W	10	90	-	70	45	S,N		20	9	3
SG12	Würzburg	0.15	0.8	0.05	160	60	E,W	10	90	-	70	45	S,N		20	9	3
SG13	Dreieck	0.15	0.8	0.05	160	60	E,W	10	90	-	70	45	S,N		20	9	3
SG14	Fränk.Alb	0.15	0.8	0.05	160	60	E,W	10	90	-	70	45	S,N		20	9	3
SG15	München	0.15	0.8	0.05	160	60	E,W	10	90	-	70	45	S,N		20	9	3
BG01	Bresse Graben	0.4	0.6	0	160	60	E,W	10	90	-	70	45	S,N		30	15	15
BG02	S_BresseGraben	0.4	0.6	0	160	60	E,W	10	90	-	70	45	S,N		30	15	15
AE01	BaselJura	0.1	0.6	0.3	150	60	NE,SW	0	90	-	80	45	SE		30	12	10
AE02	E_Jura	0.1	0.7	0.2	150	60	NE,SW	0	90	-	80	45	SE		30	12	10
AE03	Zürich-Thurgau	0.2	0.7	0.1	150	60	NE,SW	0	90	-	70	45	SE		30	12	10
AE04	Aarau-Luzern	0.1	0.8	0.1	150	60	NE,SW	0	90	-	60	45	SE		30	12	10
AE05	Biel	0	0.8	0.2	155	60	NE,SW	5	90	-	65	45	SE		30	12	10
AE06	Napf	0.1	0.8	0.1	155	60	NE,SW	5	90	-	65	45	SE		30	12	10
AE07	Fribourg	0.05	0.9	0.05	155	60	NE,SW	5	90	-	65	45	SE		30	12	10
AE08	Neuchâtel Lake	0	0.8	0.2	155	60	NE,SW	5	90	-	65	45	SE		30	12	10
AE09	Vaud	0.1	0.8	0.1	155	60	NE,SW	5	90	-	65	30	SE		30	12	10
AE10	Geneva	0.1	0.8	0.1	130	60	NE,SW	160	90	-	70	30	SE		30	12	10
AE11	Vuache	0.05	0.8	0.15	130	60	NE,SW	160	90	-	70	30	SE		30	12	10
AE12	Jura West	0.1	0.8	0.1	130	60	NE,SW	160	90	-	70	30	SE		30	12	10
AE13	Jura Center	0.1	0.8	0.1	150	60	NE,SW	0	90	-	60	30	SE		30	12	10
AC01	Grenoble	0.5	0.3	0.2	150	60	E,W	0	90	-	60	30	SE		15	9	4
AC02	Briançon	0.5	0.3	0.2	150	60	E,W	0	90	-	60	30	SE		15	9	4
AC03	Arve	0.1	0.8	0.1	150	60	E,W	0	90	-	60	30	SE		15	9	4
AC04	Préalpes	0.1	0.8	0.1	150	60	E,W	0	90	-	60	30	SE		15	9	4
AC05	Wildhorn	0.2	0.8	0	80	60	S	80	90	-	-	-	-		15	9	4
AC06	Valais	0.6	0.4	0	100	60	N,S	70	90	-	-	-	-		15	9	4
AC07	Sarnen	0.1	0.8	0.1	150	60	E,W	0	90	-	60	30	SE		15	9	4
AC08	Ticino	0.5	0.3	0.2	150	60	E,W	0	90	-	60	30	SE		15	9	4
AC09	Walensee	0	0.8	0.2	150	60	E,W	0	90	-	60	30	SE		15	9	4
AC10	Graubünden	0.3	0.7	0	160	60	E,W	20	90	-	-	-	-		15	9	4
AC11	Vorarlberg	0.3	0.7	0	170	60	E,W	10	90	-	-	-	-		15	9	4
AC12	Glorenza	0.5	0.3	0.2	150	60	E,W	0	90	-	60	30	SE		15	9	4
AC13	Allgäu	0.5	0.3	0.2	150	60	E,W	0	90	-	60	30	SE		15	9	4
AC14	Inntal	0.3	0.7	0	150	60	E,W	70	90	-	-	-	-		15	9	4
AC15	Tauern	0.5	0.3	0.2	150	60	E,W	0	90	-	60	30	SE		15	9	4
AI01	DoraMaira	0	0.6	0.4	-	-	-	60	90	-	10	45	E		37	18	10
AI02	Alpi Sud	0.333	0.334	0.333	0	60	E,W	30	90	-	90	45	S		37	18	10
AI03	Bolzano	0.333	0.334	0.333	170	60	E,W	20	90	-	80	45	S		37	18	10
PP01	Po Plain	0.333	0.334	0.333	rand	60	-	rand	90	-	rand	45	-		20	10	8

Table 3.2: Earthquake Rupture Parameters for EG1b Part 2.

Regroupings of "small scale " zones															
	style-of-faulting			Fault orientation									Depth (km)		
	%	%	%	Normal Fault			Strike Slip Fault			Thrust Fault					
label Name	Normal	Strike Slip	Thrust	Strike	dip	dip dir	Strike	dip	dip dir	Strike	dip	dip dir	max	peak	σ
Dinkelberg Area: Tucan beak															
SG5678	0.15	0.8	0.05	160	60	E,W	10	90	-	70	45	S,N	20	9	3
SG5_6_8		0.8	0.05	160	60	E,W	10	90	-	70	45	S,N	20	9	3
SG5_8	0.15	0.8	0.05	160	60	E,W	10	90	-	70	45	S,N	20	9	3
SG6_7	0.15	0.8	0.05	160	60	E,W	10	90	-	70	45	S,N	20	9	3
Basel area : Rhinozeros															
RG1_AE1	0.15	0.6	0.25	145	60	E,W	5	90	-	80	45	SE	26	13	5
AE1_2	0.1	0.6	0.3	150	60	NE,SW	0	90	-	80	45	SE	30	12	10
AE1_2_13	0.1	0.65	0.25	150	60	NE,SW	0	90	-	75	45	SE	30	12	10
AE1_13	0.1	0.7	0.2	150	60	NE,SW	0	90	-	70	45	SE	30	12	10
Schwäbisch Alp															
SG1_2	0.15	0.8	0.05	160	60	E,W	10	90	-	70	45	S,N	20	9	3

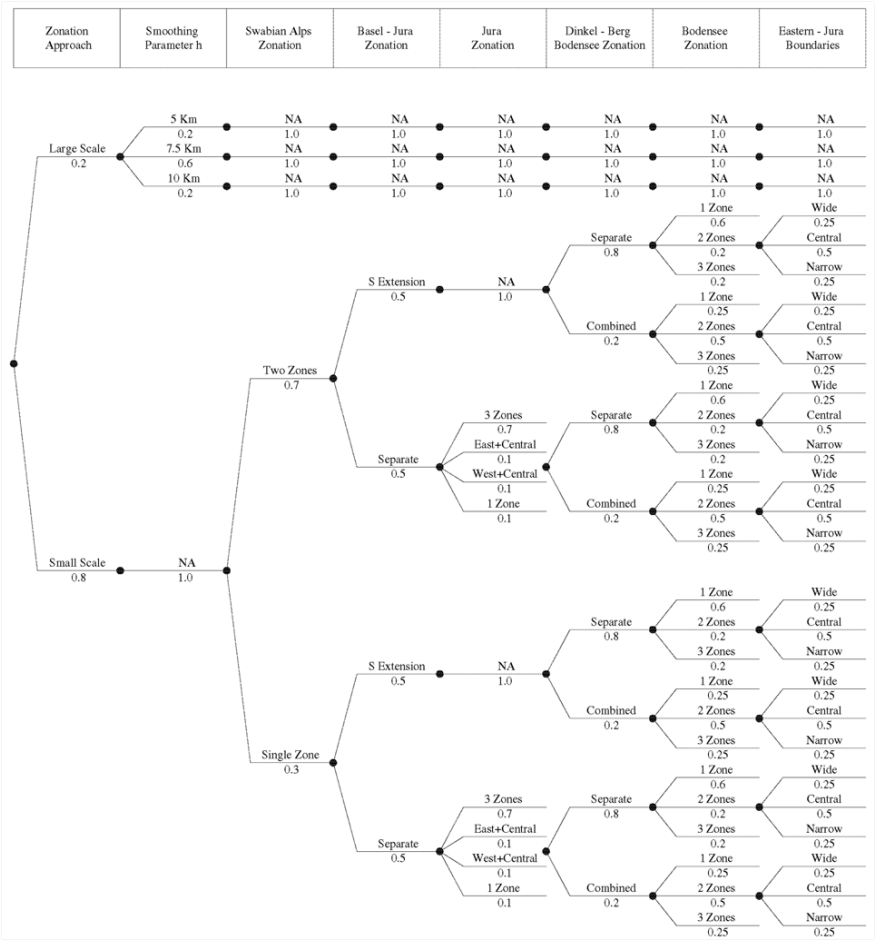

Figure 3.16: Logic tree for EG1b.

Chapter 4

QA-Certificate EG1-QC-1023

QA Certificate	PEGASOS REFINEMENT PROJECT
EG1-QC-1023	

Hazard Input Document (HID)

Expert group:	EG1b	*HID designation:*	EG1-HID-1002
Expert:	A. Cisternas, G. Grünthal	*Expert Model (EXM)*	EG1-EXM-1002

HID parameterisation of Expert Model:

TFI: N. A. Abrahamson *Hazard Input Specialist of TFI-team:* R. Youngs

HID based on Elicitation Documents: ☒ EG1-ES-1002

HID based on Exp. Assessments (EXA): ☐

Remarks on the HID model parameterisation in terms of hazard computation input:

The undersigned Hazard Input Specialist confirms that this HID includes all required (subproject specific) input information for hazard computations. No further interpretations of this input will be required and no simplifications except Algorithmic Pinching according to paragraph 2.9 of the QA-Guidelines will be applied to convert this HID into hazard software Input Files.

Signature:

HID acceptance by the Expert / Expert Group:

Date of HID review by the Expert / Expert group: Sept. 2011

HID accepted: ☒ *HID not accepted:* ☐

Reasons for non-acceptance of HID / Recommendations:

The undersigned Expert(s) accept(s) the parameterisation proposed in this HID as a faithful and adequate representation of his/their Expert Model. He/they confirm(s) that this HID is free of errors and agree(s) to its use as hazard computation input.

Signature Expert 1 / Expert:

Signature Expert 2:

Signature Expert 3:

Part IV

Assessments of EG1c

by R. Musson and S. Sellami Leinen

Chapter 1

EG1c Evaluation Summary (EG1-ES-1003)

1.1 SP1 Issues for ECOS-09

On March 31, 2010 the SP1 EG1c expert team provided its preliminary evaluations on the applicability of the SP1 EG1c PEGASOS model in the context of the new ECOS09. This report discusses the prospective changes, which might result from the new catalogue of the SED ECOS09. The catalogue ECOS09 [SED 2011], compared to ECOS02 [SED 2002] has been revised and extended with events from 2002 to 2008.

The revision consisted to a check of historical event, check of duplicates, calibration of historical events and conversion between M_L and M_W. This led to differences in magnitude and location of some of past events and to the addition of new events.

No new tectonic or geologic information was introduced, which might lead to significant difference of our logic-tree. The general framework of our elicitation is not influenced by these changes in the catalogue. We will look at the following points:

1. Zone boundaries
2. Declustering
3. Data completeness
4. Frequency-Magnitude parameters
5. M_{max} distribution
6. Depth distribution

How different is the catalogue ECOS09 compared to ECOS02?

1.1.1 Difference in Earthquake Locations

At a first glance, the difference on location between ECOS02 and ECOS09 on Figures 1.1 and 1.2 seems bigger than they are effectively. The main differences are for historical events and mainly for smaller events, less than 3. The main differences in instrumental time are outside Switzerland (in Italy). Often it is the result of a removed duplicate giving a factitious difference; this was checked on the list of differences larger than 10km.

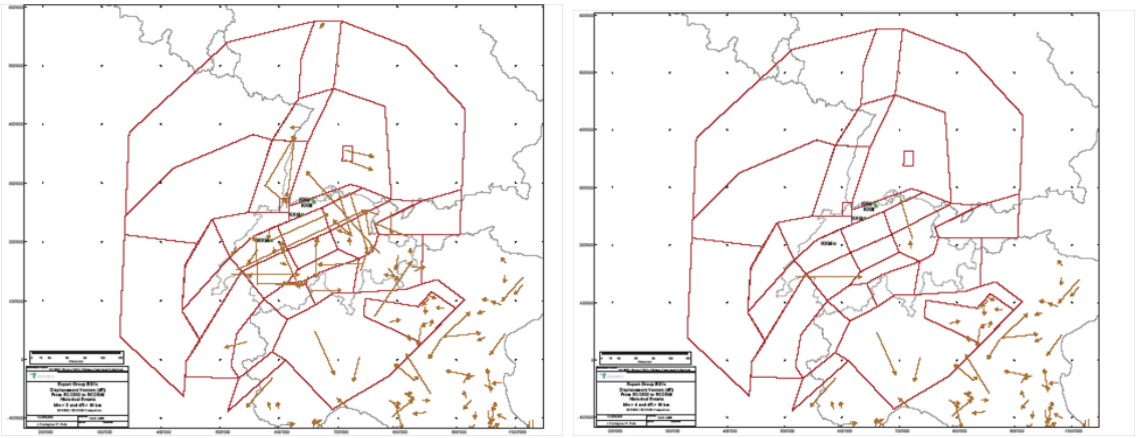

(a) $M_W > 3$ (b) $M_W > 4$

Figure 1.1: Location differences for historical events, Roth and Farrington [2010].

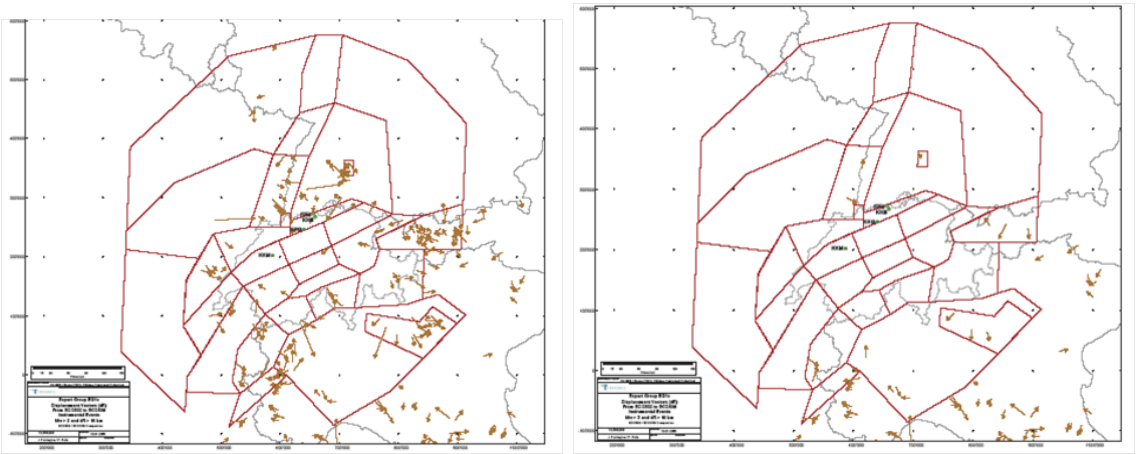

(a) $M_W > 2$ (b) $M_W > 3$

Figure 1.2: Location differences for instrumental events, Roth and Farrington [2010].

One could consider also the new events. There were no strong events with magnitude over M_W=4 since 2002 (Fig. 1.3). Because the location capability of earthquakes improved dramatically in the last year, one could consider whether alignments of smaller earthquake show patterns, which might modify the design of the zones. However, we did not identify any pressing cases. Some alignments are clearer than before in the Brig area, but these are far from the sites and not of great importance.

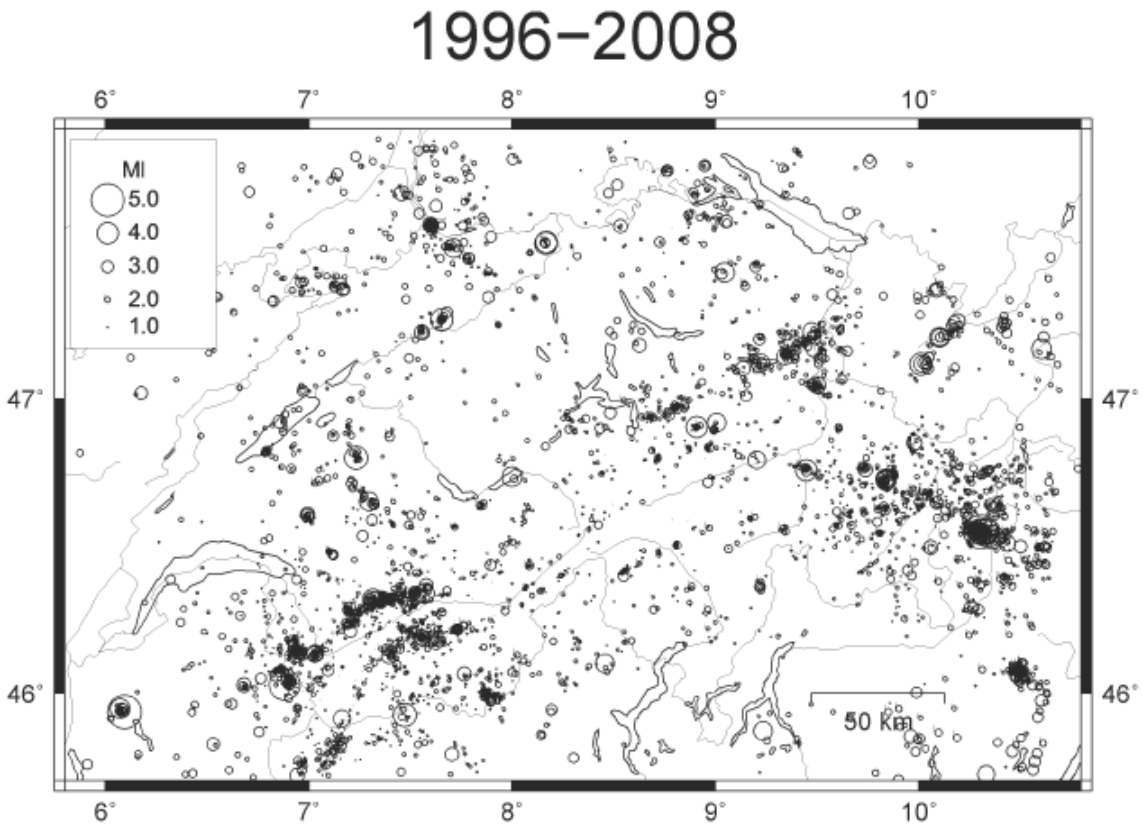

Figure 1: Epicenter map of all earthquakes (5574 events) with $M_L > 0$ in the SED data archive for the years 1996 – 2008.

Figure 1.3: Epicenter Map.

1.1.2 Differences in Magnitudes

There are three causes of difference in magnitude:

- The revision of the sources for historical events in the different catalogues.
- The calibration of historical events. The change of the calibration method induced a M_W magnitude in ECOS-09 which is often a bit smaller than the value in ECOS02. This is true for example for the Basel 1356 event, and the strong events in the Valais in the 18th, 19th and 20th centuries.
- The change in the conversion magnitude M_L to M_W.

The new conversion scheme from M_L to M_W is not linear. For a same value of M_L, the attributed M_W09 is different from the M_W02 depending of the original M_L value. A simulation compares these differences (Figure 1.4). This difference reaches 1 magnitude unit for M_L in the order of 0.2 and becomes very small at magnitude M_L about 2.7.

Ml synth.	Mw (Ecos02)	Mw (Ecos09)	Diff(Ecos09-Ecos02)
0.2	0.04	1.1	1.06
0.4	0.24	1.22	0.98
0.6	0.44	1.34	0.9
0.8	0.64	1.46	0.82
1	0.84	1.58	0.74
1.2	1.04	1.7	0.66
1.4	1.24	1.82	0.58
1.6	1.44	1.94	0.5
1.77	1.61	2.04	0.43
1.8	1.64	2.05	0.41
2	1.84	2.17	0.33
2	1.84	2.17	0.33
2.2	2.04	2.3	0.26
2.4	2.24	2.42	0.18
2.6	2.44	2.56	0.12
2.8	2.64	2.7	0.06
3	2.84	2.85	0.01
3.2	3.04	3.01	-0.03
3.4	3.24	3.17	-0.07
3.6	3.44	3.34	-0.1
3.8	3.64	3.52	-0.12
4	3.84	3.7	-0.14
4	3.84	3.7	-0.14
4.2	4.04	3.9	-0.14
4.4	4.24	4.1	-0.14
4.6	4.44	4.3	-0.14
4.8	4.64	4.5	-0.14
5	4.84	4.7	-0.14
5.2	5.04	4.9	-0.14
5.4	5.24	5.1	-0.14
5.6	5.44	5.3	-0.14
5.8	5.64	5.5	-0.14
6	5.84	5.7	-0.14
6.2	6.04	5.9	-0.14

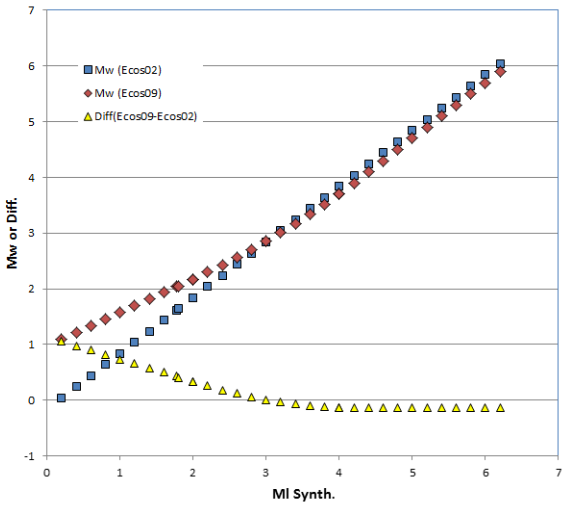

Figure 1.4: Comparison M_L/M_W.

The Figures 1.5 and 1.6 show the difference in magnitude value for historical events over magnitude 4 and instrumental with a magnitude over 3. Again the main differences are in the south of the area.

Revising the catalogue had as a consequence that the uncertainty in location and magnitude of the events increased in ECOS09 compared to ECOS02.

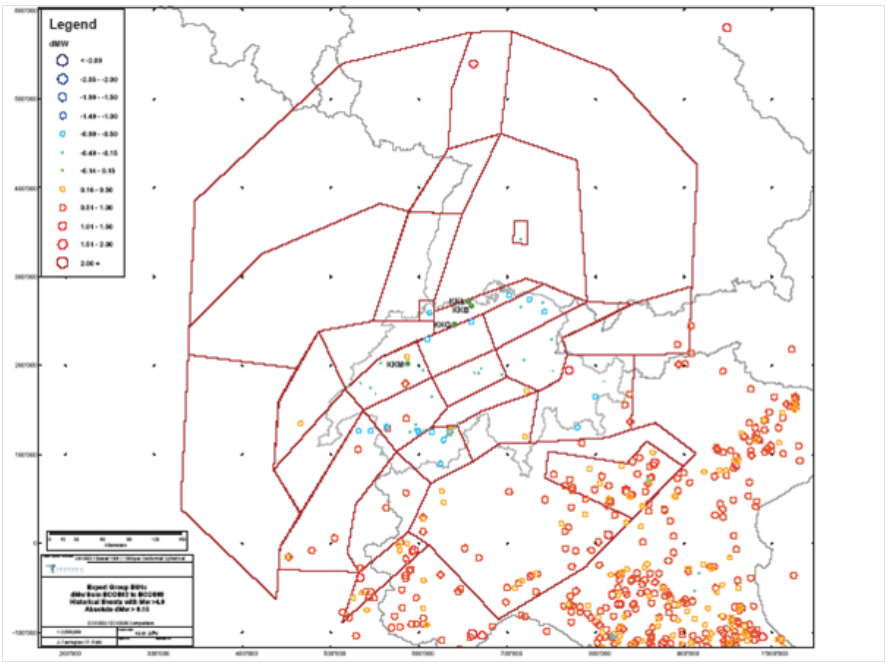

Figure 1.5: Magnitudes differences historical earthquakes with $M_W \geq 4$, Roth and Farrington [2010].

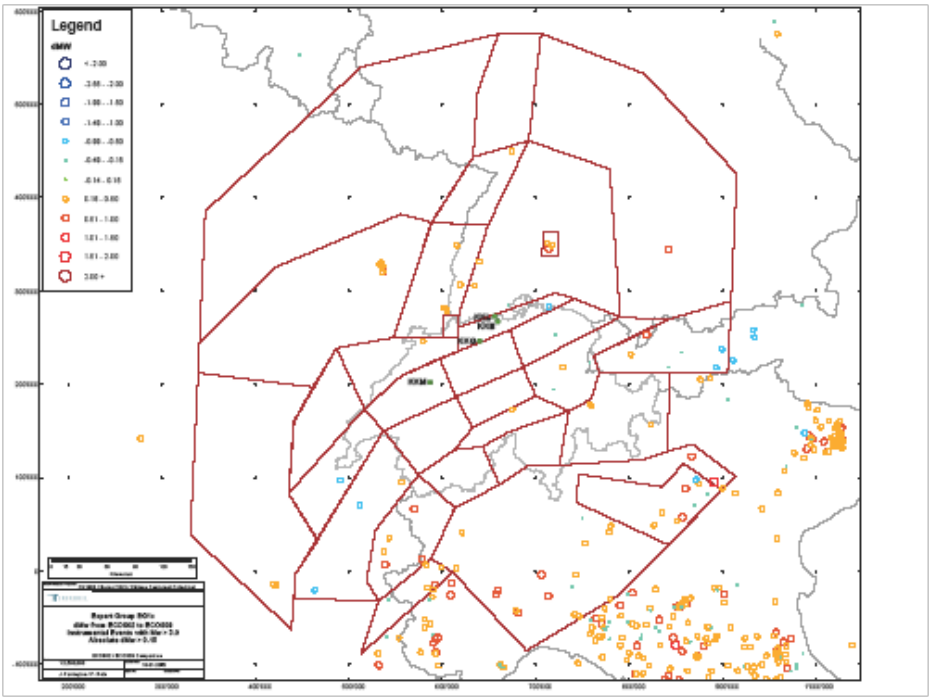

Figure 1.6: Magnitudes differences instrumental earthquakes with $M_W \geq 3$, Roth and Farrington [2010].

1.1.3 Zone Boundaries

In view of the previous information regarding the location of the events in the new catalogue, the report Roth and Farrington [2010] and the logic tree for source zone geometry shown in Figure 1.7, there is no need that our zone geometry is to be changed.

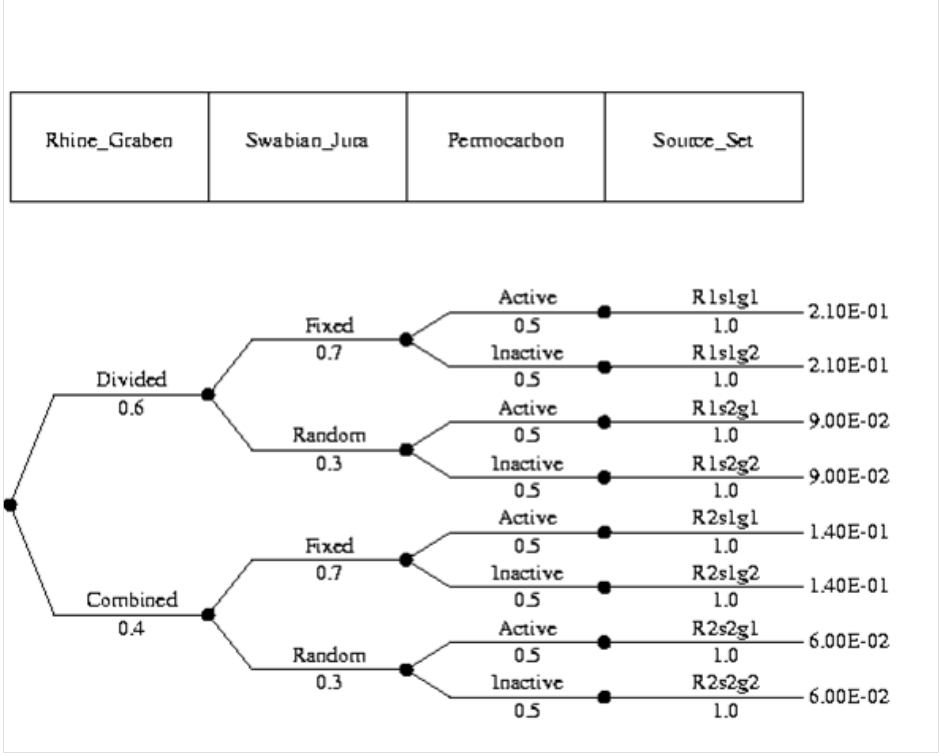

Figure 1.7: Logic tree for source zone geometry, Brüstle et al. [2003].

1.1.4 Declustering

We made a division of the catalogue into historical/modern for purposes of declustering, with the breakpoint being the beginning of 1970. The beginning of the modern period starts effectively in 1976. Neither that nor the changes in the catalogue have an influence and there is no need to change the declustering parameters. The actual declustering does have to be repeated on the new catalogue, and this has been done by r. Musson. The description of how it was done in the original report is unchanged.

1.1.5 Data Completeness

The main changes in the catalogues are for magnitude less than 3. The variation of completeness for event less than 3 is not so significant. One would either not change or keep the completeness time the same and adjust the magnitude based on the average change in the magnitude scaling. When evaluating the completeness of the most recent period, the bounds are 1961-1976 and than after 1976 (table 3 in elicitation report Brüstle et al. [2003]) this corresponds to the limit between historical and instrumental period.

Young's completeness plots (Figure 1.8 and 1.8) show some significant changes to completeness for events $\sim 4M_W$ in some cases. The reason appears to be that because of the changed

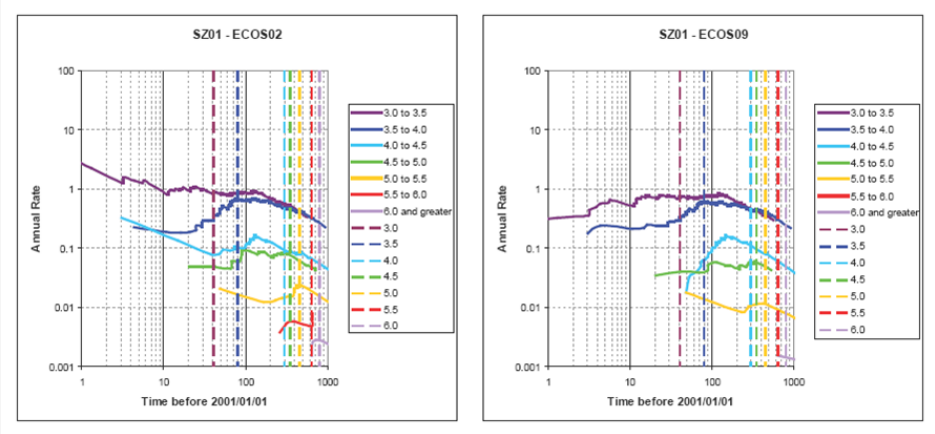

Figure 1.8: SZ01 Rheingraben and north-eastern of Switzerland, Roth and Farrington [2010].

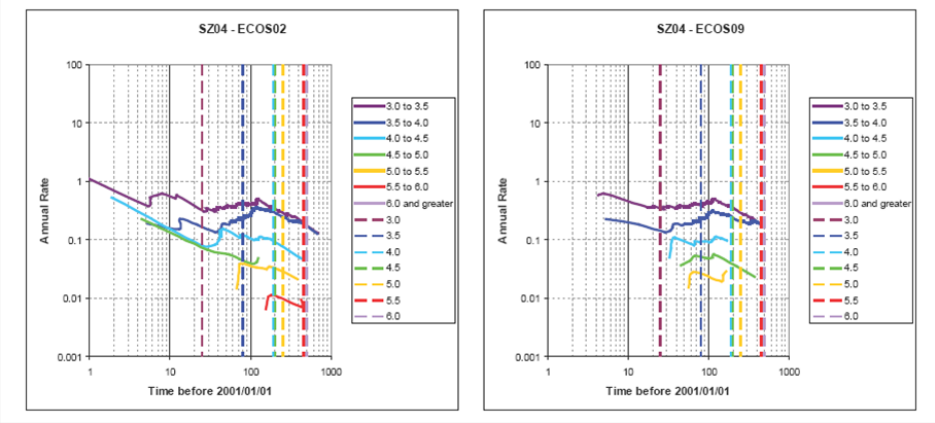

Figure 1.9: SZ04 Jura and north-western part of Switzerland, Roth and Farrington [2010].

magnitude scaling, events previously 4.0 are now 3.9. The difference between 3.9 and 4.0 is not significant regarding the uncertainty range and we do not need to change the completeness analysis. In the original report we gave the greatest weight to historical judgement as to what size of earthquake could not be missed, given the levels of documentation available in space and time. These have not changed as a result of any of the catalogue revisions.

1.1.6 Frequency-Magnitude Parameters

The recurrence rates are strongly influenced by the change in the catalogue. However it is mainly for magnitude range smaller than 3. We would like to limit the fit to $M > 2.7$ but have a evaluation of Gutenberg-Richter parameters for the different source zones. Because the catalogue has changed, the recurrence parameters all need to be recalculated, but we see no need to change the methods applied.

1.1.7 M_{max} Distribution

In the Figure 1.11 the logic tree and weights for the M_{max} evaluation in the elicitation of group EG1c are shown [Brüstle et al. 2003].

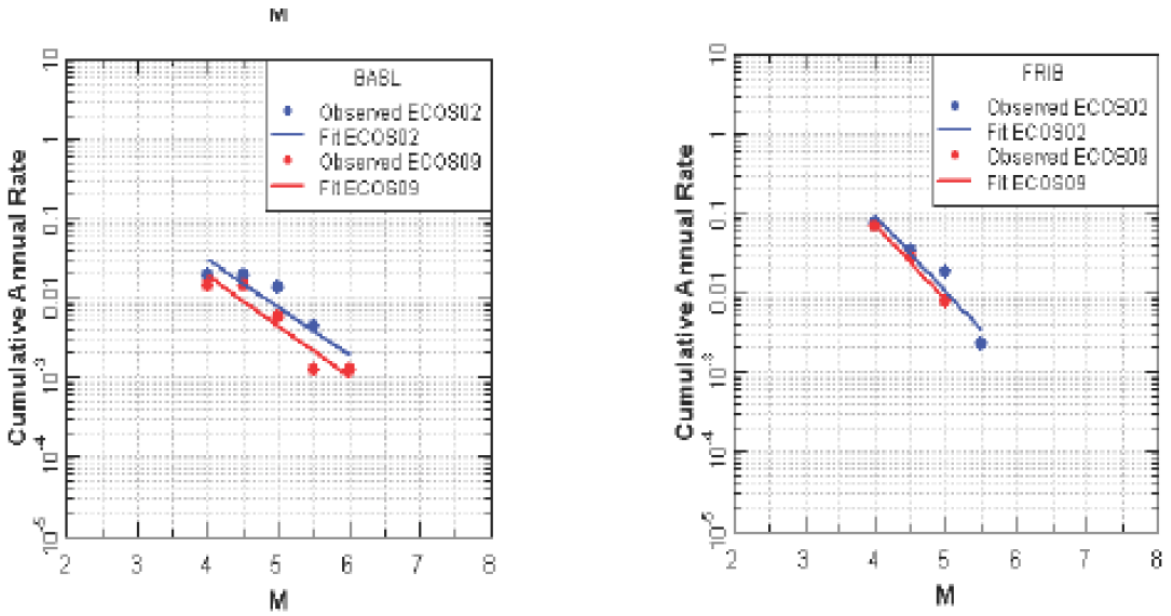

Figure 1.10: EG1C Method 2 Recurrence: Example fits to the cumulative occurrence frequencies, Youngs [2010].

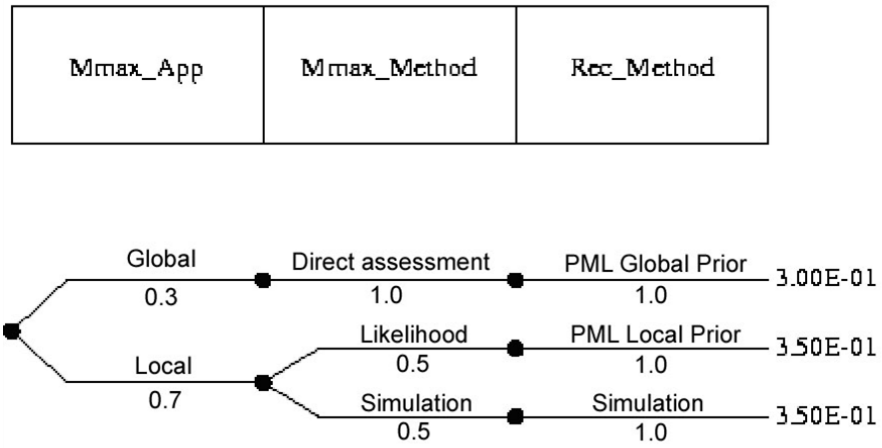

Figure 1.11: Logic tree and weights for M_{max} evaluation.

Table 1.1: Weights for M_{max} Brüstle et al. [2003].

Branch	M_{max} approach	M_{max}	M_{max} method	Recurrence method	Weight
A	Global distrib.	M6.5	Direct assessment	Likelihood distrib.	0.0375
A	Global distrib.	M7.0	Direct assessment	Likelihood distrib.	0.225
A	Global distrib.	M7.5	Direct assessment	Likelihood distrib.	0.0375
B	Local distrib.	from M5.5 or $M_{max-observed}$ to 7.25	Likelihood function	Likelihood distrib.	0.35
C	Local distrib.	from M5.5 or $M_{max-observed}$ to 7.25	Joint simulation	Joint simulation	0.35

The EG1C Method 2 for computing M_{max}, which consists of using the Bayesian approach with a non-informative prior-Used simulated catalogues to address uncertainty in size of large earthquake, was applied to the new catalogue [Youngs 2010]. The zones with a slight difference are away from the power plants. These are BRES and the zones in northern Italy.

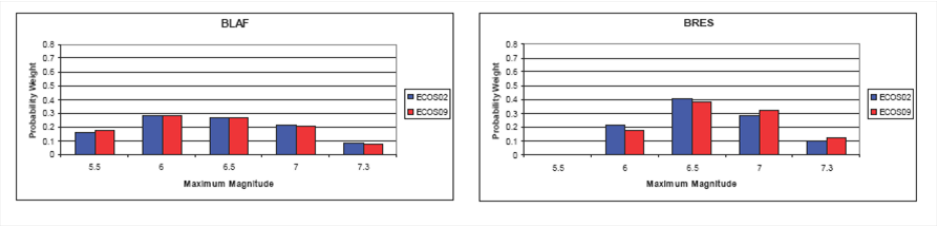

Figure 1.12: Maximum Magnitude distribution for BLAF and BRES.

Looking at the decision taken to evaluate M_{max} in our report Brüstle et al. [2003] and the differences resulting from the new catalogue, there is no change in the logic tree of M_{max} evaluation.

1.1.8 Depth Distribution

Regarding the report from Deichmann [2010] there are no significant changes since 2002, which would merit a revising our depth distribution.

Conclusion

Does the new catalogue imply that our zone geometry, or any of the procedures we describe for calculating parameters, need to be changed? No, except a re-calculation of the source zone parameters according to the new catalogue is obviously required. There are no changes to be applied in the logic tree or the procedures to calculate the parameters, nor to the basic source model.

1.2 Revision of the EG1c Model

On February 10, 2011 the SP1 EG1c expert team provided their final evaluations. This section presents the last changes applied to the source zones and parameters obtained by the group EG1c of the PEGASOS Project. These changes are a consequence of the revision of the catalogue of the SED ECOS09 and subsequently the from the revision of elicitation of the of group EG1c.

1.2.1 Frequency-Magnitude Parameters, Organization of the Logic Tree

The logic tree for the recurrence parameters had three main branches:

- Penalized maximum likelihood,
- Least square method and
- Simulation method.

The three main branches of the logic tree link estimation of M_{max} with estimation of other seismicity parameters in a dependent way.

Branch A: Penalized Maximum Likelihood The first approach consists of a directly assessed single distribution for maximum magnitude that is applied to all zones (see section 6.1.1 of the Elicitation report Brüstle et al. [2003]). The accompanying joint distributions for beta [b-value $\times \ln(10)$] and N ($M_W \geq 5$) are determined using a maximum likelihood formulation for an exponential distribution and computing relative likelihood. A prior of 0.9 (based on the global b value for the whole catalogue) was applied to all zones, with a weight of 50%. This approach is presented as three sub-branches in table 9 of Brüstle et al. [2003], because, at least in principle, the resulting values are dependant on the M_{max} value chosen. In practice here, because the M_{max} values are all rather high compared to historical experience, there is no actual difference in the distributions computed for the different M_{max} values.

Branch B: Least Squares/Maximum Likelihood Method Here the distributions were computed using the same maximum likelihood as in Branch A, with this difference - instead of a moderate prior derived from the whole catalogue, strong (weight 100%) local priors were used for each zone, derived from the b value estimates that were obtained from a least squares analysis.

Branch C: Simulation Method This approach consists of the results of a joint Monte Carlo simulation of $N(m \geq 5)$, b-value, and M_{max}. This was made by specifying a parameter search space for each zone (activity, b-value and M_{max}), choosing values at random within this space, generating a synthetic catalogue subject to the same historical completeness constraints, and comparing the result to the historical outcome. In some cases, the amount of data above magnitude 4.0 M_W was not enough for good estimates of parameters and the lower magnitude threshold was reduced from 4.0 M_W to 3.0 M_W. The analysis of each zone provides a very large set of logic-tree branches for M_{max}, b value and activity rate (i.e. one branch per triplet of values). The number of branches varied between 30 and 180 per zone. The method is described in Musson [2004].

Although it seems that an advantage of this method is that it is entirely driven by the data, and results are based on what values are shown to be feasible parameters that could result in the historical outcome we have decided to discard this branch in the Refinement Project.

Trimming of the Branch C

The principal difference in approach between branches A and B relates to the difference between a general maximum likelihood approach and a more locally-oriented approach achieved by seeding the maximum likelihood method with local priors from least squares analysis. Therefore, Branch A combines a global, conservative approach to maximum magnitude with a more generalized approach to recurrence (meaning, all earthquakes are considered equally weighted). Branch A also uses a slightly higher M_{max} than the other branches, and therefore "traps" the low possibility that a larger earthquake may occur than is supported by the other branches.

Branch B, on the other hand, represents an attempt to tackle each zone in a more precise and local-specific way, with individually determined maximum magnitude values, and recurrence

parameters estimated in a way that is relatively more sensitive to the occurrence of larger earthquakes in each zone. Finally, Branch C treats all the zones in a way that is entirely driven by the local data, without preconceptions as to what the results "should" be, and completely accepting the uncertainty as to all the possible distributions of parameters.

The results for the distribution of b values using the three branches were compared and shown in figure 17 of the original elicitation report (Version 4, PEGASOS 2004). The three maps were different, which is a good indication of the overall uncertainty in this parameter. Branch A had the least variation, which is, as it should be considering that a global prior was applied to all zones. Similarly Branch B has the most extremes, reflecting the influence of the least squares method. It also has a tendency for lower b values overall. Branch C is perhaps the most objective one and the result are covered by the two other branches.

From a sensitivity analysis perform by Ph. Roth, it appeared that the results are not sensitive to the choice of the branch C. This branch arrives at a maximum likelihood solution by different means. It also produces a huge number of branches that require effort in trimming when the hazard is calculated using FRISK.

For the choice of M_{max} approach and distribution, the branch C is equivalent to branch B, only used in the joint "simulation". So it is an alternative to "likelihood" branch B in the logic tree for the M_{max} Method and the effect of this branch is not so significant. This has been shown from sensitivity test presented by G. Toro and Ph. Roth at PEGASOS feedback meetings.

Because this branch has no influence to the hazard, it serves no particular purpose and is largely duplicates by the other branches. It is legitimate, in the refinement step to strive this branch, which only increases the amount of sub-branches and calculation time without any reasonably contribution to the hazard.

Logic Trees and Weights

In the previous assessment, the branch C gave result which range was covered by the branches A and B. It is not necessary in the new calculation to run this branch. The weight of this branch has been redistributed almost equally to the two other branches to keep their relative balance. This has the effect to change the weight of the global/local Maximum magnitude approach. The new weights are listed in the Figure 1.13 and table 1.2 below.

Table 1.2: Details of the new weights for the frequency magnitude parameters.

Branch	M_{max} **approach**	M_{max}	M_{max} **method**	**Recurrence method**	New Weights
A	Global distrib.	M6.5	Direct assessment	Likelihood distrib.	0.05
A	Global distrib.	M7.0	Direct assessment	Likelihood distrib.	0.35
A	Global distrib.	M7.5	Direct assessment	Likelihood distrib.	0.05
B	Local distrib.	from M5.5 or $M_{max-observed}$ to 7.25	Likelihood function	Likelihood distribution	0.55

1.2.2 Conclusion

The new catalog does not imply that our zone geometry, or the main procedures we describe for calculating parameters, need to be changed. A re-calculation of the source zone parameters according to the new catalogue was performed. A minor change has to be apply in the logic tree for frequency-magnitude branches describing M_{max} evaluation and a and b determination.

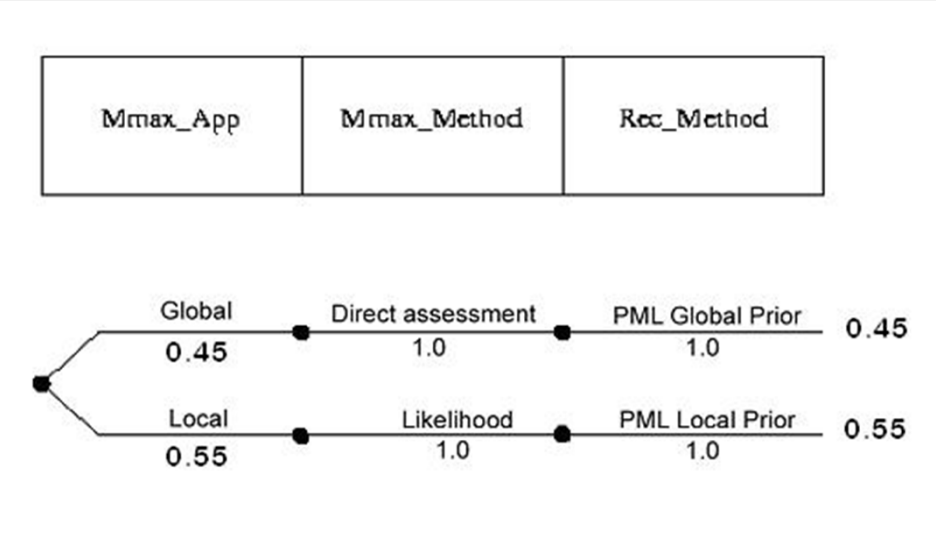

Figure 1.13: Revised sub-logic tree for the frequency magnitude parameters.

It consists of the trimming of branch C and the application of new weights on the remaining branches

1.3 Calculations with Final ECOS09 Catalog

1.3.1 Completeness Zone Recurrence Calculations

Calculations were made for the individual completeness regions and the entire study region using maximum likelihood [Youngs 2011]. The declustered version of the final ECOS09 catalog provided by Roger on October was used for the calculations. The map of the completeness regions is shown on Figure 1.14. The calculations were performed using the completeness intervals specified in PEGASOS extended to January 1, 2009 using the original 1/2 unit magnitude intervals starting with M 3.0. Figures 1.15 through 1.18 show the results for the individual completeness regions and for the entire study region. Two results are presented for the study region, one based on a assuming a homogeneous b-value and seismicity rate and one based on allowing the seismicity rate to vary among completeness regions while assuming a homogeneous b-value for the entire study region. These two approaches produce nearly the same b-value (see Figure 1.18) which is essential 0.9, unchanged from PEGASOS. As the regional b-value 0.9 have been used in the following calculations.

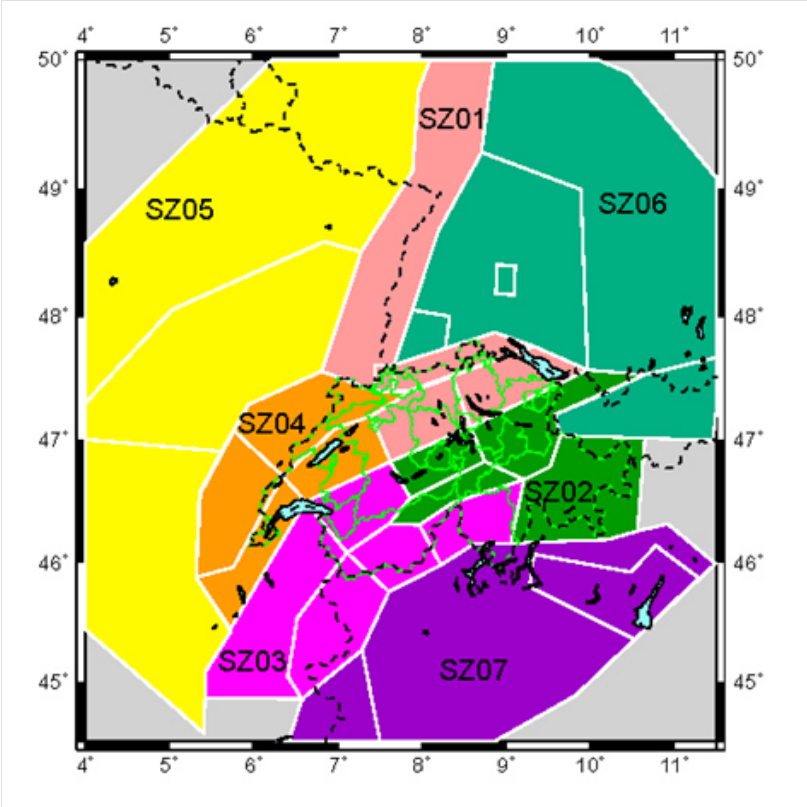

Figure 1.14: Map of EG1c Completeness Regions.

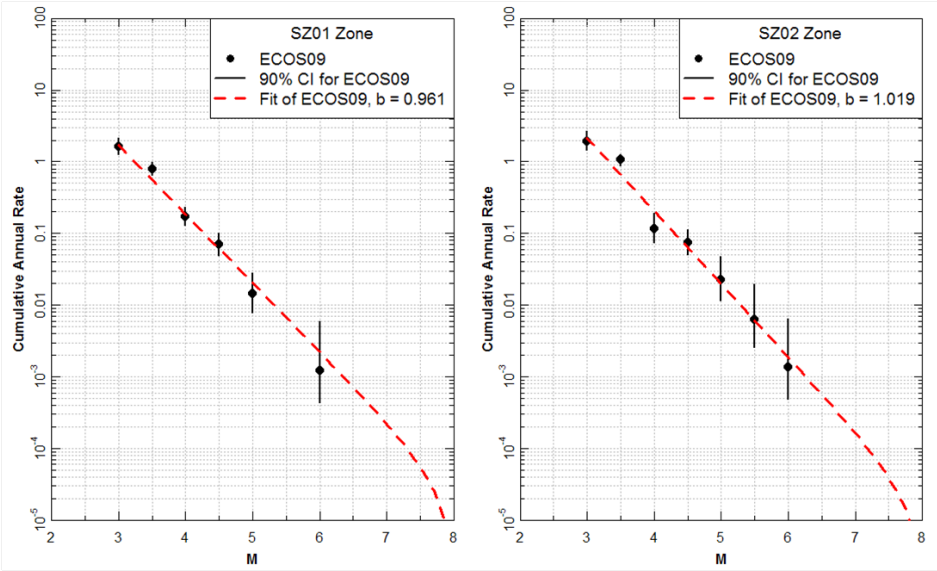

Figure 1.15: Recurrence relationships for SZ01 and SZ02.

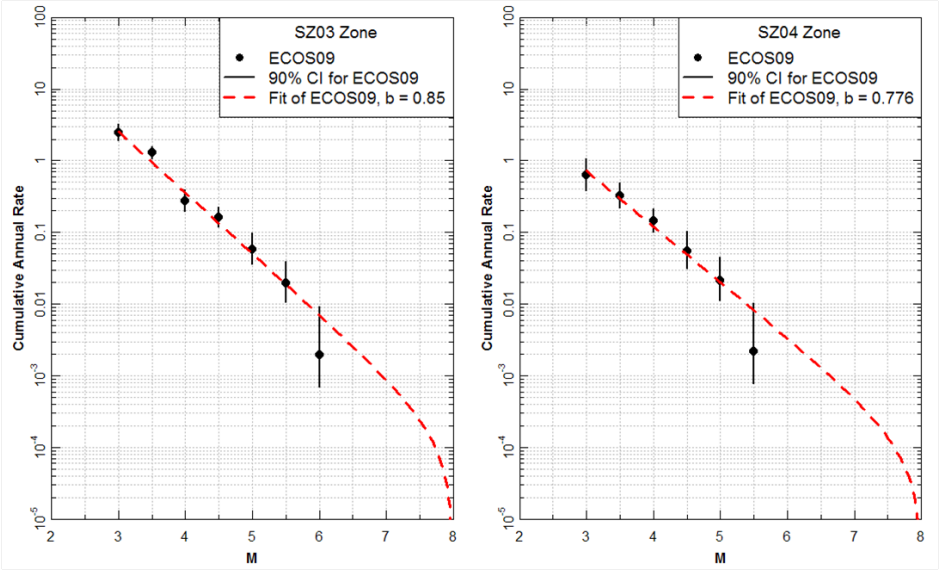

Figure 1.16: Recurrence relationships for SZ03 and SZ04.

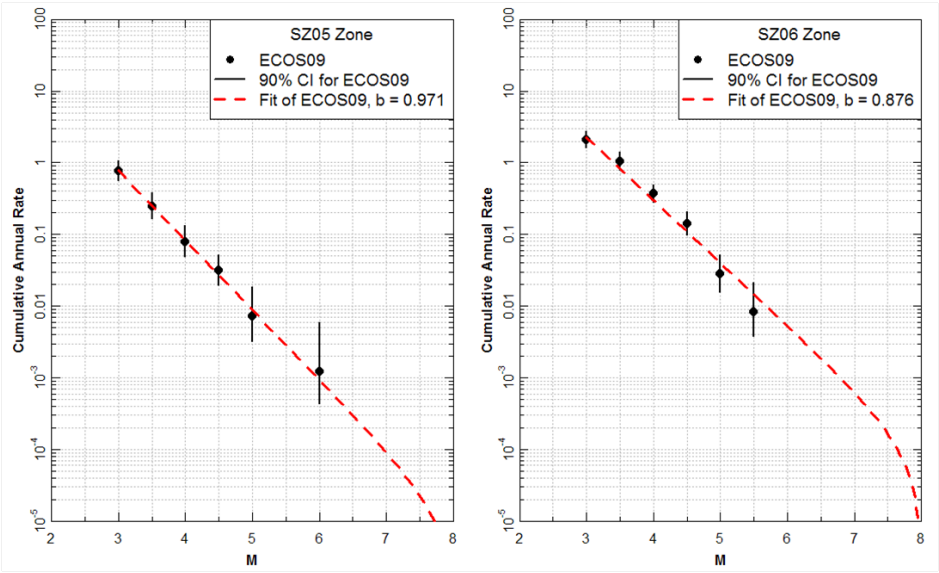

Figure 1.17: Recurrence relationships for SZ05 and SZ06.

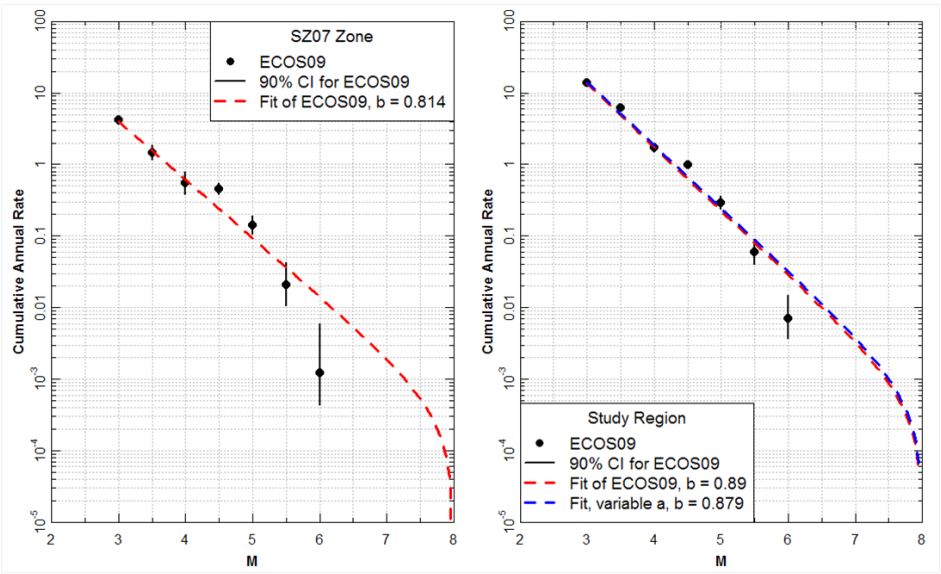

Figure 1.18: Recurrence relationships for SZ07 and Study Region.

1.3.2 M_{max} for Branch B

The table 1.3 lists the M_{max} distributions computed for the Branch B approach (uniform prior updated using likelihood function). These values were computed using a global b-value of 0.9.

Table 1.3: M_{max} for Branch B.

Source	Max Observed	Weight Assigned to Maximum Magnitude of: 5.5	6	6.5	7	7.3
ALCM	5	0.172277	0.285997	0.261982	0.203875	0.07587
ALMA	5.67		0.733791	0.191581	0.057067	0.017561
BASL	6.6				0.518496	0.481504
BAVA	5.4	0.200545	0.297069	0.250891	0.184266	0.067229
BAW2	5.6		0.320216	0.381258	0.222002	0.076524
BAWU	5.6		0.336557	0.372081	0.216876	0.074486
BW2S	5.6		0.230823	0.386021	0.280501	0.102655
BAWS	5.6		0.23684	0.386059	0.276393	0.100709
BLAF	4.5	0.161291	0.282121	0.267643	0.210422	0.078523
BRES	6		0.221506	0.405181	0.274897	0.098416
DAUP	5.36	0.216789	0.294626	0.240762	0.181065	0.066758
FRIB	5.2	0.256467	0.296481	0.223395	0.163726	0.05993
GARD	6.05			0.464085	0.414716	0.121199
GENV	5.6		0.252056	0.383736	0.267441	0.096766
GLAR	5.1	0.260946	0.297715	0.221373	0.161117	0.058849
GRAU	6.2			0.357632	0.476713	0.165655
HELV	5.8		0.30342	0.375117	0.237591	0.083872
JURA	5.4	0.148756	0.288266	0.27729	0.208745	0.076943
LORA	5.4	0.17469	0.307503	0.25615	0.191343	0.070314
MOMI	4.4	0.167763	0.284749	0.264289	0.206347	0.076852
NIDW	5.9		0.258445	0.397803	0.254051	0.089702
NSPG	4.2	0.176556	0.286642	0.260261	0.201617	0.074923
PENV	6.2			0.355286	0.479439	0.165275
POVA	5.67		0.401983	0.352242	0.184078	0.061697
RHEG	5.4	0.345418	0.318898	0.181163	0.114328	0.040191
RHGC	5.4	0.219626	0.290223	0.249853	0.17631	0.063989
RHGN	4.7	0.199598	0.295442	0.248837	0.187122	0.069002
RHGS	5	0.225859	0.299188	0.23762	0.173744	0.063589
SAVO	5.8		0.337026	0.375604	0.213803	0.073567
SBRE	5.4	0.21157	0.31238	0.241072	0.172228	0.06275
SJUR	4.3	0.152673	0.279275	0.271833	0.215575	0.080643
SWAB	5.5	0.334656	0.331405	0.178831	0.114649	0.04046
TICI	4.3	0.15985	0.281597	0.268355	0.211309	0.078889
TYRO	5.5	0.400163	0.277263	0.166532	0.114737	0.041305
ZURI	5.1	0.245151	0.298141	0.228286	0.167232	0.06119
ZUR2	5.1	0.277808	0.298654	0.214	0.153641	0.055898

1.3.3 Individual Zone Recurrence for Branched A and B

The PEGASOS recurrence parameters for the individual zones were computed using Maximum Likelihood using priors on b-value that were global (Branch A) or local based on Least Squares fits to the individual zone data (Branch B). The following set of plots shows the fits to the data for individual source zones. Presented for each zone are: a M_L fit **without a prior** (M_L, red curve), a maximum likelihood fit with a b-value prior of 0.9, weight 50% (MLP, green dashed curve) and a least squares fit using all data from M 3.0 and above (LS, blue curve). These results were presented so that EG1c could evaluate any changes to the approach they may want to make on a zone by zone basis. Afterwards, everything was rerun using EG1c's final decisions.

It should be noted that for the SJUR zone R. Youngs extended the lower magnitude bin to M 2.7-3.5 as there are no earthquakes in the M 3.0-3.5 bin.

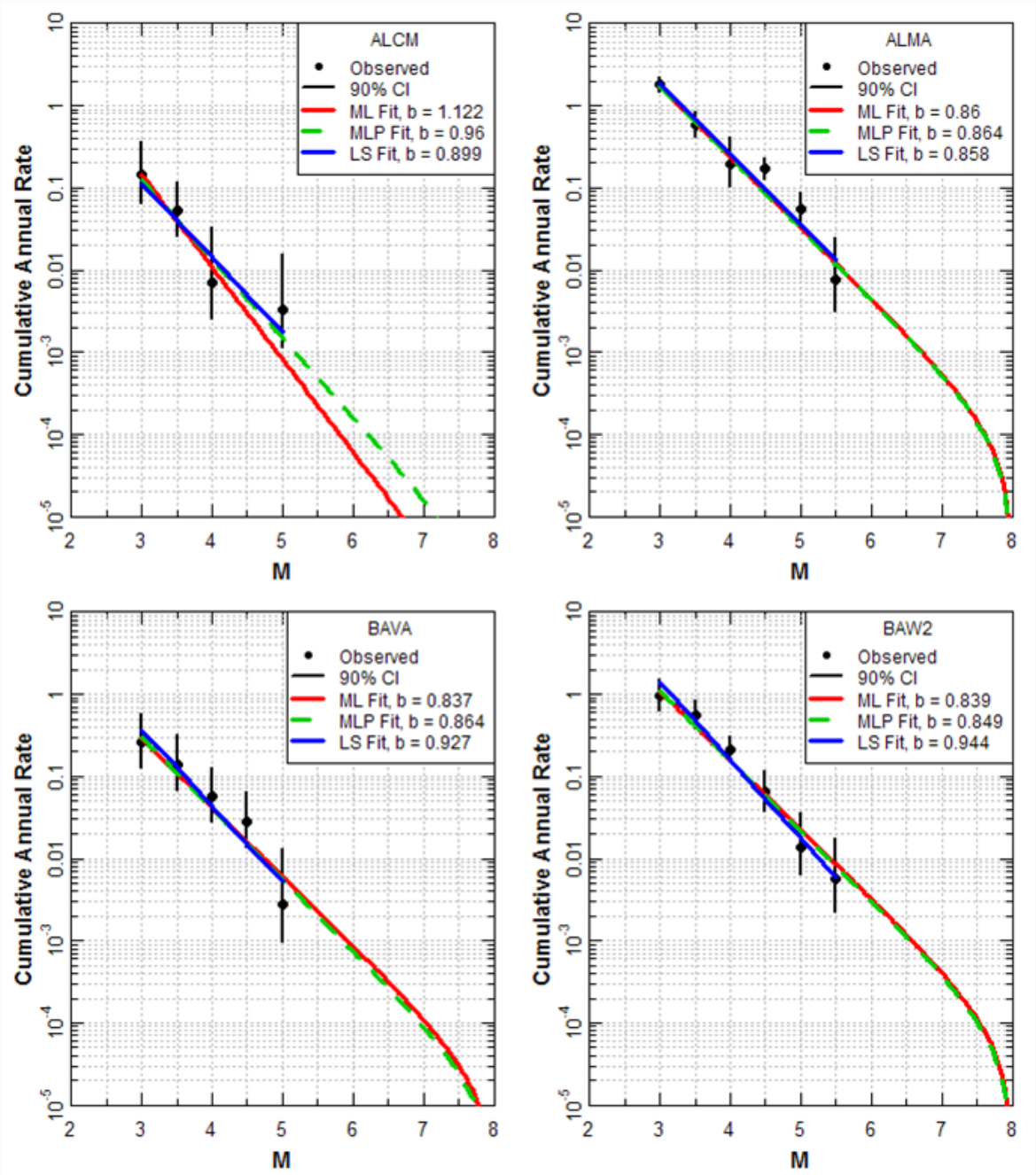

Figure 1.19: Zone Recurrence Plot 1.

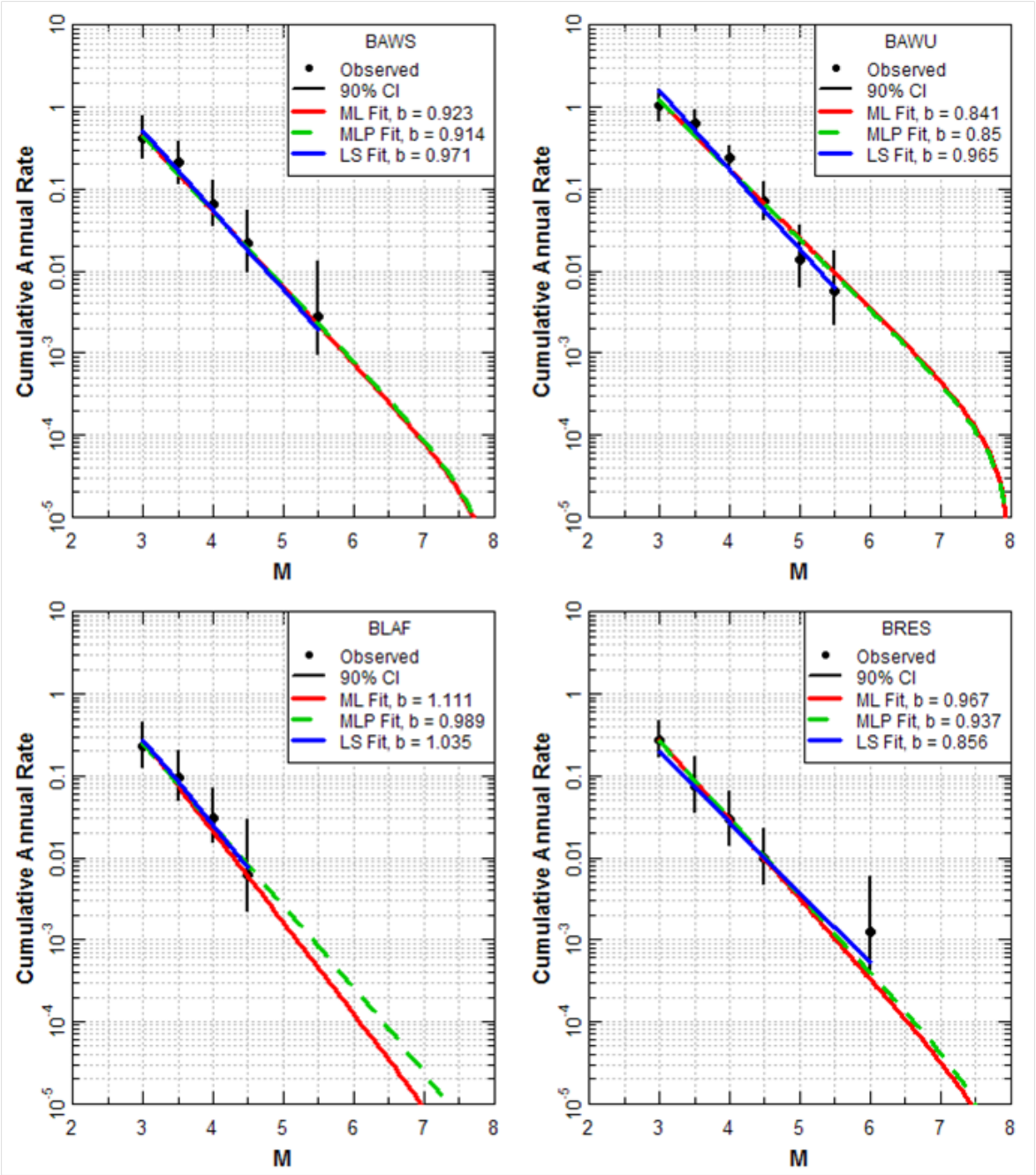

Figure 1.20: Zone Recurrence Plot 2.

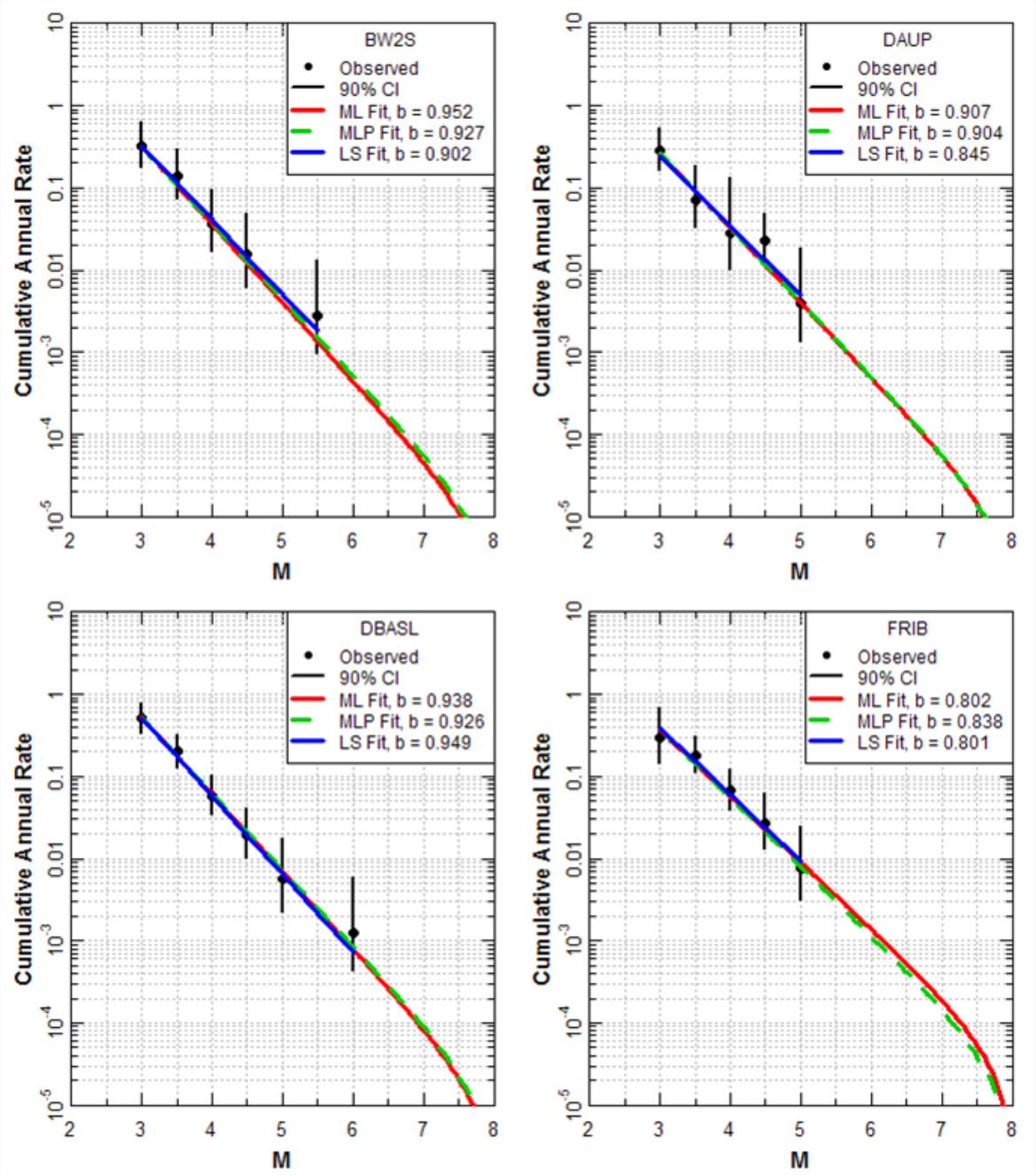

Figure 1.21: Zone Recurrence Plot 3.

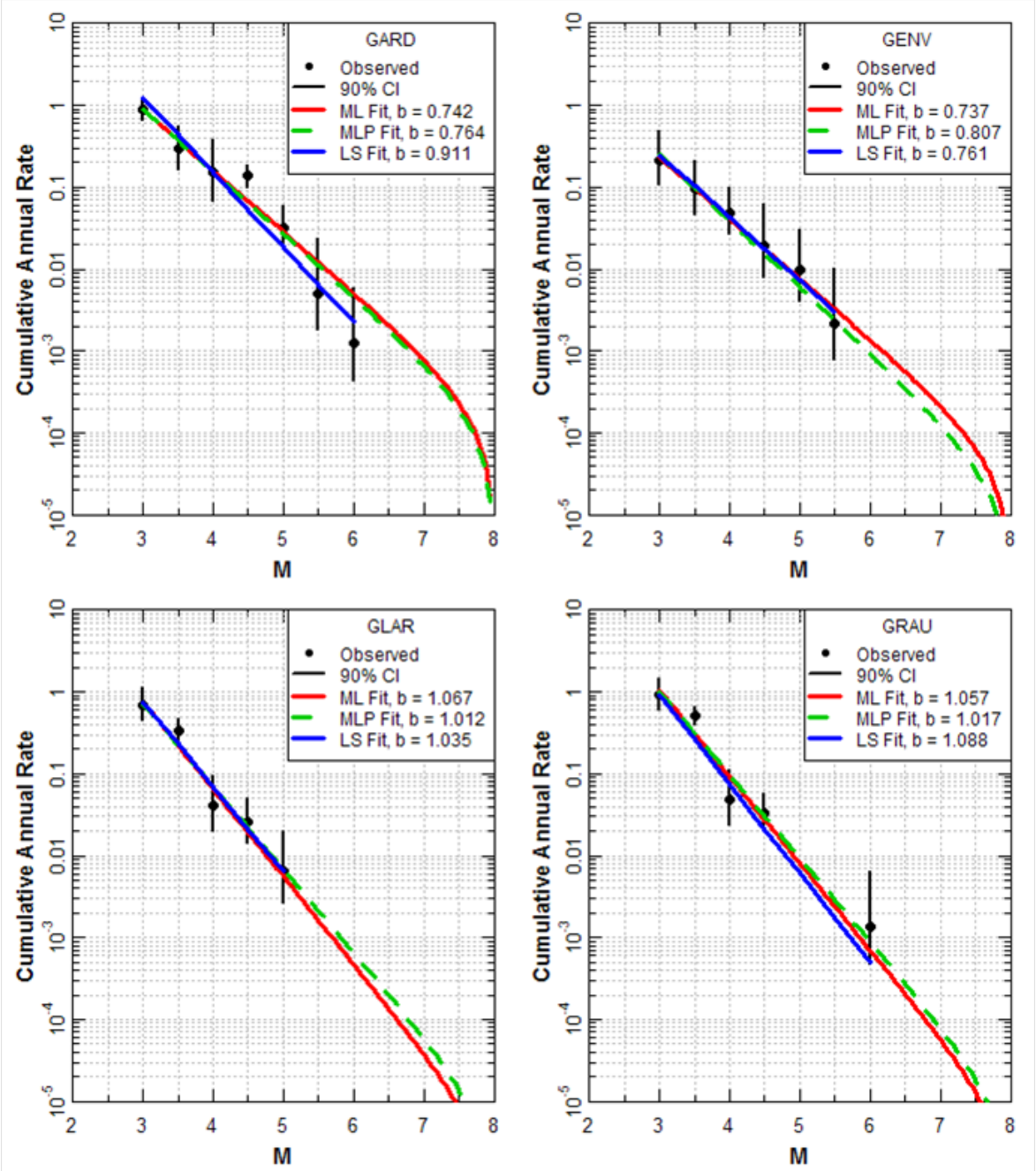

Figure 1.22: Zone Recurrence Plot 4.

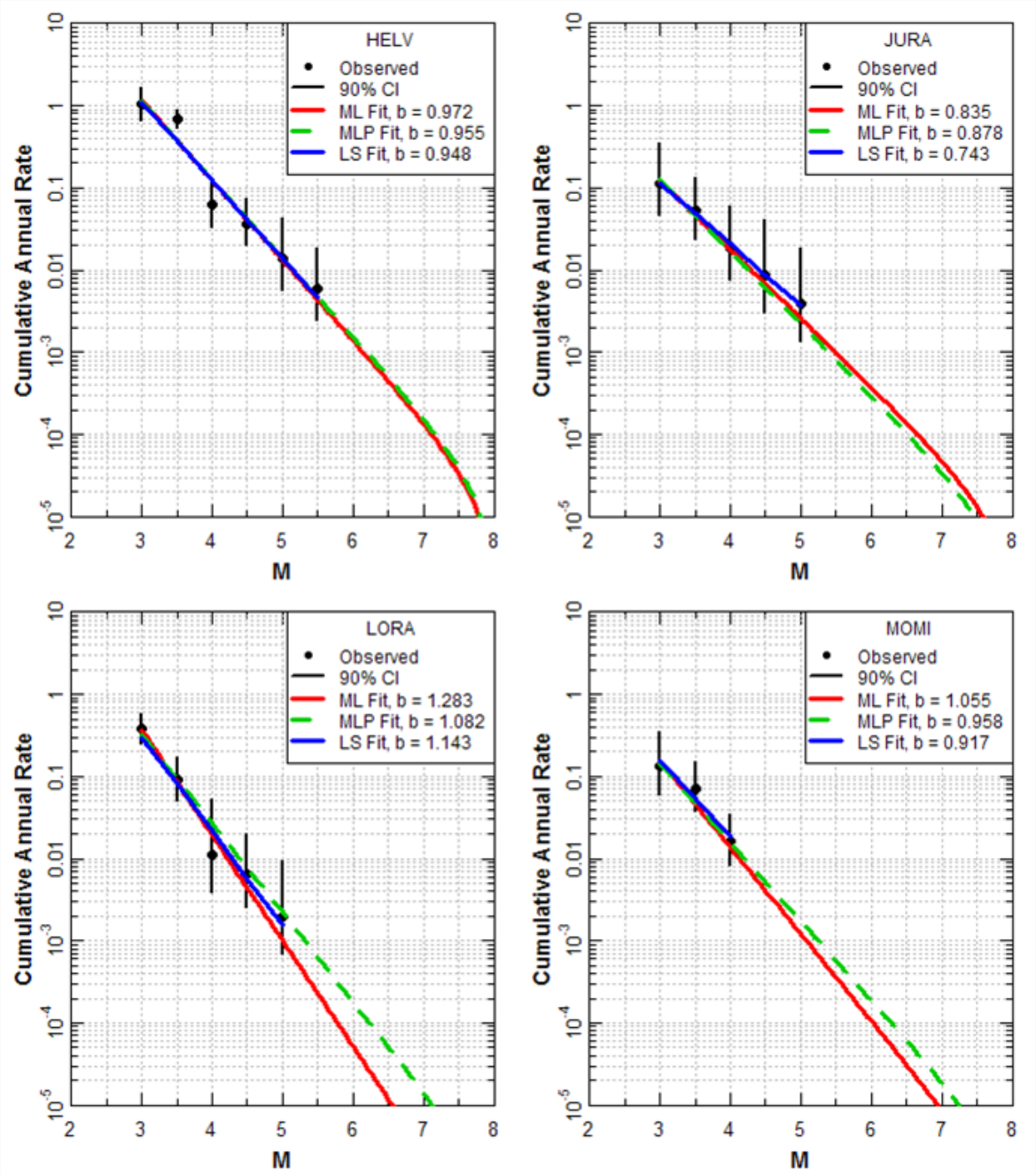

Figure 1.23: Zone Recurrence Plot 5.

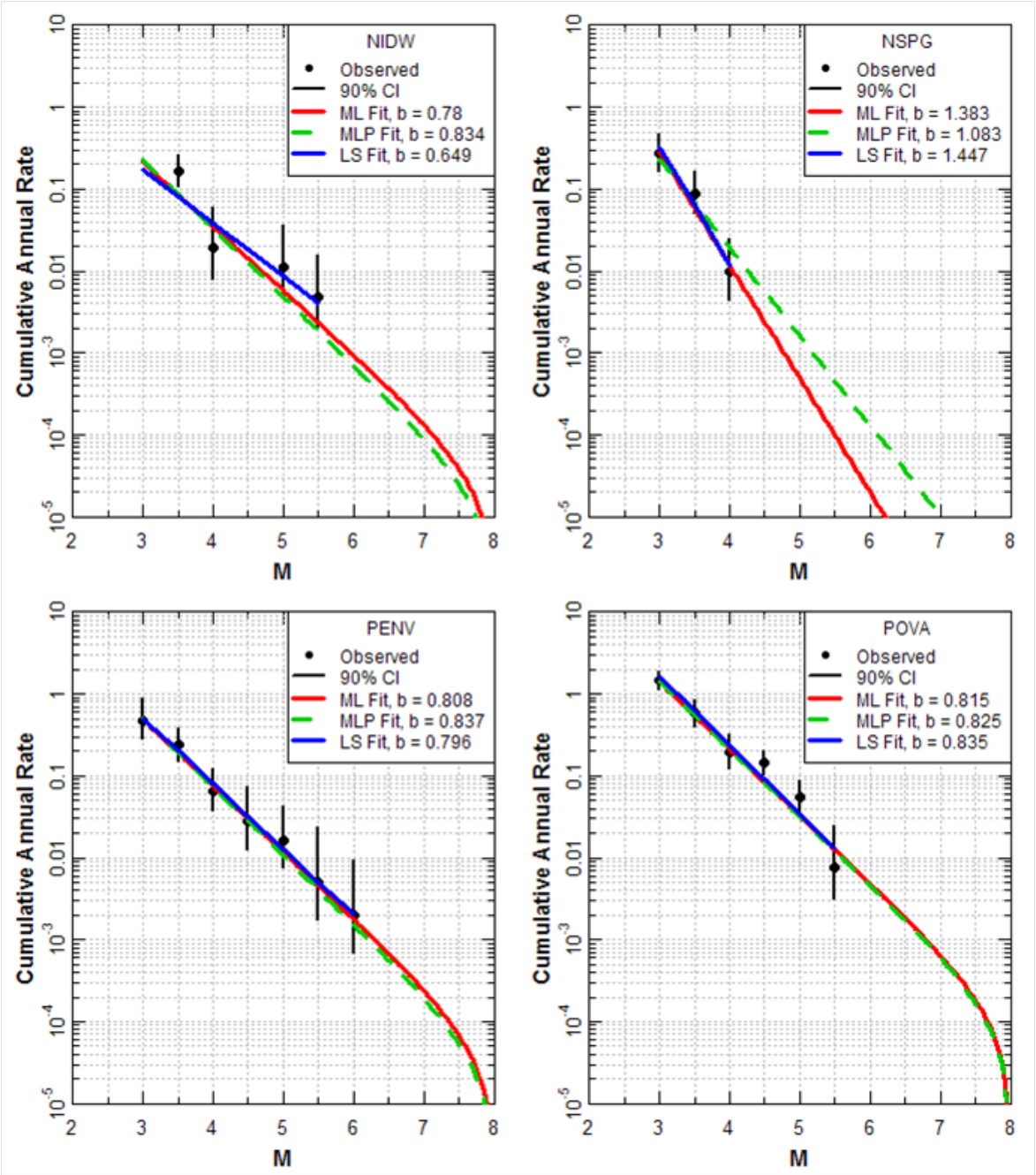

Figure 1.24: Zone Recurrence Plot 6.

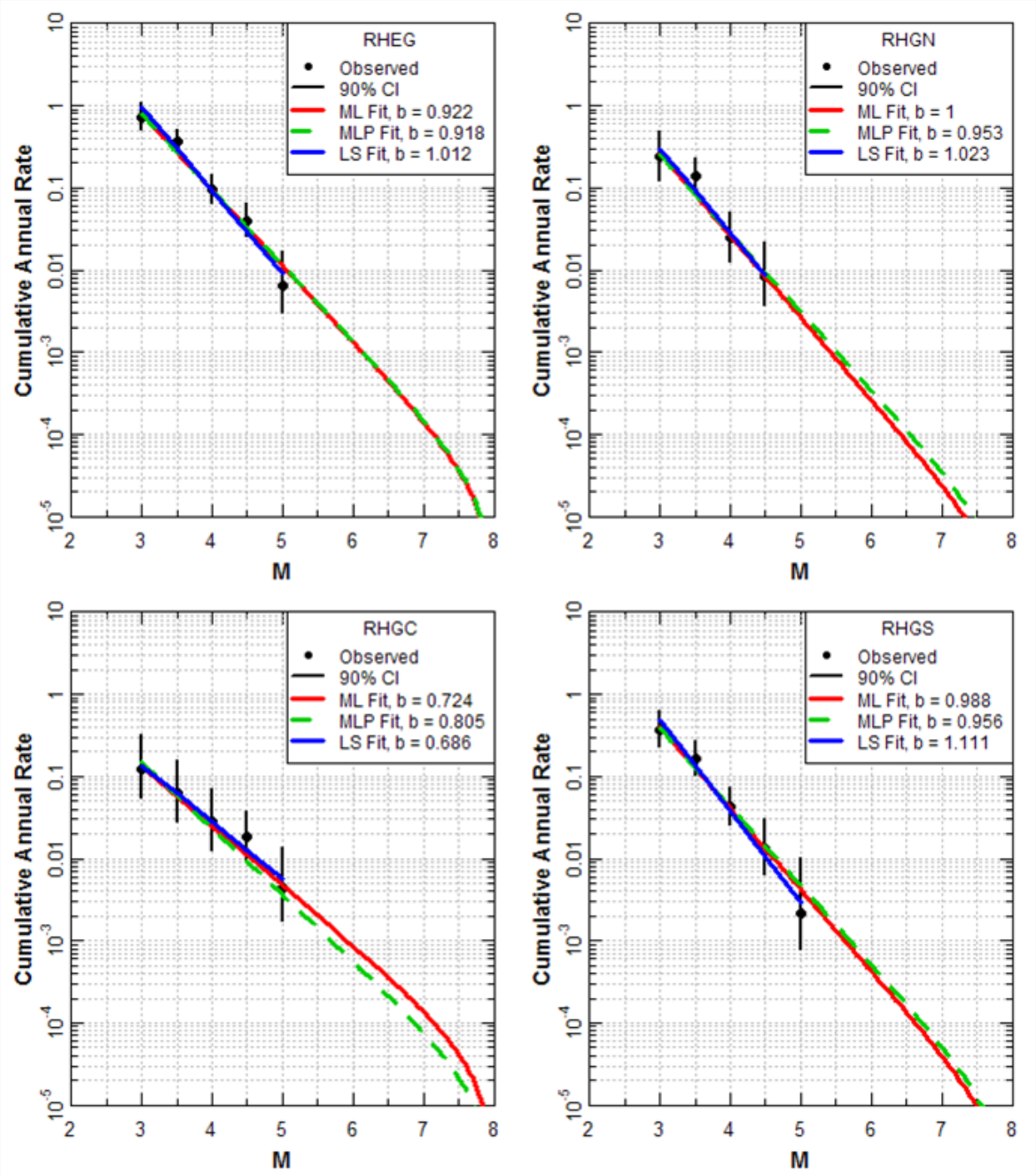

Figure 1.25: Zone Recurrence Plot 7.

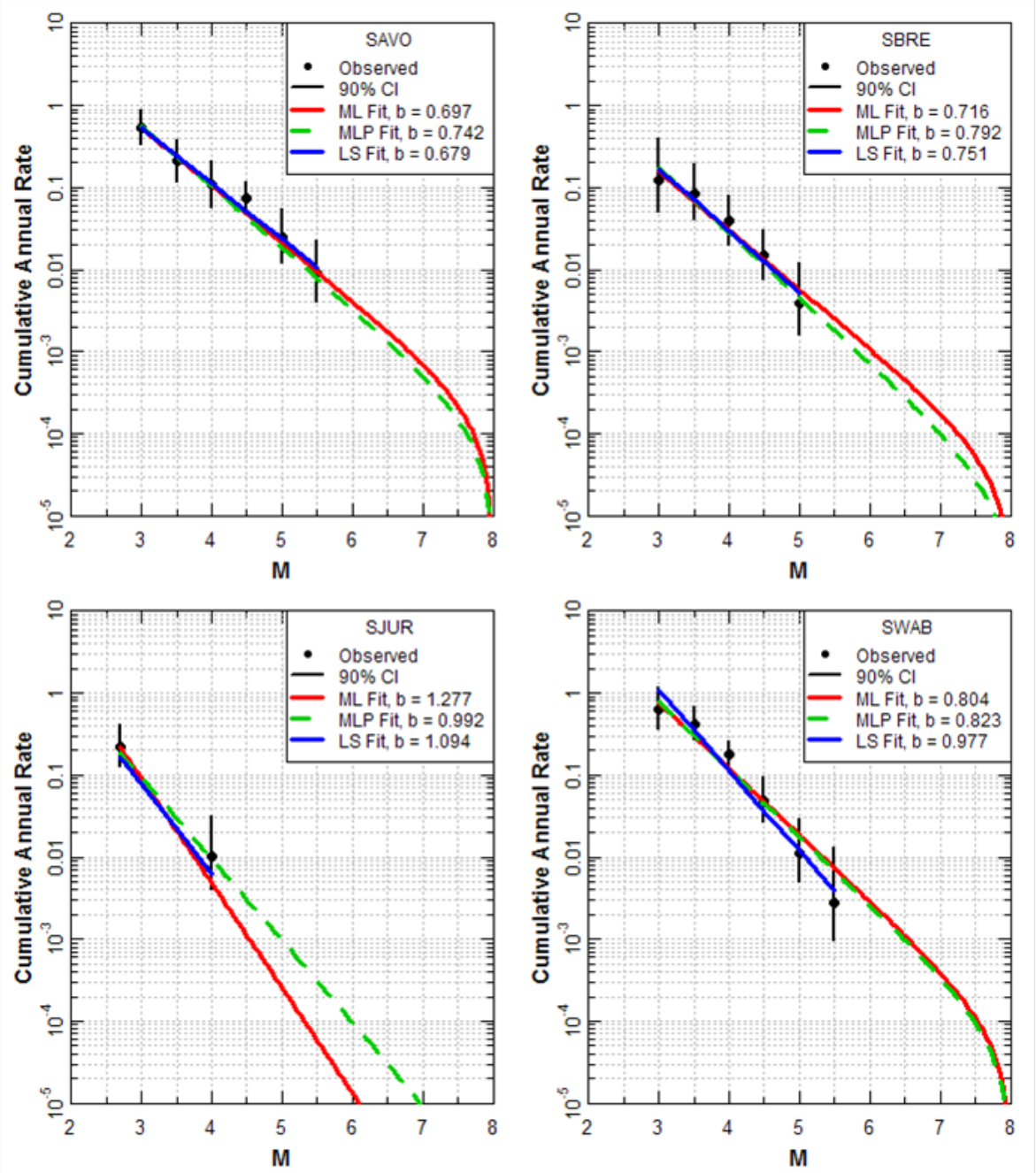

Figure 1.26: Zone Recurrence Plot 8.

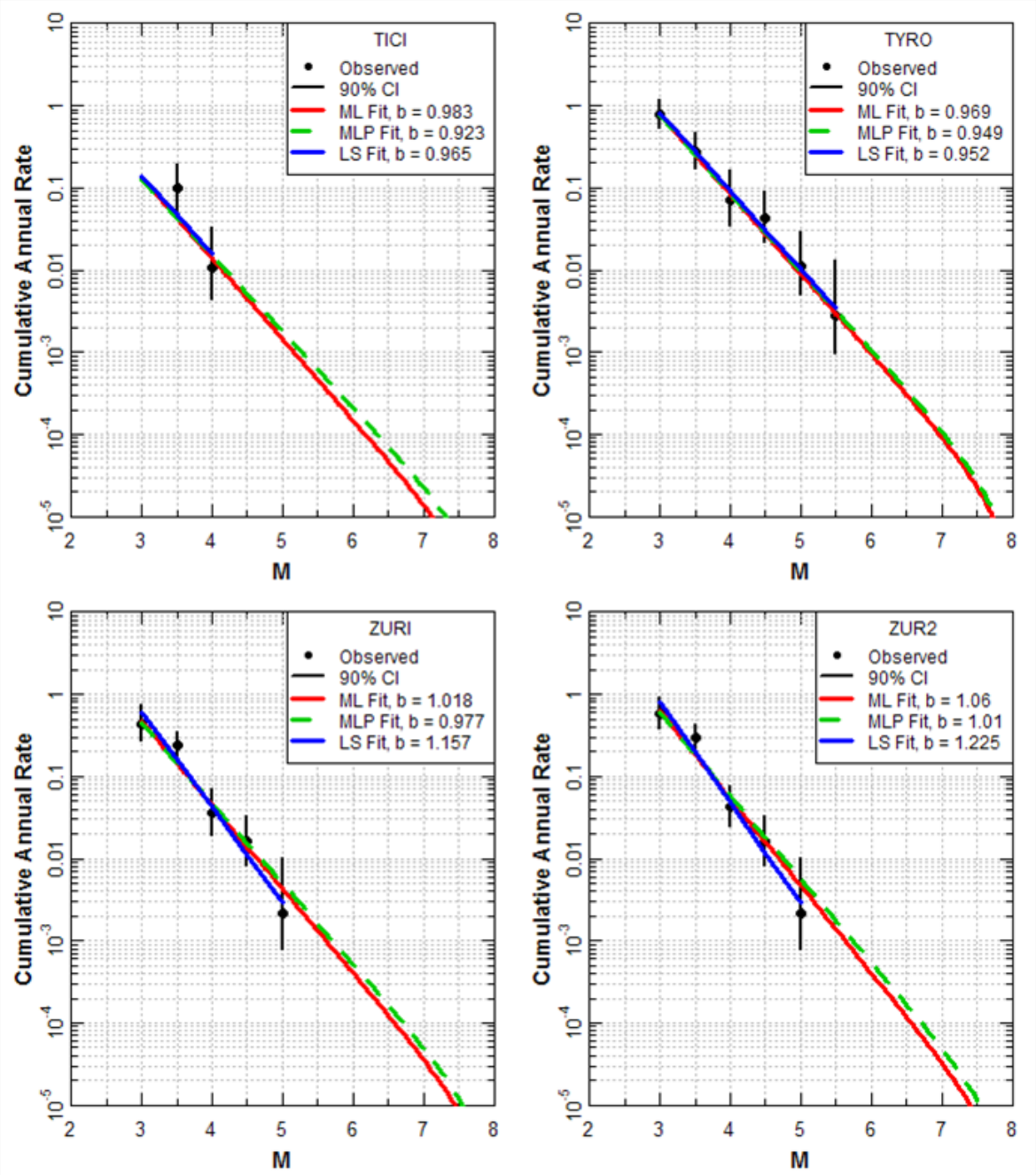

Figure 1.27: Zone Recurrence Plot 9.

Chapter 2

Supporting Calculations for EG1c by R. Youngs

2.1 Calculations for Expert Team EG1c

This section documents the calculations performed to support the EG1c Expert Team's review and finalization of the updated seismicity parameters based on the ECOS-09 catalog. These calculations are all performed using the final ECOS-09 catalog (Swiss Seismological Service, 2010) as declustered by the EG1c Expert Team.

2.2 Earthquake Recurrence Relationships

2.2.1 Earthquake Recurrence for Catalog Completeness Regions

The maximum likelihood method described in section 2.2.3 was used to compute seismicity parameters for the eight EG1c catalog completeness regions (Figure 2.36). The calculations were performed using the catalog completeness periods extended through the end of 2008 and the magnitude intervals originally specified for PEGASOS. Table 2.1 lists the catalog completeness periods used for the calculations. Figures 2.1 through 2.4 show the seismicity data for each completeness region and the maximum likelihood recurrence relationship. The second panel of Figure 2.4 shows the seismicity data for the entire study region. Two maximum likelihood fits to the study region data are shown one assuming a homogeneous seismicity rate and one assuming a common b-value but allowing for differences in the seismicity rate among the catalog completeness regions. These two assessments produce essentially the same b-value.

2.2.2 Initial Earthquake Recurrence for Seismic Source Zones

Initial calculations of earthquake recurrence relationships were performed for each of the EG1c seismic sources to provide a basis for evaluation the performance of various approached using the ECOS-09 earthquake catalog. These results are shown on Figures 2.5 to 2.13.

Table 2.1: EG1c Earthquake Catalog Completeness Periods.

Magnitude Interval	Beginning Year of Complete Reporting for Completeness Zone:						
	SZ01	SZ02	SZ03	SZ04*	SZ05	SZ06	SZ07
3.0 – 3.5	1960	1976	1976	1976	1960	1976	1960
3.5 – 4.0	1920	1920	1940	1920	1920	1960	1960
4.0 – 4.5	1700	1750	1820	1810	1800	1870	1800
4.5 – 5.0	1650	1700	1750	1800	1550	1850	1750
5.0 – 5.5	1550	1700	1750	1750	1500	1650	1750
5.5 – 6.0	1350	1600	1670	1550	1500	1650	1750
6.0 – 7.0	1200	1270	1500	1500	1200	1200	1200
7.0 – 8.0	1100	1100	1200	1200	1100	1100	1100

* First magnitude interval adjusted to 2.7 to 3.5 for zone SZ04

Three approaches were used for each source zone: a maximum likelihood fit (section 2.2.3) without a prior on the b-value (red curves labeled M_L), a maximum likelihood fit with a b-value prior of 0.9 and weight of 50% (green dashed curve labeled MLP) and a least squares fit (section 2.4.2) (blue curve labeled LS). For the SJUR zone the magnitude interval for the lowest magnitude bin was extended to M 2.7-3.5 as there are no earthquakes in the M 3.0-3.5 bin.

2.2.3 Final Earthquake Recurrence for Seismic Source Zones

The final earthquake recurrence relationships for each of the EG1c seismic sources were performed as follows. For branch A of the EG1c seismic source logic tree the earthquake recurrence relationships for each source were computed using maximum likelihood with a global prior on b of 0.9 with weight 50. For branch B of the EG1c seismic source logic tree the earthquake recurrence relationships B for each source were computed using maximum likelihood with a local prior on b based on least squares (shown on Figures 2.5 to 2.13) with a weight of 100%. Figures 2.14 to 2.22 show the resulting earthquake recurrence relationships.

2.3 Maximum Magnitude Distributions

Maximum magnitude distributions were computed for the EG1c seismic sources using the Bayesian (EPRI) approach described in section 2.2.4. A non-informative (uniform) prior on 5.5 or the largest observed earthquake rounded up to the nearest $\frac{1}{2}$ magnitude. The upper bound of the range was set at M $7\frac{1}{4}$ (rounded to 7.3 for application). The likelihood function based on the maximum observed was computed using the global b-value of 0.9. Table 2.2 lists the resulting maximum magnitude distributions for the EG1c seismic sources.

Table 2.2: Maximum Magnitude Distributions for EG1c Seismic Sources.

Source	Max Observed	Weight Assigned to Maximum Magnitude of: 5.5	6	6.5	7	7.3
ALCM	5	0.172277	0.285997	0.261982	0.203875	0.07587
ALMA	5.67		0.733791	0.191581	0.057067	0.017561
BASL	6.6				0.518496	0.481504
BAVA	5.4	0.200545	0.297069	0.250891	0.184266	0.067229
BAW2	5.6		0.320216	0.381258	0.222002	0.076524
BAWU	5.6		0.336557	0.372081	0.216876	0.074486
BW2S	5.6		0.230823	0.386021	0.280501	0.102655
BAWS	5.6		0.23684	0.386059	0.276393	0.100709
BLAF	4.5	0.161291	0.282121	0.267643	0.210422	0.078523
BRES	6		0.221506	0.405181	0.274897	0.098416
DAUP	5.36	0.216789	0.294626	0.240762	0.181065	0.066758
FRIB	5.2	0.256467	0.296481	0.223395	0.163726	0.05993
GARD	6.05			0.464085	0.414716	0.121199
GENV	5.6		0.252056	0.383736	0.267441	0.096766
GLAR	5.1	0.260946	0.297715	0.221373	0.161117	0.058849
GRAU	6.2			0.357632	0.476713	0.165655
HELV	5.8		0.30342	0.375117	0.237591	0.083872
JURA	5.4	0.148756	0.288266	0.27729	0.208745	0.076943
LORA	5.4	0.17469	0.307503	0.25615	0.191343	0.070314
MOMI	4.4	0.167763	0.284749	0.264289	0.206347	0.076852
NIDW	5.9		0.258445	0.397803	0.254051	0.089702
NSPG	4.2	0.176556	0.286642	0.260261	0.201617	0.074923
PENV	6.2			0.355286	0.479439	0.165275
POVA	5.67		0.401983	0.352242	0.184078	0.061697
RHEG	5.4	0.345418	0.318898	0.181163	0.114328	0.040191
RHGC	5.4	0.173571	0.30735	0.264599	0.186715	0.067765
RHGN	4.7	0.199598	0.295442	0.248837	0.187122	0.069002
RHGS	5	0.225859	0.299188	0.23762	0.173744	0.063589
SAVO	5.8		0.337026	0.375604	0.213803	0.073567
SBRE	5.4	0.21157	0.31238	0.241072	0.172228	0.06275
SJUR	4.3	0.152673	0.279275	0.271833	0.215575	0.080643
SWAB	5.5	0.334656	0.331405	0.178831	0.114649	0.04046
TICI	4.3	0.15985	0.281597	0.268355	0.211309	0.078889
TYRO	5.5	0.400163	0.277263	0.166532	0.114737	0.041305
ZURI	5.1	0.245151	0.298141	0.228286	0.167232	0.06119
ZUR2	5.1	0.277808	0.298654	0.214	0.153641	0.055898

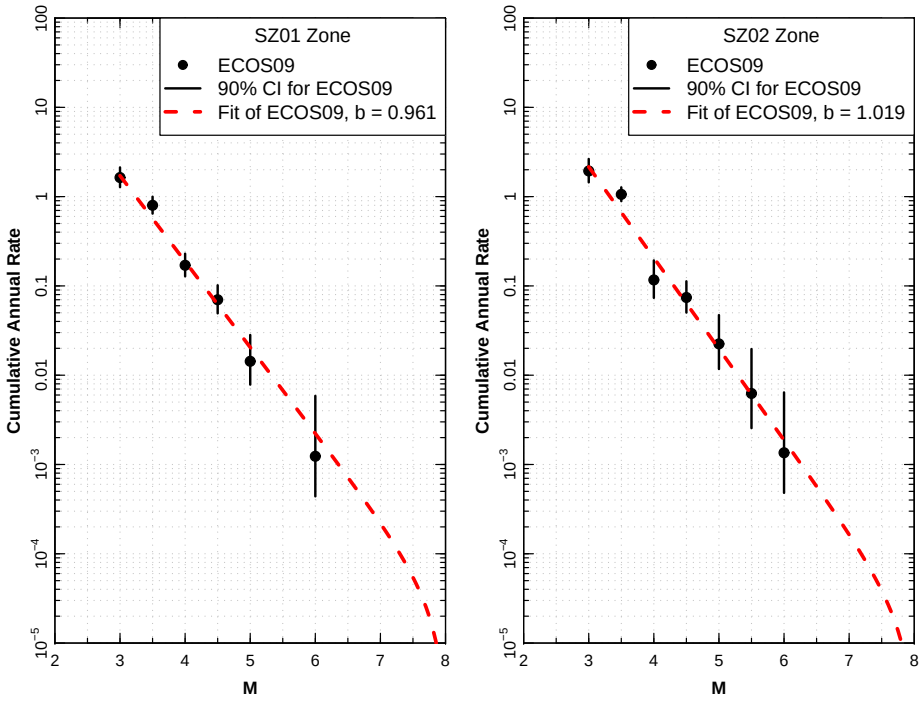

Figure 2.1: Earthquake Recurrence relationships for EG1c completeness regions SZ01 and SZ02.

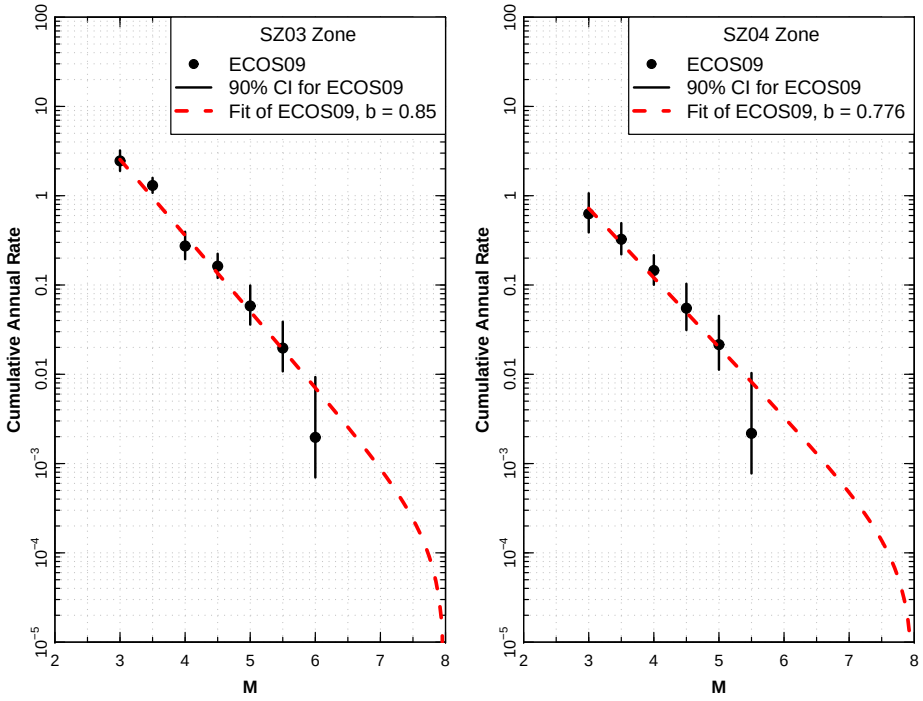

Figure 2.2: Earthquake Recurrence relationships for EG1c completeness regions SZ03 and SZ04.

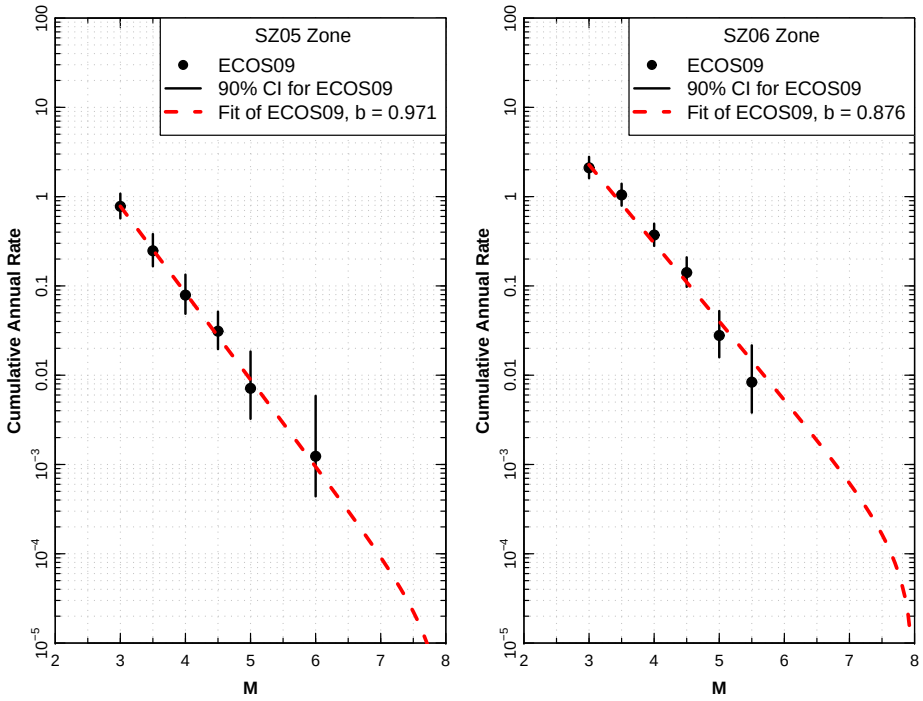

Figure 2.3: Earthquake Recurrence relationships for EG1c completeness regions SZ05 and SZ06.

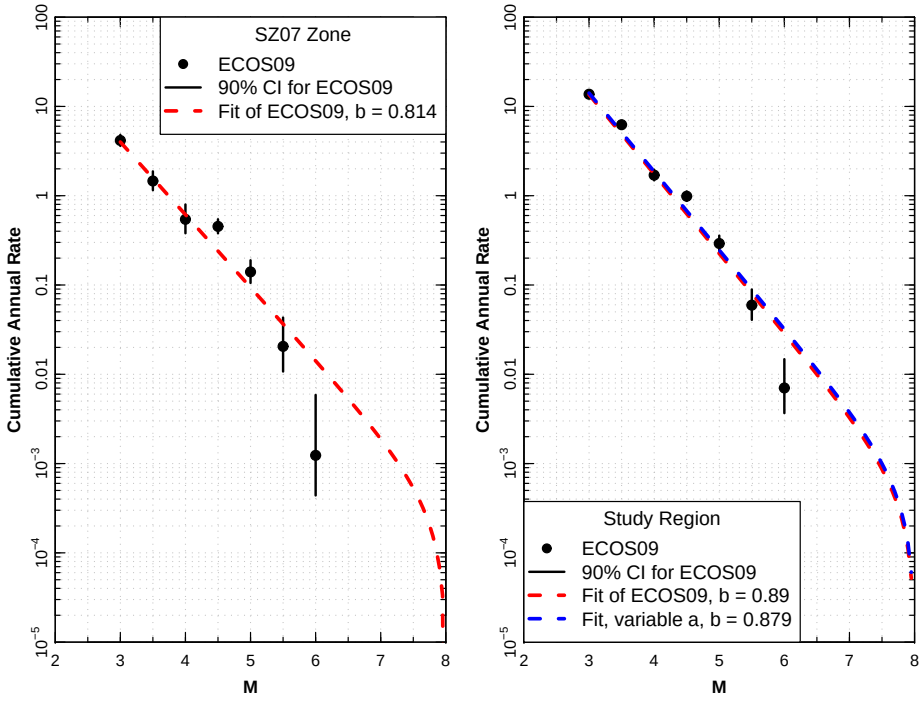

Figure 2.4: Earthquake Recurrence relationships for EG1c completeness region SZ07 and Study Region.

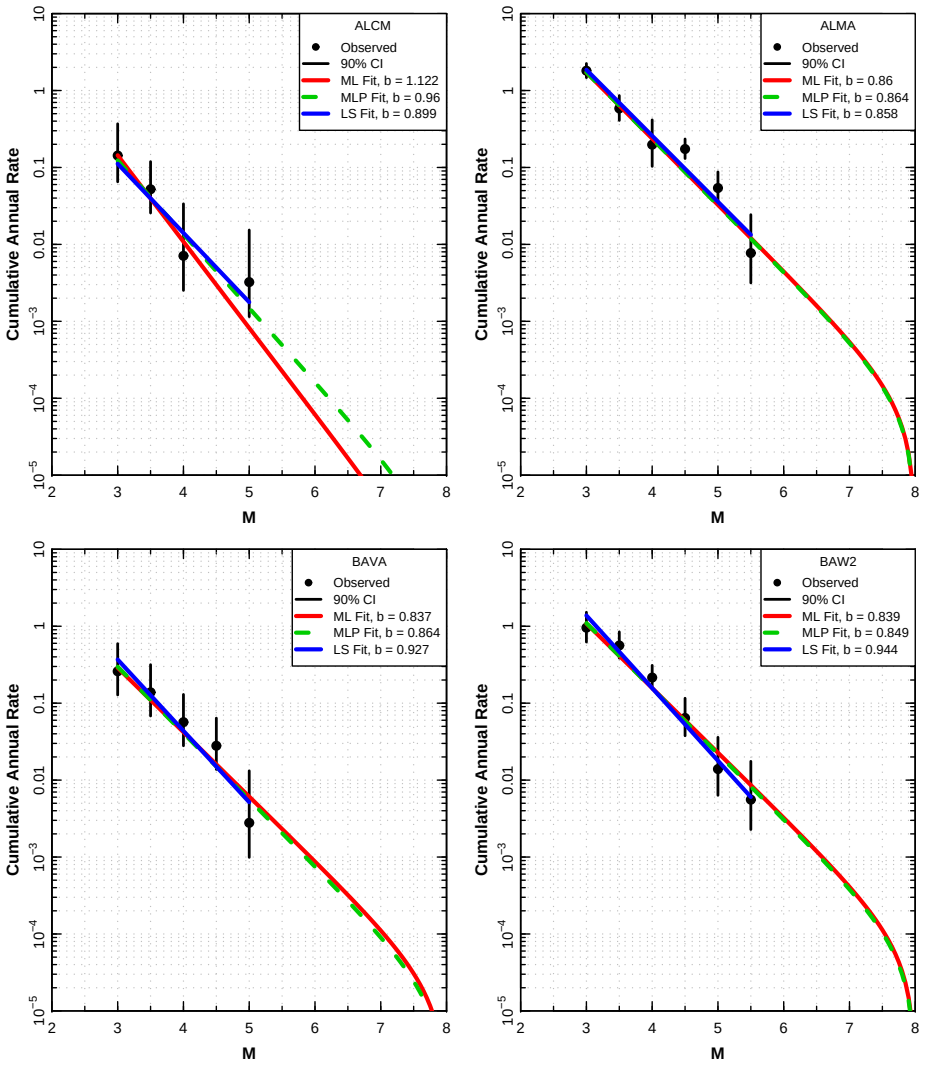

Figure 2.5: Initial earthquake recurrence relationships for EG1c source zones (1 of 9).

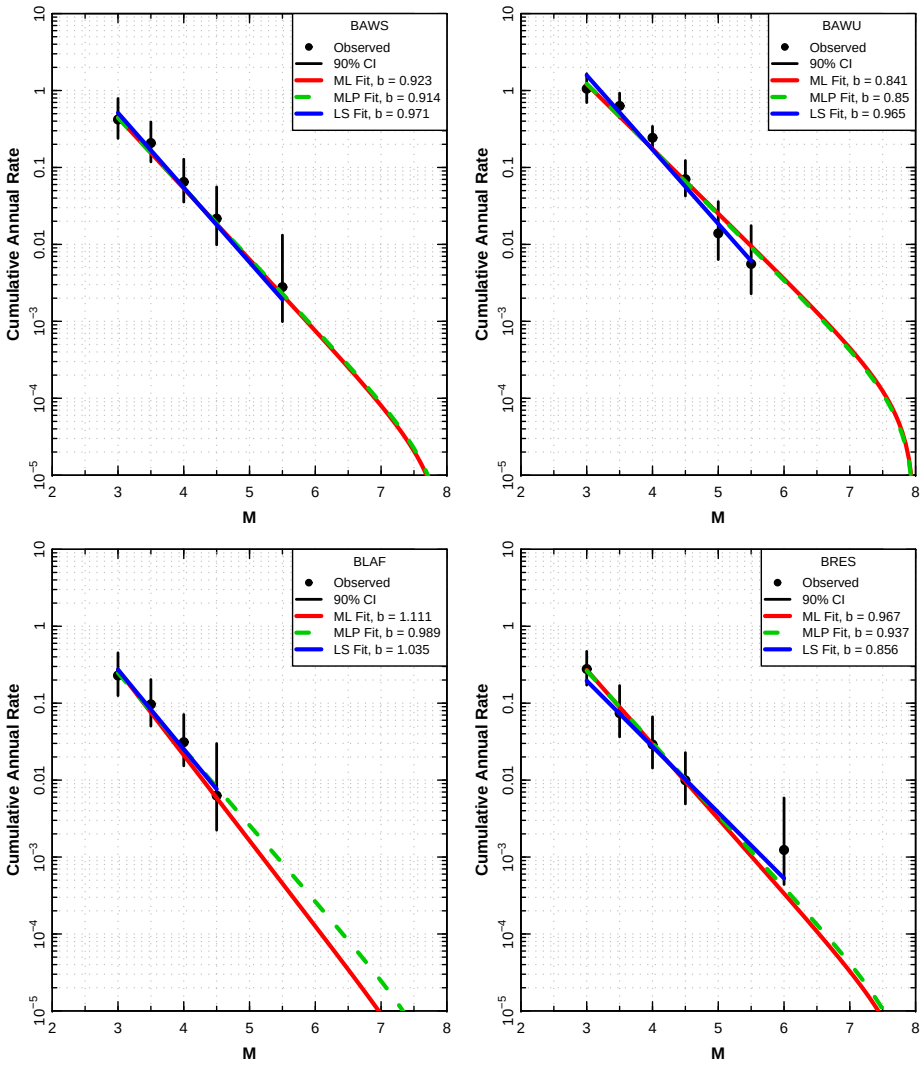

Figure 2.6: Initial earthquake recurrence relationships for EG1c source zones (2 of 9).

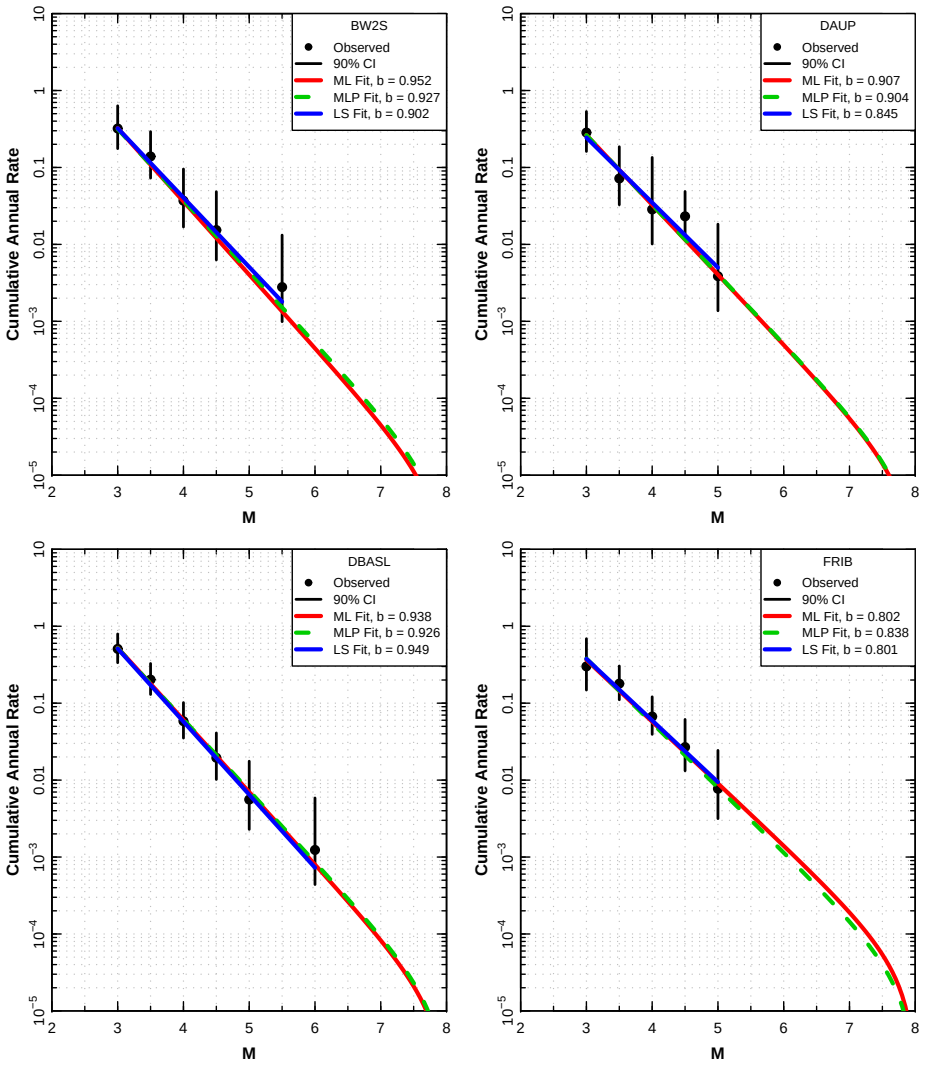

Figure 2.7: Initial earthquake recurrence relationships for EG1c source zones (3 of 9).

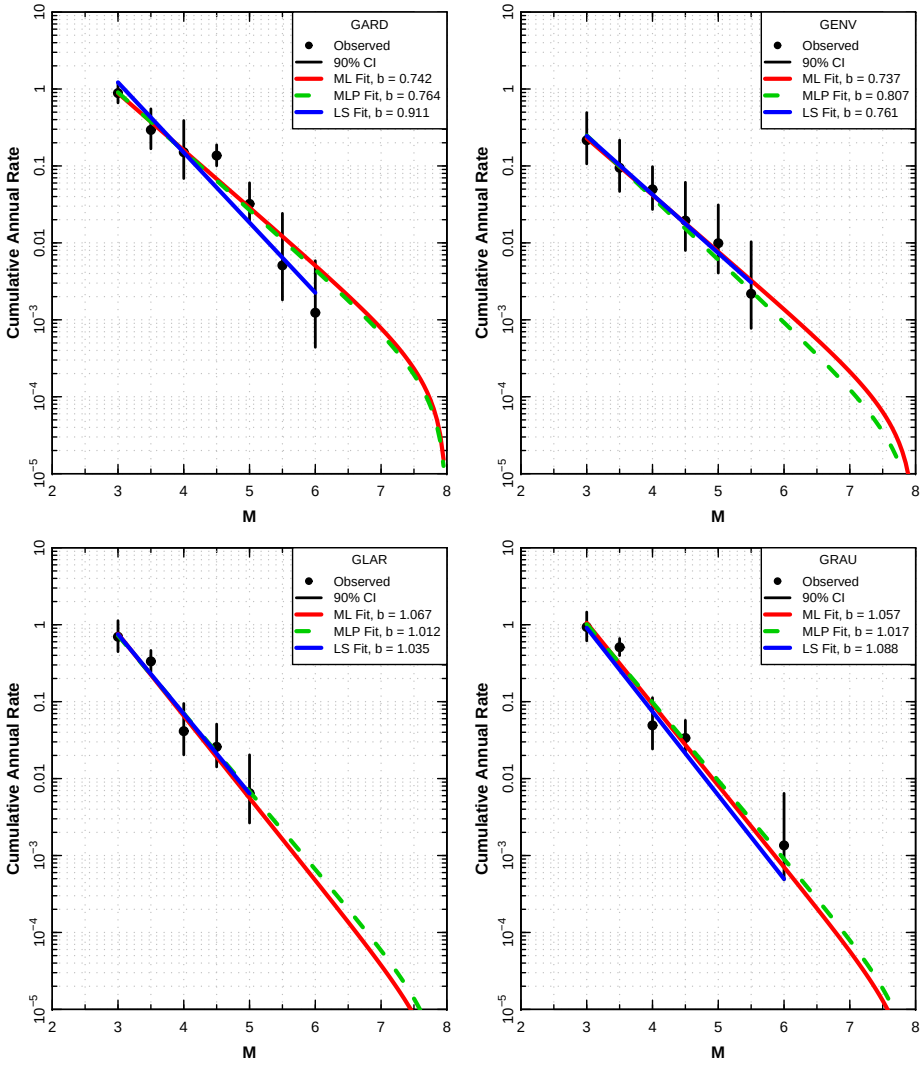

Figure 2.8: Initial earthquake recurrence relationships for EG1c source zones (4 of 9).

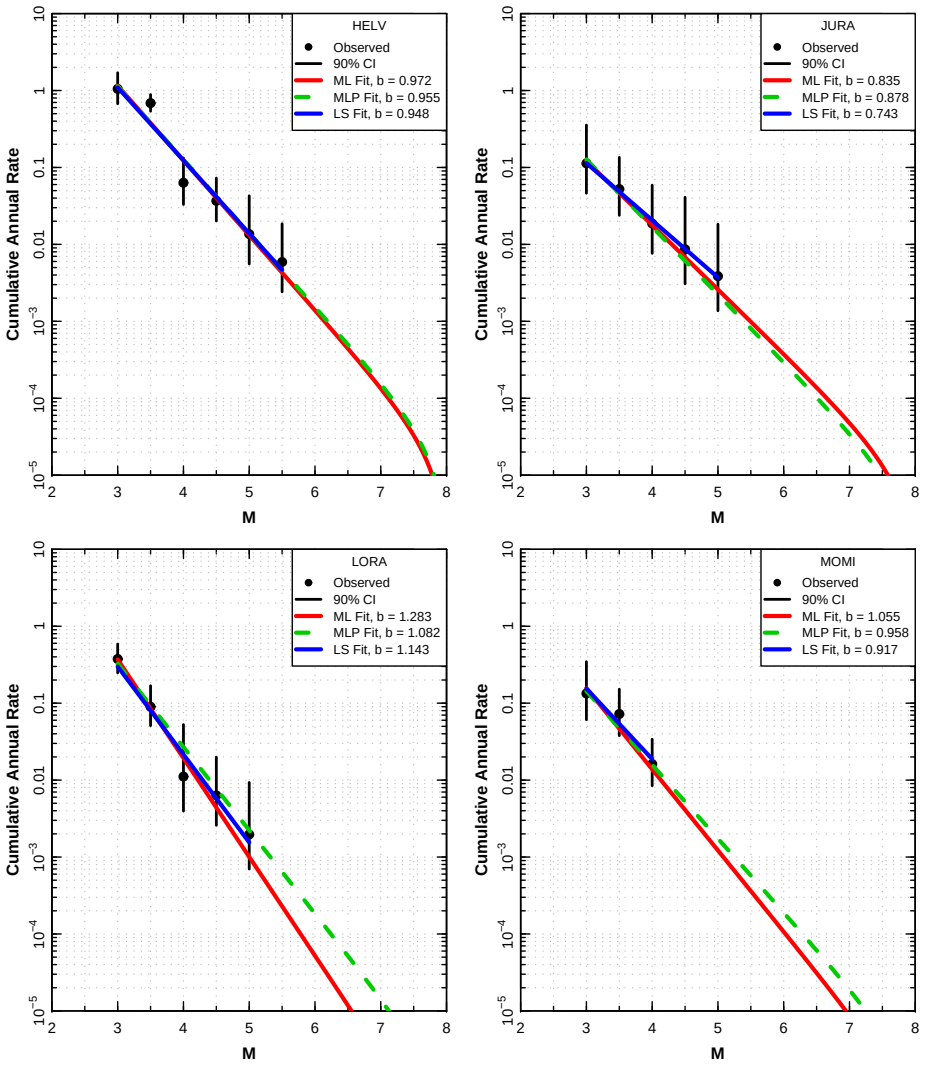

Figure 2.9: Initial earthquake recurrence relationships for EG1c source zones (5 of 9).

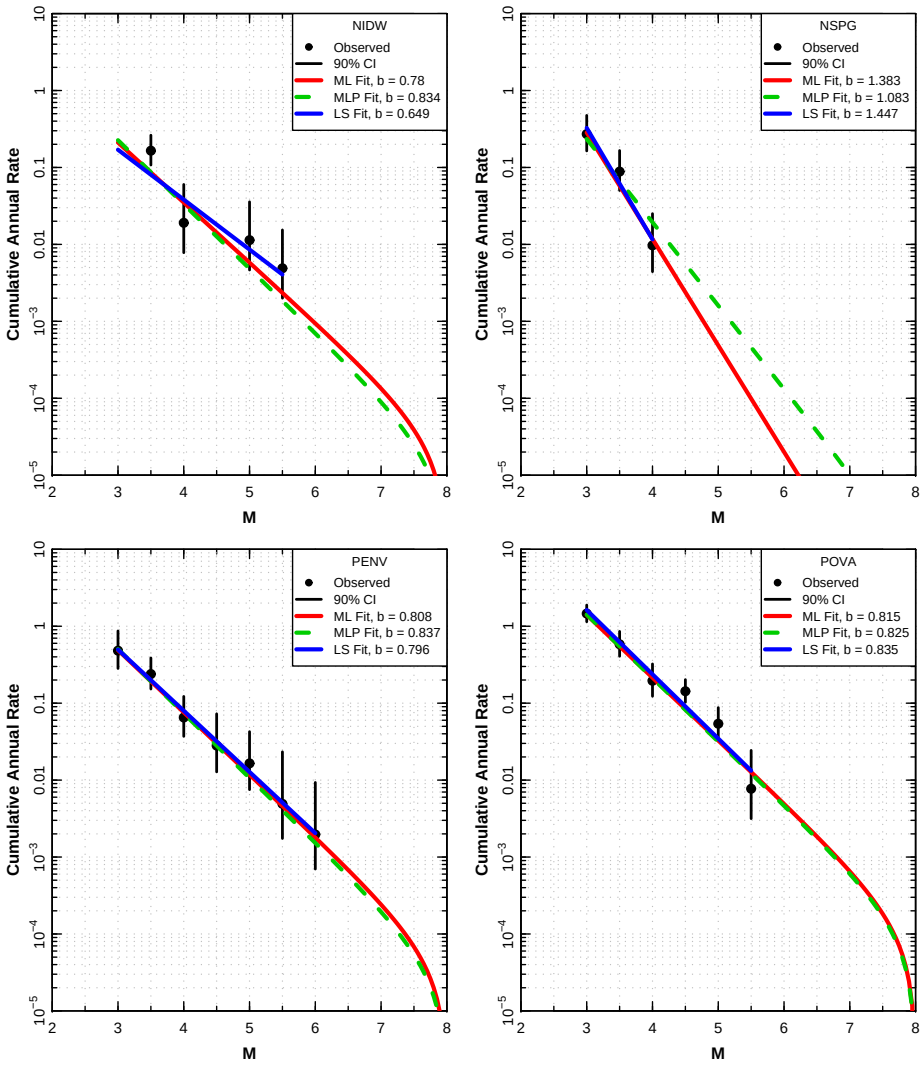

Figure 2.10: Initial earthquake recurrence relationships for EG1c source zones (6 of 9).

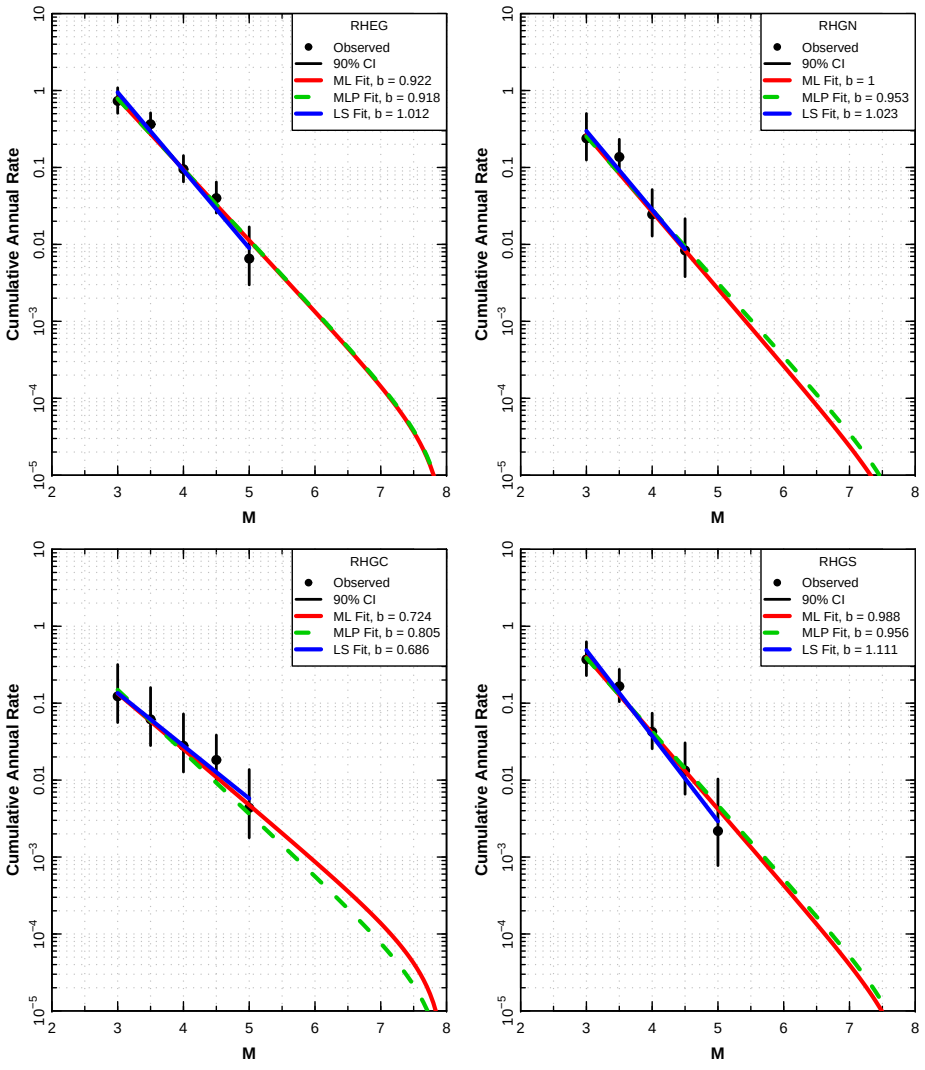

Figure 2.11: Initial earthquake recurrence relationships for EG1c source zones (7 of 9).

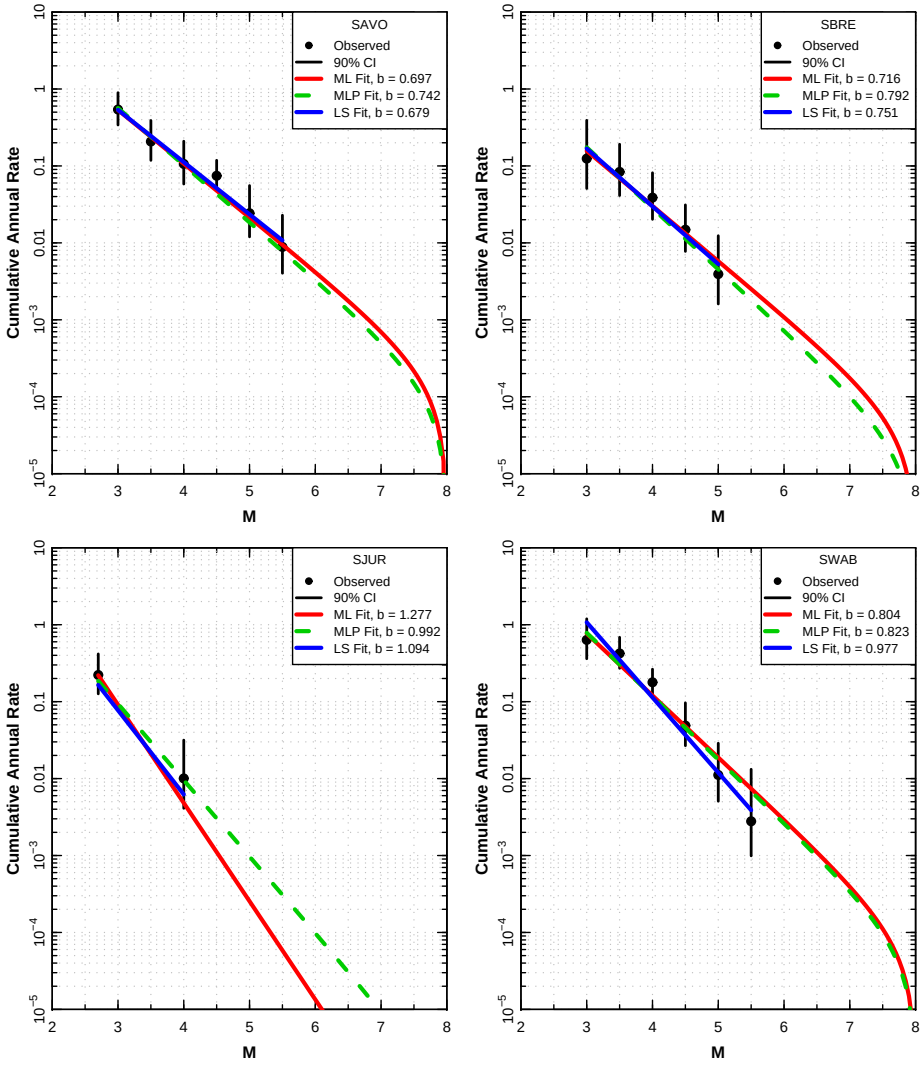

Figure 2.12: Initial earthquake recurrence relationships for EG1c source zones (8 of 9).

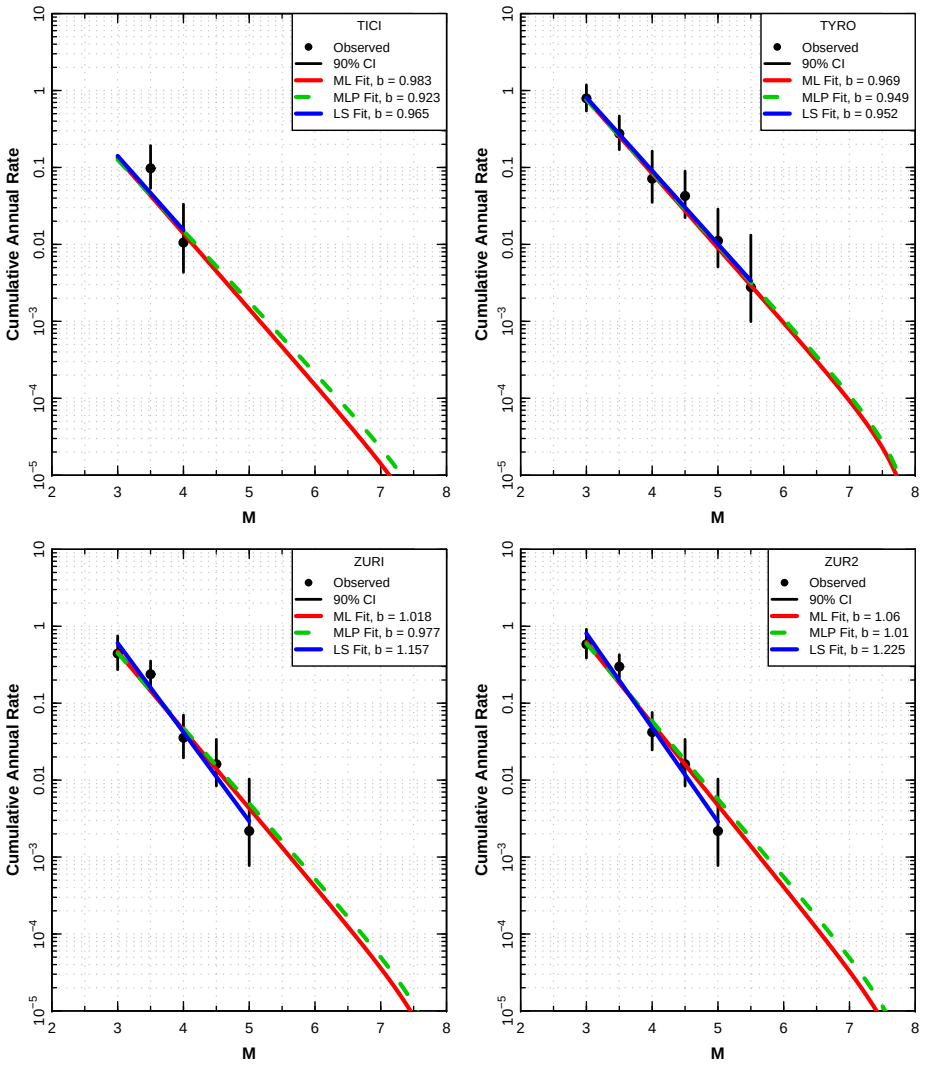

Figure 2.13: Initial earthquake recurrence relationships for EG1c source zones (9 of 9).

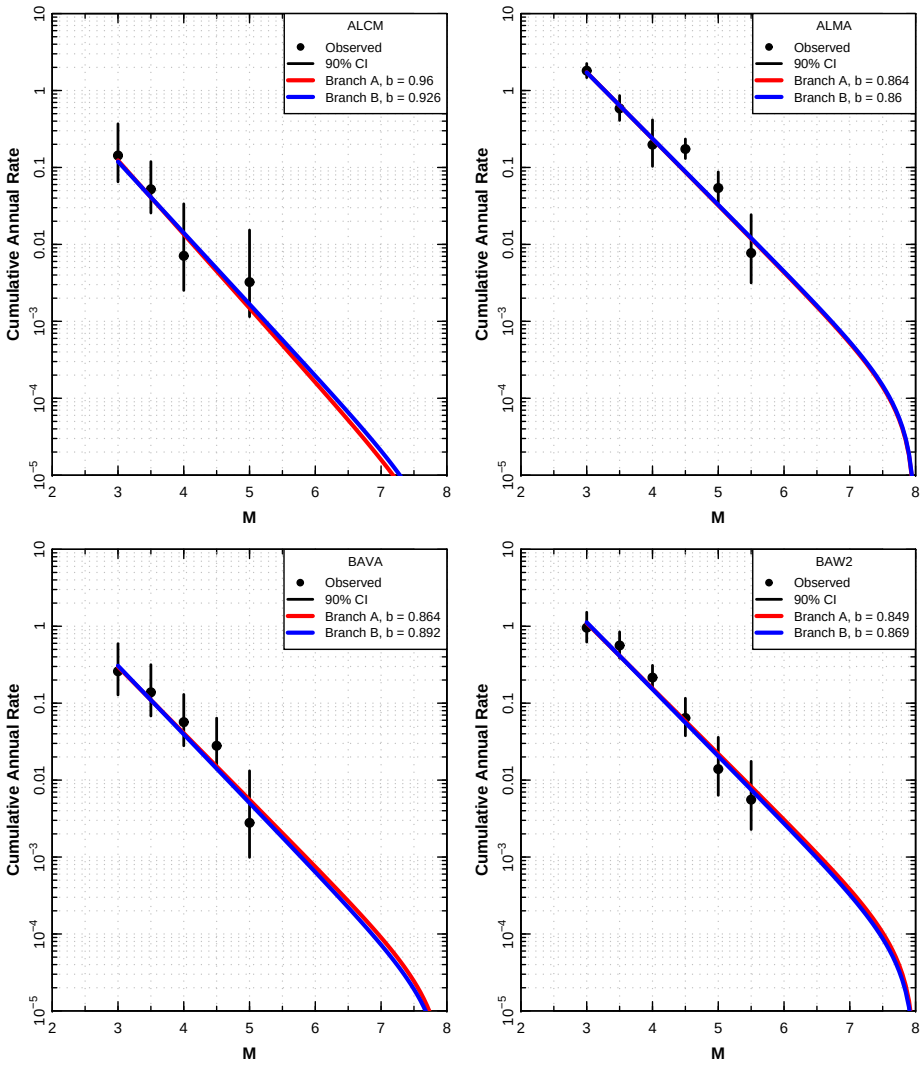

Figure 2.14: Final earthquake recurrence relationships for EG1c source zones (1 of 9).

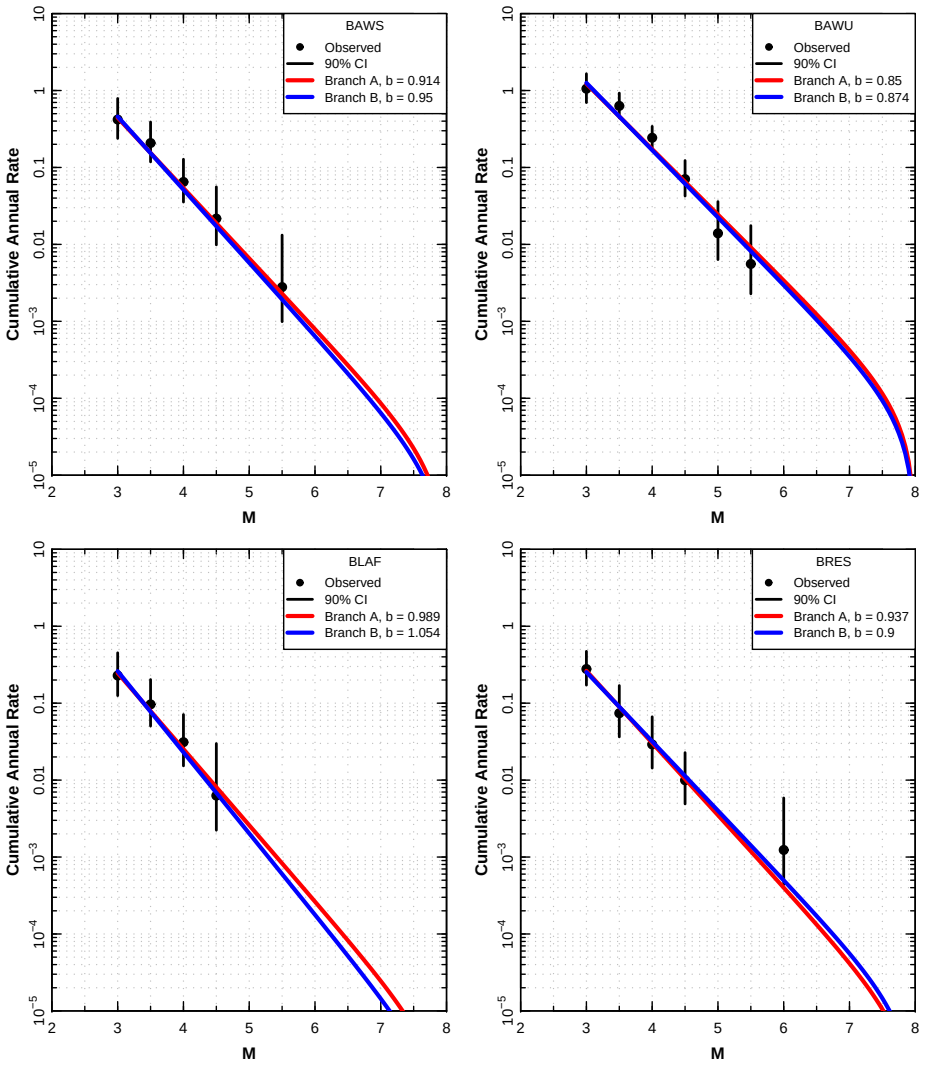

Figure 2.15: Final earthquake recurrence relationships for EG1c source zones (2 of 9).

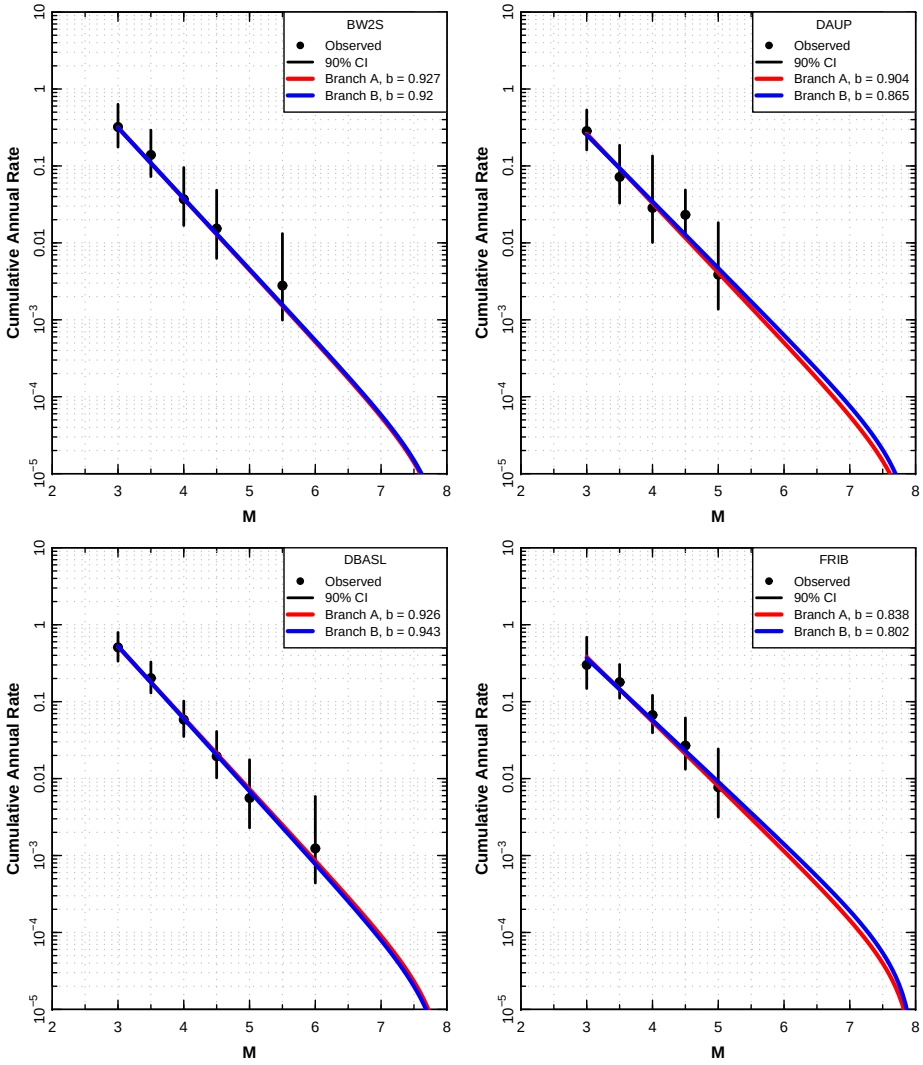

Figure 2.16: Final earthquake recurrence relationships for EG1c source zones (3 of 9).

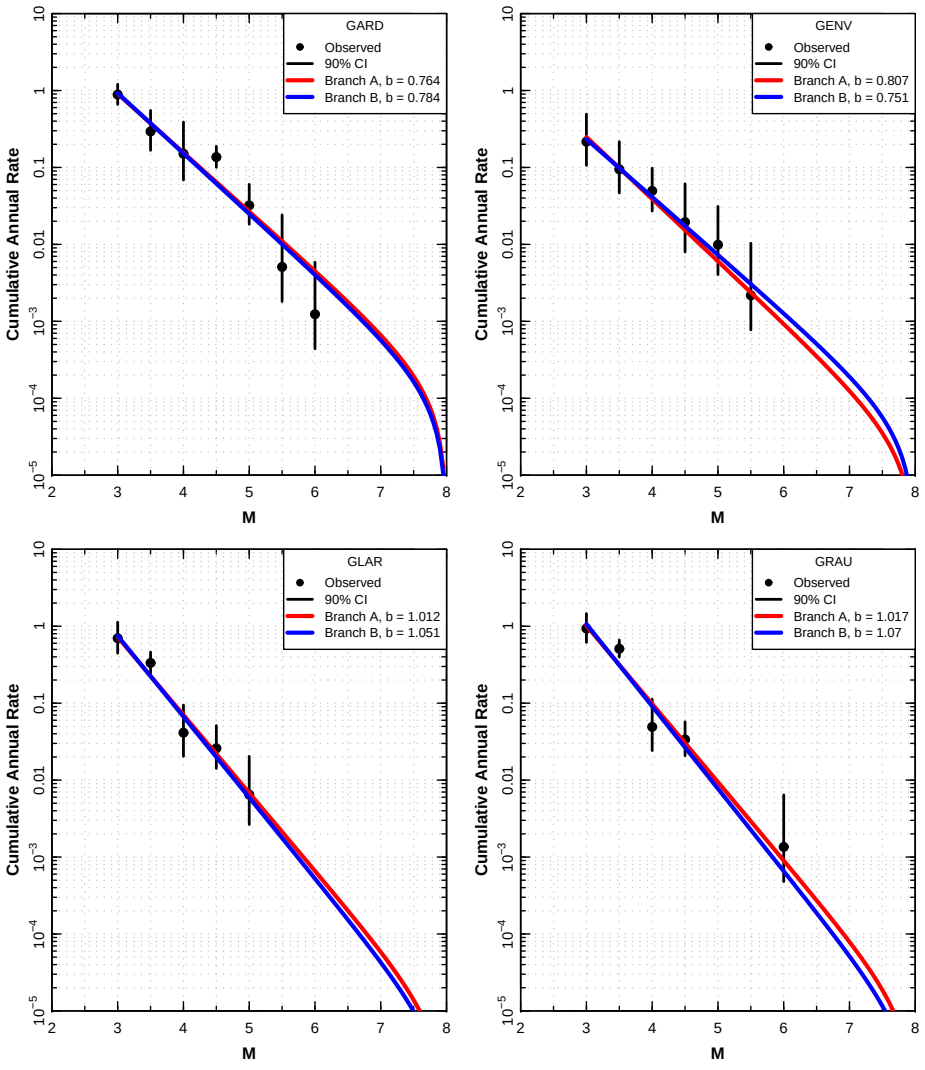

Figure 2.17: Final earthquake recurrence relationships for EG1c source zones (4 of 9).

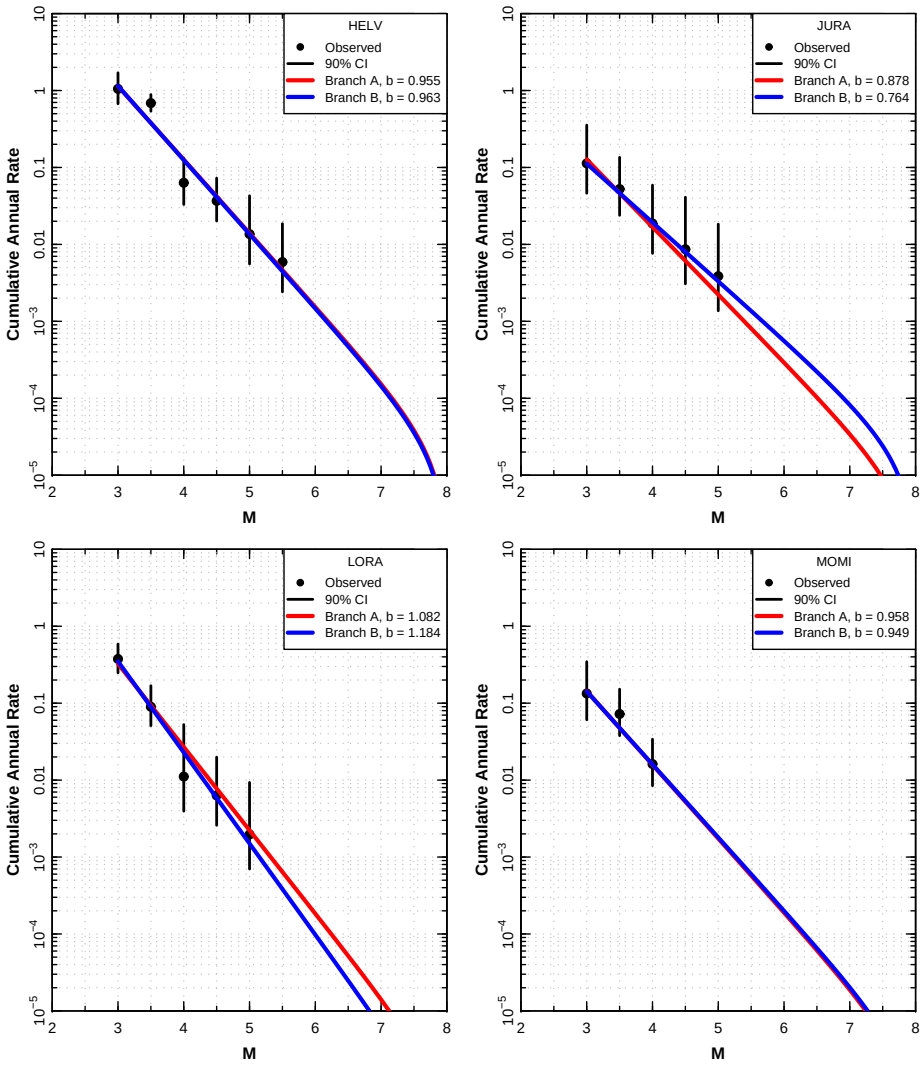

Figure 2.18: Final earthquake recurrence relationships for EG1c source zones (5 of 9).

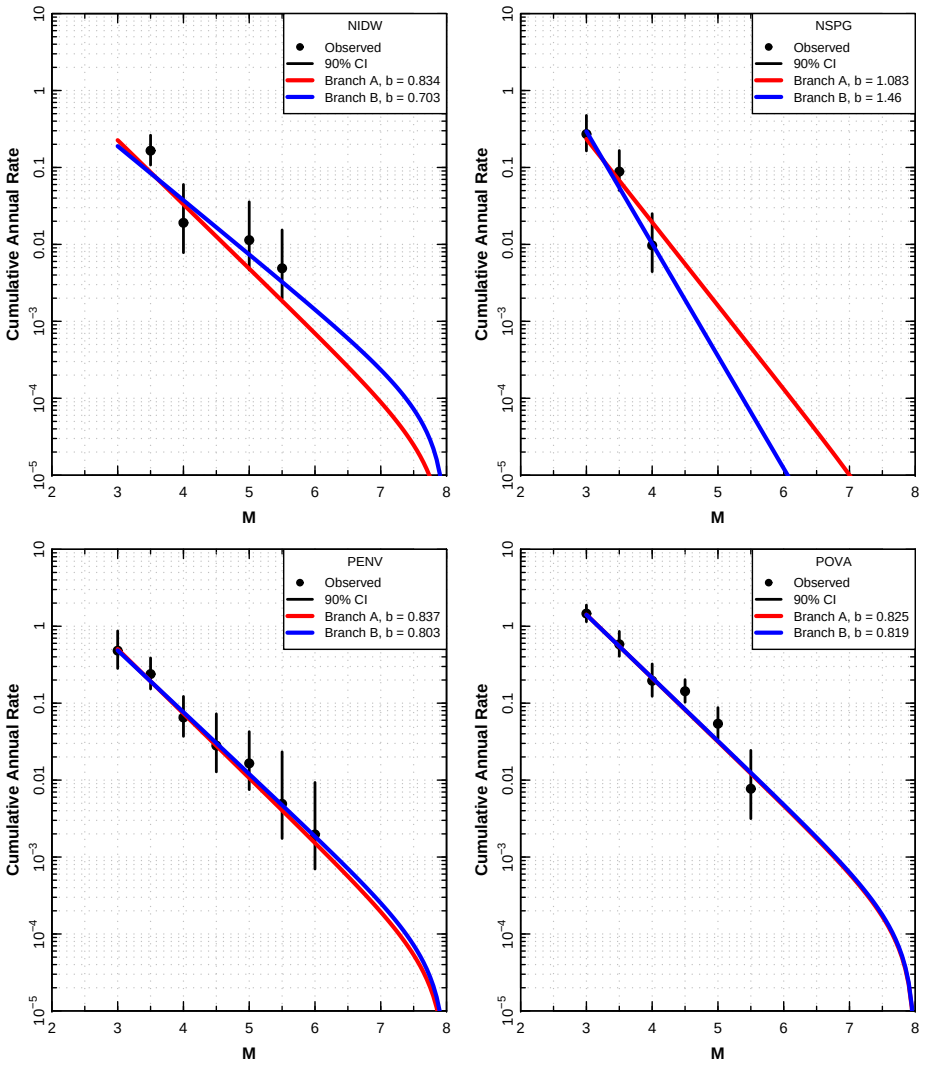

Figure 2.19: Final earthquake recurrence relationships for EG1c source zones (6 of 9).

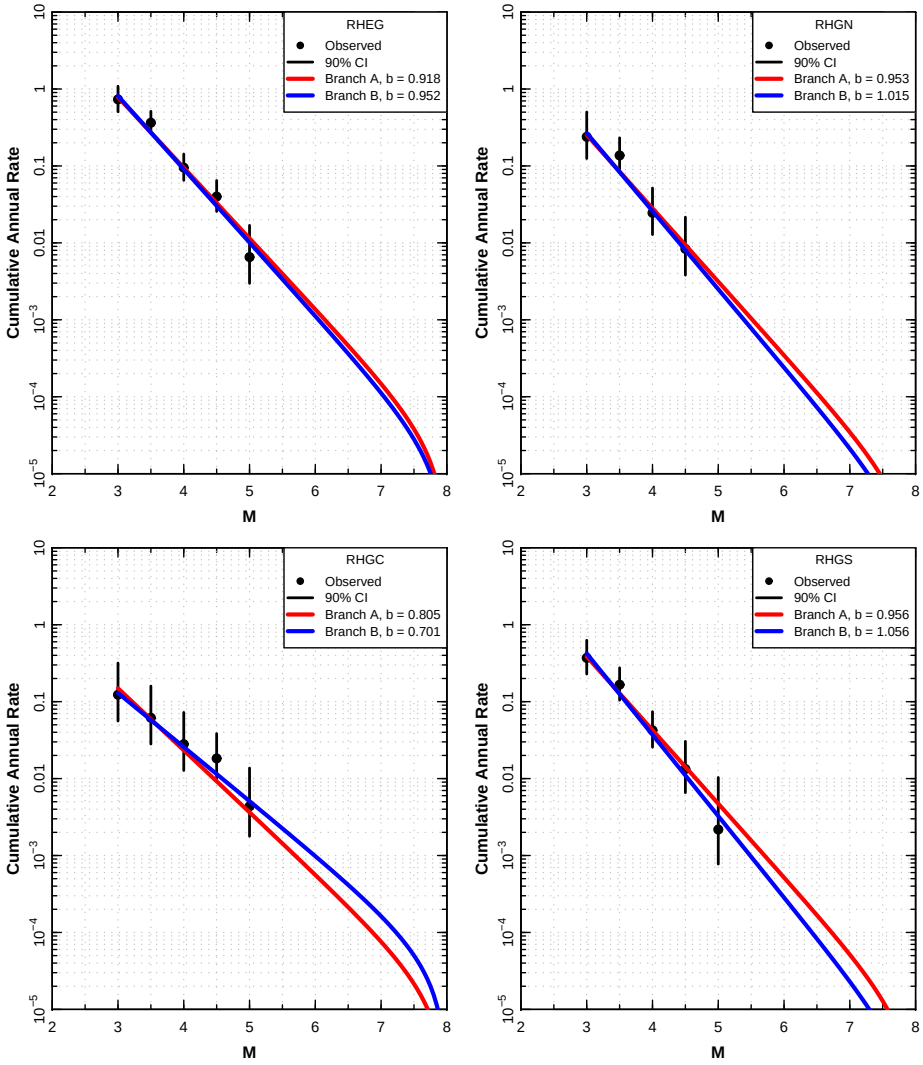

Figure 2.20: Final earthquake recurrence relationships for EG1c source zones (7 of 9).

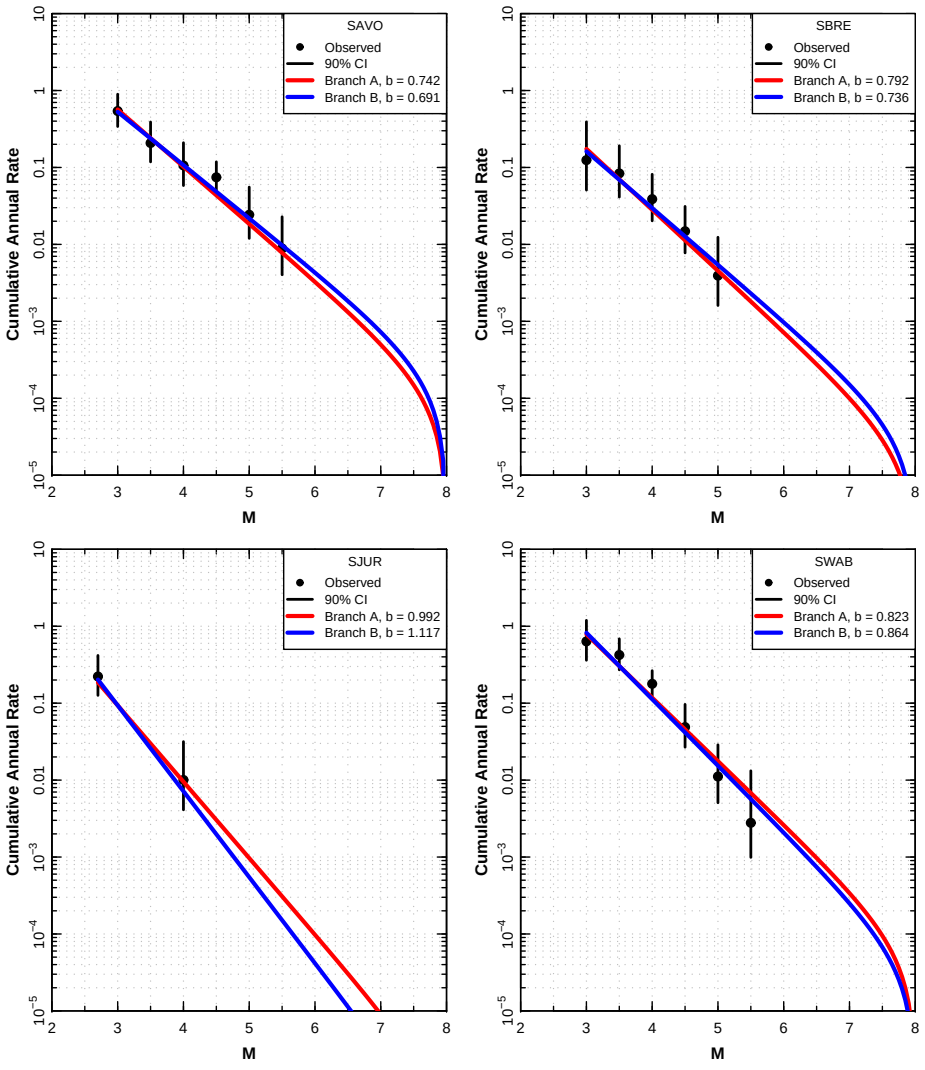

Figure 2.21: Final earthquake recurrence relationships for EG1c source zones (8 of 9).

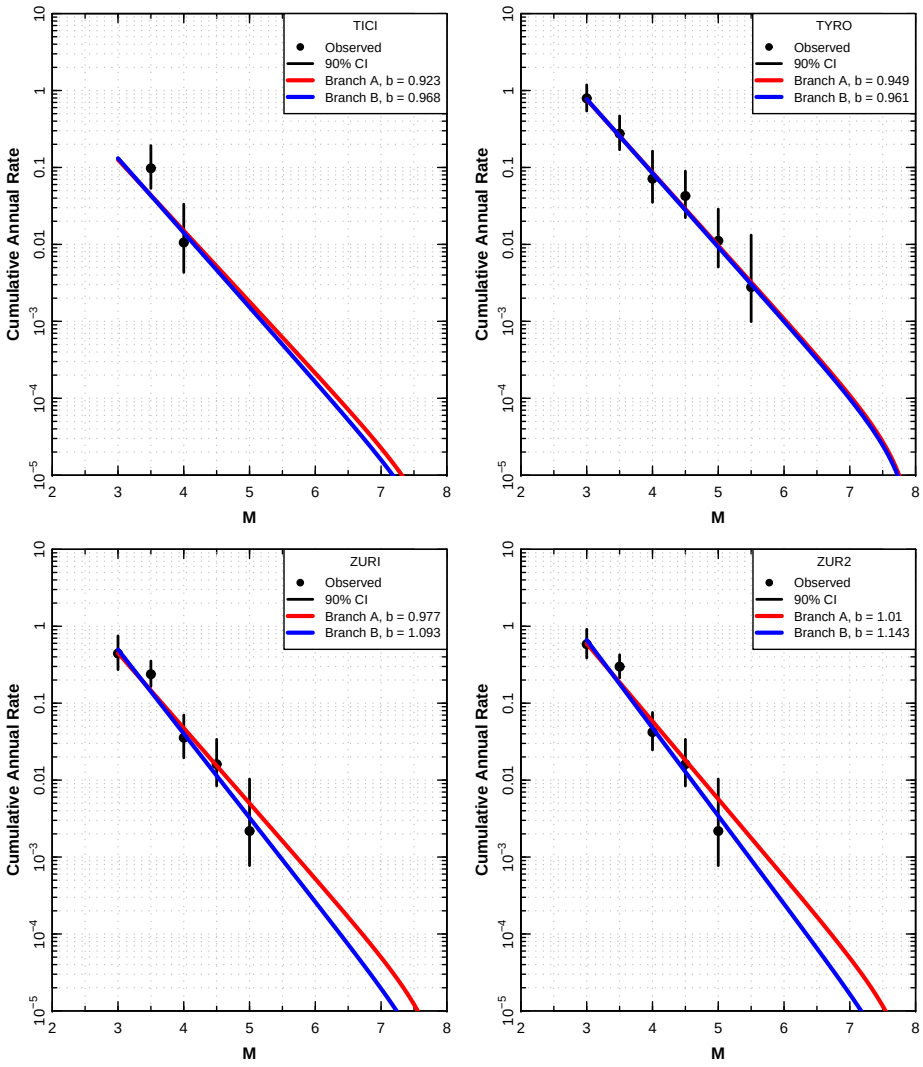

Figure 2.22: Final earthquake recurrence relationships for EG1c source zones (9 of 9).

Chapter 3

Hazard Input Document for EG1c (EG1-HID-1003) of March 31, 2011

Written by the PMT, SP4 and TFI

This document describes the final seismic source model developed by Expert Team EG1c in the PRP project. The data files associated with this seismic source model are located in the zip file EG1-HID-1003_EG1c_data.zip. This document is based on the PEGASOS Hazard Input Document EG1-HID-0040. Based on the new earthquake ECOS09 catalog published in March 2010 the EG1c team revised its model, updating the seismicity parameters that go with that seismic source model and removing one alternative for the recurrence parameters calculations. This document repeats for the most part the content of the PEGASOS Hazard Input Document EG1-HID-0040. The modifications caused by the model revision are highlighted in blue.

3.1 Seismic Source Zonation

The basic seismic source model consists of areal source zones defined by simple polygons. Seismicity is assumed to be spatially homogeneous within these sources, with the exception of the distributed Basel source described below. The source zone files are located in directory: `./ZONES`.

The seismic source zonation for team EG1c is described on Figures 3.1, 3.2, 3.3, 3.4 and 3.5. Figure 3.1 shows the logic tree structure for source zonation. The tree consists of three levels. The first address whether the Rhine Graben should be treated as a single source (RHEG) or divided into three sources (RHGN, RHGC, and RHGS). These alternative sources are shown on Figure 3.2.

The second level addresses the treatment of the Swabian Jura active zone. In one model, the seismicity is confined to the distinct stationary source SWAB embedded in the larger zone BAWS or BW2S. These zones are shown on the right had side of Figure 3.3. Zone files BAWS and BW2S were created to be simple polygons wrapping around zone SWAB. The alternative model considers the elevated seismicity in SWAB not to be a stationary source, but rather may occur anywhere within the larger BAWU zones. As a result, just zones BAWU or BAW2

are used, as shown on the left of Figure 3.3. BAWU is equivalent to BAWS plus SWAB; BAW2 is equivalent to BW2S plus SWAB.

The third level addresses whether or not the permocarboniferous troughs are an active source zone or not. If they are an active, then source NSPG is used as a source zone and the Zurich and BAWU sources have configurations ZURI, BAWU or BAWS as shown on the bottom of Figure 3.3. If they are not an active, then the Black Forest source BLAF is used as a source zone and the Zurich and BAWU sources have configurations ZUR2, BAW2 or BW2S as shown on the top of Figure 3.3.

In addition, there are 22 sources whose boundaries are unaffected by the alternatives discussed above. These are shown on Figure 3.4.

The final source is the distributed Basel source. EG1c defined a source zone around the cluster of seismicity near Basel. However, they considered that the concentration was in part due the process of recording historical earthquakes and the seismicity should be dispersed outward from the modeled source zone using a Gaussian decay in rate over a distance of 30 km, with a standard deviation of 10 km. Polygon `DBASL.ZON` was created to encompass the distributed Basel source (Figure 3.5). The seismicity rate varies spatially within this source. File `DBASL.XYG` contains a grid of longitude-latitude pairs with the fraction of the total rate for the source that is assigned to each grid point. Note that this spatial grid overlaps the adjacent sources by intent.

As indicated on the right hand side of Figure 3.1, the above alternative models lead to eight different source sets. These are listed in table 3.1. The first row of the table lists the source set "UC" that includes the 22 zones shown on Figure 3.4 plus DBASL. These sources do not change with the alternative zonations and are to be included in each set.

Table 3.1: EG1c Seismic Source Sets.

Source Set	**Sources**
UC (unchanging)	DBASL, ALCM, ALMA, BAVA, BRES, DAUP, FRIB, GARD, GENV, GLAR, GRAU, HELV, JURA, LORA, MOMI, NIDW, PENV, POVA, SAVO, SBRE, SJUR, TICI, TYRO
R1S1G1	RHGN, RHGC, RHGS, SWAB, BAWS, NSPG, ZURI + UC
R1S1G2	RHGN, RHGC, RHGS, SWAB, BW2S, BLAF, ZUR2 + UC
R1S2G1	RHGN, RHGC, RHGS, BAWU, NSPG, ZURI + UC
R1S2G2	RHGN, RHGC, RHGS, BAW2, BLAF, ZUR2 + UC
R2S1G1	RHEG, SWAB, BAWS, NSPG, ZURI + UC
R2S1G2	RHEG, SWAB, BW2S, BLAF, ZUR2 + UC
R2S2G1	RHEG, BAWU, NSPG, ZURI + UC
R2S2G2	RHEG, BAW2, BLAF, ZUR2 + UC

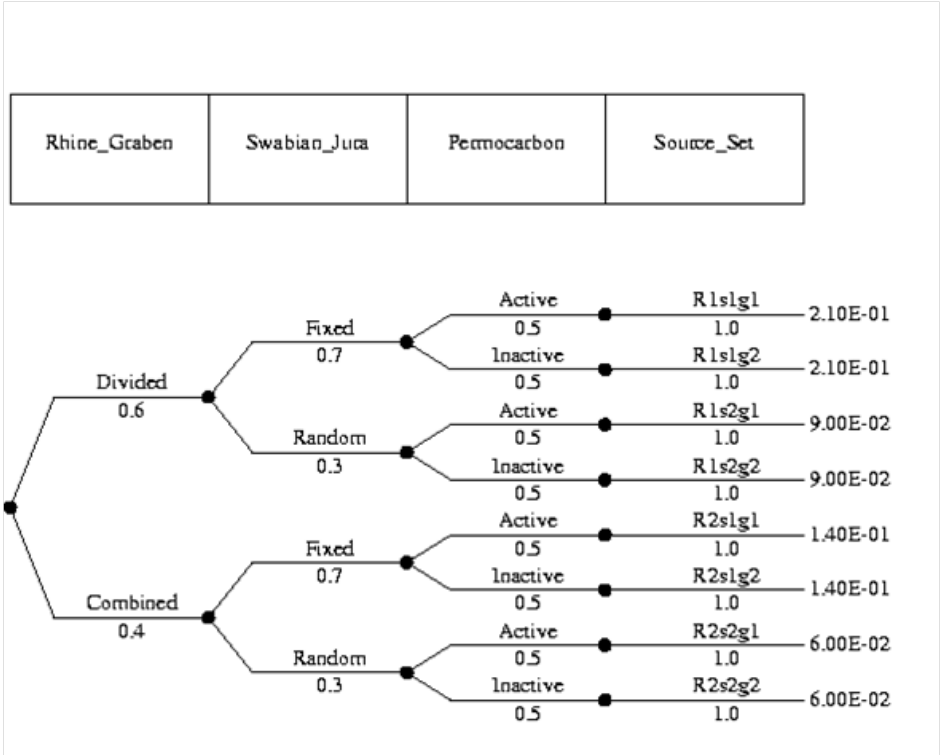

Figure 3.1: Logic tree for EG1c seismic source zonation.

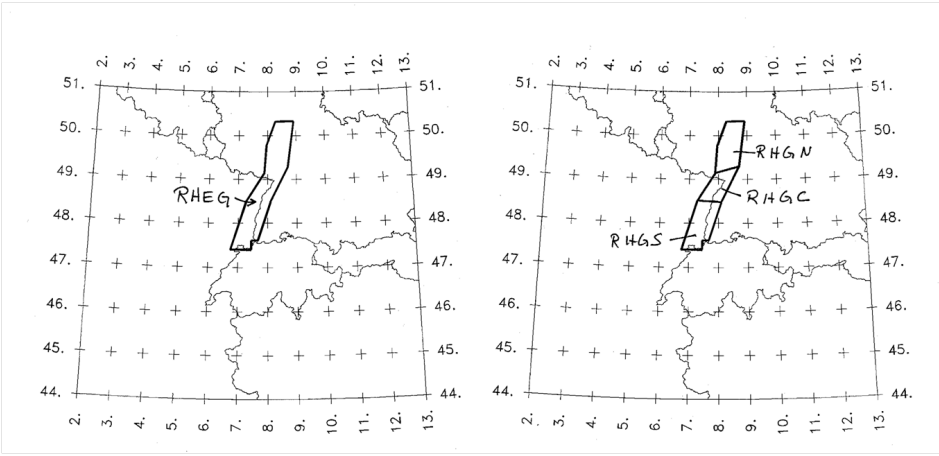

Figure 3.2: EG1c alternative source zonations of the Rhine Graben.

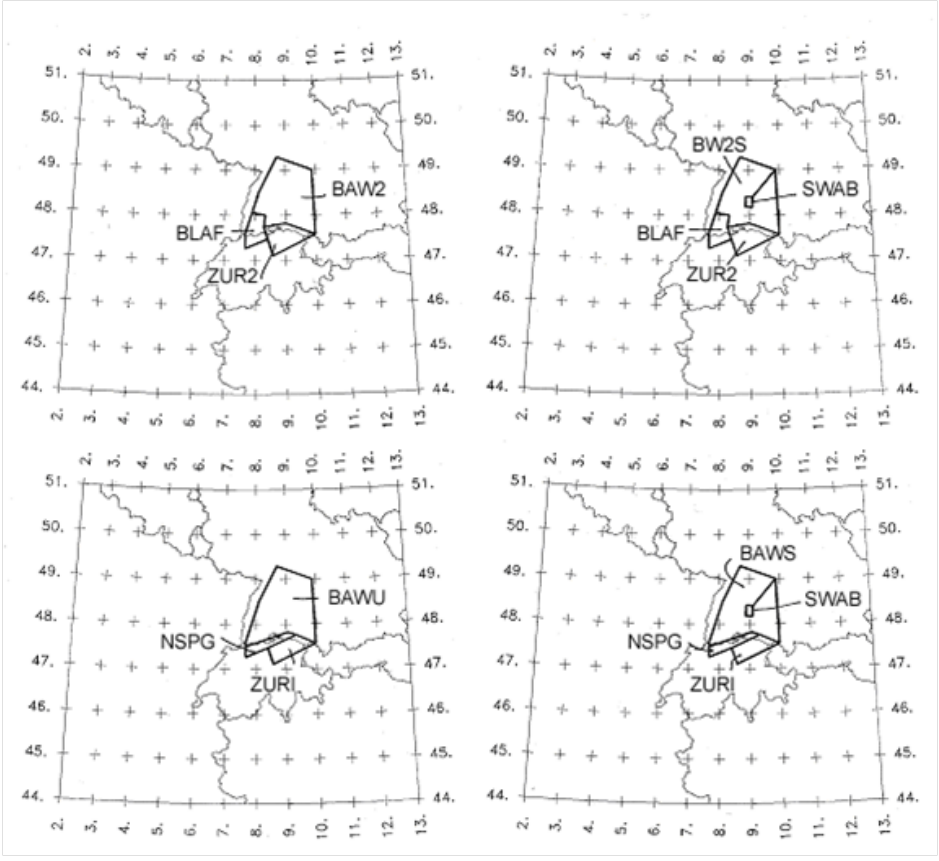

Figure 3.3: EG1c alternative source zonations for the Swabian Jura and permocarboniferous troughs.

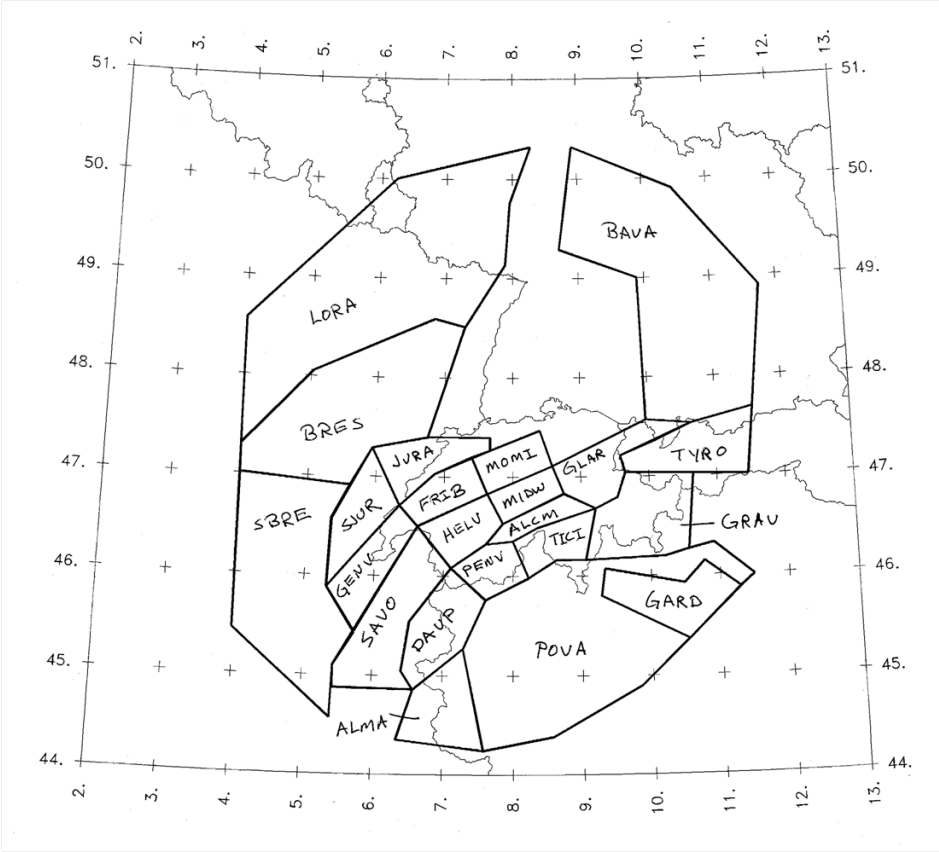

Figure 3.4: EG1c source zones that do not change with the alternatives listed on Figure 3.1.

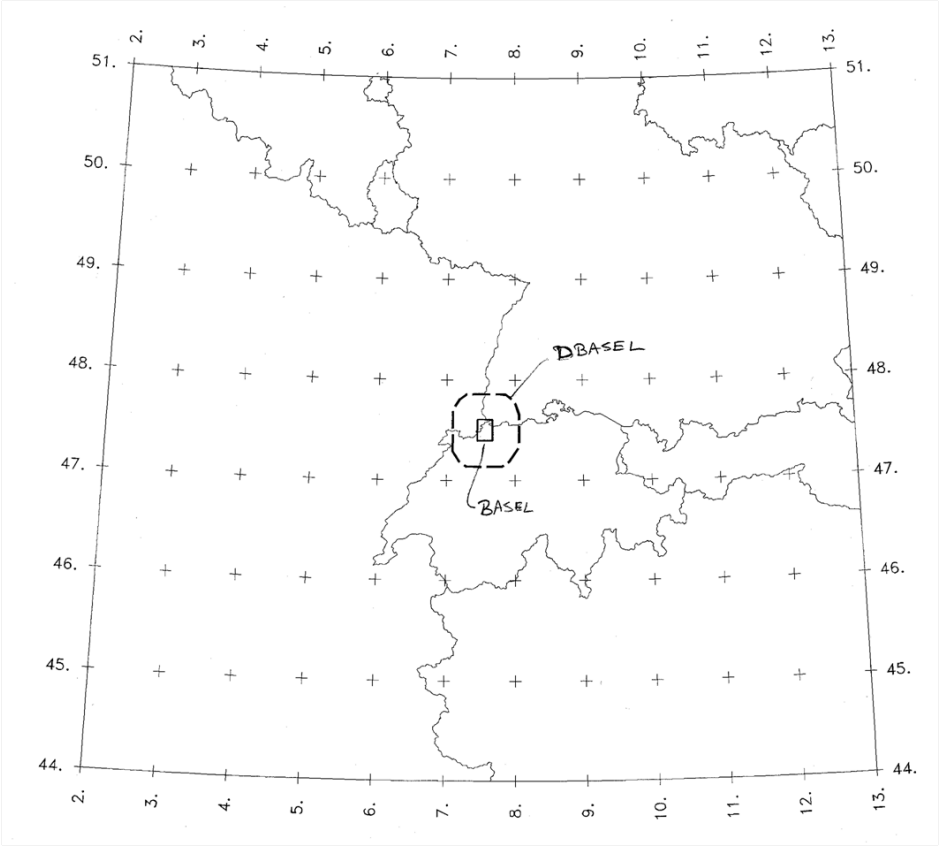

Figure 3.5: The nominal BASL polygon and the limits of the distributed Basel source, DBASL.

3.2 Earthquake Rupture Geometry

The size of earthquake ruptures is defined by the relationship:

$$\text{Mean}\log_{10}(\text{rupture area}) = 1.04M - 4.31 \quad (3.1)$$

$$\sigma\log_{10}(\text{rupture area}) = 0.24 \quad (3.2)$$

Using the relationship for the expectation of a lognormal distribution, the mean (expected) rupture area is given by the relationship:

$$\text{mean rupture area} = 10^{(1.04M-4.244)} \quad (3.3)$$

The relationship for the mean rupture area will be used in the hazard computations. The rupture length and width have an aspect ratio of 1:1 until the maximum rupture width for a source is reached. The maximum rupture width is determined on the basis of the maximum depth and fault dip, as defined below. For larger ruptures, the width is held constant at the maximum width and the length is obtained by dividing the rupture area by this width.

Earthquake epicenters are uniformly distributed within each source except for the distributed Basel source DBASL where a spatial density grid is provided. Earthquake ruptures are located symmetrically on the epicenters (the epicenter is at the midpoint of the rupture). For those epicenters located closer than 1/2 rupture length to the source zone boundary, the ruptures are allowed to extend beyond the source boundary except for the following cases. Figure 3.6 shows regional boundaries that ruptures cannot cross. Because the sites of interest are all located within the central region where ruptures can cross source boundaries, the objective of Figure 6 can be achieved by truncating ruptures at the source boundaries for sources RHEG, RHGS, BRES, SBRE, LORA, POVA, and BAVA. This will prevent ruptures originating outside of the central region from crossing the heavy boundaries on shown of Figure 3.6 and extending closer to the sites. The boundary condition for each source is listed in table 3.2.

Table 3.2 defined the relative frequency of rupture orientations and styles-of-faulting for the individual sources. Two specific styles-of-faulting are considered for larger events ($> M5.5$), strike-slip and reverse. A possible third condition may exist in which the specified fraction of earthquakes are to have random orientation (uniform distribution for azimuth) and random style-of-faulting (equally likely to be strike-slip or reverse faulting). The relative frequency of styles-of-faulting and rupture orientation for the larger earthquakes specified in table 3.2 are to be used for all earthquakes.

The depth distribution of hypocenters for small events is defined by a trapezoidal distribution with the parameters listed in table 3.3. Listed are the minimum and maximum depths and the upper and lower depths for the plateau in the trapezoidal distribution. Figure 3.7 shows an example distribution. For larger earthquakes, a magnitude-dependent depth distribution is to be developed using the weighted approach outlined in Toro [2003] (TP1-TN-0373) with T = 0.5 (hypocenter in lower half of rupture).

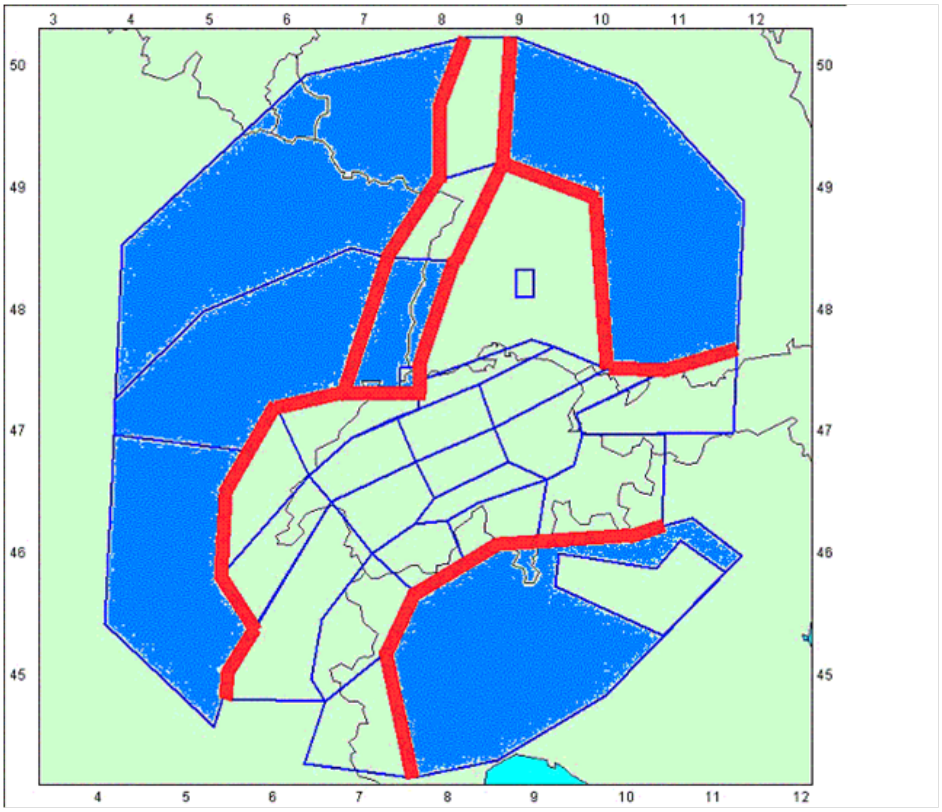

Figure 3.6: Restrictions on propagation of fault rupture. The darker blue sources have boundaries that may not be crossed by ruptures, except in the case of events originating from the BASL (DBASL) source.

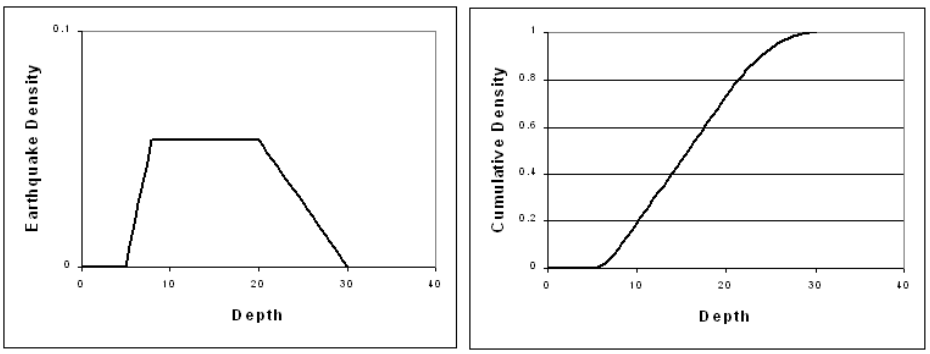

Figure 3.7: Example depth distribution with a minimum depth of 5, upper plateau depth of 8, lower plateau depth of 20, and a maximum depth of 30.

Table 3.2: Rupture Orientation, Style of Faulting, and Source Boundary Conditions.

Source	Strike Slip*	Reverse*	Random	Ruptures can Cross Source Boundary Source Boundary
DBASL	0.4, N20E	0.4 N75E	0.2	Yes
RHEG	1.0, N20E	0	0	No
RHGN	1.0, N20E	0	0	Yes
RHGC	1.0, N20E	0	0	Yes
RHGS	1.0, N20E	0	0	No
LORA	0	0	1	No
BRES	0	0	1	No
SBRE	0	0	1	No
BAVA	0	0	1	No
SWAB	1.0, N10E	0	0	Yes
BAWU	0	0	1	Yes
BAW2	0	0	1	Yes
BAWS	0	0	1	Yes
BW2S	0	0	1	Yes
BLAF	0	0	1	Yes
NSPG	0	0.6, N75E	0.4	Yes
ZURI	0.1, N20E	0.4, N75E	0.5	Yes
ZUR2	0.1, N20E	0.4, N75E	0.5	Yes
MOMI	0.1, N20E	0.4, N60E	0.5	Yes
FRIB	0.1, N00E	0.4, N50E	0.5	Yes
JURA	0.1, N00E	0.4, N50E	0.5	Yes
SJUR	0.1, N10W	0.4, N40E	0.5	Yes
GENV	0.1, N10W	0.4, N40E	0.5	Yes
GLAR	0.1, N00E	0.6, N60E	0.3	Yes
NIDW	0	0.7, N60E	0.3	Yes
HELV	0	0.7, N50E	0.3	Yes
SAVO	0	0.7, N10E	0.3	Yes
GRAU	0	0	1	Yes
TICI	0	0	1	Yes
PENV	0	0	1	Yes
DAUP	0	0	1	Yes
ALMA	0	0	1	Yes
ALCM	0	0	1	Yes
TYRO	0	0	1	Yes
GARD	0	0	1	Yes
POVA	0	0	1	No

* First number is the relative frequency and second number is the rupture orientation. Note that strike-slip earthquakes have a dip of 90 degrees and reverse earthquakes have a dip of 45 degrees to the south, southeast, or east, depending on the strike.

Table 3.3: Hypocenter Depth Distribution Parameters.

Source	Minimum	Upper Plateau	Lower Plateau	Maximum
DBASL	5	8	20	30
RHEG	5	8	20	30
RHGN	5	8	20	30
RHGC	5	8	20	30
RHGS	5	8	20	30
NSPG	3	8	20	30
BAVA	5	8	15	30
BAWU	5	8	15	30
BAW2	5	8	15	30
BAWS	5	8	15	30
BW2S	5	8	15	30
SWAB	5	8	15	30
BLAF	5	8	15	30
MOMI	5	8	20	30
ZURI	5	8	25	30
ZUR2	5	8	25	30
FRIB	5	8	20	30
GENV	5	8	20	30
JURA	5	8	15	20
SJUR	5	8	15	20
ALCM	3	6	12	20
GLAR	3	6	12	20
NIDW	3	6	12	20
HELV	3	6	12	20
SAVO	3	6	12	20
DAUP	3	6	12	20
PENV	3	6	12	20
TICI	5	6	12	20
GRAU	3	6	12	20
TYRO	5	8	15	30
BRES	5	8	15	25
LORA	5	8	15	25
SBRE	5	8	15	25
ALMA	5	8	15	50
GARD	5	8	15	50
POVA	5	8	15	50

3.3 Earthquake Recurrence Parameters

The alternatives for defining the maximum magnitude and earthquake recurrence parameters are shown on Figure 3.8. The approaches for assessing maximum magnitude and recurrence parameter distributions are linked as indicated in the logic tree, resulting in two sets of parameter distributions. Note that for all sources, a truncated exponential earthquake recurrence relationship is used to define the relative frequency of earthquakes of different sizes.

The first set consists of a directly assessed single distribution for maximum magnitude that is applied globally to all zones: M_{max} being 6.5 M_W (weighted 0.111), 7.0 M_W (weighted 0.778) and 7.5 M_W (weighted 0.111). Individual M_{max} distribution files for each source zone are contained in subdirectory `./RECMOD1.MMX`. These individual source zone M_{max} distributions are dependent across all sources, that is M_{max} in all sources is simultaneously either 6.5, 7, or 7.5. The accompanying joint distributions for beta $[b - value \times \ln(10)] and N(m \geq 5)$ are determined using a maximum likelihood formulation for an exponential distribution with a global prior derived from the whole catalogue and computing relative likelihoods. Individual distribution files for each source zone are contained in subdirectory `./RECMOD1.ABD`. The recurrence parameter distributions for each zone are independent. This set of parameters corresponds to the path through the logic tree (Figure 3.8) designated by "Global" for M_{max} approach, "Direct Assessment" for M_{max} method and "PML Global Prior" for recurrence method.

The second set consists of individual source M_{max} distributions computed using a sample likelihood function based on the maximum observed event or 5.5 M_W, whichever is the larger, and the number of earthquakes in the zone. The likelihood function is truncated at a maximum of 7.3 in order to generate a proper probability distribution. Individual M_{max} distribution files for each source zone are contained in subdirectory `./RECMOD2.MMX`. The accompanying joint distributions for beta [b-value $\times \ln(10)$] and $N(m \geq 5)$ are determined using a maximum likelihood formulation but instead of a moderate prior derived from the whole catalogue (as in branch A), strong local priors were used for each zone, derived from least-squares analysis. Individual distribution files for each source zone are in subdirectory `./RECMOD2.ABD`. This set of parameters corresponds to the path through the logic tree (Figure 3.8) designated by "Local" for M_{max} approach, "Likelihood" for M_{max} method and "PML Local Prior" for recurrence method.

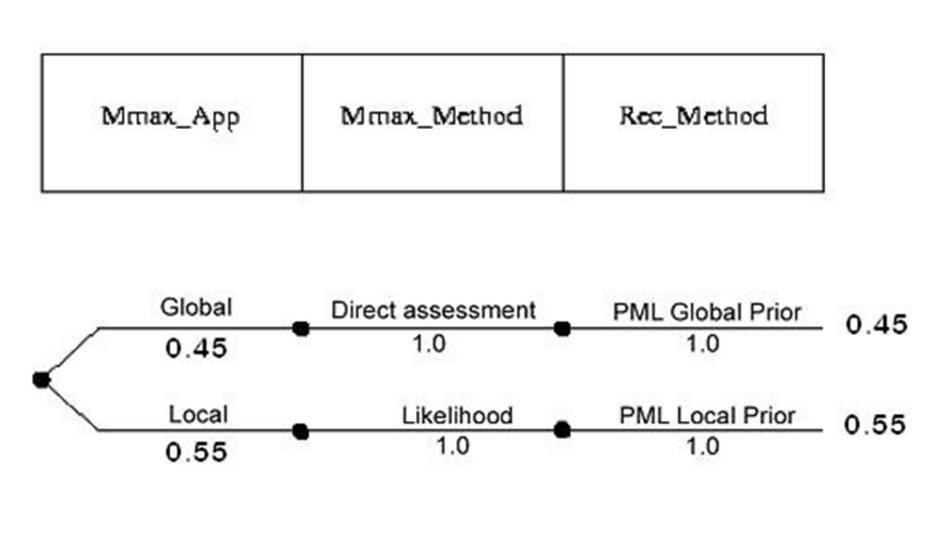

Figure 3.8: EG1c maximum magnitude and earthquake recurrence parameter logic tree.

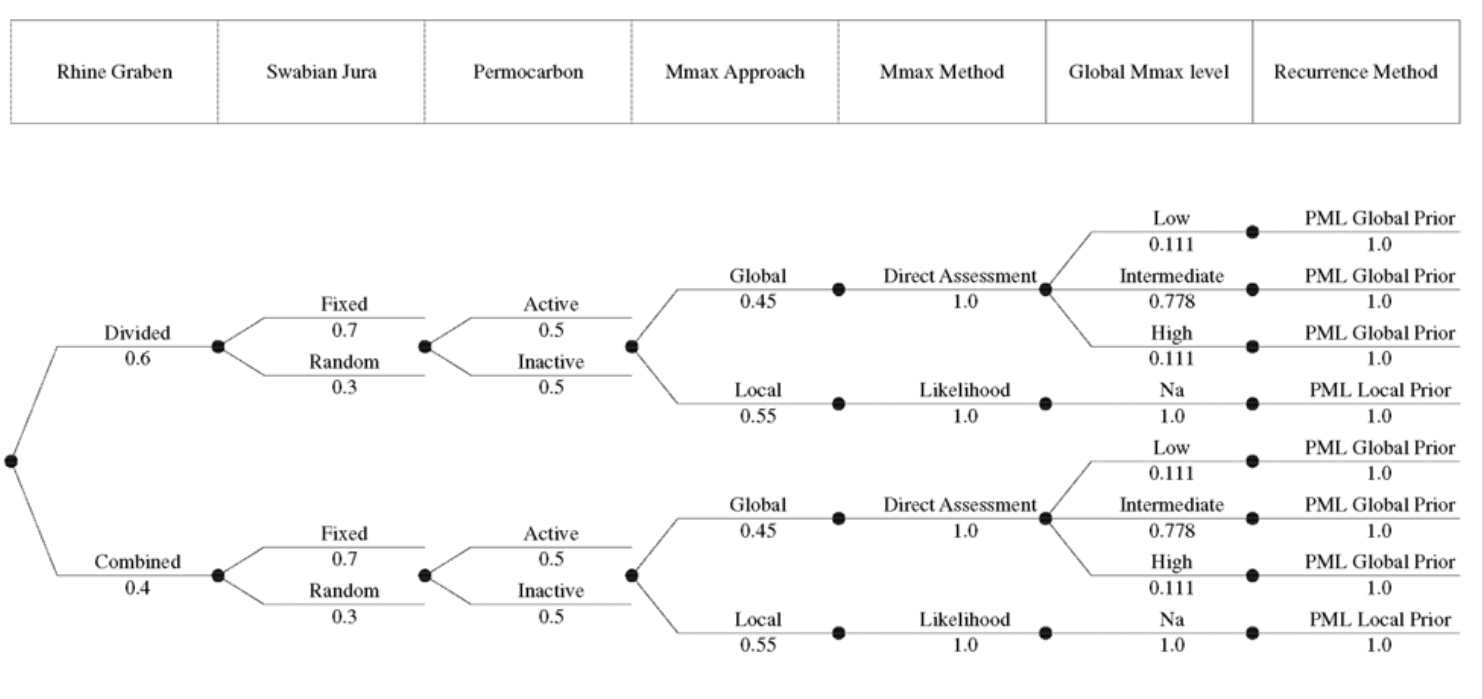

Figure 3.9: Logic tree for EG1c.

Chapter 4

QA-Certificate EG1-QC-1024

QA Certificate	PEGASOS REFINEMENT PROJECT
EG1-QC-1024	

Hazard Input Document (HID)

Expert group:	**EG1c**	***HID designation:***	**EG1-HID-1003**
Expert:	R. M.W. Musson, S. Sellami Leinen	***Expert Model (EXM)***	EG1-EXM-1003

HID parameterisation of Expert Model:

TFI: N. A. Abrahamson ***Hazard Input Specialist of TFI-team:*** Ph. Roth

HID based on Elicitation Documents: ☒ EG1-ES-1003

HID based on Exp. Assessments (EXA): ☐

Remarks on the HID model parameterisation in terms of hazard computation input:

The undersigned Hazard Input Specialist confirms that this HID includes all required (subproject specific) input information for hazard computations. No further interpretations of this input will be required and no simplifications except Algorithmic Pinching according to paragraph 2.9 of the QA-Guidelines will be applied to convert this HID into hazard software Input Files.

Signature:

HID acceptance by the Expert / Expert Group:

Date of HID review by the Expert / Expert group: 23.08.2011

HID accepted: ☒ ***HID not accepted:*** ☐

Reasons for non-acceptance of HID / Recommendations:

The undersigned Expert(s) accept(s) the parameterisation proposed in this HID as a faithful and adequate representation of his/their Expert Model. He/they confirm(s) that this HID is free of errors and agree(s) to its use as hazard computation input.

Signature Expert 1 / Expert:

Signature Expert 2:

Signature Expert 3:

Part V

Assessments of EG1d

by J.-P. Burg, G. Fernández and S. Wiemer

Chapter 1

EG1d Evaluation Summary (EG1-ES-1004)

1.1 Assessment of EG1d by March 2010

On March 25, 2010 the SP1 EG1d expert team provided its assessments and conclusions on the applicability of the SP1 EG1d PEGASOS model for the PRP. This document conveys the assessment and requests of Expert group EG1d with respect to the recurrence, M_{max}, and hazard sensitivity calculations based on the final ECOS09. This assessment is intended as input for he calculations performed by R. Young's and Ph. Roth. A summary and overview of the underlying PEGASOS models of EG1d can be found in Wiemer et al. [2009].

The modified ECOS09 catalog has a potential impact on the EG1d logic tree in a number of places (see Figure 1.1). Based on the feedback provided to us during the three SP1 workshops, we have assessed the impact expected on our hazard model, and come to the following conclusions:

1. The changes in epicenter locations when comparing ECOS02 and ECOS09 are minor, specifically for larger events, and they do not seem to be systematic. We do not see the need to update our zonation model, or smoothing kernel, because of ECOS09. This is particularly so since in our model we are explicitly including the uncertainty in hypocenter, which should make the model less sensitive to small changes.

2. The changes in hypocenter distributions, likewise, seem minor to us, and we do not see the need to update the depth distribution used in our model.

3. The addition of earthquake data since 2002 is welcome and should of course be used in deriving the recurrence parameters. While we are fully aware that the completeness has significantly improved since 2002, we do not want to introduce a new completeness period 2002-2009, because we do not want more weight in our model to the very small events ($M < 2.2$). We therefore extend for each completeness region the most recent period to 2009.

4. The change in the M_W to M_L scaling introduces a significant change in the completeness of the instrumental data. The completeness periods are unchanged, but the absolute levels do change. This was investigated in detail in a report by Wiemer and Wössner [2010] and through the Stepp plots provided by R. Youngs. Because the EG1d model uses small magnitudes since 1975 onwards, we need to take this change in M_C into account. The change observed in the data when mapping M_C is indeed close to the theoretical curve introduced by the M_W/M_L conversion (Figure 1.2). We therefore will use for the instrumental period adjusted completeness windows according to the conversion shown in Figure 1.2.
   For the historical data, the situation is more complex. Many historical events are smaller now due to the different set of calibration events used (see also Figure 11 of Wiemer and Wössner [2010]). Because historical completeness was assigned partially due to the historical record of events, it is conceivable that the completeness magnitudes of the historical record derived based on ECOS02 is slightly too high when using ECOS09 magnitudes, at least for the range $M_C > 5.0$. For the M_C range 3-5, the situation is even less clear. Because the effect is small and not very clear in the data, we will use for the historical completeness the same M_C thresholds as used in our ECOS02 based assessment.

5. b-values: The possibility of a non-linear compression of the M_W scale relative to the M_L scale, and the lingering question in which scale a Gutenberg-Richter power law may in fact be valid, is unresolved right now. The attempt to introduce a modified Truncated Exponential (mTE) fit that "corrects" the small magnitudes back to a M_W ECOS02 compatible version (model three in EG1D-rec_corrected.ppt provided by B. Young's) is successful in reproducing the ECOS02 results. However, the fact that the larger events now have s smaller magnitude leads to a significant discrepancy between the observed rates and forecasted ones when using the mTE approach (slide 11 of the presentation). The ECOS09 with modified completeness intervals (green curves in slide 10) seem a reasonable fit, they also result in overall b-value that seem more reasonable than the ones obtained for ECOS02. The red curves, while visually pleasing, have the problem of using an obviously "wrong" M_C, so we do not consider them adequate. We therefore like to use the Model ECOS09 with modiefied M_C intervals.
   In addition to running the "green" model with the normal TE, we would like to see rate and hazard sensitivity calculations for a new model where the minimum completeness of the instrumental period is set to 3.0. At this M_C, the effect of the non-linear M_W/M_L conversion is minimal.

6. M_{max}: We decide to use the approach "ECOS09 with Mod. Comp. Intervals" (purple bars in EG1D-M_{max} corrected.ppt), because as outlined before we do not see the mTE as a good model, and we do believe that the M_C needs to be adjusted (but only for the instrumental data). We also like to evaluate if the "equal binning" approach proposed and request by G. Grünthal has an effect on our M_{max} distribution and potentially on the hazard.

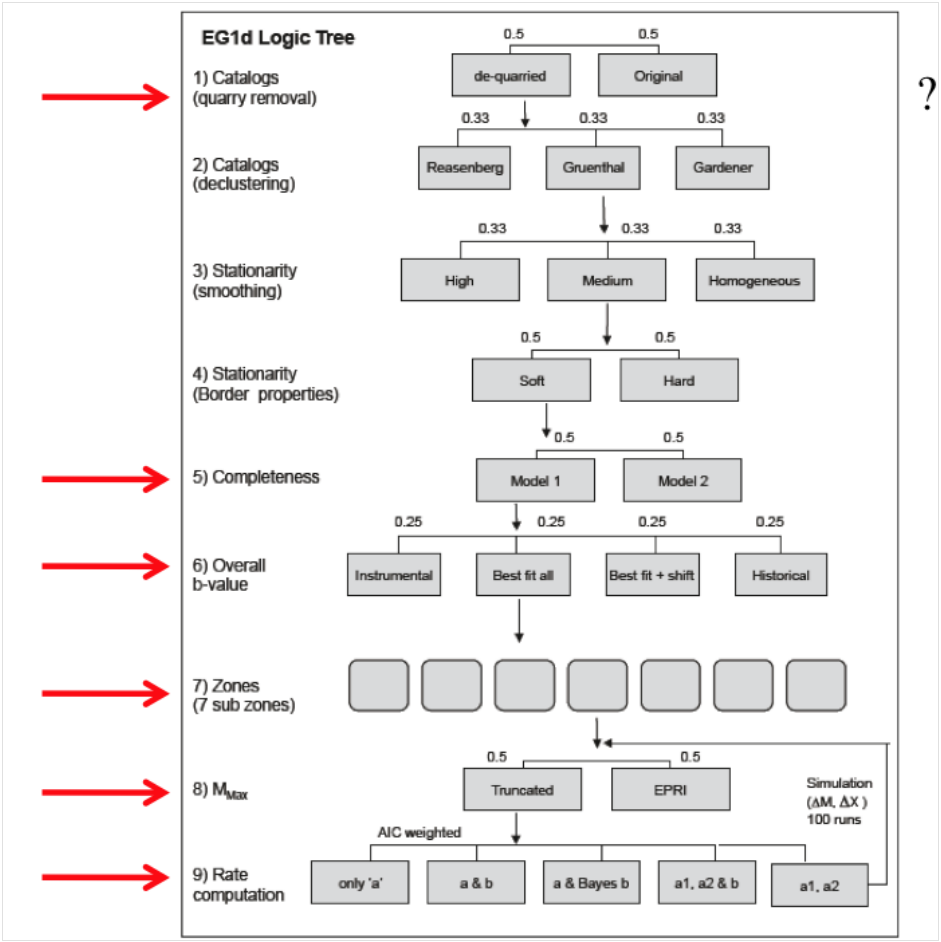

Figure 1.1: The EG1D logic tree. Red arrows mark decisons in the logic tree that could be impacted by the new ECOS09 catalog.

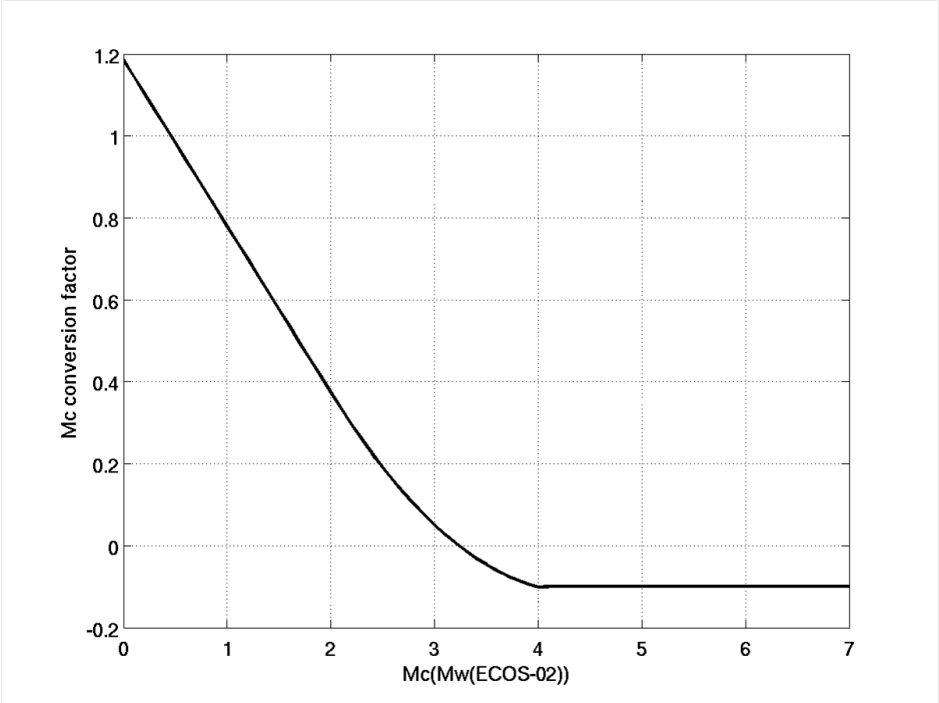

Figure 1.2: M_C conversion factor as a function of magnitude between from $M_C(M_W(\text{ECOS-02}))$and $M_C(M_W(\text{ECOS-09}))$. The factor needs to be added to the completeness estimated during the completeness assessment for ECOS-02.

Chapter 2

Support Calculations for EG1d by R. Youngs

2.1 Calculations for Expert Team EG1d

This section documents the calculations performed to support the EG1d Expert Team's review and finalization of the updated seismicity parameters based on the ECOS-09 catalog. These calculations are all performed using the final ECOS-09 catalog (Swiss Seismological Service, 2010) declustered by S. Wiemer utilizing Gardner and Knopoff [1974] approach with the time and distance windows developed by Grünthal [1985] as published in Burkhard and Grünthal [2009].

2.2 Regional b-values

The maximum likelihood method described in section 2.2.3 was used to compute regional b-values for the study region using the final ECOS-09 catalog. The regional b-values are computed using four sets of catalog completeness parameters.

- Completeness Set 1 is the original ECOS02 completeness Set 1 with modified magnitude intervals based on Equation 2.11 and extending the completeness periods to the catalog end date of 2009/01/01.
- Completeness Set 2 is the original ECOS02 completeness Set 2 with modified magnitude intervals based on Equation 2.11 and extending the completeness periods to the catalog end date of 2009/01/01.
- Completeness Set 3 is the new ECOS09 Set 1, considering only magnitudes $\geq M3.007$
- Completeness Set 4 is the new ECOS09 Set 2, considering only magnitudes $\geq M3.007$

These completeness sets are listed in tables 2.1 through 2.4.

The regional b-values are computed assuming that there is a uniform b-value throughout the study region but allowing for differences in the seismicity rate among the five catalog completeness regions defined by EG1d (shown in Figure 2.100). The plots are grouped in the order of the four different regional b-value estimates used by EG1d. Figures 2.1 through 2.4 show the results obtained by fitting all of the catalog data. Figures 2.5 through 2.8 show the results obtained by fitting the catalog data allowing for a change in recurrence rate between the instrumental period (post 1/1/1975) and the pre-instrumental period (prior to 1975). Figures 2.9 through 2.12 show the results obtained by fitting only the post 1/1/1975 data. Figures 2.13 through 2.16 show the results obtained by fitting only the historical (pre 1880) data. The resulting regional b-values are listed in table 2.5.

2.3 Maximum Magnitude Distributions

Maximum magnitude distributions were computed for the EG1d seismic sources using the Bayesian (EPRI) approach described in section 2.2.4 with the Extended Crust prior distribution [Johnston et al. 1994]. Uncertainty in magnitude and earthquake location was incorporated in the assessment by simulation of 100 catalogs using the magnitude and location errors reported in the ECOS-09 catalog. The posterior distributions were then binned in 1/2 magnitude intervals. The likelihood function based on the maximum observed was computed using the 16 alternative regional b-values assessed above in section 2.2 and listed in table 2.5. These completeness regions are shown on Figure 2.100. As shown on Figure 2.155, the source zones defined by EG1d overlap areas of different catalog completeness. Therefore, average values of catalog completeness were developed for each source zone for use in computing the maximum magnitude distributions by considering which completeness regions are representative of each source zone. Table 2.6 lists these approximate catalog completeness values used for computing the maximum magnitude distributions.

Figures 2.17 through 2.51 show the resulting maximum magnitude distributions. The results obtained using the different regional b-values are denoted by C1 through C1 for Completeness Sets 1 through 4 and by BA for all data, BI for post 1/1/1975, BH for pre 1880, and BS for separate seismicity rates before and after 1/1/1975. Each figure shows the results for the two alternative upper bound truncation values specified by EG1d, M 7.5 and M 8.0.

2.4 Earthquake Recurrence Rates

The maximum likelihood formulation presented in section 2.2.3 was used to compute earthquake recurrence rates for each of the seismic sources defined by EG1d. The approach used follows that developed by EG1d in PEGASOS. Recurrence rate parameter distributions are developed for the four alternative Completeness Sets. The four alternative regional b-values associated with each Completeness Set are used as priors for b with a weight equal to the inverse of the standard error for b-value obtained in the maximum likelihood calculations shown in section 2.2.

For each case defined by a Completeness Set and a regional b-value five alternative estimates of the seismicity parameters for each source are obtained

- b-value fixed at b-prior, all data used to estimate seismicity rate

- b-value fixed at b-prior, all data used to estimate seismicity rate with difference in rate pre and post 1/1/1975 allowed
- maximum likelihood fit of both seismicity rate and b-value, all data used
- maximum likelihood fit of both seismicity rate and b-value, all data used with difference in rate pre and post 1/1/1975 allowed
- maximum likelihood fit of both seismicity rate and b-value, all data used, Bayesian b-value obtained (see EG1d PEGAGOS Report).

The five alternative seismicity parameter distributions are weighted based on their relative Akaike Information Criterion (AIC) score. The process used is described in the EG1d PEGASOS Report.

EG1d also explored two methods for discretizing the Bayesian maximum magnitude distributions. The first follows the practice used in the PEGASOS of binning the posterior distribution into 1/2 magnitude unit bins. These are the distributions shown in section 2.3. This approach is designated as 0.5 delta M_{max} in the follow plot legends. The second method was to represent the posterior M_{max} distribution with a 5-point discrete approximation [Miller and Rice 1983]. This is designated as 5-point M_{max} in the plot legends.

Figures 2.52 through 2.69 show predicted earthquake recurrence rates for the six major source zones defined by EG1d. In each plot the earthquake occurrence rates are computed using the full logic tree for the four alternative regional b-values, the five alternative methods for computing the seismicity parameters, the two alternative upper bound truncations on the M_{max} distributions and the resulting M_{max} distribution for each source. The resulting mean, 5th percentile and 95th percentile predicted cumulative magnitude occurrence rates are shown.

The first two plots for each source show that the two alternative representations of the posterior M_{max} distributions produce similar predicted earthquake recurrence rates. The third plot for each source indicates the effect of the alternative minimum magnitudes used to estimate the seismicity parameters. The choice of the alternative minimum magnitude of M 3.007 does have some effect in various zones, typically resulting in higher predicted frequencies for earthquakes in the magnitude range of interest to the hazard calculations.
For Zone J the results for C2 are somewhat unusual. The reason is that for this zone the F2 option (free b-value, split rates for instrumental and historical periods) produces a high b-value (1.16). The time weighted a-value favors the historical rate. When this rate is projected back to $M < 4$, it gives high rates. For the C2 case the AIC weighting gives ∼10 to 15 % weight to the F2 case. Similar high b-values are obtained for F2 for C1, but the AIC weights are ~ 0. Thus, the values shown on the plot are an artifact of attempting to present a composite rate for all events based on the rates for $M > 5$ used in the hazard.

For Zone SA the small differences between C1 & C3 and C2 & C4 are due to the effect of the different regional b-values for these cases.

Figure 2.70 presents a comparison of the observed and predicted for all of Switzerland using the region defined by the Swiss completeness regions. The C2 results are affected by the results for Source J, which makes up a significant portion of Switzerland.

Table 2.1: EG1d Catalog Completeness Set C1.

Magnitude	Beginning Year for Complete Reporting in Completeness Region:				
	Austria	France	Germany	Italy	Switzerland
2.173					1977
2.424		1978			1977
2.702	1978	1978			1977
3.007	1896	1978	1870		1880
3.427	1896	1978	1870	1979	1880
3.7	1896	1880	1870	1979	1880
4.1	1896	1880	1870	1880	1880
4.5	1896	1880	1870	1880	1750
4.9	1896	1880	1870	1880	1750
5.4	1700	1700	1620	1775	1600
5.9	1700	1700	1300	1775	1300
6.4	1700	1700	1300	1775	1300

Table 2.2: EG1d Catalog Completeness Set C2.

Magnitude	Beginning Year for Complete Reporting in Completeness Region:				
	Austria	France	Germany	Italy	Switzerland
2.173					
2.424		1978			1977
2.702	1978	1978			1977
3.007	1978	1978	1980		1977
3.427	1896	1978	1870	1979	1977
3.7	1896	1978	1870	1979	1977
4.1	1896	1880	1870	1880	1880
4.5	1896	1880	1870	1880	1880
4.9	1896	1880	1870	1880	1750
5.4	1896	1700	1620	1775	1600
5.9	1700	1700	1620	1775	1300
6.4	1700	1700	1300	1775	1300

Table 2.3: EG1d Catalog Completeness Set C3.

Magnitude	Beginning Year for Complete Reporting in Completeness Region:				
	Austria	France	Germany	Italy	Switzerland
2.173					
2.424					
2.702					
3.007	1896	1978	1870		1880
3.427	1896	1978	1870	1979	1880
3.7	1896	1880	1870	1979	1880
4.1	1896	1880	1870	1880	1880
4.5	1896	1880	1870	1880	1750
4.9	1896	1880	1870	1880	1750
5.4	1700	1700	1620	1775	1600
5.9	1700	1700	1300	1775	1300
6.4	1700	1700	1300	1775	1300

Table 2.4: EG1d Catalog Completeness Set C4.

Magnitude	Beginning Year for Complete Reporting in Completeness Region:				
	Austria	France	Germany	Italy	Switzerland
2.173					
2.424					
2.702					
3.007	1978	1978	1980		1977
3.427	1896	1978	1870	1979	1977
3.7	1896	1978	1870	1979	1977
4.1	1896	1880	1870	1880	1880
4.5	1896	1880	1870	1880	1880
4.9	1896	1880	1870	1880	1750
5.4	1896	1700	1620	1775	1600
5.9	1700	1700	1620	1775	1300
6.4	1700	1700	1300	1775	1300

Table 2.5: Regional *b*-values for EG1d.

Catalog Completeness Set	*b*-value Approach	Regional *b*-value
C1	All data	0.919
	Prior to 1880	1.067
	Post 1975	1.238
	Split Pre and Post 1975	1.025
C2	All data	0.899
	Prior to 1880	1.185
	Post 1975	1.109
	Split Pre and Post 1975	1.002
C3	All data	0.877
	Prior to 1880	1.067
	Post 1975	0.955
	Split Pre and Post 1975	0.915
C4	All data	0.803
	Prior to 1880	1.185
	Post 1975	0.928
	Split Pre and Post 1975	0.895

Table 2.6: EG1d Catalog Completeness Values Uses for Maximum Magnitude Calculations.

Source Zone	Catalog Completeness Regions Used	Catalog Completeness Set	Catalog Completeness Values	
			Magnitude	Year
SA, XWCA,	Italy	C1, C2,	3.427	1979
XCA, XWA		C3 & C4	4.1	1880
			5.4	1775
			6.4	1500*
XHHA, XHA,	Switzerland	C1, C3	3.007	1880
HA, J, TZ			4.5	1750
			5.4	1600
			5.9	1300
		C2, C4	3.007	1977
			4.1	1880
			4.9	1750
			5.4	1600
			5.9	1300
E, B, RG, SRB,	Germany	C1, C3	3.007	1870
NRG, FKZ, SWA			5.4	1620
			5.9	1300
		C2, C4	3.007	1980
			3.427	1870
			5.4	1620
			5.9	1300

* Extended to capture older earthquakes

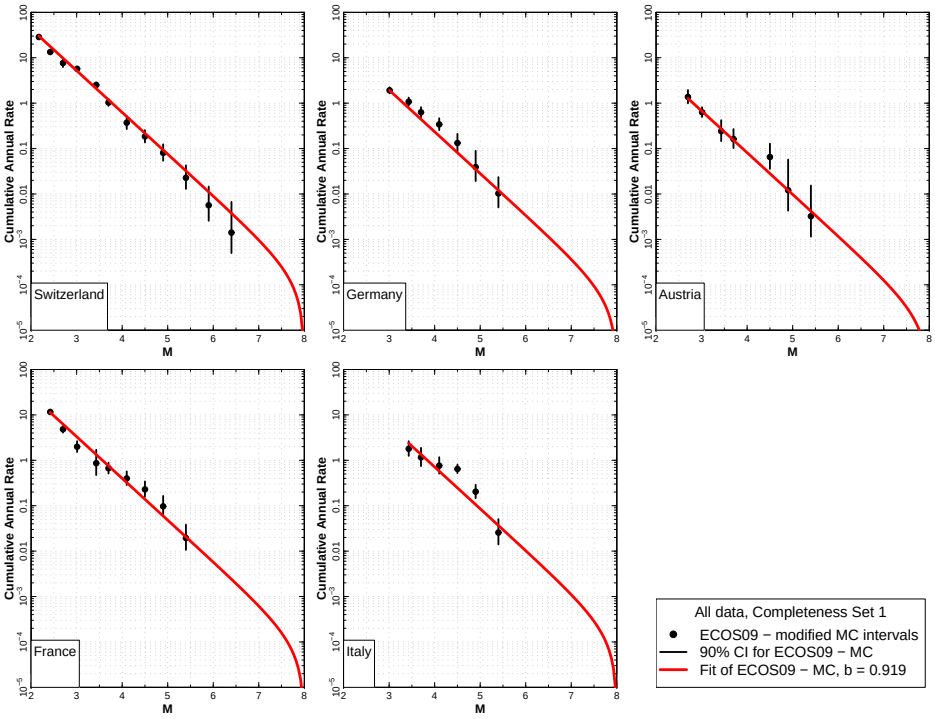

Figure 2.1: Regional *b*-value for EG1d Completeness Set 1 using all data.

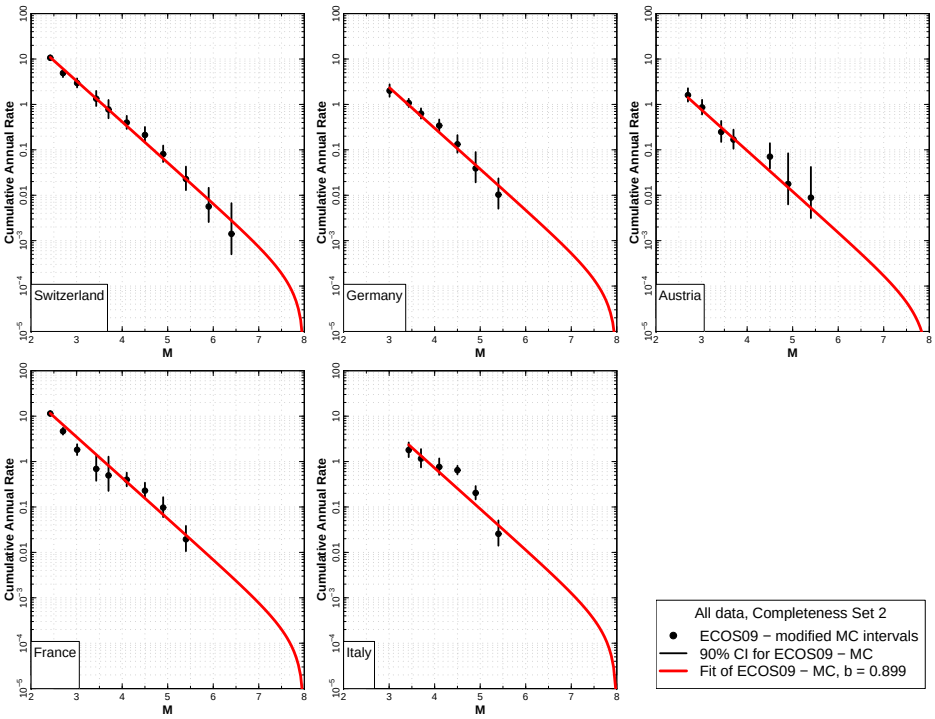

Figure 2.2: Regional *b*-value for EG1d Completeness Set 2 using all data.

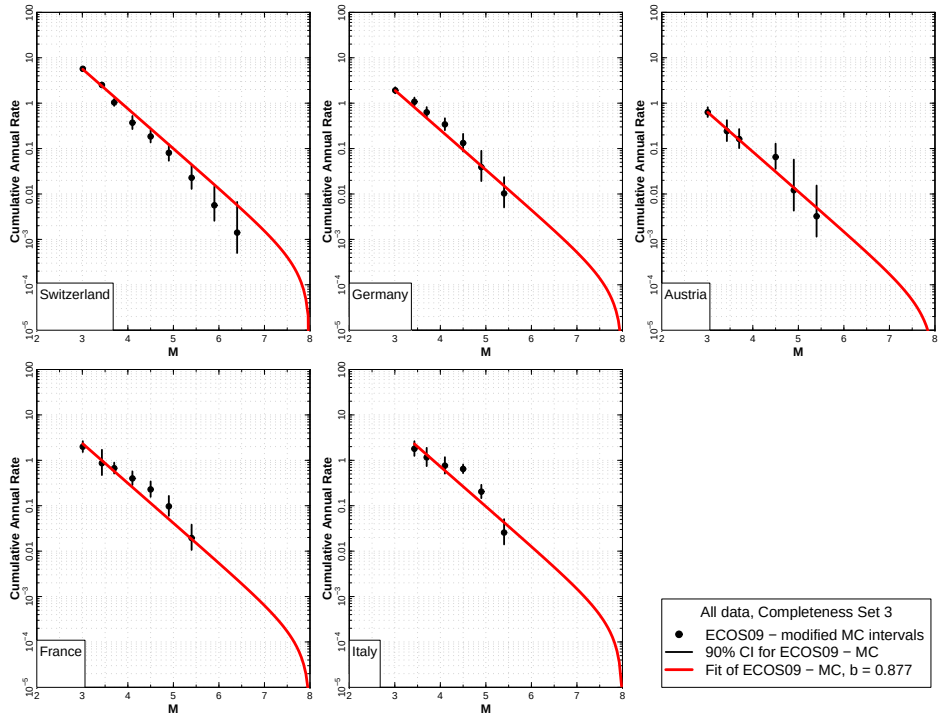

Figure 2.3: Regional *b*-value for EG1d Completeness Set 3 using all data.

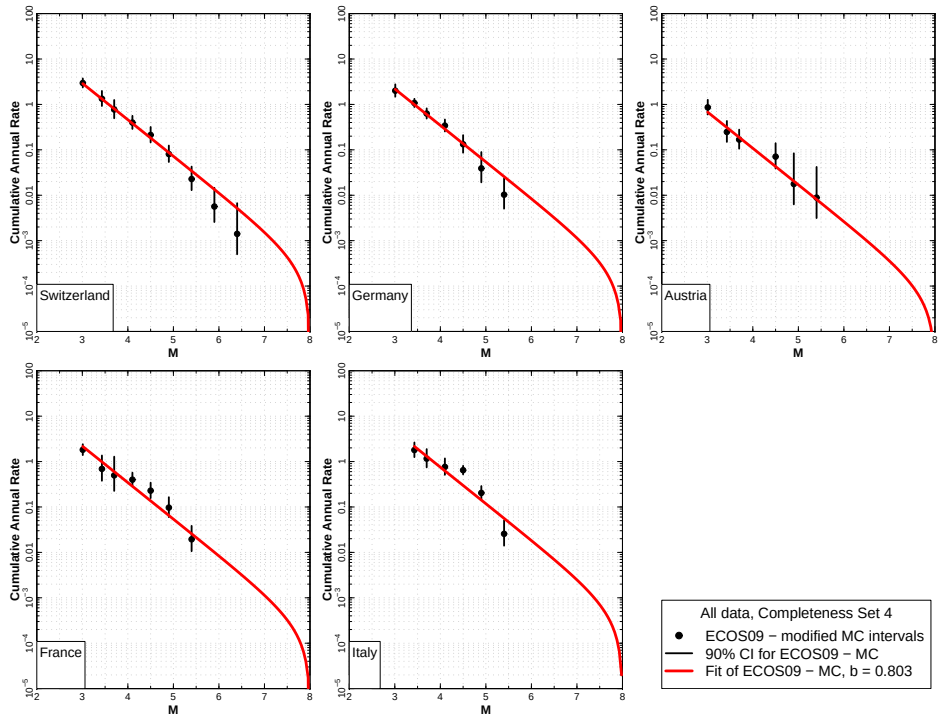

Figure 2.4: Regional *b*-value for EG1d Completeness Set 4 using all data.

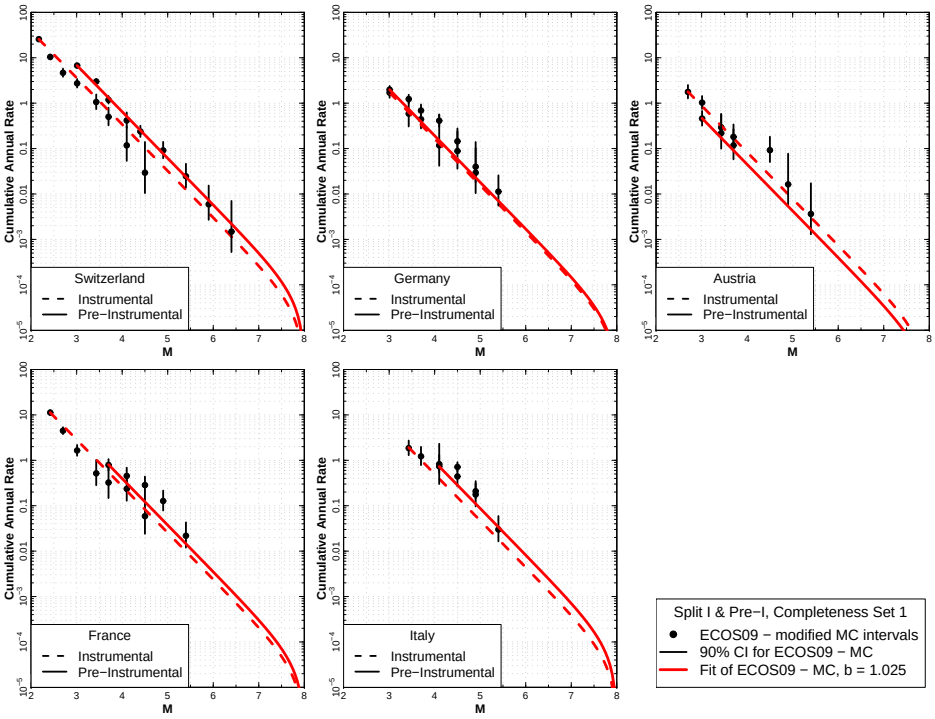

Figure 2.5: Regional *b*-value for EG1d Completeness Set 1 allowing for difference in recurrence rates in the instrumental (post 1/1/1975) and pre-instrumental (prior to 1/1/1975) periods.

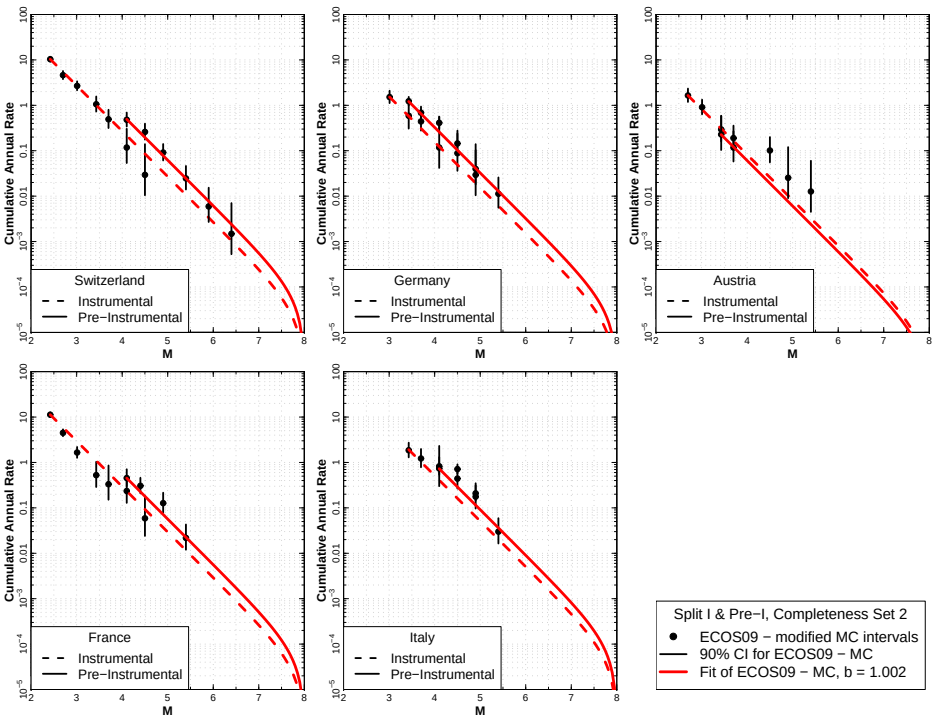

Figure 2.6: Regional *b*-value for EG1d Completeness Set 2 allowing for difference in recurrence rates in the instrumental (post 1/1/1975) and pre-instrumental (prior to 1/1/1975) periods.

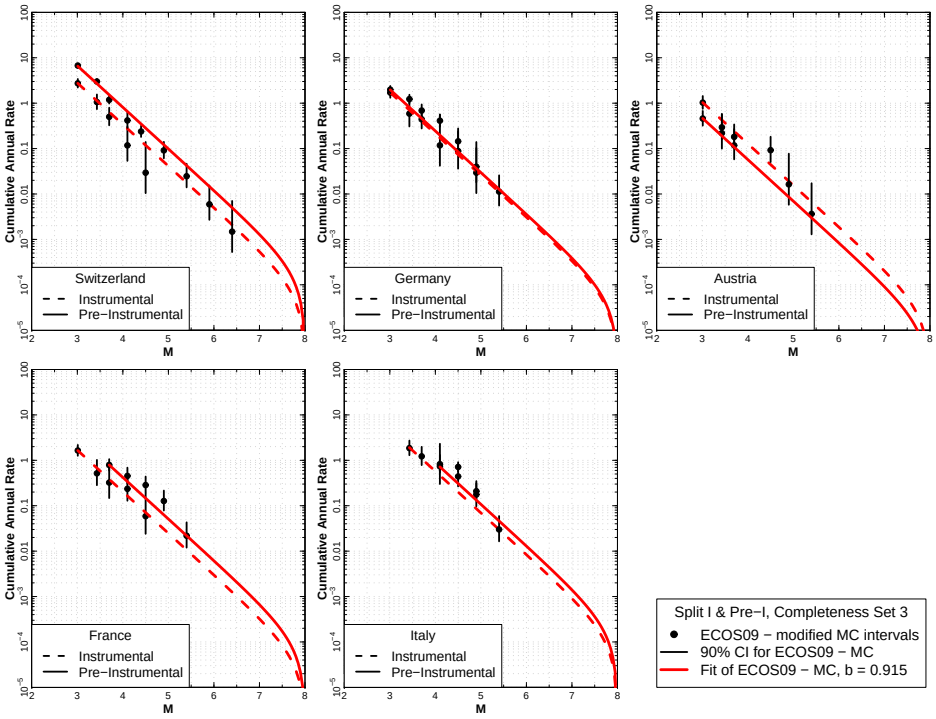

Figure 2.7: Regional *b*-value for EG1d Completeness Set 3 allowing for difference in recurrence rates in the instrumental (post 1/1/1975) and pre-instrumental (prior to 1/1/1975) periods.

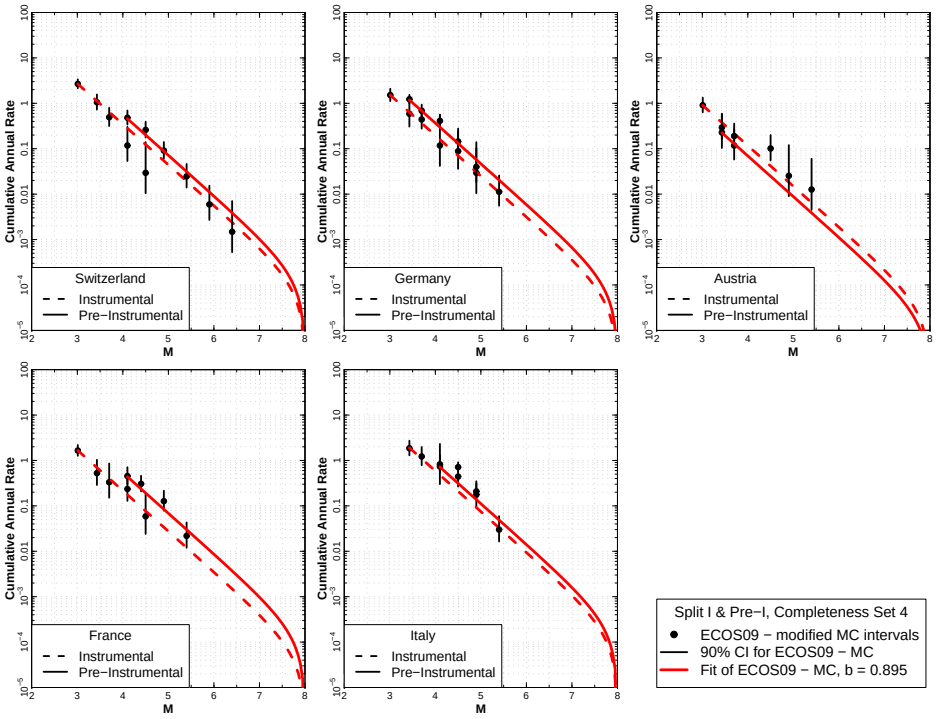

Figure 2.8: Regional *b*-value for EG1d Completeness Set 4 allowing for difference in recurrence rates in the instrumental (post 1/1/1975) and pre-instrumental (prior to 1/1/1975) periods.

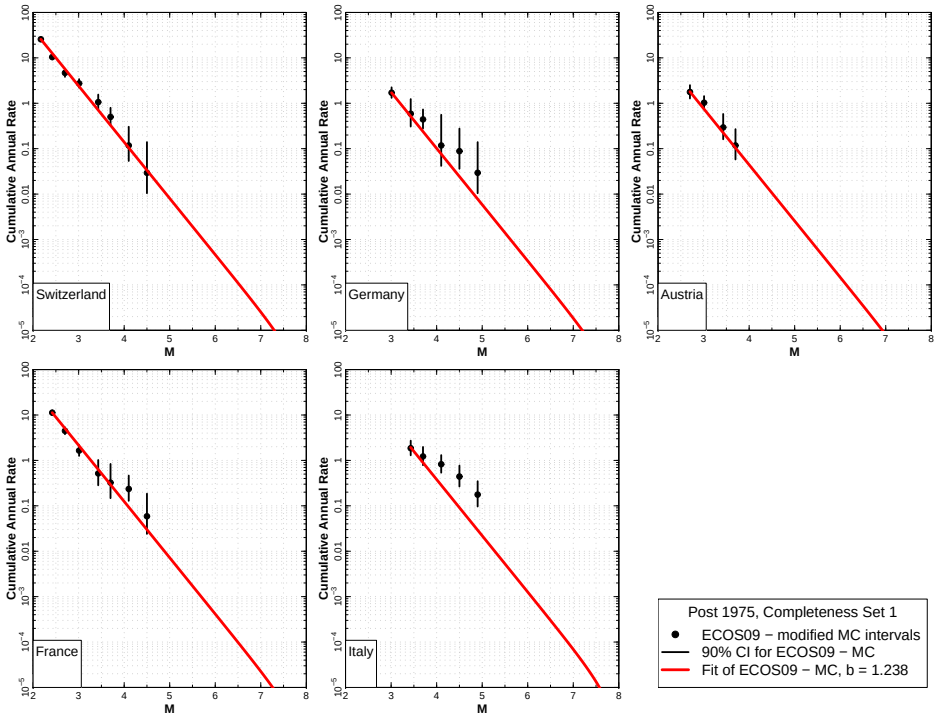

Figure 2.9: Regional b-value for EG1d Completeness Set 1 fitting only post 1/1/1975 data.

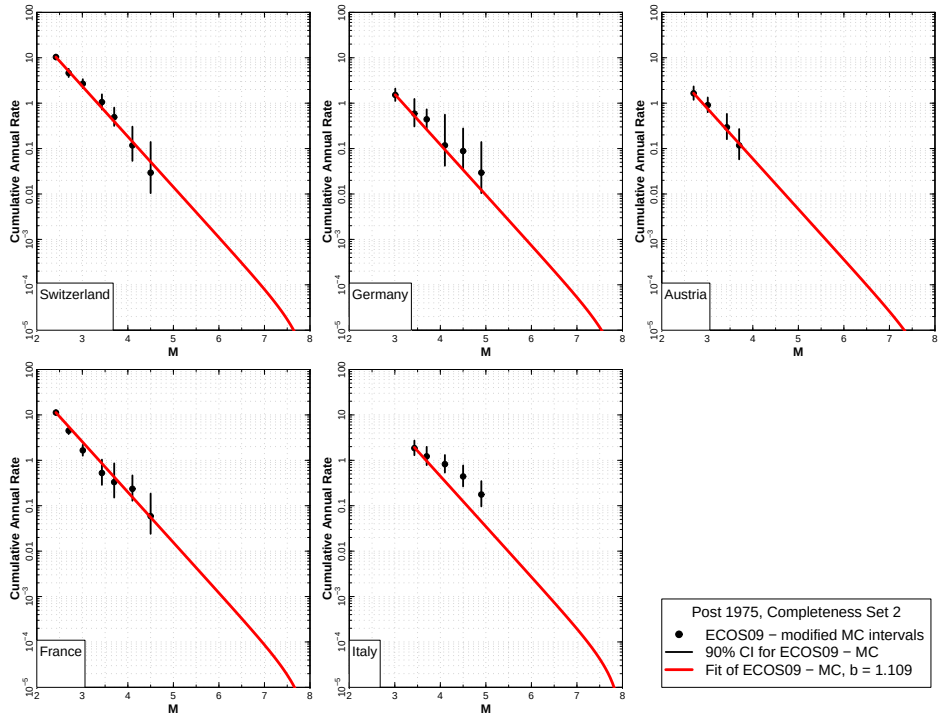

Figure 2.10: Regional *b*-value for EG1d Completeness Set 2 fitting only post 1/1/1975 data.

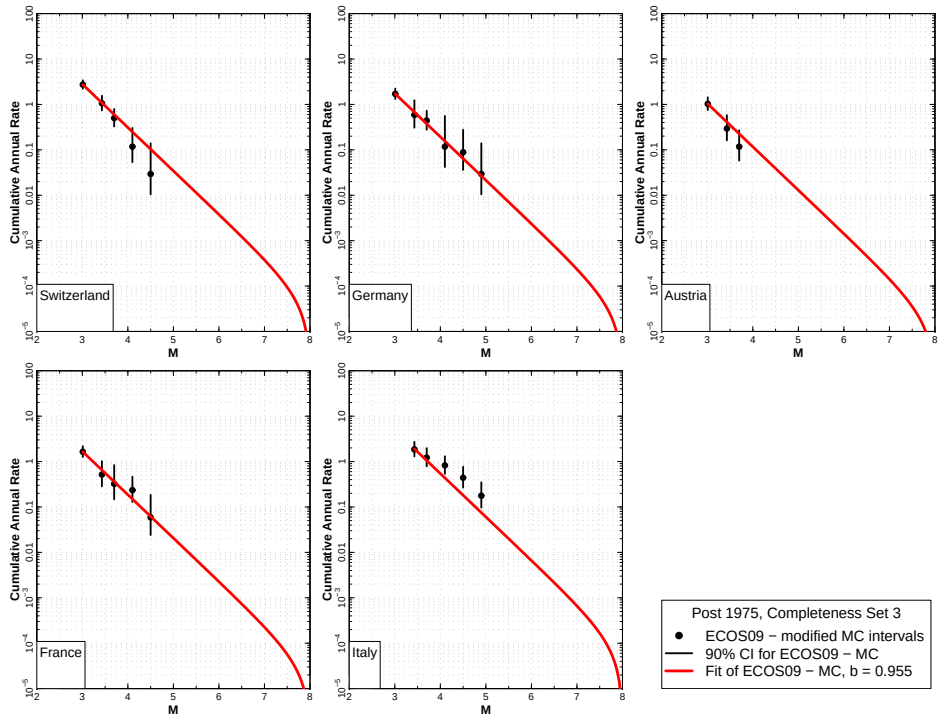

Figure 2.11: Regional *b*-value for EG1d Completeness Set 3 fitting only post 1/1/1975 data.

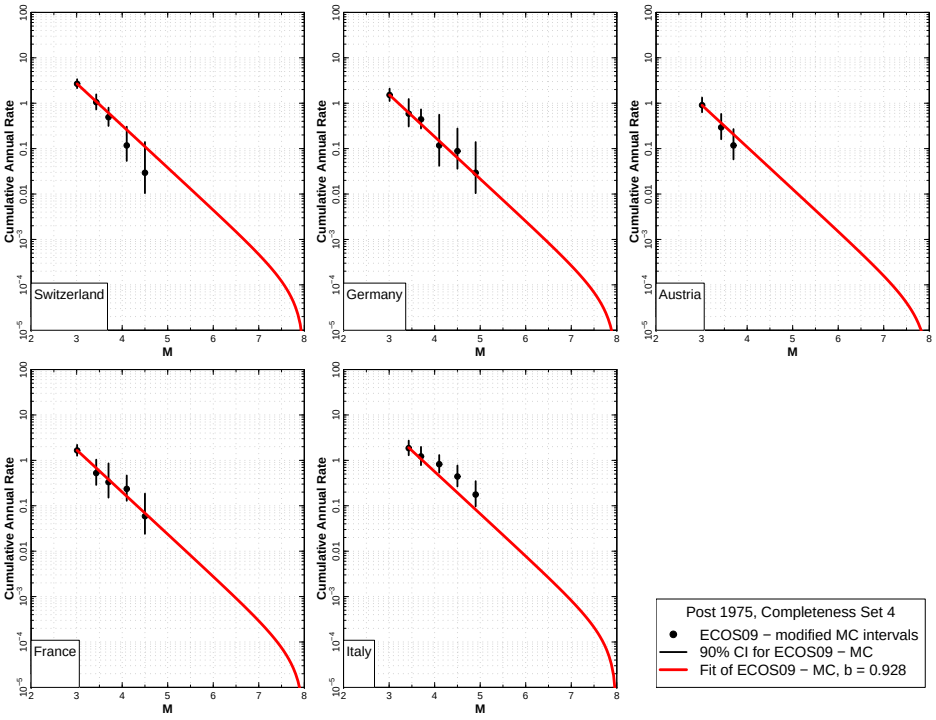

Figure 2.12: Regional *b*-value for EG1d Completeness Set 4 fitting only post 1/1/1975 data.

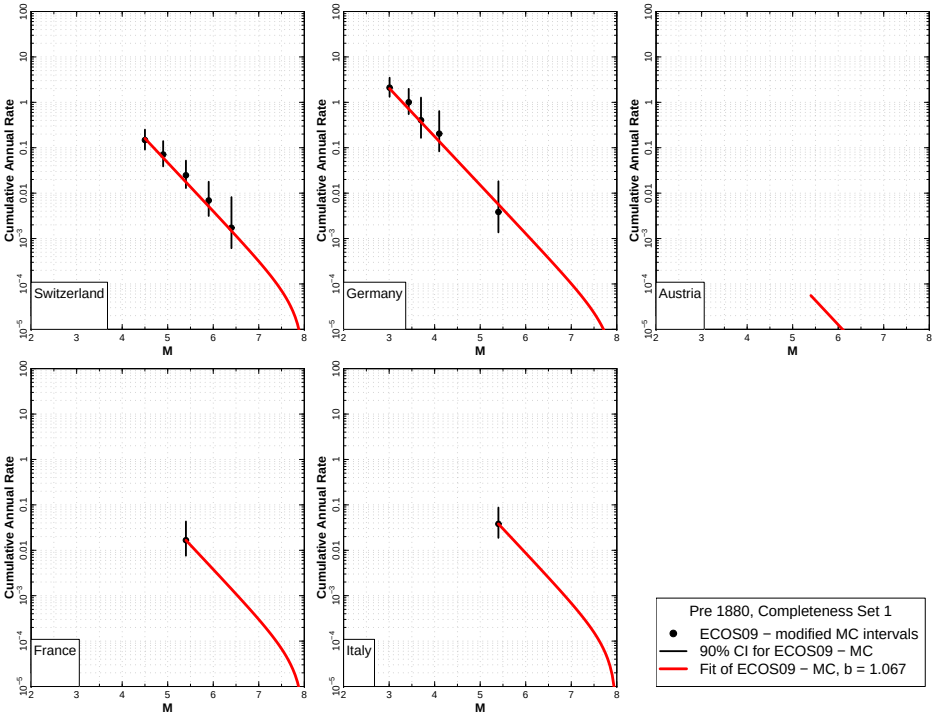

Figure 2.13: Regional *b*-value for EG1d Completeness Set 1 fitting only pre 1880 data.

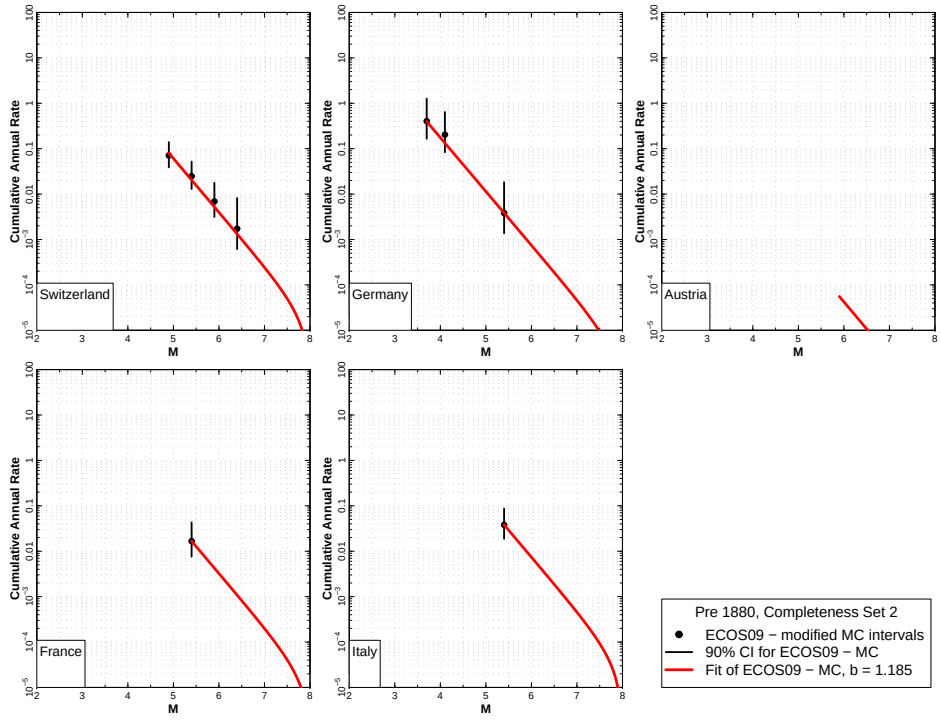

Figure 2.14: Regional *b*-value for EG1d Completeness Set 2 fitting only pre 1880 data.

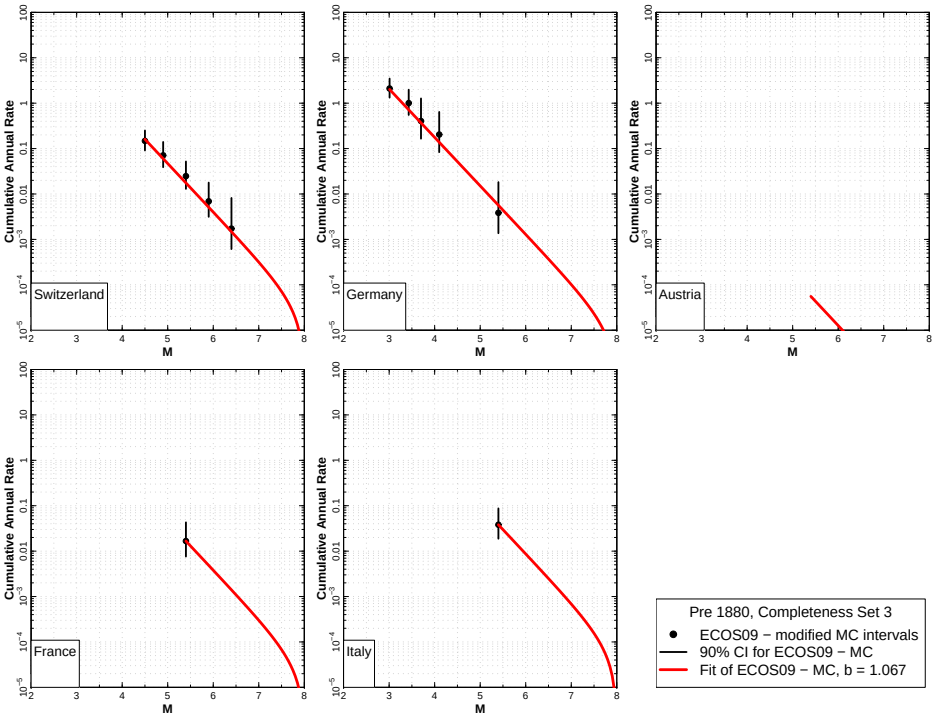

Figure 2.15: Regional *b*-value for EG1d Completeness Set 3 fitting only pre 1880 data.

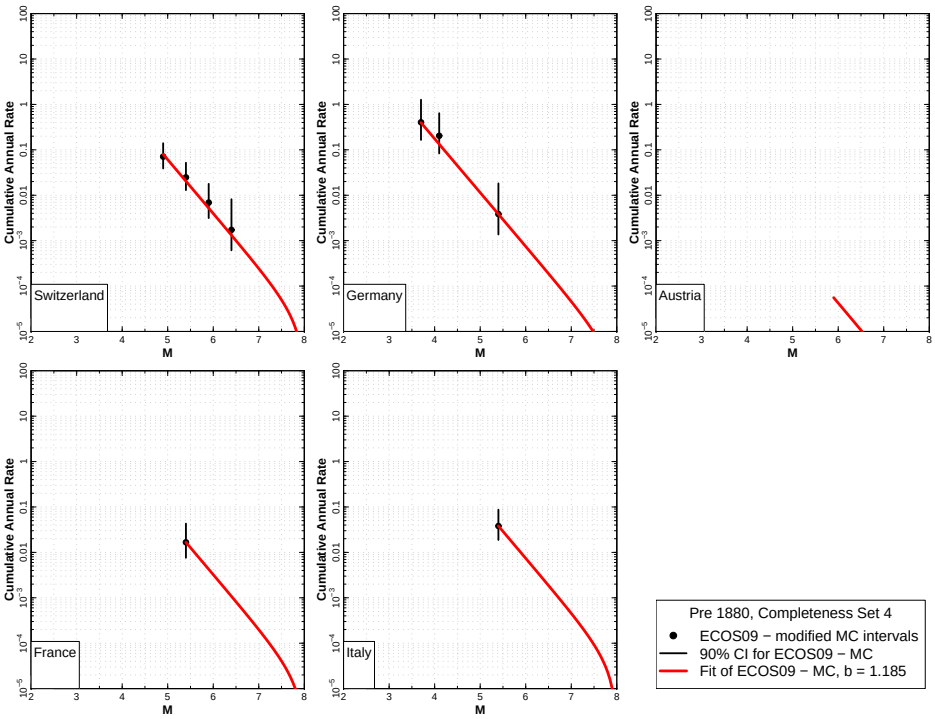

Figure 2.16: Regional *b*-value for EG1d Completeness Set 4 fitting only pre 1880 data.

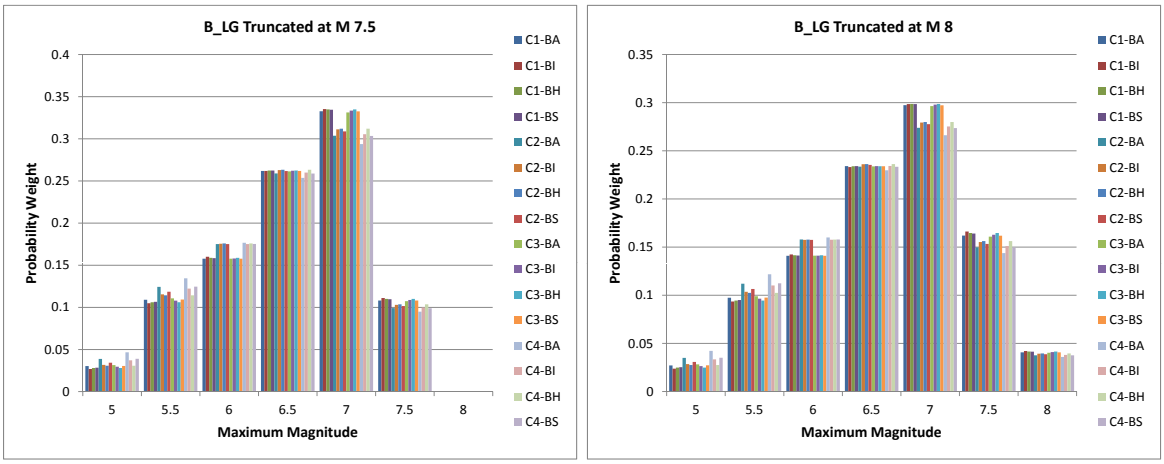

Figure 2.17: Maximum Magnitude Distributions for B_LG.

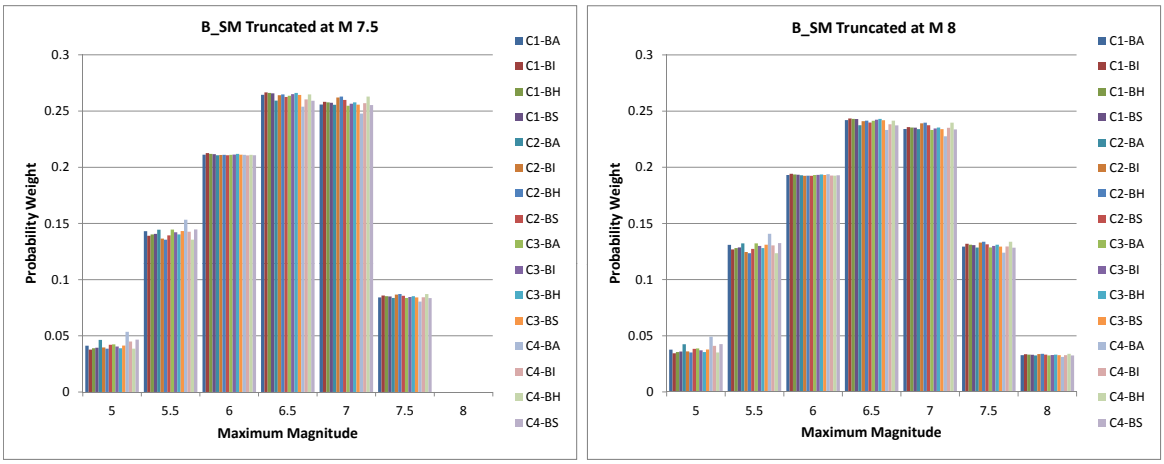

Figure 2.18: Maximum Magnitude Distributions for B_SM.

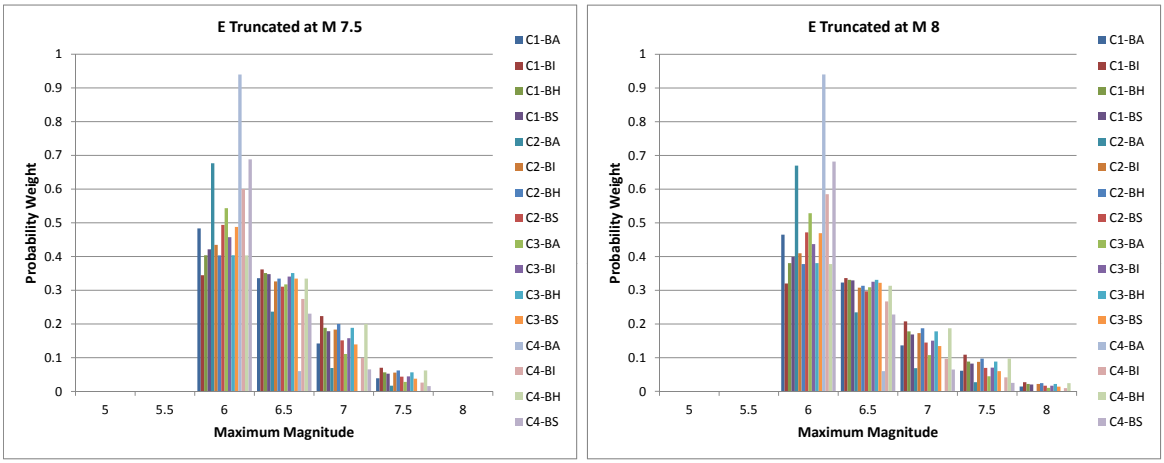

Figure 2.19: Maximum Magnitude Distributions for E.

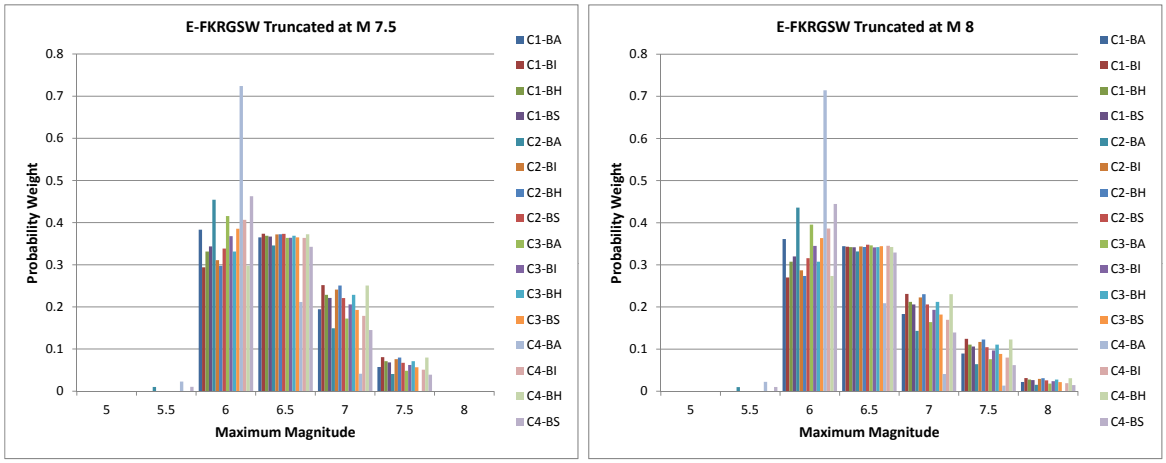

Figure 2.20: Maximum Magnitude Distributions for E-FKRGSW.

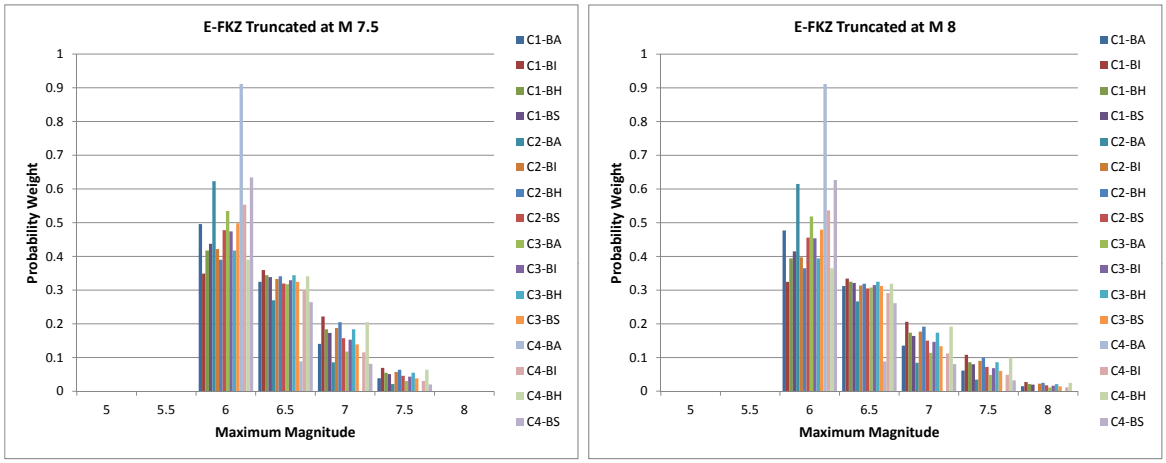

Figure 2.21: Maximum Magnitude Distributions for E-FKZ.

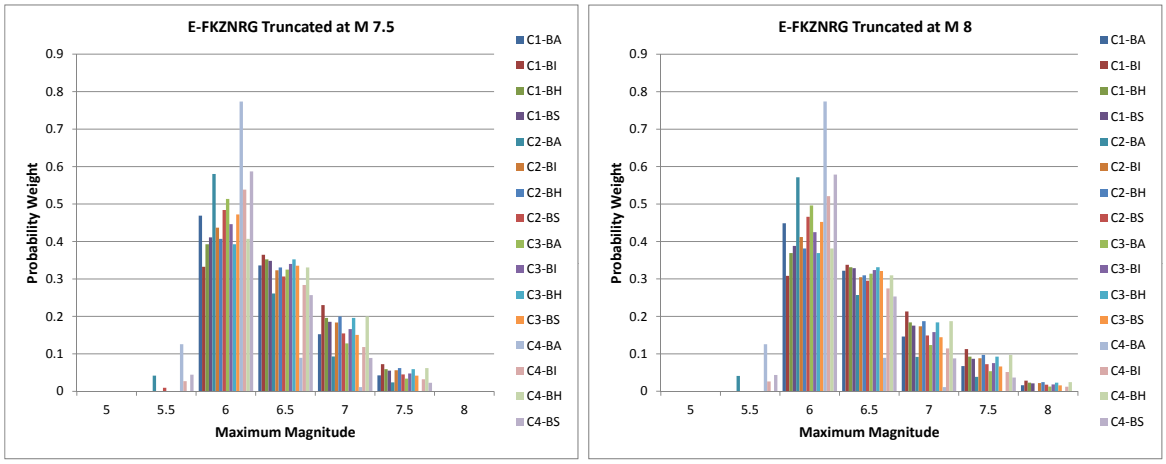

Figure 2.22: Maximum Magnitude Distributions for E-FKZNRG.

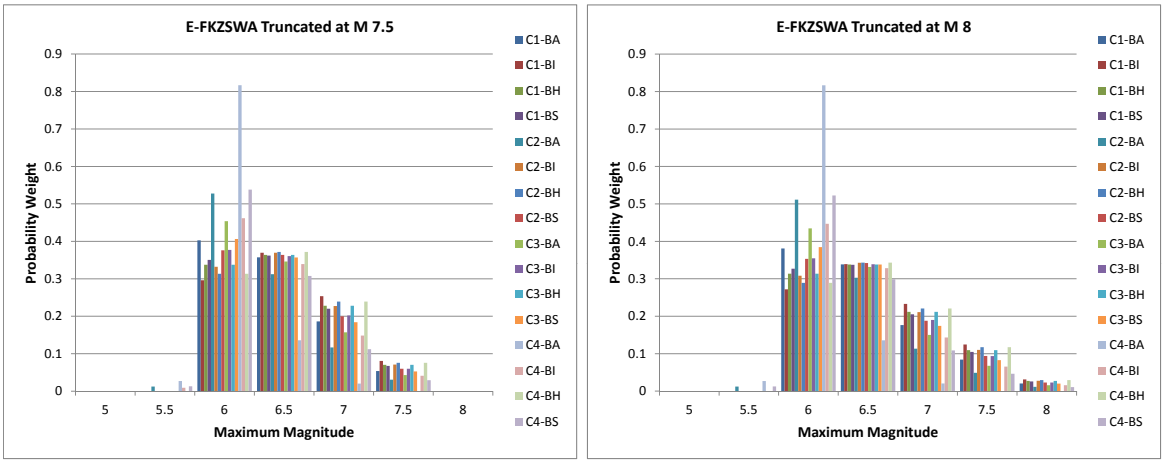

Figure 2.23: Maximum Magnitude Distributions for E-FKZSWA.

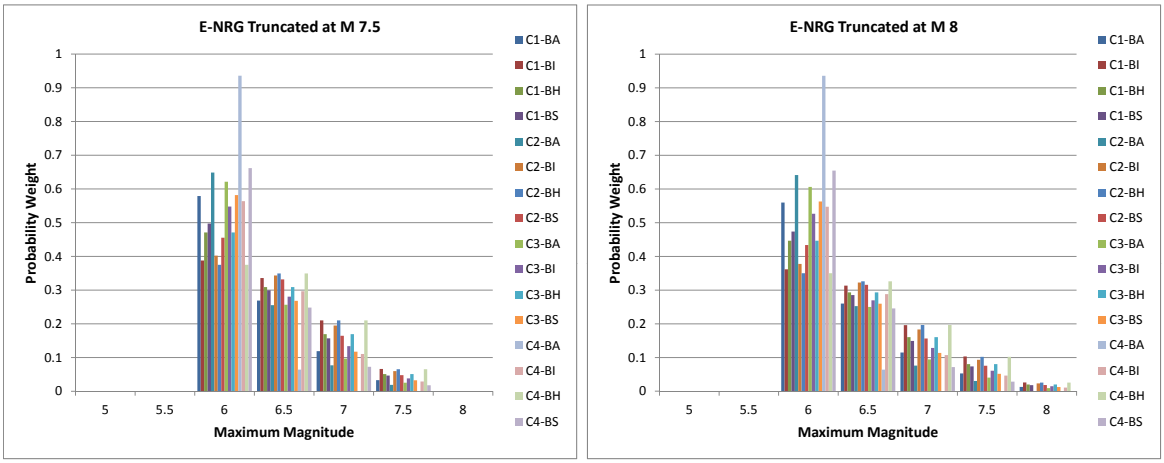

Figure 2.24: Maximum Magnitude Distributions for E-NRG.

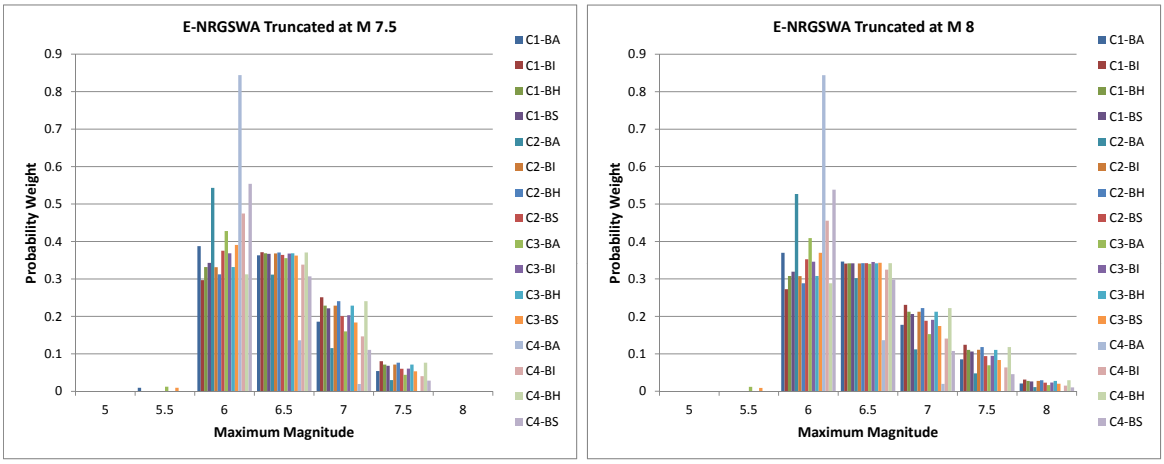

Figure 2.25: Maximum Magnitude Distributions for E-NRGSWA.

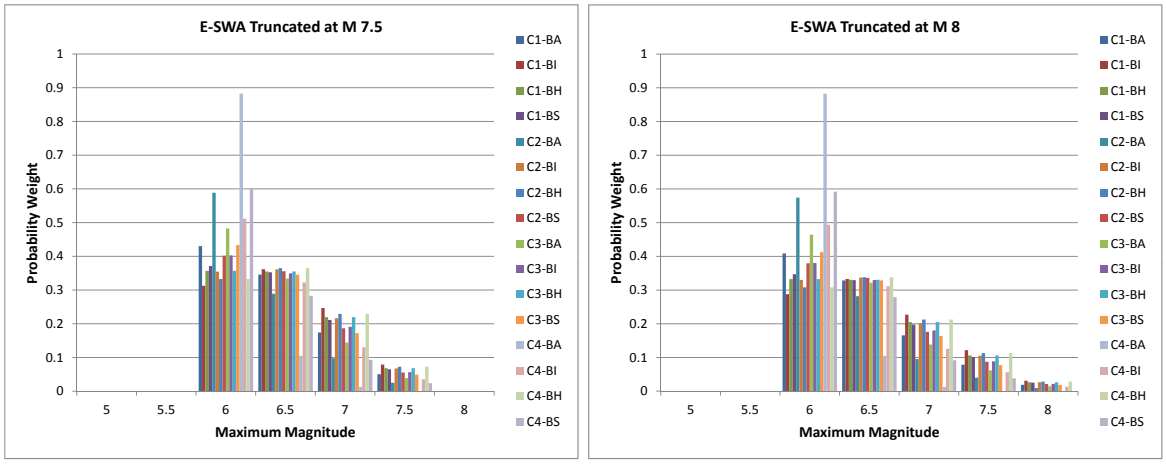

Figure 2.26: Maximum Magnitude Distributions for E-SWA.

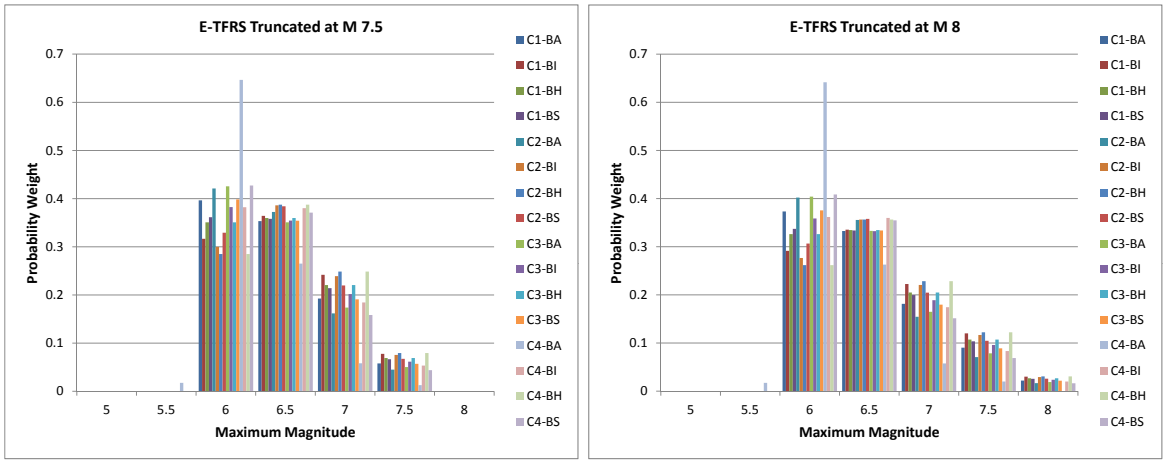

Figure 2.27: Maximum Magnitude Distributions for E-TFRS.

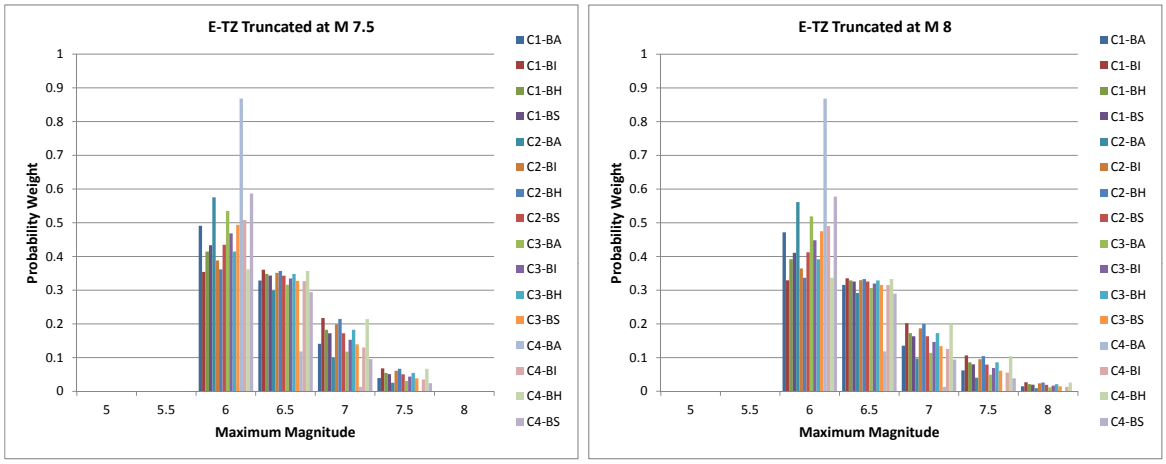

Figure 2.28: Maximum Magnitude Distributions for E-TZ.

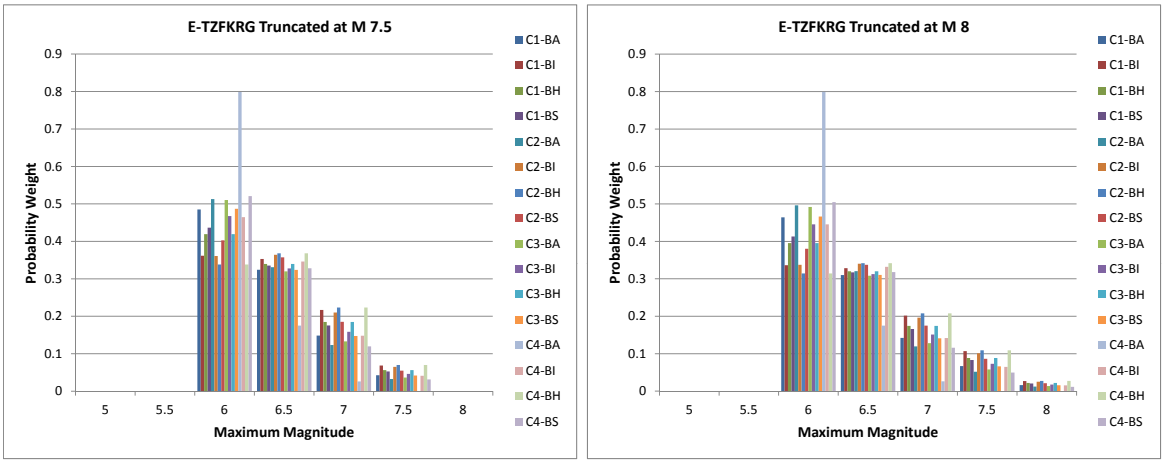

Figure 2.29: Maximum Magnitude Distributions for E-TZFKRG.

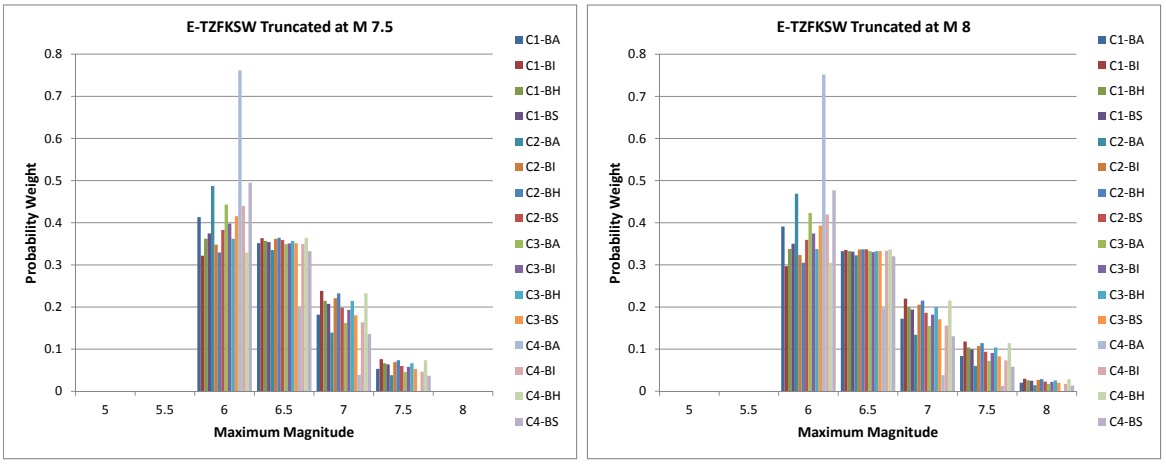

Figure 2.30: Maximum Magnitude Distributions for E-TZFKSW.

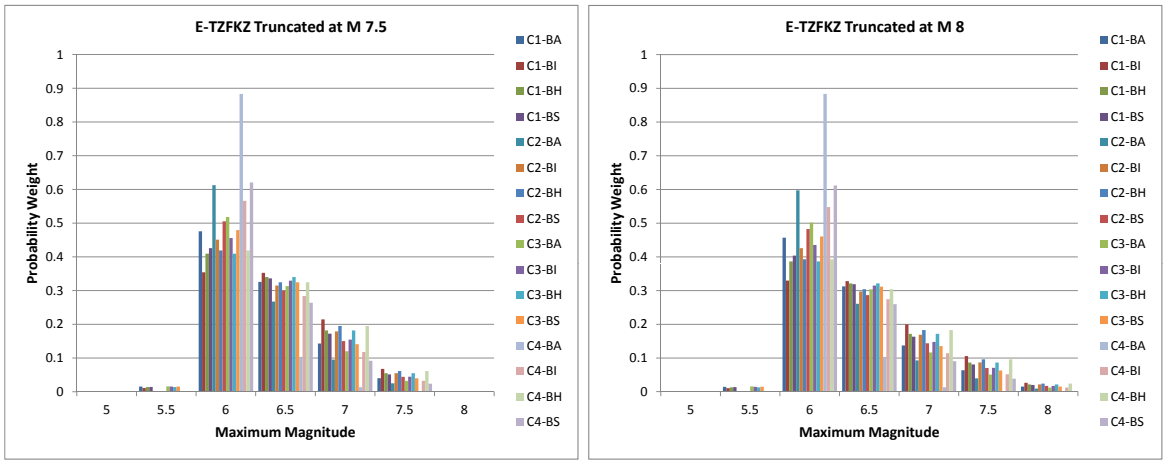

Figure 2.31: Maximum Magnitude Distributions for E-TZFKZ.

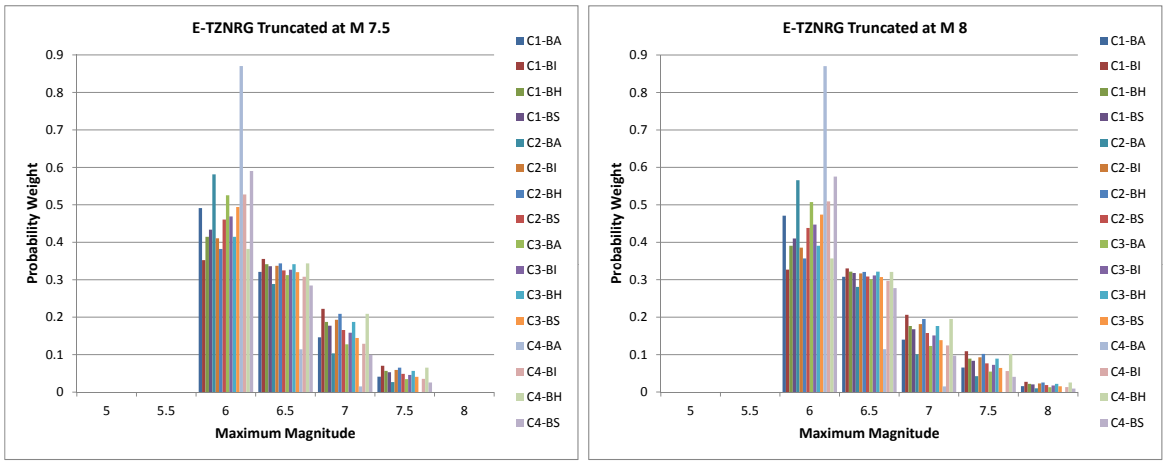

Figure 2.32: Maximum Magnitude Distributions for E-TZNRG.

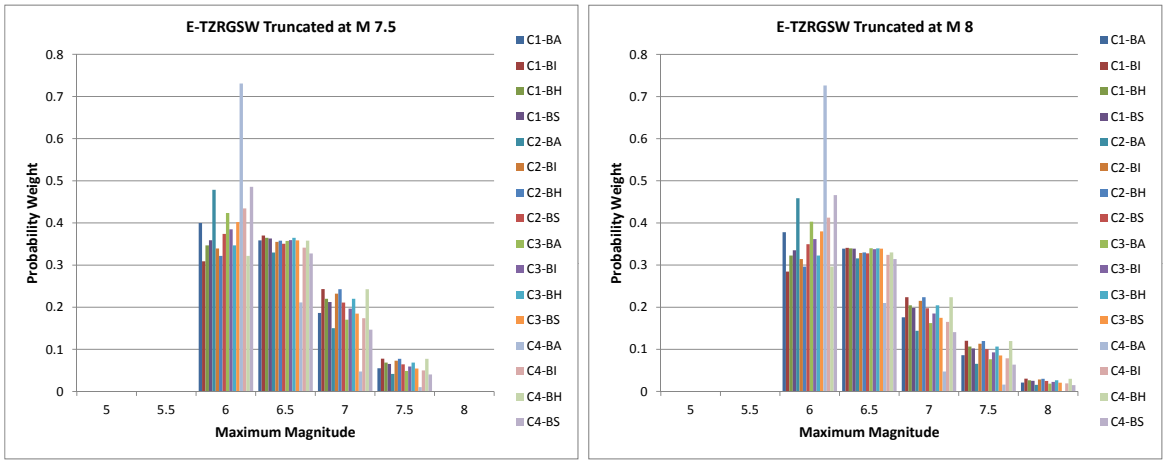

Figure 2.33: Maximum Magnitude Distributions for E-TZRGSW.

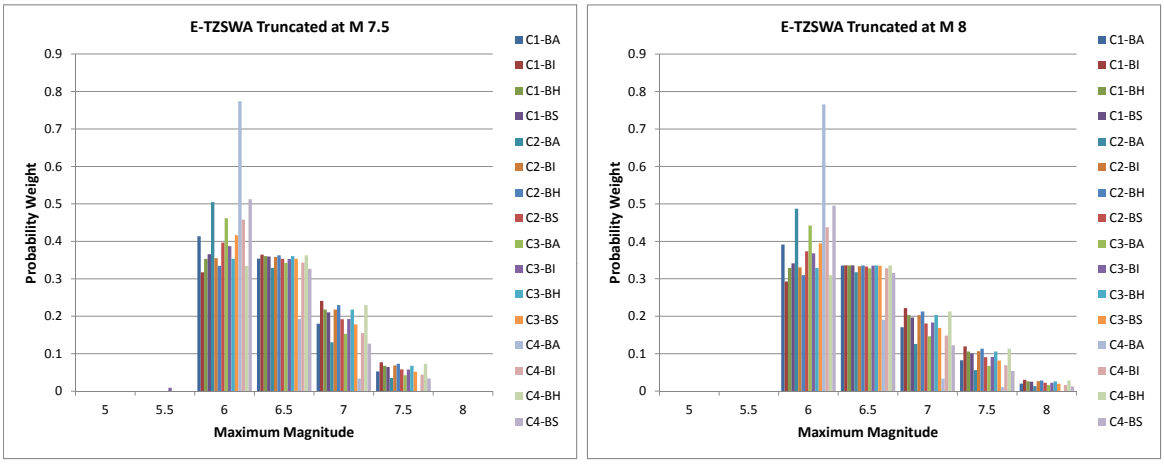

Figure 2.34: Maximum Magnitude Distributions for E-TZSWA.

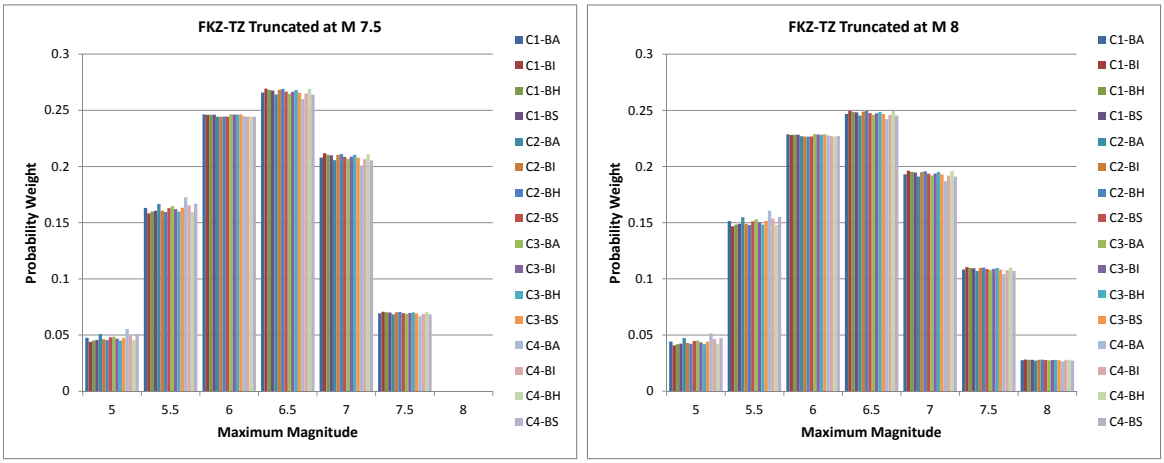

Figure 2.35: Maximum Magnitude Distributions for FKZ-TZ.

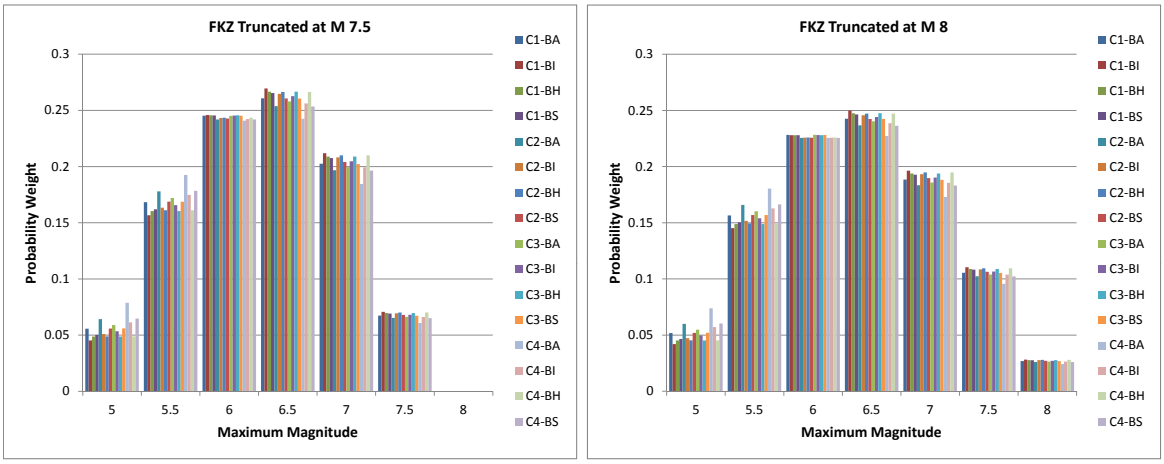

Figure 2.36: Maximum Magnitude Distributions for FKZ.

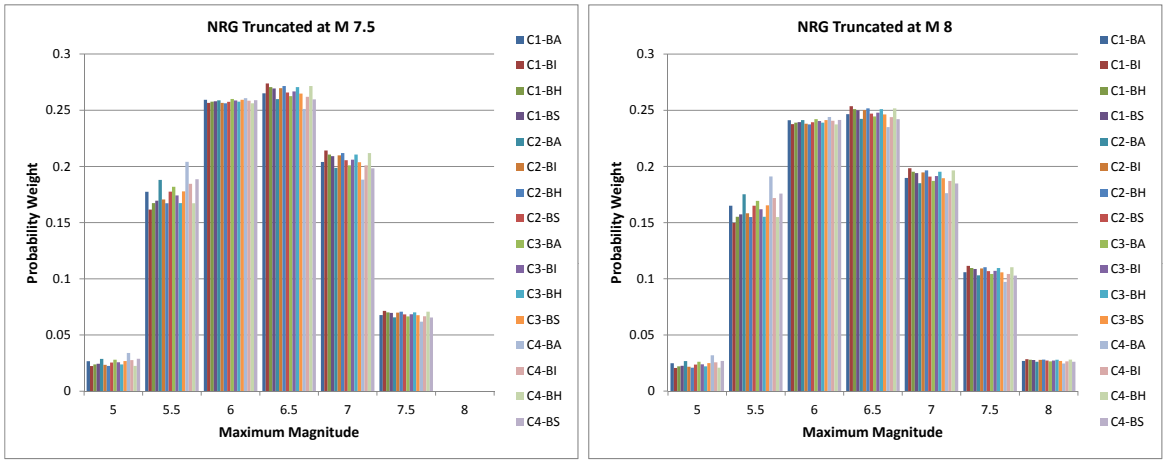

Figure 2.37: Maximum Magnitude Distributions for NRG.

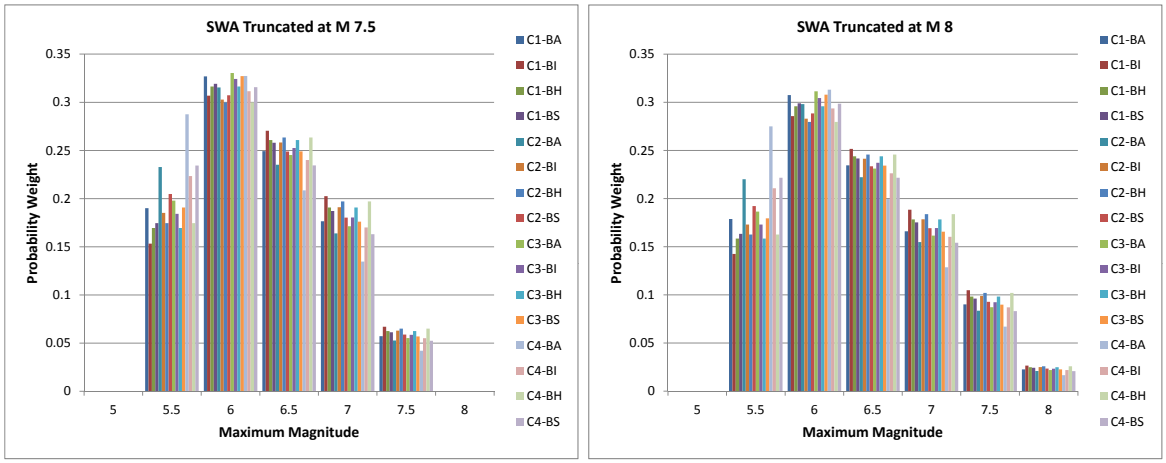

Figure 2.38: Maximum Magnitude Distributions for SWA.

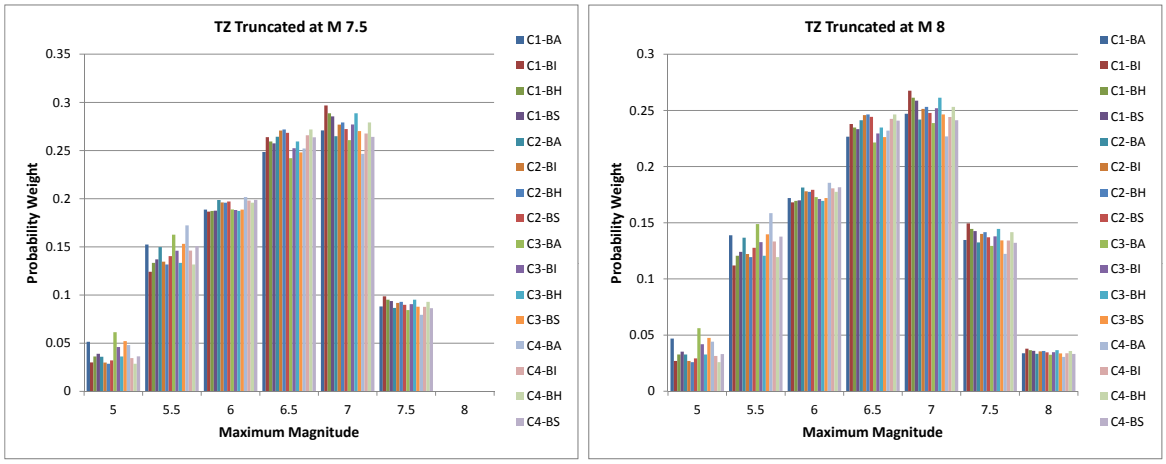

Figure 2.39: Maximum Magnitude Distributions for TZ.

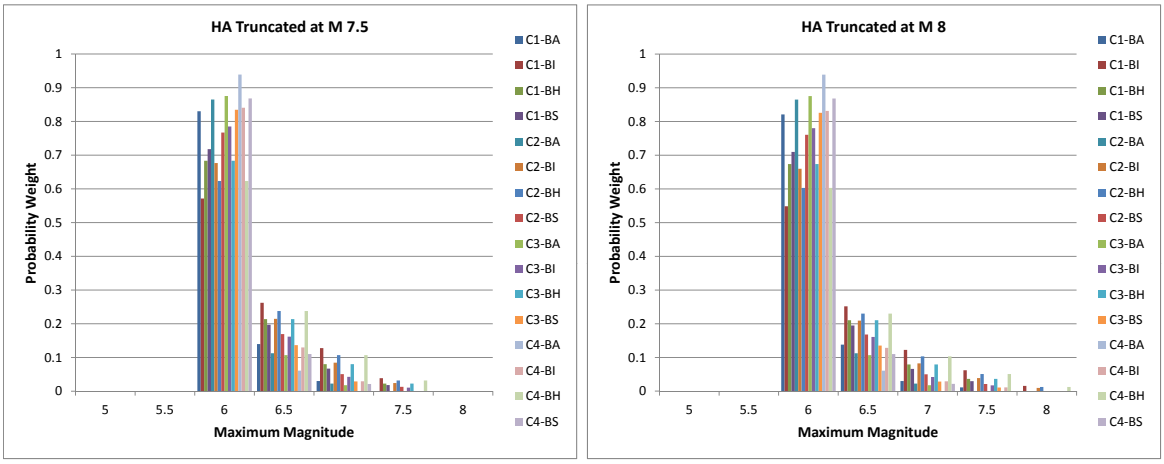

Figure 2.40: Maximum Magnitude Distributions for HA.

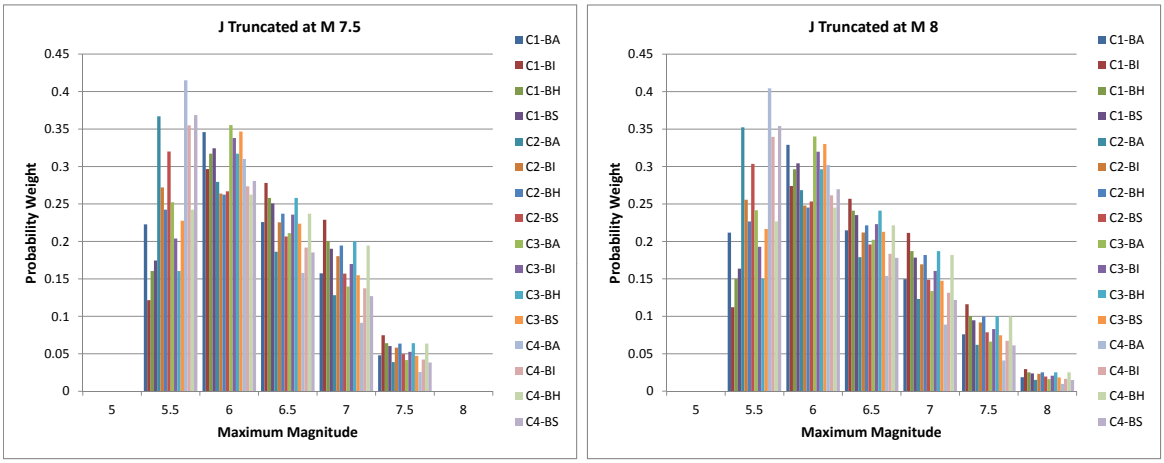

Figure 2.41: Maximum Magnitude Distributions for J.

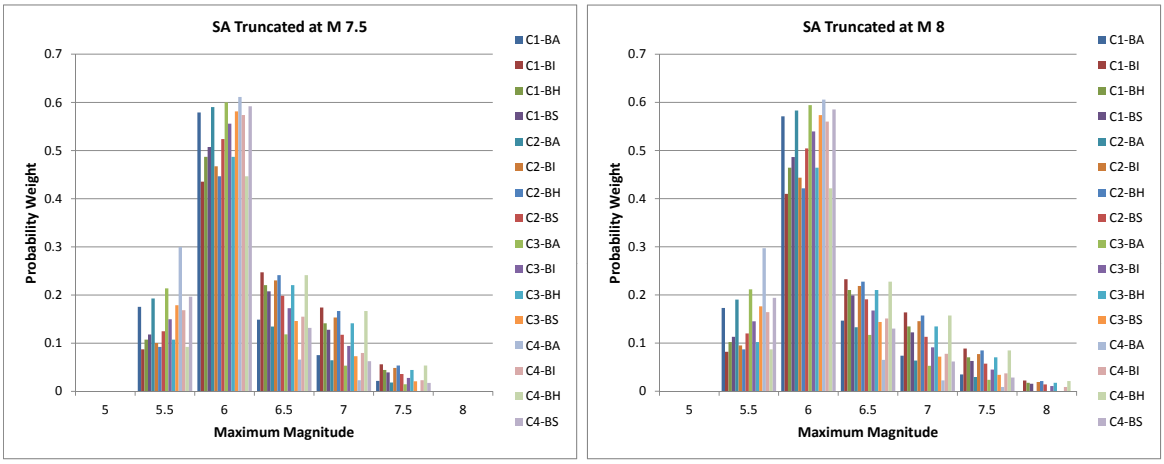

Figure 2.42: Maximum Magnitude Distributions for SA.

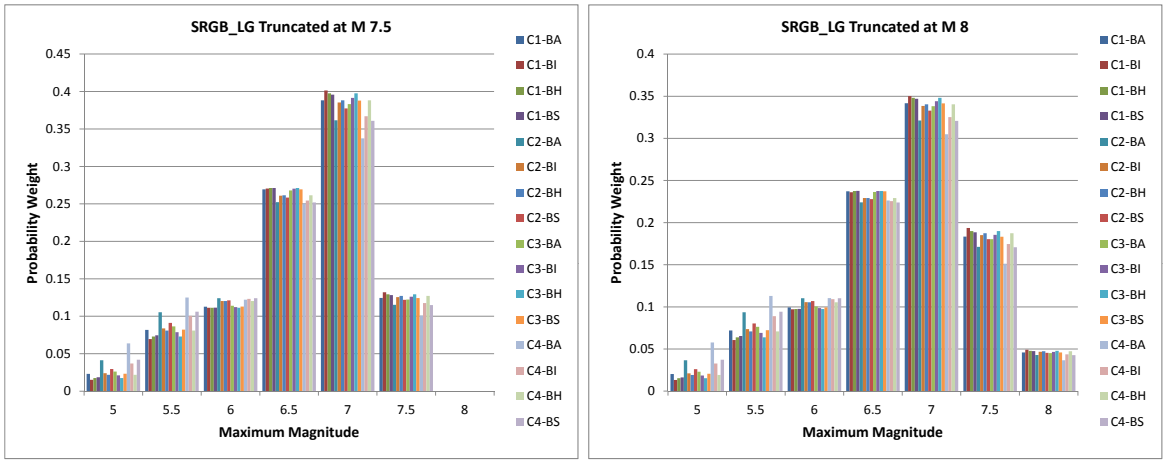

Figure 2.43: Maximum Magnitude Distributions for SRGB_LG.

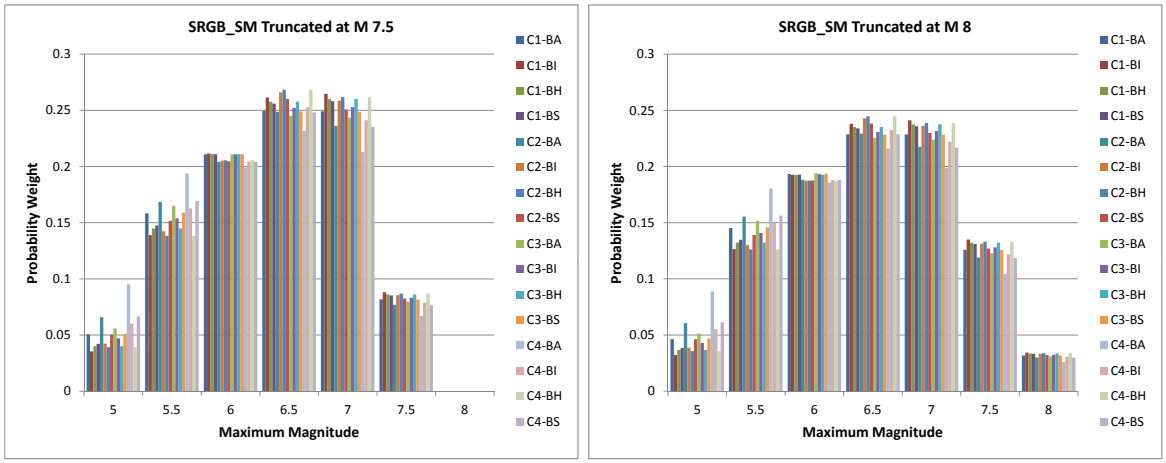

Figure 2.44: Maximum Magnitude Distributions for SRGB_SM.

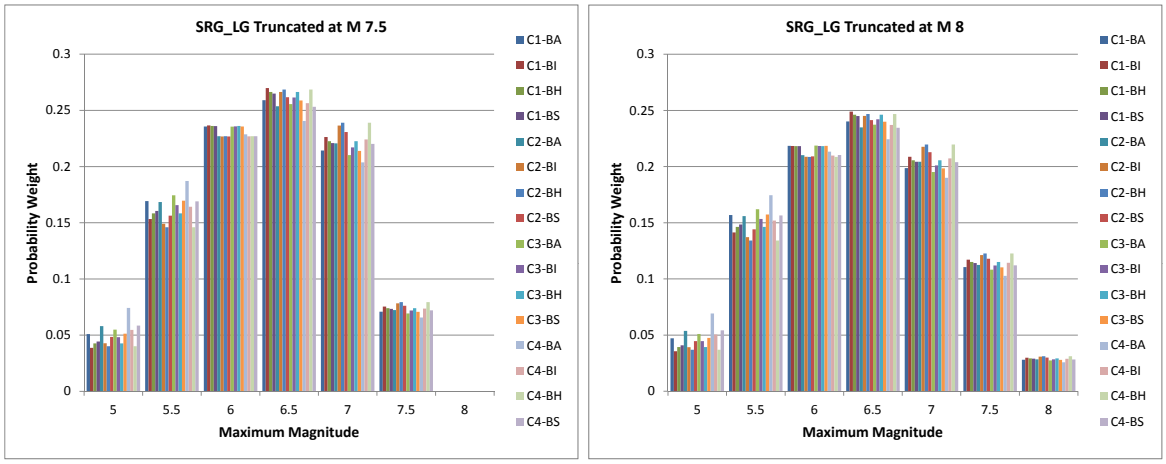

Figure 2.45: Maximum Magnitude Distributions for SRG_LG.

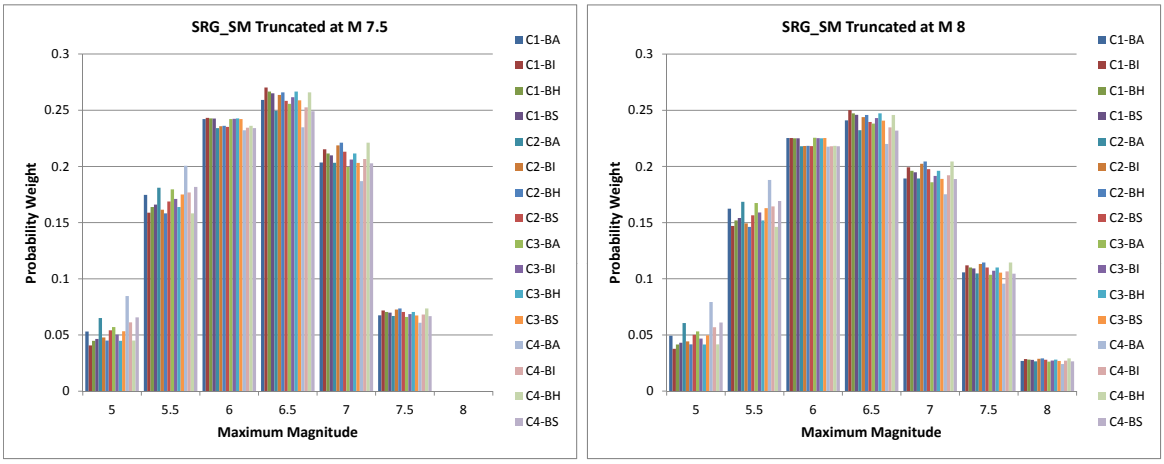

Figure 2.46: Maximum Magnitude Distributions for SRG_SM.

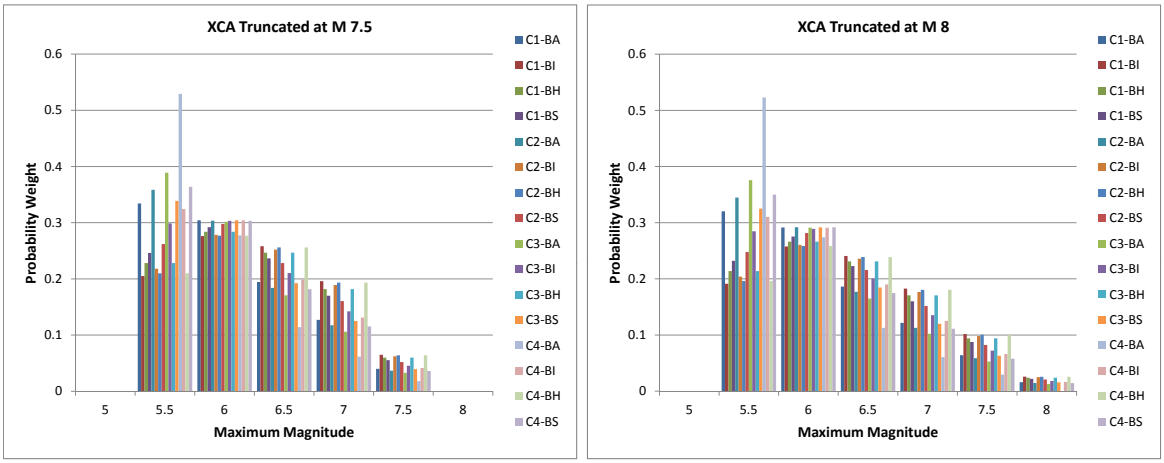

Figure 2.47: Maximum Magnitude Distributions for XCA.

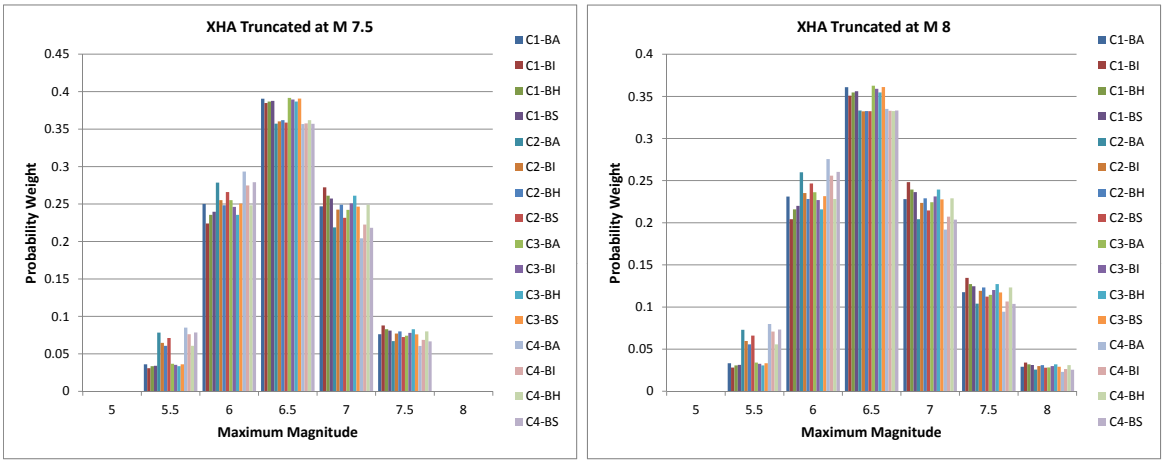

Figure 2.48: Maximum Magnitude Distributions for XHA.

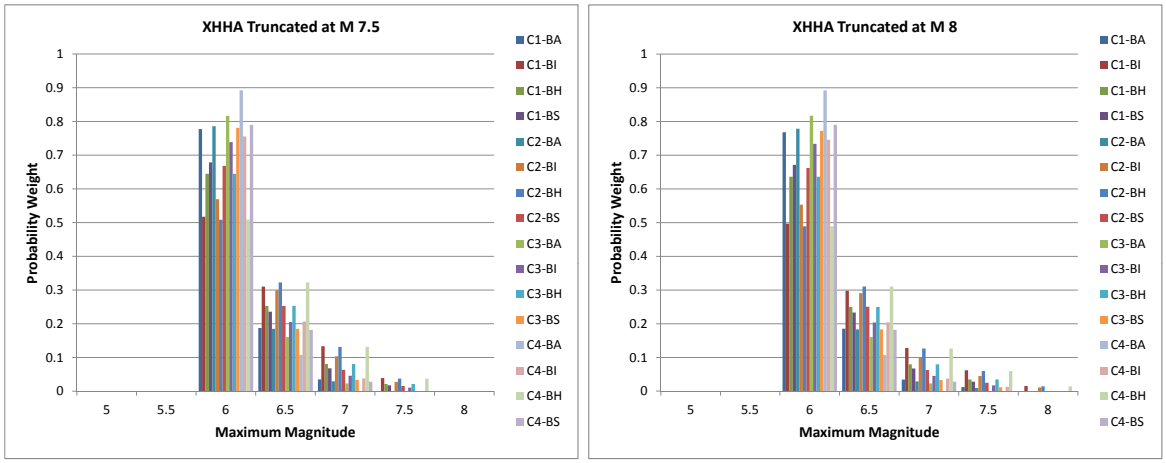

Figure 2.49: Maximum Magnitude Distributions for XHHA.

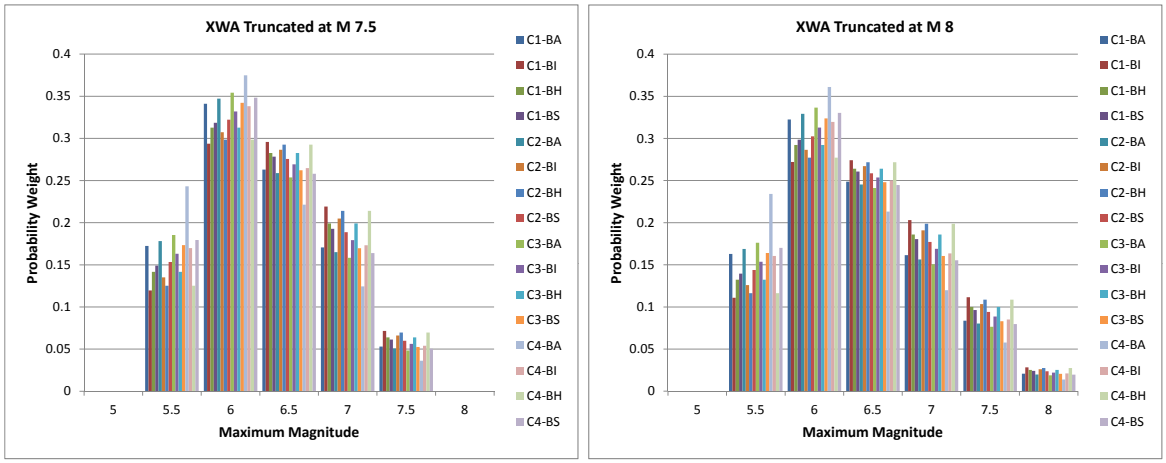

Figure 2.50: Maximum Magnitude Distributions for XWA.

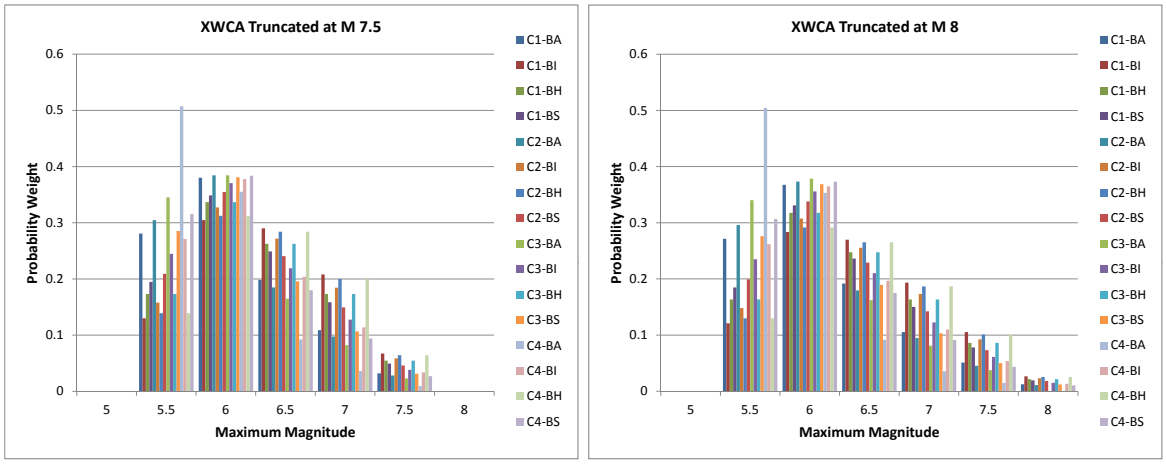

Figure 2.51: Maximum Magnitude Distributions for XWCA.

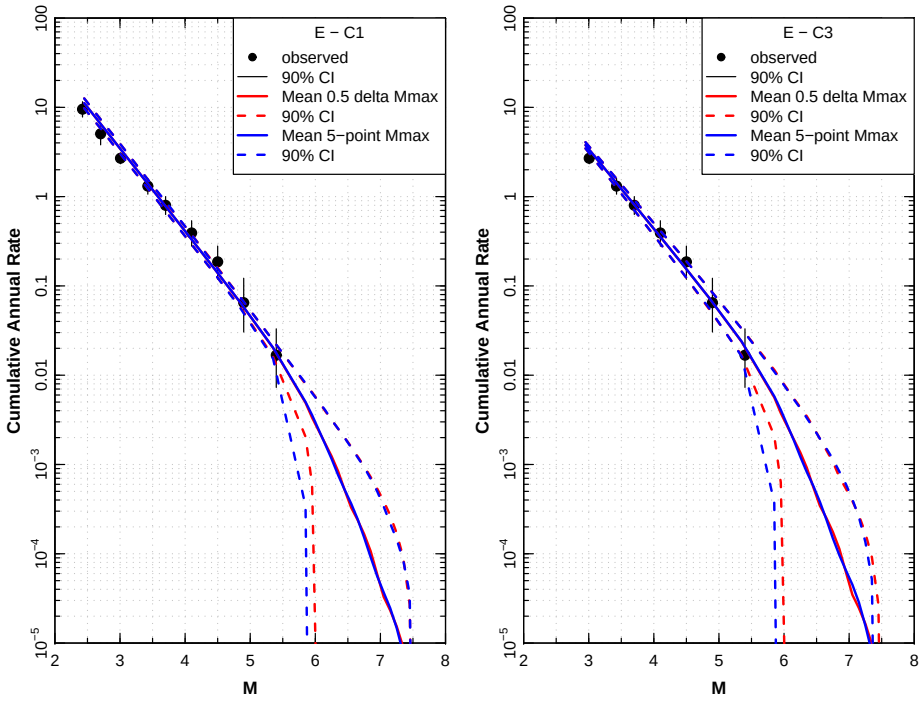

Figure 2.52: Zone E - Comparison of computed earthquake occurrence rates using alternative completeness and M_{max} distributions.

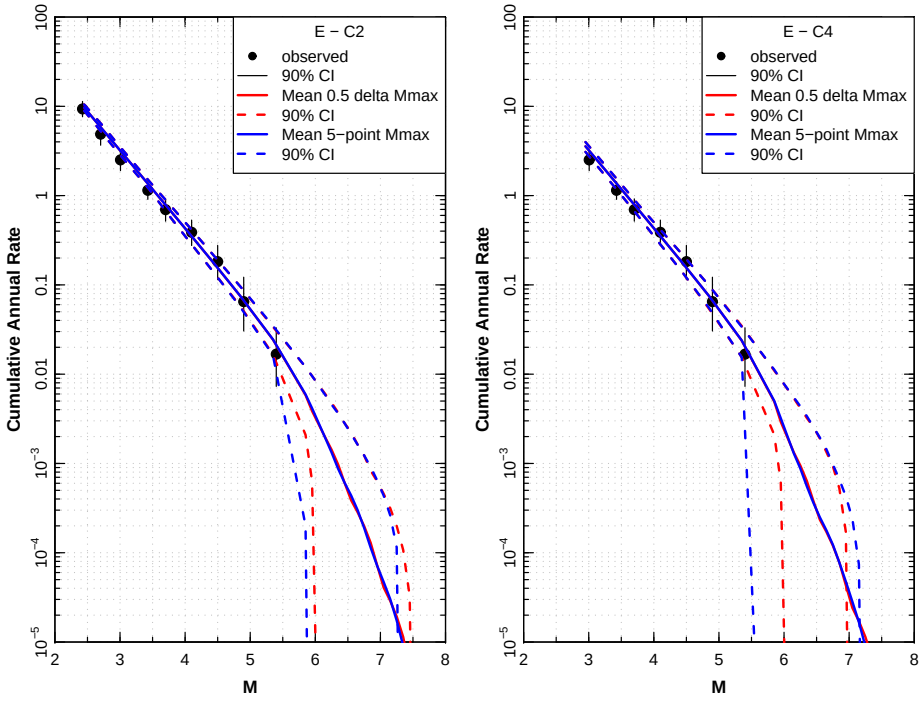

Figure 2.53: Zone E - Comparison of computed earthquake occurrence rates using alternative completeness and M_{max} distributions.

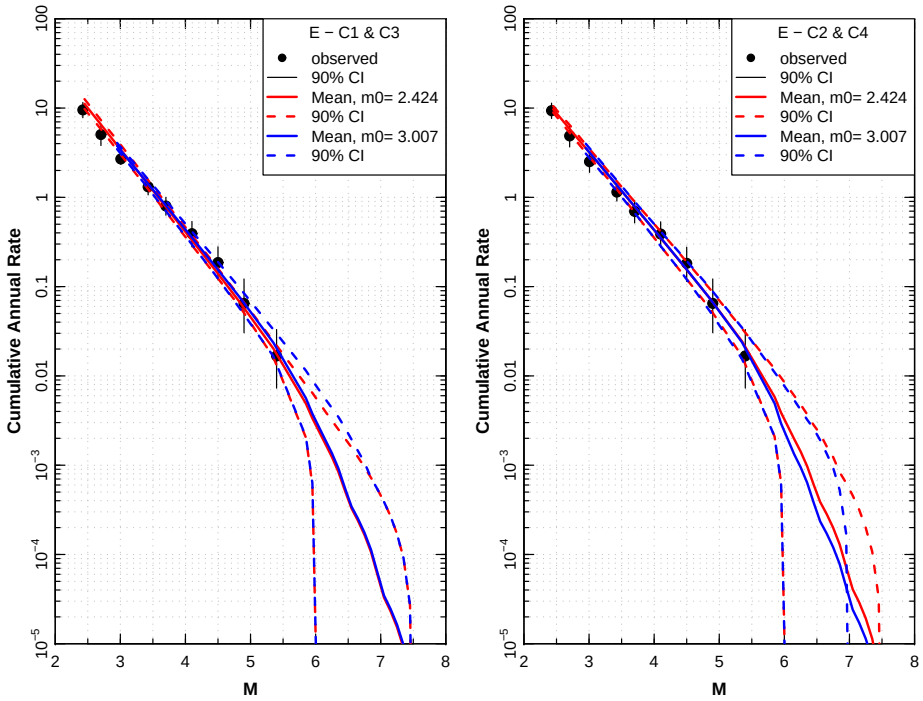

Figure 2.54: Zone E - Comparison of earthquake occurrence rates for alternative minimum magnitudes. C1 and C2 use minimum defined in completeness region for France, C3 and C4 use 3.007. M_{max} distribution based on 0.5 magnitude unit binning.

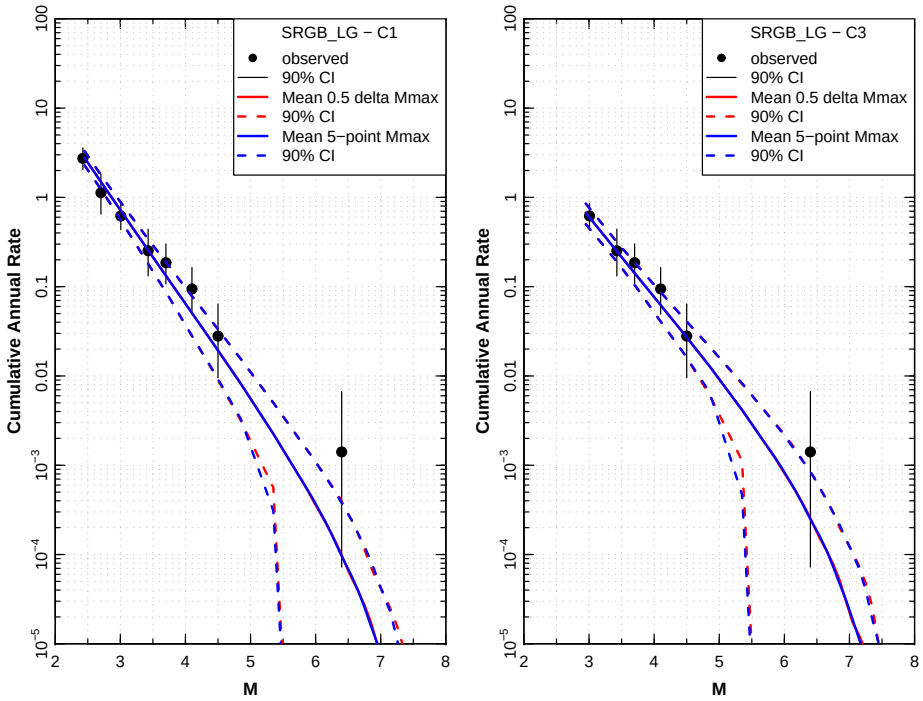

Figure 2.55: Zone SRGB_LG - Comparison of computed earthquake occurrence rates using alternative completeness and M_{max} distributions.

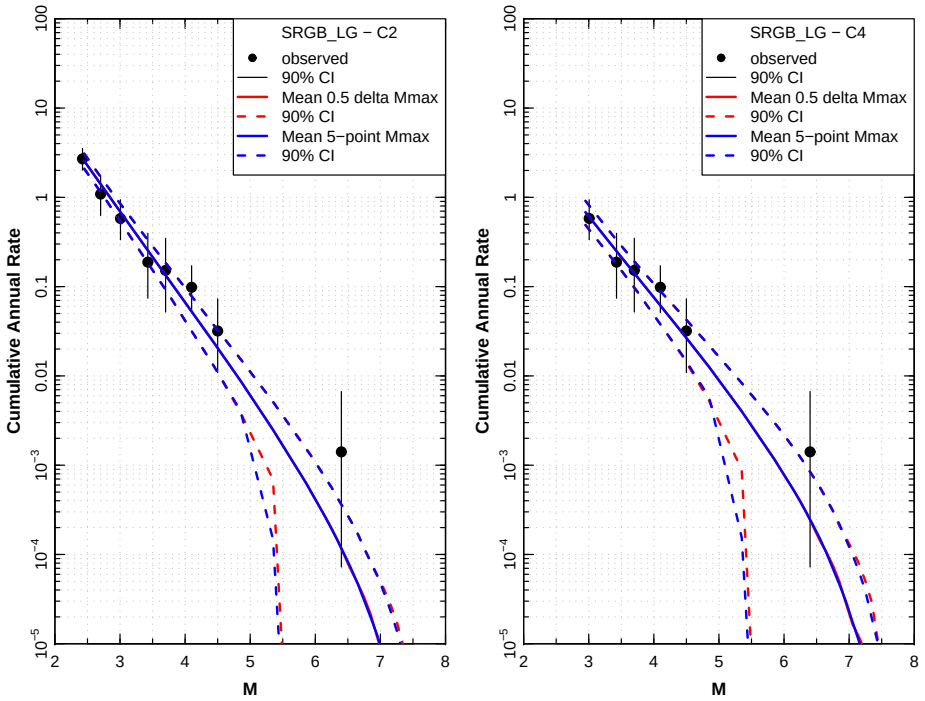

Figure 2.56: Zone SRGB_LG - Comparison of computed earthquake occurrence rates using alternative completeness and M_{max} distributions.

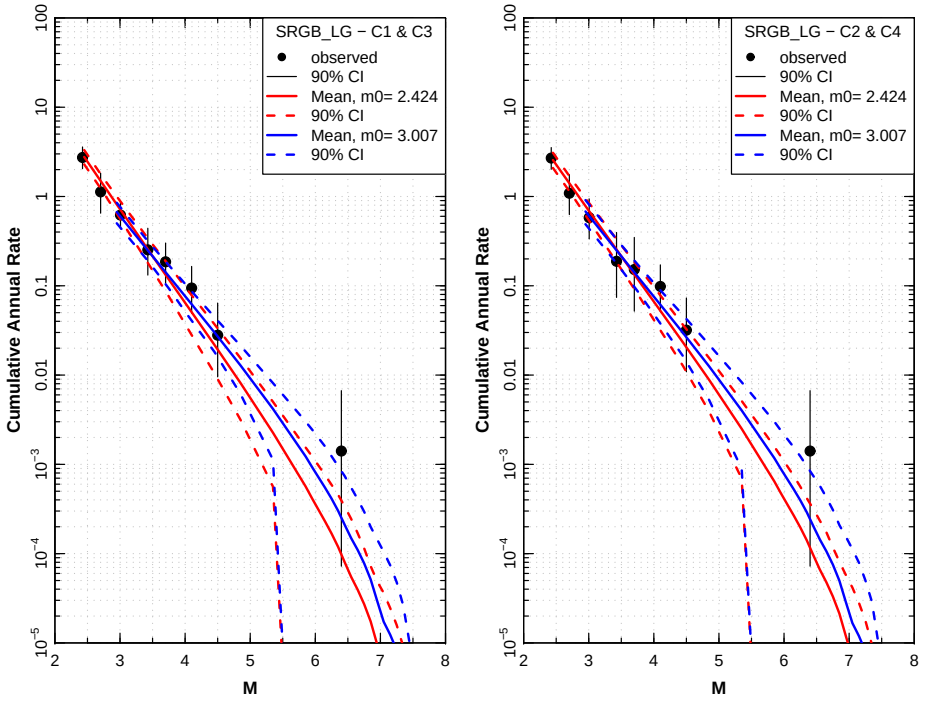

Figure 2.57: Zone SRGB_LG - Comparison of earthquake occurrence rates for alternative minimum magnitudes. C1 and C2 use minimum defined in completeness region for France, C3 and C4 use 3.007. M_{max} distribution based on 0.5 magnitude unit binning.

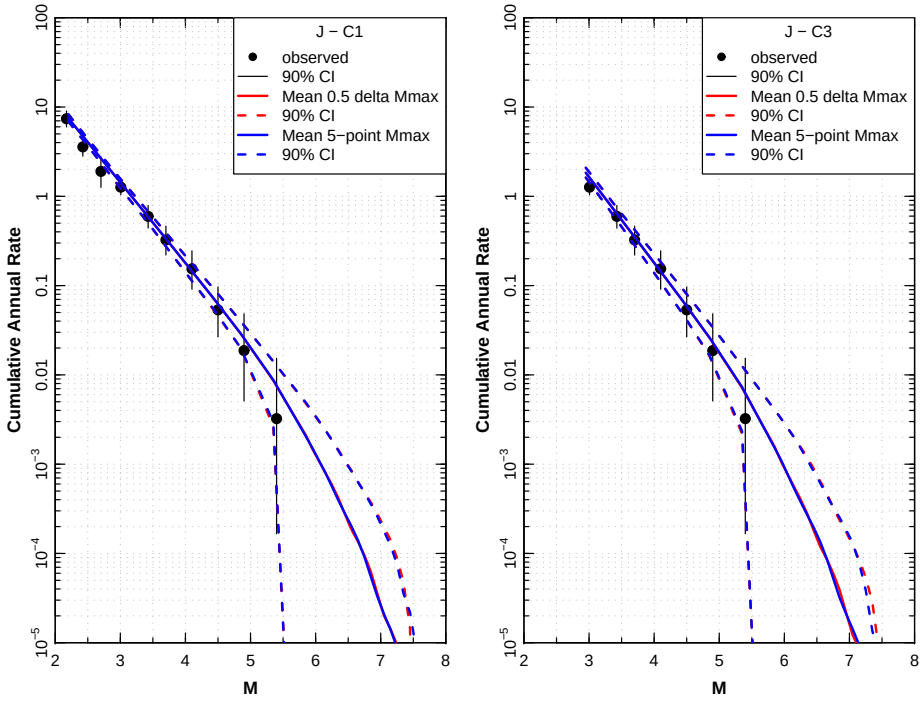

Figure 2.58: Zone J - Comparison of computed earthquake occurrence rates using alternative completeness and M_{max} distributions.

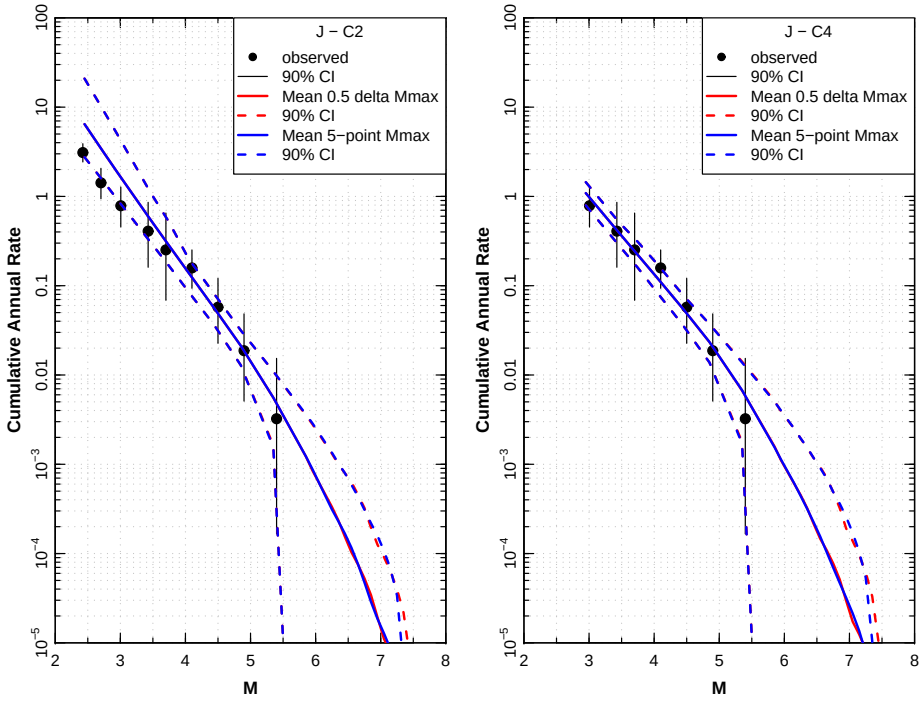

Figure 2.59: Zone J - Comparison of computed earthquake occurrence rates using alternative completeness and M_{max} distributions.

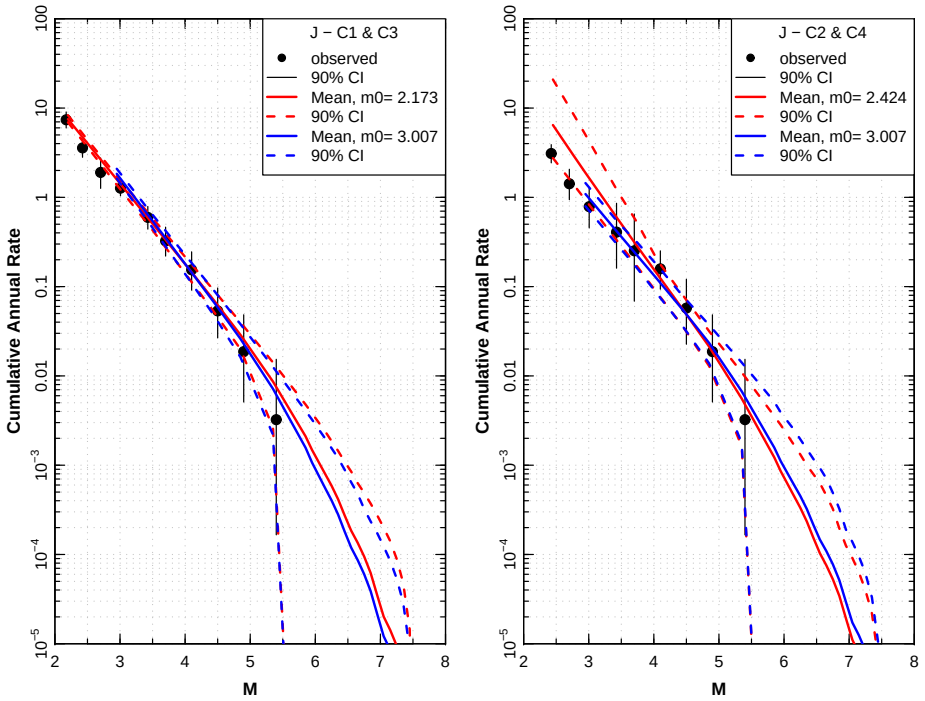

Figure 2.60: Zone J - Comparison of earthquake occurrence rates for alternative minimum magnitudes. C1 and C2 use minimum defined in completeness region for France, C3 and C4 use 3.007. M_{max} distribution based on 0.5 magnitude unit binning.

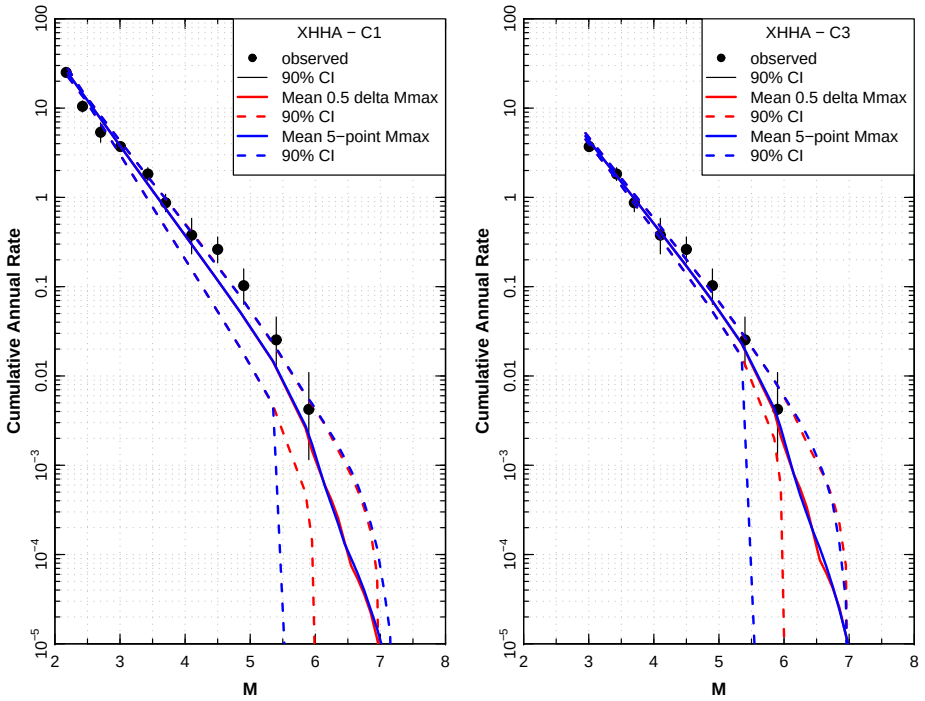

Figure 2.61: Zone XHHA - Comparison of computed earthquake occurrence rates using alternative completeness and M_{max} distributions.

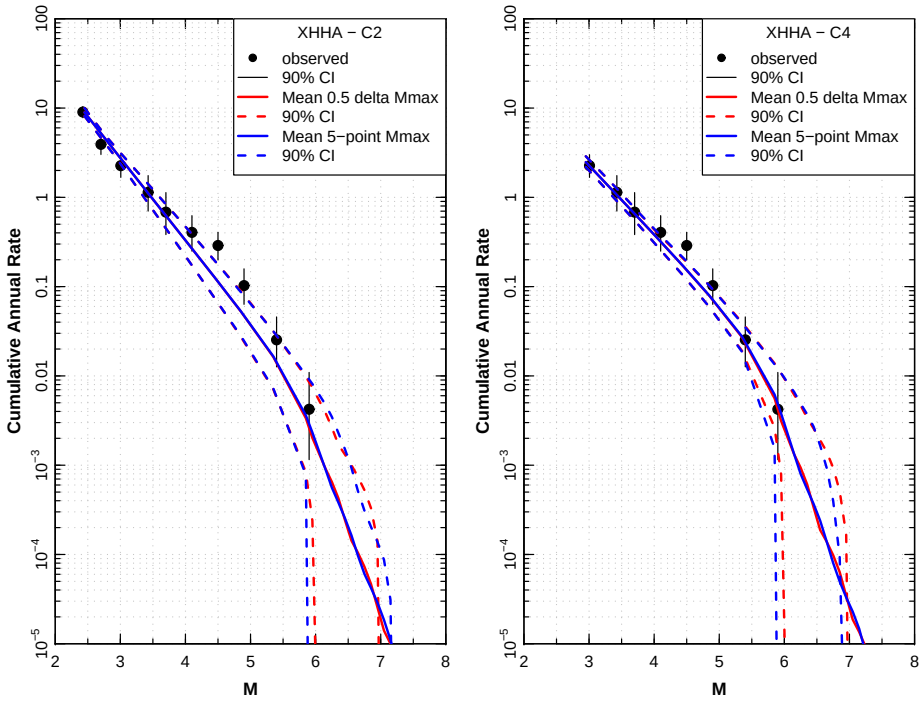

Figure 2.62: Zone XHHA - Comparison of computed earthquake occurrence rates using alternative completeness and M_{max} distributions.

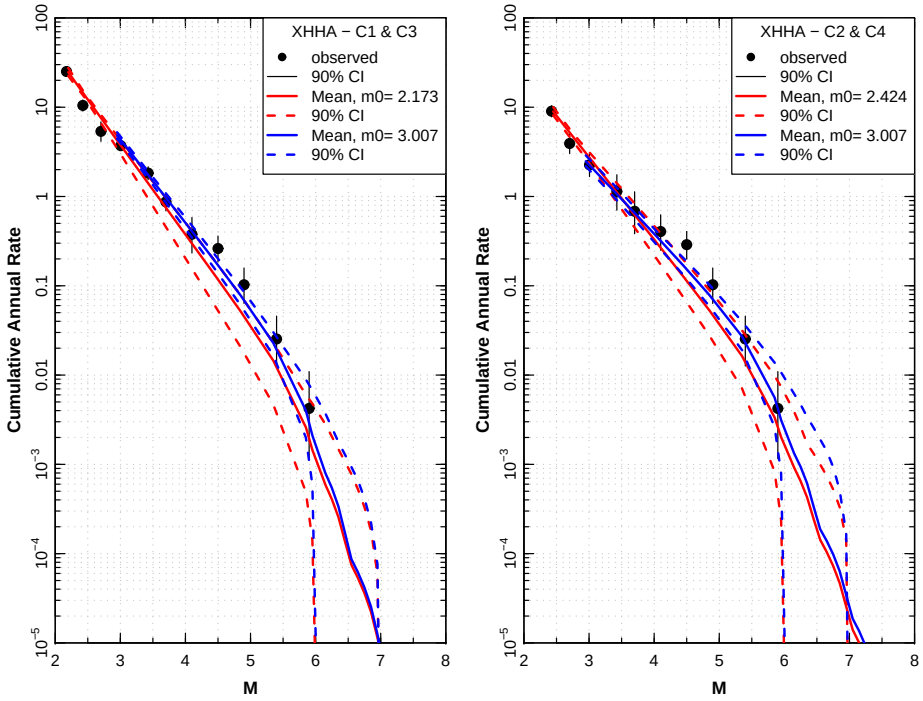

Figure 2.63: Zone XHHA - Comparison of earthquake occurrence rates for alternative minimum magnitudes. C1 and C2 use minimum defined in completeness region for France, C3 and C4 use 3.007. M_{max} distribution based on 0.5 magnitude unit binning.

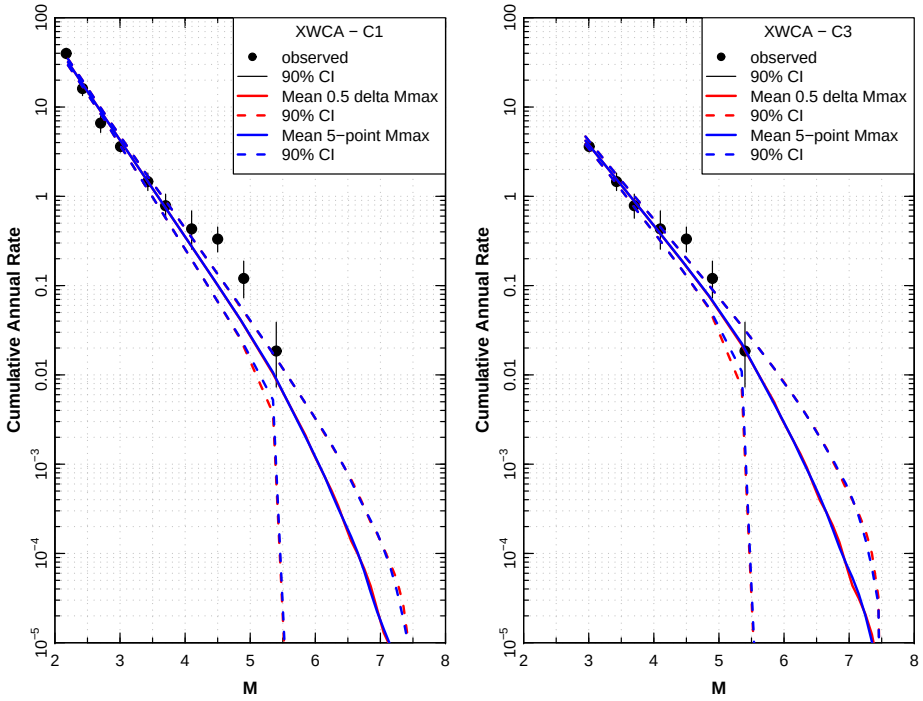

Figure 2.64: Zone XWCA - Comparison of computed earthquake occurrence rates using alternative completeness and M_{max} distributions.

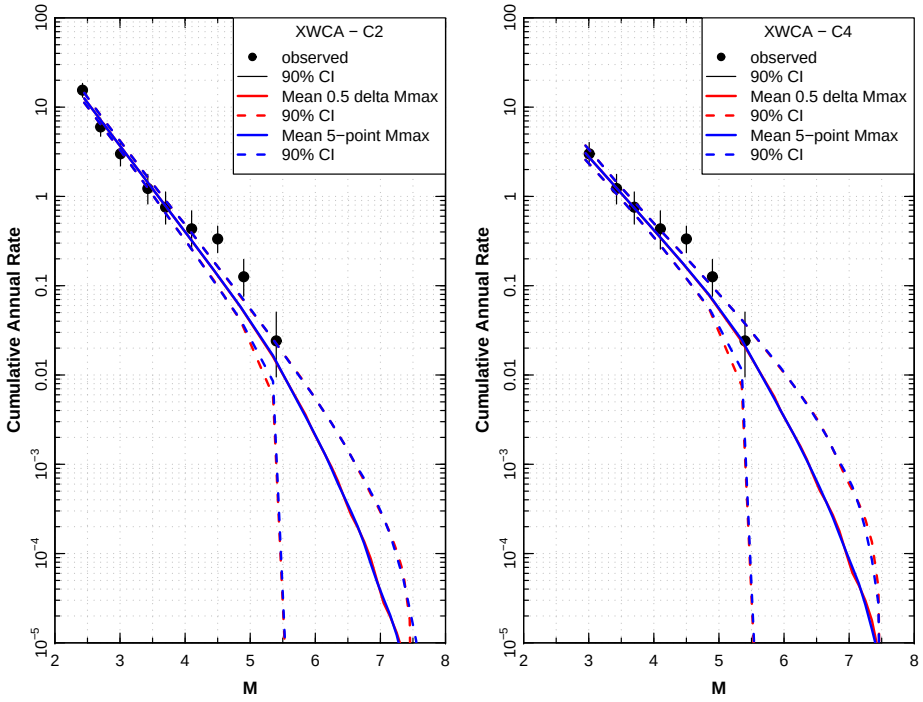

Figure 2.65: Zone XWCA - Comparison of computed earthquake occurrence rates using alternative completeness and M_{max} distributions.

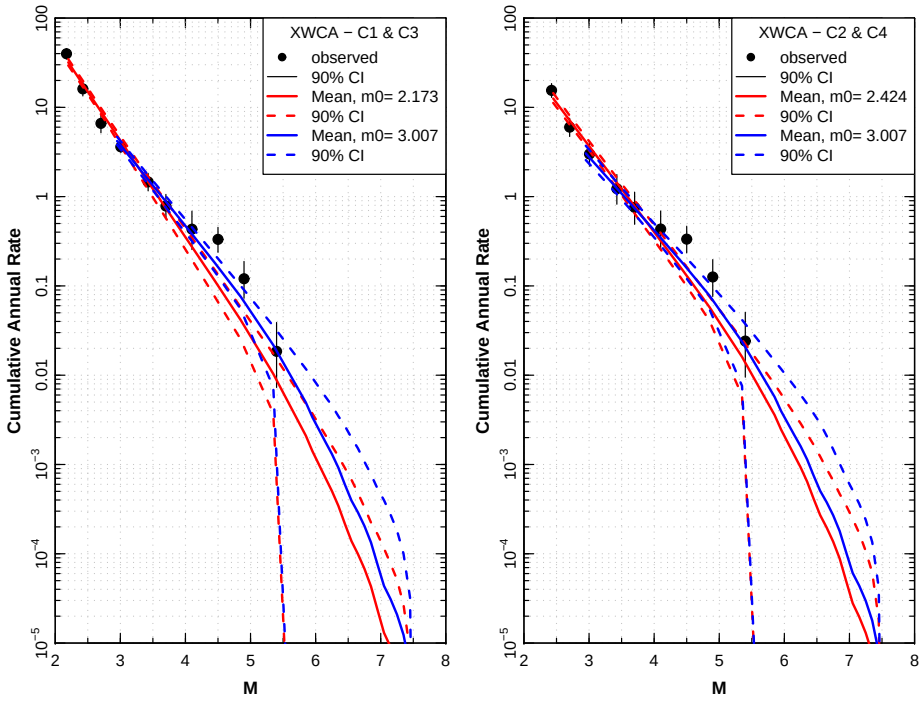

Figure 2.66: Zone XWCA - Comparison of earthquake occurrence rates for alternative minimum magnitudes. C1 and C2 use minimum defined in completeness region for Switzerland, C3 and C4 use 3.007. M_{max} distribution based on 0.5 magnitude unit binning.

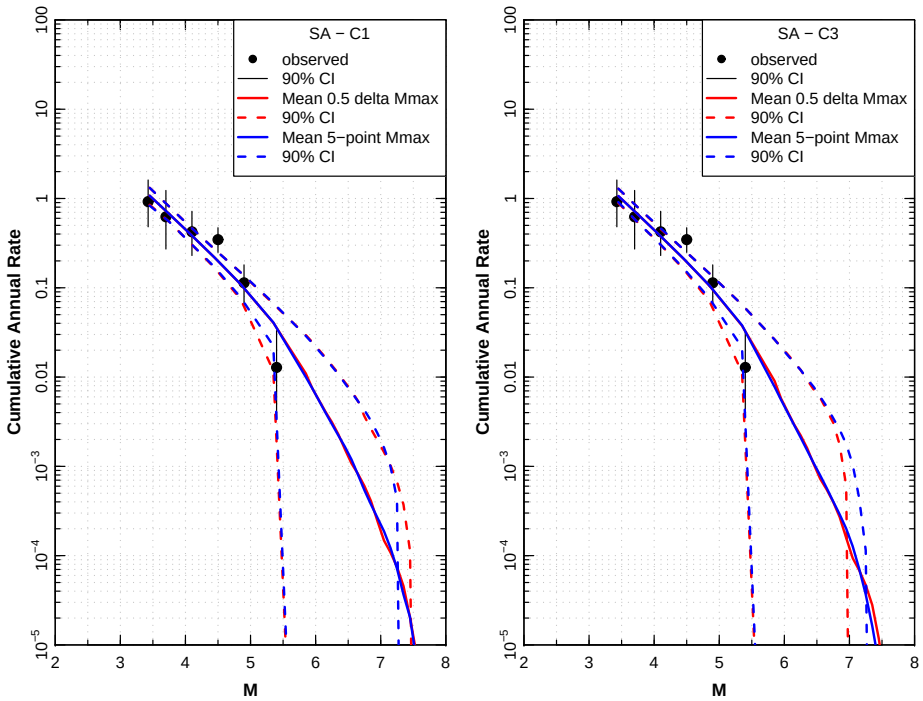

Figure 2.67: Zone SA - Comparison of computed earthquake occurrence rates using alternative completeness and M_{max} distributions.

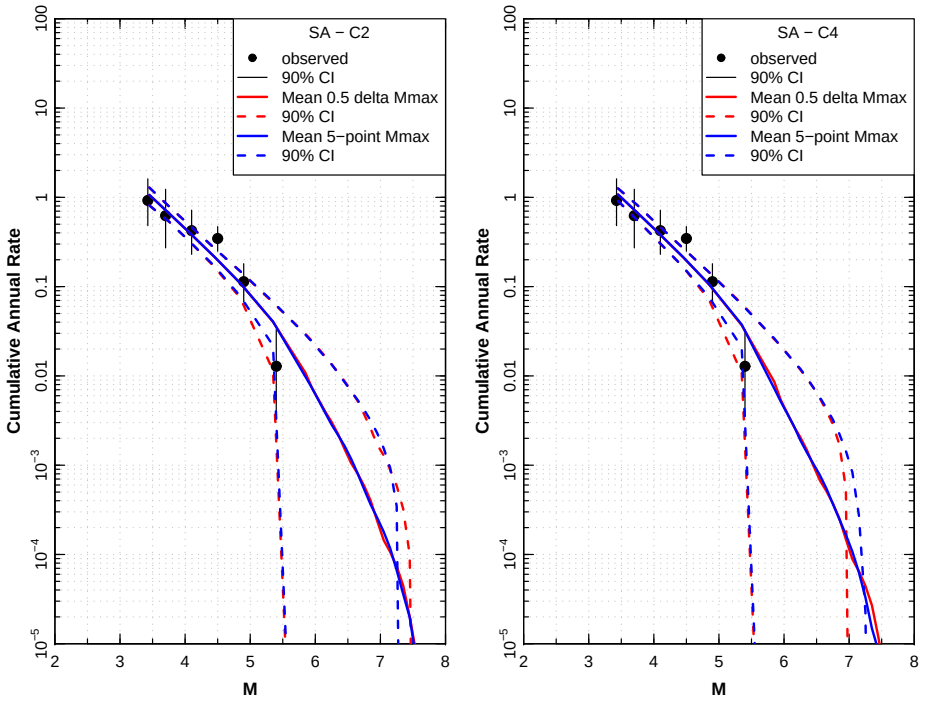

Figure 2.68: Zone SA - Comparison of computed earthquake occurrence rates using alternative completeness and M_{max} distributions.

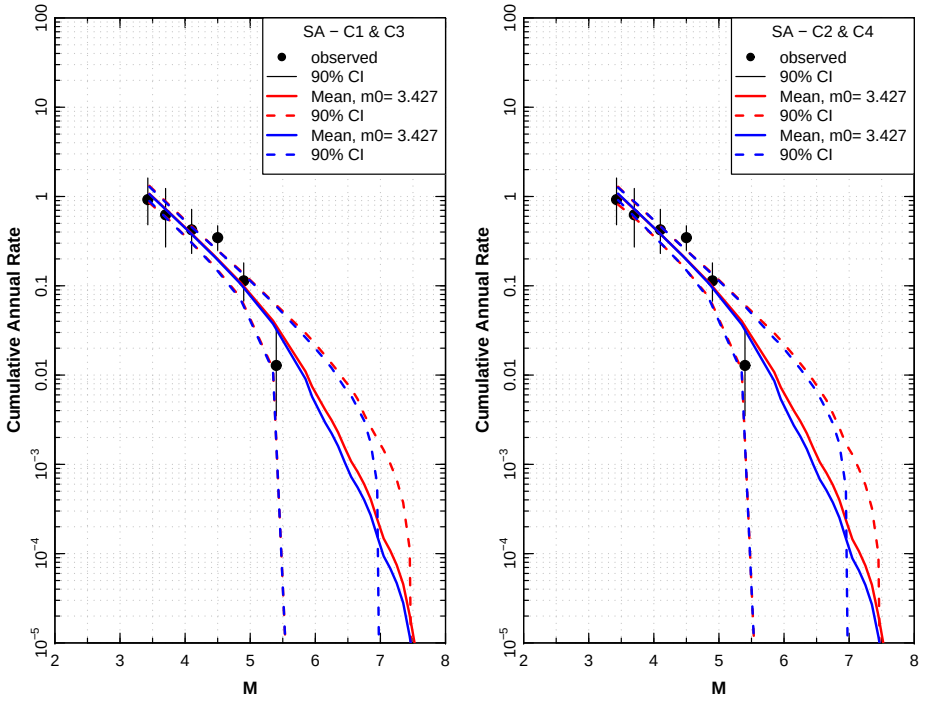

Figure 2.69: Zone SA - Comparison of earthquake occurrence rates for alternative minimum magnitudes. C1 and C2 use minimum defined in completeness region for Italy, C3 and C4 use 3.007. M_{max} distribution based on 0.5 magnitude unit binning.

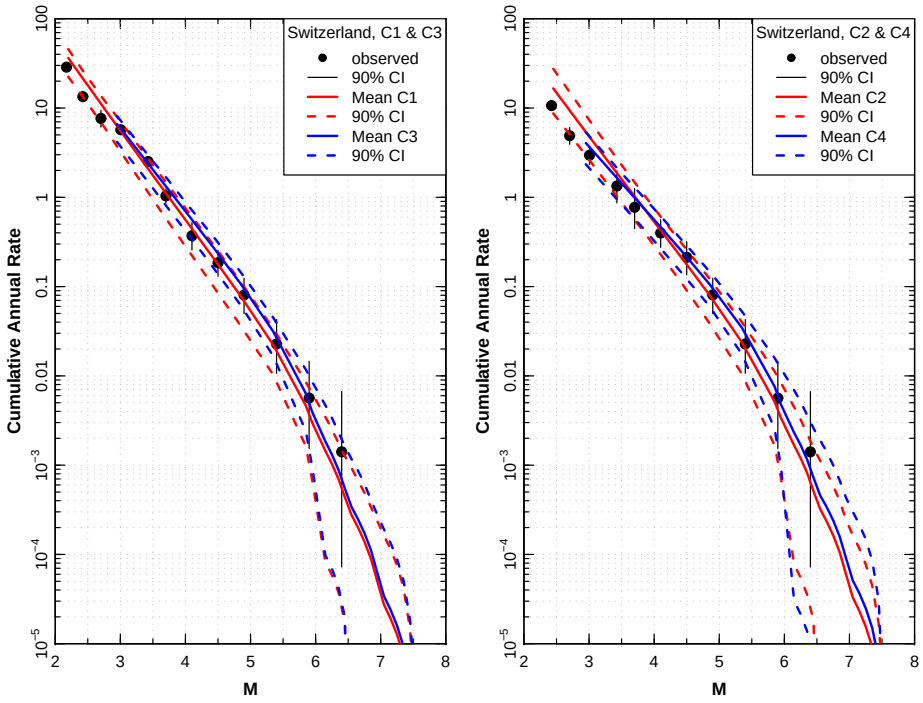

Figure 2.70: Comparison of predicted rates for the Swiss Completeness region.

Chapter 3

Hazard Input Document for EG1d (EG1-HID-1004) of March 8, 2011

Written by the PMT, SP4 and TFI

This document describes the final seismic source model developed by Expert Team EG1d in the PRP project. The data files associated with this seismic source model are located in the zip file EG1-HID-1004_EG1d_data_16_11_2010.zip. This document is based on the PEGASOS Hazard Input Document EG1-HID-0035. Based on the new earthquake ECOS09 catalog published in March 2010 the EG1d team revised its model, updating the seismicity parameters that go with that seismic source model and adding some complexities in the number of completeness models. This document repeats for the most part the content of the PEGASOS Hazard Input Document EG1-HID-0035. The modifications caused by the model revision are highlighted in blue.

3.1 Seismic Zonation

Figure 3.1 shows the global assessment that applies to modeling of the spatial distribution of seismicity. Three alternatives are considered. The first alternative is a low degree of stationarity in which seismicity is assumed to be homogeneously distributed with the boundaries of the seismic source zones. The second alternative is a moderate level of stationarity in which the spatial distribution of seismicity is modeled using a Gaussian kernel density function with the smoothing parameter h=15 km. The third is a high level of stationarity in which the spatial distribution of seismicity is modeled using a Gaussian kernel density function with the smoothing parameter h=5 km. These three alternatives are considered to be completely dependent across all sources.

The study region was divided into a number of large regional zones, as shown on Figure 3.2. There are a number of alternative subdivisions of these zones as indicated on the logic trees shown on Figures 3.3 and 3.4.

Figure 3.3 shows the logic tree for the alternative models for zones XHHA, XWCA, and SRGB_LG (and the related zone SRGB_SM). Zone XHHA is either treated as a single zone

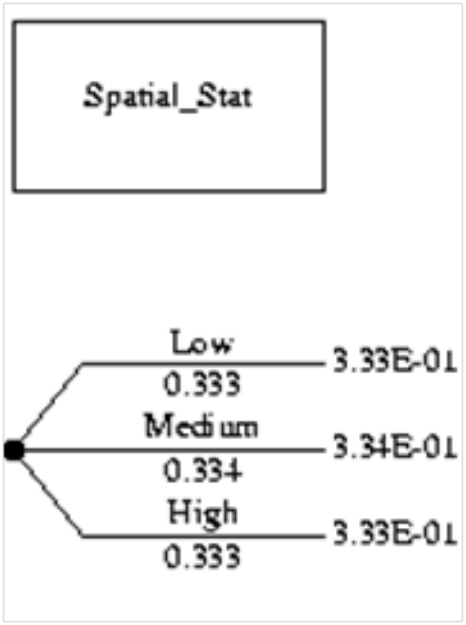

Figure 3.1: Spatial stationarity logic tree for EG1d.

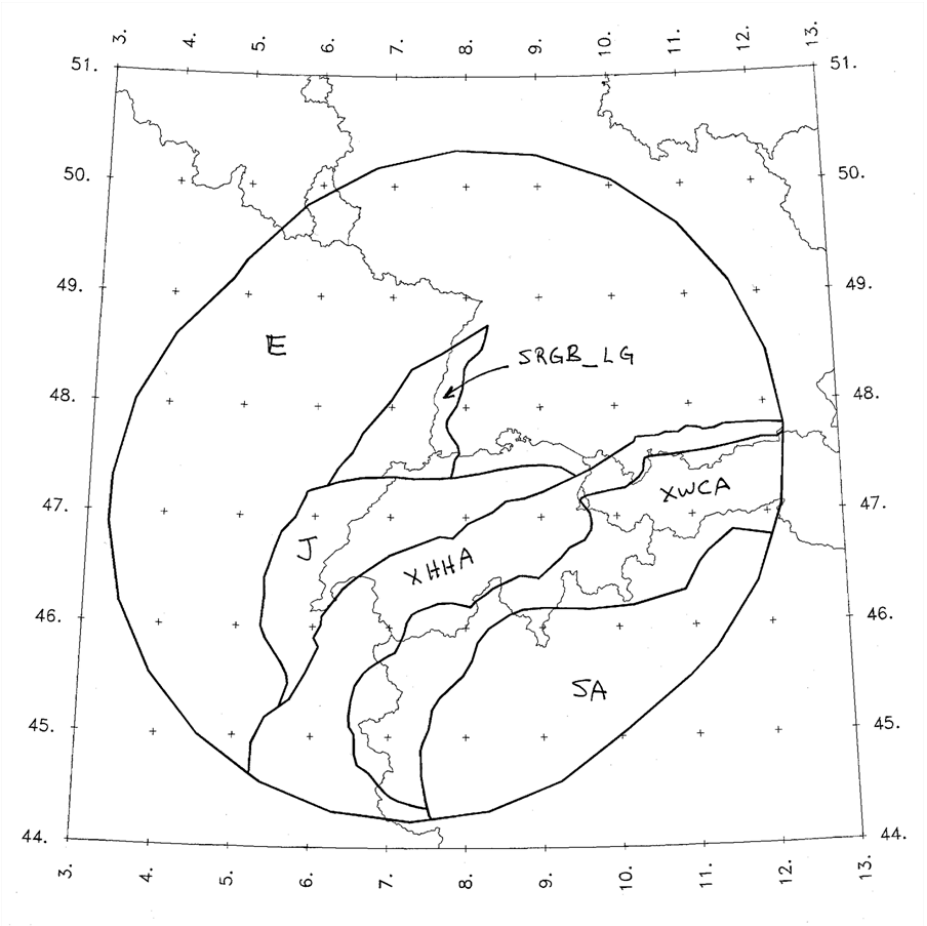

Figure 3.2: Regional zones for EG1d.

or is divided into two zones XHA and HA. These are shown on Figure 3.5. Similarly, zone XWCA is either treated as a single zone or is divided into two zones XWA and XCA, shown on Figure 3.5. The southern Rhine Graben source SRGB_LG is either a single zone, or the Basel region is a separate zone, B_LG from the rest of the southern Rhine Graben, SRG_LG. These alternatives are shown on the top of Figure 3.6. If zone TZ (discussed below) is present, then the southern Rhine Graben sources have alternative geometries SRGB_SM, SRG_SM, and B_SM, as shown on the bottom of Figure 3.6.

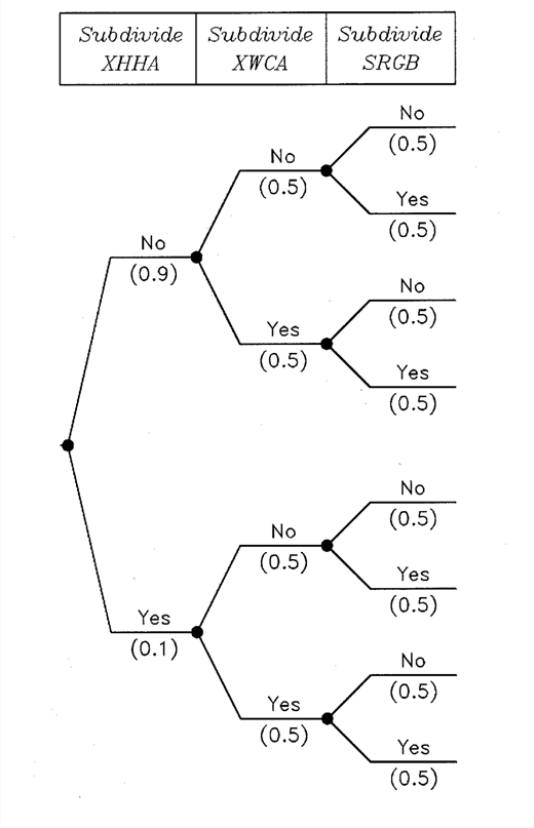

Figure 3.3: Logic tree for alternative zonations of the Alps and the Rhine Graben.

Figure 3.4 shows the logic tree for zonation alternatives within northern Switzerland and southern Germany. The basic model consists of a large zone representing Europe north-northwest of the Alps and Jura (zone E on Figure 3.2). Within this region, four alternative subzones are defined, SWA, NRG, FKZ, and TZ. The probabilities that each of these is present are independent. As a result, there are 16 alternative configurations for zone E. These are listed o the right-hand side off the logic tree Figure 3.4 and are shown on Figures 3.7, 3.8, 3.9 through 3.10. The alternatives for zone E are defined as simple polygons by wrapping the zone around narrow gaps between the other zones were necessary (for example between zones FKZ and SRG_LG).

The various logic tree branches produce 35 distinct source zone alternatives. Table 3.1 lists the various combinations of sources corresponding to end branches of the logic trees shown on Figures 3.3 and 3.4. The zone files are located in directory `./ZONES`. The spatial smoothing grid files are located in subdirectories within directory `./ZONES`. These are named to identify the earthquake catalog used to generate the kernel density function. These files have extensions

`*.h05` and `*.h15` for h values of 5 and 15 km, respectively.

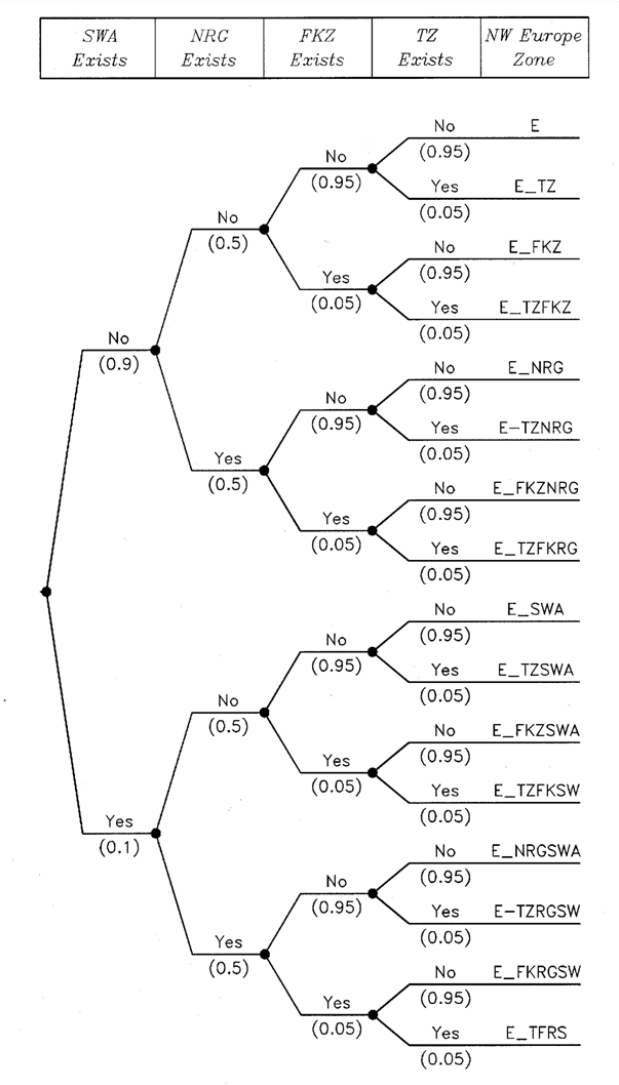

Figure 3.4: Logic tree for alternative sources within northern Switzerland and southern Germany.

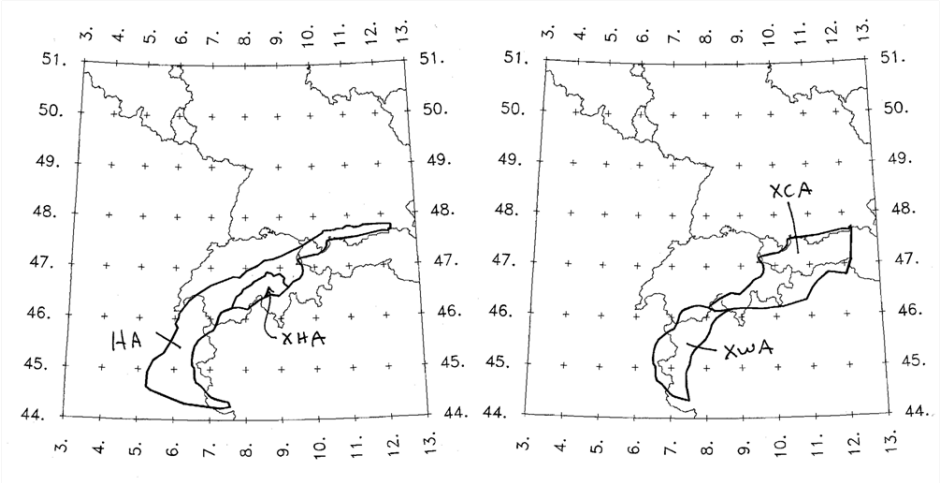

Figure 3.5: Left: division of zone XHHA into XHA and HA. Right: division of zone XWCA into XWA and XCA.

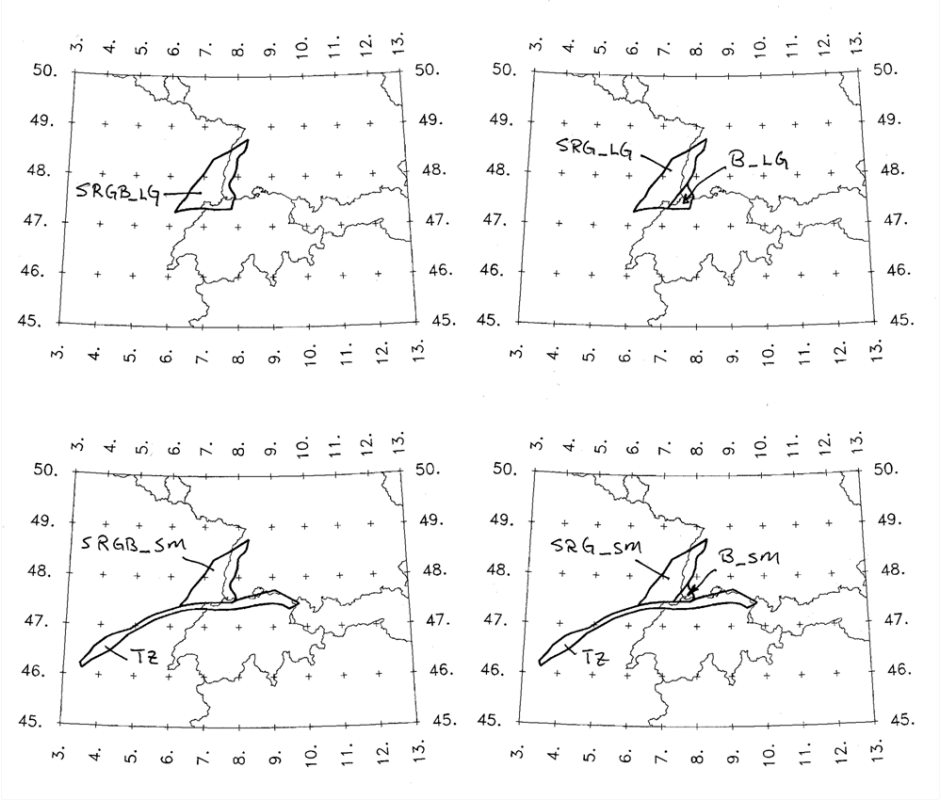

Figure 3.6: Alternative models for SRGB zone. Top left: SRGB_LG. Top right: division into SRG_LG and B_LG. Bottom plots show alternative geometry when zone TZ is present. Sources SRG_LG and B_LG are replaced with SRG_SM and B_SM, respectively.

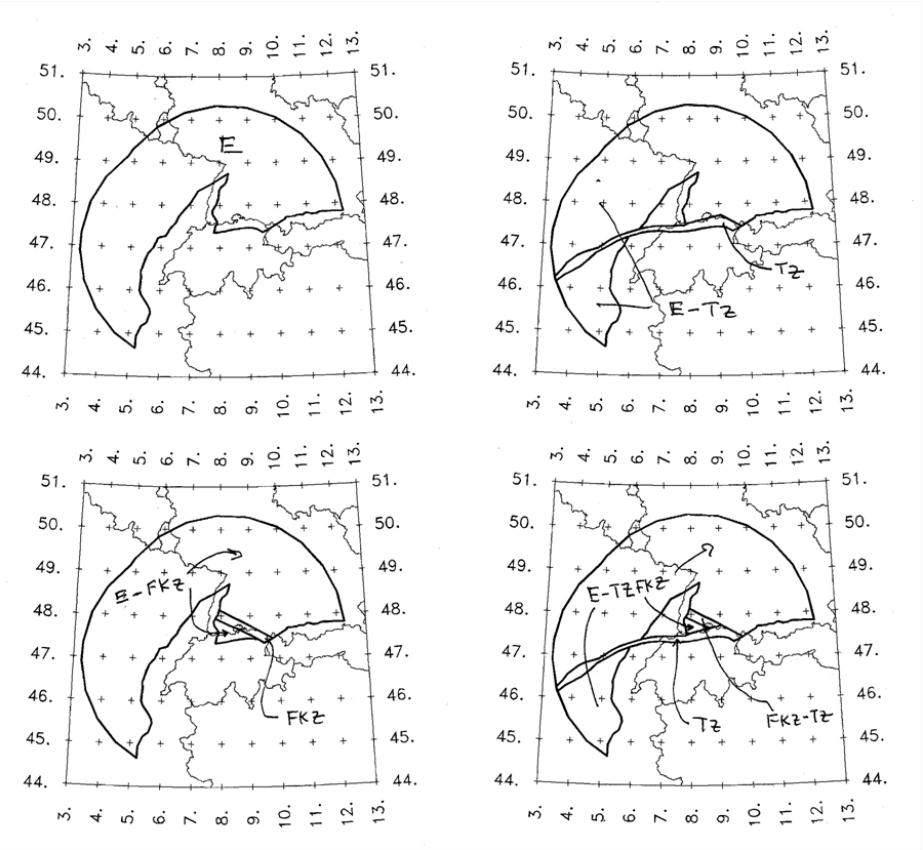

Figure 3.7: Alternative models of zone E reflecting the presence of zones TZ and FKZ.

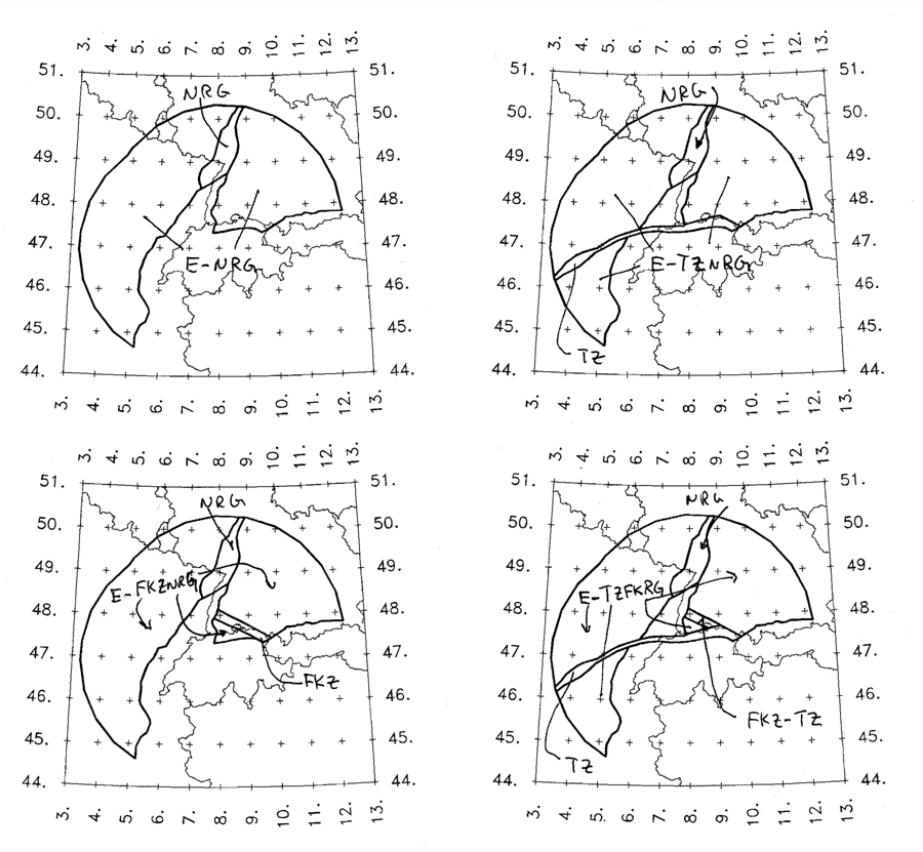

Figure 3.8: Alternative models of zone E reflecting the presence of zones NRG, TZ and FKZ.

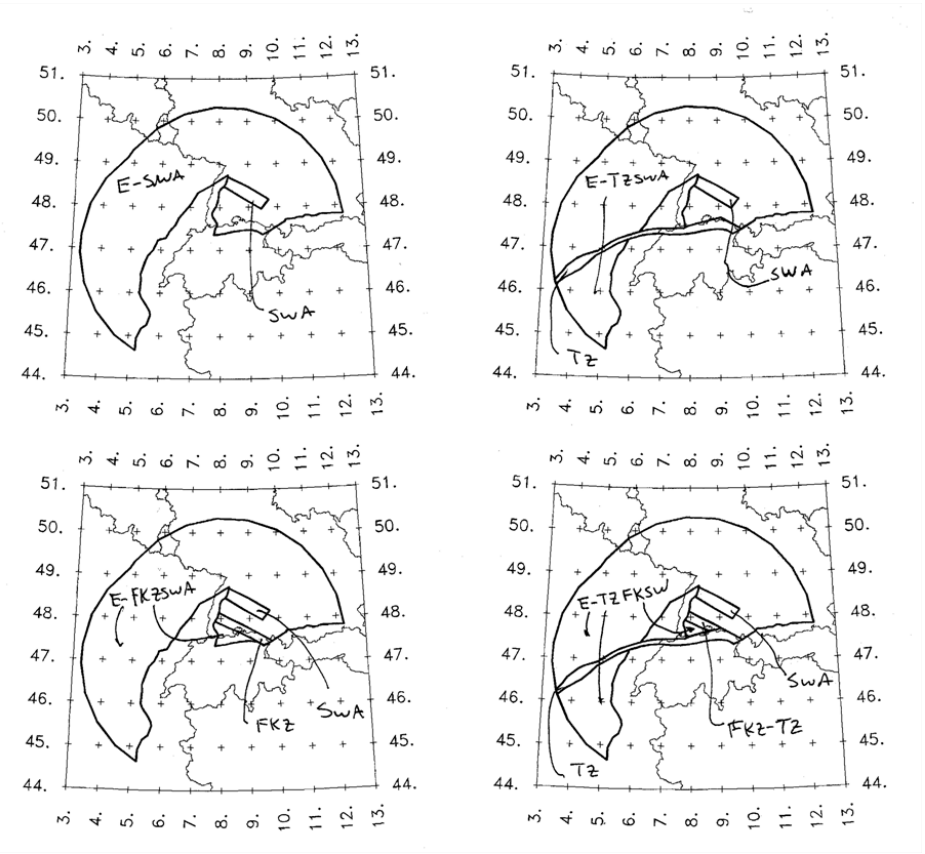

Figure 3.9: Alternative models of zone E reflecting the presence of zones SWA, TZ and FKZ.

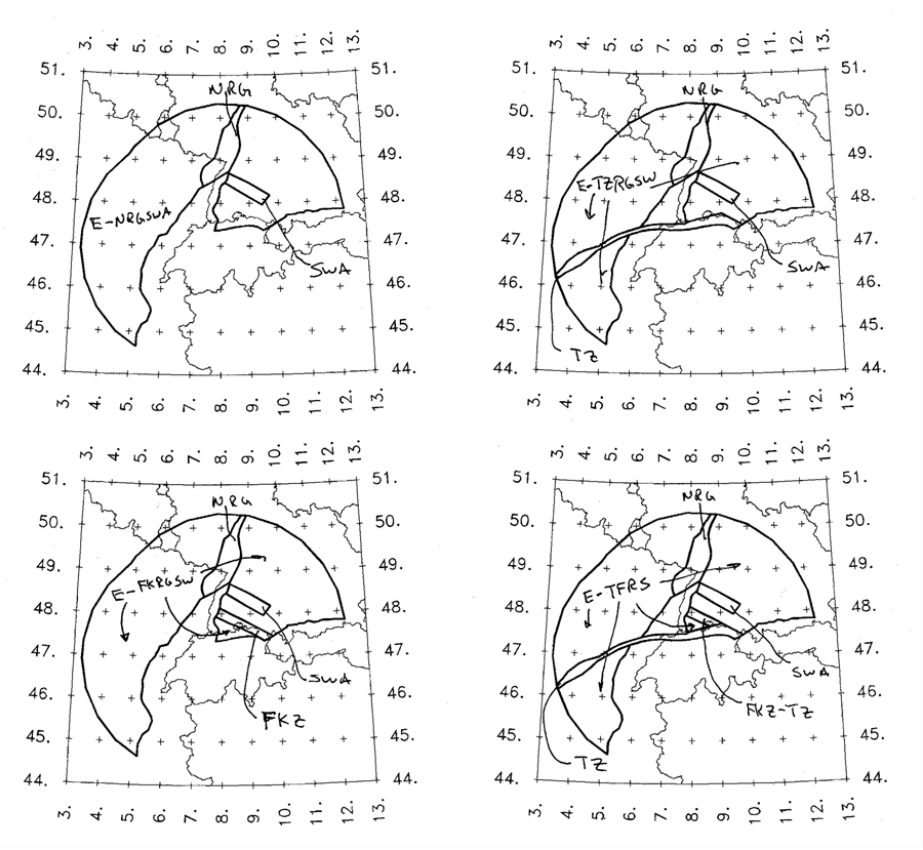

Figure 3.10: Alternative models of zone E reflecting the presence of zones SWA, NRG, FKZ and TZ.

Table 3.1: Source Zone Combinations for EG1d .

Subdivide XHHA	Subdivide XWCA	Subdivide SRGB	SWA Exists	NRG Exists	FKZ Exists	TZ Exists	Sources
No (0.9)	No (0.5)	No (0.5)	No (0.9)	No (0.5)	No (0.95)	No (0.95)	J, SA, XHHA, XWCA, SRGB_LG, E
No (0.9)	No (0.5)	No (0.5)	No (0.9)	No (0.5)	No (0.95)	Yes (0.05)	J, SA, XHHA, XWCA, SRGB_SM, TZ, E-TZ
No (0.9)	No (0.5)	No (0.5)	No (0.9)	No (0.5)	Yes (0.05)	No (0.95)	J, SA, XHHA, XWCA, SRGB_LG, FKZ, E-FKZ
No (0.9)	No (0.5)	No (0.5)	No (0.9)	No (0.5)	Yes (0.05)	Yes (0.05)	J, SA, XHHA, XWCA, SRGB_SM, TZ, FKZ-TZ, E-TZFKZ
No (0.9)	No (0.5)	No (0.5)	No (0.9)	Yes (0.5)	No (0.95)	No (0.95)	J, SA, XHHA, XWCA, SRGB_LG, NRG, E-NRG
No (0.9)	No (0.5)	No (0.5)	No (0.9)	Yes (0.5)	No (0.95)	Yes (0.05)	J, SA, XHHA, XWCA, SRGB_SM, TZ, NRG, E-TZNRG
No (0.9)	No (0.5)	No (0.5)	No (0.9)	Yes (0.5)	Yes (0.05)	No (0.95)	J, SA, XHHA, XWCA, SRGB_LG, FKZ, NRG, E-FKZNRG
No (0.9)	No (0.5)	No (0.5)	No (0.9)	Yes (0.5)	Yes (0.05)	Yes (0.05)	J, SA, XHHA, XWCA, SRGB_SM, TZ, FKZ-TZ, NRG, E-TZFKRG
No (0.9)	No (0.5)	No (0.5)	Yes (0.1)	No (0.5)	No (0.95)	No (0.95)	J, SA, XHHA, XWCA, SRGB_LG, SWA, E-SWA
No (0.9)	No (0.5)	No (0.5)	Yes (0.1)	No (0.5)	No (0.95)	Yes (0.05)	J, SA, XHHA, XWCA, SRGB_SM, TZ, SWA, E-TZSWA
No (0.9)	No (0.5)	No (0.5)	Yes (0.1)	No (0.5)	Yes (0.05)	No (0.95)	J, SA, XHHA, XWCA, SRGB_LG, FKZ, SWA, E-FKZSWA
No (0.9)	No (0.5)	No (0.5)	Yes (0.1)	No (0.5)	Yes (0.05)	Yes (0.05)	J, SA, XHHA, XWCA, SRGB_SM, TZ, FKZ-TZ, SWA, E-TZFKSW
No (0.9)	No (0.5)	No (0.5)	Yes (0.1)	Yes (0.5)	No (0.95)	No (0.95)	J, SA, XHHA, XWCA, SRGB_LG, NRG, SWA, E-NRGSWA
No (0.9)	No (0.5)	No (0.5)	Yes (0.1)	Yes (0.5)	No (0.95)	Yes (0.05)	J, SA, XHHA, XWCA, SRGB_SM, TZ, NRG, SWA, E-TZRGSW
No (0.9)	No (0.5)	No (0.5)	Yes (0.1)	Yes (0.5)	Yes (0.05)	No (0.95)	J, SA, XHHA, XWCA, SRGB_LG, FKZ, NRG, SWA, E-FKRGSW
No (0.9)	No (0.5)	No (0.5)	Yes (0.1)	Yes (0.5)	Yes (0.05)	Yes (0.05)	J, SA, XHHA, XWCA, SRGB_SM, TZ, FKZ-TZ, NRG, SWA, E-TFRS
No (0.9)	No (0.5)	Yes (0.5)	No (0.9)	No (0.5)	No (0.95)	No (0.95)	J, SA, XHHA, XWCA, SRG_LG, B_LG, E
No (0.9)	No (0.5)	Yes (0.5)	No (0.9)	No (0.5)	No (0.95)	Yes (0.05)	J, SA, XHHA, XWCA, SRG_SM, B_SM, TZ, E-TZ
No (0.9)	No (0.5)	Yes (0.5)	No (0.9)	No (0.5)	Yes (0.05)	No (0.95)	J, SA, XHHA, XWCA, SRG_LG, B_LG, FKZ, E-FKZ
No (0.9)	No (0.5)	Yes (0.5)	No (0.9)	No (0.5)	Yes (0.05)	Yes (0.05)	J, SA, XHHA, XWCA, SRG_SM, B_SM, TZ, FKZ-TZ, E-TZFKZ
No (0.9)	No (0.5)	Yes (0.5)	No (0.9)	Yes (0.5)	No (0.95)	No (0.95)	J, SA, XHHA, XWCA, SRG_LG, B_LG, NRG, E-NRG
No (0.9)	No (0.5)	Yes (0.5)	No (0.9)	Yes (0.5)	No (0.95)	Yes (0.05)	J, SA, XHHA, XWCA, SRG_SM, B_SM, TZ, NRG, E-TZNRG
No (0.9)	No (0.5)	Yes (0.5)	No (0.9)	Yes (0.5)	Yes (0.05)	No (0.95)	J, SA, XHHA, XWCA, SRG_LG, B_LG, FKZ, NRG, E-FKZNRG
No (0.9)	No (0.5)	Yes (0.5)	No (0.9)	Yes (0.5)	Yes (0.05)	Yes (0.05)	J, SA, XHHA, XWCA, SRG_SM, B_SM, TZ, FKZ-TZ, NRG, E-TZFKRG
No (0.9)	No (0.5)	Yes (0.5)	Yes (0.1)	No (0.5)	No (0.95)	No (0.95)	J, SA, XHHA, XWCA, SRG_LG, B_LG, SWA, E-SWA
No (0.9)	No (0.5)	Yes (0.5)	Yes (0.1)	No (0.5)	No (0.95)	Yes (0.05)	J, SA, XHHA, XWCA, SRG_SM, B_SM, TZ, SWA, E-TZSWA
No (0.9)	No (0.5)	Yes (0.5)	Yes (0.1)	No (0.5)	Yes (0.05)	No (0.95)	J, SA, XHHA, XWCA, SRG_LG, B_LG, FKZ, SWA, E-FKZSWA
No (0.9)	No (0.5)	Yes (0.5)	Yes (0.1)	No (0.5)	Yes (0.05)	Yes (0.05)	J, SA, XHHA, XWCA, SRG_SM, B_SM, TZ, FKZ-TZ, SWA, E-TZFKSW
No (0.9)	No (0.5)	Yes (0.5)	Yes (0.1)	Yes (0.5)	No (0.95)	No (0.95)	J, SA, XHHA, XWCA, SRG_LG, B_LG, NRG, SWA, E-NRGSWA
No (0.9)	No (0.5)	Yes (0.5)	Yes (0.1)	Yes (0.5)	No (0.95)	Yes (0.05)	J, SA, XHHA, XWCA, SRG_SM, B_SM, TZ, NRG, SWA, E-TZRGSW
No (0.9)	No (0.5)	Yes (0.5)	Yes (0.1)	Yes (0.5)	Yes (0.05)	No (0.95)	J, SA, XHHA, XWCA, SRG_LG, B_LG, FKZ, NRG, SWA, E-FKRGSW
No (0.9)	No (0.5)	Yes (0.5)	Yes (0.1)	Yes (0.5)	Yes (0.05)	Yes (0.05)	J, SA, XHHA, XWCA, SRG_SM, B_SM, TZ, FKZ-TZ, NRG, SWA, E-TFRS
No (0.9)	Yes (0.5)	No (0.5)	No (0.9)	No (0.5)	No (0.95)	No (0.95)	J, SA, XHHA, XCA, XWA, SRGB_LG, E
No (0.9)	Yes (0.5)	No (0.5)	No (0.9)	No (0.5)	No (0.95)	Yes (0.05)	J, SA, XHHA, XCA, XWA, SRGB_SM, TZ, E-TZ
No (0.9)	Yes (0.5)	No (0.5)	No (0.9)	No (0.5)	Yes (0.05)	No (0.95)	J, SA, XHHA, XCA, XWA, SRGB_LG, FKZ, E-FKZ
No (0.9)	Yes (0.5)	No (0.5)	No (0.9)	No (0.5)	Yes (0.05)	Yes (0.05)	J, SA, XHHA, XCA, XWA, SRGB_SM, TZ, FKZ-TZ, E-TZFKZ

Continued on next page...

Table 3.1 – continued from previous page

Subdivide XHHA	Subdivide XWCA	Subdivide SRGB	SWA Exists	NRG Exists	FKZ Exists	TZ Exists	Sources
No (0.9)	Yes (0.5)	No (0.5)	No (0.9)	Yes (0.5)	No (0.95)	No (0.95)	J, SA, XHHA, XCA, XWA, SRGB_LG, NRG, E-NRG
No (0.9)	Yes (0.5)	No (0.5)	No (0.9)	Yes (0.5)	No (0.95)	Yes (0.05)	J, SA, XHHA, XCA, XWA, SRGB_SM, TZ, NRG, E-TZNRG
No (0.9)	Yes (0.5)	No (0.5)	No (0.9)	Yes (0.5)	Yes (0.05)	No (0.95)	J, SA, XHHA, XCA, XWA, SRGB_LG, FKZ, NRG, E-FKZNRG
No (0.9)	Yes (0.5)	No (0.5)	No (0.9)	Yes (0.5)	Yes (0.05)	Yes (0.05)	J, SA, XHHA, XCA, XWA, SRGB_SM, TZ, FKZ-TZ, NRG, E-TZFKRG
No (0.9)	Yes (0.5)	No (0.5)	Yes (0.1)	No (0.5)	No (0.95)	No (0.95)	J, SA, XHHA, XCA, XWA, SRGB_LG, SWA, E-SWA
No (0.9)	Yes (0.5)	No (0.5)	Yes (0.1)	No (0.5)	No (0.95)	Yes (0.05)	J, SA, XHHA, XCA, XWA, SRGB_SM, TZ, SWA, E-TZSWA
No (0.9)	Yes (0.5)	No (0.5)	Yes (0.1)	No (0.5)	Yes (0.05)	No (0.95)	J, SA, XHHA, XCA, XWA, SRGB_LG, FKZ, SWA, E-FKZSWA
No (0.9)	Yes (0.5)	No (0.5)	Yes (0.1)	No (0.5)	Yes (0.05)	Yes (0.05)	J, SA, XHHA, XCA, XWA, SRGB_SM, TZ, FKZ-TZ, SWA, E-TZFKSW
No (0.9)	Yes (0.5)	No (0.5)	Yes (0.1)	Yes (0.5)	No (0.95)	No (0.95)	J, SA, XHHA, XCA, XWA, SRGB_LG, NRG, SWA, E-NRGSWA
No (0.9)	Yes (0.5)	No (0.5)	Yes (0.1)	Yes (0.5)	No (0.95)	Yes (0.05)	J, SA, XHHA, XCA, XWA, SRGB_SM, TZ, NRG, SWA, E-TZRGSW
No (0.9)	Yes (0.5)	No (0.5)	Yes (0.1)	Yes (0.5)	Yes (0.05)	No (0.95)	J, SA, XHHA, XCA, XWA, SRGB_LG, FKZ, NRG, SWA, E-FKRGSW
No (0.9)	Yes (0.5)	No (0.5)	Yes (0.1)	Yes (0.5)	Yes (0.05)	Yes (0.05)	J, SA, XHHA, XCA, XWA, SRGB_SM, TZ, FKZ-TZ, NRG, SWA, E-TFRS
No (0.9)	Yes (0.5)	Yes (0.5)	No (0.9)	No (0.5)	No (0.95)	No (0.95)	J, SA, XHHA, XCA, XWA, SRG_LG, B_LG, E
No (0.9)	Yes (0.5)	Yes (0.5)	No (0.9)	No (0.5)	No (0.95)	Yes (0.05)	J, SA, XHHA, XCA, XWA, SRG_SM, B_SM, TZ, E-TZ
No (0.9)	Yes (0.5)	Yes (0.5)	No (0.9)	No (0.5)	Yes (0.05)	No (0.95)	J, SA, XHHA, XCA, XWA, SRG_LG, B_LG, FKZ, E-FKZ
No (0.9)	Yes (0.5)	Yes (0.5)	No (0.9)	No (0.5)	Yes (0.05)	Yes (0.05)	J, SA, XHHA, XCA, XWA, SRG_SM, B_SM, TZ, FKZ-TZ, E-TZFKZ
No (0.9)	Yes (0.5)	Yes (0.5)	No (0.9)	Yes (0.5)	No (0.95)	No (0.95)	J, SA, XHHA, XCA, XWA, SRG_LG, B_LG, NRG, E-NRG
No (0.9)	Yes (0.5)	Yes (0.5)	No (0.9)	Yes (0.5)	No (0.95)	Yes (0.05)	J, SA, XHHA, XCA, XWA, SRG_SM, B_SM, TZ, NRG, E-TZNRG
No (0.9)	Yes (0.5)	Yes (0.5)	No (0.9)	Yes (0.5)	Yes (0.05)	No (0.95)	J, SA, XHHA, XCA, XWA, SRG_LG, B_LG, FKZ, NRG, E-FKZNRG
No (0.9)	Yes (0.5)	Yes (0.5)	No (0.9)	Yes (0.5)	Yes (0.05)	Yes (0.05)	J, SA, XHHA, XCA, XWA, SRG_SM, B_SM, TZ, FKZ-TZ, NRG, E-TZFKRG
No (0.9)	Yes (0.5)	Yes (0.5)	Yes (0.1)	No (0.5)	No (0.95)	No (0.95)	J, SA, XHHA, XCA, XWA, SRG_LG, B_LG, SWA, E-SWA
No (0.9)	Yes (0.5)	Yes (0.5)	Yes (0.1)	No (0.5)	No (0.95)	Yes (0.05)	J, SA, XHHA, XCA, XWA, SRG_SM, B_SM, TZ, SWA, E-TZSWA
No (0.9)	Yes (0.5)	Yes (0.5)	Yes (0.1)	No (0.5)	Yes (0.05)	No (0.95)	J, SA, XHHA, XCA, XWA, SRG_LG, B_LG, FKZ, SWA, E-FKZSWA
No (0.9)	Yes (0.5)	Yes (0.5)	Yes (0.1)	No (0.5)	Yes (0.05)	Yes (0.05)	J, SA, XHHA, XCA, XWA, SRG_SM, B_SM, TZ, FKZ-TZ, SWA, E-TZFKSW
No (0.9)	Yes (0.5)	Yes (0.5)	Yes (0.1)	Yes (0.5)	No (0.95)	No (0.95)	J, SA, XHHA, XCA, XWA, SRG_LG, B_LG, NRG, SWA, E-NRGSWA
No (0.9)	Yes (0.5)	Yes (0.5)	Yes (0.1)	Yes (0.5)	No (0.95)	Yes (0.05)	J, SA, XHHA, XCA, XWA, SRG_SM, B_SM, TZ, NRG, SWA, E-TZRGSW
No (0.9)	Yes (0.5)	Yes (0.5)	Yes (0.1)	Yes (0.5)	Yes (0.05)	No (0.95)	J, SA, XHHA, XCA, XWA, SRG_LG, B_LG, FKZ, NRG, SWA, E-FKRGSW
No (0.9)	Yes (0.5)	Yes (0.5)	Yes (0.1)	Yes (0.5)	Yes (0.05)	Yes (0.05)	J, SA, XHHA, XCA, XWA, SRG_SM, B_SM, TZ, FKZ-TZ, NRG, SWA, E-TFRS
Yes (0.1)	No (0.5)	No (0.5)	No (0.9)	No (0.5)	No (0.95)	No (0.95)	J, SA, XHA, HA, XWCA, SRGB_LG, E
Yes (0.1)	No (0.5)	No (0.5)	No (0.9)	No (0.5)	No (0.95)	Yes (0.05)	J, SA, XHA, HA, XWCA, SRGB_SM, TZ, E-TZ
Yes (0.1)	No (0.5)	No (0.5)	No (0.9)	No (0.5)	Yes (0.05)	No (0.95)	J, SA, XHA, HA, XWCA, SRGB_LG, FKZ, E-FKZ
Yes (0.1)	No (0.5)	No (0.5)	No (0.9)	No (0.5)	Yes (0.05)	Yes (0.05)	J, SA, XHA, HA, XWCA, SRGB_SM, TZ, FKZ-TZ, E-TZFKZ
Yes (0.1)	No (0.5)	No (0.5)	No (0.9)	Yes (0.5)	No (0.95)	No (0.95)	J, SA, XHA, HA, XWCA, SRGB_LG, NRG, E-NRG
Yes (0.1)	No (0.5)	No (0.5)	No (0.9)	Yes (0.5)	No (0.95)	Yes (0.05)	J, SA, XHA, HA, XWCA, SRGB_SM, TZ, NRG, E-TZNRG
Yes (0.1)	No (0.5)	No (0.5)	No (0.9)	Yes (0.5)	Yes (0.05)	No (0.95)	J, SA, XHA, HA, XWCA, SRGB_LG, FKZ, NRG, E-FKZNRG
Yes (0.1)	No (0.5)	No (0.5)	No (0.9)	Yes (0.5)	Yes (0.05)	Yes (0.05)	J, SA, XHA, HA, XWCA, SRGB_SM, TZ, FKZ-TZ, NRG, E-TZFKRG

Continued on next page. . .

Table 3.1 – continued from previous page

Subdivide XHHA	Subdivide XWCA	Subdivide SRGB	SWA Exists	NRG Exists	FKZ Exists	TZ Exists	Sources
Yes (0.1)	No (0.5)	No (0.5)	Yes (0.1)	No (0.5)	No (0.95)	No (0.95)	J, SA, XHA, HA, XWCA, SRGB_LG, SWA, E-SWA
Yes (0.1)	No (0.5)	No (0.5)	Yes (0.1)	No (0.5)	No (0.95)	Yes (0.05)	J, SA, XHA, HA, XWCA, SRGB_SM, TZ, SWA, E-TZSWA
Yes (0.1)	No (0.5)	No (0.5)	Yes (0.1)	No (0.5)	Yes (0.05)	No (0.95)	J, SA, XHA, HA, XWCA, SRGB_LG, FKZ, SWA, E-FKZSWA
Yes (0.1)	No (0.5)	No (0.5)	Yes (0.1)	No (0.5)	Yes (0.05)	Yes (0.05)	J, SA, XHA, HA, XWCA, SRGB_SM, TZ, FKZ-TZ, SWA, E-TZFKSW
Yes (0.1)	No (0.5)	No (0.5)	Yes (0.1)	Yes (0.5)	No (0.95)	No (0.95)	J, SA, XHA, HA, XWCA, SRGB_LG, NRG, SWA, E-NRGSWA
Yes (0.1)	No (0.5)	No (0.5)	Yes (0.1)	Yes (0.5)	No (0.95)	Yes (0.05)	J, SA, XHA, HA, XWCA, SRGB_SM, TZ, NRG, SWA, E-TZRGSW
Yes (0.1)	No (0.5)	No (0.5)	Yes (0.1)	Yes (0.5)	Yes (0.05)	No (0.95)	J, SA, XHA, HA, XWCA, SRGB_LG, FKZ, NRG, SWA, E-FKRGSW
Yes (0.1)	No (0.5)	No (0.5)	Yes (0.1)	Yes (0.5)	Yes (0.05)	Yes (0.05)	J, SA, XHA, HA, XWCA, SRGB_SM, TZ, FKZ-TZ, NRG, SWA, E-TFRS
Yes (0.1)	No (0.5)	Yes (0.5)	No (0.9)	No (0.5)	No (0.95)	No (0.95)	J, SA, XHA, HA, XWCA, SRG_LG, B_LG, E
Yes (0.1)	No (0.5)	Yes (0.5)	No (0.9)	No (0.5)	No (0.95)	Yes (0.05)	J, SA, XHA, HA, XWCA, SRG_SM, B_SM, TZ, E-TZ
Yes (0.1)	No (0.5)	Yes (0.5)	No (0.9)	No (0.5)	Yes (0.05)	No (0.95)	J, SA, XHA, HA, XWCA, SRG_LG, B_LG, FKZ, E-FKZ
Yes (0.1)	No (0.5)	Yes (0.5)	No (0.9)	No (0.5)	Yes (0.05)	Yes (0.05)	J, SA, XHA, HA, XWCA, SRG_SM, B_SM, TZ, FKZ-TZ, E-TZFKZ
Yes (0.1)	No (0.5)	Yes (0.5)	No (0.9)	Yes (0.5)	No (0.95)	No (0.95)	J, SA, XHA, HA, XWCA, SRG_LG, B_LG, NRG, E-NRG
Yes (0.1)	No (0.5)	Yes (0.5)	No (0.9)	Yes (0.5)	No (0.95)	Yes (0.05)	J, SA, XHA, HA, XWCA, SRG_SM, B_SM, TZ, NRG, E-TZNRG
Yes (0.1)	No (0.5)	Yes (0.5)	No (0.9)	Yes (0.5)	Yes (0.05)	No (0.95)	J, SA, XHA, HA, XWCA, SRG_LG, B_LG, FKZ, NRG, E-FKZNRG
Yes (0.1)	No (0.5)	Yes (0.5)	No (0.9)	Yes (0.5)	Yes (0.05)	Yes (0.05)	J, SA, XHA, HA, XWCA, SRG_SM, B_SM, TZ, FKZ-TZ, NRG, E-TZFKRG
Yes (0.1)	No (0.5)	Yes (0.5)	Yes (0.1)	No (0.5)	No (0.95)	No (0.95)	J, SA, XHA, HA, XWCA, SRG_LG, B_LG, SWA, E-SWA
Yes (0.1)	No (0.5)	Yes (0.5)	Yes (0.1)	No (0.5)	No (0.95)	Yes (0.05)	J, SA, XHA, HA, XWCA, SRG_SM, B_SM, TZ, SWA, E-TZSWA
Yes (0.1)	No (0.5)	Yes (0.5)	Yes (0.1)	No (0.5)	Yes (0.05)	No (0.95)	J, SA, XHA, HA, XWCA, SRG_LG, B_LG, FKZ, SWA, E-FKZSWA
Yes (0.1)	No (0.5)	Yes (0.5)	Yes (0.1)	No (0.5)	Yes (0.05)	Yes (0.05)	J, SA, XHA, HA, XWCA, SRG_SM, B_SM, TZ, FKZ-TZ, SWA, E-TZFKSW
Yes (0.1)	No (0.5)	Yes (0.5)	Yes (0.1)	Yes (0.5)	No (0.95)	No (0.95)	J, SA, XHA, HA, XWCA, SRG_LG, B_LG, NRG, SWA, E-NRGSWA
Yes (0.1)	No (0.5)	Yes (0.5)	Yes (0.1)	Yes (0.5)	No (0.95)	Yes (0.05)	J, SA, XHA, HA, XWCA, SRG_SM, B_SM, TZ, NRG, SWA, E-TZRGSW
Yes (0.1)	No (0.5)	Yes (0.5)	Yes (0.1)	Yes (0.5)	Yes (0.05)	No (0.95)	J, SA, XHA, HA, XWCA, SRG_LG, B_LG, FKZ, NRG, SWA, E-FKRGSW
Yes (0.1)	No (0.5)	Yes (0.5)	Yes (0.1)	Yes (0.5)	Yes (0.05)	Yes (0.05)	J, SA, XHA, HA, XWCA, SRG_SM, B_SM, TZ, FKZ-TZ, NRG, SWA, E-TFRS
Yes (0.1)	Yes (0.5)	No (0.5)	No (0.9)	No (0.5)	No (0.95)	No (0.95)	J, SA, XHA, HA, XCA, XWA, SRGB_LG, E
Yes (0.1)	Yes (0.5)	No (0.5)	No (0.9)	No (0.5)	No (0.95)	Yes (0.05)	J, SA, XHA, HA, XCA, XWA, SRGB_SM, TZ, E-TZ
Yes (0.1)	Yes (0.5)	No (0.5)	No (0.9)	No (0.5)	Yes (0.05)	No (0.95)	J, SA, XHA, HA, XCA, XWA, SRGB_LG, FKZ, E-FKZ
Yes (0.1)	Yes (0.5)	No (0.5)	No (0.9)	No (0.5)	Yes (0.05)	Yes (0.05)	J, SA, XHA, HA, XCA, XWA, SRGB_SM, TZ, FKZ-TZ, E-TZFKZ
Yes (0.1)	Yes (0.5)	No (0.5)	No (0.9)	Yes (0.5)	No (0.95)	No (0.95)	J, SA, XHA, HA, XCA, XWA, SRGB_LG, NRG, E-NRG
Yes (0.1)	Yes (0.5)	No (0.5)	No (0.9)	Yes (0.5)	No (0.95)	Yes (0.05)	J, SA, XHA, HA, XCA, XWA, SRGB_SM, TZ, NRG, E-TZNRG
Yes (0.1)	Yes (0.5)	No (0.5)	No (0.9)	Yes (0.5)	Yes (0.05)	No (0.95)	J, SA, XHA, HA, XCA, XWA, SRGB_LG, FKZ, NRG, E-FKZNRG
Yes (0.1)	Yes (0.5)	No (0.5)	No (0.9)	Yes (0.5)	Yes (0.05)	Yes (0.05)	J, SA, XHA, HA, XCA, XWA, SRGB_SM, TZ, FKZ-TZ, NRG, E-TZFKRG
Yes (0.1)	Yes (0.5)	No (0.5)	Yes (0.1)	No (0.5)	No (0.95)	No (0.95)	J, SA, XHA, HA, XCA, XWA, SRGB_LG, SWA, E-SWA
Yes (0.1)	Yes (0.5)	No (0.5)	Yes (0.1)	No (0.5)	No (0.95)	Yes (0.05)	J, SA, XHA, HA, XCA, XWA, SRGB_SM, TZ, SWA, E-TZSWA
Yes (0.1)	Yes (0.5)	No (0.5)	Yes (0.1)	No (0.5)	Yes (0.05)	No (0.95)	J, SA, XHA, HA, XCA, XWA, SRGB_LG, FKZ, SWA, E-FKZSWA

Continued on next page...

Table 3.1 – continued from previous page

Subdivide XHHA	Subdivide XWCA	Subdivide SRGB	SWA Exists	NRG Exists	FKZ Exists	TZ Exists	Sources
Yes (0.1)	Yes (0.5)	No (0.5)	Yes (0.1)	No (0.5)	Yes (0.05)	Yes (0.05)	J, SA, XHA, HA, XCA, XWA, SRGB_SM, TZ, FKZ-TZ, SWA, E-TZFKSW
Yes (0.1)	Yes (0.5)	No (0.5)	Yes (0.1)	Yes (0.5)	No (0.95)	No (0.95)	J, SA, XHA, HA, XCA, XWA, SRGB_LG, NRG, SWA, E-NRGSWA
Yes (0.1)	Yes (0.5)	No (0.5)	Yes (0.1)	Yes (0.5)	No (0.95)	Yes (0.05)	J, SA, XHA, HA, XCA, XWA, SRGB_SM, TZ, NRG, SWA, E-TZRGSW
Yes (0.1)	Yes (0.5)	No (0.5)	Yes (0.1)	Yes (0.5)	Yes (0.05)	No (0.95)	J, SA, XHA, HA, XCA, XWA, SRGB_LG, FKZ, NRG, SWA, E-FKRGSW
Yes (0.1)	Yes (0.5)	No (0.5)	Yes (0.1)	Yes (0.5)	Yes (0.05)	Yes (0.05)	J, SA, XHA, HA, XCA, XWA, SRGB_SM, TZ, FKZ-TZ, NRG, SWA, E-TFRS
Yes (0.1)	Yes (0.5)	Yes (0.5)	No (0.9)	No (0.5)	No (0.95)	No (0.95)	J, SA, XHA, HA, XCA, XWA, SRG_LG, B_LG, E
Yes (0.1)	Yes (0.5)	Yes (0.5)	No (0.9)	No (0.5)	No (0.95)	Yes (0.05)	J, SA, XHA, HA, XCA, XWA, SRG_SM, B_SM, TZ, E-TZ
Yes (0.1)	Yes (0.5)	Yes (0.5)	No (0.9)	No (0.5)	Yes (0.05)	No (0.95)	J, SA, XHA, HA, XCA, XWA, SRG_LG, B_LG, FKZ, E-FKZ
Yes (0.1)	Yes (0.5)	Yes (0.5)	No (0.9)	No (0.5)	Yes (0.05)	Yes (0.05)	J, SA, XHA, HA, XCA, XWA, SRG_SM, B_SM, TZ, FKZ-TZ, E-TZFKZ
Yes (0.1)	Yes (0.5)	Yes (0.5)	No (0.9)	Yes (0.5)	No (0.95)	No (0.95)	J, SA, XHA, HA, XCA, XWA, SRG_LG, B_LG, NRG, E-NRG
Yes (0.1)	Yes (0.5)	Yes (0.5)	No (0.9)	Yes (0.5)	No (0.95)	Yes (0.05)	J, SA, XHA, HA, XCA, XWA, SRG_SM, B_SM, TZ, NRG, E-TZNRG
Yes (0.1)	Yes (0.5)	Yes (0.5)	No (0.9)	Yes (0.5)	Yes (0.05)	No (0.95)	J, SA, XHA, HA, XCA, XWA, SRG_LG, B_LG, FKZ, NRG, E-FKZNRG
Yes (0.1)	Yes (0.5)	Yes (0.5)	No (0.9)	Yes (0.5)	Yes (0.05)	Yes (0.05)	J, SA, XHA, HA, XCA, XWA, SRG_SM, B_SM, TZ, FKZ-TZ, NRG, E-TZFKRG
Yes (0.1)	Yes (0.5)	Yes (0.5)	Yes (0.1)	No (0.5)	No (0.95)	No (0.95)	J, SA, XHA, HA, XCA, XWA, SRG_LG, B_LG, SWA, E-SWA
Yes (0.1)	Yes (0.5)	Yes (0.5)	Yes (0.1)	No (0.5)	No (0.95)	Yes (0.05)	J, SA, XHA, HA, XCA, XWA, SRG_SM, B_SM, TZ, SWA, E-TZSWA
Yes (0.1)	Yes (0.5)	Yes (0.5)	Yes (0.1)	No (0.5)	Yes (0.05)	No (0.95)	J, SA, XHA, HA, XCA, XWA, SRG_LG, B_LG, FKZ, SWA, E-FKZSWA
Yes (0.1)	Yes (0.5)	Yes (0.5)	Yes (0.1)	No (0.5)	Yes (0.05)	Yes (0.05)	J, SA, XHA, HA, XCA, XWA, SRG_SM, B_SM, TZ, FKZ-TZ, SWA, E-TZFKSW
Yes (0.1)	Yes (0.5)	Yes (0.5)	Yes (0.1)	Yes (0.5)	No (0.95)	No (0.95)	J, SA, XHA, HA, XCA, XWA, SRG_LG, B_LG, NRG, SWA, E-NRGSWA
Yes (0.1)	Yes (0.5)	Yes (0.5)	Yes (0.1)	Yes (0.5)	No (0.95)	Yes (0.05)	J, SA, XHA, HA, XCA, XWA, SRG_SM, B_SM, TZ, NRG, SWA, E-TZRGSW
Yes (0.1)	Yes (0.5)	Yes (0.5)	Yes (0.1)	Yes (0.5)	Yes (0.05)	No (0.95)	J, SA, XHA, HA, XCA, XWA, SRG_LG, B_LG, FKZ, NRG, SWA, E-FKRGSW
Yes (0.1)	Yes (0.5)	Yes (0.5)	Yes (0.1)	Yes (0.5)	Yes (0.05)	Yes (0.05)	J, SA, XHA, HA, XCA, XWA, SRG_SM, B_SM, TZ, FKZ-TZ, NRG, SWA, E-TFRS

3.2 Earthquake Rupture Geometry

The size of earthquake ruptures is defined by the relationship:

$$\text{Mean}\log_{10}(\text{rupture area}) = 0.91M - 3.49 \quad (3.1)$$

$$\sigma\log_{10}(\text{rupture area}) = 0.24 \quad (3.2)$$

Using the relationship for the expectation of a lognormal distribution, the mean (expected) rupture area is given by the relationship:

$$\text{mean rupture area} = 10^{(0.91M-3.424)} \quad (3.3)$$

The relationship for the mean rupture area will be used in the hazard computations. The rupture length and width have an aspect ratio of 2.5:1 until the maximum rupture width for a source is reached. The maximum rupture width is determined on the basis of the maximum depth and fault dip, as defined below. For larger ruptures, the width is held constant at the maximum width and the length is obtained by dividing the rupture area by this width. Earthquake epicenters are distributed within each source either uniformly or according to a kernel density function (Figure 3.1). Earthquake ruptures are located symmetrically on the epicenters (the epicenter is at the midpoint of the rupture). For those epicenters located closer than 1/2 rupture length to the source zone boundary, the ruptures are allowed to extend beyond the source boundary.

Table 3.2 defines the relative frequency of the style-of-faulting for the individual sources. Three specific styles-of-faulting are considered, normal, strike-slip and reverse. Rupture orientation should be uniformly distributed over the range of 0 to 360 degrees within each source (no preferred orientation of rupture). The dip angles for each style-of-faulting are specified by two (for strike-slip) or three (for dip slip) equally weighted angles representing aleatory variability in the dip of ruptures. These dip angles are: 70 (0.5) and 90 (0.5) degrees for strike-slip faulting; 40 (0.333), 60 (0.333), and 80 (0.333) degrees for normal faulting; and 10 (0.333), 30 (0.333), and 50 (0.333) degrees for thrust faulting.

Table 3.2: Styles of Faulting for EG1d Source Zones.

Region	**Fraction (%) of Earthquakes with Style of Faulting:**		
	Strike Slip	**Normal**	**Thrust**
Europe (E, SWA, FKZ, TZ)	85	5	10
Southern Rhine Graben (SRG, SRGB, B)	75	20	5
Northern Rhine Graben (NRG)	85	10	5
Jura (J)	75	5	20
Italy (SA)	70	10	20
Alps (XWCA, XHHA, HA, XHA, XCA, XWA)	70	15	15

The depth distribution of small earthquakes for the sources is defined by the two distributions shown in Figure 3.11 and listed in table 3.3. For larger earthquakes, a magnitude-dependent

depth distribution is to be developed using the weighted approach outlined in Toro [2003] (TP1-TN-0373) with T = 0.5 (hypocenter in lower half of rupture).

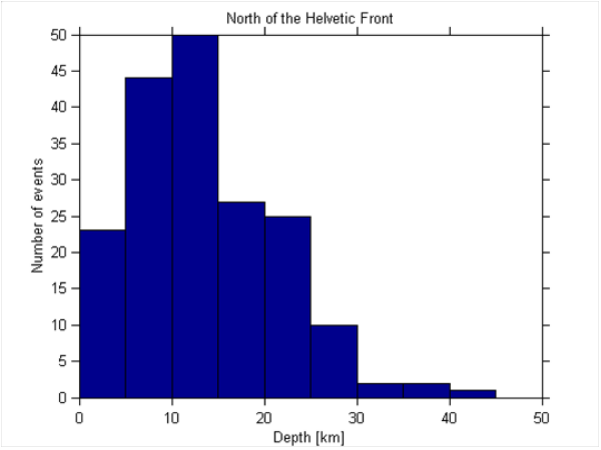

(a) left

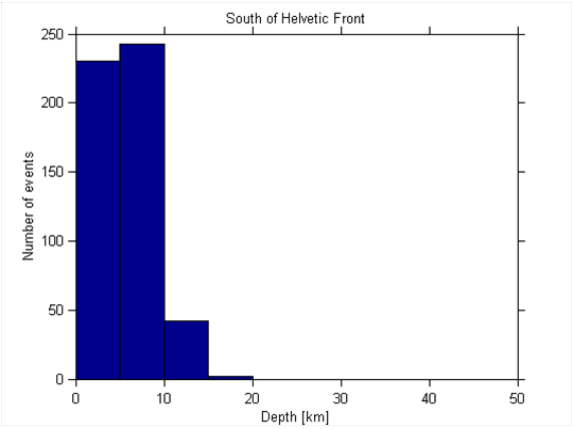

(b) right

Figure 3.11: Focal depth distributions.

Table 3.3: Focal Depth Distributions.

Depth Range [km]	North of HF [%]	South of HF [%]
0-4.99	12.5	44.48
5-9.99	23.91	47
10-14.99	27.17	8.02
15-19.99	14.67	0.38
20-24.99	13.58	0.1
25-29.99	5.43	0
30-34.99	1.08	0
35-39.99	1.08	0
40-44.99	0.54	0
45-49.99	0	0

The distribution labeled South of the Helvetic Front applies to sources SA, XHHA, XHA, HA, XWCA, XCA, and XWA. The distribution labeled North of the Helvetic Front applies to all other sources. Within each depth range, the distribution is assumed to be uniform.

3.3 Earthquake Recurrence Parameters

Figure 3.12 show the logic tree that defines the global alternatives for assessing earthquake recurrence parameters and maximum magnitudes. The global alternatives are dependent across all sources. The earthquake recurrence parameters are based on the ECOS09 catalog declustered using the Grünthal parameters. This is designated as the GR catalog.

The first level of the logic tree Figure 3.12 addresses the assessment of catalog completeness. Two alternative models, designated C1 and C2 are used for all assessments. Earthquake recurrence parameters are derived for C1 and C2 using the minimum magnitudes designated for each completeness model. A second set of recurrence parameters are derived using a minimum magnitude of Mmin 3.007. These are designated with completeness codes C3 and C4.

The second node of the logic tree shown on Figure 3.12 addresses the alternatives for defining a regional b-value for use in maximum magnitude and recurrence parameter estimation. The four alternatives are: the use of all data (designated ba), the use of only post-1975 data (designated *bi*), the use of only historical data prior to 1880 (designated *bh*), and the use of all data allowing for a rate change in 1975 (designated *bs*). The result is 16 alternative datasets for maximum magnitude and recurrence parameter calculations. The results of these calculations are stored in subdirectories labeled by the two-letter catalog designation GR, by C1, C2, C3, or C4 for the completeness model, and by one of the four regional b-value designations. Table 3.4 lists the 16 alternative datasets. These alternatives are dependent across all sources and all have equal weight at this time.

Table 3.4: Catalog and Completeness Data Sets used for Maximum Magnitude and Recurrence Parameter Distributions.

Completeness Model	Regional b-value	Catalog Data Set
Model C1	All data	GRC1-ba
Model C1	Post 1975	GRC1-bi
Model C1	Pre 1880	GRC1-bh
Model C1	Split at 1975	GRC1-bs
Model C2	All data	GRC2-ba
Model C2	Post 1975	GRC2-bi
Model C2	Pre 1880	GRC2-bh
Model C2	Split at 1975	GRC2-bs
Model C3	All data	GRC3-ba
Model C3	Post 1975	GRC3-bi
Model C3	Pre 1880	GRC3-bh
Model C3	Split at 1975	GRC3-bs
Model C4	All data	GRC4-ba
Model C4	Post 1975	GRC4-bi
Model C4	Pre 1880	GRC4-bh
Model C4	Split at 1975	GRC4-bs

Maximum magnitude distributions were derived using the EPRI approach. Two global options are included for the upper tail truncation of the distributions, one at magnitude M 7.5 and one at M 8.0. The two global alternative truncation values have equal weight. The distribution files are located in directory `./MMAX` in subdirectories that designate the 16 alternative datasets identified in table 3.4.

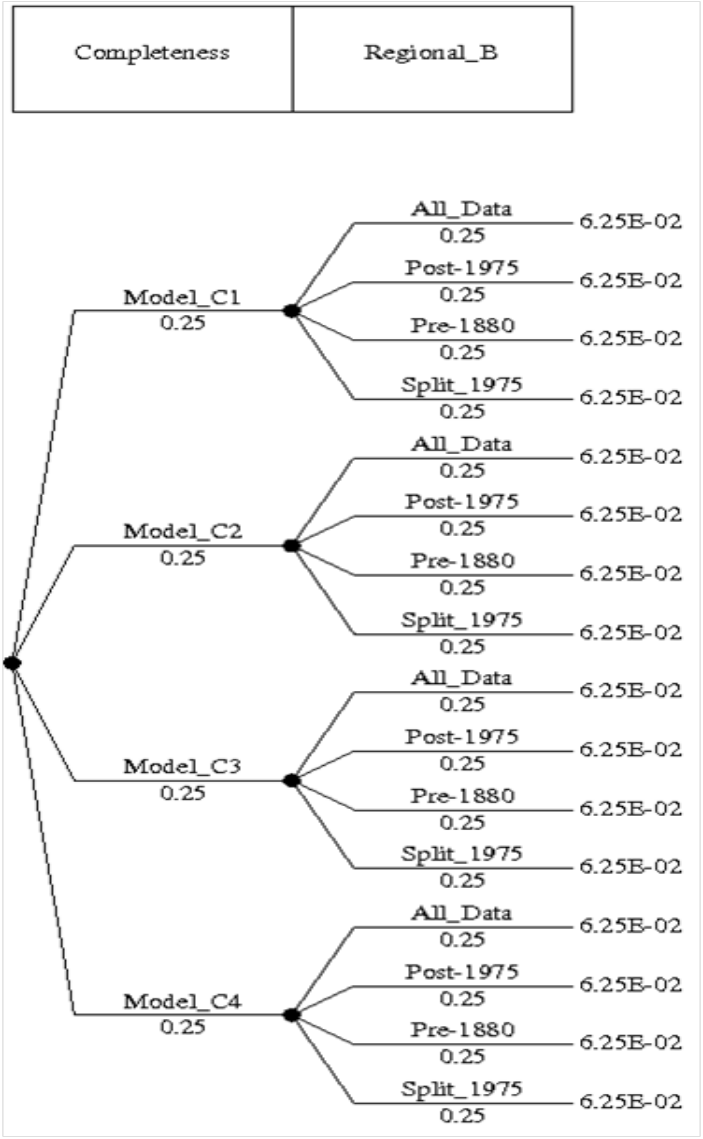

Figure 3.12: Global catalog and regional b-value alternatives.

The distributions for the individual sources are in separate files with the source name. The extensions `*.mx7` correspond to the distributions truncated at M 7.5 and the extensions `*.mx8` correspond to the distributions truncated at M 8.0.

Earthquake recurrence rates for each source are defined in terms of joint discrete distributions for $N(m \geq 5)$ and $\beta[b \ln(10)]$. Again, 16 sets of distributions were developed corresponding to the 16 datasets identified above. The distribution files are located in directory `./REC` in subdirectories that designate the 16 alternative datasets listed in table 3.4.

Five alternative approaches were used to develop these distributions and five distribution files exist for each source and dataset. The first approach is to use the regional b-value and its uncertainty to define the zone recurrence. The distribution file names for this approach have the extension `*.bx`. The second approach is to fit the b-value to the local zone data. The distribution file names for this approach have the extension `*.bf`. The third approach is to again use the regional b-value, but allow for a rate change in 1975. The distribution file names

for this approach have the extension `*.bx2`. The fourth approach is fit the b-value to the local zone data, allowing for a rate change in 1975. The distribution file names for this approach have the extension `*.bf2`. The fifth approach is to define a Bayesian-weighted b-value and use this to compute the recurrence parameter distribution. The distribution file names for this approach have the extension `*.bb`.

Relative weights for these five alternatives were developed on a zone-by-zone basis. The main directory `./REC` contains files with the file name indicating the global dataset and the extension `*.wts`. These files give the relative weight for the five alternative recurrence parameter distributions for each source zone.

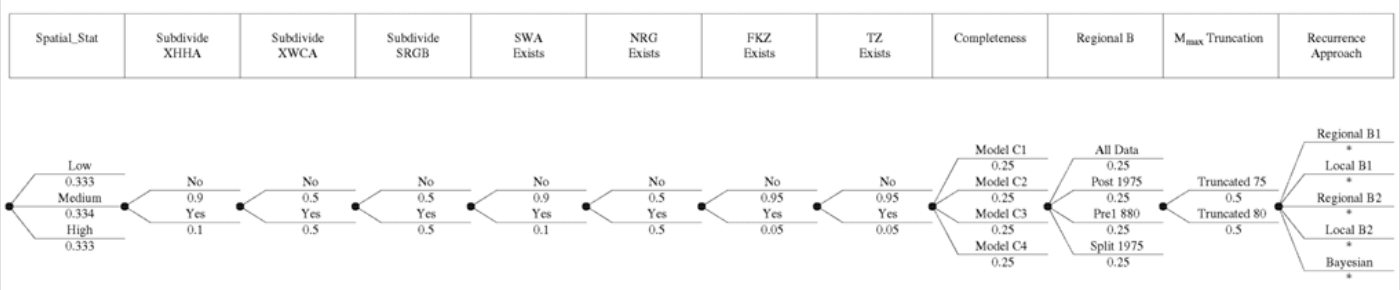

Figure 3.13: Generic logic tree for EG1d. The tree is specific to the source and differ in the weights of the last global variable (Recurrence Approach) alternatives.

Chapter 4

QA-Certificate EG1-QC-1025

QA Certificate	PEGASOS REFINEMENT PROJECT
EG1-QC-1025	

Hazard Input Document (HID)

Expert group:	**EG1d**	***HID designation:***	**EG1-HID-1004**
Expert:	J.-P. Burg, M. Garcia Fernandez, S. Wiemer	***Expert Model (EXM)***	EG1-EXM-1004

HID parameterisation of Expert Model:

TFI: N. A. Abrahamson ***Hazard Input Specialist of TFI-team:*** Ph. Roth

HID based on Elicitation Documents: ☒ EG1-ES-1004

HID based on Exp. Assessments (EXA): ☐

Remarks on the HID model parameterisation in terms of hazard computation input:

The undersigned Hazard Input Specialist confirms that this HID includes all required (subproject specific) input information for hazard computations. No further interpretations of this input will be required and no simplifications except Algorithmic Pinching according to paragraph 2.9 of the QA-Guidelines will be applied to convert this HID into hazard software Input Files.

Signature:

HID acceptance by the Expert / Expert Group:

Date of HID review by the Expert / Expert group: 02.11.2011

HID accepted: ☒ ***HID not accepted:*** ☐

Reasons for non-acceptance of HID / Recommendations:

The undersigned Expert(s) accept(s) the parameterisation proposed in this HID as a faithful and adequate representation of his/their Expert Model. He/they confirm(s) that this HID is free of errors and agree(s) to its use as hazard computation input.

Signature Expert 1 / Expert:

Signature Expert 2:

Signature Expert 3:

Bibliography

Allmann et al. 2009 Allmann, B. ; Edwards, B. ; Bethmann, F. ; Deichmann, N.: Appendix I - Determination of M_W and calibration of M_L (SED) - M_W regression / SED - ETH Zürich, prepared for PRP - PEGASOS Refinement Project. 2009. – Internal Report. SP1 [cited at p. 141]

Brüstle et al. 2003 Brüstle, W. ; Musson, R. ; Sellami, S.: Elicitation report. 2003 (EG1c-HID-005). – Technical Report [cited at p. 358, 359, 360, 361, 362, 499, 504]

Burkhard and Grünthal 2009 Burkhard, M. ; Grünthal, G.: Seismic source zone characterization for the seismic hazard assessment project PEGASOS by the Expert Group 2 (EG 1b). In: *Swiss Journal of Geosciences* 102 (2009), p. 149–188 [cited at p. 3, 5, 169, 261, 267, 423]

Deichmann 2010 Deichmann, N.: Summary of focal depth distributions of earthquakes in Switzerland / SED, prepared for PRP - PEGASOS Refinement Project. 2010 (TP1-TN-1066). – Technical Note. SP1 [cited at p. 361]

Deichmann et al. 2003 Deichmann, N. ; Schmid, S.M. ; Slejko, D.: SP1a Team - Seismic source characterization for PSHA (Probabilistic seismic hazard analysis) of Swiss nuclear power plan sites (Pegasos) - Elicitation summary. 2003. – Internal Report. Pegasos internal report, 133 pp. [cited at p. 141, 142, 149]

Gardner and Knopoff 1974 Gardner, J.K ; Knopoff, L: Is the sequence of earthquakes in South California, with aftershocks removed, Poissonian? In: *Bulletin of the Se* 64 (1974), p. 1363–1367 [cited at p. 5, 169, 267, 423]

Grünthal 1985 Grünthal, G..: The up-dated earthquake catalogue - statistical data characteristics and conclusions for hazard assessment. In: *Intern. Symp. Analyses of Seismic and Seismic Risk, Liblice, Prague* (1985), p. 19–25 [cited at p. 5, 169, 267, 423]

Grünthal et al. 2009a Grünthal, G. ; Bosse, C. ; Stromeyer, D.: Die neue Generation der probabilistischen seismischen Gefährdungseinschätzung der Bundesrepublik Deutschland: Version 2007 mit Anwendung für die Erdbeben-Lastfälle der DIN 19700:2004-07 "Stauanlagen" / GFZ (Deutsches GeoForschungsZentrum). Version: 2009. URL http://edoc.gfz-potsdam.de/gfz/get/13837/0/216508cfbe2f861a4d283e4ae8abae93/0907.pdf. – Scientific Technical Report STR 09/07. – Electronic Resource [cited at p. 263, 264, 265]

Grünthal et al. 2009b Grünthal, G. ; Stromeyer, D. ; Wahlström, R.: Harmonization check of Mw within the central, northern, and northwestern European earthquake catalogue (CENEC). In: *Journal of Seismology* "online first" (2009), p. "online first". http://dx.doi.org/10.1007/s10950-009-9154-2. – DOI 10.1007/s10950–009–9154–2 [cited at p. 261]

Grünthal and Wahlström 2003 Grünthal, G. ; Wahlström, R.: An Mw based earthquake catalogue for central, northern and northwestern Europe using a hierarchy of magnitude conversions. In: *Journal of Seismology* 7 (2003), p. 507–531 [cited at p. 262]

Grünthal and Wahlström 2006 Grünthal, G. ; Wahlström, R.: New Generation of probabilistic seismic hazard assessment for the area Cologne/ Aachen considering the uncertainties of the input data. In: *Natural Hazards* 1-2 (2006), No. 38, p. 159–176 [cited at p. 263]

Grünthal et al. 2009c Grünthal, G. ; Wahlström, R. ; Stromeyer, D.: The unified catalogue of earthquakes in central, northern, and northwestern Europe (CENEC)-updated and expanded to the last millennium. In: Journal of Seismology [**Stromeyer et al. 2004**], p. "online first". – DOI 10.1007/s10950–008–9144–9 [cited at p. 262]

Gruppo di Lavoro 2004 Gruppo di Lavoro: Redazione della mappa di pericolosità sismica prevista dall'Ordinanza PCM 3274 del 20 marzo 2003 / INGV. Milano - Roma, 2004. – Rapporto conclusivo per il Dipartimento della Protezione Civile. 65 pp. + 5 App. [cited at p. 160]

Johnston et al. 1994 Johnston, A.C. ; Coppersmith, K.J ; Kanter, L.R. ; Cornell, C. A.: The earthquakes of stable continental regions, Assemssment of large earthquake potential / Electric Power Research Institute (EPRI). Palo Alto, California, 1994 (TR-102261). – Technical Report. Vol.1-Vol.4 (Vol.5-Vol.6 not available) [cited at p. 7, 8, 10, 269, 424]

Kastrup et al. 2007 Kastrup, U. ; Deichmann, N. ; Fröhlich, A. ; Giardini, D.: Evidence for an active fault below the northwestern Alpine foreland of Switzerland. In: *Geophysical Journal International* 169 (2007), p. 1273–1288. http://dx.doi.org/10.1111/j.1365-246X.2007.03413.x. – DOI 10.1111/j.1365–246X.2007.03413.x [cited at p. 261]

Kijko and Graham 1998 Kijko, A. ; Graham, G.: "Parametric-historic" procedure for probabilistic seismic hazard analysis: Assessment of maximum regional magnitude mmax. In: *Pure and Applied Geophysics* 152 (1998), p. 413–442 [cited at p. 165]

Miller and Rice 1983 Miller, A. C. ; Rice, T. R.: Discrete Approximations of Probability Distributions. In: *The Institute of Management Science* 29 (1983), March, No. 3, p. 352–362 [cited at p. 269, 425]

Musson 2004 Musson, R. M. W.: Joint solution of seismic parameters for seismic source zones through simulation. In: *Bollettino Di Geofisica Teorica Ed Applicata* 45 (2004), p. 1–13 [cited at p. 362]

Musson et al. 2009 Musson, R. M. W. ; Sellami, S. ; Brüstle, W.: Preparing a seismic hazard model for Switzerland: the view from PEGASOS Expert Group 3 (EG1c). In: *Swiss Journal of Geosciences* 102 (2009), p. 107–120. http://dx.doi.org/10.1007/s00015-008-1301-1. – DOI 10.1007/s00015–008–1301–1 [cited at p. 3]

Roth and Farrington 2010 Roth, P. ; Farrington, P. J.: ECOS02-ECOS09, Comparison In Terms of Magnitude and Location / Interoil, prepared for PRP - PEGASOS Refinement Project. 2010 (TP1-TN-1063). – Technical Note. SP1 [cited at p. 354, 357, 358, 359, 499]

Schmid 2009 Schmid, D.: Seismic source characterization of the Alpine foreland in the context of a probabilistic seismic hazard analysis by PEGASOS Expert Group 1 (EG1a). In: *Swiss Journal of Geosciences* 102 (2009), p. 121–148. http://dx.doi.org/10.1007/s00015-008-1300-2. – DOI 10.1007/s00015–008–1300–2 [cited at p. 3]

SED 2002 SED: ECOS02 - Earthquake Catalog of Switzerland / Swiss Seismological Service (SED). 2002 (PEGASOS technical report EXT-TB-0043). – Technical Report. ECOS Report to PEGASOS, Version 31.03.2002; ECOS Catalogue, Version 31.03.2002 [cited at p. 6, 353]

SED 2010 SED: SED ECOS-09: Earthquake Catalogue of Switzerland, Release 2009 / ETH Report, Swiss Seismological Service, prepared for PRP - PEGASOS Refinement Project. 2010 (TP1-TB-1022). – Technical Report. SP1 [cited at p. 5, 152, 158, 169]

SED 2011 SED: SED ECOS-09: Earthquake Catalogie of Switzerland, release 2010 / ETH Report, Swiss Seismological Service, prepared for PRP - PEGASOS Refinement Project. 2011 (SED/PRP/R/008/20100331). – not public catalogue [cited at p. 5, 6, 57, 267, 353]

Stepp 1972 Stepp, J.C.: Analysis of Completeness of the Earthquake Sample in the Puget Sound Area and its Effect on Statistical Estimates of Earthquake Hazard. In: *Proceedings of the International Conference on Microzonation* 2 (1972), p. 897–910 [cited at p. 6, 9]

Stromeyer et al. 2004 Stromeyer, D. ; Gruenthal, G. ; Wahlström, R.: Chi-square regression for seismic strength parameter relations, and their uncertainties, with applications to an Mw based earthquake catalogue for central, northern and northewestern Europe. In: *Journal of Seismology* 1 (2004), No. 8, p. 143–153. http://dx.doi.org/10.1023/B:JOSE.0000009503.80673.51. – DOI 10.1023/B:JOSE.0000009503.80673.51 [cited at p. 262, 482]

Toro 2003 Toro, G.: TP1-TH-0373 / Risk Engineering, Inc., prepared for PEGASOS Project. 2003 (TP1-TH-0373). – Technical Note. SP1 [cited at p. 250, 345, 409, 475]

Weichert 1980 Weichert, D. H.: Estimation of the Earthquake recurrence parameters for unequal observation periods for differtent magnitudes. In: *Bull. Seismmol. Soc. Am.* 4 (1980), No. 70, p. 1337–1346 [cited at p. 6]

Wells and Coppersmith 1994 Wells, D. L. ; Coppersmith, K. J.: New Empirical Relationships among Magnitude, Rupture Length, Rupture Width, Rupture Area, and Surface Displacement. In: *Bulletin of the Seismological Society of America* 84 (1994), August, No. 4, p. 974–1002 [cited at p. 265]

Wiemer et al. 2009 Wiemer, S. ; Garcia-FernANDez, M. ; Burg, J.-P.: Development of a seismic source model for Probabilistic Seismic Hazard Assessment of Nuclear Power Plant Sites in Switzerland: the view from PEGASOS Expert Group 4 (EG1d). In: *Swiss Journal of Geosciences* 102 (2009), p. 189–209. http://dx.doi.org/10.1007/s00015-009-1311-7. – DOI 10.1007/s00015–009–1311–7 [cited at p. 3, 419]

Wiemer and Wössner 2010 Wiemer, S. ; Wössner, J.: Completeness in magnitude reporting of the ECOS2009 catalog: A preliminary study / ETH, Zürich prepared for PRP. 2010. – Internal Report. SP1 [cited at p. 5, 57, 141, 262, 420]

Youngs 2011 Youngs, B.: EG1c Calculations with Final ECOS09 Catalog / AMEC Geomatrix Inc., prepared for PRP - PEGASOS Refinement Project. 2011. – Technical Report [cited at p. 364]

Youngs 2010 Youngs, R.: Feedback plots for ECOS09 Working Meeting 26.01.2010 / AMEC Geomatrix Inc., prepared for PRP - PEGASOS Refinement Project. 2010 (TP1-RF-1162). – Presentation Slides. SP1 [cited at p. 360, 361]

Appendices

Appendix A

Hazard Feedback

A direct link to files for the final SP1 hazard feedback is given here:

- Open external file: TP4-TN-1179 Hazard feedback for SP1 - Explanations.
- Open external file: TP4-RHZ-1002 EG1a Hazard Feedback.
- Open external file: TP4-RHZ-1003 EG1b Hazard Feedback.
- Open external file: TP4-RHZ-1004 EG1c Hazard Feedback.
- Open external file: TP4-RHZ-1005 EG1d Hazard Feedback.

List of Figures

List of Tables